VISIT…

DRUGS AND THE PHARMACEUTICAL SCIENCES VOLUME 137

Freeze-Drying/Lyophilization of Pharmaceutical and Biological Products

Second Edition, Revised and Expanded

edited by
Louis Rey
Joan C. May

Freeze-Drying/Lyophilization of Pharmaceutical and Biological Products

Second Edition, Revised and Expanded

edited by

Louis Rey

Cabinet d'Études
Lausanne, Switzerland

Joan C. May

Center for Biologics Evaluation and Research
Food and Drug Administration
Rockville, Maryland, U.S.A.

Copyright 2004 by Marcel Dekker, Inc. All Rights Reserved.

Although great care has been taken to provide accurate and current information, neither the author(s) nor the publisher, nor anyone else associated with this publication, shall be liable for any loss, damage, or liability directly or indirectly caused or alleged to be caused by this book. The material contained herein is not intended to provide specific advice or recommendations for any specific situation.

Trademark notice: Product or corporate names may be trademarks or registered trademarks and are used only for identification and explanation without intent to infringe.

Library of Congress Cataloging-in-Publication Data
A catalog record for this book is available from the Library of Congress.

ISBN: 0-8247-4868-9

This book is printed on acid-free paper.

Headquarters
Marcel Dekker, Inc., 270 Madison Avenue, New York, NY 10016, U.S.A.
tel: 212-696-9000; fax: 212-685-4540

Distribution and Customer Service
Marcel Dekker, Inc., Cimarron Road, Monticello, New York 12701, U.S.A.
tel: 800-228-1160; fax: 845-796-1772

Eastern Hemisphere Distribution
Marcel Dekker AG, Hutgasse 4, Postfach 812, CH-4001 Basel, Switzerland
tel: 41-61-260-6300; fax: 41-61-260-6333

World Wide Web
http://www.dekker.com

The publisher offers discounts on this book when ordered in bulk quantities. For more information, write to Special Sales/Professional Marketing at the headquarters address above.

Copyright © 2004 by Marcel Dekker, Inc. All Rights Reserved.

Neither this book nor any part may be reproduced or transmitted in any form or by any means, electronic or mechanical, including photocopying, microfilming, and recording, or by any information storage and retrieval system, without permission in writing from the publisher.

Current printing (last digit):

10 9 8 7 6 5 4 3 2 1

PRINTED IN THE UNITED STATES OF AMERICA

Copyright 2004 by Marcel Dekker, Inc. All Rights Reserved.

DRUGS AND THE PHARMACEUTICAL SCIENCES

Executive Editor

James Swarbrick
PharmaceuTech, Inc.
Pinehurst, North Carolina

Advisory Board

Larry L. Augsburger
University of Maryland
Baltimore, Maryland

Harry G. Brittain
Center for Pharmaceutical Physics
Milford, New Jersey

Jennifer B. Dressman
Johann Wolfgang Goethe-University
Frankfurt, Germany

Anthony J. Hickey
University of North Carolina School of Pharmacy
Chapel Hill, North Carolina

Jeffrey A. Hughes
University of Florida College of Pharmacy
Gainesville, Florida

Ajaz Hussain
U.S. Food and Drug Administration
Frederick, Maryland

Trevor M. Jones
The Association of the
British Pharmaceutical Industry
London, United Kingdom

Hans E. Junginger
Leiden/Amsterdam Center
for Drug Research
Leiden, The Netherlands

Vincent H. L. Lee
University of Southern California
Los Angeles, California

Stephen G. Schulman
University of Florida
Gainesville, Florida

Jerome P. Skelly
Alexandria, Virginia

Elizabeth M. Topp
University of Kansas School of Pharmacy
Lawrence, Kansas

Geoffrey T. Tucker
University of Sheffield
Royal Hallamshire Hospital
Sheffield, United Kingdom

Peter York
University of Bradford School of Pharmacy
Bradford, United Kingdom

Copyright 2004 by Marcel Dekker, Inc. All Rights Reserved.

DRUGS AND THE PHARMACEUTICAL SCIENCES

A Series of Textbooks and Monographs

1. Pharmacokinetics, *Milo Gibaldi and Donald Perrier*
2. Good Manufacturing Practices for Pharmaceuticals: A Plan for Total Quality Control, *Sidney H. Willig, Murray M. Tuckerman, and William S. Hitchings IV*
3. Microencapsulation, *edited by J. R. Nixon*
4. Drug Metabolism: Chemical and Biochemical Aspects, *Bernard Testa and Peter Jenner*
5. New Drugs: Discovery and Development, *edited by Alan A. Rubin*
6. Sustained and Controlled Release Drug Delivery Systems, *edited by Joseph R. Robinson*
7. Modern Pharmaceutics, *edited by Gilbert S. Banker and Christopher T. Rhodes*
8. Prescription Drugs in Short Supply: Case Histories, *Michael A. Schwartz*
9. Activated Charcoal: Antidotal and Other Medical Uses, *David O. Cooney*
10. Concepts in Drug Metabolism (in two parts), *edited by Peter Jenner and Bernard Testa*
11. Pharmaceutical Analysis: Modern Methods (in two parts), *edited by James W. Munson*
12. Techniques of Solubilization of Drugs, *edited by Samuel H. Yalkowsky*
13. Orphan Drugs, *edited by Fred E. Karch*
14. Novel Drug Delivery Systems: Fundamentals, Developmental Concepts, Biomedical Assessments, *Yie W. Chien*
15. Pharmacokinetics: Second Edition, Revised and Expanded, *Milo Gibaldi and Donald Perrier*
16. Good Manufacturing Practices for Pharmaceuticals: A Plan for Total Quality Control, Second Edition, Revised and Expanded, *Sidney H. Willig, Murray M. Tuckerman, and William S. Hitchings IV*
17. Formulation of Veterinary Dosage Forms, *edited by Jack Blodinger*
18. Dermatological Formulations: Percutaneous Absorption, *Brian W. Barry*
19. The Clinical Research Process in the Pharmaceutical Industry, *edited by Gary M. Matoren*
20. Microencapsulation and Related Drug Processes, *Patrick B. Deasy*
21. Drugs and Nutrients: The Interactive Effects, *edited by Daphne A. Roe and T. Colin Campbell*
22. Biotechnology of Industrial Antibiotics, *Erick J. Vandamme*

Copyright 2004 by Marcel Dekker, Inc. All Rights Reserved.

23. Pharmaceutical Process Validation, *edited by Bernard T. Loftus and Robert A. Nash*
24. Anticancer and Interferon Agents: Synthesis and Properties, *edited by Raphael M. Ottenbrite and George B. Butler*
25. Pharmaceutical Statistics: Practical and Clinical Applications, *Sanford Bolton*
26. Drug Dynamics for Analytical, Clinical, and Biological Chemists, *Benjamin J. Gudzinowicz, Burrows T. Younkin, Jr., and Michael J. Gudzinowicz*
27. Modern Analysis of Antibiotics, *edited by Adjoran Aszalos*
28. Solubility and Related Properties, *Kenneth C. James*
29. Controlled Drug Delivery: Fundamentals and Applications, Second Edition, Revised and Expanded, *edited by Joseph R. Robinson and Vincent H. Lee*
30. New Drug Approval Process: Clinical and Regulatory Management, *edited by Richard A. Guarino*
31. Transdermal Controlled Systemic Medications, *edited by Yie W. Chien*
32. Drug Delivery Devices: Fundamentals and Applications, *edited by Praveen Tyle*
33. Pharmacokinetics: Regulatory • Industrial • Academic Perspectives, *edited by Peter G. Welling and Francis L. S. Tse*
34. Clinical Drug Trials and Tribulations, *edited by Allen E. Cato*
35. Transdermal Drug Delivery: Developmental Issues and Research Initiatives, *edited by Jonathan Hadgraft and Richard H. Guy*
36. Aqueous Polymeric Coatings for Pharmaceutical Dosage Forms, *edited by James W. McGinity*
37. Pharmaceutical Pelletization Technology, *edited by Isaac Ghebre-Sellassie*
38. Good Laboratory Practice Regulations, *edited by Allen F. Hirsch*
39. Nasal Systemic Drug Delivery, *Yie W. Chien, Kenneth S. E. Su, and Shyi-Feu Chang*
40. Modern Pharmaceutics: Second Edition, Revised and Expanded, *edited by Gilbert S. Banker and Christopher T. Rhodes*
41. Specialized Drug Delivery Systems: Manufacturing and Production Technology, *edited by Praveen Tyle*
42. Topical Drug Delivery Formulations, *edited by David W. Osborne and Anton H. Amann*
43. Drug Stability: Principles and Practices, *Jens T. Carstensen*
44. Pharmaceutical Statistics: Practical and Clinical Applications, Second Edition, Revised and Expanded, *Sanford Bolton*
45. Biodegradable Polymers as Drug Delivery Systems, *edited by Mark Chasin and Robert Langer*
46. Preclinical Drug Disposition: A Laboratory Handbook, *Francis L. S. Tse and James J. Jaffe*
47. HPLC in the Pharmaceutical Industry, *edited by Godwin W. Fong and Stanley K. Lam*

Copyright 2004 by Marcel Dekker, Inc. All Rights Reserved.

48. Pharmaceutical Bioequivalence, *edited by Peter G. Welling, Francis L. S. Tse, and Shrikant V. Dinghe*
49. Pharmaceutical Dissolution Testing, *Umesh V. Banakar*
50. Novel Drug Delivery Systems: Second Edition, Revised and Expanded, *Yie W. Chien*
51. Managing the Clinical Drug Development Process, *David M. Cocchetto and Ronald V. Nardi*
52. Good Manufacturing Practices for Pharmaceuticals: A Plan for Total Quality Control, Third Edition, *edited by Sidney H. Willig and James R. Stoker*
53. Prodrugs: Topical and Ocular Drug Delivery, *edited by Kenneth B. Sloan*
54. Pharmaceutical Inhalation Aerosol Technology, *edited by Anthony J. Hickey*
55. Radiopharmaceuticals: Chemistry and Pharmacology, *edited by Adrian D. Nunn*
56. New Drug Approval Process: Second Edition, Revised and Expanded, *edited by Richard A. Guarino*
57. Pharmaceutical Process Validation: Second Edition, Revised and Expanded, *edited by Ira R. Berry and Robert A. Nash*
58. Ophthalmic Drug Delivery Systems, *edited by Ashim K. Mitra*
59. Pharmaceutical Skin Penetration Enhancement, *edited by Kenneth A. Walters and Jonathan Hadgraft*
60. Colonic Drug Absorption and Metabolism, *edited by Peter R. Bieck*
61. Pharmaceutical Particulate Carriers: Therapeutic Applications, *edited by Alain Rolland*
62. Drug Permeation Enhancement: Theory and Applications, *edited by Dean S. Hsieh*
63. Glycopeptide Antibiotics, *edited by Ramakrishnan Nagarajan*
64. Achieving Sterility in Medical and Pharmaceutical Products, *Nigel A. Halls*
65. Multiparticulate Oral Drug Delivery, *edited by Isaac Ghebre-Sellassie*
66. Colloidal Drug Delivery Systems, *edited by Jörg Kreuter*
67. Pharmacokinetics: Regulatory • Industrial • Academic Perspectives, Second Edition, *edited by Peter G. Welling and Francis L. S. Tse*
68. Drug Stability: Principles and Practices, Second Edition, Revised and Expanded, *Jens T. Carstensen*
69. Good Laboratory Practice Regulations: Second Edition, Revised and Expanded, *edited by Sandy Weinberg*
70. Physical Characterization of Pharmaceutical Solids, *edited by Harry G. Brittain*
71. Pharmaceutical Powder Compaction Technology, *edited by Göran Alderborn and Christer Nyström*
72. Modern Pharmaceutics: Third Edition, Revised and Expanded, *edited by Gilbert S. Banker and Christopher T. Rhodes*

Copyright 2004 by Marcel Dekker, Inc. All Rights Reserved.

73. Microencapsulation: Methods and Industrial Applications, *edited by Simon Benita*
74. Oral Mucosal Drug Delivery, *edited by Michael J. Rathbone*
75. Clinical Research in Pharmaceutical Development, *edited by Barry Bleidt and Michael Montagne*
76. The Drug Development Process: Increasing Efficiency and Cost Effectiveness, *edited by Peter G. Welling, Louis Lasagna, and Umesh V. Banakar*
77. Microparticulate Systems for the Delivery of Proteins and Vaccines, *edited by Smadar Cohen and Howard Bernstein*
78. Good Manufacturing Practices for Pharmaceuticals: A Plan for Total Quality Control, Fourth Edition, Revised and Expanded, *Sidney H. Willig and James R. Stoker*
79. Aqueous Polymeric Coatings for Pharmaceutical Dosage Forms: Second Edition, Revised and Expanded, *edited by James W. McGinity*
80. Pharmaceutical Statistics: Practical and Clinical Applications, Third Edition, *Sanford Bolton*
81. Handbook of Pharmaceutical Granulation Technology, *edited by Dilip M. Parikh*
82. Biotechnology of Antibiotics: Second Edition, Revised and Expanded, *edited by William R. Strohl*
83. Mechanisms of Transdermal Drug Delivery, *edited by Russell O. Potts and Richard H. Guy*
84. Pharmaceutical Enzymes, *edited by Albert Lauwers and Simon Scharpé*
85. Development of Biopharmaceutical Parenteral Dosage Forms, *edited by John A. Bontempo*
86. Pharmaceutical Project Management, *edited by Tony Kennedy*
87. Drug Products for Clinical Trials: An International Guide to Formulation • Production • Quality Control, *edited by Donald C. Monkhouse and Christopher T. Rhodes*
88. Development and Formulation of Veterinary Dosage Forms: Second Edition, Revised and Expanded, *edited by Gregory E. Hardee and J. Desmond Baggot*
89. Receptor-Based Drug Design, *edited by Paul Leff*
90. Automation and Validation of Information in Pharmaceutical Processing, *edited by Joseph F. deSpautz*
91. Dermal Absorption and Toxicity Assessment, *edited by Michael S. Roberts and Kenneth A. Walters*
92. Pharmaceutical Experimental Design, *Gareth A. Lewis, Didier Mathieu, and Roger Phan-Tan-Luu*
93. Preparing for FDA Pre-Approval Inspections, *edited by Martin D. Hynes III*
94. Pharmaceutical Excipients: Characterization by IR, Raman, and NMR Spectroscopy, *David E. Bugay and W. Paul Findlay*
95. Polymorphism in Pharmaceutical Solids, *edited by Harry G. Brittain*

Copyright 2004 by Marcel Dekker, Inc. All Rights Reserved.

96. Freeze-Drying/Lyophilization of Pharmaceutical and Biological Products, *edited by Louis Rey and Joan C. May*
97. Percutaneous Absorption: Drugs–Cosmetics–Mechanisms–Methodology, Third Edition, Revised and Expanded, *edited by Robert L. Bronaugh and Howard I. Maibach*
98. Bioadhesive Drug Delivery Systems: Fundamentals, Novel Approaches, and Development, *edited by Edith Mathiowitz, Donald E. Chickering III, and Claus-Michael Lehr*
99. Protein Formulation and Delivery, *edited by Eugene J. McNally*
100. New Drug Approval Process: Third Edition, The Global Challenge, *edited by Richard A. Guarino*
101. Peptide and Protein Drug Analysis, *edited by Ronald E. Reid*
102. Transport Processes in Pharmaceutical Systems, *edited by Gordon L. Amidon, Ping I. Lee, and Elizabeth M. Topp*
103. Excipient Toxicity and Safety, *edited by Myra L. Weiner and Lois A. Kotkoskie*
104. The Clinical Audit in Pharmaceutical Development, *edited by Michael R. Hamrell*
105. Pharmaceutical Emulsions and Suspensions, *edited by Francoise Nielloud and Gilberte Marti-Mestres*
106. Oral Drug Absorption: Prediction and Assessment, *edited by Jennifer B. Dressman and Hans Lennernäs*
107. Drug Stability: Principles and Practices, Third Edition, Revised and Expanded, *edited by Jens T. Carstensen and C. T. Rhodes*
108. Containment in the Pharmaceutical Industry, *edited by James P. Wood*
109. Good Manufacturing Practices for Pharmaceuticals: A Plan for Total Quality Control from Manufacturer to Consumer, Fifth Edition, Revised and Expanded, *Sidney H. Willig*
110. Advanced Pharmaceutical Solids, *Jens T. Carstensen*
111. Endotoxins: Pyrogens, LAL Testing, and Depyrogenation, Second Edition, Revised and Expanded, *Kevin L. Williams*
112. Pharmaceutical Process Engineering, *Anthony J. Hickey and David Ganderton*
113. Pharmacogenomics, *edited by Werner Kalow, Urs A. Meyer, and Rachel F. Tyndale*
114. Handbook of Drug Screening, *edited by Ramakrishna Seethala and Prabhavathi B. Fernandes*
115. Drug Targeting Technology: Physical • Chemical • Biological Methods, *edited by Hans Schreier*
116. Drug–Drug Interactions, *edited by A. David Rodrigues*
117. Handbook of Pharmaceutical Analysis, *edited by Lena Ohannesian and Anthony J. Streeter*
118. Pharmaceutical Process Scale-Up, *edited by Michael Levin*
119. Dermatological and Transdermal Formulations, *edited by Kenneth A. Walters*

Copyright 2004 by Marcel Dekker, Inc. All Rights Reserved.

120. Clinical Drug Trials and Tribulations: Second Edition, Revised and Expanded, *edited by Allen Cato, Lynda Sutton, and Allen Cato III*
121. Modern Pharmaceutics: Fourth Edition, Revised and Expanded, *edited by Gilbert S. Banker and Christopher T. Rhodes*
122. Surfactants and Polymers in Drug Delivery, *Martin Malmsten*
123. Transdermal Drug Delivery: Second Edition, Revised and Expanded, *edited by Richard H. Guy and Jonathan Hadgraft*
124. Good Laboratory Practice Regulations: Second Edition, Revised and Expanded, *edited by Sandy Weinberg*
125. Parenteral Quality Control: Sterility, Pyrogen, Particulate, and Package Integrity Testing: Third Edition, Revised and Expanded, *Michael J. Akers, Daniel S. Larrimore, and Dana Morton Guazzo*
126. Modified-Release Drug Delivery Technology, *edited by Michael J. Rathbone, Jonathan Hadgraft, and Michael S. Roberts*
127. Simulation for Designing Clinical Trials: A Pharmacokinetic-Pharmacodynamic Modeling Perspective, *edited by Hui C. Kimko and Stephen B. Duffull*
128. Affinity Capillary Electrophoresis in Pharmaceutics and Biopharmaceutics, *edited by Reinhard H. H. Neubert and Hans-Hermann Rü ttinger*
129. Pharmaceutical Process Validation: An International Third Edition, Revised and Expanded, *edited by Robert A. Nash and Alfred H. Wachter*
130. Ophthalmic Drug Delivery Systems: Second Edition, Revised and Expanded, *edited by Ashim K. Mitra*
131. Pharmaceutical Gene Delivery Systems, *edited by Alain Rolland and Sean M. Sullivan*
132. Biomarkers in Clinical Drug Development, *edited by John C. Bloom and Robert A. Dean*
133. Pharmaceutical Extrusion Technology, *edited by Isaac Ghebre-Sellassie and Charles Martin*
134. Pharmaceutical Inhalation Aerosol Technology: Second Edition, Revised and Expanded, *edited by Anthony J. Hickey*
135. Pharmaceutical Statistics: Practical and Clinical Applications, Fourth Edition, *Sanford Bolton and Charles Bon*
136. Compliance Handbook for Pharmaceuticals, Medical Devices, and Biologics, *edited by Carmen Medina*
137. Freeze-Drying/Lyophilization of Pharmaceutical and Biological Products: Second Edition, Revised and Expanded, *edited by Louis Rey and Joan C. May*

ADDITIONAL VOLUMES IN PREPARATION

New Drug Approval Process: Fourth Edition, Accelerating Global Registrations, *edited by Richard A. Guarino*

Microbial Contamination Control in Parenteral Manufacturing, *edited by Kevin L. Williams*

Copyright 2004 by Marcel Dekker, Inc. All Rights Reserved.

Foreword

Like most of today's technological success stories, the history of freeze-drying has been pretty much limited to the 20th century. Whereas Altmann (1), in 1890, reported drying frozen tissues to make histological sections, it was not until 1909 that an application to biologicals was first reported (2). Although the first patent was filed in 1927 (3), there appears to have been little interest in commercial uses until 1935 with a publication by Flosdorf and Mudd (4) that introduced the concept of the cold trap. In the early 1940s Flosdorf et al. (5) in the United States and Greaves (6), working quite independently in England, constructed plants for the large-scale production of dried plasma for wartime use, establishing both the principles and the commercial potential of a new industry.

During the subsequent half-century, the potential of freeze-drying captured the imagination of both scientists and industrial engineers, often without full appreciation of the economic limitations imposed by the immutable thermodynamic costs of freezing and the subsequent sublimation of the frozen water. The food industry in particular was attracted by the potential of prolonged room-temperature storage at a time when home freezers were not yet a staple in every kitchen. It is surprising how long it took to recognize the inappropriateness of this demanding technology for use with a low-cost, high-volume product.

It is the biological and pharmaceutical industries that have been best able to capitalize on the unique virtues of lyophilization and that have stimulated continuing research into the biophysics of both freezing and freeze-drying, some of which is displayed in the initial chapters of this volume. These are the studies that are progressively converting the pioneering and somewhat "brute force" demonstrations by Flosdorf and Greaves into modern, more finely tuned procedures, the importance of which cannot be underestimated. At present it is the pharmaceutical industry with its high-cost product that drives the development of this demanding technology that is increasingly delivering great benefits to our society.

Copyright 2004 by Marcel Dekker, Inc. All Rights Reserved.

This volume provides clear evidence of the mature state of freeze-drying technology, from the mundane to the sophisticated, all of which are essential to a quality product. And, paradoxically, it is the potential for a high-quality product that will stimulate efforts for still higher quality. The more faithfully the lyophilized product resembles the starting material, the more the focus will fall on the quality of the starting material.

The ability to maintain the complex and delicate structural relationships of biologically active compounds during storage at ambient temperatures has been a boon to manufacturers but with an impact well beyond the manufacturing process itself. Analyses of the freeze-drying process are beginning to shift from the physical aspects of freezing and sublimation to a more sophisticated examination of the effects of the process on the chemical structures and the biological properties of the products themselves.

It is here that the technology of freeze-drying may ultimately make its greatest contribution. Protein function and protein conformation are inexorably linked, and the forces that maintain functional conformations can be substantially and often irreversibly altered by cold and by dehydration (7,8). As those in the pharmaceutical industry look more closely at how these forces may be altering the structure and jeopardizing the function of biologicals during lyophilization, they will inevitably find that many of these alterations, particularly those induced by cold, are not limited only to the freeze-drying process but are inherent in many of the isolation and purification procedures conducted well before final processing begins.

An active site on a protein may be a very small proportion of the total molecule. Is maintaining the function of the active site good enough? Why is the rest of the molecule there? Does it make an unrecognized contribution and should we worry about its integrity? The human body is exquisitely designed to reject malformed and altered proteins. Will denaturation of "inactive" portions of a protein alter its physiological function? Can such denaturation be responsible for unrelated side effects? The resolution of technical concerns such as freezing rates, drying temperatures, and product solubility will permit a more critical reassessment of product quality.

As the technology of lyophilization is perfected, it is creating an environment in which attention will be increasingly focused on the stability of product at the molecular level, not just after or even during lyophilization but throughout the entire manufacturing process. The benefits to society of safe and more effective pharmaceuticals are indisputable and for those of us

Copyright 2004 by Marcel Dekker, Inc. All Rights Reserved.

who have participated in the development of freeze-drying technology, it is a privilege to have been part of that history.

Harold T. Meryman, M.D.
Founding Member and Past-President
The Society of Cryobiology
Rockville, Maryland, U.S.A.

REFERENCES

1. R Altmann. "Die Elementarorganismen und ihre Beziehungen zu den Lellen." Veit and Co., Leipzig, 1890.
2. L Shackell. *Amer. J. Physiol.* **24:**325, 1909.
3. HL Tival. U.S. Patent No. 1,630,985, 1927 (and 1932, No. RE 18,364).
4. EW Flosdorf and S Mudd. *J. Immunol.* **29:**389, 1935.
5. EW Flosdorf, F Stokes, and S Mudd. *J. Amer. Med. Ass.* **115:**1095, 1940.
6. RIN Greaves. "The Preservation of Proteins by Drying," H.M.S.O., London, 1946.
7. JF Carpenter, BS Chang. Lyophilization of protein pharmaceuticals. *Biotechnology and Biopharmaceutical Manufacturing, Processing and Preservation*. Edited by KE Avis and VL Wu, Volume 2, 199–264, 1996.
8. LI Tsonev and AG Hirsh. Fluorescence ratio intrinsic basic states analysis: a novel approach to monitor and analyze protein unfolding by fluorescence. *J. of Biochemical and Biophysical Methods* **45,** Issue 1, 1–21.

Copyright 2004 by Marcel Dekker, Inc. All Rights Reserved.

Foreword

When I first became aware of the freezing process, some 30 years ago, the process appeared to me to be rather simple and straightforward. At that time I was employed by a major manufacturer of freeze-dryers but working in the field of microelectronics. Given my background in physical chemistry, I found myself becoming increasingly involved in the field of freeze-drying. I must admit I was surprised and somewhat puzzled to learn that some of those using this process were experiencing difficulties. Many formulations of lyophilized products were made isotonic and contained a host of other recipients such as bulking compounds, cryoprotectants, surfactants, and pH modifiers. It was then that I started to read publications concerning the freeze-drying process, particularly those that offered any explanation regarding why some freeze-drying processes were not successful. It was at that time that I realized that the freeze-drying process was more complex than my first impression. That viewpoint has not been altered and perhaps has only been reinforced as the years have passed. However, a great deal of research has been and continues to be done in this field to enhance our understanding.

The actual number of factors we should take into account with a freeze-drying or lyophilization process I simply never stopped to count. But I am certain that they will exceed the 10 fingers on our hands. While not wishing to examine every possible aspect of this process, let me just share with the reader just three areas that I feel to be of major concern.

The first and foremost is the thermal properties of the formulation, without which one is reduced to process development by trial and error. With knowledge of the thermal properties, one is able to quickly develop and validate a lyophilization process. Without such knowledge one has no reference point on which to rely should a change occur in the properties of the formulation. Knowledge of the thermal properties is paramount to the development of a lyophilization process.

The stability of a lyophilized product will be dependent on the residual moisture content. The industry is certainly very much in need of a means

Copyright 2004 by Marcel Dekker, Inc. All Rights Reserved.

of determining the residual moisture in a product that is both nondestructive and noninvasive. The method should determine the moisture without destroying the dried product, nor should the measurement cause any changes in the product properties such as a loss in activity.

Finally, although the equipment should only provide a safe environment for the product and the necessary operating parameters for the lyophilization process, differences in freeze-drying equipment can affect the process. One should be aware of such differences, especially when transferring a process from one dryer to another. So in any discussion of the lyophilization process, the freeze-drying equipment should not be overlooked.

It is the intent of this Foreword to provide the reader with an appreciation that considerable efforts are being made to enhance our knowledge of the lyophilization process and its associated instrumentation and equipment. While admittedly we will need more information to complete our knowledge of this process, the advances described in this book will take us closer to achieving this final objective.

Thomas A. Jennings, Ph.D.
President
The International Society for Lyophilization–Freeze-Drying, Inc.
Bala Cynwyd, Pennsylvania, U.S.A.

Copyright 2004 by Marcel Dekker, Inc. All Rights Reserved.

Preface

In the middle of the 1950s, when I was actively engaged in low-temperature preservation of living tissues and organs, and tissue banking, I discovered with surprise that in 1902, in St. Petersburg, the participants of the International Congress on Paleontology were given mammoth meat at the banquet. That curiosity actually came from Iakoutia, where a whole frozen mammoth suddenly appeared in the collapsed bank of a Siberian river. Apparently this body had been stored there in the permafrost for 15,000 years and the wolves still found it palatable, as did the conference participants.

I learned then that this discovery was not uncommon and that, from time to time, well-preserved mammoth were found in Northern Siberia. Quite excited by this news I started to investigate whether I could get a sample of that unique material. Numerous requests made at all levels of the administration were fruitless and I had almost forgotten the issue when, in the late 1960s, I received in Switzerland a big box from the USSR Academy of Sciences and—what a surprise—inside there was a big mammoth steak with its fur still attached to the skin. Instead of being frozen it was perfectly freeze-dried and, of course, naturally so. Apparently the big animal had broken its backbone falling into a crevasse and was buried under snow, almost immediately and relatively close to the surface, where it sublimed for millennia, which kept its anatomical features almost intact. We made many scientific investigations of this sample and obtained excellent electron micrographs of the dried muscles. Less successful, by far, was the "stew" that the Nestlé cooks managed to prepare with it: it definitely was no delicacy!

Much more recently, when opening a microbiological conference in Morocco, I came across in my preparation work, on several interesting papers dealing with lithopanspermia, the fantastic ride of living cells in suspended animation, dashing throughout outer space on a rock's back. Quite certainly freeze-dried, they traveled there for maybe millions of years before being captured by the earth's gravity field and falling into the depths

Copyright 2004 by Marcel Dekker, Inc. All Rights Reserved.

of the ocean, where—it is claimed by some scientists—they "seeded" life on our planet. Freeze-drying, as a natural phenomenon, was again in the limelight.

A scientific curiosity for almost 40 years after the publication of Bordas and d'Arsonval in 1906, freeze-drying, later called lyophilization by Earl Flosdorf at the time of World War II, has bloomed again within the past 20 years to become an almost unavoidable technology to preserve rare and sensitive biochemicals and drugs. Concomitantly, new challenges appeared in basic and applied engineering fields and required more and more sophisticated approaches.

This is the reason that Joan May and I found it useful, if not compulsory, to prepare a second edition of our 1999 book *Freeze-Drying/Lyophilization of Pharmaceutical and Biological Products*. Indeed, our understanding of the fundamentals of freeze-drying has been continuously improving in such areas as confined water, annealing, NMR assessment of mobility in dried products, formulation, protein stabilization, and the role of additives. We witness rising interest in some fields which have been long considered as collateral but which are of prime importance today: properties and behavior of glass and elastomeres in the always present container-closer system. In parallel, industrial operations are becoming more diversified and offer numerous different problems: scaling up towards production from the laboratory bench throughout the pilot plant, cleaning and environmental concerns, and sterile handling of bulk material with the associated qualification and validation strategies. Moreover, new technologies are starting to develop: the use of co-solvents and irradiation. However, in all cases, an absolute duty of care still remains for the operators to provide both security and quality and keep their outgoing products in line with the international standards, a field which is quickly expanding.

Thus, year after year, lyophilization is becoming a vast, diversified field for research and development, engineering, and production, still under the close eye of the administration and of the compliance officers.

Therefore, it comes as no surprise that the publisher and the editors decided to prepare this revised and expanded second edition. In so doing, it is a privilege and pleasure for Joan May and I to extend our warm appreciation to all our devoted, competent contributors and acknowledge once more the generous support and professional skill of the staff at Marcel Dekker, Inc.

Louis Rey, Ph.D.

Copyright 2004 by Marcel Dekker, Inc. All Rights Reserved.

Contents

Foreword *Harold T. Meryman*
Foreword *Thomas A. Jennings*
Preface *Louis Rey*
Contributors

1 Glimpses into the Realm of Freeze-Drying: Fundamental Issues
Louis Rey

2 Structural and Dynamic Properties of Bulk and Confined Water
M.-C. Bellissent-Funel and J. Teixeira

3 Mechanisms of Protein Stabilization During Freeze-Drying and Storage: The Relative Importance of Thermodynamic Stabilization and Glassy State Relaxation Dynamics
Michael J. Pikal

4 Freezing and Annealing Phenomena in Lyophilization
James A. Searles

5 Freezing- and Drying-Induced Perturbations of Protein Structure and Mechanisms of Protein Protection by Stabilizing Additives
John F. Carpenter, Ken-ichi Izutsu, and Theodore W. Randolph

6 Molecular Mobility of Freeze-Dried Formulations as Determined by NMR Relaxation, and its Effect on Storage Stability
Sumie Yoshioka

7 Formulation Characterization
D. Q. Wang

Copyright 2004 by Marcel Dekker, Inc. All Rights Reserved.

8 Practical Aspects of Freeze-Drying of Pharmaceutical and Biological Products Using Non-Aqueous Co-Solvent Systems
Dirk L. Teagarden and David S. Baker

9 Closure and Container Considerations in Lyophilization
Frances L. DeGrazio

10 Advanced Glassware for Freeze-Drying
Jürgen Thürk and Peter Knaus

11 Critical Steps in the Preparation of Elastomeric Closures for Biopharmaceutical Freeze-Dried Products
Maninder S. Hora and Sidney N. Wolfe

12 Development of a New Concept for Bulk Freeze-Drying: LYOGUARD® Freeze-Dry Packaging
Meagan Gassler and Louis Rey

13 Regulatory Control of Freeze-Dried Products: Importance and Evaluation of Residual Moisture
Joan C. May

14 Freeze-Drying of Biological Standards
Paul Matejtschuk, Michelle Andersen, and Peter Phillips

15 Industrial Freeze-Drying for Pharmaceutical Applications
Georg-Wilhelm Oetjen

16 Development of Process Data in a Pilot Plant Transferable to Production
Hanna Willemer

17 Technical Procedures for Operation of Cleaning-in-Place/Sterilization-in-Place Process for Production Freeze-Drying Equipment
Gilles A. Beurel

18 Global Validation of Freeze-Drying Cycle Parameters by Using Integral HFT Systems
Gilles A. Beurel

Copyright 2004 by Marcel Dekker, Inc. All Rights Reserved.

19 Lyophilizer Qualification: Some Practical Advice
Thorsten Fischer

20 Lyophilization Process Validation
Christian Bindschaedler

21 A New Development: Irradiation of Freeze-Dried Vaccine and Other Select Biological Products
Louis Rey and Joan C. May

22 Some Leading Edge Prospects in Lyophilization
Louis Rey

Copyright 2004 by Marcel Dekker, Inc. All Rights Reserved.

Contributors

Michelle Andersen Standards Division, National Institute for Biological Standards & Control (NIBSC), Hertfordshire, England

David S. Baker Pfizer Corporation, Kalamazoo, Michigan, U.S.A.

M.-C. Bellissent-Funel Laboratoire Léon-Brillouin (CEA-CNRS), CEA Saclay, Gif-sur-Yvette, France

Gilles A. Beurel S.G.D. Serail, Argenteuil, France

Christian Bindschaedler Serono Laboratories S.A., Aubonne, Switzerland

John F. Carpenter University of Colorado Health Sciences Center, Denver, Colorado, U.S.A.

Frances L. DeGrazio West Pharmaceutical Services, Inc., Lionville, Pennsylvania, U.S.A.

Thorsten Fischer Aventis Behring GmbH, Marburg, Germany

Meagan Gassler W. L. Gore & Associates, Inc., Elkton, Maryland, U.S.A.

Maninder S. Hora Chiron Corporation, Emeryville, California, U.S.A.

Ken-ichi Izutsu University of Colorado Health Sciences Center, Denver, Colorado, U.S.A.

Peter Knaus Forma Vitrum, Schott Pharmaceutical Packaging, St. Gallen, Switzerland

Paul Matejtschuk Standards Division, National Institute for Biological Standards & Control (NIBSC), Hertfordshire, England

Joan C. May Center for Biologics Evaluation and Research, Food and Drug Administration, Rockville, Maryland, U.S.A.

Georg-Wilhelm Oetjen Lübeck, Germany

Copyright 2004 by Marcel Dekker, Inc. All Rights Reserved.

Peter Phillips Standards Division, National Institute for Biological Standards & Control (NIBSC), Hertfordshire, England

Michael J. Pikal School of Pharmacy, University of Connecticut, Storrs, Connecticut, U.S.A.

Theodore W. Randolph University of Colorado, Boulder, Colorado, U.S.A.

Louis Rey Cabinet d'Études, Lausanne, Switzerland

James A. Searles Global Parenteral Products, Manufacturing Science and Technology, Eli Lilly and Company, Indianapolis, Indiana, U.S.A.

Dirk L. Teagarden Pfizer Corporation, Kalamazoo, Michigan, U.S.A.

J. Teixeira Laboratoire Léon-Brillouin (CEA-CNRS), CEA Saclay, Gif-sur-Yvette, France

Jürgen Thürk Forma Vitrum, Schott Pharmaceutical Packaging, St. Gallen, Switzerland

D. Q. Wang Bayer Corporation, Berkeley, California, U.S.A.

Hanna Willemer Köln, Germany

Sidney N. Wolfe Chiron Corporation, Emeryville, California, U.S.A.

Sumie Yoshioka National Institute of Health Sciences, Tokyo, Japan

Copyright 2004 by Marcel Dekker, Inc. All Rights Reserved.

1

Glimpses into the Realm of Freeze-Drying: Fundamental Issues

Louis Rey
*Cabinet d'Études, Lausanne, Switzerland**

In their 1906 paper to the Académie des Sciences in Paris (almost a century ago), Bordas and d'Arsonval [1] demonstrated for the first time that it was possible to dry a delicate product from the frozen state under moderate vacuum. In that state it would be stable at room temperature for a long time and the authors described, in a set of successive notes, that this technique could be applied to the preservation of sera and vaccines. Freeze-drying was then officially borne, despite its having been in use centuries ago by the Incas who dried their frozen meat in the radiant heat of the sun in the rarified atmosphere of the Altiplano.

However, we had to wait until 1935 to witness a major development in the field when Earl W. Flosdorf and his coworkers [2] published some very important research on what they called, at the time, lyophilization (this name was derived from the term *lyophile* coming from the Greek λυος and φιλειν, which means "likes the solvent," describing the great ability of the dry product to rehydrate again). Freeze-drying had then received a new name that has been in current use since, together with cryodesiccation.

Many authors, in different comprehensive books dedicated to freeze-drying, have already described in full detail the scientific history of this

**Mailing address*: 2 Chemin de Verdonnet, CH-1010 Lausanne, Switzerland.

Copyright 2004 by Marcel Dekker, Inc. All Rights Reserved.

method [3], and we will not attempt to do it again. Moreover, in the last 60 years, much research and substantial development have been devoted to freeze-drying, and it would be of little use to list papers that are well known and available to all of the specialists concerned.

This, indeed, is the very reason why the present book has been designed to present to the readers essentially new experimental methods and data, as well as recent developments on our own basic understanding of the physical and chemical mechanisms involved in cryodesiccation.

Nevertheless, it would not be fair to skip the names of some of the great pioneers in the field. Earl Flosdorf, Ronald Greaves, and François Henaff fought the difficult battle of the mass production of freeze-dried human plasma, which was used extensively during World War II. To that end, they engineered the appropriate large-scale equipment. Sir Ernst Boris Chain, the Noble Laureate for penicillin, introduced freeze-drying for the preparation of antibiotics and sensitive biochemicals. Isidore Gersh and, later on, Tokio Nei and Fritjof Sjøstrand produced remarkable photographs of biological structures prepared by freeze-drying for electron microscopy. Charles Merieux, on his side, opened wide new areas for the industrial production of sera and vaccines. In parallel, he developed a bone bank, a first move in a field where the U.S. Navy Medical Corps invested heavily a few years later under Captain Georges Hyatt.

At the same time, cryobiology was getting its credentials with many devoted and gifted scientists such as Basil Luyet, Alan Parkes, Audrey Smith, Harry Meryman, Christopher Polge, Peter Mazur, and others. We had the privilege of living in this exciting period together with all of these people since 1954 and most of them were present in Lyons in 1958 when Charles Merieux and I opened the first International Course on Lyophilization, with the sad exception of Earl Flosdorf who had agreed to deliver the opening address but died tragically a few weeks before the conference.

Today, 40 years later, we are pleased to see that freeze-drying still holds a remarkable place in our multiple panel of advanced technologies and more particularly in the pharmaceutical field. It was thus a wise and sound decision of our publisher to propose that a collective book be devoted to that topic.

I. BASIC FREEZE-DRYING

Lyophilization is a multistage operation in which, quite obviously, each step is critical. The main actors of this scenario are all well known and should be under strict control to achieve a successful operation.

Copyright 2004 by Marcel Dekker, Inc. All Rights Reserved.

The product, i.e., the ''active'' substance which needs to keep its prime properties.

The surrounding ''*medium*'' and its complex cohort of bulking agents, stabilizers, emulsifiers, antioxidants, cryoprotectors, moisture-buffering agents.

The equipment, which needs to be flexible, fully reliable, and geared to the ultimate goal (mass production of sterile/nonsterile drugs or ingredients, experimental research, technical development).

The process, which has to be adapted to individual cases according to the specific requirements and low-temperature behavior of the different products under treatment.

The final conditioning and storage parameters of the finished product, which will vary not only from one substance to another, but in relationship with its ''expected therapeutic life'' and marketing conditions (i.e., vaccines for remote tropical countries, international biological standards, etc.). In other words, a freeze-dryer is not a conventional balance; it does not perform in the same way with different products. *There is no universal recipe for a successful freeze-drying operation* and the repetitive claim that ''this material cannot be freeze-dried'' has no meaning until each successive step of the process has been duly challenged with the product in a systematic and professional way and not by the all-too-common ''trial-and-error'' game.

The freeze-drying cycle. It is now well established that a freeze-drying operation includes:

The ad hoc *preparation of the material* (solid, liquid, paste, emulsion) to be processed taking great care not to impede its fundamental properties.

The freezing step during which the material is hardened by low temperatures. During this very critical period, all fluids present become solid bodies, either crystalline, amorphous, or glass. Most often, water gives rise to a complex ice network but it might also be imbedded in glassy structures or remain more or less firmly bound within the interstitial structures. Solutes do concentrate and might finally crystallize out. At the same time, the volumetric expansion of the system might induce powerful mechanical stresses that combine with the osmotic shock given by the increasing concentration of interstitial fluids.

The *sublimation phase or primary drying* will follow when the frozen material, placed under vacuum, is progressively heated to deliver enough energy for the ice to sublimate. During this very critical

Copyright 2004 by Marcel Dekker, Inc. All Rights Reserved.

period a correct balance has to be adjusted between heat input (heat transfer) and water sublimation (mass transfer) so that drying can proceed without inducing adverse reactions in the frozen material such as back melting, puffing, or collapse. A continuous and precise adjustment of the operating pressure is then compulsory in order to link the heat input to the "evaporative possibilities" of the frozen material.

The *desorption phase or secondary drying* starts when ice is being distilled away and a higher vacuum allows the progressive extraction of bound water at above zero temperatures. This, again, is not an easy tack since overdrying might be as bad as underdrying. For each product, an appropriate residual moisture has to be reached under given temperatures and pressures.

Final conditioning and storage begins with the extraction of the product from the equipment. During this operation great care has to be taken not to lose the refined qualities that have been achieved during the preceding steps. Thus, for vials, stoppering under vacuum or neutral gas within the chamber is the current practice. For products in bulk or in ampoules, extraction might be done in a tight gas chamber by remote operation. Water, oxygen, light, and contaminants are all important threats and must be monitored and controlled.

Ultimate storage has to be done according to the specific "sensitivities" of the products (at room temperature, $+4^{\circ}C$, $-20^{\circ}C$). Again uncontrolled exposures to water vapor, oxygen (air), light, excess heat, or nonsterile environment are major factors to be considered. This obviously includes the composition and quality of the container itself, i.e., glass, elastomers of the stoppers, plastic or organic membranes.

At the end, we find the *reconstitution phase*. This can be done in many different ways with water, balanced salt solutions, or solvents either to restore the concentration of the initial product or to reach a more concentrated or diluted product. For surgical grafts or wound dressings, special procedures might be requested. It is also possible to use the product as such, in its dry state, in a subsequent solvent extraction process when very dilute biochemicals have to be isolated from a large hydrated mass, as is the case for marine invertebrates.

Figure 1 summarizes the freeze-drying cycle and indicates for each step the different limits that have to be taken into consideration. Figure 2 gives an example of a typical freeze-drying cycle.

Copyright 2004 by Marcel Dekker, Inc. All Rights Reserved.

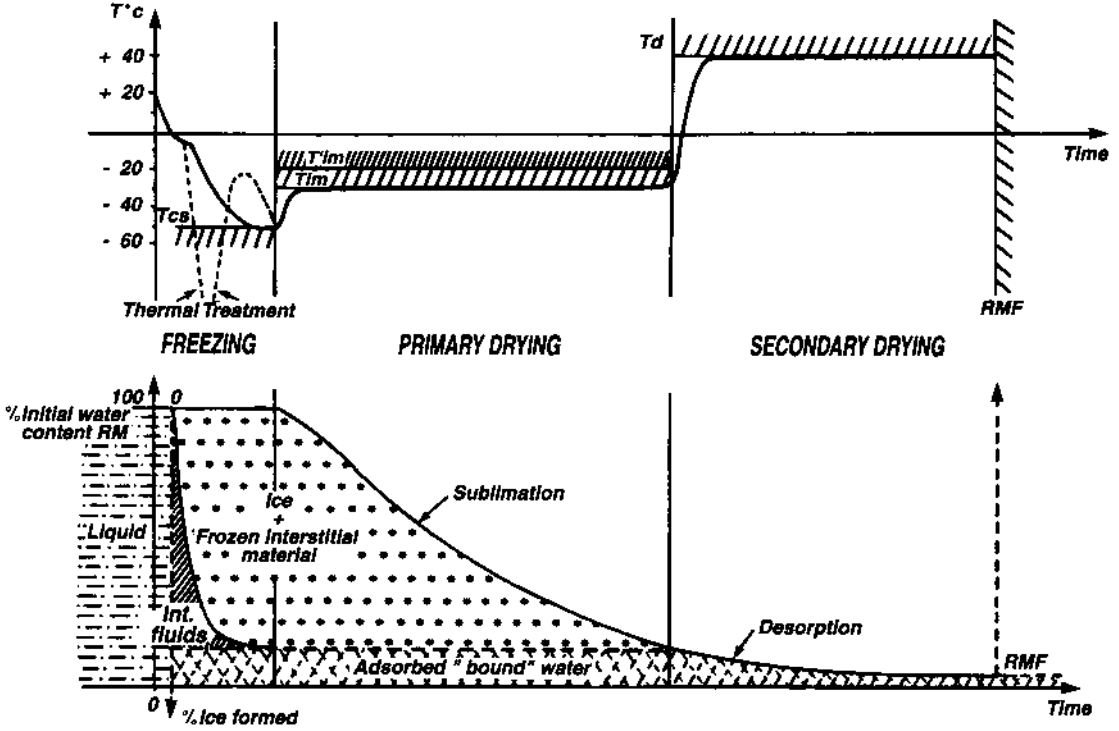

Figure 1 Schematic evolution of the freeze-drying process. Temperatures (upper curve) and water content (lower curve) are indicated versus time. In the temperature diagram T_{CS} = maximum temperature of complete solidification; T_{im} = minimum temperature of incipient melting; T_{lm} = absolute limit for fast process; T_d = maximum allowed temperature for the dry product; RMF, final requested residual moisture.

Copyright 2004 by Marcel Dekker, Inc. All Rights Reserved.

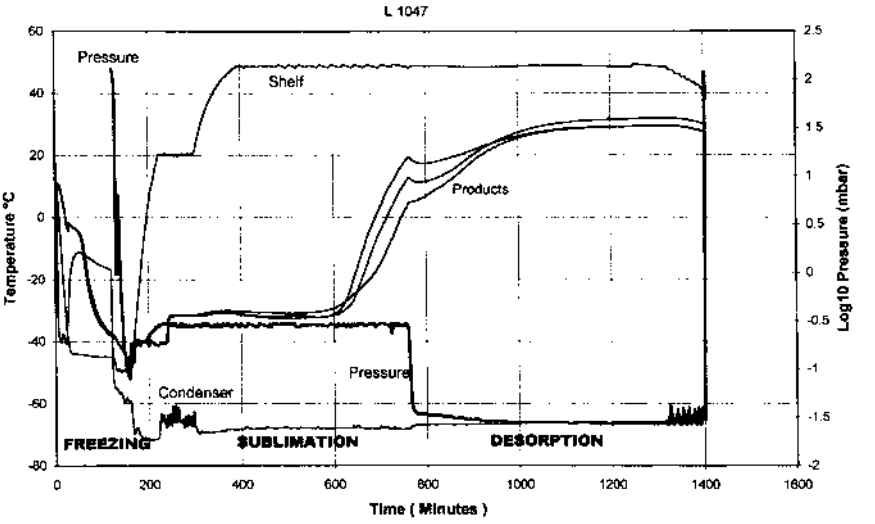

Figure 2 A typical freeze-drying cycle. Note that the pressure is raised to 0.3 mbar to increase the heat transfer during sublimation and then lowered to 0.02 mbar for desorption.

II. INSIGHT INTO THE BEHAVIOR OF PRODUCTS AT LOW TEMPERATURE

A. Thermal and Electric Properties

A fundamental paradigm of freeze-drying is to understand that, in almost every case, there is no direct correlation between the structure of a frozen product and its temperature since all structural features depend essentially on the "thermal history" of the material. In other words, the knowledge of the temperature of a frozen solution is not enough to allow the operator to know its structure since this latter depends, essentially, upon the way this temperature has been reached, i.e., upon the freezing cycle,

For instance, we did show in 1960 [4] that an aqueous solution of sodium chloride at $-25^{\circ}C$ could be

Either a sponge-like ice network soaked with highly concentrated fluids if the system has been cooled progressively from $+20^{\circ}C$ to $-25^{\circ}C$.

Or else a totally frozen solid where all the interstitial fluids have crystallized as eutectics if the system has been cooled, first to $-40^{\circ}C$ and then rewarmed to $-25^{\circ}C$.

Copyright 2004 by Marcel Dekker, Inc. All Rights Reserved.

Actually, when water separates as pure ice, as is the case for diluted solutions, there might be a considerable degree of supercooling in the remaining interstitial fluids. It is, then, compulsory to go to much lower temperatures to "rupture" these metastable states and provoke their separation as solid phases. This, indeed, has a great significance because it is precisely within those hypertonic concentrated fluids that the "active substances" lie whether they are virus particles, bacteria, or delicate proteins, and where they can undergo serious alterations in this aggressive environment. This is the reason why we advised cooling the product at sufficiently low levels to reach what we have called T_{cs}: the maximum temperature of completes solidification [4,5]. However, when frozen, the material will only start to melt when it reaches either eutectic temperature or what we called T_{im}, the minimum temperature of incipient melting [4,5].

Differential thermal analysis (DTA) and differential scanning calorimetry (DSC) are useful techniques to proceed to this determination [4,5]. They can be very advantageously coupled with LF electric measurements since the impedance of the frozen system drops in a spectacular way when melting occurs (see Figures 3 and 4). In other terms, a high electric impedance is always related to a state of utter rigidity. Moreover, the electric measurements are more reliable than DTA/DSC alone. Indeed, when we are dealing with a complex system—more particularly when it contains high

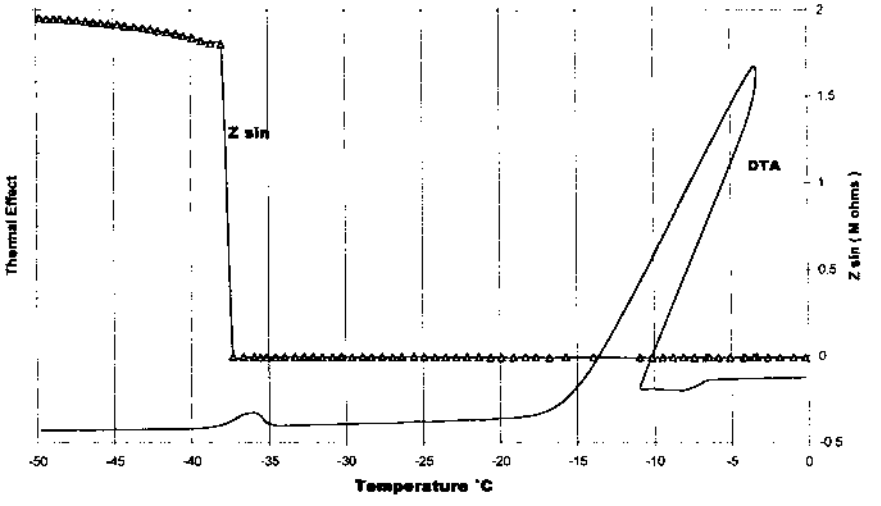

Figure 3 Differential thermal analysis (DTA) and impedance (1000 Hz – $Z \sin \varphi$) of a 2 p. 100 solution of Cl Na in water during controlled freezing.

Copyright 2004 by Marcel Dekker, Inc. All Rights Reserved.

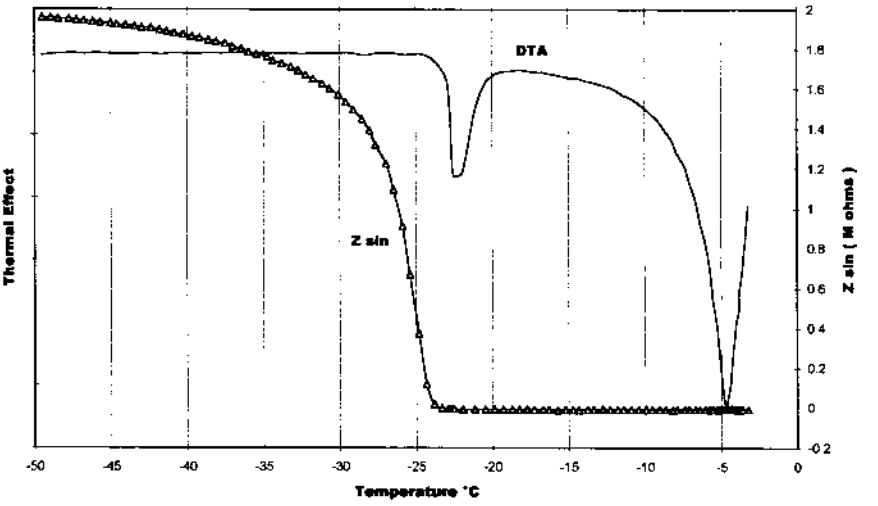

Figure 4 Differential thermal analysis (DTA) and impedance (1000 Hz – $Z \sin \varphi$) of a 2 p. 100 solution of Cl Na in water during controlled rewarming.

molecular weight compounds—the material hardens progressively during freezing and, often, in the course of rewarming shows incipient melting only at relatively high temperatures. Until that point the DTA curve remains "silent." Unfortunately, this is not always a sign of absolute stability since, quite often, a "softening" of the structure appears much earlier. It is our experience that a sharp decrease in electric impedance is a clear warning for an operator who should try and maintain the product during primary drying at temperatures below this limit. Figure 5 demonstrates this phenomenon in the case of the U.S. Standard for Pertussis vaccine lot 9, and Figure 6 shows the same behavior for the Saizen mass 10 mg from Serono. In both cases it is quite obvious that sublimation has to be done at temperatures much lower than those that could be derived from the DTA curves alone.

The evolution of electric properties is, thus, at least for us, a major parameter in the design and follow-up of a freeze-drying cycle. It can even be used for automatic control of the whole operation as we proposed in the past [6].

B. Glass and Vitreous Transformations

It is well known that certain solutions/systems do not crystallize when they are cooled down, especially when this is done in a rapid process.

Copyright 2004 by Marcel Dekker, Inc. All Rights Reserved.

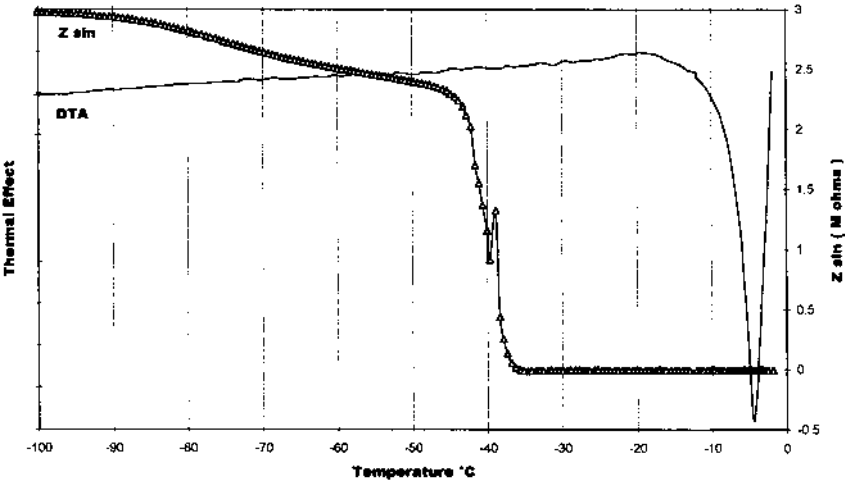

Figure 5 Differential thermal analysis (DTA) and impedance (1000 Hz – $Z \sin \varphi$) of U.S. FDA Standard Pertussis vaccine, lot no. 9.

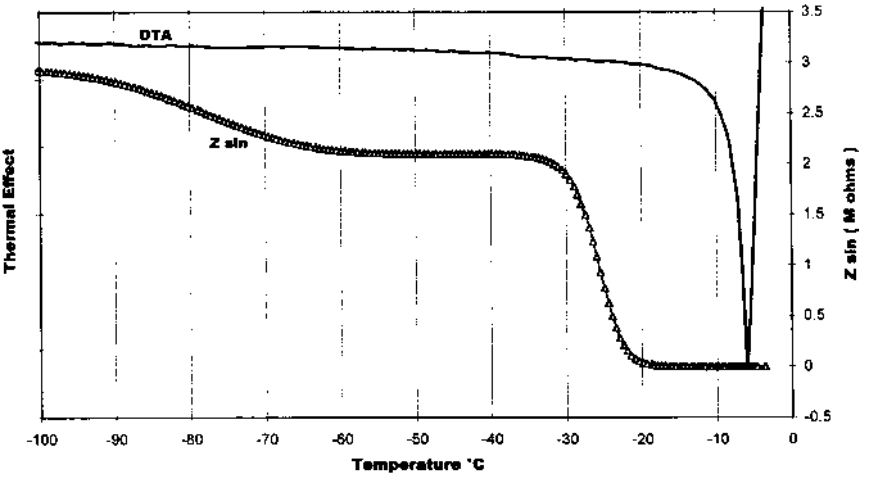

Figure 6 Differential thermal analysis (DTA) and impedance (1000 Hz – $Z \sin \varphi$) of Serono Saizen mass 10 mg.

(Quenching in cryogenic fluids has long been in use by electron microscopy specialists to prepare their samples.) Cooling results in that particular case in the formation of a hard material that has the properties of a glass. This vitreous body can prove to be stable, and when rewarmed it softens

Copyright 2004 by Marcel Dekker, Inc. All Rights Reserved.

progressively and goes back to liquid again. However, in the course of rewarming it generally undergoes a major structural change known as the vitreous transformation. During this process the glass, still in the solid phase, evolves from a solid-like state (with low specific heat and low specific volume) to a liquid-like state with a sharp increase in specific heat and specific volume. This occurs at a well-known temperature, the temperature of vitreous transformation, generally quoted as T_g. A typical example, pure glycerol, is shown in Figure 7. This phenomenon is fully reversible.

In some other cases the glass, when rewarmed, becomes highly unstable, and when the *vitreous transformation* is completed (or sometimes during this transformation itself), it crystallizes out abruptly showing a marked exothermic peak. This, to the contrary, is an irreversible process called *devitrification*. All of the glass might then disappear or it might devitrify only partially. If the material is then cooled again and rewarmed a second time the initial vitreous transformation disappears or is substantially reduced (and sometimes shifted to a higher temperature) and the exothermic peak no longer exists. During this cycle, which we called "thermal Treatment" in 1960 [4–7], the metastable system became unstable and has been "annealed." Figure 8 shows this type of evolution in a glycerol–water–Cl Na system. It is worthwhile mentioning that in both cases the vitreous transformation initiates a marked decrease of the electric

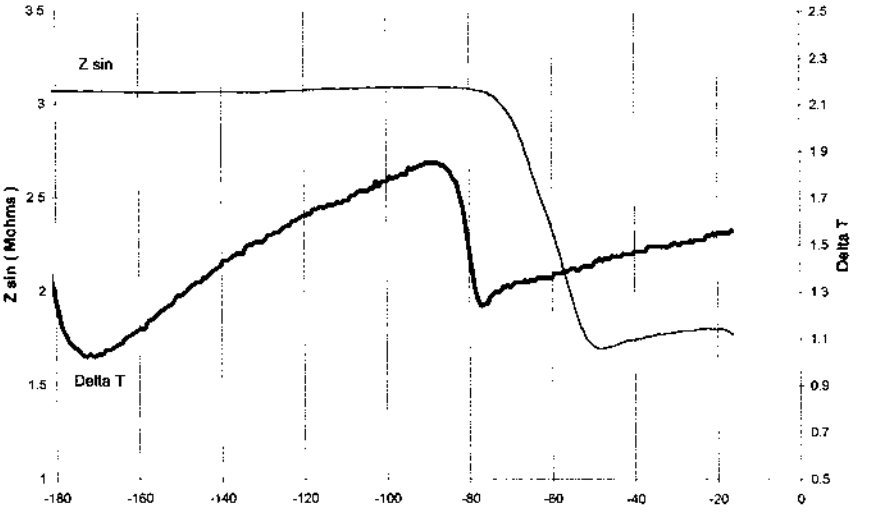

Figure 7 Differential thermal analysis and impedance (1000 Hz) of pure glycerol.

Copyright 2004 by Marcel Dekker, Inc. All Rights Reserved.

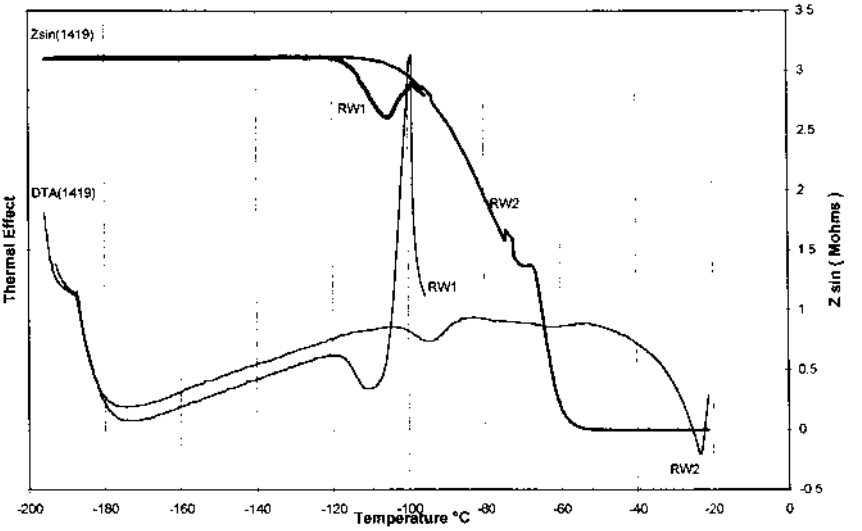

Figure 8 Low-temperature behavior of a 50:50 glycerol–H_2O system containing 10 per 1000 Cl Na. RW1: recordings of DTA and $Z \sin \varphi$ during the first rewarming from $-196°C$ to $-95°C$. When the devitrification peak is completed ($-95°C$), the sample is immediately cooled back to $-196°C$. RW2: Second analysis from $-196°C$ to $-20°C$ after "thermal treatment."

impedance, though at first sight the system remains a compact solid. Figure 9 summarizes this evolution.

The magnitude and temperature of these events are, of course, dependent on the system under investigation, as can be seen in Figure 10 which compares D_2O/glycerol and H_2O/glycerol mixtures.

This type of behavior is not uncommon in pharmaceutical preparations. Indeed, it is often required that a thermal treatment be applied to the material in order to secure a steady and successful freeze-drying operation. In the example depicted in Figure 11 a and b, it was discovered that a refined biochemical (recombinant glycoprotein Mol-2 from the Center for Molecular Immunology in Havana, Cuba) needed to be stabilized by thermal treatment in order to raise the softening temperature (as witnessed by the evolution of the electric impedance) from $-32°C$ to $-19°C$ and allow an easy freezing-drying.

In other instances—as this will be developed later in this book by Carpenter and Pikal—it appears essential to safeguard the glassy state, which is indeed an absolute prerequisite to secure the tertiary structures of active proteins. Here, again, a precise knowledge of the boundaries and sensitivities of this glass is definitely needed.

Copyright 2004 by Marcel Dekker, Inc. All Rights Reserved.

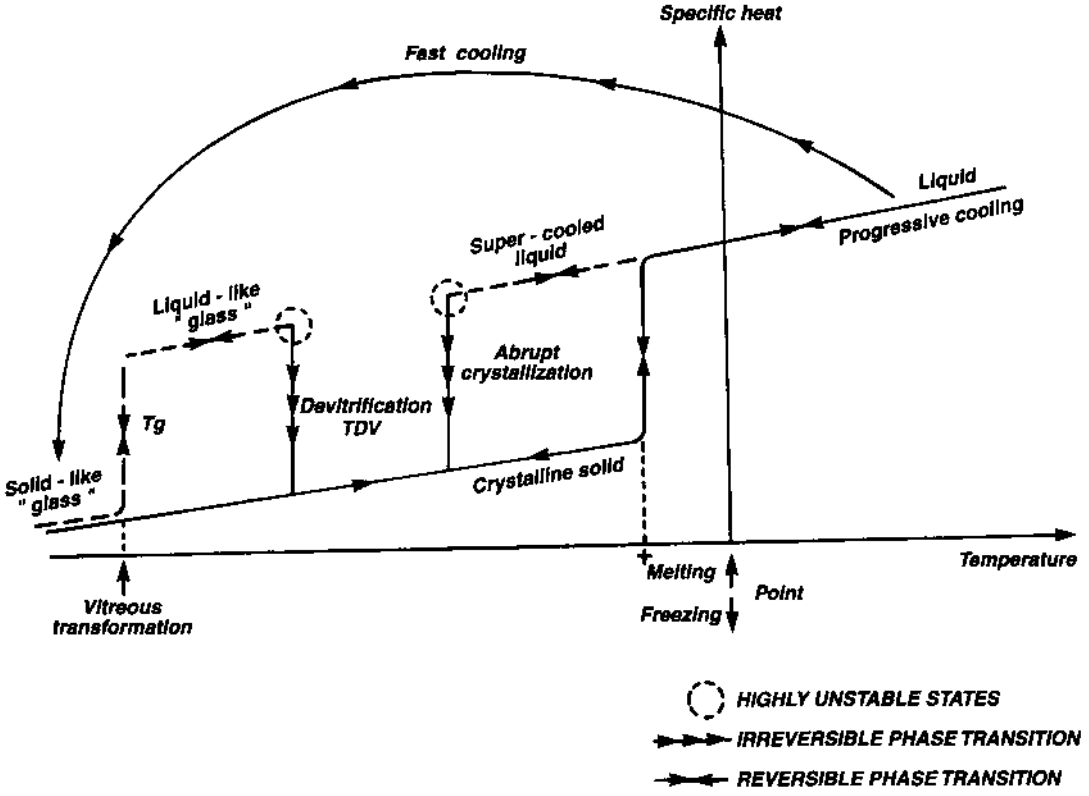

Figure 9 Theoretical diagram of the low-temperature behavior of a system susceptible to present glass formation. Specific heat has been taken as the "maker."

Copyright 2004 by Marcel Dekker, Inc. All Rights Reserved.

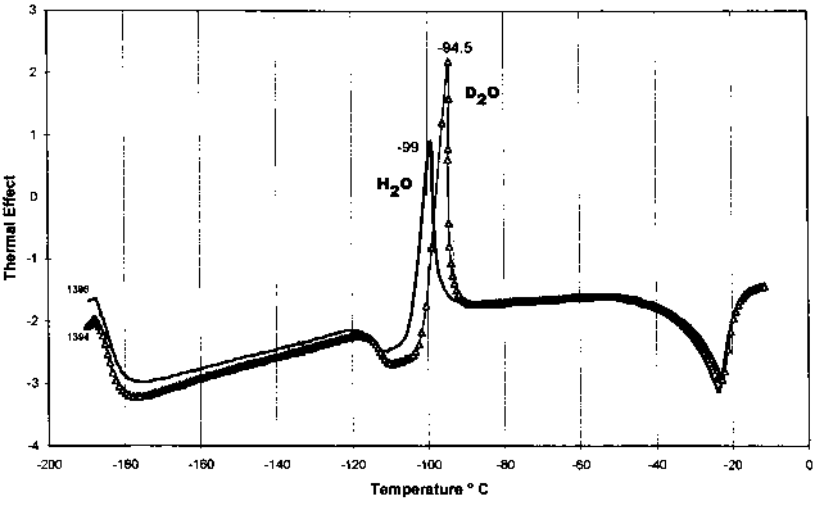

Figure 10 Differential thermal analysis of 50:50/100 mixtures of glycerol and D_2O/H_2O. Both normal and "heavy" water–glycerol mixtures demonstrate the same behavior but the transition temperatures for D_2O are shifted upward by 4.5°C.

Finally, let us mention the interesting case of the sucrose/water systems, which after drying give a very sensitive porous cake susceptible to undergoing adverse transformations at *above zero* temperatures and *in the dry state* because of the existence of a rather high T_g (57°C). It is, thus, compulsory to keep these products at temperatures low enough to prevent the shrinkage of the pellet by what has been called a "rubber behavior".

C. A New Tool to Investigate the Structure of Liquids: Low-Temperature Thermoluminescence

The primary "structure" of the fluids that are bound to undergo freeze-drying is, of course, of great interest. In that wake, the structure of water itself is a determinant item. This is why two chapters in this book relate directly to that topic (Watts and Bellissent-Funel/Teixeira). Accordingly, we will not deal with it. However, we would like to share with our readers and colleagues some ideas that evolved from recent experiments that we have carried out on the low-temperature thermoluminescence of different systems and, in particular, on water itself (see Fig. 12).

Copyright 2004 by Marcel Dekker, Inc. All Rights Reserved.

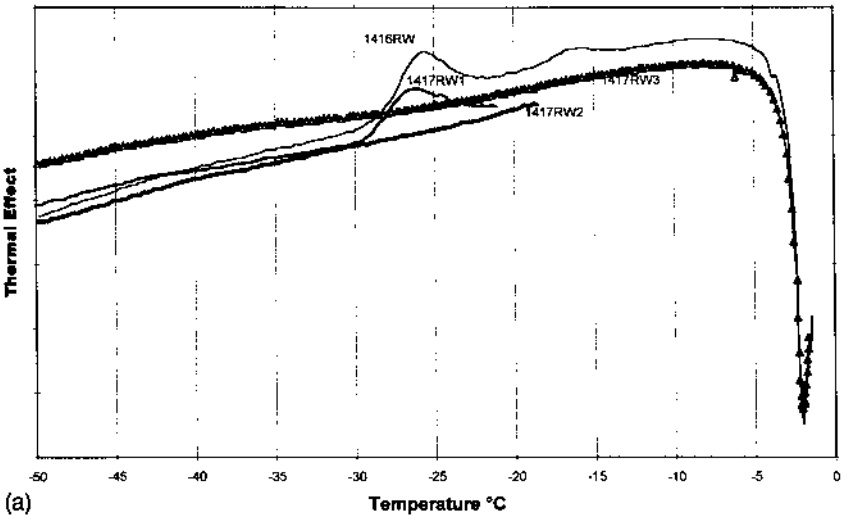

Figure 11 (a and b) Recombinant glycoprotein-Mol-2. *1416 RW*: In a preliminary analysis two slight exothermic phenomena were observed by DTA at $-25.5°C$ and $-16.4°C$, followed by a progressive melting starting around $-8°C$. However, the electrical measurements already showed a marked decrease in rigidity starting at $-32°C$. *1417 RW 1*: "Thermal treatment" was applied by cooling the solution down from $-20°C$ to $-50°C$, then rewarming to $-21°C$. The thermal curve is almost identical to the *1416 RW* one and the first exothermic peak shows up. The systems is then cooled back from $-21°C$ to $-50°C$ and rewarmed again to $-18°C$. *1417 RW* 2 shows, during the second rewarming, that the first exothermic phenomenon has disappeared. As a consequence, the $Z \sin \varphi$ is by far higher and "rigidity" good until $-20°C$. To improve, once more, the low-temperature stability of the system, it is cooled back a third from $-18°C$ to $-50°C$ and then rewarmed for analysis. *1417 RW 3* shows that, in the course of the third rewarming, all "accidents" have disappeared on the DTA curve, which only indicates progressive melting from $-8°C$ upward. Moreover, the stability of the frozen structure has been substantially improved since now $Z \sin \varphi$ remains almost constant during the whole period and only start to drop at $-19°C$ instead of $-32°C$ without thermal treatment. It is then easy to freeze-dry the solution at $-20°C$ or slightly below.

1. Method

Small samples of liquid (0.5 to 1 cm^3) are deposited in open aluminum capsules and frozen down to liquid nitrogen temperatures under well-controlled conditions (generally a two-step freezing: down to $-20°C$ in 10 min with a 5–6 h equilibrium time at this temperature followed by quenching to $-196°C$). The capsules are then "activated" by gamma

Copyright 2004 by Marcel Dekker, Inc. All Rights Reserved.

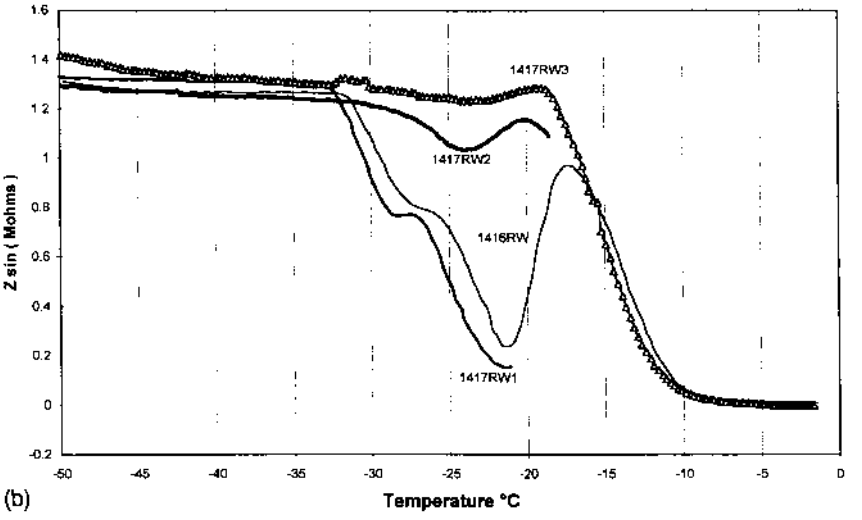

Figure 11 Continued.

irradiation from cobalt-60 sources at liquid nitrogen temperature (courtesy of COGEMA, Celestin Reactor staff in Marcoule, France, and of Cigal Irradiator, C.E.A., D.E.V.M., Cadarache, France). Thus, a high dose (30 kGy = 3 Mrad) is delivered in a short time (45 min). The treated samples are brought back to the laboratory, taken out of the Dewar flask, placed under the window of a very high sensibility photomultiplier, and rewarmed at a constant rate (1.5°C/min) to room temperature. During that time, the samples deactivate by recombination of free radicals, electron-hole pairs, etc., and emit light when the excited states go back to the fundamental level. In some experiments we have been able to record the frequency spectrum of the glow thanks to a high-performance digital CCD camera coupled with a visible- to near-IR ACTON spectrograph (Princeton Instruments).

2. Results

It is generally assumed that the thermoluminescence centers are located preferentially in the defects of the crystalline network and that those defects, in turn, are a mere reflexion of the structure of the original liquid. We can, thus, expect to know a little more about our starting solutions.

Figure 13 shows the thermoluminescence curves for pure H_2O and D_2O. For H_2O they confirm prior measurements made by Grossweiner and Matheson [8]. Several major peaks can be identified. We can also see that for

Copyright 2004 by Marcel Dekker, Inc. All Rights Reserved.

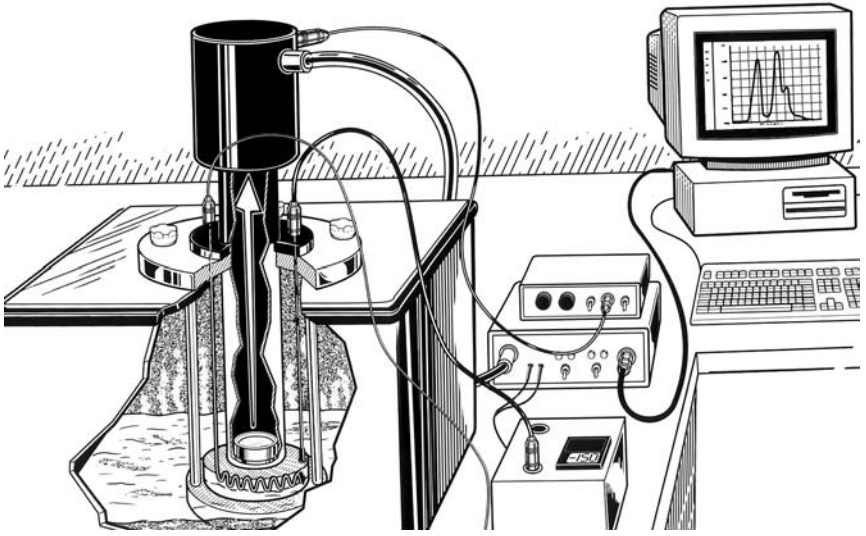

Figure 12 Low-temperature thermoluminescence set-up. A previously irradiated frozen sample, placed in a liquid N_2 cryostat, emits light during controlled rewarming. The corresponding glow is recorded by a photomultiplier versus temperature.

Copyright 2004 by Marcel Dekker, Inc. All Rights Reserved.

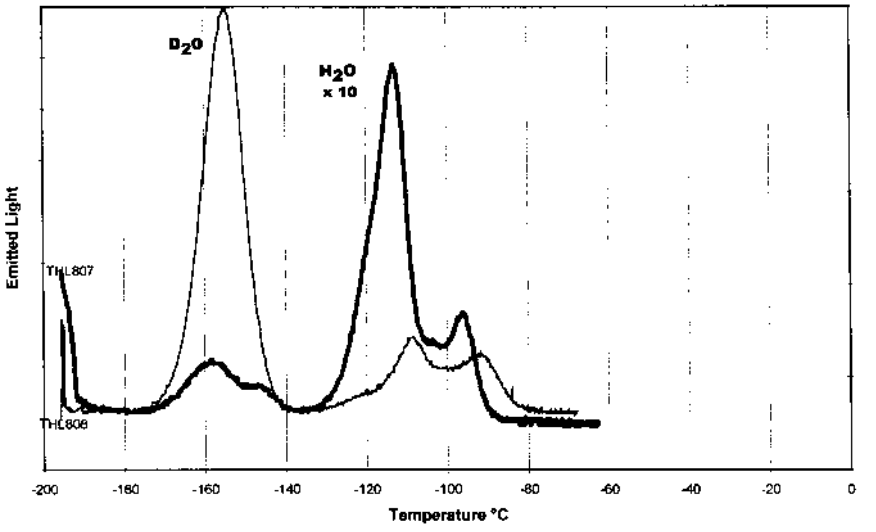

Figure 13 Thermoluminescence of D_2O and H_2O after gamma irradiation at $-196°C$ (30 kGy). The D_2O light emission is more than 10 times more intense than the H_2O glow and shows a predominant peak at $-155°C$, whereas the maximum emission is at $-113°C$ for H_2O.

D_2O the level of emission is much higher than for H_2O. Figure 14 a and b shows the emission spectrum for different regions of the rewarming curve.

At that point we are still unclear as to the deciphering of this emission but we can assume that the lower peaks (at $-158°C$ for H_2O, $-155°C$ for D_2O) are linked to the internal structure of the water molecule itself since they show such a major isotopic dependence. Conversely, the higher temperature emissions (from $-120°C$ to $-80°C$) appear to be more directly connected to the structure of the crystalline lattice itself and, more particularly, to the state and position of the network defects.

We got some support for this idea when we discovered that, in glycerol and in glycerol/water systems, the main luminescence emission did coincide with the temperature range during which structural events occur and, more precisely, when the vitreous transformation takes place. Figures 15 and 16 present these data. Thus, we are inclined to believe that the application of this technique to numerous systems presenting low-temperature evolutions such as sugar, polymers, and alcohols might be of interest.

This is one of the reasons why we could not resist applying low-temperature thermoluminescence to dilutions of the type used by homeopathy. Indeed, the scientists who have been working in this field have often

Copyright 2004 by Marcel Dekker, Inc. All Rights Reserved.

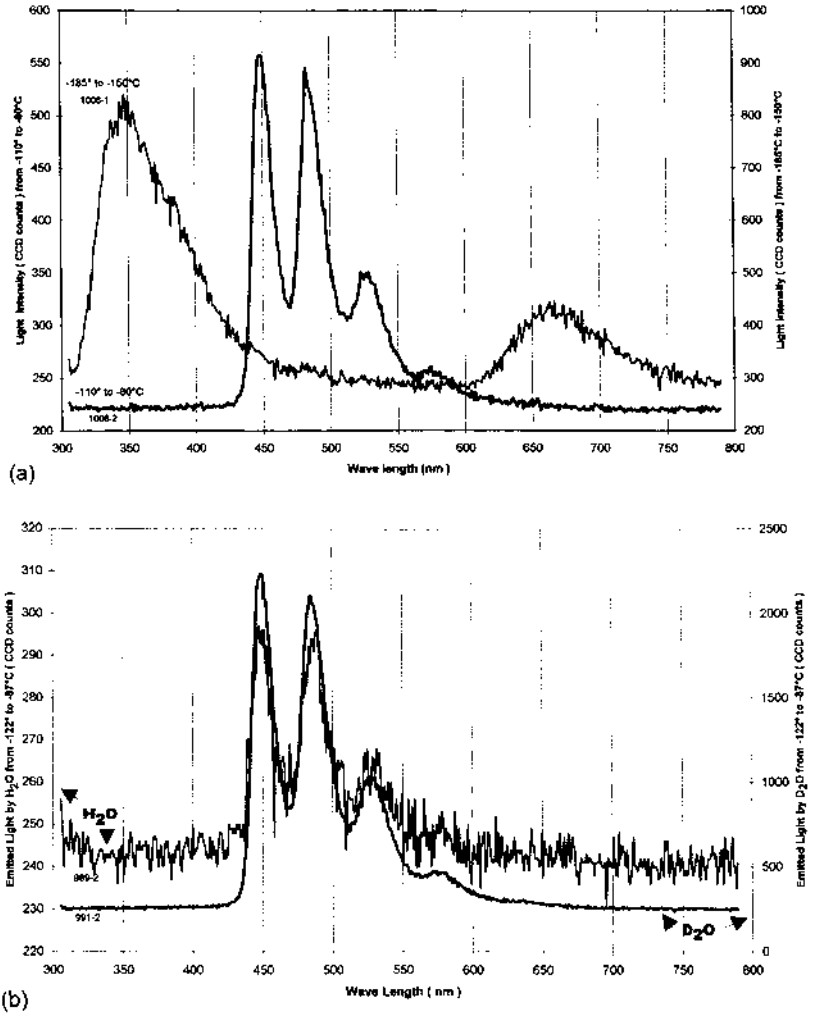
-185° to -150°C
1006-1
-110° to -80°C
1006-2
Light Intensity (CCD counts) from -110° to -80°C
Light Intensity (CCD counts) from -185°C to -150°C
Wave length (nm)
(a)
H2O
989-2
991-2
D2O
Emitted Light by H2O from -122° to -87°C (CCD counts)
Emitted Light by D2O from -122° to -87°C (CCD counts)
Wave Length (nm)
(b)

Figure 14 (a) Thermoluminescence emission spectra of D_2O irradiated by gamma rays (10 kGy) at $-196°C$ and reactivated by rewarming. The spectrographic analysis of the thermoluminescence glow of D_2O irradiated by gamma rays (10 kGy at $-196°C = 77\,K$) has been performed by integrating the light emission during rewarming, respectively, between $-182°C$ and $-122°C$ and between $-122°C$ and $-87°C$. The well-defined peaks are different for these two temperature ranges (High sensibility Princeton Instruments CCD camera). (b) Thermoluminescence emission spectra of gamma-irradiated H_2O and D_2O (10 kGy at $-196°C$). The thermoluminescence glow of H_2O is more than seven times lower than the one for D_2O but the wavelengths of the major peaks do coincide exactly.

Copyright 2004 by Marcel Dekker, Inc. All Rights Reserved.

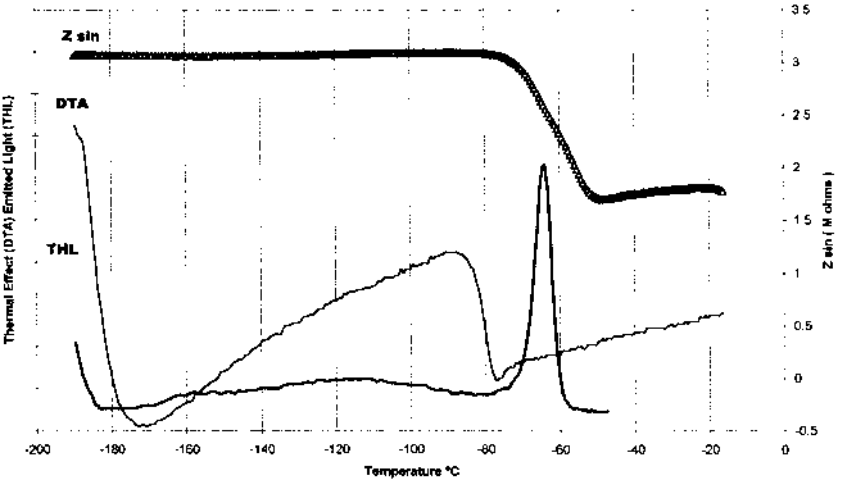

Figure 15 In pure glycerol submitted to a strong gamma irradiation (30 kGy) in the frozen state (−196°C) we can see that, during rewarming, the electric rigidity (impedance) starts to drop almost at the same time as the system undergoes vitreous transformation ($T_g = -81°C$). The subsequent rapid fall in $Z \sin \varphi$ also coincides with the thermoluminescence peak (−64°C), which is a clear indication that a major transition is taking place within the frozen system.

claimed that the successive dilutions, with their associated dynamizations, do create, within the solutions, a selective network where water molecules group in cages and clusters around the diluted substance—and even around its "ghost' when they reach higher dilutions. We wanted to challenge this idea without any preconceived opinion and we carried out a substantial number of tests along these lines. Though some of them gave rise to somewhat questionable results, we found a majority of positive answers [9a, 9b]. As a mere example, we present here, for the first time, a set of two experiments done with dilutions of Cl Na prepared by the Laboratories Boiron (Figures 17 and 18). As the reader will see, these results are most surprising and seem to indicate that there is indeed a progressive, stable, structural modification that is induced in the original solution by the successive dilutions/dynamizations. It is definitely interesting to note that these modifications not only resist low-temperature freezing but, moreover, seem to orient the crystallization patterns.

We do know that we enter here a controversial area where, unfortunately, emotional issues have often been predominant. However, facts are facts and it is simply honest to present them, as understanding of their basic mechanisms has an implication for the future.

Copyright 2004 by Marcel Dekker, Inc. All Rights Reserved.

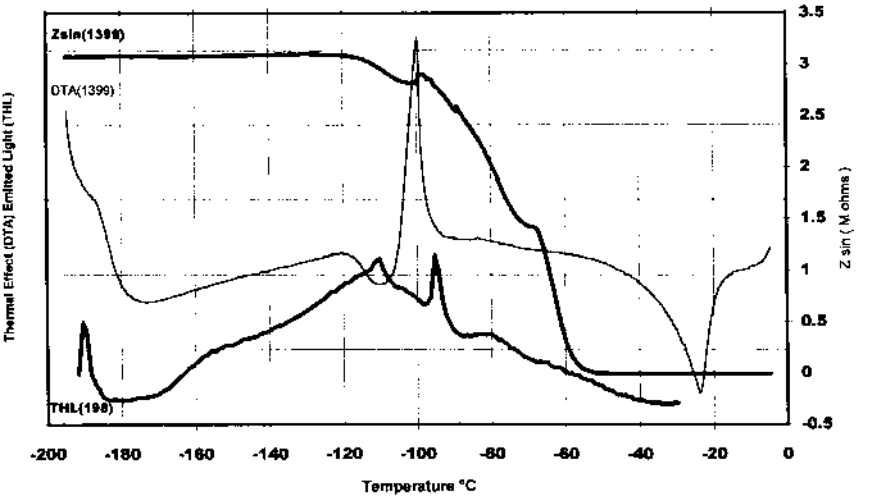

Figure 16 Differential thermal analysis/1000 Hz impedance/thermoluminescence after gamma irradiation at −196°C (30 kGy) of a 50/50 mixture of glycerol/H_2O plus 10 p. 1000 Cl Na. A more complex system containing an electrolyte (Cl Na) displays a quite analogous behavior to the one of pure glycerol: $Z \sin \varphi$ starts to drop while the vitreous transformation is taking place (−114°C) and quite abruptly again after the devitrification peak (−100°C). This second fall is concomitant with the thermoluminescence peak (−95°C).

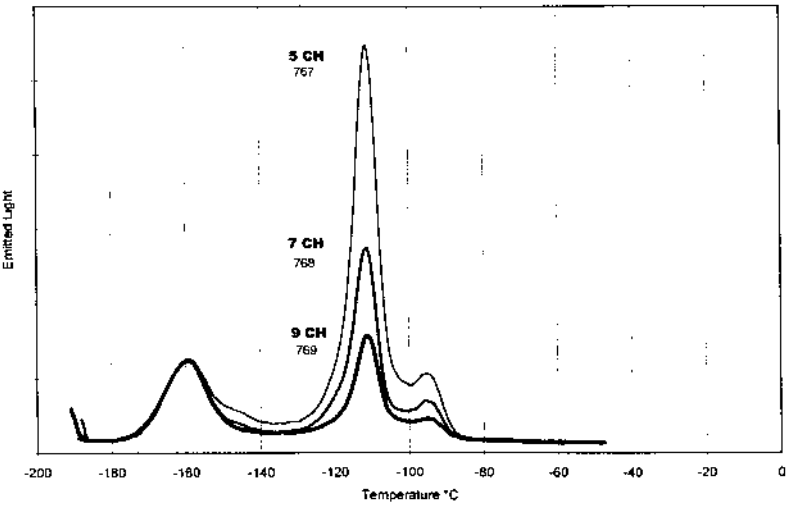

Figure 17 Thermoluminescence of dilutions of natrum muriaticum after gamma irradiation at −196°C (30 kGy).

Copyright 2004 by Marcel Dekker, Inc. All Rights Reserved.

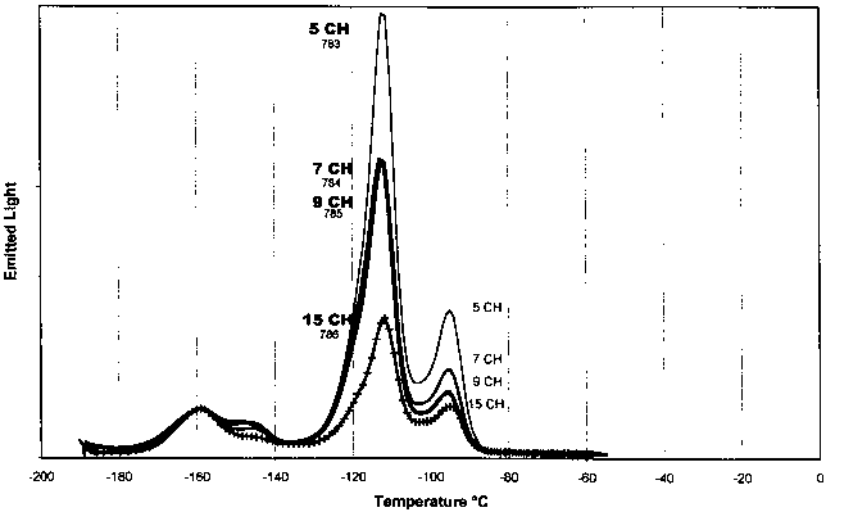

Figure 18 Thermoluminescence of dilutions of natrum muriaticum after gamma irradiation at −196°C (30 kGy).

III. OPERATING PRESSURE

Numerous books and papers have been written on the physics of primary and secondary drying. In the present book, G. W. Oetjen reviews quite extensively the different parameters involved. Therefore, it is pointless deal with this topic in the introductory chapter. However, we would like to stress one single point that has not always been clearly understood: the central role of the operating pressure. Indeed, as we have shown in Figure 2, freeze-drying deserves an accurate and continuous control of the pressure in the chamber during the whole operation.

With the exception of vacuum freezing (or "snap"-freezing), the *initial cooling* is always done at atmospheric pressure, sometimes in a separate cabinet.

Primary drying, to the contrary, is performed under vacuum. Whereas in the young days of the technique it was felt by more specialists that the higher the vacuum the better the process could be, it was shown by Neumann [10] and Oetjen et al. [11] that throttling the water vapor flow between the chamber and the condenser was increasing the speed and efficiency of the operations. Later on, Rieutord and I patented the air injection process [12], which could be applied to any equipment whether the condenser coils were placed in a separate

Copyright 2004 by Marcel Dekker, Inc. All Rights Reserved.

chamber or in the drying cabinet itself. Since then, the "air bleed' has been used almost universally since a substantial rise in the pressure (between 0.1 and 0.5 mbar according to the T_{im} of the treated product) proved to increase considerably the heat transfer to the sublimation interface essentially by gas conduction–convection. As a consequence, the temperature of the heaters could be substantially reduced, which prevented melting of the still-frozen core and/or scorching of the already existing dry layer. Monitoring and control of this pressure is still an essential part of the process, and they can be geared to the intrinsic properties of the product such as its temperature or, better, its electric impedance [4–6,12]. At any rate, during this whole sublimation period, the vacuum level is the master key to the heat transfer and can help to "rescue" a product that is becoming too hot and starting to soften dangerously. Indeed, in such a situation, pulling the vacuum down immediately works as a real thermal switch with an instantaneous result, whereas cooling the shelves requires a longer time.

Secondary drying is generally carried out under higher vacuum when the product has reached and above-zero temperature (or its electric impedance has reached the upper limit). Indeed, it has been shown by different authors that isothermal desorption was *faster* and allowed *lower final residual moistures* when the pressure lay in the level of 10^{-2} mbar, but that higher vacuums (10^{-3} mbar) did not drastically improve the operation.

Final conditioning has always been much discussed and, in the last decades, vacuum and dry neutral gas both got their supporters. Today, stoppering the vials under a slightly reduced pressure of dry nitrogen gas looks to be the favorite option. Some experiments that we did in the past and that remained unpublished push us to think that stoppering under dry argon could give better results for long-term storage, as is the case, for instance, for international biological standards.

IV. THREE CHALLENGING WAYS TO INVESTIGATE THE FINAL DRY PRODUCT

The dry freeze-dried cake undoubtedly has a very peculiar structure since it has been "carved" under vacuum from a solid matrix. At the end of this process and when it is still under vacuum, its internal surface is quite "clean" and very reactive. It can be easily understood that its first contact with a foreign element, such as the gas used to rupture

Copyright 2004 by Marcel Dekker, Inc. All Rights Reserved.

the vacuum, is determinant. This is, in fact, why the choice of this gas as well as the procedure to introduce it are critical. In that context the properties of the dry cake internal surface constitute a major element.

Another important factor is the level of the residual moisture in the pellet and its evolution—if any—during storage.

Finally, it is definitely of interest to know how this internal water is bound to the structure.

These are three recurrent problems in freeze-drying, among many others. We shall propose some selected experimental means for their investigation.

A. Internal Surface: BET

Applying the Brunner, Emmett, and Teller (BET) method to pharmaceuticals, whether ingredients or finished products, is of common use in powders for the determination of their specific area and pore sizes. However, generally, the operator has a reasonable amount of substance in hand and most often this material is relatively resistant to water vapor and can be manipulated without too many risks in the open space of a laboratory or, if needed, within a conventional glove box.

The situation is quite different with sensitive freeze-dried specimens contained in sealed vials or ampoules, which present both a very reduced weight and, of course, a very low density as well as a high hygroscopicity. In that case, the prolonged contact with moist air can provoke a real 'collapse'' of the internal structure, which cannot be restored to its original state by prolonged pumping. A very precise methodology has, then, to be followed to get a reliable measurement. We would like to explain how we proceed to that end:

The sample to be checked (5–100 mg of dry product in a sealed vial or ampoule) is quickly opened with a diamond saw and the bottom part, containing the plug, placed in a special stainless steal BET cell that is immediately capped, weighted, and connected to the manifold of the pumping device. Vacuum is then pulled over the sample at room temperature.

Two to three days later the vacuum is broken with dry nitrogen gas and the BET cell connected to an automatic, computerized analyzer (Den-Ar-Mat 1000).

Vacuum is pulled again and repetitively checked until the leak rate (combined with the gas release from the product) falls to the order of $2-3 \times 10^{-4}$ mbar/s.

Copyright 2004 by Marcel Dekker, Inc. All Rights Reserved.

The BET cell is then flooded with helium for the determination of the sample volume, which allows the determination of its real density and porosity since we already know both its weight and its apparent volume.

The BET cell is again pumped and immersed in liquid nitrogen.

When temperature and pressure are stable, known amounts of helium are introduced in the measuring chamber thanks to special gas-tight microsyringes (7 µl for the smallest one) in order to perform the calibration of the cavity before adsorption.

The BET cell is pumped again and then the measurement can start. Known amounts of the adsorption gas are then introduced in the specimen chamber and each time we wait for a steady equilibrium. The adsorption isotherm is, thus, constructed progressively throughout the BET range.

When saturation is reached, the BET cell is slowly pumped down, stepwise, to ensure controlled desorption in order to measure pore size and distribution.

For absolute surfaces ranging from 50 to 5 m^2 the measuring gas to be used is nitrogen. For absolute surfaces of 5–0.5 m^2 the measuring gas is argon. For absolute surfaces below this level we use krypton. In the last case, the only possible determination is that of the specific area since, with krypton being solid at liquid nitrogen temperature, it is not feasible to perform a complete adsorption–desorption cycle for the evaluation of pore distribution and sizes. For obvious reasons, krypton measurement is bound to become the routine one for most freeze-dried pharmaceuticals.

Figure 19, for instance, represents the krypton adsorption curve for a sample of Gonal F75 UI from Serono and we can see that it gives a pretty accurate reading despite the fact that the absolute surface measured is only 0.07 m^2.

It is beyond the scope of this chapter to indulge in more details about this technique, but it might be of interest to note that it allows the evaluation of the influence, on the product structure, of different factors such as the initial concentration of the starting fluid, the rate of freezing (macro- or microcrystalline structures), the pertinence of the drying cycle and of the final conditioning.

Since many functional properties of the dry cake derive from its internal surface and porosity such as solubility, oxygen, and water sensitivity, these measurements might be of great interest, especially for the assessment of the reliability of a new process in view of its potential validation.

Some people will ask why we did not use penetration by mercury for the measurement of pores. Our answer is that for delicate, flexible products

Copyright 2004 by Marcel Dekker, Inc. All Rights Reserved.

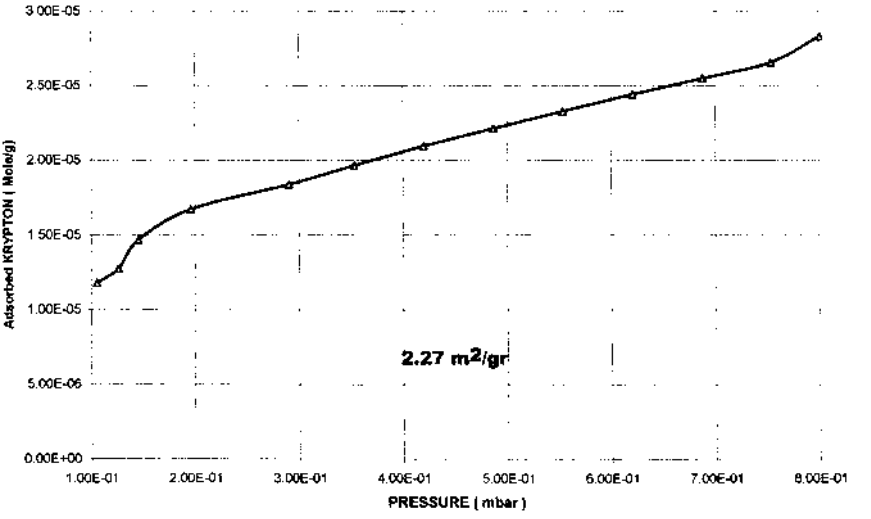

Figure 19 Determination of the specific area of freeze-dried Serono Gonal F75 Ul by BET (sample weight 0.0325 g).

that can be easily crushed or simply distorted in their morphology by outside constraints, we found that the application on the cake of pressures ranging to a few thousand bars could be considered irrelevant.

B. Equilibrium Water Vapor Measurement in a Sealed Vial

For the reasons that we have just described, the measurement of residual moisture within an isolated vial or ampoule is a difficult undertaking. Joan May, in this book, also deals with this topic and she explains how the FDA developed very accurate standardized techniques to execute these determinations by chemical Karl Fischer titration or thermogravimetric techniques. The only drawback is that, in both cases, the material is destroyed.

It is, in fact, because of that specific point that our approach has followed a different route:

Use a nonintrusive method leaving the product intact.
Be able, under those conditions, to do repetitive measurements on the *same vial* in the course of time to assess its evolution during storage.

Figure 20 shows the principle of the method we developed jointly with J. Mosnier (deceased). The selected vial or ampoule is placed in a thermostatic metallic block where temperature can be maintained constant

Copyright 2004 by Marcel Dekker, Inc. All Rights Reserved.

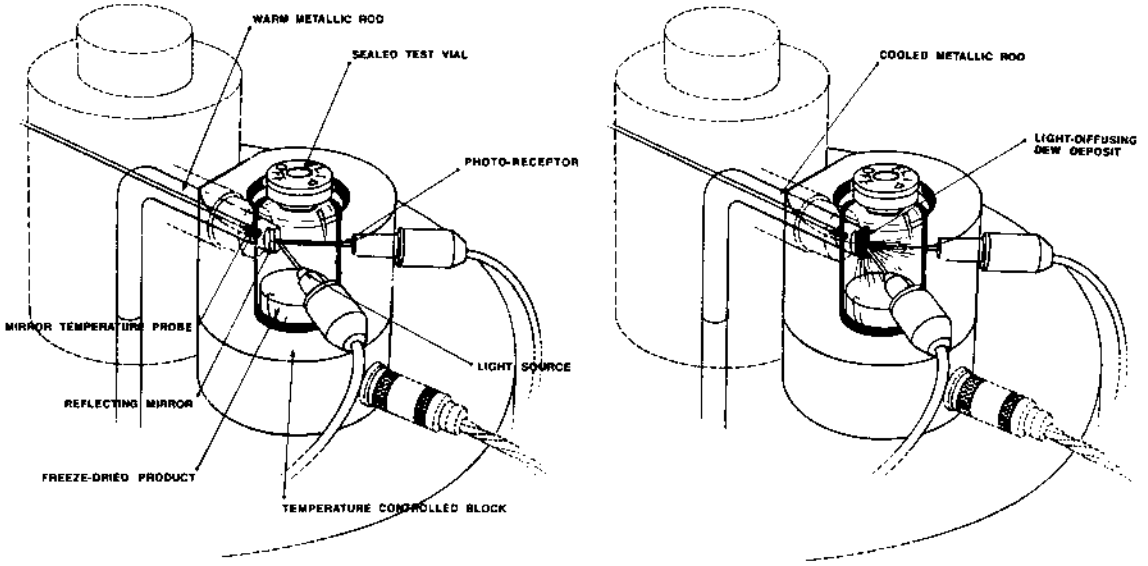

Figure 20 Operating principle of the device made to measure the equilibrium water vapor pressure inside a sealed vial.

Copyright 2004 by Marcel Dekker, Inc. All Rights Reserved.

from $-10°C$ to $+60°C$. On one side of the block a metallic "finger" having at its end a tiny polished stainless steel cylindrical mirror (2×6 mm) is pushed toward the outside wall of the glass vessel and the connection is made optically and thermally tight thanks to a trace of silicon grease. On the other side is placed a near IR diode that beams light throughout the vial on the mirror which, in turn, reflects that light on to a phototransistor placed in a symmetrical position.

When the temperature of the mirror is equal to or higher than that of the metallic block (hence the temperature of the sample) the level of reflected light is steady. To start the measurement, the temperature of the mirror is progressively decreased thanks to combined Peltier and cold nitrogen gas. Because of the good thermal contact on a very limited surface (12 mm^2) the internal wall of the flask is equally cooled on a small isolated spot. When, finally, the temperature of the mirror (and the temperature of the spot on the internal surface) reaches the value corresponding to the saturated water vapor pressure within the flask, some dew (or ice) is deposited on the internal wall that immediately becomes diffusive. The reflected light drops sharply. The measurement is done. The mirror can thus be warmed again, dew evaporates, light is restored, and the sample can be placed back into the storage cabinet for further determination. Figure 21 gives an example of this determination for a sample of Novartis Calcitonin dry substance in a sealed ampoule measured at $+25°C$. At the corresponding condensation temperature of $-15.8°C$, the water vapor pressure inside the ampoule is 1.53 mbar.

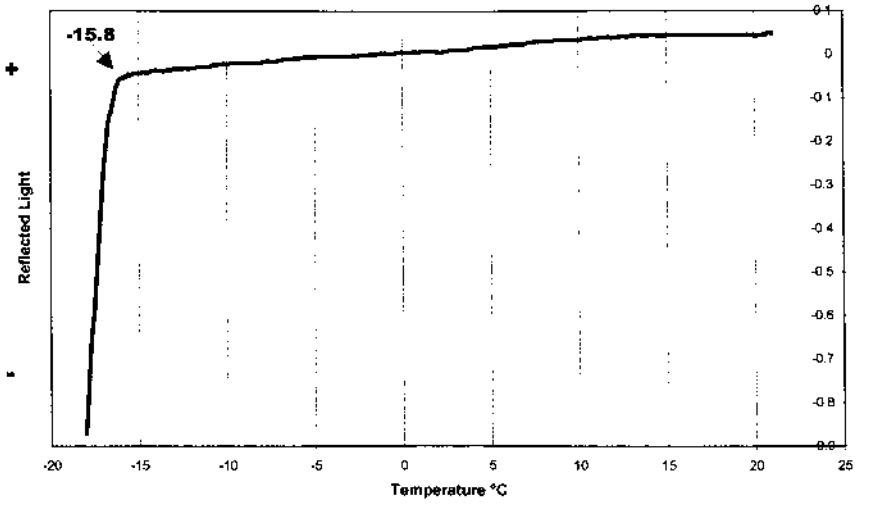

Figure 21 Novartis Calcitonin dry substance in ampoules.

Copyright 2004 by Marcel Dekker, Inc. All Rights Reserved.

The sensitivity of this method is very high since measurements are still possible for condensation temperatures of $-60^{\circ}C$, which, in a vial of 10 cm^3, means that less than 0.1 μg of water is present in the overhead space above the pellet.

Over the last three years, systematic determinations have been done in collaboration with Dr. May from the FDA and with several drug companies on a vast number of products. Most of them have been followed during storage (at $-20^{\circ}C$, $+4^{\circ}C$, or room temperature) for more than two years. Dr. May reports on some of her findings later in this book.

Without going into too much detail, let us mention some of the key issues of this particular work:

In sealed glass ampoules and for the same product we found substantial differences in the equilibrium water vapor pressures according to batches and, within a given batch, according to the position of the ampoule on the shelves of the freeze-dryer. The so-called wall, door, condenser, and corner effects could then be analyzed and amended.

In sealed glass ampoules we also witnessed an evolution in the course of storage showing that often the remaining water was "restructured" in the course of time going from a rather mobile form to a more firmly bound form displaying a lower water vapor equilibrium pressure (Figure 22).

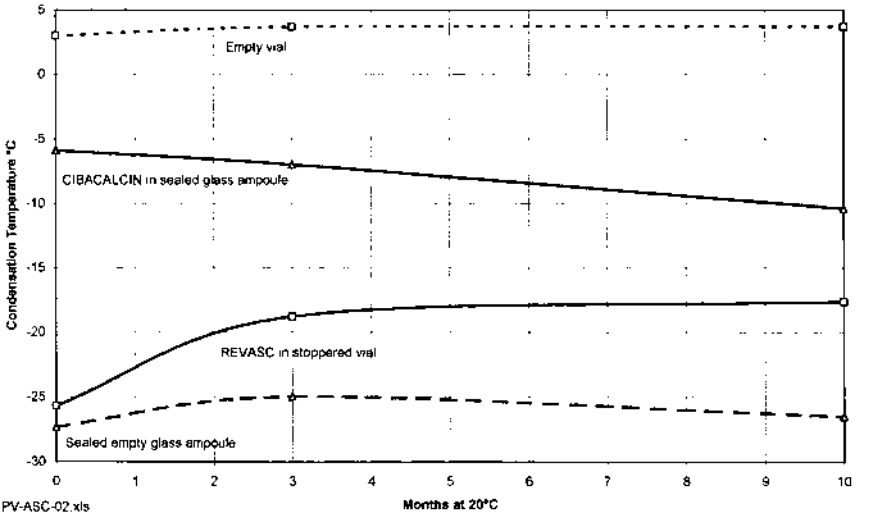

Figure 22 Evolution of the condensation temperatures of freeze-dried CIBACALCIN and REVASC (Novartis) in the course of storage at 20°C.

Copyright 2004 by Marcel Dekker, Inc. All Rights Reserved.

In stoppered vials we could follow quite easily the transfer of moisture from the stopper toward the plug, which acted as a ''getter pump'' until a new equilibrium was reached (Figure 22). This allowed us, for instance, to understand why in a certain BCG vaccine the Karl Fischer titration went up when the equilibrium water vapor went down reaching condensation points as low as $-50^{\circ}C$.

Sometimes our method helped the pharmaceutical technicians to modify the formula of the excipients and stabilize the water content. They could also better understand the as-yet-unknown behavior of certain additives like heavy polyalcohols, glycerol, or tensioactive agents.

Today we are convinced that there are numerous applications for this new analytical tool, especially when controls have to be performed on rare, high-cost, or infectious material for which a nonintrusive remote technique is compulsory or that repetitive measurements need to be done on the same sample over prolonged periods.

C. Low-Temperature Thermoluminescence of Dry Material

Thermoluminescence analysis has been applied to solids for quite a long time in archaeological research and radiation dosimetry. In both cases the samples that have been activated by natural and/or man-made radiation sources present a certain number of energy traps that can be emptied by heating. For the datation of ceramics, the heating cycle is extremely fast and brings the sample to more than $300^{\circ}C$ in less than a couple of minutes. The magnitude of the light emission under well-standardized conditions is directly linked to the age of the material, which can be determined over several centuries with an accuracy of a few percentage points.

For radiation dosimetry, within or around nuclear plants as well as in open green fields and in the environment at large, the analysts make use, generally, of so-called thermoluminescent solids which are susceptible to ''activation'' over a large span of doses. Espagnan et al. [13] developed a refined method to that end using lithium fluoride tablets, which are first totally deactivated at $400^{\circ}C$, then exposed to the radiation field at ambient temperature. Reading is done by recording the emission peaks during their progressive 'extraction'' in the course of a constant-speed ($1^{\circ}C/s$) heating, which generally show up between $200^{\circ}C$ and $400^{\circ}C$.

At the onset of our research work, we tried to operate in the same way with freeze-dried products that had received a strong gamma irradiation (40–60 kGy) at room temperature. The results were disappointing because we were limited to rather low temperatures (below $100^{\circ}C$) and, even so,

Copyright 2004 by Marcel Dekker, Inc. All Rights Reserved.

when the material could stand high temperatures like freeze-dried silica. This is why we attempted to apply to these products the same methodology that we used previously for our investigation on water and solutions.

The dry samples are irradiated at $-196°C$ and deactivated by a gentle rewarming (1.5°C/min) to room temperature. Our preliminary results look promising.

Figure 23, for instance, shows the behavior of a freeze-dried plug of mannitol (residual moisture 1.5%). We can see that, in comparison with the initial solution (at 10% mannitol), the thermoluminescence of the dry material is some 20 times stronger and does not follow the same pattern. The lower peak (at $-152°C$) is very narrow whereas the higher one (near $-118°C$) is substantially depressed. This is not surprising if we assume, as we have already done, that the first peak is directly connected to the water molecule itself while the second one seems to be geared to the tridimensional network of the water molecules within the crystalline lattice.

Additional studies done on freeze-dried silica gels (microbead gels from Rhodia, Salindres) give some support to this idea. In Figure 24, for instance, we can see that when we shift from a largely hydrated material (like the fresh starting material at around 40% residual moisture) to the low residual moisture freeze-dried gels, the $-120°C/-40°C$ emission is first almost completely erased and then disappears (for 2% residual moisture). At the same time the low-temperature peak increases and sharpens.

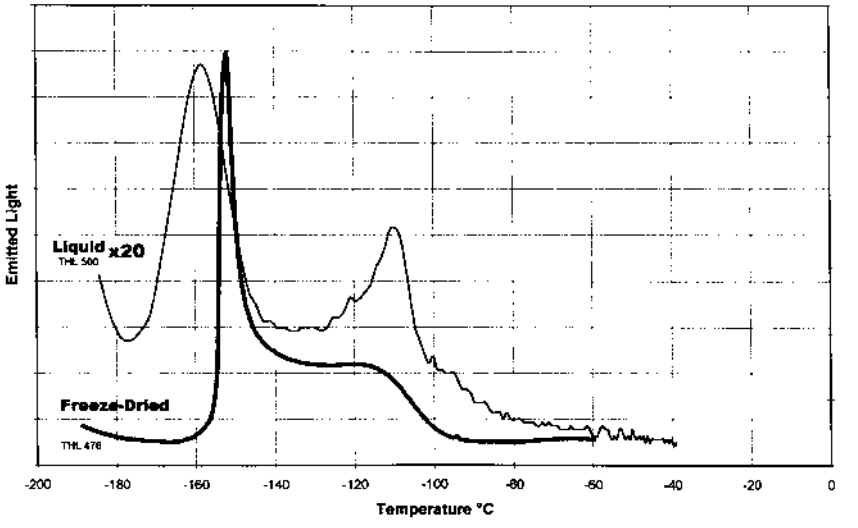

Figure 23 Thermoluminescence of a 10 p. 100 mannitol–H_2O system after gamma irradiation at $-196°C$ (30 kGy).

Copyright 2004 by Marcel Dekker, Inc. All Rights Reserved.

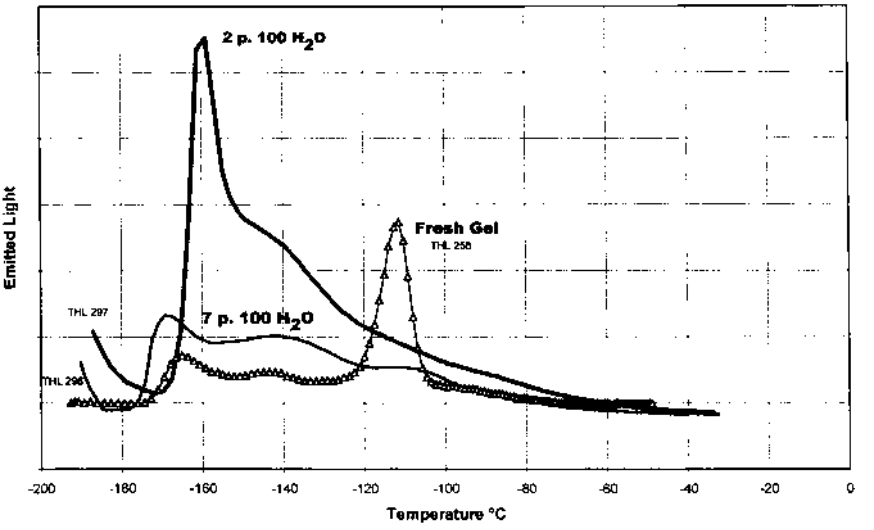

Figure 24 Thermoluminescence of fresh and freeze-dried SiO_2 gels (microbeads) after gamma irradiation at $-196°C$ (30 kGy).

We are now at the very beginning of these investigations, but we think that low-temperature thermoluminescence applied to freeze-dried solids is susceptible to give us new information on the water "traps" within the solid material, and that with a better knowledge of the temperature, magnitude, and shape of the emission peaks we might be able to shine some light on the role of residual moisture in freeze-dried products and on the mechanisms of water molecules binding to their supporting matrix.

REFERENCES

1. F Bordas, M d'Arsonval. C R Acad Sci Paris 142:1058 and 1079; 143:567, 1906.
2. EW Flosdorf, S. Mudd. Procedure and apparatus for preservation in "lyophile" form of serum and other biological substances. J Immunol 29:389, 1935. See also EW Flosdorf. Freezing and Drying. New York: Reinhold, 1949, pp 1–280.
3. P Hauduroy. Histoire de la technique de lyophilisation. In: Traîté de Lyophilisation. Paris: Hermann, 1960, pp 3–16.
4. LR Rey. Thermal analysis of eutectics in freezing solutions. Ann N Y Acad Sci 85:513–534, 1960.
5. LR Rey. Fundamental aspects of lyophilization. In: Research and Development in Freeze-Drying. Pairs: Hermann, 1964, pp 23–43.

Copyright 2004 by Marcel Dekker, Inc. All Rights Reserved.

6. LR Rey. Automatic regulation of the freeze-drying of complex systems. Biodynamica 8:241–260, 1961.
7. LR Rey. Glimpses into the fundamental aspects of freeze-drying. In: Freeze-Drying of Biological Products, Biological Standardization Series, vol. 36. Basel: S. Karger, 1977, pp 19–27.
8. LI Grossweiner, MS Matheson. Fluorescence and thermoluminescence of ice. J Chem Phys 22:1514–1526, 1954.
9a. LR Rey. Low temperature thermoluminescence. Nature 391:418, 1998.
9b. LR Rey. Thermoluminescence of ultra-high dilutions of lithium chloride and sodium chloride. Physica A 323: 67–74, 2003.
10. K Neumann. Les Problèmes de mesure et de réglage en lyophilisation. In: Traîté de Lyophilisation, Paris: Hermann, 1960, pp 1–411.
11. GW Oetjen, W Ehlers, U Hackenberg, J Moll, K Neumann. Temperature measurements and control of freeze-drying process. In: Freeze-Drying of Foods, Natl. Acad. of Sciences, Natl. Res. Council, ed., Washington, D.C., 1962, pp 25–42.
12. L Rieutord. International patents, 1961.
13. M Espagnan, P Plume, G Marcellin. Dosimétrie des doses élevées par Thermoluminescence des pics profonds du Fluorure de Lithium: Fli: Mg, Ti. Radioprotection 26:51–64, 1991.

Copyright 2004 by Marcel Dekker, Inc. All Rights Reserved.

2

Structural and Dynamic Properties of Bulk and Confined Water

M.-C. Bellissent-Funel and J. Teixeira
Laboratoire Léon-Brillouin (CEA-CNRS), CEA Saclay, Gif-sur-Yvette, France

I. INTRODUCTION

The structural and dynamic properties of bulk water are now mostly well understood in some ranges of temperatures and pressures. In particular many investigations using different techniques such as x-ray diffraction, neutron scattering, nuclear magnetic resonance (NMR), differential scanning calorimetry (DSC), molecular dynamics (MD), and Monte Carlo (MC) simulations have been performed in the deeply supercooled regime [1–10] and, in a situation where the effects due to the hydrogen bonding are dominant.

However, in many technologically important situations, water is not in its bulk form but instead attached to some substrates or filling small cavities. Common examples are water in porous media, such as rock or sandstones, and water in biological material as in the interior of cells or attached to surfaces of biological macromolecules and membranes. This is what we define here as the "confined" or the "interfacial water."

Water in a confined space has attracted considerable interest in recent years. It is commonly believed that the structure and dynamics of water are modified by the presence of solid surfaces, both by a change of hydrogen bonding and by modification of the molecular motion, which depends on the distance of water molecules from the surface.

Copyright 2004 by Marcel Dekker, Inc. All Rights Reserved.

Understanding of the modification from bulk liquid water behavior when water is introduced into pores of porous media or confined in the vicinity of metallic surfaces is important in technological problems such as oil recovery from natural reservoirs, mining, heterogeneous catalysis, corrosion inhibition, and numerous other electrochemical processes. Water in porous materials such as Vycor glass, silica gel, and zeolites has been actively under investigation because of their relevance in catalytic and separation processes. In particular, the structure of water near layer-like clay minerals [11,12], condensed on hydroxylated oxide surface [13], confined in various types of porous silica [14–22] or in carbon powder [23] has been studied by neutron and/or x-ray diffraction.

In the field of biology, the effects of hydration on equilibrium protein structure and dynamics are fundamental to the relationship between structure and biological function [24–30]. In particular, the assessment of perturbation of liquid water structure and dynamics by hydrophilic and hydrophobic molecular surfaces is fundamental to the quantitative understanding of the stability and enzymatic activity of globular proteins and functions of membranes. Examples of structures that impose spatial restriction on water molecules include polymer gels, micelles, vesicles, and microemulsions. In the last three cases, since the hydrophobic effect is the primary cause for the self-organization of these structures, obviously the configuration of water molecules near the hydrophilic–hydrophobic interfaces is of considerable relevance.

The microscopic structure of bulk and confined water is currently studied by using x-ray and/or neutron diffraction techniques, which are complementary techniques. These diffraction techniques allow access to the intermolecular pair correlation function $g(r)$ [31] of a system that is the probability density of finding another atom lying in another molecule at a distance r from any atom. In x-ray measurements $g(r)$ is the pair correlation function of the molecular centers, to a good approximation equal to the oxygen–oxygen correlation function. In neutron measurements $g(r)$ is the weighed sum of the three partial functions relative, respectively, to the oxygen–oxygen pairs, oxygen–deuterium pairs, and deuterium–deuterium pairs. In particular, it is heavily weighted toward deuterium–deuterium and oxygen–deuterium partial correlation functions.

The structural and dynamic properties of water may be affected by both purely geometrical confinement and/or interaction forces at the interface. Therefore, a detailed description of these properties must take into account the nature of the substrate and its affinity to form bonds with water molecules, and the hydration level or number of water layers. In order to discriminate between these effects, reliable model systems exhibiting hydrophilic or hydrophobic interactions with water are required.

Copyright 2004 by Marcel Dekker, Inc. All Rights Reserved.

This chapter looks at the appropriate strategy to be developed to obtain some understanding of the behavior of water close to a biological macromolecule, as presented in the following.

In the last few years, computer simulations and theoretical treatments of the structure and dynamics of water in different kinds of environments have been undertaken [32–41]. Some important results are now available. For instance, molecular dynamics simulations indicate that the water density increases up to $1.5\,g/cm^3$ in the first few angstroms of the shell around a protein and give information concerning the pair correlation functions and orientations of water molecules [42].

The purpose of this chapter is to account for the more recent developments on the structure and the dynamics of bulk and confined water as a function of temperature. Examples relative to interactions of water molecules with model systems as well as with biological macromolecules will be presented.

II. THE STRUCTURE AND DYNAMICS OF LIQUID WATER: A SHORT REVIEW

In spite of an enormous number of experiments performed with liquid water under different external conditions [1–9], many of its properties remain not fully understood. The main reason is the complexity of the intermolecular potential resulting from the formation of intermolecular hydrogen bonds. Such bonds are strongly directional and their study requires consideration of quantum effects.

Most of the recent theoretical developments have been achieved by computer simulations of the molecular dynamics using several sophisticated effective potentials [3,10]. Such potentials are written ad hoc in order to simulate at best both the microscopic structure and the thermodynamic and transport properties. A general problem is that the potential either imposes a much too strong and ice-like structure in order to reproduce the thermodynamic properties, or it reproduces well the pair correlation function $g(r)$ but then the so-called water anomalies are not taken into account. Much progress has been achieved recently and one can classify the different effective potentials in several categories: rigid molecule, flexible molecule (including internal degrees of motion), with enhanced dipole, ab initio potential, etc.

Heuristic approaches remain, probably for a long time, extremely useful and we will show here that a simple model that focusses on the statistics of the hydrogen bonds is qualitatively sufficient for explaining some of the water anomalous properties.

Copyright 2004 by Marcel Dekker, Inc. All Rights Reserved.

Every study of liquid water at a molecular level must take into account three features that, together, characterize the microscopic behavior and the thermodynamic properties. These are the tetrahedral symmetry of the molecule, the large number of hydrogen bonds formed between near-neighbor molecules, and the very short characteristic lifetime of these bonds.

The first feature is a result of the molecular orbital hybridization, which yields an HOH angle very close to the ideal tetrahedral angle (109°). As a consequence, in all circumstances, one observes that the coordination number (number of nearest neighbors) is around 4. This is a small number, meaning that there is a large amount of "free space" available for movements such as the O–O–O bending. This is apparent on the pair correlation function $d(r)$ as defined by:

$$d(r) = 4\pi\rho r[g(r) - 1] \tag{1}$$

where ρ is the molecular number density.

The function $d(r)$ is obtained by Fourier transforming the scattering function $S(Q)$ measured by x-rays or neutron scattering. In the case of x-rays, $d(r)$ gives the oxygen positions because the contribution of hydrogen atoms to the scattered intensity is negligible. It shows a well-defined first peak at 2.8 Å, corresponding to the first shell of neighbors, a broad second-neighbor peak at 4.5 Å, and dies rapidly beyond the third-neighbor distance (Figure 1 a) [43]. This is in contrast with simple atomic liquids, such as argon, for which long-range order is clearly observed. Thus with x-rays, the scattering is dominated by $g_{OO}(r)$ while with neutrons all the three partials ($g_{OO}(r)$, $g_{OD}(r)$, and $g_{DD}(r)$) contribute to the total scattered intensity. With neutron scattering combined with H/D isotopic substitution, we can actually measure all three of the $g(r)$ in water with reasonable precision. Figure 1 b depicts the total pair correlation function, $g(r)$ [44], obtained by neutron scattering, and shows the three partial correlation functions $g_{OO}(r)$, $g_{OD}(r)$, and $g_{DD}(r)$ (Figure 1 c, 1 d, 1 e) [6,45].

The O–D distribution has a well-defined peak at 1.85 Å consisting of about 1.8 hydrogen atoms out to a distance of 2.35 Å from an oxygen atom at the origin. The O–O distribution, in agreement with x-ray diffraction, has a well-defined peak at 2.8 Å consisting of about 4.5 oxygen atoms out to a distance of 3.3 Å from an oxygen atom at the origin. These numbers and distances suggest that the near-neighbor coordination of water molecules is well defined and roughly tetrahedral at any instant in time but that a substantial number of molecules are to be found in other configurations.

The second property is the existence of intermolecular bonds. Spectroscopic studies traditionally classify the bonds in two categories,

Copyright 2004 by Marcel Dekker, Inc. All Rights Reserved.

intact and broken bonds, essentially because of the shape of the intramolecular stretching band of the Raman spectrum of liquid water and its temperature dependence. Such an interpretation is questionable but, whatever the definition used for the classification of the bonds, a large number of molecules have a strong attractive interaction with their neighbors.

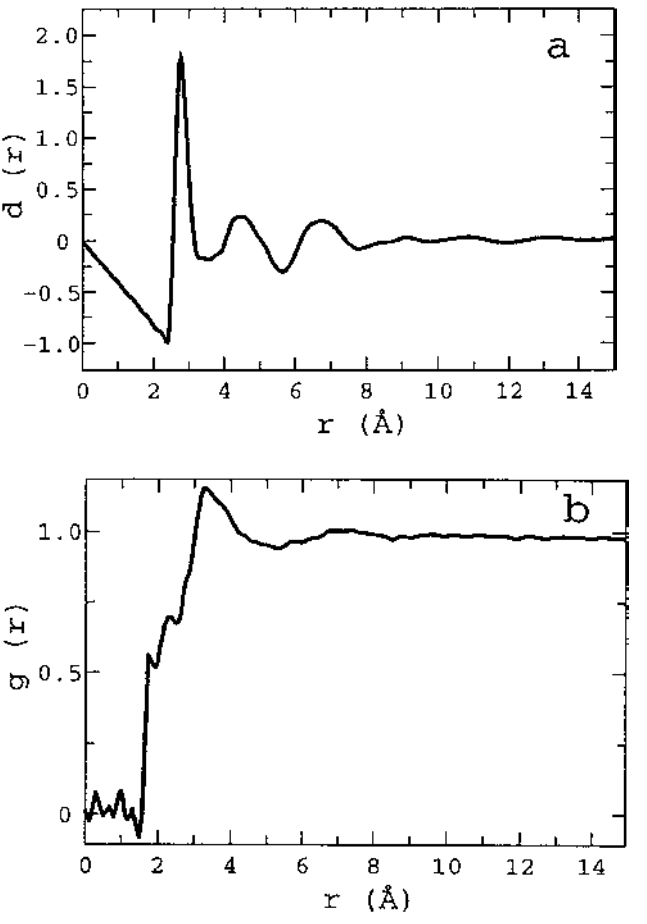

Figure 1 (a) The function $d(r)$, related to the pair correlation function, $g(r)$, by $d(r) = 4\pi r\rho[g(r)^{-1}]$, evaluated from the $S(Q)$ measured by x-rays (Ref. 43). (b) The pair correlation function, $g(r)$, obtained from neutron scattering data (Ref. 44) is shown with the three different partial correlation functions $g_{OO}(r)$, $g_{OD}(r)$ and $g_{DD}(r)$ (c, d and e). Solid line: results of M-C Bellissent-Funel (Ref. 6); dashed line: results of A.K. Soper and M.G. Philips (Ref. 45).

Copyright 2004 by Marcel Dekker, Inc. All Rights Reserved.

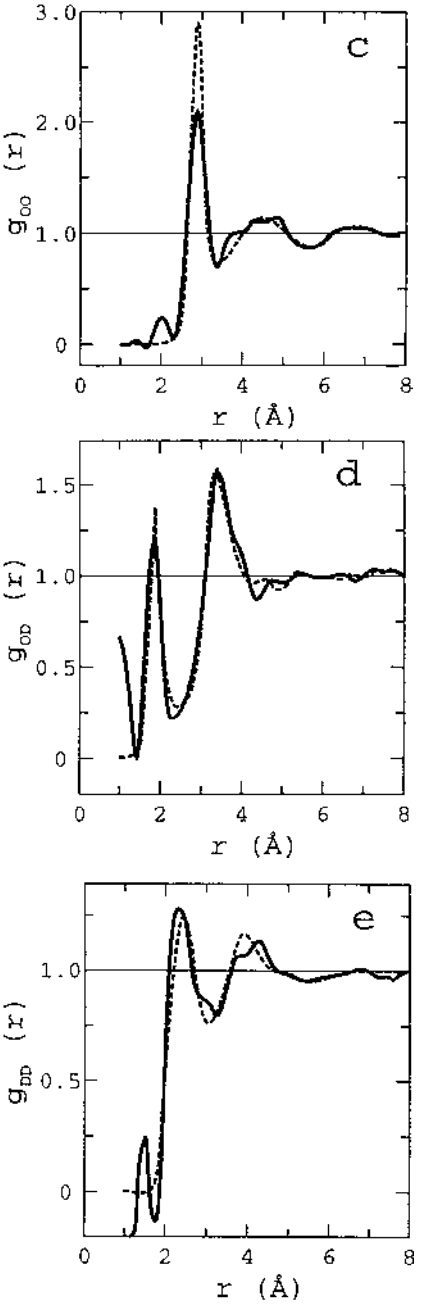

Figure 1 Continued.

Copyright 2004 by Marcel Dekker, Inc. All Rights Reserved.

In a simple way, one can say that the ensemble of the intact (or with energy beyond some reference energy) bonds constitutes a network well above its percolation threshold. As a consequence, at a given time, essentially all the molecules are part of an "instantaneous gel" [9]. It is worth noting that the two preceding properties of water structure explain that, in spite of a very short-range local order, the connectivity length of the hydrogen bond network is infinite.

However, and this is the third aspect, the characteristic lifetime of a hydrogen bond is very short, between 10^{-13} and 10^{-12} s, and this is why viscoelastic properties of a gel structure will never be observed even in short characteristic time experiments. The explanation of such a short time is that hydrogen bond lifetimes are determined by the proton dynamics [3,8]. In particular, large-amplitude librational movements easily take the proton from the region between two oxygen atoms, where the energy of the bond is sufficiently large.

Many of the thermodynamic and transport properties of liquid water can be qualitatively understood if one focusses attention on the statistical properties of the hydrogen bond network [9]. As an example, let us observe the temperature dependence of density and entropy. As temperature decreases, the number of intact bonds increases and the coordination number is closer to the ideal value 4. Because of the large free volume available, this means that the temperature decrease is associated with an increase of the local molecular volume. Of course, this effect superimposes on the classical anharmonic effects, which dominate at high temperature, when the number of intact bonds is smaller. The consequence of both effects is a maximum on the temperature dependence of the liquid density. This maximum is actually at 4°C for normal water and at 11°C for heavy water. Such a large isotopic effect can also be understood because the larger mass of the deuterium makes the hydrogen bonds more stable.

Entropy decreases with decreasing temperature due to an increase of the local order following the hydrogen bond formation. Similar arguments to those developed above explain the minimum of the temperature dependence of heat capacity.

A more complete discussion of these effects has been done and gives a good explanation of the enhanced anomalies of water observed at low temperature [1,2]. More important is to notice the minimum of the isothermal compressibility at 46°C and a sharp increase of the heat capacity at temperatures close to and below the melting point, when liquid water is undercooled. The first corresponds microscopically to enhanced density fluctuations corresponding to the existence of short-lifetime, low-density regions in liquid water [3]. These regions are formed by molecules strongly bound together. Clearly, the percolation mechanism yields a dramatic

Copyright 2004 by Marcel Dekker, Inc. All Rights Reserved.

increase in the size and number of these regions explaining, incidentally, why homogeneous nucleation takes place at about the same temperature (about 228 K), as the thermodynamic properties seem to diverge. This temperature is also well above the glass transition temperature of liquid water, which is around 140 K. The second corresponds to a rapid decrease of the entropy which approaches the entropy of the crystal also around 228 K.

The transport properties of liquid water also have a strongly anomalous behavior, in particular at low temperature [1,2]. Properties such as self-diffusion, viscosity, and different relaxation times show a strong non-Arrhenius temperature dependence, the characteristic activation energy increasing with decreasing temperature. This also corresponds to the fact that, with decreasing temperature, more bonds must be simultaneously broken to allow the movement of a given molecule. At high temperature, when the number of intact bonds is relatively small, the dynamics is similar to that of a classical liquid. As the temperature decreases, the activation energy increases until values three times larger corresponding to the energy necessary to break, on average, a larger number of bonds.

When water is mixed with another liquid, the number of bonds can increase, as for instance in water–ethanol solutions (structure formers), or decrease (structure breakers). However, in all cases, the tetrahedral structure vanishes (except, of course, for isotopic mixtures of light and heavy water). As a consequence, the anomalies of liquid water are strongly reduced upon addition of other components. For instance, 7% of ethanol is sufficient to completely suppress the maximum in the temperature dependence of the density of the mixture [9].

A more detailed study of the properties of water solutions is clearly of major importance in many applications. One can say that it is impossible to speak about a general behavior. Different compounds solubilized in water correspond a priori to different local structures. A very extensive study of salt solutions has been done by Enderby and coworkers [46]. Careful neutron scattering experiments allow the determination of the hydrogen shell around several ions. Around a cation, the water molecule is oriented with the oxygen closer to the cation corresponding to a minimization of the energy between the ion and the water dipole. Instead, around an anion, the hydrogen atoms are closer to the ion. The coordination numbers, i.e., the number of water molecules present inside the first hydration shell, and the lifetimes depend very much on the nature of the solute and on its concentration. Around hydrophobic molecules, such as methane, water forms large cages (clathrates) probably with a geometry close to that of polyhedra such as icosahedra. Finally, in the presence of a solid substratum, water may form bonds. This is the case, for instance, in glasses where silanol groups Si–O–H are present at the water–silica interface. It is worth noting

Copyright 2004 by Marcel Dekker, Inc. All Rights Reserved.

that in the presence of biological macromolecules, such as peptides, enzymes, proteins, DNA, etc., all these behaviors can be found depending more or less on the hydrophilic or hydrophobic nature of each site or residue. Bonds, in particular, certainly play a major role in the structure of these macromolecules.

III. STRUCTURE OF CONFINED WATER

A. Model Systems–Water Interactions

The choice of porous media as model systems is dependent on the conditions: a well-characterized pore size distribution and surface details. Among the hydrophilic model systems where the structure of confined water has been studied by neutron diffraction, let us mention clay minerals [11,12] and various types of porous silica [14–22]. In the last case, the authors have interpreted their results in terms of a thin layer of surface water with more extensive H-bonding, lower density and mobility, and lower nucleation temperature as compared to bulk water. Recently the structure of water confined in the cylindrical pores of MCM-41 zeolites with two different pore sizes (21 Å and 28 Å) has been studied by x-ray diffraction [21] over a temperature range of 223–298 K. For the capillary-condensed samples, there is a tendency to form a more tetrahedral-like hydrogen-bonded water structure at subzero temperatures in both pore sizes.

The more extensive results concern the structure of water confined in a Vycor glass [47], which is a porous silica glass characterized by quite a sharp distribution of cylindrical interconnected pores, and hydrophilic surfaces. Results have been obtained as functions of level of hydration from full hydration (0.25 g water/g dry Vycor) down to 25% hydration and temperature [48]. Based on the information that the dry density of Vycor is 1.45 g/ml, the porosity of 28% and the internal cylindrical pores of cross-sectional diameter 50 Å, the 50% hydrated sample has three layers of water molecules on its internal surface. A 25% hydrated sample corresponds roughly to a monolayer coverage of water molecules.

Results for two levels of hydration of Vycor demonstrate that the fully hydrated case is almost identical to the bulk water and the partially hydrated case is of little difference (Figure 2). However, the three site–site radial correlation functions are indeed required for a sensible study of the orientational correlations between neighboring molecules, and the results of three neutron diffraction experiments on three different isotopic mixtures of light and heavy water have been reported in a recent publication [49].

It is interesting, however, to comment on the level of supercooling possible for heavy water in Vycor. According to Ref. 48, for partially

Copyright 2004 by Marcel Dekker, Inc. All Rights Reserved.

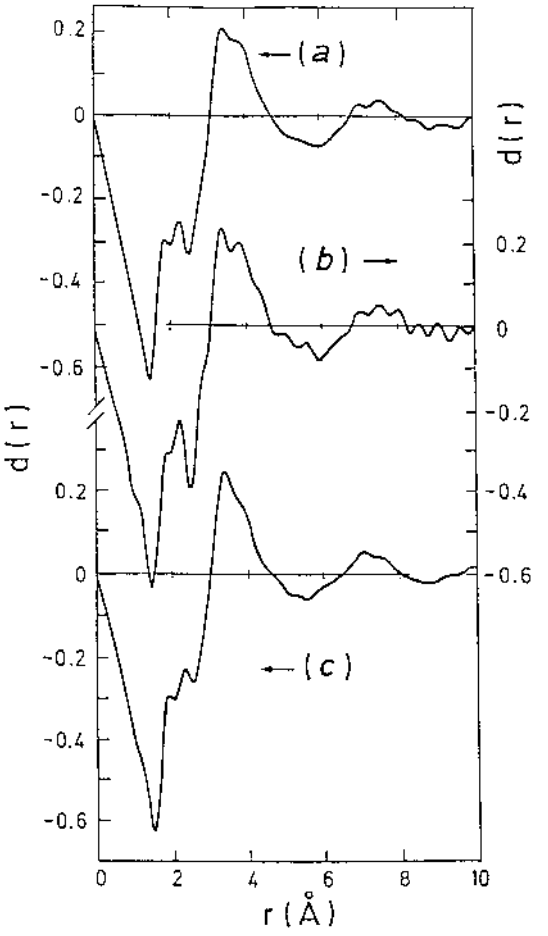

Figure 2 Pair correlation function $d(r)$ for (a) confined D_2O from fully hydrated Vycor (27°C); (b) confined D_2O from partially hydrated Vycor (35°C) compared with (c) bulk water (27°C) (Ref. 48).

hydrated samples, the deepest supercooling is −27°C, while for the fully hydrated sample it is −8°C. As temperature goes below the limit of supercooling, part of the confined water nucleates into cubic ice. The proportion of cubic ice increases with decreasing temperature. This is in sharp contrast to bulk water, which always nucleates into hexagonal ice.

Results relative to a 25% hydrated Vycor sample indicates that, at room temperature, interfacial water has a structure similar to that of bulk

Copyright 2004 by Marcel Dekker, Inc. All Rights Reserved.

supercooled water at a temperature of about 0°C which corresponds to a shift of about 30 K [50]. The structure of interfacial water is characterized by an increase of the long-range correlations, which corresponds to the building of the H-bond network as it appears in low-density amorphous ice [51]. There is no evidence of ice formation when the sample is cooled from room temperature down to −96°C (liquid nitrogen temperature).

Among hydrophobic model systems, one experimental investigation of particular interest concerns the structure of water contained in a carbon powder [23]. The structure of water has been determined by both x-ray and neutron diffraction, as functions of hydration, from room temperature down to 77 K. In agreement with previous work [14–18,48,52,53], this study gave support to the existence of a region near the interface where the properties of water are markedly different from those of the bulk liquid. From x-ray measurements, which yield information about the oxygen–oxygen distribution function, it appears that, at the lowest investigated water content, the 42% hydration level, a distortion of the tetrahedral ordering is clearly observed (Figure 3). Neutron scattering experiments can be analyzed to describe the intermolecular correlations (Figure 4): At the same lower level of hydration the hydrogen bonding is modified and water molecules are more ordered. It is not possible to determine the thickness of the affected layer. However, a crude determination from the specific area indicates that for an hydration equal to 50%, the thickness does not exceed 5 Å. This value must be compared with the computer simulation data [32–37], which indicate that structural modifications do not extend beyond 10 Å from the solid surface.

When partially hydrated samples are cooled down to 77 K, no crystallization peak is detected by differential thermal analysis. X-rays and neutrons show that an amorphous form is obtained and its structure is different from those of low- and high-density amorphous ices already known [5]. Samples with lower levels of hydration corresponding to one monolayer coverage of water molecules are under investigation. This phenomenon looks similar in both hydrophilic and hydrophobic model systems. However, in order to characterize more precisely the nature of the amorphous phase, the site–site partial correlation functions need to be experimentally obtained and compared with those deduced from molecular dynamics simulations.

B. Macromolecules–Water Interactions

The structure of water near polymeric membranes [52] has been studied by neutron diffraction. The structure of water confined in a hydro-gel has been

Copyright 2004 by Marcel Dekker, Inc. All Rights Reserved.

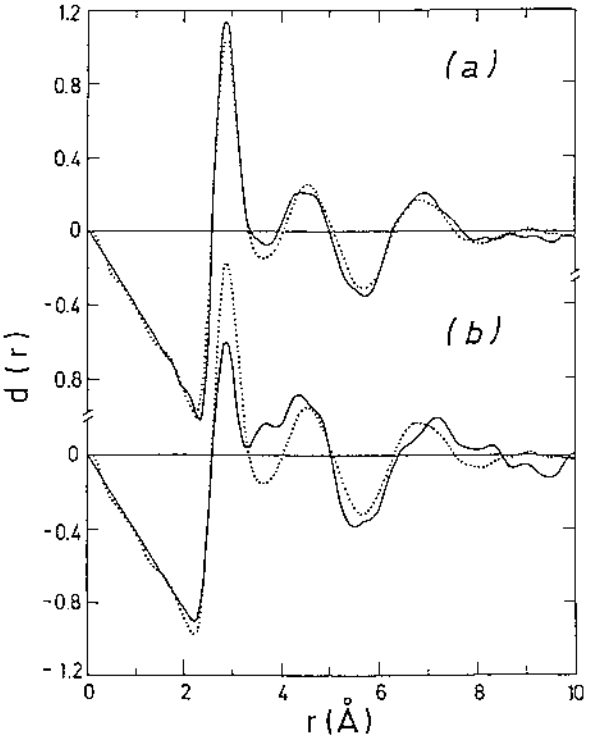

Figure 3 X-ray pair correlation function $d(r)$ of water contained in activated carbon, at room temperature, shown by solid lines for 188% (curve a) and 42% hydration (curve b). For comparison, $d(r)$ of bulk water at the same temperature is also drawn (dotted line) (Ref. 43).

investigated by x-ray scattering [54]; the distortion seen at the level of the second-nearest neighbors has been attributed to the bending of H-bonds.

The amount of information about protein–water correlations is small. For neutron diffraction, deuterated samples are required and difficult to obtain. However, the first results have been obtained in the case of a photosynthetic C-phycocyanin protein for which the x-ray crystallographic structure is known to a resolution of 1.66 Å [55].

C-phycocyanin is abundant in blue-green algae. Nearly 99% of the deuterated samples of this phycobiliprotein were isolated from the cyanobacteria which were grown in perdeuterated cultures [56] (99% pure D_2O) at Argonne National Laboratory. This process yielded deuterated C-phycocyanin proteins (d-CPC) that had virtually all the ^1H–C bonds replaced by ^2H–C bonds. One can obtain a lyophilized sample that is similar

Copyright 2004 by Marcel Dekker, Inc. All Rights Reserved.

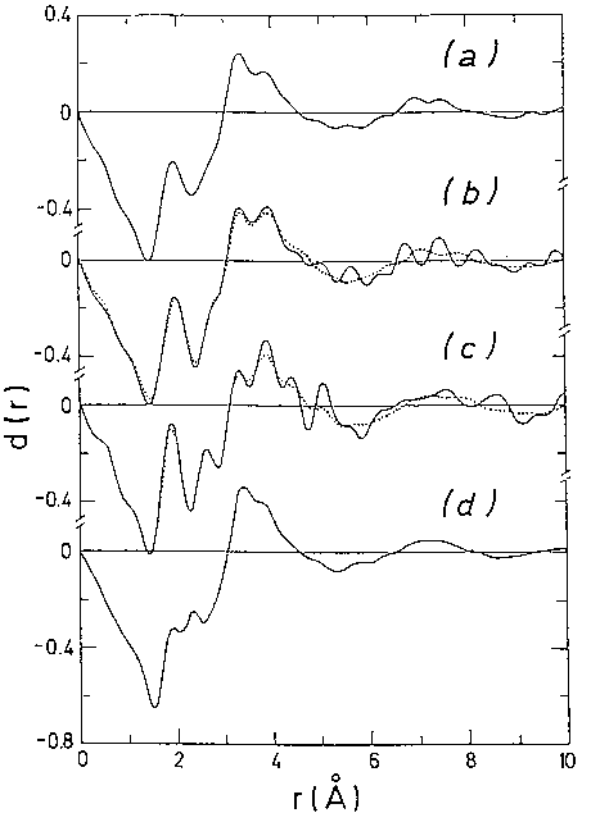

Figure 4 Neutron pair correlation function $d(r)$ of water contained in activated carbon, at room temperature, shown by solid lines for 200% (curve a), 42% (curve b), and 25% hydration (curve c). For comparison, $d(r)$ of bulk water at the same temperature is also drawn (curve d) (Ref. 43). The dotted lines show the result of smoothing the experimental data before the Fourier transformation. This demonstrates that the additive oscillations, which appear between 3 and 6 Å, have a physical meaning the opposite of that appearing at higher r values.

to amorphous solids as determined by neutron diffraction [53]. As defined in previous papers [57–59], the level of hydration $h = 0.5$ corresponds to 100% hydration of C-phycocyanin which leads to a coverage of about 1.5 monolayers of water molecules on the surface of the protein [60].

Fairly recently, the water (D_2O)–protein correlations at the surface of a fully deuterated amorphous protein C-phycocyanin have been studied by neutron diffraction as functions of temperature and hydration level [53].

Copyright 2004 by Marcel Dekker, Inc. All Rights Reserved.

The correlation distance of 3.5 Å measured in these diffraction experiments compared well with computer simulation work on polypeptides and proteins [34,61] and has been interpreted as resulting from some increase in the clustering of water molecules (Figure 5). For the highest hydrated sample ($h = 0.365$), a definite peak appears at 3.5 Å. This is the average distance between the centre of mass of a water molecule in the first hydration layer and amino-acid residues on the surface of the protein. In the case of the lowest hydrated sample ($h = 0.175$), the perturbation to the structure of protein due to water of hydration is not detectable. It is generally viewed in the literature that at full hydration ($h = 0.5$), there is a complete monolayer of water surrounding the protein [62].

Some similarity between the behavior of water close to C-phycocyanin protein and close to hydrophilic model systems can be stressed. In fact, for

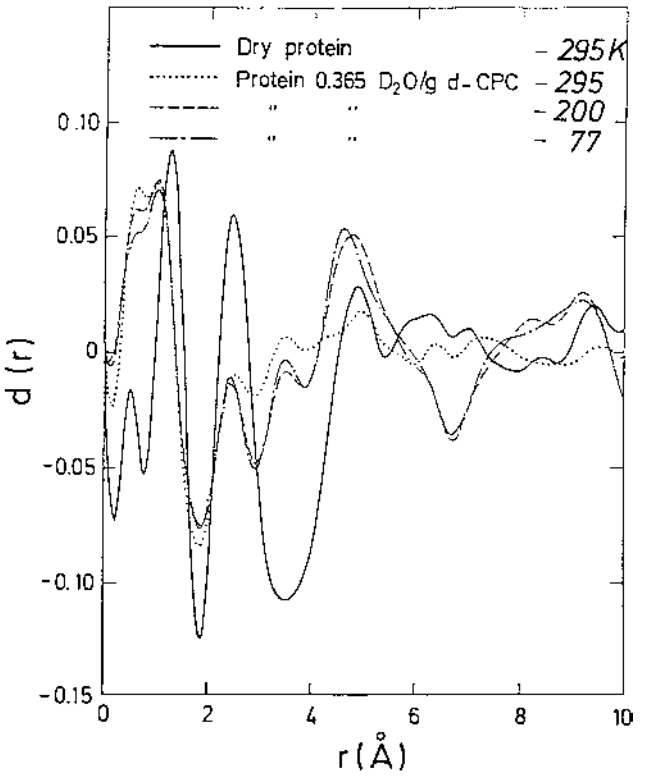

Figure 5 Pair correlation function $d(r)$ for a dry d-CPC protein at 295 K and for a D_2O-hydrated ($h = 0.365$) d-CPC protein at different temperatures (Ref. 53).

Copyright 2004 by Marcel Dekker, Inc. All Rights Reserved.

low hydrated protein samples, no crystallization of water is detectable, while for more than one monolayer coverage there is the appearance of hexagonal crystalline ice. Moreover, the peak at 3.5 Å is also detected. However, it should be noted that at the highest hydration level, water nucleates into hexagonal ice at low temperature; this is in contrast with hydrated Vycor where water nucleates into cubic ice.

Some other interesting findings have come from the study of the glass–liquid transition and crystallization behavior of water trapped in loops of methemoglobin chains [63].

IV. DYNAMICS OF CONFINED WATER

Traditionally, the dynamics of interfacial water has been studied by nuclear magnetic relaxation techniques. Halle and coworkers [64–66] have shown that ^{17}O magnetic relaxation in water is dominated by a quadrupolar coupling to the electric field gradient of intramolecular origin. Thus, it is a particularly suitable method for investigating the single-particle dynamics of interfacial water and thus the protein–water interaction. The main general findings from these techniques are a reduced lateral mobility of water molecules (10–100 times) and a long residence time (10–100 ps). With regard to the solvent diffusion constant near protein and silica surfaces there are reports from other groups that it is reduced by a factor of about 5 compared with that of bulk water [67,68].

An ideally microscopically detailed method for exploring the change in hydrogen-bonding patterns as well as the translational and rotational diffusion constants and residence times of water molecules, when they are near surfaces, is computer molecular dynamics (CMD). For example, Rossky and coworkers [32,33,35–37] have investigated changes of the structure, hydrogen bonding, and dynamics of water molecules when they are adjacent to an atomically detailed hydrophobic surface and to a hydroxylated silica surface. Results of CMD simulations [32,33,35–37] generally indicate that the dynamics of water molecules on protein and silica surfaces where hydrophilic interactions are dominant suffers only a mild slowing down compared to bulk water. More specifically, it has been reported that the retardation is by a factor of about 2 in the protein case and about a factor of 5 in the silica case. Residence times of water in the first hydration layer are typically of the order of 100 ps.

Linse [69] carried out a similar simulation for water near a charged surface with mobile counter-ions constituting an electric double layer such as in the interior of a reverse micelle formed with ionic surfactants in oil.

Copyright 2004 by Marcel Dekker, Inc. All Rights Reserved.

He reported that water in the aqueous core of reverse micelles has a reduced rate of translational and rotational motions by a factor of 2–4.

These CMD results are still qualitative and conflict somewhat with the available experimental data [65], largely because of the simplified models used for the surfaces and more certainly due to difficulties in choosing suitable potential functions for the simulations. However, fairly recently, molecular dynamics simulations of the hen egg–white lysozyme–Fab D1.3 complex have been reported; both the crystal state and the complex in solution were studied [42]. The findings are consistent with the observation by various experimentalists of a reduced water mobility in a region extending several angstroms beyond the first hydration layer [64–67] as reported also from CMD simulations [70].

From the above comparison it seems clear that there are considerable discrepancies in the degrees of slowing down between NMR experiments and CMD. This is especially true for the translational diffusion constant.

One way to resolve these discrepancies has been recently attempted by quasi-elastic and inelastic neutron scattering. Neutron scattering is a powerful and unique tool for studying the self-dynamics of interfacial water; actually the large incoherent scattering cross-section of the protons yields unambiguous results about the individual motions of water molecules [31]. In fact, this technique is a method for studying the diffusive motion of atoms in solids and liquids [71]. It gives access to the correlation function for the atomic motions which are explored over a space domain of a few angstroms and for times of the order of 10^{-12} s. This space and time domain justifies the comparison between neutron scattering and CMD. The correlation function can be calculated for various models for the assumed motion of the diffusing particles (e.g., Brownian motion, jump diffusion, diffusion in a confined space, rotational motion, etc.) and the microscopic properties of the environment of the scattering atoms, e.g., the residence time, the jump length, the diffusion coefficients, and the H-bond lifetime become available.

Another quantity that can be obtained is the density of states of mobile protons, in particular the translational and librational modes for water of hydration as compared to that of bulk water.

This method has been used with success for studying the self-dynamics of bulk water as a function of temperature [72] as previously reported.

Previous studies on the dynamics of water near interfaces by quasi-elastic neutron scattering involved the mobility of water on the surface of Nafion membranes [73,74], the diffusive motions and the density of states of water in silica gels [75], and the interfacial melting of ice in graphite and talc powders [76]. It is interesting to note that quasi-elastic scattering, like the effects for extremely small wavevectors, can be observed in the pulsed

Copyright 2004 by Marcel Dekker, Inc. All Rights Reserved.

gradient spin–echo NMR experiments. The latter technique has been used for studying the diffusion of water in both permeable [77] and connected structures where the effects of confinement can be clearly identified [78].

A. Model Surface–Water Systems

A complete study of the self-dynamics of water close to some well-defined hydrophilic surface such as the Vycor surface has been performed by quasi-elastic and inelastic neutron scattering. It has been done for levels of hydration ranging from full hydration down to the lowest one (25%), corresponding to one monolayer coverage of water molecules. The effect of temperature has also been studied. We report the main results here [79].

The short-time diffusion (a few picoseconds) of water molecules close to the Vycor surface has been described in terms of simple models for all the samples studied [80]. At short times, the water molecules, close to some hydrophilic surface, perform very local rotational jumps characterized by D_t and τ_1 as in bulk water, but with a longer residence time τ_0 on a given site before diffusing to an adjacent site along the surface with a diffusion coefficient equal to D_{local}. This diffusion is limited to some volume estimated as spherical. For the 25% hydrated sample, the diffusion coefficient measured by NMR appears to be smaller than D_t, which is smaller than D_{local} [81]. This is due to the fact that the NMR technique measures the long-time and long-range diffusion coefficient.

The effect of the temperature has been followed down to -35°C. The radius of the spherical volume of confinement varies between 5 and 2 Å; it decreases when the temperature is lowered, which means that water molecules are more localized at low temperatures. The observed trend seems reasonable.

The values obtained for D_{local} are low, which demonstrate the influence of the hydrophilic groups when one reaches a monolayer coverage of water molecules. Moreover, these values are close to the values of the diffusion coefficient of water molecules, at the immediate hydrophilic interface, as determined in a molecular dynamics simulation by Lee and Rossky [36].

Figure 6 shows the vibrational density of states for confined water (52% hydrated Vycor) compared with that of bulk water at room temperature [3]. The density of states of confined water exhibits striking features. The peak associated with the hindered translational motions, centered on 6 meV, is much attenuated, indicating the reduction of this degree of freedom upon confinement. There is an upshift of the librational peak at 70 meV, indicating some hindrance of the librational motions because of the presence of the surface. The hindrance of the motions increases when the temperature is lowered.

Copyright 2004 by Marcel Dekker, Inc. All Rights Reserved.

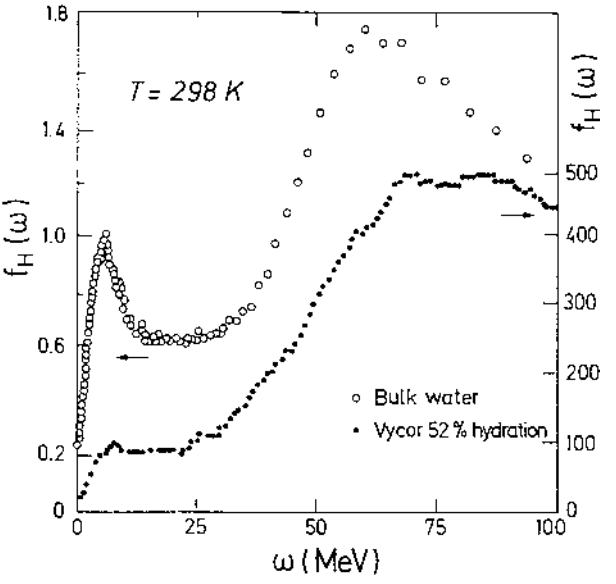

Figure 6 Proton vibrational density of states f_H for water contained in 52% hydrated Vycor at 298 K (full circles). For comparison the corresponding quantity for bulk water (open circles) is also given (Ref. 59).

In hydrophobic environments such as activated carbon powder, the vibrational density of states for confined water has been determined by inelastic neutron scattering as a function of temperature and compared with bulk water. For the lowest level of hydration, the translational peak around 6 meV and the vibrational peak at 70 meV, are less affected than in the Vycor case. However, an up-shift of the librational peak at 70 meV, characteristic of hindered motions, is observed [50].

B. Biopolymer–Water Systems

The volume of neutron data on biopolymer–water systems is small [60,82,83]. In fact, the case of water close to different residues of a biological material is certainly more interesting for future applications. However, the situation is also more complex due to contributions such as the hydrogen atoms of the protein itself, the possibility of their exchange with water molecules, and the presence of hydrophilic and hydrophobic regions. Studies of the single-particle dynamics of hydration water in proteins have been hampered by the fact that about 40% of the constituent

Copyright 2004 by Marcel Dekker, Inc. All Rights Reserved.

atoms in a typical protein molecule are hydrogen atoms, present in the backbone and in the side chains. The elastic contribution is thus too large for an accurate determination of the dynamical parameters which are characteristic of hydration process. However, by working with a deuterated protein/H_2O system, it has been possible recently to focus on the water dynamics at and near the protein surface [57–59].

In the vicinity of biomolecules, water may adopt very different behavior depending on the nature of the sites, on the available free volume, on temperature, etc. Due to the difficulty of experiments that can identify local properties among a variety of possibilities, the number of unambiguous results remains scarce. It is plausible that the development of computer simulations of molecular dynamics will soon take into account more precisely local environments [39–41].

Quasi-elastic neutron scattering has been used to describe the motions of water molecules in the vicinity of proteins and other macromolecules. One of the more successful results has been obtained with C-phycocyanin, a protein extracted from blue-green algae, which can be obtained nearly fully deuterated from perdeuterated cultures as mentioned previously [56]. In this way, and because of the very large incoherent cross-section of hydrogen atoms, only the motions of water molecules are observed in a quasi-elastic neutron scattering experiment [57–59]. The results presented in Figure 7 show clearly that the total scattered intensity contains two components. The width of the narrow component is imposed by the instrumental resolution. Its area is proportional to the number of water molecules with motions that are too slow to be observed by the technique, i.e., typically with a characteristic time longer than several tens of picoseconds. Instead, the wider component depicts the diffusive motions of the other water molecules through a Lorentzian line $L(\omega)$. Its intensity and width can be analyzed as functions of the degree of hydration and of temperature.

The simplest expression that can be written separates the two components in the following way:

$$S_{\text{inc}}(Q,\omega) = [P + (1 - P)A_0]\delta(\omega) + (1 - P)(1 - A_0)L(\omega) \tag{2}$$

where $P = p + q(1 - p)$ contains both the contributions of the p nonlabile protons of the protein and the fraction q of water molecules with a slow dynamics. $A_0(Qa)$ is a mathematical factor, called the *elastic incoherent scattering factor*, which takes into account the confinement of the motions within a small volume of size a, assumed spherical for simplicity [80].

Typical results are shown in Figure 8. Figure 8 a shows that the number q of "immobile" water molecules increases gradually from 40%,

Copyright 2004 by Marcel Dekker, Inc. All Rights Reserved.

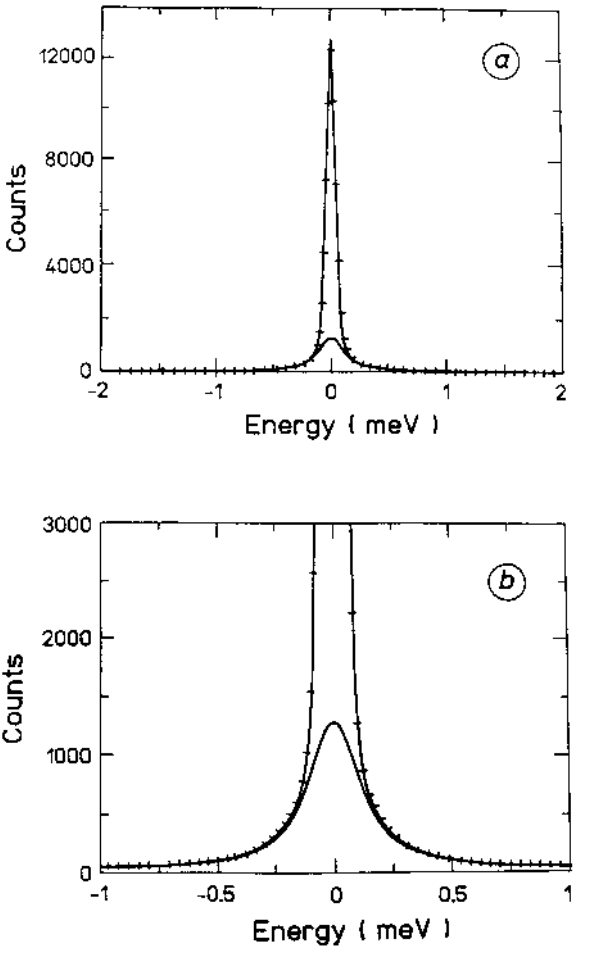

Figure 7 A typical quasi-elastic spectrum for the fully hydrated C-phycocyanin ($h = 0.5$ g water/g protein) at a scattering angle $\theta = 65.4^\circ$ and for $T = 293$ K. (a) Spectrum of the quasi-electric scattered intensity. (b) Enlarged representation of the same spectrum showing the Lorentzian component. Symbols (+) are experimental points and the solid line is the fit using equation (2) (Ref. 58).

at high temperature, to 100% around 200 K. This result shows that the number of confined water molecules is small at room temperature but, in contrast, that only at very low temperature (typically at -50°C) are their motions totally frozen. The curve shown in Figure 8 b depicts the linewidth of the Lorentzian $L(\omega)$ versus the square of the momentum transfer Q.

Copyright 2004 by Marcel Dekker, Inc. All Rights Reserved.

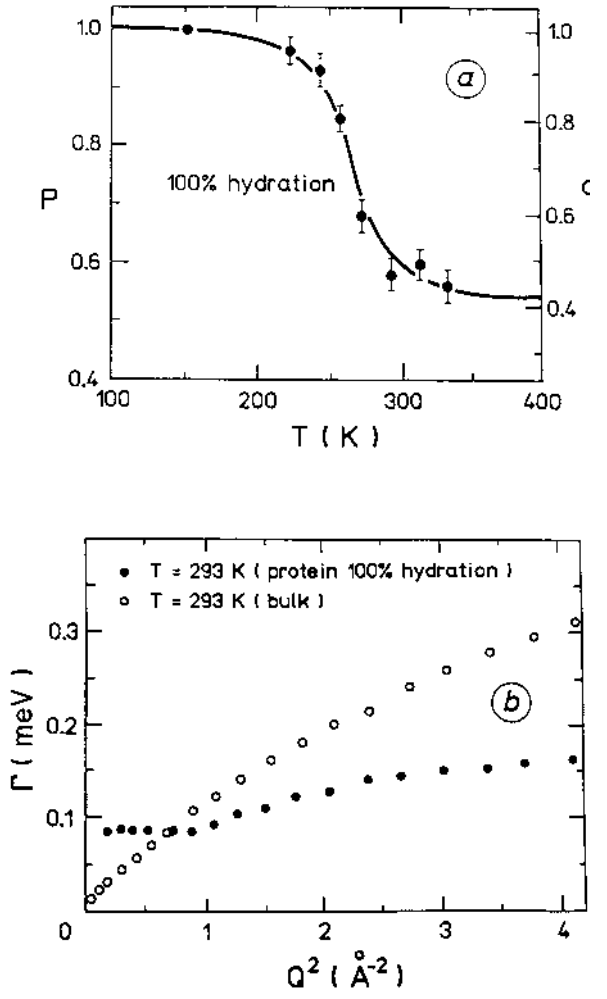

Figure 8 (a) The variation of the measured P parameter and of the fraction of "immobile water" q versus T for the fully hydrated C-phycocyanin ($h = 0.5$ g water/g protein) (Ref. 58). (b) Half width at half maximum of the Lorentzian quasi-elastic line (Γ) versus Q^2, for $T = 293$ K, for the fully hydrated C-phycocyanin and for the bulk water (Ref. 58).

It shows that, at low values of Q, i.e., when one investigates the system at large scales, the molecules appear confined. This is evident from the plateau seen below $Q = 1\ \text{Å}^{-1}$. The resulting confinement yields a volume of confinement of molecular size ($a \approx 3$ Å). This is in contrast with the

Copyright 2004 by Marcel Dekker, Inc. All Rights Reserved.

behavior of bulk water at the same temperature. The same figure shows that, in the case of bulk water, diffusive motions take place at all scales, as expected for a liquid. Indeed, the linewidth corresponding to bulk water goes to zero at small values of Q, following Fick's law, $\Gamma = DQ^2$, where D is the self-diffusion coefficient. At intermediate values of Q, the slope of $\Gamma(Q^2)$ is smaller for confined water than for bulk water. This means that, even in the small volume of confinement, the dynamics is hindered.

Numerical analysis of the data obtained at different temperatures shows that the dynamics of confined water molecules is analogous to that of bulk water at temperatures typically 30°C lower [84]. This can be understood in the following way: at hydrophilic sites of the protein, water molecules form relatively stable hydrogen bonds which keep the molecule confined in a small region of the surface of the protein. Water molecules form alternatively hydrogen bonds with the hydrophilic sites and their characteristic lifetime is longer than in bulk water. At the time scale of the neutron scattering experiment, the dynamics of hydrogen bond formation concerns only three bonds among the four possible intermolecular bonds, one of them being "blocked" by the hydrophilic site of the protein.

The behavior that we describe appears very general, at least qualitatively. Hydration water from other biomolecules, as well as water confined in small pores, show a similar slowing down of dynamic properties and a decrease of the temperature at which all the diffusive motions are frozen [59,79,83].

The common features arising from quasi-elastic neutron scattering studies of water at a Vycor surface or close to a more complex protein surface are presented below. In particular, the results of a C-phycocyanin protein at a hydration level $h = 0.4$ are important since a monolayer coverage of water molecules allows the protein to initiate its function [24]. Tables 1 and 2 give respectively for hydrated protein ($h = 0.4$) and for 25%

Table 1 Parameters for Water Near Surface of a C-Phycocyanin Protein (Hydrated Lyophilized Sample, $h = 0.40$)

T (°C)	a (Å)	D_{local} confined water (10^{-5} cm^2/s)	D_t confined water (10^{-5} cm^2/s)	D_t bulk water (10^{-5} cm^2/s)	τ_0 confined water (ps)	τ_0 bulk water (ps)
40	4.5	1.28	1.52	3.20	5.9	0.90
25	4.3	0.97	1.20	2.30	6.6	1.10
0	4.0	0.84	0.76	1.10	8.2	3.00

Copyright 2004 by Marcel Dekker, Inc. All Rights Reserved.

Table 2 Parameters for Water Confined in a 25% Hydrated Vycor Sample

T (°C)	a (Å)	D_{local} confined water (10^{-5} cm^2/s)	D_t confined water (10^{-5} cm^2/s)	D_t bulk water (10^{-5} cm^2/s)	τ_0 confined water (ps)	τ_0 bulk water (ps)	τ_1 confined water (ps)	τ_1 bulk water (ps)
25	4	0.92	2.45	2.30	15	1.10	1.5	1.10
−5	3	0.38	1.36	0.907	20	4.66	1.8	1.57
−15	3	0.26	1.20	0.574	25	8.90	2.0	1.92
−35	2						3.1	

hydrated Vycor the values of the diffusion coefficients D_{local} and D_t for confined water compared with the diffusion coefficient D_t of bulk water. The residence times τ_0 [59,79] and the H-bond lifetimes τ_1 [59,79] are also given as a function of temperature.

For hydrated protein (Table 1), the values obtained for D_{local} are lower than those of bulk water. They are close to those obtained at the same temperature for 25% H_2O-hydrated Vycor (Table 2) which demonstrates the influence of the hydrophilic groups on the water molecules when one reaches a monolayer coverage. This shows that the diffusive motion of water molecules is strongly retarded by interactions with a protein surface.

However, in contrast with the case of water in hydrated Vycor, the values of D_t for water of hydration in protein are smaller than that of bulk water. This is due to some influence of hydrophobic residues of protein, at the vicinity of the protein surface, which, in fact, is not as hydrophilic as that of Vycor. We are thus able to detect the effect of the substrate [59].

Figure 9 a gives the Arrhenius plots of τ_0 for water of hydration at the surface of a protein [59] compared with those of water in Vycor at different levels of hydration [79] and bulk water [72].

The residence times τ_0 of confined water from 25% hydrated Vycor and from hydrated protein are always longer than the residence time of bulk water, at the same temperature. They increase rapidly as either the temperature or the level of hydration decreases. For example, for the 25% hydrated Vycor sample $\tau_0 = 25$ ps at -5°C.

The H-bond lifetimes τ_1 for confined water are close to that of bulk water [79]. They have an Arrhenius temperature dependence (Figure 9b) while the residence time τ_0 does not exhibit such a behavior (Figure 9a).

Figure 10 shows the evolution of the vibrational density of states for H_2O-hydrated protein C-phycocyanin as a function of temperature for two levels of hydration, $h = 0.5$ and $h = 0.25$.

Copyright 2004 by Marcel Dekker, Inc. All Rights Reserved.

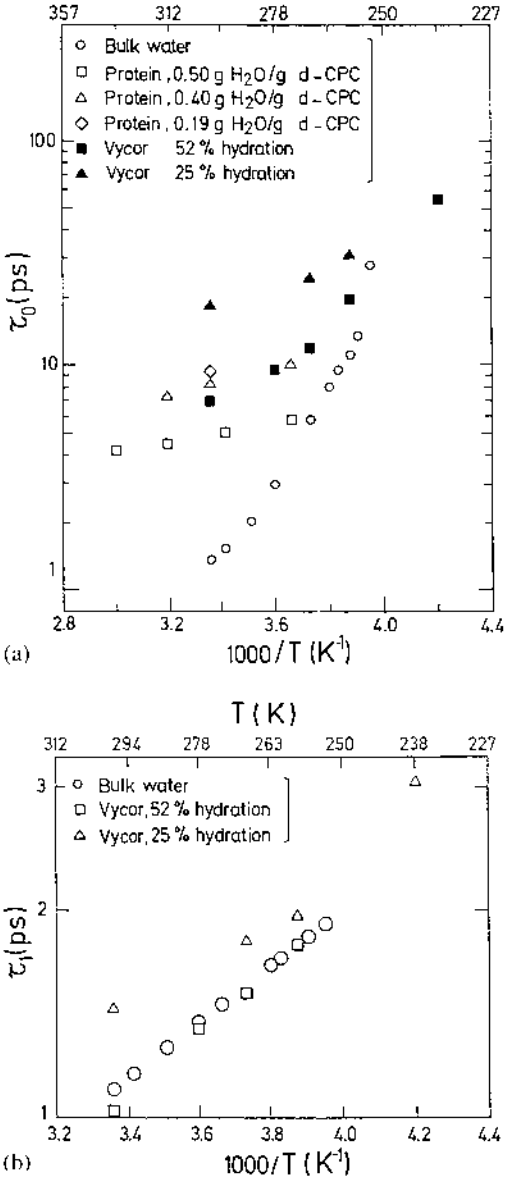

Figure 9 (a) Arrhenius plot of the residence time τ_0 for different levels of hydration of water: at the surface of H_2O-hydrated d-CPC protein (open symbols); contained in hydrated Vycor (full symbols); compared with bulk water (open circles) (Refs. 59, 79). (b) Arrhenius plot of the hindered rotations characteristic time, τ_1. This time can be associated with the hydrogen bond lifetime (Refs. 59, 79).

Copyright 2004 by Marcel Dekker, Inc. All Rights Reserved.

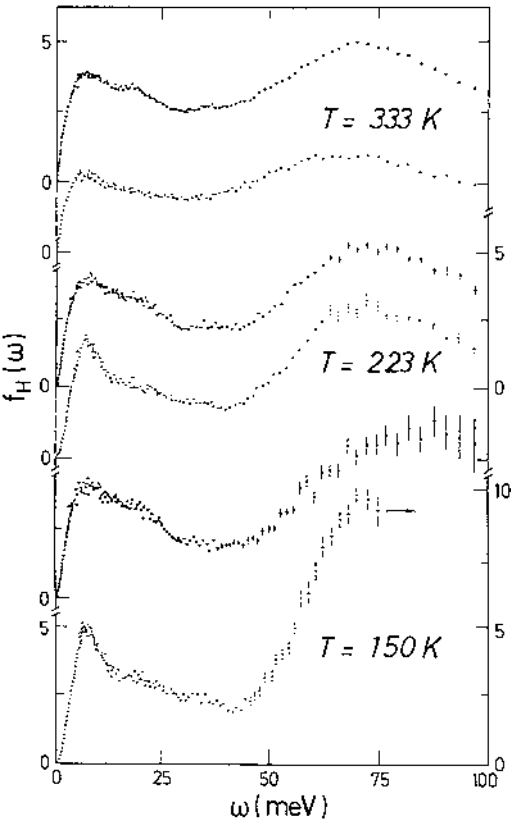

Figure 10 Proton vibrational density of states f_H for water at surface of H_2O-hydrated d-CPC protein $\theta = 27.5°$, for three temperatures 333, 223, and 150 K and two levels of hydration $h = 0.50$ (crosses) and $h = 0.25$ (full circles) (Ref. 59).

One can see that the corresponding peaks for hydration water in protein are also shifted upward slightly compared to the bulk water at the same temperature and as is observed for water confined in Vycor (Figure 6). The upshift of the librational peak increases either as the temperature is lowered or the level of hydratation is decreased, which reflects the amplified effect of confinement [59]. This indicates that both the translational and librational motions of water molecules, at or near a protein surface, are slightly more hindered, in agreement with observations from computer simulations.

Moreover, in the case of a low level of hydration ($h = 0.25$) the evolution of the density of states of hydrated protein as a function of

Copyright 2004 by Marcel Dekker, Inc. All Rights Reserved.

the temperature is less pronounced than in the case of $h = 0.5$. This is in agreement with the structural study [53] at the lower hydration ($h = 0.175$) which only detected small changes when the temperature is lowered from room temperature down to 77 K, and with further structural studies of low hydrated Vycor samples. Low temperatures do not significantly affect the overall structure of the protein and the bound water molecule and no crystallization of water has been observed. This could reflect the fact that at room temperature the interfacial water behaves like a dense supercooled liquid.

V. CONCLUSION

From the more recent findings combining neutron techniques and molecular dynamics simulations, it is now possible to have a more precise picture of confined water. Water, in the vicinity of a hydrophilic surface, is in a state equivalent to bulk water at a lower temperature. As previously demonstrated; this depends on the degree of hydration of the sample. In particular, at room temperature, interfacial water shows a dynamic behavior similar to that of bulk water at a temperature 30 K lower. It behaves like bulk supercooled water.

It appears that the short-time dynamics of water molecules at or near a hydrophilic model surface and at a soluble protein surface is much slower compared to that of bulk water. It is important to notice that the more significant slow dynamics of interfacial water is reflected in the long residence time for jump diffusion. This suggests that there may be a common underlying mechanism for the slowing down of the single-particle dynamics of interfacial water.

This is a consequence of the confined diffusion theory, which has been used to analyze the quasi-elastic neutron scattering data. This simple theory gives information on the confinement volume and the slow dynamics of the single-particle motions. In order to understand the microscopic origin of the confinement and slowing down of motions of water molecules and the exact role played in this context, the theory of kinetic glass transition in dense supercooled liquids [85,86] has been used. This theory leads to some description of the dynamics of confined water in terms of correlated jump diffusion [87] instead of jump diffusion [72]. This description seems to be consistent with molecular dynamics simulations of supercooled water [88] and has been confirmed by high-resolution quasi-elastic neutron scattering experiments of water from hydrated Vycor [89] and from hydrated C-phycocyanin protein [90].

Copyright 2004 by Marcel Dekker, Inc. All Rights Reserved.

This more sophisticated way shows a large distribution of residence times for water molecules in the cage formed by the neighboring molecules, which is a more realistic view than the sharp separation of water molecules into two classes, according to their mobility [59]. Short-time dynamics results on hydrated myoglobin have been recently interpreted by using this same theory of kinetic glass transition in dense supercooled liquids [83].

Finally, recent progress has been made in understanding the origin of the temperature shift, of the order of 30 K, proper to water close to some hydrophilic surface. That can be explained within the reliable percolation model of water [91], assuming that only three hydrogen bonds can be formed between interfacial water molecules instead of four in bulk water. This lowest number of H-bonds appears to be in good agreement with the more recent experimental findings on water in Vycor [49].

ACKNOWLEDGMENTS

We are grateful to H. L. Crespi for his continuing collaboration in the preparation of the perdeuterated protein C-phycocyanin.

REFERENCES

1. CA Angell. In: F Franks, ed. Water: A Comprehensive Treatise. Vol. 7, Chap. 1. New York: Plenum Press, 1981.
2. EW Lang, HD Ludemann. Angew Chem Int Ed Engl 21:315, 1982.
3. SH Chen, J Teixeira. Adv Chem Phys 64:1, 1985.
4. JC Dore. In: F Franks, ed. Water Science Reviews. Vol. 1. Cambridge University Press, 1985.
5. M-C Bellissent-Funel, J Teixeira, L Bosio. J Chem Phys 87:2231, 1987.
6. M-C Bellissent-Funel. Hydrogen bonded liquids. In: JC Dore, J Teixeira, eds. NATO ASI Series C. Dordrecht: Kluwer Academic Publishers, 1991, p 117.
7. M-C Bellissent-Funel, J Teixeira. J Mol Struct 250:213, 1991.
8. SH Chen. Hydrogen-bonded liquids. In: JC Dore, J Teixeira, eds. NATO ASI Series C329. Dordrecht: Kluwer Academic Publishers, 1991, p 289.
9. J Teixeira. J Phys IV 3:C1-163, 1993 and references therein.
10. PH Poole, F Sciortino, U Essman, HE Stanley. Nature 360:324 and references therein.
11. RK Hawkins, PA Egelstaff. Clays Clay Miner 28:19, 1980.
12. AK Soper. Hydrogen-bonded liquids. In: JC Dore, J Teixeira, eds. NATO ASI Series C329. Dordrecht: Kluwer Academic Publisher, 1991, p 147.
13. Y Kuroda, S Kittaka, S Takahara, T Yamaguchi, M-C Bellissent-Funel. J Phys Chem B 103:11064, 1999.

Copyright 2004 by Marcel Dekker, Inc. All Rights Reserved.

14. DC Steytler, JC Dore. J Chem Phys 87:2458, 1983.
15. DC Steytler, JC Dore, CJ Wright. Mol Phys 48:1031, 1983.
16. DC Steytler, JC Dore. Mol Phys 5:1001, 1985.
17. JC Dore, M Dunn, P Chieux. J Physique 48:C1-457, 1987.
18. JC Dore, F Coveney, M-C Bellissent-Funel. In: WS Howells, K Soper, eds. Recent Developments in the Physics of Fluids. Bristol: Adam Hilger, 1992, p 299.
19. MJ Benham, JC Cook, JC Li, ADK Ross, PL Hall, B Sarkissian. Phys Rev B 39:633, 1989.
20. SH Chen, MC Bellissent-Funel. Hydrogen bond networks. In: MC Bellissent-Funel, JC Dore, eds. NATO ASI C435. Dordrecht: Kluwer Academic Publisher, 1994, p 307.
21. P Smirnov, T Yamaguchi, S Kittaka, S Takahara, Y Kuroda. J Phys Chem B 104:5498, 2000.
22. V Venuti, V Crupi, S Magazu, D Majolino, P Migliardo, M-C Bellissent-Funel. J Phys IV 10:Pr7-211, 2000.
23. M-C Bellissent-Funel, R Sridi-Dorbez, L Bosio. J Chem Phys 104:10023, 1996.
24. JA Rupley, G Careri. Adv Prot Chem 41:37, 1991.
25. MF Colombo, DC Rau, VA Parsegian. Science 256:655, 1992.
26. J Smith. Q Rev Biophys 24:227, 1991.
27. PJ Steinbach, BR Brooks. Proc Natl Acad Sci USA 90:9135, 1993.
28. V Lounnas, BM Pettitt, L Findsen, S Subramaniam. J Phys Chem 96:7157, 1992.
29. V Lounnas, BM Pettitt. Proteins Struct Funct Gen 18:148, 1994.
30. V Lounnas, BM Pettitt, GN Phillips Jr. Biophys J 66:601, 1994.
31. SW Lovesey. Theory of Neutron Scattering from Condensed Matter. 3rd ed. Oxford: Clarendon Press, 1987.
32. CY Lee, JA McCammon, PJ Rossky. J Chem Phys 80:4448, 1984.
33. SH Lee, PJ Rossky. Proceedings of the 10th Korean Scientists and Engineers Conference, Inchen, Korea, 1987, p 150.
34. M Levitt, R Sharon. Proc Natl Acad Sci USA: Biophys 85:7557, 1988.
35. PJ Rossky, SH Lee. Chem Scr 29A:93, 1989.
36. SH Lee, PJ Rossky. J Chem Phys 100:3334, 1994.
37. PJ Rossky. Hydrogen bond networks. In: MC Bellissent-Funel, JC Dore, eds. NATO ASI C435. Dordrecht: Kluwer Academic Publisher, 1994, p 337.
38. PA Netz, T Dorfmüller. J Phys Chem B 102:4875, 1998.
39. M Marchi, F Sterpone, M Ceccarelli. J Am Chem Soc 124:6787, 2002.
40. AR Bizzarri, S Cannistraro. J Phys Chem B 106:6617, 2002.
41. A Luzar, D Chandler. Phys Rev Lett 76:928, 1996.
42. F Alary, J Durup, Y-H Sanejouand. J Phys Chem 97:13864, 1993.
43. M-C Bellissent-Funel, R Sridi-Dorbez, L Bosio. J Chem Phys 104:10023, 1996.
44. M-C Bellissent-Funel, L Bosio, J Teixeira. J Phys Condens Matter 3:4065, 1991.

Copyright 2004 by Marcel Dekker, Inc. All Rights Reserved.

45. AK Soper, MG Phillips. Chem Phys 107:47, 1986.
46. JE Enderby. The physics and chemistry of aqueous ionic solutions. In: MC Bellissent-Funel, GW Neilson, eds. NATO ASI C205. Dordrecht: D. Reidel, 1987, p 129 and references therein.
47. General information on Vycor Brand Porous "thirsty glass," no. 7930, Corning Glass Works, is available from OEM Sales Service, Box 5000, Corning, NY 14830, U.S.A.
48. M-C Bellissent-Funel, L Bosio, J Lal. J Chem Phys 98:4246, 1993.
49. F Bruni, MA Ricci, AK Soper. J Chem Phys 109:1478, 1998.
50. J-M Zanotti. Ph.D. Thesis, University of Orsay, France, 1997.
51. M-C Bellissent-Funel, L Bosio, A Hallbrucker, E Mayer, R Sridi-Dorbez. J Chem Phys 97:1282, 1992.
52. PM Wiggins. Prog Polym Sci 13:1, 1988.
53. M-C Bellissent-Funel, J Lal, KF Bradley, SH Chen. Biophys J 64:1542, 1993.
54. L Bosio, GP Johari, M Oumezzine, J Teixeira. Chem Phys Lett 188:113, 1992.
55. M Duerring, GB Schmidt, R Huber. J Mol Biol 217:577, 1987.
56. HL Crespi. In: Stable Isotopes in the Life Science, III. Vienna: IAEA, 1977.
57. M-C Bellissent-Funel, J Teixeira, KF Bradley, SH Chen, HL Crespi. Physica B 180–181:740, 1992.
58. M-C Bellissent-Funel, J Teixeira, KF Bradley, SH Chen. J Phys I France 2:995, 1992.
59. M-C Bellissent-Funel, J-M Zanotti, SH Chen. Faraday Discuss 103, 1996, p 281.
60. HD Middendorf. In: M Peyrard, ed. Nonlinear Excitations in Biomolecules. Les Ulis: Les Editions de Physique, 1995, p 369.
61. PJ Rossky, M Karplus. J Am Chem Soc 101:1913, 1979.
62. B Lee, FM Richard. J Mol Biol 55:379, 1971.
63. G Sartor, A Hallbrucker, H Hofer, E Mayer. Conference Proceedings on Water Biomolecule Interactions. Bologna: SIF, 1993, pp 143–146.
64. B Halle, T Andersson, S Forsen, B Lindman. J Am Chem Soc 103:500, 1981.
65. L Piculell, B Halle. In: GW Neilson, JE Enderby, eds. Water and Aqueous Solutions. Bristol: Adam Hilger, 1986, p 219 and references therein.
66. G Carlstroem, B Halle. Langmuir 4:1346, 1988.
67. CF Polnaszek, RG Bryant. J Am Chem Soc 106:428, 1984; J Chem Phys 81:4038.
68. CF Polnaszek, DA Hanggi, PW Carr, RG Bryant. Anal Chim Acta 194:311, 1987.
69. P Linse. J Chem Phys 90:4992, 1989.
70. CF Wong, JA McCammon. Isr J Chem Phys 27:211, 1986.
71. T Springer. Quasi-elastic neutron scattering for the investigation of diffusive motions in solids and liquids, Springer Series in Modern Physics. Vol. 64, 1972.
72. J Teixeira, M-C Bellissent-Funel, SH Chen, AJ Dianoux. Phys Rev A31:1913, 1985.
73. F Volino, M Pineri, AJ Dianoux, A de Geyer. J Polym Sci 20:481, 1982.

Copyright 2004 by Marcel Dekker, Inc. All Rights Reserved.

74. AJ Dianoux. The physics and chemistry of aqueous ionic solutions. In: MC Bellissent-Funel, GW Neilson, eds. NATO ASI C205. Dordrecht: D. Reidel, and references therein, 1987, p 129.
75. JDF Ramsay, C Poinsignon. Langmuir 3:320, 1987.
76. M Maruyama, M Bienfait, JG Dash, G Coddens. J Cryst Growth 118:33, 1992.
77. PT Callaghan, A Coy, TPJ Halpin, D MacGowan, KJ Packer, FO Zelaya. J Chem Phys 97:651, 1992.
78. PT Callaghan, A Coy, D MacGowan, KJ Packer, FO Zelaya. Nature 351:467, 1991.
79. MC Bellissent-Funel, SH Chen, J-M Zanotti. Phys Rev E 51:4558, 1995.
80. F Volino, AJ Dianoux. Mol Phys 41:271, 1980.
81. M-C Bellissent-Funel, JRC van der Maarel. Unpublished results.
82. HD Middendorf, D Di Cola, F Cavatorta, A Deriu, CJ Carlile. Biophys Chem 53:145, 1994.
83. M Settles, W Doster. Faraday Discuss 103, 1996, p 269.
84. J Teixeira, J-M Zanotti, M-C Bellissent-Funel, S-H Chen. Physica B 234–236:370, 1997.
85. W Gotze, L Sjogren. Rep Prog Phys 55:241, 1992.
86. HZ Cummins, G Li, WM Du, WM Hernandez. Physica A204:169, 1994.
87. SH Chen, P Gallo, M-C Bellissent-Funel. Non Equilibrium Phenomena in Supercooled Fluids, Glasses and Materials. Singapore: World Scientific, 1996.
88. P Gallo, F Sciortino, P Tartaglia, SH Chen. Phys Rev Lett 76:2730, 1996.
89. J-M Zanotti, M-C Bellissent-Funel, S-H Chen. Phys Rev E 59:3084, 1999.
90. S Dellerue, M-C Bellissent-Funel. Chem Phys 258:315, 2000.
91. HE Stanley, J Teixeira. J Chem Phys 73:3404, 1980.

Copyright 2004 by Marcel Dekker, Inc. All Rights Reserved.

3

Mechanisms of Protein Stabilization During Freeze-Drying and Storage: The Relative Importance of Thermodynamic Stabilization and Glassy State Relaxation Dynamics

Michael J. Pikal
School of Pharmacy, University of Connecticut, Storrs, Connecticut, U.S.A.

I. INTRODUCTION

Partly because of chemical complexity and partly due to the marginal stability of higher order structure (i.e., conformation), therapeutic proteins often present significant stability problems. While proteins are generally quite stable in aqueous solution for short periods of time, a pharmaceutical product must have adequate stability over storage periods of many months, typically several years. Many proteins do not possess this long-term stability in the aqueous state. Ironically, while the nature of water is an important contributing factor to the conformational stability of a protein, water is a destabilizing factor in the long-term preservation of the chemical and structural integrity of a protein. With proteins, as with most labile molecules, removal of water to form a solid generally improves storage stability. Thus, proteins are typically freeze-dried in an attempt to achieve

Copyright 2004 by Marcel Dekker, Inc. All Rights Reserved.

adequate storage stability. However, some proteins suffer *irreversible* damage during freeze-drying, and even if the protein survives freeze-drying without damage, the freeze-dried solid does not always have the desired storage stability. Stability problems are normally minimized by a combination of proper process control and formulation optimization.

In the context of proteins, "stability" has two distinct meanings. The term pharmaceutical stability refers to the ability of a protein to be processed, distributed, and used without *irreversible* change in primary structure, conformation, or state of aggregation. We refer to pharmaceutical *instability* as "degradation." The phrase "protein stability" is also commonly used to describe the position of the equilibrium between native and unfolded conformations. If a protein formulation requires a high level of chemical denaturant, or a high temperature, to shift the equilibrium between native and unfolded in favor of the unfolded state, the protein is said to be "stable." This meaning of stability we denote "thermodynamic stability." The time scale for manifestation of thermodynamic *instability* in aqueous solutions is normally quite short, i.e., time constants for unfolding are typically seconds to hours [1,2]. While pharmaceutical *instability* during processing may also occur on a short time scale, degradation during storage involves a time scale on the order of years. Thermodynamic *instability* involves physical changes, somewhat analogous to a thermodynamic change of state. Pharmaceutical *instability* may be purely a result of a physical change (i.e., noncovalent aggregation), but may also involve changes in primary structure or "chemical degradation."

Pharmaceutical stability and thermodynamic stability are not necessarily directly related. For example, a protein may exhibit thermodynamic *instability* during freeze-drying and unfold, but if no *irreversible* reactions occur during storage or during reconstitution, the reconstituted protein may refold completely within seconds and therefore display perfect pharmaceutical stability. A protein that remains in the native state, and is thermodynamically stable, may still degrade via chemical reactions such as deamidation and methionine oxidation over storage times of years, particularly if the reactive moiety is located on the protein surface. Conversely, thermodynamic *instability* may well be a prelude to degradation. Certainly an unfolded protein could expose normally buried and "protected" methionine and asparagine residues to the solution environment and render these residues more reactive. Also, degradation via *irreversible* aggregation is believed to often proceed through unfolded or partially unfolded conformations as intermediates [3].

While the literature does contain some general guidelines for process and formulation optimization [4,5], mechanisms of stabilization are incompletely understood. Consequently, formulation and process development

Copyright 2004 by Marcel Dekker, Inc. All Rights Reserved.

efforts remain somewhat empirical in practice. Mechanisms suggested to rationalize the stabilization of proteins by added formulation components generally fall into two general classifications, ''thermodynamic mechanisms'' and ''pure kinetic mechanisms.'' A stabilizer that functions by increasing the free energy of denaturation operates via a thermodynamic stabilization mechanism. Stability is conferred by shifting the equilibrium between ''stable'' native conformation and ''unstable'' unfolded conformations toward the native state. The ''solute exclusion hypothesis,'' generally believed to be a major factor in stabilization during freezing, and the ''water substitute hypothesis,'' often used to rationalize the stabilizing effect of saccharides during drying, are examples of thermodynamic stabilization mechanisms [6]. Conversely, a stabilization strategy that functions by slowing the rate of the degradation process, without significantly affecting the equilibrium constants, operates via a pure kinetic mechanism. That is, if the rate constant for unfolding is sufficiently reduced to prevent unfolding on the experimental time scale, the protein will not unfold regardless of what the free energy of unfolding might become, and stabilization in purely kinetic. The ''vitrification hypothesis'' [7], which in its simplest form states that a system below its glass transition temperature is stabilized due to immobilization of the reactive entity in a solid-like glassy system, is the primary example of a pure kinetic stabilization mechanism. Thus, since mobility is required for reaction, and if one postulates that mobility is insignificant in the glassy state, the glassy state is a stable state.

Most protein stability studies have focussed their interpretation either on a thermodynamic mechanism or on a pure kinetic mechanism, and consequently, there is some controversy and confusion over which mechanism is ''correct.'' Since the direction of a formulation development effort may depend upon which ''theory'' is being followed, clarification of the roles of thermodynamic stabilization and kinetic stabilization in given stability problems would provide some practical benefit. This review is an effort to provide such clarification. To this end, the major stresses, or destabilizing effects, that operate during the freeze-drying process are discussed, selected empirical observations regarding pharmaceutical stability in protein systems are presented, and the structure and dynamics in amorphous protein formulations are discussed.

II. STRESSES DURING FREEZE-DRYING: THERMODYNAMIC DESTABILIZATION FACTORS

As a sample is cooled during the freezing process, the solution normally supercools to a temperature about 10–20°C below the equilibrium freezing

Copyright 2004 by Marcel Dekker, Inc. All Rights Reserved.

point before ice first nucleates and crystallizes. Once crystallization does begin, the product temperature rises rapidly to near the equilibrium freezing point, decreases slowly until most of the water has crystallized, and then decreases sharply to finally approach the shelf temperature. The process of ice formation is accompanied by an increase in solute concentration between the growing ice crystals and an increase in solution viscosity. Solutes that tend to crystallize easily from aqueous solution, such as sodium chloride and buffer salts, may crystallize, but the protein itself and most carbohydrate excipients do not crystallize. Rather, they remain amorphous, and at the end of the freezing process exist in a glassy state containing a relatively large amount of unfrozen water (i.e., $\approx 20\%$ w/w).

As an example of freeze concentration and the corresponding viscosity increase, the time profiles of product temperature, solute concentration, and viscosity are illustrated in Figure 1 for the freezing of 3% aqueous sucrose contained in glass vials. These data were calculated from freezing point

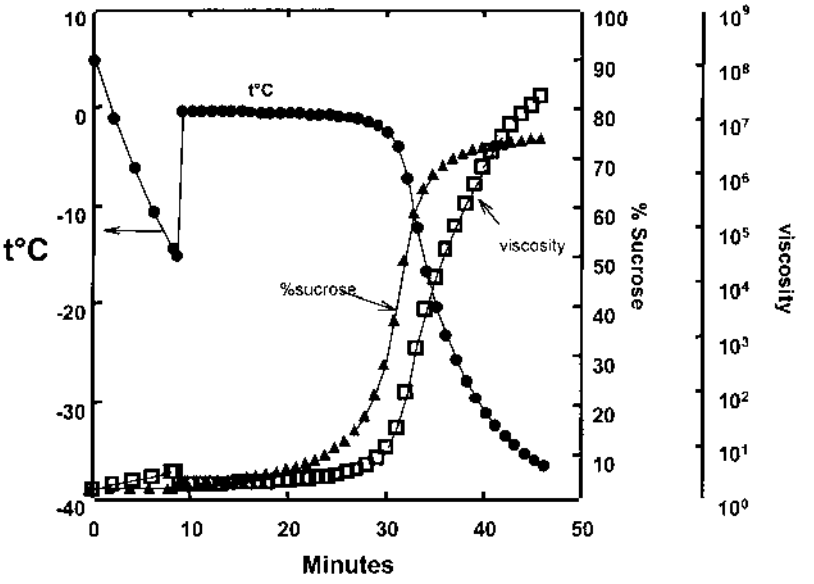

Figure 1 Time profile of temperature, concentration, and viscosity during freezing of 3% sucrose. Data are calculated assuming ice crystallization begins at $-15°C$ and that the solution composition follows the equilibrium freezing point depression curve (*data taken from Ref. 8*). Viscosities are estimated from a fit of viscosity data over a wide range of composition and temperature (*data taken from Refs. 7 and 8*) to a VTF-type equation.

Copyright 2004 by Marcel Dekker, Inc. All Rights Reserved.

depression data and viscosity data in the literature [8,9]. Here, the solution supercools to about −15°C before ice begins to form, after which the temperature abruptly rises. During the initial portion of the ice growth stage between 10 and about 25 min, temperature remains nearly constant as the heat removed from the product is nearly balanced by the heat liberated by ice formation. Near the 25 min mark, as the amount of unfrozen water becomes depleted, the sucrose concentration begins to increase sharply, and the temperature abruptly decreases. At the 30 min mark, when most of the freezable water has been converted to ice, the sucrose concentration and the viscosity of the freeze concentrate increase very sharply. At about the 45 min mark, viscosity is about seven orders of magnitude higher than for the starting solution. At this point, the freeze concentrate is nearly a glass.

Since most of the water is removed from the protein phase during freezing, most of the drying is actually accomplished during the freezing process. A number of stresses or perturbations of the free energy of unfolding may develop. First, since it is the unique nature of water that is often credited with stabilization of the native conformation via hydrophobic interactions, one might expect the thermodynamic stability of the native conformation would be decreased as most of the water is transformed to ice. Also, the phenomenon of freeze concentration will increase the protein concentration as well as increase the concentration of any potential reactant, thereby increasing the rate of bimolecular degradation reactions. Thus, as the system freezes, degradation rates may actually increase in spite of the decrease in temperature. Figure 2 gives an illustration of the impact of freeze concentration on degradation rate as well as demonstrating the impact of increasing viscosity on reactivity in the freeze concentrate. The data were calculated for the case of a trace amount of drug in 3% sucrose, using the viscosity and sucrose concentration data from Figure 1 and assuming an Arrhenius activation energy of 20 kcal/mol for the case where rate is independent of viscosity. If one assumes the degradation rate is completely uncoupled from macroscopic viscosity, the rate of degradation is nearly two orders of magnitude higher at the maximum than in the solution at the beginning of the freezing process. Eventually, as the temperature decreases sharply around 30 min, the Arrhenius factor dominates, and the rate of reaction decreases. However, since a degradation pathway requires motion or mobility of some kind, most reactions would likely slow as the viscosity increases [7], at least for very high viscosities when the system approaches the glassy state.

The extreme example of coupling is with a diffusion-controlled reaction with the diffusion constant being inversely proportional to viscosity, as in the Stokes–Einstein equation. The curve defined by the

Copyright 2004 by Marcel Dekker, Inc. All Rights Reserved.

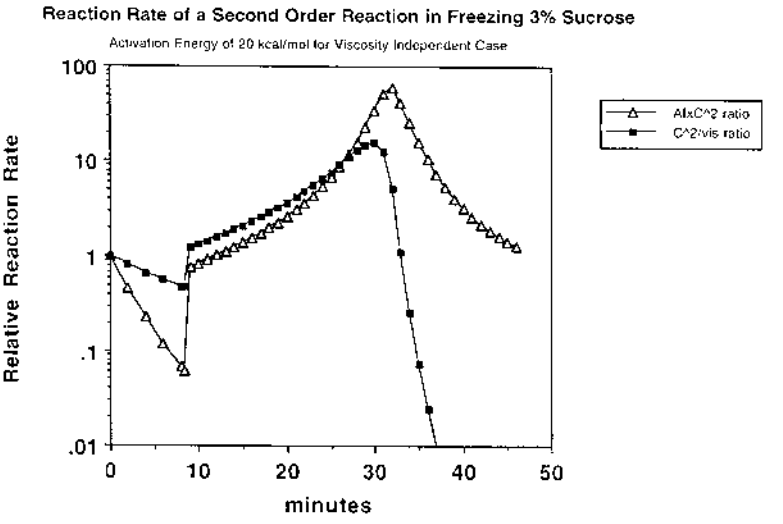

Figure 2 Calculated reaction rates for a second-order reaction in freezing 3% sucrose. Key: triangles = rate independent of viscosity with Arrhenius temperature dependence and a 20 kcal/mol activation energy; squares = reaction rate inversely proportional to viscosity.

square symbols in Figure 2 represents this extreme case. However, even with complete coupling of the reaction rate to viscosity, the degradation rate reaches a maximum about one order of magnitude higher than in the starting solution. However, once the increase in viscosity dominates, the reaction rate decreases sharply toward extremely low values. While a protein formulation of interest may deviate from the quantitative behavior shown in Figure 2, two generalizations seem valid. First, due to increasing solute concentration, bimolecular processes will be accelerated during the freezing stage in spite of decreasing temperature. Direct experimental observation of this phenomenon has been reported [10]. Secondly, at least for reactions that are viscosity dependent, the rates will decrease dramatically near the end of freezing. Indeed, the principle of stabilization by vitrification [7] is based upon the concept that viscosity increases near the glass transition temperature depress or eliminate degradation reactions. Experimental studies of three different reactions in frozen maltodextrin systems lend support to this view, although not all reactions are viscosity dependent [11]. Rate constants for enzymatic hydrolysis of a substrate, aggregation of a protein, and oxidation of ascorbic acid were obtained in frozen maltodextrin solutions near the T'_g of -10°C. The data show about an order of magnitude

Copyright 2004 by Marcel Dekker, Inc. All Rights Reserved.

reduction in rate constant between $-5^{\circ}C$ and $-10^{\circ}C$ for enzymatic hydrolysis and for ascorbic acid oxidation, but the protein aggregation reaction studied shows only a small temperature dependence throughout the range studied. Surprisingly, the rate determining step for aggregation appears not to be viscosity dependent. However, the possibility of significant dilution with ice melt above T_g' confounds the interpretation of these data.

While sucrose and most excipients fail to crystallize during freezing, mannitol, glycine, sodium chloride, and phosphate buffers will crystallize, if present as the major component, once freeze concentration provides sufficient supersaturation. It should also be noted that very high concentrations may be reached before crystallization occurs (i.e., about 6 molal for NaCl), so the ionic strength environment of the protein during freezing may be quite different than in the starting formulation and could present a "stress" for protein stability [4,5]. Crystallization of buffer components, resulting in massive pH shifts, may present an even greater stress for proteins. Under equilibrium conditions attained by seeding, the sodium phosphate buffer system shows a dramatic decrease in pH of about 4 pH units due to crystallization of the basic buffer component, $Na_2HPO_4{\cdot}2H_2O$ [12]. Conversely, the potassium phosphate system shows only a modest increase in pH of about 0.8 pH units. Under nonequilibrium conditions (i.e., no seeding) and with lower buffer concentrations, the degree of crystallization is less, and the resulting pH shifts are moderated [13]. Table 1 shows data accumulated [14,15] during freezing of phosphate buffer solutions in large volumes at cooling rates intended to mimic freezing in vials. For the concentrated buffer solutions (100 mM), the frozen pH values are close to the equilibrium values. However, lowering the buffer concentration by an order of magnitude considerably reduces the pH shift

Table 1 Shifts in pH During Nonequilibrium Freezing with Phosphate Buffer Systems

Concentration (mm)	Initial pH	Frozen pH	Δ pH
Sodium phosphate buffer			
100	7.5	4.1	−3.4
8	7.5	5.1	−2.4
Potassium phosphate buffer			
100	7.0	8.7	+1.7
100	5.5	8.6	+3.1
10	5.5	6.6	+1.1

Source: Data taken from Refs.13 and 14.

Copyright 2004 by Marcel Dekker, Inc. All Rights Reserved.

observed during freezing. It should also be noted that, under some conditions, potassium phosphate buffers also give large pH shifts during freezing. As shown in Table 1, if the initial pH is 5.5, the 100 mM potassium phosphate buffer increases in pH by 3.1 units during freezing. Clearly, if a protein's structural integrity is sensitive to pH shifts, buffer crystallization must be avoided. In our experience, the best solution is to formulate such that the weight ratio of buffer to other solutes is very low [16,17].

It is well known [18] that protein adsorption to surfaces, such as the air–water interface, may result in a perturbation of the conformation. That is, adsorption is a possible "stress." While the surface area of the air–water interface is minimal during a well-designed freezing process, liberation of dissolved air during thawing may generate numerous bubbles, thereby providing a significant surface area for protein adsorption and conformational change. During the freezing process itself, the major interfacial area is the aqueous–ice interface. As the degree of supercooling increases (normally, as the rate of cooling increases), the number of ice crystals increases, thereby increasing the aqueous–ice interfacial area. It is clear that if a protein were to adsorb on the ice crystals and suffer a loss of conformational stability, the formation of ice itself would be a significant "stress" during freezing. Several observations suggest this speculation has merit. Freezing studies with human growth hormone [19] show more insoluble aggregates develop during rapid freezing in a $-80^{\circ}C$ bath than during freezing procedures that cool more slowly. Classically, one expects less aggregation during a fast cooling process since the residence time in the potentially reactive freeze concentrate is much less than in a slow cooling process (i.e., the time required to reach the glassy state is much less). However, since the fast cooling process will generate a greater aqueous–ice interface, which would maximize the fraction of protein adsorbed, the authors concluded that human growth hormone (hGH) was denatured by adsorption on ice. We have observed that more rapid freezing to lower temperatures results in more air bubbles on thawing, so an alternate interpretation of the hGH data might be made in terms of denaturation at air bubbles.

A recent study of unfolding during freezing provides strong evidence that proteins can indeed unfold as a result of adsorption to the ice surface [20]. A summary of the major findings of this study is given in Figure 3 where the solid circles represent the average phosphorescence lifetime of Trp-48 of azurin in a 1 mM potassium phosphate buffer. All these systems contain ice at subzero temperatures and were formed by seeding with ice at $-2^{\circ}C$ followed by rapid equilibration to the temperature of interest. The heavy line gives the corresponding lifetime data for a 1:1 mix of buffered protein and ethylene glycol, a system intended to illustrate behavior for a

Copyright 2004 by Marcel Dekker, Inc. All Rights Reserved.

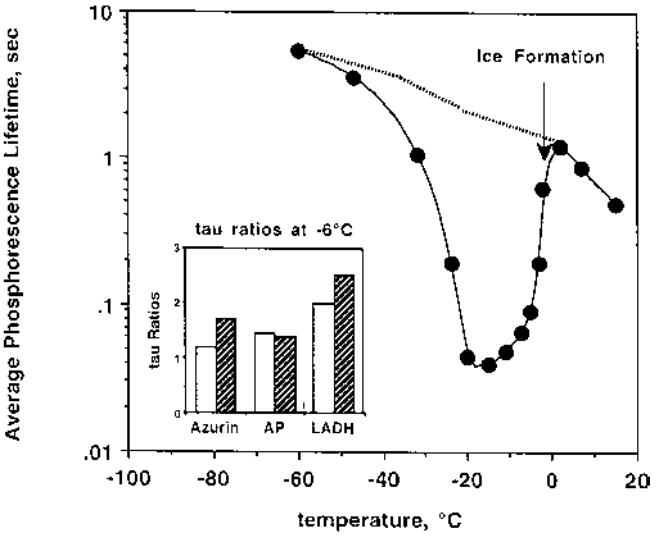

Figure 3 The effect of freezing on the average phosphorescence lifetime of Trp-48 of azurin. The circles represent data for protein in 1 mM phosphate buffer. Frozen samples were prepared by seeding a solution at $-2^{\circ}C$ with ice and quickly bringing the sample to the temperature of interest. The dashed line without symbols gives the behavior of protein in a 1 : 1 phosphate buffer : ethylene glycol system that does not freeze. The inset shows ratios of lifetimes, low ice surface area divided by high surface area, for the freezing rate variation experiment (light shaded bars) and the annealing experiment (dark shaded bars). The proteins studied were azurin, liver alcohol dehydrogenase (LADH), and alkaline phosphatase (AP) (*data taken from Ref. 20*).

system that does not freeze. It should be noted that such data show a sharp decrease in lifetime when the protein undergoes unfolding. As the temperature is lowered, the lifetime increases reflecting the lower temperature and increased viscosity. However, as soon as ice is introduced, the lifetime decreases abruptly by roughly two orders of magnitude, signaling denaturation of the protein. Of course, as soon as ice forms, a significant amount of freeze concentration occurs, and one could argue that several mechanisms other than adsorption of protein to ice are causing the denaturation. However, the authors [20] provide additional data, given in the inset in Figure 3, that are difficult to interpret unless one admits that denaturation at the ice surface is at least a critical factor. Samples of both high and low surface area of ice were prepared by first seeding with ice at $-2^{\circ}C$, followed by cooling rapidly ($\approx 200^{\circ}C$/min) or slowly ($\approx 1^{\circ}C$/min) to

Copyright 2004 by Marcel Dekker, Inc. All Rights Reserved.

a final temperature of −6°C. The fast-cooled samples were assumed to have higher surface area than the slowly cooled samples. Additional low surface area samples were prepared by allowing the fast cooled samples to "anneal" at −6°C for 10 h to increase the size of the ice crystals and decrease the surface area. The inset in Figure 3 gives ratios of the lifetime of a low surface area sample to the lifetime for the corresponding high surface area sample. A value greater than unity means that the extent of denaturation is less for the low surface area sample. The light shaded bars represent the freezing rate variation experiment, and the dark bars give the ratios for the annealing experiment. For all six examples, the ratio is greater than unity, indicating that denaturation was indeed less for the low surface area samples. Since all samples were studied at the same temperature, −6°C, and the experiments were so well controlled, one is left with the conclusion that, at least with these proteins, denaturation at the ice surface is a significant factor in protein denaturation during freezing. From a mechanistic viewpoint, it is not clear why a protein should denature at the ice surface. One might speculate that the mechanism involves the very strong electric fields that can be generated during crystallization of ice via preferential incorporation of one ionic species into the ice lattice [21]. However, except for noting that the fields increase with increasing crystal growth rate, and the effect on the protein would obviously be more severe the larger the ratio of ice surface area to protein concentration, there is no evidence known to this author that would link the electric field effect to protein denaturation. In any event, it is clear that ice itself is a "stress" to protein stability during freezing.

One might speculate that a major role of a surfactant in stabilization during freezing might involve adsorption at the aqueous–ice interface to prevent adsorption of protein with subsequent denaturation. A recent work [22] summarizes the literature precedents for this view and provides a convincing set of data to support the hypothesis. Freezing protocols which should produce a higher specific interfacial area produce greater levels of particulates (i.e., insoluble aggregates), and for a series of proteins, particulate levels after freeze:thaw are well correlated with particulate levels after shaking protein solutions with small teflon beads. Thus, it does appear that formation of insoluble aggregates during freezing does arise from surface denaturation, and the surface involved is the surface of ice! In all cases, addition of low levels ($\approx 0.01\%$) of surfactants greatly retards particulate formation.

The conformational stability of a protein is normally a rather delicate balance between various interactions or "forces," and these interactions may well be modified by changes in the solution environment and/or temperature. Increases in temperature will ultimately decrease the free energy of unfolding to the point where the thermodynamically stable form

Copyright 2004 by Marcel Dekker, Inc. All Rights Reserved.

of the protein is the unfolded or denatured form. At this point, provided the unfolding process is not kinetically hindered, the protein spontaneously unfolds, normally providing a moiety that is much more prone to *irreversible* (i.e., degradation) processes. Solution environments, particularly pH and the presence of chemical denaturants, significantly impact the onset of denaturation. Of course, since freeze-drying is a low-temperature process, high-temperature denaturation is not directly relevant to destabilization during freeze-drying. However, just as proteins undergo thermal denaturation at elevated temperature, proteins also undergo spontaneous unfolding at very low temperature, denoted "cold denaturation" [23,24]. Estimated cold denaturation temperatures are often well below freeze-drying temperatures and therefore are of questionable relevance to freeze-drying. However, estimates of cold denaturation temperatures are based upon thermodynamic parameters measured in dilute aqueous solutions. The impact of perturbations caused by freeze concentration are largely unknown, and therefore the role of cold denaturation in protein inactivation during a practical freeze-drying process is uncertain.

The preceding discussion has focussed on stresses that develop during the freezing process. However, since it seems unlikely these stresses would be relieved during drying, the same stresses must also exist during the drying process. In addition, during drying, the moisture content in the protein phase is reduced from on the order of 20% water to very low levels, often less than 1%. This additional drying may be considered an additional stress. Indeed, the water substitute hypothesis [6] is based upon the proposition that a significant thermodynamic destabilization occurs when the hydrogen bonding between protein and water is lost during the last stages of drying. The use of a "water substitute" as a lyoprotectant allows a hydrogen bonding interaction between protein and the water substitute which thermodynamically stabilizes the native conformation and preserves activity.

During the early portions of freezing, the system is mostly aqueous and of low or moderate viscosity. During the last stages of freezing, and during both primary and secondary drying, the system is a glass or at least not much above the glass transition temperature. These differences are potentially important in the protein's response to a given thermodynamic stress. The time scales of the various stages of freeze-drying are also different. Relative to drying, freezing is relatively fast. Freezing is typically over within a few hours while drying often requires days. However, it must be noted that primary drying, or ice sublimation, constitutes the longest portion of the drying process. Although some water desorption does occur during primary drying, low water content in the solute phase is not achieved until all ice has been removed, and the process enters the secondary drying

Copyright 2004 by Marcel Dekker, Inc. All Rights Reserved.

stage [25]. During the early portion of secondary drying, the water content decreases quickly from roughly 10%–20% to less than 5% within a few hours. Thus, assuming that it is during this drying period that the "drying stress" occurs, the time scale is roughly the same as the freezing time scale.

Since both the last part of freezing and the entire drying stages are normally carried out in a glassy or near glassy state, molecular mobility should be greatly restricted relative to the fluid state that prevails during early freezing, and the dynamic response to a thermodynamic stress will be significantly slower than for a fluid system, assuming the dynamic response depends upon viscosity. If the dynamic response is sufficiently slow, thermodynamic *instability* will have no consequence as insufficient time is available for unfolding and subsequent degradation. Recent (unpublished) studies in our laboratories of the kinetics of protein unfolding in highly viscous aqueous systems demonstrate that the protein unfolding rate is strongly coupled to viscosity, at least for the two proteins studied, phosphoglycerate kinase and β-lactoglobulin, in high sucrose content systems. These data (see also Figure 1 and Figure 2) suggest that unfolding is on the time scale of months, even at temperatures 10–20°C above the glass transition temperature. The fact that protein inactivation during drying does occur suggests that the mobility needed for inactivation is nearly completely decoupled from viscosity in these systems. Of course, if the mechanism for inactivation does not involve protein unfolding, we do not necessarily expect inactivation kinetics to track with unfolding kinetics.

III. STABILIZATION OF PROTEINS FOR FREEZE-DRYING: SELECTED EMPIRICAL OBSERVATIONS

A. In-Process Stability: Freeze–Thaw and Freeze-Dry Stability

While many proteins survive the freeze-drying process with little or no degradation, other proteins exhibit significant degradation and loss of activity during processing. Multimeric proteins seem particularly prone to degradation during freeze-drying [26–29]. Degradation during the freeze-drying process may arise during freezing and/or during drying. As a measure of the degradation during freezing, "freeze–thaw" stability studies are carried out, and to estimate (roughly) the degradation during drying, stability during freeze-drying is compared to stability during freeze–thaw. The basic assumption is that degradation during thawing is comparable to degradation during reconstitution, and therefore the difference in activity between a freeze-dried:reconstituted sample and a freeze:thawed sample is a measure of the loss in activity during drying. This assumption is likely a

Copyright 2004 by Marcel Dekker, Inc. All Rights Reserved.

reasonable approximation for a fast thawing process, at least if air bubbles released during thawing are not a major factor. One observation of particular significance is that some excipients stabilize during both freezing *and* drying (denoted "lyoprotectants"), while others stabilize only during freezing (denoted "cryoprotectants") [26,30,31]. Data for phosphofructokinase (PFK), active as a tetramer, illustrate this observation quite well (Figure 4). With no "stabilizer" added to the formulation, PFK is completely deactivated during freeze–thaw. With all "stabilizers" at the relatively high level of 0.5 M, some stabilize reasonably well during freeze–thaw but offer no protection during freeze-drying (proline and trimethylamine N-oxide). The disaccharides (trehalose, sucrose, maltose) stabilize both during freezing and drying, and therefore, at a level of 0.5 M, are effective "lyoprotectants." Low levels of disaccharides are not good cryoprotectants [31] and therefore cannot be good lyoprotectants. Of course, if a given formulation offers no protection during freezing, any potential protection during drying will be invisible with the usual experimental design. Polyethylene glycol (PEG) is found to be an exceptionally efficient "cryoprotectant" for PFK but offers no protection

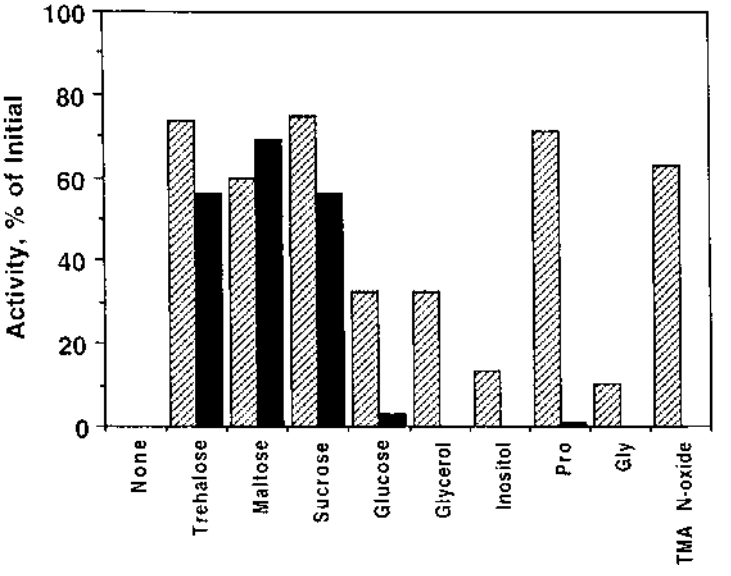

Figure 4 Comparison of freeze–thaw stability with freeze–dry stability: phosphofructokinase with additives at 0.5 M. Key: shaded bar = freeze–thaw, solid bar = freeze-dry (*data from Ref. 26*).

Copyright 2004 by Marcel Dekker, Inc. All Rights Reserved.

during drying [31]. Trehalose and glucose at low levels (≈ 0.1 M) offer essentially no protection during freeze-drying because, at low levels, they are not cryoprotectants. However, when PEG is used in combination with a low level of trehalose (or glucose), nearly complete stabilization during freeze-drying is obtained. Studies with lactate dehydrogenase give essentially the same results [31]. The conclusion is that PEG stabilizes during freezing while the sugar stabilizes during drying, even at relatively low levels. Thus, the combination of stabilizers is a good lyoprotectant. Sugars are effective cryoprotectants only when used at relatively high concentrations, but are generally effective drying stabilizers when used at much lower concentrations. As a general rule, the relevant concentration unit for stabilization during freezing is the molar concentration *in solution*, whereas for stabilization during drying, the relevant concentration unit is the weight ratio of stabilizer to protein (or protein plus buffer) [30–32]. Since different formulation strategies are needed for stabilization during freezing than are required for stabilization during drying, it is concluded that the "stresses" during freezing are different from those during drying, meaning that the mechanisms of destabilization (and stabilization) are different [26,30,31].

Catalase is an example of a multimeric protein that is relatively stable during freeze–thaw, but without a suitable stabilizer suffers significant loss of activity during drying. Without stabilizers, loss of activity during freeze–thaw is only about 20% [33] but loss during freeze-drying is 65% [27]. Addition of glucose or sucrose reduces the loss on both freeze–thaw and freeze-drying to about 10%, suggesting that the roughly 45% loss on drying the pure enzyme has been reduced to near zero by these excipients. Mannitol and a variety of saccharides also stabilize during freeze-drying. The degree of stabilization is not correlated with the glass transition temperature of the pure excipient but does appear correlated with the molecular weight of the saccharide. As the molecular weight increases, protein activity remains constant through maltotriose but then decreases, with the high molecular weight dextran [150 kD] being the least effective of the excipients studied.

L-asparaginase provides another example of a multimeric protein that suffers severe degradation during drying due to de-aggregation of the active tetramer [28]. Without stabilizers, L-asparaginase loses about 80% of its initial activity during freeze-drying. Glucose, tetramethylglucose (TMG), mannose, sucrose, and poly(vinylpyrrolidone) (PVP) are all extremely effective lyoprotectants, preserving essentially 100% of the initial activity. Mannitol preserves only about 50% of the initial activity, perhaps due to partial crystallization of the mannitol. Here, as with catalase, a monosaccharide is as effective as a disaccharide. Stability does not correlate with residual water after freeze-drying [28], and since the glass transition temperatures of the effective stabilizers range from 39°C for glucose to

Copyright 2004 by Marcel Dekker, Inc. All Rights Reserved.

about 170°C for PVP, it is obvious that stabilization is not correlated with T_g. The effectiveness of TMG and PVP demonstrates that "sugar-type" hydrogen bonding to the protein is *not* essential for stability.

B. Storage Stability

Storage stability has generally been the more serious stability issue faced by therapeutic proteins. Storage stability can be extremely formulation specific [16,32,34,35], and even with a knowledge of the major degradation pathways in solution, selection of the optimum formulation for a solid is far from obvious. We illustrate the sensitivity of stability to formulation details with studies of an important protein product, human growth hormone.

Human growth hormone (hGH) is a monomeric 22 kD protein marketed as a freeze-dried solid with refrigerated storage recommended. While hGH is easily freeze-dried with little or no degradation [16], degradation does occur during storage of the freeze-dried solid at 25°C and 40°C. Chemical degradation proceeds by both methionine oxidation and asparagine deamidation, and aggregation (mostly dimer) develops after storage and reconstitution [16,36,37]. Formulation with mannitol or glycine improves storage stability slightly, but a combination of mannitol and glycine (weight ratio of hGH:glycine:mannitol of 1:1:5) provides better stability than an equivalent amount of either mannitol or glycine alone [16], a result attributed to the observation that glycine remains mostly amorphous in the combination formulation. An excipient system of mannitol alone or glycine alone results in nearly 100% crystalline excipient, and therefore would not be expected to improve stability greatly, i.e., very little excipient could be in the protein phase. Formulation with lactose provides a completely amorphous system that does reduce aggregation dramatically. However, lactose is a reducing sugar, and as might be expected, a massive amount of a degradation product, likely representing an adduct of lactose and hGH, is formed after only one month of storage at 25°C [16]. Thus, while a 100% amorphous excipient system offers the best potential for stabilization, a "reactive" excipient system, such as a reducing sugar, is clearly unacceptable.

Chemical and aggregation stability of hGH in several other 100% amorphous systems are compared with corresponding stability in pure protein and the glycine:mannitol formulation in Figure 5 [38]. Hydroxyethyl starch (HES), stachyose, and trehalose are formulated in a 1:1 weight ratio of excipient:hGH, whereas the dextran formulation is 6:1 dextran:hGH. While the concept that an excipient system must remain at least partially amorphous to improve protein stability is not in question, it is clear that

Copyright 2004 by Marcel Dekker, Inc. All Rights Reserved.

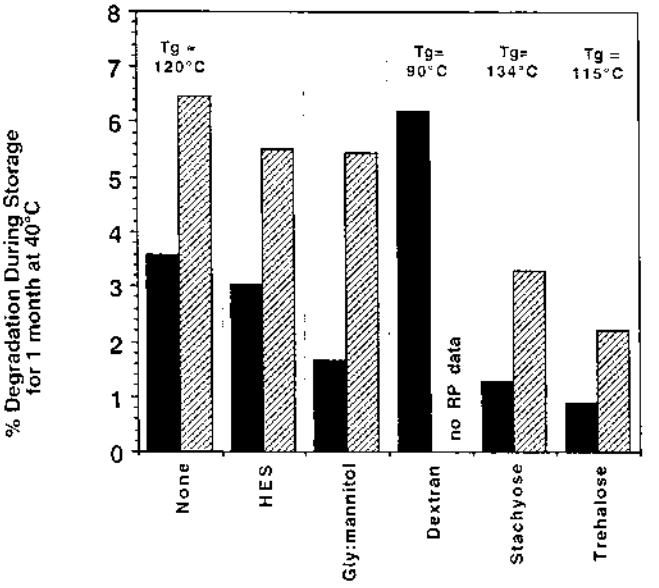

Figure 5 The effect of excipients on the storage stability of freeze-dried human growth hormone (hGH). Samples were stored for 1 month at 40°C. Key: solid bars = aggregation (primarily dimer), shaded bar = chemical degradation via methionine oxidation and asparagine deamidation. The glass transition temperatures of the "initial" freeze-dried formulations are given above the bars when a glass transition temperature could be measured by DSC. The glycine:mannitol formulation is a weight ratio of hGH:glycine:mannitol of 1:1:5, the dextran formulation is 1:6 hGH:dextran 40, "none" means no stabilizer, and the others are 1:1 hGH: stabilizer. All formulations contain sodium phosphate buffer (pH 7.4) at 15% of the hGH content. Initial moisture contents are all ≈1%.

remaining amorphous is not a sufficient condition for stability. Apparent aggregation in the dextran formulation is greater than in the pure protein. Hydroxyethyl starch shows a slight improvement in stability over the pure protein, but is not nearly as effective as the glycine:mannitol formulation, and increasing the level of HES to 3:1 HES:hGH does not improve stability [38]. Conversely, both stachyose and trehalose provide better stability than the glycine:mannitol system, with trehalose superior to stachyose. All systems are glasses at the storage temperature of 40°C, and for those formulations where glass transition temperatures are available, it is clear that storage is well below the T_g, and there is no simple relationship between T_g and stability. While one might speculate that a glass is more "solid," and

Copyright 2004 by Marcel Dekker, Inc. All Rights Reserved.

therefore more stable, the higher the difference between T_g and the storage temperature, the data are not consistent with this speculation. Comparing the stachyose and trehalose formulations, which are both 1:1 formulations with hGH, the T_g of the stachyose formulation is nearly 20°C higher than the trehalose formulation, but trehalose offers slightly better stability than does stachyose. These observations and other similar results [38] suggest that while it is necessary for the formulation to have a T_g well above the highest anticipated storage temperature for both elegance and stability reasons, T_g is not a relevant stability variable for systems stored well below their glass transition temperatures.

IV. STRUCTURE AND DYNAMICS IN AMORPHOUS PROTEIN FORMULATIONS

A. Protein Formulations as Amorphous Solids

Freeze-dried protein formulations are amorphous systems, at least in part, and the physical and chemical behavior of such products depends on the characteristics of amorphous systems, perhaps as much as their behavior depends upon the unique behavior of proteins. Amorphous materials below their glass transition temperatures are termed glasses, and in many respects are solids in the same sense as are crystalline solids. That is, while the long-range order characteristic of crystalline solids is absent, short-range order does exist, and the dynamics in glasses more closely resembles crystalline solids than liquids above their equilibrium fusion temperatures. Glasses differ from liquids in another important respect. The short-range order or structure in liquids represents an equilibrium between possible configurations that responds essentially immediately to changes in temperature. The short-range order in glasses does not represent an equilibrium distribution of configurations. Rather, as a first approximation, the short-range order or configurations characteristic of the liquid at T_g are "frozen in" by cooling quickly through the glass transition, and the resulting glass is in a metastable state. With aging, transitions to lower energy states or enthalpy relaxations occur [39]. In short, sufficient mobility exists even well below the glass transition temperature to allow changes in configuration. These relaxations are typically nonexponential in time due to contributions from a number of substates in the glass [39]. Dynamics is important in amorphous materials since nearly any degradation reaction will require some degree of motion, or molecular mobility, for the reaction to proceed at a significant rate. The glass transition temperature, T_g, marks the division between mostly solid dynamics and mostly liquid state dynamics. It is important to emphasize, however, that solid dynamics does not mean zero mobility.

Copyright 2004 by Marcel Dekker, Inc. All Rights Reserved.

A protein dissolved in another glassy component (i.e., sucrose) could behave as a two-phase system with regard to mobility. That is, the protein molecules themselves could undergo internal motion in a rigid matrix, and have a pseudo glass transition or mobility transition which is not strongly coupled with the glass transition of the sucrose matrix. Using Fourier transform infrared (FTIR) spectroscopy to study internal protein motion in carbonmonoxymyoglobin (MbCO) dissolved in aqueous glycerol, protein internal ''glass transitions'' were determined and compared to the glass transition temperatures of the systems as a whole determined by differential scanning calorimetry (DSC) [40]. The protein glass transition temperatures were very close to the corresponding glass transition temperatures determined by DSC. For 65% glycerol and 75% glycerol, the DSC glass transition temperatures are $-124^{\circ}C$ and $-98^{\circ}C$, respectively. The corresponding protein glass transition temperatures are $-118^{\circ}C$ and $-95^{\circ}C$. Thus, at least in these systems, the solvent and the protein dynamics are strongly coupled, likely due to the hydrogen bonding interactions between the solvent and the protein surface [40]. While it is perhaps somewhat unusual to refer to the mobility transition in the protein as a glass transition, it should also be noted that the glassy MbCO systems studied also show protein intramolecular relaxation process (i.e., transitions between protein substates) that are both nonexponential in time and non-Arrhenius in temperature dependence, a property characteristic of glasses [40].

Evidence for coupling between glassy matrix dynamics and protein dynamics is not restricted to low-temperature aqueous systems. Studies of the kinetics of ligand binding in MbCO [41] dissolved in *dry* glassy trehalose demonstrates that the glassy trehalose matrix suppresses the equilibrium between protein conformational substates on the time scale of the ligand binding reaction at least up to room temperature. While a protein glass transition temperature was not obtained, the data do demonstrate significant coupling between internal protein motions and the dynamics of the glassy matrix, trehalose.

Coupling between matrix dynamics and internal protein dynamics could have significant pharmaceutical stability implications. While limitations on translational diffusion would be expected to moderate bimolecular reactions regardless of the degree of coupling between protein internal dynamics and the matrix dynamics, degradation processes which depend only upon motions within the protein molecule would not necessarily be quenched in the glassy state unless the protein internal dynamics was strongly coupled with the dynamics of the glassy system as a whole. Thus, one would expect optimal stability in those glassy systems which provide effective coupling of the protein dynamics with the dynamics of the glassy matrix.

Copyright 2004 by Marcel Dekker, Inc. All Rights Reserved.

B. Molecular Motion, Relaxation, and the Glass Transition

The Stokes–Einstein equation,

$$D = kT/6\pi\eta a \tag{1}$$

predicts that the translational diffusion coefficient, D, is inversely proportional to the coefficient of viscosity, η, where k is Boltzmann's constant and "a" is the effective hydrodynamic radius of the diffusing species. Thus, while the point at which a material becomes a glass is historically defined in terms of the viscosity (i.e., $\eta > 10^{14}$ poise) [42], if the Stokes–Einstein relationship is valid, the corresponding definition of a glass could also be based upon the diffusion coefficient. The translational diffusion coefficient is given in terms of the "jump distance," x, and the diffusional correlation time, τ, or "relaxation time" by

$$D = x^2/2\tau \tag{2}$$

so the diffusion coefficient is inversely proportional to the diffusional "relaxation time." A similar relationship holds for rotational motion. Since the electrical mobility of an ion is directly related to the diffusion coefficient [43], electrical conductance is also inversely proportional to the coefficient of viscosity given the validity of the Stokes–Einstein equation. We use the term "mobility" in a general sense to refer to translational or rotational diffusion constant, or reciprocal of "relaxation time." Assuming validity of the Stokes–Einstein equation, mobility and viscosity are inversely related.

As a liquid is cooled near the glass transition, viscosity increases sharply, and the temperature dependence of viscosity becomes distinctly non-Arrhenius. That is, the apparent activation energy increases as the temperature decreases. The Adam–Gibbs equation is a theoretical result describing relaxation behavior in highly viscous systems that was developed using a statistical mechanical analysis of configurational changes in highly viscous systems [44]. Configurational changes in systems close to the glass transition temperature take place by highly cooperative motions involving rearrangements in a region whose size is determined by the configurational entropy of the system. As the temperature in a highly viscous system decreases, the configurational entropy decreases, and the size of the cooperatively rearranging region increases, thereby increasing the total free energy barrier to the configurational change and slowing the process. The relationship between configurational entropy, S_c, and the relaxation time is given by

$$\tau(T) = A\exp\left(\frac{C}{TS_c}\right) \tag{3}$$

Copyright 2004 by Marcel Dekker, Inc. All Rights Reserved.

where C is a constant which is proportional to the molar (or segmental, for polymers) change in chemical potential for a transition, and A is a pre-exponential factor practically independent of temperature. The configurational entropy must vanish at some temperature, T_0, otherwise one is faced with the "unphysical" conclusion that the configurational entropy will become negative at some low temperature. This result is based upon the observation that extrapolations of configurational entropy from temperatures above T_g to lower temperatures predict negative values roughly 50° below T_g (i.e., at T_0). Thus, the temperature, T_0, marks the temperature at which the system, at equilibrium, must undergo a second-order phase transition losing the configurational heat capacity. Below T_0 the configurational entropy is zero. With $S_c = 0$ for $T \leq T_0$, the configurational entropy at temperature T, $S_c(T)$, becomes

$$S_c(T) = \int_{T_0}^{T} \left(\frac{\Delta C_p}{T} \right) dT \tag{4}$$

where ΔC_p is the configurational part of the heat capacity, frequently taken to be the difference in heat capacity between the equilibrium melt and the glass. In cases where the heat capacity of the glass is significantly larger than the heat capacity of the crystalline phase, ΔC_p should perhaps be taken as the difference between the heat capacity of the melt and the crystal.

Angell [45] takes the configurational heat capacity as inversely proportional to absolute temperature, $\Delta C_p = K/T$, where K is a constant of the material. With this relationship, the relaxation time in equation (3) becomes

$$\tau(T) = A \exp\left(\frac{DT_0}{T - T_0} \right) \tag{5}$$

where D is a constant characteristic of the material ($D = C/K$). Since "C" is directly proportional to the molar change in chemical potential for a transition, so also is "D." This result is of the same form as another empirical equation known to represent the behavior of highly viscous systems, commonly referred to as the VTF equation (Vogel–Tammann–Fulcher equation). If one insists that the relaxation time for all glasses is (roughly) the same at the glass transition temperature, ≈ 100 s, and further insists that τ is the same for all materials at the extreme high-temperature limit (16 orders of magnitude change between T_g

Copyright 2004 by Marcel Dekker, Inc. All Rights Reserved.

and the high-temperature limit), a relationship between D and T_0 results* [45]:

$$T_g/T_0 = 1 + D/36.85 \tag{6}$$

Thus, a large value of D means a larger difference between the glass transition temperature and the zero mobility temperature (i.e., larger ratio of T_g/T_0). From equation (5), it is apparent that a larger difference between T_g and T_0 means that as $T \rightarrow T_g$, the temperature dependence of relaxation time is smaller. That is, the effective activation energy is smaller, and the deviation from Arrhenius behavior is less for large D. Depending upon the nature of the amorphous material, values of D do vary [45]. Amorphous materials with large values of D are denoted "strong glasses" while materials with small values of D are "fragile glasses" [45]. In short, not all glasses are equivalent in the temperature dependence of relaxation time, and therefore are not equivalent in the deviation from Arrhenius behavior.

The traditional "derivation" of the Adam–Gibbs equation as given above assumes the configurations are always in thermal equilibrium, and therefore the results given by equations (4) and (5) do not apply below the glass transition, as the configurations in a glass are *not* in thermal equilibrium. If one assumes that the configurational heat capacity, ΔC_p is equal to the difference in heat capacity between the melt and the glass at T_g (i.e., no configurational contribution to the heat capacity of a glass), the configurational enthalpy and entropy do not change as the temperature is decreased below the glass transition region. Thus, the configurational entropy of the glass is equal to the configurational entropy of the "equilibrium" glass at the glass transition temperature at all temperatures below T_g. In this case, the temperature dependence of the relaxation time becomes Arrhenius below T_g [46]. However, the observation that, at least for some materials [47,48], the heat capacity of the glassy phase is significantly higher than the heat capacity of the crystalline phase, suggests that one should use the difference in heat capacity between melt and crystalline phase as the configurational heat capacity. With this choice, the configurational heat capacity of the real glass is not identically zero below the glass transition temperature, and the configurational entropy does not remain absolutely constant below T_g, although the configurational entropy curve of

*When using the VTF equation in viscosity form, one assumes a difference between the viscosity at T_g and the high-temperature limit of 17 orders of magnitude [43], which changes the numerical value of 36.85 to 39.14

Copyright 2004 by Marcel Dekker, Inc. All Rights Reserved.

the real glass does lie well above the corresponding curve for the equilibrium glass (Figure 6). The configurational entropy of the real glass at temperature, T, is equal to the configurational entropy of the equilibrium glass at a higher temperature, T_f, termed the "fictive temperature" [49]. Thus, we may write

$$S_c(T) = S_c^e(T_f) = \int_{T_0}^{T_f} \frac{\Delta C_p}{T} dT \tag{7}$$

where "S_c^e" denotes the configurational entropy of the equilibrium glass (i.e., the dotted line in Figure 6), and the configurational heat capacity, ΔC_p, is the difference between the heat capacity of the melt and the crystalline phase at T_g. Substitution of equation (7) for the configurational entropy of the real glass into the expression for relaxation time, equation (3), and assuming $\Delta C_p T$ is constant, then gives

$$\tau(T,T_f) = \tau_0 \exp\left(\frac{DT_0}{T - (T/T_f)T_0}\right) \tag{8}$$

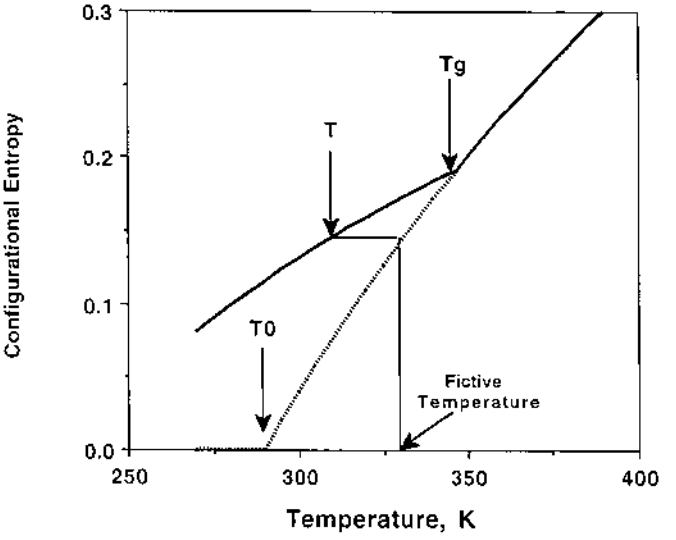

Figure 6 A schematic of the temperature dependence of configurational entropy: definition of fictive temperature. Data calculated using input data for sucrose (see text).

Copyright 2004 by Marcel Dekker, Inc. All Rights Reserved.

From the schematic given by Figure 6, it is clear that the fictive temperature is between the temperature, T, and the glass transition temperature, T_g. A quantitative relationship for fictive temperature may be developed using the expression for the difference in configurational entropy between the real glass and the equilibrium glass, as given by

$$S_c(T) - S_c^e(T) = \int_T^{T_g} \frac{\Delta C_p^{l,g}}{T} dT, \qquad \Delta C_p^{l,g} = C_p^l - C_p^g \tag{9}$$

where C_p^l is the heat capacity of the liquid or "equilibrium glass," and C_p^g is the heat capacity of the "real" glass. Performing the integration in equation (9), assuming the quantity $T\Delta C_p^{l,g}$ is independent of temperature, and combination with the integrated forms of equation (7) then leads to the desired expression for fictive temperature

$$\begin{aligned} &\frac{1}{T_f} = \frac{(1-\gamma_c)}{T} + \frac{\gamma_c}{T_g}; \qquad T \le T_g \\ &\gamma_c \equiv \frac{\Delta C_p^{l,g}}{\Delta C_p} = \frac{C_p^l - C_p^g}{C_p^l - C_p^{xstal}} \end{aligned} \tag{10}$$

where C_p^{xstal} is the heat capacity of the crystalline phase. All heat capacities are evaluated at the glass transition temperature. The combination of equations (8) and (10) constitutes a generalization of the Adam–Gibb theory for the temperature dependence of the structural relaxation time. Above the glass transition temperature, fictive temperature and temperature are identical, and the expression for relaxation time given by equation (8) reduces to the usual expression (i.e., equation 5). Below T_g, equation (10) is used to evaluate the fictive temperature, and the expression for relaxation time differs from the usual expression, the magnitude of the change depending upon the value of γ_c. Note that if the configurational heat capacity of the real glass is zero (i.e., the heat capacities of the real glass and the crystal are identical), $\gamma_c = 1$, and the fictive temperature is equal to the glass transition temperature at all temperatures below T_g. In this case, the relaxation time shows Arrhenius temperature dependence below T_g. At the other extreme, if the configurational heat capacities of the real glass and the liquid differ only slightly, $\gamma_c \approx 0$, $T_f \approx T$, and the relaxation time expression is the same both below and above T_g. We note that since enthalpy relaxation is nonexponential, a real glass consists of a number of substates, each having a different configurational entropy and a different

Copyright 2004 by Marcel Dekker, Inc. All Rights Reserved.

fictive temperature. Thus, the results given in equations (8)–(10) refer to an average of substates for temperatures below T_g.

While most treatments of this subject assume that the heat capacities of the crystalline and glassy phases are essentially the same, and therefore Arrhenius temperature dependence is predicted below T_g, experimental heat capacity data for sucrose [47,48,50] indicate that the heat capacity of glassy sucrose is significantly higher than the heat capacity of crystalline sucrose, and $\gamma_c \approx 0.8$. Figure 7 shows calculated relaxation times for two hypothetical amorphous materials with $T_g = 70°C$, but different fragilities (i.e., $D = 7$ and $\gamma_c = 0.8$ for a fragile glass like sucrose and $D = 23$ and $\gamma_c = 0.94$ for a representative strong glass). Above the glass transition temperature in the fluid state, the "strong glass" has the longer relaxation time, but in the glassy state, the fragile glass has a longer relaxation time. Thus, assuming that pharmaceutical stability is correlated with structural relaxation, a protein formulation above T_g would be more stable in the strong glass, but below T_g the fragile glass would provide better stability. For the strong glass, temperature dependence is nearly Arrhenius both above and below T_g. For the fragile glass, significant deviations from linearity in the plot indicate non-Arrhenius temperature dependence

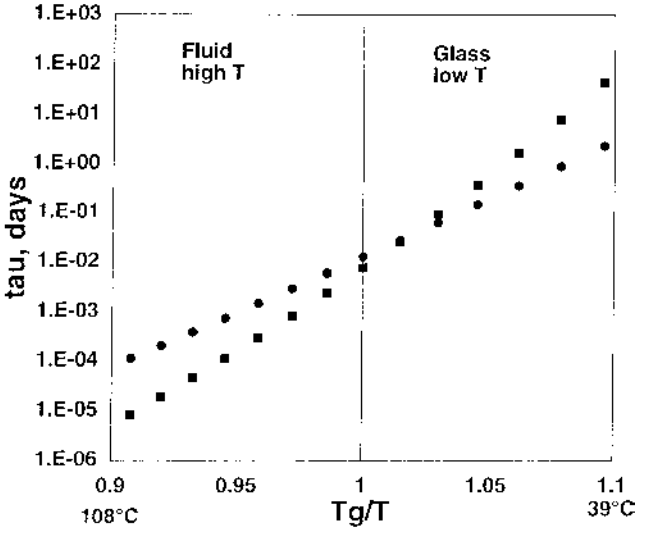

Figure 7 Comparison of structural relaxation times for fragile and strong glasses with glass transition temperatures of 70°C. The data were calculated using input data characteristic of sucrose except for the strength parameter, D. Key: circles = strong glass ($D = 23$), squares = fragile glass ($D = 7$).

Copyright 2004 by Marcel Dekker, Inc. All Rights Reserved.

both above and below T_g, although the non-Arrhenius behavior is more pronounced above T_g. To the extent that the thermal history of the glass will impact the value of γ_c, thermal history will impact the value of τ. Thus, one might speculate that thermal history may well impact pharmaceutical stability in a glassy formulation. Evidence for such an effect is meager, but several studies do suggest greater chemical stability for samples annealed below T_g [51,52].

Structural relaxation times determined from enthalpy relaxation studies with sucrose and trehalose [39,53] are given in Figure 8. The structural relaxation times observed are qualitatively similar to those estimated for the fragile glass example in Figure 7. While there is considerable scatter in the data, it seems clear that the temperature dependence for sucrose is nonlinear and therefore non-Arrhenius. Insufficient data are available for trehalose to judge linearity. The trehalose structural

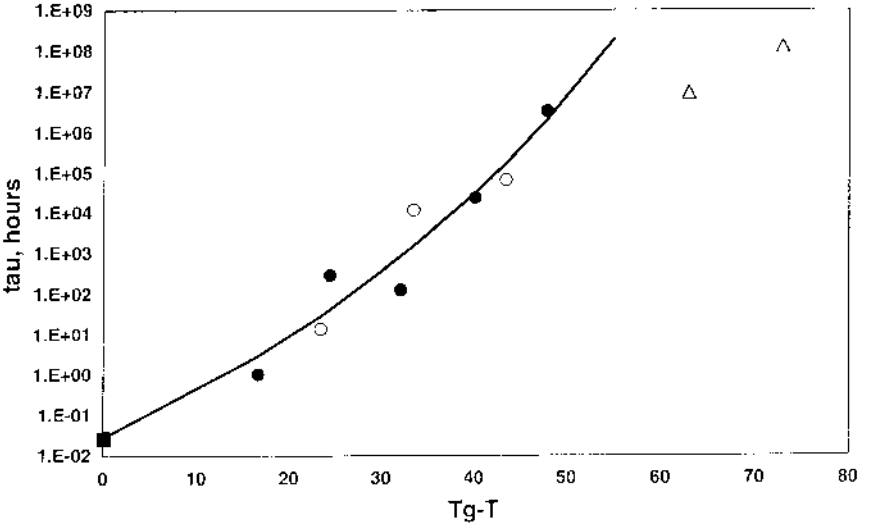

Figure 8 Structural relaxation times for quench-cooled glassy disaccharides as determined from enthalpy relaxation data. Structural relaxation times were obtained by a fit of the data to the stretched exponential function (see Refs. 39, 52, and 53). Key: full circles = data for sucrose obtained by differential scanning calorimetry on annealed samples (*data taken from Ref. 39*), open circles = data for sucrose obtained by isothermal microcalorimetry (*data taken from Refs. 52 and 53*), open triangles = data for trehalose obtained by isothermal microcalorimetry (*data taken from Ref. 53*).

Copyright 2004 by Marcel Dekker, Inc. All Rights Reserved.

relaxation times are lower than those for sucrose at the same T_g/T, indicating different fragility and/or a different value of γ_c.

C. Instability and the Glass Transition: Coupling of Reaction Mobility with Structural Relaxation

The "vitrification hypothesis" assumes that the mobility relevant to pharmaceutical *instability* is strongly correlated with viscosity and structural relaxation time such that high viscosity and large structural relaxation time mean very slow, hopefully insignificant, degradation rate. The mobility required for a given reaction is thought of in terms of a series of diffusional jumps to produce the change in configuration required for the physical or chemical change. These diffusional jumps may involve the entire molecule as in a bimolecular aggregation process, the segmental diffusional motion of amino acid residues as in an unfolding reaction, or the motion on a smaller scale such as formation of the cyclic intermediate in a deamidation pathway. It is further assumed that these diffusional jumps require corresponding motion in the surrounding amorphous medium, otherwise reaction mobility would not couple with (i.e., be dependent upon) medium viscosity. Thus, the rate constant for the reaction is proportional to a diffusion constant for the reaction motion, and through equation (2), the rate constant is inversely proportional to the reaction relaxation time. Perfect coupling with viscosity (i.e., validity of the Stokes–Einstein equation) would mean the reaction relaxation time and the structural relaxation time are directly proportional. However, the Stokes–Einstein equation is not entirely appropriate for the high-viscosity systems of interest to protein stability, and not all types of mobility are strongly coupled to viscosity [54].

It is well known that while values of T_0 determined from ionic conductivity studies are usually identical to those determined from viscosity data on the same systems [9], the values of the strength parameters, D, do differ. Conductivity typically produces slightly smaller "D" values, meaning the structural relaxation times determined from viscosity "decouple" from the conductivity relaxation times with the differences becoming more marked as temperature decreases [9,54]. With some inorganic glasses, the decoupling of conductivity from viscosity becomes extreme with the conductivity relaxation time being nearly 12 orders of magnitude smaller than the (viscosity) structural relaxation time [54]. Small-molecule diffusion in glassy polymers also appears to be nearly completely decoupled from structural relaxation [55,56].

A study of mobilities for three different kinds of motion in a polymer having a glass transition at 35°C demonstrates that, even in the same polymer, not all types of motion couple with the viscosity in equal fashion [57].

Copyright 2004 by Marcel Dekker, Inc. All Rights Reserved.

The mobilities are derived from D-NMR correlation times. Complete coupling with the glass transition would imply roughly nine orders of magnitude reduction in mobility between $1000/T = 2.7$ and the glass transition temperature. The data show (Figure 9) that while chain fluctuation (i.e., chain diffusion) mobility appears to be strongly coupled to the glass transition, chain rotation is only moderately coupled, and ring flip motion of a side chain is nearly completely decoupled. Ring flip "mobility" shows Arrhenius behavior above and below the glass transition with essentially the same activation energy. The only impact of the glass transition on ring flip is a sharp but small decrease in mobility as the temperature decreases through T_g. It appears that mobility involving motion on a larger scale (i.e., more displacement and/or more generation of free volume needed for a "jump") correlates best with viscosity and the glass transition phenomenon, a conclusion also consistent with the observation made above regarding diffusion of small molecules in polymer glasses.

The physical basis of variable coupling between mobility and structural relaxation time likely has its origin in the differences between free volume requirements, or in the context of the Adam–Gibbs theory, differences in the molar chemical potential change between structural relaxation and the relevant diffusional jump [54]. Since the strength parameter for structural relaxation, D, is proportional to the molar

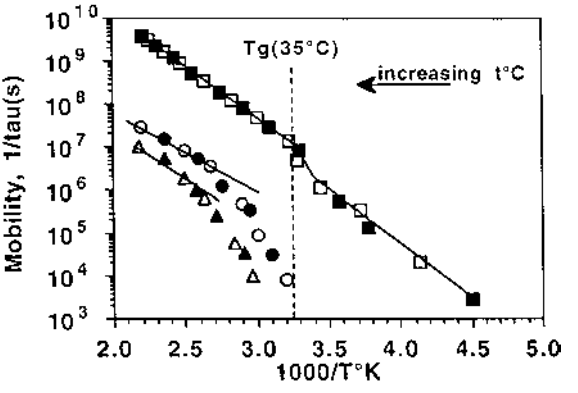

Figure 9 Coupling of mobility with the glass transition in a polymer system. Mobility is the reciprocal of the correlation time for the type of motion indicated. Correlation times were evaluated from deuteron NMR relaxation data. Key: triangles = reorientation or "fluctuation" of the chain axis; circles = rotation about the chain axis; squares = 180° ring flips of side chain aromatic rings. Open and full symbols refer to different degrees of deuteration (*original data taken from Ref. 57*).

Copyright 2004 by Marcel Dekker, Inc. All Rights Reserved.

chemical potential change, one might speculate that the reaction relaxation time could be written in the same form as the structural relaxation time but with a different strength parameter, D_{rx}, where $D_{rx} = gD$, and where the "coupling constant," g, would be expected to be less than unity unless the degradation process required translational diffusion of the entire protein molecule. Thus, with the degradation rate constant, k, being inversely proportional to the reaction relaxation time, one might expect a relationship of the form

$$k = A_k \exp\left(-\frac{gDT_0}{[T-(T/T_f)T_0]}\right) \tag{11}$$

where the A_k is a pre-exponential constant depending upon the details of the degradation mechanism. One would expect the value of A_k to decrease as the number of "diffusional jumps" needed to complete a reaction increases. Given a distribution of substates in the glass, the values of g and T_f would represent averages for the populated substates. Whether equation (11) is valid is a matter of speculation as no degradation studies have been determined in a series of amorphous systems where D, T_0, and T_f are also available. However, as discussed above, mobility data do provide experimental justification for at least the qualitative features of equation (11). That is, as long as degradation in a highly viscous amorphous material or glass is limited by diffusional motion of some kind, the degradation rate is likely to depend on the factors emphasized in equation (11): (1) the zero mobility temperature, T_0; (2) the strength parameter, D, or the glass transition temperature, T_g (i.e., only two of the three parameters, T_g, T_0, and D are independent if equation (6) is valid); (3) for a glass, thermal history through fictive temperature, T_f; and (4) the degree of coupling as expressed in equation (11) via the coupling coefficient, g. Clearly, while $T \ll T_g$ is important for good stability, other material characteristics of the formulation are also important and may dominate.

D. Instability and the Glass Transition: Experimental Observations

A number of systems show marked deterioration of stability as temperature exceeds the glass transition temperature, but for storage well below the glass transition temperature, stability does not appear to depend directly on the difference between T_g and the storage temperature (i.e., see Figure 5). The correlation between reactivity and T_g is most easily discussed in terms of the WLF equation. The WLF equation [58] is an expression for relaxation

Copyright 2004 by Marcel Dekker, Inc. All Rights Reserved.

time, roughly equivalent to the VTF equation, that may be "derived" using free volume concepts. With fixed constants, the WLF equation states that the ratio of relaxation time at any temperature to the relaxation time at T_g depends only on the difference between temperature and the glass transition temperature. Assuming that reaction rate is inversely proportional to structural relaxation time in the amorphous phase, degradation rates normalized to the corresponding rates at T_g should depend only on $T - T_g$. Thus, in an experiment where both temperature and glass transition temperature are varied, stability is a function of only one variable, $T - T_g$. Degradation in a monoclonal antibody:vinca alkaloid conjugate system is consistent with the "$T - T_g$" dependence of relative reaction rate [59]. Rates of dimerization, hydrolysis of the antibody–vinca linkage, and degradation of the vinca moiety (mostly oxidation) were obtained at two temperatures and three water contents (i.e., three T_g). The rate normalized to the rate at the glass transition temperature is a function only of "$T - T_g$", as suggested by the WLF equation (Figure 10). All three degradation reactions form a single curve (a straight line), indicating the WLF constants are a characteristic of the amorphous system and independent of the nature of the degradation pathway, as expected.

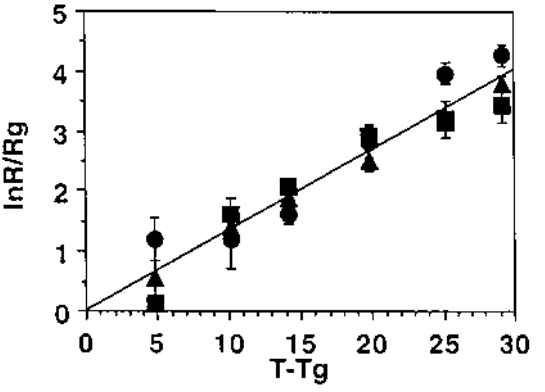

Figure 10 The stability of a freeze-dried monoclonal antibody:vinca alkaloid conjugate formulation. Desacetylvinblastine hydrazide is linked to the KS1/4 monoclonal antibody via aldehyde residues of the oxidized carbohydrate groups on the antibody. The formulation is conjugate:glycine:mannitol in a 1:1:1 weight ratio. Storage temperatures are 25°C and 40°C for samples with moisture contents of 1.4%, 3.0%, and 4.7%. Key: circles = dimer formation; triangles = free vinca generation (hydrolysis); squares = vinca degradation; solid line = best fit to the WLF equation (*reproduced with permission from Ref. 59*).

Copyright 2004 by Marcel Dekker, Inc. All Rights Reserved.

The effect of residual water on the chemical degradation of hGH in a trehalose formulation provides another example of a correlation between stability and the glass transition [60]. The trehalose formulation shows a well-defined glass transition temperature with DSC, with the expected decrease in T_g as the water content is increased. The pseudo first-order rate constant for chemical degradation is essentially independent of water content while the system remains glassy, but at least for the 50°C data, degradation increases sharply as increasing water content depresses the system glass transition temperature significantly below the storage temperature (Figure 11). Rates of aggregation show essentially the same behavior. However, since stability is not sensitive to water content in the glassy state, stability is not correlated with $T - T_g$ below the glass transition temperature. The study of formulation effects on hGH stability (Figure 5)

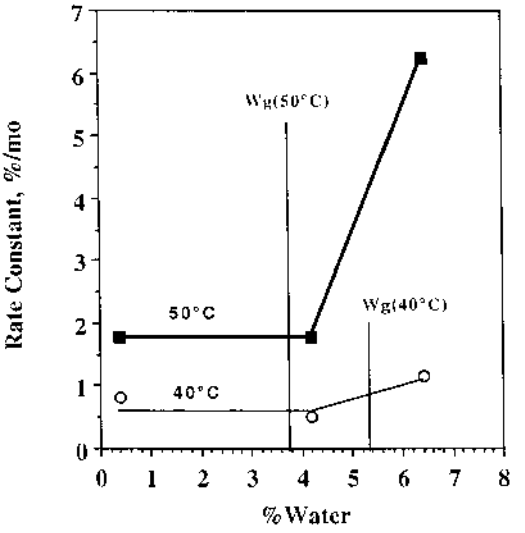

Figure 11 Chemical degradation in freeze-dried hGH formulated with trehalose as a function of water content at 40°C and 50°C. The pseudo first-order rate constant for degradation (%/month) is given for the combination of asparagine deamidation and methionine oxidation. The formulation is hGH:trehalose in a 1:6 weight ratio with sodium phosphate buffer (pH 7.4) at 15% of the hGH content. The highest moisture content samples were collapsed after storage at both 40°C (moderate collapse) and 50°C (severe collapse). The water content that reduces the glass transition temperature of the formulation to the storage temperature is denoted W_g. Key: open circles = 40°C storage, full squares = 50°C storage (*original data from Ref. 60*).

Copyright 2004 by Marcel Dekker, Inc. All Rights Reserved.

suggests the same conclusion. That is, for glassy systems, stability is not directly related to the precise difference between storage temperature and T_g.

E. Structure of Proteins in the Amorphous Solid State

While it is clear that many proteins may be freeze-dried and reconstituted with little or no loss in activity, it is usually not obvious whether the freeze-dried protein is basically native in conformation or whether the solid state conformation is distinctly "non-native," with the native and active conformation quickly forming during rehydration. The observation that lysozyme regains enzymatic activity *in the "solid" state* above about 20% water [61] demonstrates that a protein need not be in a predominantly aqueous system to maintain activity and presumably posses native structure. However, this observation does not necessarily imply that the structure is non-native at lower water contents where the enzymatic activity disappears. The loss of activity at lower water contents [61] could simply be a consequence of greatly slowed kinetic processes (i.e., greatly restricted molecular mobility as the system passes into the glassy state).

Even very dry proteins in the glassy state commonly show denaturation endotherms via DSC [36,62–65], where the heat of denaturation and heat capacity change on denaturation [65] are roughly comparable to solution values. These data provide direct evidence of significant tertiary structure in the dry glass, but do not necessarily mean the structure is fully native. Vibrational spectroscopy perhaps provides the best methodology for study of the conformational changes induced by freeze-drying. An early Raman study suggested perturbations in the tertiary structure of freeze-dried ribonuclease [66], and FTIR spectroscopy has been employed recently to document changes in the IR spectra of proteins upon freeze-drying, presumably reflecting changes in secondary structure [30,67–71]. In studies with freeze-dried solids, quantitative comparison between spectra may be made using the spectral correlation coefficient, r, defined by [67,69]

$$r = \frac{\sum_n x_i y_i}{\sqrt{\left(\sum_n x_i^2 \sum_n y_i^2\right)}} \tag{12}$$

where x_i and y_i are the spectral absorbance values of the reference (i.e., normally the "native" aqueous solution) and the sample of interest (i.e., the freeze-dried solid). Analysis is restricted to the amide I region (i.e., 1720 to 1610 per cm) using smoothed second-derivative spectra [67,69]. Changes in the FTIR spectra upon freeze-drying vary from slight to dramatic, with corresponding "r" values from greater than 0.9 to less than 0.5. In general,

Copyright 2004 by Marcel Dekker, Inc. All Rights Reserved.

bandwidths are greater for freeze-dried solids, suggesting configurational disorder. New bands may appear in the solid, and solution bands may disappear, suggesting major conformational changes. Small shifts in band positions also occur on freeze-drying. Studies with poly-L-lysine [67] suggest that the loss of water during freeze-drying favors formation of β-sheet secondary structure. It is concluded [67] that dehydration alone, without conformational changes, could produce small shifts in protein bands to higher wavenumber, but most of the loss of correspondence between solution and solid spectra arises from conformational changes. The conformational changes involve, at least in part, formation of β-sheet structure. The changes in spectra, and conformation, are not necessarily *irreversible*. In general, the spectral correlation coefficient of a *reconstituted* freeze-dried sample is higher than for the solid. Formulation with good lyoprotectants (i.e., sucrose or trehalose) moderates the change in FTIR spectra on freeze-drying, with a corresponding increase in the spectral correlation coefficient relative to that obtained by freeze-drying from buffer alone. Formulation with disaccharides appears to provide a hydrogen bonding opportunity for the protein that does not involve a shift in conformation to β-sheet, thereby stabilizing the native conformation [67].

While FTIR spectroscopy may have some limitations as a quantitative predictor of the pharmaceutical stability of a protein since only changes in secondary structure are measured, it does seem clear that protein structure is often altered during the freeze-drying process, and the degree of structural perturbation is specific to the protein and quite specific to the formulation.

While one certainly cannot maintain that preserving a protein in the native state is a *sufficient* condition for good storage stability (i.e., otherwise, why freeze-dry?), it does seem intuitive that a ''native'' freeze-dried protein will generally be *more* stable than the same freeze-dried protein in an unfolded conformation. Whether the native state is retained via a thermodynamic mechanism or through a purely kinetic mechanism is immaterial! While the volume of relevant data is not large, it does appear that this intuitive concept does have validity for freeze-dried proteins. For example, loss of activity of lactate dehydrogenase (LDH) during freeze-drying from various sugar and polyol formulations does correlate reasonably well with the FTIR spectral correlation coefficients [67]. Recently, it has also been demonstrated that storage stability of freeze-dried proteins is well correlated with the FTIR spectral correlation coefficient [72,73]. Apparent first-order rate constants for aggregation of freeze-dried rIL-2 decrease with decreasing pH in a manner fully consistent with the increase in spectral correlation coefficient with decreasing pH, producing an excellent correlation between storage stability and spectral correlation coefficient (Figure 12). Therefore, there is some experimental base for the proposition

Copyright 2004 by Marcel Dekker, Inc. All Rights Reserved.

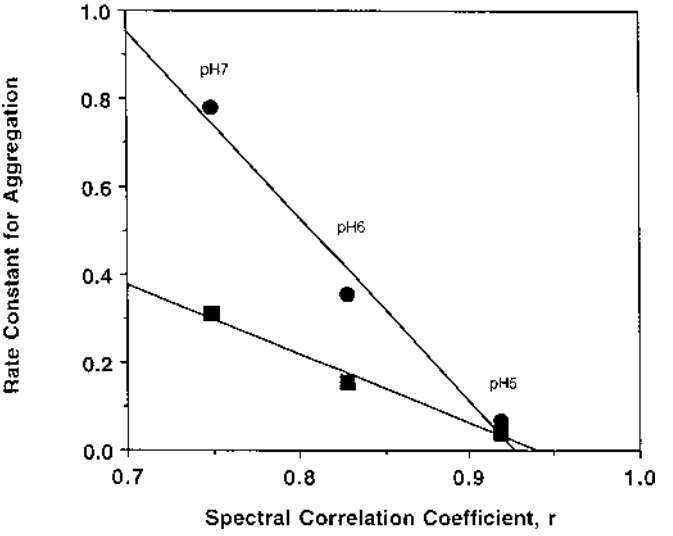

Figure 12 The correlation of storage stability with protein structure as determined by Fourier transform infrared (FTIR) spectroscopy: apparent first-order rate constants for aggregation of freeze-dried rIL-2. Key: circles = 45°C storage, squares = 29°C storage (*data taken from Ref. 72*).

that one requirement for stability during freeze-drying and storage is retention of native conformation in the glassy protein. It should be noted, however, that the correlation between residual activity and spectral correlation coefficient need not necessarily be a direct proportion or even a linear function.

V. MECHANISMS OF STABILIZATION

A. Stabilization During Freezing: the "Excluded Solute" Concept

Although many stress factors may operate during freezing, the protein does exist in an aqueous environment during most of the freezing process. Only near the end of freezing does freeze concentration proceed to the point where the protein phase becomes mostly solutes, viscosity becomes high, and mobility becomes slow on the time scale of the experiment (Figure 1). Assuming the critical stress factors develop before the system becomes a solute-rich high-viscosity system, it is understandable that solutes that stabilize during freezing, or cryoprotectants, are generally those solutes that

Copyright 2004 by Marcel Dekker, Inc. All Rights Reserved.

stabilize the native conformation at more normal concentrations and temperatures [5]. Given the chemical diversity of such stabilizers (i.e., amino acids, polyols, sugars, and poly(ethylene) glycols), it is obvious that specific chemical interactions are not the common stabilization mechanism. Such solutes tend to be "excluded" from the surface of the protein and therefore induce "preferential hydration" of the protein. The thermodynamics of this phenomenon is analogous to solute "surface excess" at the air–water interface. A negative surface excess means the solute is partly excluded from the interface, thereby increasing the surface tension of the solution. Indeed, there is a good correlation between those solutes that increase the surface tension of water and those that are "excluded" from the surface of a protein [6]. The thermodynamic consequence of "solute exclusion" and "preferential hydration" is to increase the chemical potential of the protein. The first assumption in relating this thermodynamic result to cryoprotection may be stated as: if the increase in chemical potential of the native protein caused by "solute exclusion" is denoted, $\Delta\mu_N$, the corresponding increase for the unfolded protein is $k\Delta\mu_N$, where $k > 1$. Thus, the free energy of unfolding would be increased by the solute, which is equivalent to stabilization of the native conformation [6]. Secondly, it is assumed that pharmaceutical stability, or degradation, is directly related to thermodynamic stability. Finally, it is assumed that the solution state concepts are valid throughout the freezing process, or at least valid over the period where unfolding in the absence of a cryoprotectant is both thermodynamically favored and kinetically allowed.

The extent of "solute exclusion," $(\partial m_s/\partial m_p)_{T,\mu_w,\mu_p}$, can be measured, and the corresponding effect on chemical potential of the protein, $(\partial\mu_p/\partial m_s)_{T,P,m_p}$, can then be calculated [6,74–77]:

$$\left(\frac{\partial\mu_p}{\partial m_s}\right)_{T,P,m_p} = -\left(\frac{\partial m_s}{\partial m_p}\right)_{T,\mu_w,\mu_p}\left(\frac{\partial\mu_s}{\partial m_s}\right)_{T,P,m_p} \tag{13}$$

where the solute exclusion parameter is the partial derivative of the molal concentration of stabilizer in the domain of the protein, m_s, with respect to the molal concentration of protein, m_p, at constant temperature, T, and constant chemical potentials of water, μ_w, and protein, μ_p. The relationship also involves the concentration dependence of the chemical potential of stabilizer, μ_s, which may be written

$$\left(\frac{\partial\mu_s}{\partial m_s}\right)_{T,P,m_p} = \frac{RT}{m_s} + RT\left(\frac{\partial \ln\gamma_s}{\partial m_s}\right)_{T,P,m_2} \tag{14}$$

Copyright 2004 by Marcel Dekker, Inc. All Rights Reserved.

The first term on the right hand side is the "ideal solution" contribution while the "nonideal" part involves the concentration dependence of the activity coefficient of the stabilizer in water, γ_s. Since equation (14) involves the reciprocal of stabilizer concentration, it appears that the response of the chemical potential of the protein to a stabilizer, $(\partial\mu_p/\partial m_s)_{T,P,m_p}$, becomes infinite as the stabilizer concentration approaches zero. However, the molal "solute exclusion" parameter, $(\partial m_s/\partial m_p)_{T,\mu_w,\mu_p}$, is actually directly proportional to concentration, so the chemical potential derivative, $(\partial\mu_p/\partial m_s)_{T,P,m_p}$, is roughly independent of concentration for most of the systems studied [74–77]. The factors impacting the chemical potential derivative are more transparent if we first convert from molal concentration units to mass-based concentrations (i.e., weight ratios, where the weight ratio of component "i" to water is symbolized, g_i); g_i is related to molality and molecular weight, M_i, by

$$g_i = m_i \frac{M_i}{1000} \tag{15}$$

The "solute exclusion" parameter then becomes, $(\partial g_s/\partial g_P)_{T,\mu_w,\mu_p}$, in "mass concentration form." This mass-based "solute exclusion" parameter may be related to the mass-based "preferential hydration" parameter, $(\partial g_w/\partial g_P)_{T,\mu_w,\mu_p}$, by the identity [6,74–77],

$$\left(\frac{\partial g_w}{\partial g_p}\right)_{T,\mu_w,\mu_s} = -\left(\frac{1}{g_s}\right)\cdot\left(\frac{\partial g_s}{\partial g_p}\right)_{T,\mu_w,\mu_s} \tag{16}$$

The "preferential hydration" parameter is nearly independent of concentration, and for most small molecular weight "excluded solutes" is in the range 0.2–0.6 [6,74–77]. Thus, the chemical potential derivative, in terms of mass-based concentrations, becomes

$$\left(\frac{\partial\mu_p}{\partial g_s}\right)_{T,P,g_P} = RT\frac{M_p}{M_s}\left(\frac{\partial g_w}{\partial g_P}\right)_{T,\mu_w,\mu_s}\left[1 + g_s\left(\frac{\partial \ln\gamma_s}{\partial g_s}\right)\right] \tag{17}$$

The nonideality term, $1 + g_s(\partial \ln\gamma_s/\partial g_s)$, is normally relatively close to unity even in concentrated solutions. The exceptions are some polymers such as higher molecular weight PEGs. For example, for 1 M sucrose, 2 M glycine, and 1 M proline, the nonideality terms are 1.19, 0.67, and 1.1, respectively [78,79], but for 2% PEG 6000, the nonideality term is 2.6 [77]. The quantity most directly relevant to stabilization is the free energy of transfer, which is

Copyright 2004 by Marcel Dekker, Inc. All Rights Reserved.

given by the integral of the chemical potential derivative from zero concentration of stabilizer to the concentration of interest, g_s:

$$\Delta\mu_p \text{ (transfer)} = \int_0^{g_s} \left(\frac{\partial\mu_p}{\partial g_s}\right) dg_s = g_s\left\langle\frac{\partial\mu_p}{\partial g_s}\right\rangle \tag{18}$$

where $\langle\partial\mu_p/\partial g_s\rangle$ is the average value of the derivative over the concentration range from zero to g_s. Since the "experimental" values of $\partial\mu_p/\partial g_s$ are relatively insensitive to concentration, the average value may be treated as a constant for a given protein:stabilizer combination, at least as a good first approximation within the range of concentrations studied, typically $g_s < 0.7$. It does not seem reasonable to assume, however, that $\partial\mu_p/\partial g_s$ will continue to remain constant as the system moves toward the high concentrations found in the freeze-concentrated glass, i.e., as $g_s \to 4$. However, since the rate constants for unfolding and folding may slow sufficiently to prevent equilibrium from being maintained on the time scale of a relatively fast freeze (Figure 7), thermodynamic stabilization may be irrelevant near the glass transition temperature. The free energy of transfer given by equation (18) is the increase in free energy of the protein caused by addition of the stabilizer at concentration g_s, earlier denoted "$\Delta\mu_N$" for the protein in the native conformation. Again, while equation (18) also applies to a protein in the denatured state, data are available only for proteins in their native conformation. Assuming that the corresponding free energy of transfer of the denatured protein is given by $k\ \Delta\mu_{N,}$ where $k > 1$, the stabilization free energy is given by $(k-1)\Delta\mu_N$, which is greater than zero when a stabilizer increases the chemical potential of the native protein. Thus, in a series of stabilizers, the stability enhancement should correlate with the free energies of transfers evaluated for the protein in the native conformation. Of course, this conclusion is based upon the assumption that $k-1$ is not a major variable in the context of the study.

A selection of data are given in Table 2, where mean values of preferential hydration coefficients, $\partial g_w/\partial g_p$, and chemical potential derivatives, $\partial\mu_p/\partial g_s$, are tabulated for some stabilizers of pharmaceutical significance. The nonideality terms for glycerol and mannitol were assumed to be identical to that for glucose. Since the nonideality is less than the estimated error in $\partial\mu_p/\partial g_s$, the uncertainty in the nonideality term is of no practical significance. Except for the high molecular weight PEGs, which have very high preferential hydration coefficients, the preferential hydration values are all of the same magnitude, although they are specific to the stabilizer:protein combination. Of the small molecule stabilizers tabulated, glycine is the most effective "preferential hydration inducer," and because of

Copyright 2004 by Marcel Dekker, Inc. All Rights Reserved.

Table 2 The Effect of Solutes on the Preferential Hydration and Chemical Potential of Proteins. Uncertainties in the data are typically ±10–20%

Protein	Stabilizer	$(\partial g_w/\partial g_p)_{T,\mu_w,\mu_s}$	$(\partial \mu_p/\partial g_s)_{T,P,m_p}$ (kcal/mol)
RNASE	Sucrose, ≤ 1 M	0.46	12
BSA	Lactose, ≤ 0.4 M	0.30	37
BSA	Glucose, ≤ 2 M	0.23	59
BSA	Mannitol, ≤ 15%	0.20	48
BSA	Inositol, ≤ 10%	0.40	96
BSA	Glycerol, ≤ 40%	0.17	80
BSA	Glycine, ≤ 2 M	0.43	200
BSA	PEG 400, ≤ 10%	0.61	70
BSA	PEG 1000, ≤ 10%	1.18	74
BSA	PEG 3000, ≤ 6%	2.36	56
BSA	PEG 6000, ≤ 4%	3.76	67
Lysozyme	Glycine, ≤ 2 M	0.58	56
Lysozyme	Proline, 1 M	0.32	26
Lysozyme	PEG 400, ≤ 10%	0.26	6.0
Lysozyme	PEG 1000, ≤ 10%	0.83	11.3
Lysozyme	PEG 3000, ≤ 4%	2.55	12.5
Lysozyme	PEG 6000, ≤ 2%	8.6	21

its small molecular weight, the chemical potential derivative is by far the highest of the stabilizers in Table 2. Thus, on a weight basis, glycine gives the highest free energy of transfer. The high molecular weight PEGs are exceptional "preferential hydration inducers," but because of the inverse relationship of the chemical potential derivative to molecular weight, the chemical potential derivatives and the free energies of transfer are not exceptionally high. Assuming, for the moment, that stability enhancement should correlate with the free energy of transfer, the implication of the data given in Table 2 is that, when compared on a fixed mass-based concentration, high molecular weight PEGs will *not* be outstanding stabilizers. This conclusion seems contrary to implications in the literature [6,74–77]. Values of the chemical potential derivative are typically given in the literature in terms of molal concentration, i.e., $\partial \mu_p/\partial m_s$ is the reported parameter. While values of $\partial \mu_p/\partial m_s$ for high molecular weight PEGs are extremely high, a comparison based upon molal concentration is not practically relevant for pharmaceutical purposes, which is the primary reason why mass-based concentration is used in this presentation. However, stabilization during freeze:thaw is reported to be superior for high molecular

Copyright 2004 by Marcel Dekker, Inc. All Rights Reserved.

weight PEGs, even when comparing stabilizers at constant weight percent [31]. Moreover, the trends in stability during freeze:thaw of PFK given in Figure 4 are not consistent with the data given in Table 2. At constant molar concentration of stabilizer (0.5 M), the order of free energies of transfer are (for Lysozyme): glycine > proline. For BSA, the order is: inositol > lactose > glucose > glycerol. For retention of activity on freeze: thaw (of PFK), the order is: proline $\gg$ glycine, and disaccharide > glucose = glycerol > inositol. While the correlation with the preferential hydration coefficient is somewhat better, the "theory" is really based upon a correlation with free energies of transfer.

The lack of a quantitative correlation between the thermodynamics of "solute exclusion" and stability during freeze:thaw described above may have several contributing factors. First, the discussion above is limited to only a few proteins and includes only excipients which are "excluded solutes." That is, a correlation would certainly appear better if one were to include known denaturing solutes such as urea, although the pharmaceutical significance of such a comparison is questionable. Even the sparse data in Table 2 demonstrate that the relative effectiveness of the PEGs varies somewhat with the protein, so a wider protein database could improve the correlation. Also, the data in Table 2 refer to free energies of transfer at room temperature. Free energies are obviously temperature dependent, and whether the rank order of free energies at room temperature will persist at the subzero temperatures encountered during freezing is far from obvious. One must also question the validity of assuming the relationship between the increase in chemical potential of the native form and the denatured form are coupled by a k value that is really a constant for a variety of stabilizers. It must also be recognized that other factors may be controlling *instability* and stability. One possibility that has been largely ignored is the role of denaturation at the aqueous–ice interface and the role of the stabilizer in minimizing protein adsorption on the ice surface. While minimization of protein adsorption is a thermodynamic mechanism, it is a mechanism that does not directly involve thermodynamic stabilization of the aqueous protein. An additional factor, likely important if the stress occurs late in freezing, is the increasing viscosity of the freeze concentrate. Near the end of freezing, the protein is dispersed in an excipient matrix where the viscosity becomes very high (Figure 1). Both dilution of the protein in the matrix and the low molecular mobility generally associated with high viscosity would tend to slow the rate of denaturation or at least retard aggregation of partially denatured protein, assuming that the mobility critical for degradation is coupled, at least to some extent, to viscosity. Finally, there is at least one example of the stabilizer operating, at least in part, through its ability to prevent crystallization of a buffer component, thereby preventing

Copyright 2004 by Marcel Dekker, Inc. All Rights Reserved.

a large pH shift that destabilizes the protein [80,81]. Thus, while solute exclusion is likely a major factor in stabilization during freezing, other stabilization mechanisms are possible and even probable in some cases. It is not the purpose of this discussion to refute the concept of stabilization during freezing via the "excluded solute" concept, at least as a significant factor. Indeed, in this author's opinion, the concept does have merit and may dominate in many cases. Rather, the intent is to demonstrate that the predictive power of the thermodynamic results, such as in Table 2, for selecting the "optimum" stabilizer system for a "new protein" is quite limited and this limitation should not come as a surprise.

B. Stabilization During Drying

As discussed earlier, all stresses that develop during freezing are still present during drying, but the normal implicit assumption is that if degradation during freezing did not occur, the freezing stresses are not sufficient to thermodynamically destabilize the protein. Thus, the critical stress during drying is normally assumed to be the removal of the water that is part of the freeze concentrate. This assumption is likely correct as long as degradation occurs during secondary drying where the time scale is similar to that for freezing. Even assuming the critical stress factor in drying is the reduction of water to low levels, thereby removing the assumed stabilizing influence of hydrogen bonding interactions between protein and water, it is not obvious that the role of a stabilizer is to replace water in the hydrogen bonding interactions and thermodynamically stabilize the native conformation. If the stabilizer were to effectively couple the internal motions of the protein to structural relaxation in the glass, thereby reducing the rate of unfolding of a thermodynamically unstable system to insignificant levels, the net result would be a freeze-dried protein in the native conformation. That is, the protein would not unfold, regardless of what the free energy of unfolding might become, and stabilization would be purely kinetic.

Many experimental studies of the relative effectiveness of various solutes in preventing drying damage can be interpreted according to either the water substitute hypothesis, which is a thermodynamic stabilization mechanism, or a purely kinetic stabilization argument based upon the effective coupling of the protein motions to the glass. There are studies, however, which do not appear to be consistent with both classes of stabilization mechanisms. For example, the l-asparaginase study discussed earlier demonstrates that the water substitute hypothesis cannot always provide a satisfactory explanation of the data. Neither tetramethylglucose or poly(vinylpyrrolidone) can hydrogen-bond as water substitutes but yet are effective in preventing inactivation during drying. The catalase example

Copyright 2004 by Marcel Dekker, Inc. All Rights Reserved.

discussed earlier illustrates that a high glass transition temperature for the excipient is not the critical factor in stabilization during drying. Even glucose ($T_g = 39°C$) and mannitol (which frequently crystallizes) stabilize as effectively as do materials that readily form glasses with glass transition temperatures on the order of 100°C. While the catalase data do appear to be better interpreted in terms of the water substitute hypothesis than by protein immobilization in a glass, it must be acknowledged that mobility of the protein in a glass is not necessarily well measured by the difference between the glass transition temperature of the pure excipient and the sample temperature. First, since the catalase formulations were 1:1 weight ratio mixtures of excipient and catalase, the glass transition temperatures of the formulations will be intermediate between the glass transition temperature of the pure excipient and the glass transition temperature of the protein. Since protein T_g values are normally quite high [64,65], the differences in formulation glass transition temperatures will be much less than the differences in excipient glass transition temperatures. Secondly, glass fragility, thermal history, and perhaps most important, the degree of coupling of the protein motion to motion in the glass, are important factors in determining protein mobility at a given value of $T_g - T$.

Stabilization by a thermodynamic mechanism requires that the rates of unfolding and refolding are fast on the time scale of the experiment, which for drying is on the order of hours. Thus, equilibrium is established quickly, and it is the position of the equilibrium (i.e., the ratio of ''unfolded'' to ''native'' species) that determines degradation rate and loss of activity. Assuming that drying is carried out close to the glass transition temperature [4], the structural relaxation time is on the order of minutes to tens of minutes (Figure 7). Therefore, structural relaxation is moderately fast on the drying time scale. However, one can argue that the unfolding time is likely to be significantly greater than the structural relaxation time. Since unfolding involves rather large-scale motion, analogous to polymer chain diffusion, it is likely that coupling to structural relaxation will be strong. Recall that polymer chain diffusion appears to couple well with viscosity and the glass transition (Figure 9). Further, since a large number of diffusional jumps would be required to complete the unfolding reaction, the total time required for unfolding would be much greater than the time for a single diffusional jump. Thus, one might expect that the unfolding time would consist of a large number of diffusional jump times, each of which is similar in duration to the structural relaxation time. We also note that crystallization of sucrose from an amorphous system near T_g, likely also a diffusion-controlled process, seems to require a reaction time significantly longer than the structural relaxation time. Onset of nucleation and crystallization requires about 1 day when carried out 10°C above the

Copyright 2004 by Marcel Dekker, Inc. All Rights Reserved.

glass transition temperature of the system [82]. The estimated structural relaxation time (Figure 7) 10°C above the glass transition is $\approx 5 \times 10^{-6}$ days, so at least for sucrose crystallization, the ratio of the reaction time to the relaxation time is on the order of 10^5. Thus, we tentatively conclude that protein unfolding times in stabilized glassy formulations near T_g are likely of the same order of magnitude as the drying time or longer. Given these considerations, the rates of unfolding and refolding do *not* appear to be fast on the drying time scale, and thermodynamic stabilization mechanisms do not appear plausible. However, uncertainty in the degree of coupling between the diffusional jump process and structural relaxation introduces considerable uncertainty in the above conclusion. Further, it is significant to note that the temperature denoted, T_g', may be about 20°C higher than the true glass transition temperature [83]. If this interpretation is correct, primary drying and early secondary drying are typically carried out well above the glass transition temperature. For a process carried out at a temperature 20°C above a glass transition temperature, the structural relaxation time is in the range of 10^{-8} to 10^{-5} days, depending upon fragility, and one might argue that the rates of unfolding and refolding would be fast compared to the time scale of drying. Thermodynamic stabilization concepts would then become quite viable! However, as mentioned earlier, our data (unpublished) on rates of unfolding in viscous systems suggest unfolding rates can be on the time scale of months even 20°C above a glass transition temperature. To the extent this observation is general, one would not expect unfolding to occur during the usual drying process. However, since *instability* does occur during drying, either the *instability* does not depend on unfolding or the unfolding dynamics is not well coupled to the system mobility in these unstable systems.

C. Storage Stability

The stresses during storage are exactly those stresses that operate during drying. The major differences between drying stabilization and storage stabilization are the time scales. The time scale available for a stress to produce significant degradation is hours during drying but is months or years for storage. Further, it should also be noted that while the product temperature may closely approach the glass transition temperature during normal processing [4], storage temperatures are typically much below the system glass transition temperature, so relaxation times will also be much longer than during processing. Using the data in Figure 7 as a guide, the structural relaxation time at 40°C may vary from several days to many months, depending upon glass fragility. The variation could be far more if possible differences in coupling coefficient were also taken into

Copyright 2004 by Marcel Dekker, Inc. All Rights Reserved.

consideration. Thus, kinetic control of degradation via coupling with the structural relaxation time is certainly consistent with large differences in stability between different formulations. Experimental data (Figure 8) indicate that the structural relaxation times for sucrose at 25°C and 40°C are 570 years and 3 months, respectively, and the structural relaxation time for trehalose at 40°C is over 10,000 years! It is clear that, at least for a protein in a sucrose or trehalose matrix at 25°C, the structural relaxation times are much longer than storage times. Indirect evidence was used earlier to argue that unfolding times are long compared to structural relaxation times. Thus, we conclude that protein unfolding times in stabilized glassy formulations well below T_g are generally vastly greater than storage times, and any mechanism based upon equilibrium between folded and unfolded forms (i.e., thermodynamic mechanism) cannot be correct. Of course, even in stabilized systems, aggregation does occur after storage and reconstitution, which suggests that either some partial unfolding does occur well below T_g, or alternately, aggregation of partially unfolded molecules occurs via small-scale motion which is poorly coupled with structural relaxation.

If we assume that a structurally perturbed protein may have different reactivity than a protein in the native conformation, the observation that proteins do suffer structural perturbations upon freeze-drying, which are often highly formulation dependent, suggests that a realistic model of protein degradation in the solid state must recognize the existence of these substates of the protein. Thus, degradation in any given sample is a function of the distribution and reactivities of the substates. Specifically, one might write the rate constant for degradation, k, in terms of substate rate constants, k_i, and the fraction of such substates, w_i, in the general form

$$k = \sum_i w_i k_i = \sum_i w_i A_{ki} \exp\left(-\frac{g_i D T_0}{[T - (T/T_f)T_0]}\right) \tag{19}$$

where eq. 11 has been used to express the substate rate constants, k_i. Presumably, a substate that is partially unfolded would have fewer diffusional jumps to complete the reaction process and its A_{ki} would be larger than the corresponding pre-exponential factor for the native conformation. It is also quite possible that partial unfolding would mean a lower coupling coefficient, g_i, for the perturbed state. Both effects would give a larger substate rate constant for the partially unfolded protein. Equation (19) is not necessarily intended to be quantitative or correct in detail. However, the qualitative message is believed valid and consistent with the available data. That is, degradation in a glassy protein formulation depends upon both the dynamic properties of the glass and the specific

Copyright 2004 by Marcel Dekker, Inc. All Rights Reserved.

properties of the substates that are created during the freeze-drying process. While thermodynamic stabilization is not required for storage stability, thermodynamic stabilization during processing could well play a significant role in providing stable substate structures.

REFERENCES

1. TY Tsong. Biopolymers 17:1669–1678, 1978.
2. T Kiefhaber, R Quaas, U Hahn, FX Schmid. Biochemistry 29:3053–3061, 1990.
3. DN Brems. Biochemistry 27:4541–4546, 1988.
4. JF Carpenter, MJ Pikal, BS Chang, TW Randoph. Pharm Res 14(8): 969–975, 1997.
5. MJ Pikal. Freeze Drying. In: J Swaarbrick and JC Boylan, eds. Encyclopedia of Pharmaceutical Technology. Vol. 6. New york: Marcel Dekker, 2001.
6. T Arakawa, Y Kita, JF Carpenter. Pharm Res 8:285–291, 1991.
7. F Franks. Cryo-Letters 11:93–110, 1990.
8. CRC Handbook. Boca Raton, FL: Chemical Rubber Publishing Co, 1957.
9. CA Angell, RD Bressel, JL Green, H Kanno, M Oguni, FJ Sare. J Food Eng 22:115–142, 1994.
10. TE Kiovsky, RE Pincock. J Am Chem Soc 88:7704–7710, 1966.
11. M Lim, D Reid. In: H Levine and L Slade, eds. Water Relationships in Food. New York: Plenum Press, 1991, pp 103–122.
12. SS Larsen. Arch Pharm Chemi Sci Ed 1:41–53, 1973.
13. N Murase, F Franks. Biophys Chem 34:293–300, 1989.
14. G Gomez, N Rodriguez-Hornedo, MJ Pikal. Pharm Res 11:S-265, PPD 7364, 1994.
15. BA Szkudlarek, N Rodriguez-Hornedo, MJ Pikal. Mid-Western AAPS Meeting, Chicago, poster #24, 1994.
16. MJ Pikal, KM Dellerman, ML Roy, RM Riggin. Pharm Res 8:427–436, 1991.
17. ML Roy, MJ Pikal, EC Rickard, AM Maloney. Dev Biol Stand 74: 323–340, 1991.
18. JD Andrade, V Hlady. Adv Poly Sci 79:3–63, 1986.
19. BM Eckhardt, JQ Oeswein, TA Bewley. Pharm Res 8:1360–1364, 1991.
20. GB Strambini, E Gabellieri. Biophys J 70:971–976, 1996.
21. A Hubel, C Korber, E Cravalho, G Rau. J Cryst Growth 87:69–78, 1988.
22. BS Chang, BS Kendrick, JF Carpenter. J Pharm Sci 85:1325–1330, 1996.
23. F Franks. Biophysics biochemistry at low temperatures. Cambridge University Press, 1985.
24. P Privalov. Biochem Mol Biol 25:281–305, 1990.
25. MJ Pikal, S Shah, ML Roy, R Putman. Int J Pharm 60:203–217, 1990.
26. J Carpenter, J Crowe, T Arakawa. J Dairy Sci 73:3627–3636, 1990.
27. R Tanaka, T Takeda, K Miyajima. Chem Pharm Bull 39:1091–1094, 1991.
28. K Hellman, D Miller, K Cammack. Biochim Biophys Acta 749:133–142, 1983.

Copyright 2004 by Marcel Dekker, Inc. All Rights Reserved.

29. ME Ressing, W Jiskoot, H Talsma, CW van Ingen, EC Beuvery. DJA Crommelin, Pharm Res 9:266–270, 1992.
30. T Arakawa, S Prestrelski, W Kinney, JF Carpenter. Adv Drug Delivery Rev 10:1–28, 1993.
31. JF Carpenter, S Prestrelski, T Arakawa. Arch Biochem Biophys 303:456–464, 1993.
32. MJ Pikal. Biopharm 3(9):26–30, 1990.
33. K Shikama, I Yamazake. Nature 190:83–84, 1961.
34. K Izutsu and S Yoshioka. Drug Stability 1:11–21, 1995.
35. MW Townsend PP DeLuca, J Parenter. Sci Technol 42:190–199, 1988.
36. MJ Pikal, K Dellerman, ML Roy. Dev Biol Stand 74:323–340, 1991.
37. R Pearlman, TH Nguyen. Therapeutic Peptides and Proteins: Formulations, Delivery, Targeting. In: D Marshak and D Liu, eds. Current Communications in Molecular Biology, Cold Spring Harbon Laboratory. NY: Cold Spring Harbor, 1989, pp 23–30.
38. MJ Pikal, Eli Lilly & Co, unpublished observations.
39. BC Hancock, SL Shamblin, G Zografi. Pharm Res 12:799–806, 1995.
40. ET Iben, D Braunstein, W Doster, H Frauenfelder, MK Hong, JB Johnson, S Luck, P Ormos, A Schulte, PJ Steinbach, AH Xie, RD Young. Phys Rev Lett 62:1916–1919, 1989.
41. SJ Hagen, J Hofrichter, WA Eaton. Science 269:959–962, 1995.
42. R Roy. J Non-Cryst Soids 3:33–40, 1970.
43. MJ Pikal. J Phys Chem 75:3124, 1971.
44. G Adam, JH Gibbs. J Chem Phys 43:139–146, 1965.
45. CA Angell. J Non-Cryst Solids 102:205–221, 1988.
46. IM Hodge. J Non-Cryst Solids 202:164–172, 1996.
47. L Finegold, F Franks, RHM Hatley. Faraday Trans 89:2945–2951, 1989.
48. SL Shamblin, X Tang, L Chang, BC Hancock, MJ Pikal. J Phys Chem 103:4113–4121, 1999.
49. IM Hodge. J Non-Cryst Solids 169:211–266, 1994.
50. RL Putnam, J Boerio-Goates. J Chem Thermodyn 25:607–613, 1993.
51. IR Mardaleishvili, VM Anisimov. Izv Akad Nauk SSR, Ser Khim. No 6:1431–1432, 1987.
52. MJ Pikal, DR Rigsbee. Thermometric Seminars on Calorimetry in Materials Sciences. Stockholm, Sweden, May 23, 1996.
53. J Liu, D Rigsbee, C Stotz, MJ Pikal. J Pharm Sci 91:1853–1862, 2002.
54. CA Angell. Chem Rev 523–542, 1990.
55. CA Oksanen, G Zografi. Pharm Res 10:791–799, 1993.
56. P Meares. J Am Chem Soc 76:3415–3422, 1954.
57. K Kohlhammer, G Kothe, B Reck, H Ringsdorf, Ber Bunsenges. Phys Chem 93:1323–1325, 1989.
58. ML Williams, RF Landel, JD Ferry. J Am Chem Soc 77:3701 1955.
59. ML Roy, MJ Pikal, EC Rickard, AM Maloney. Dev Biol Stand 74:323–340, 1991.
60. MJ Pikal, ML Roy, DR Rigsbee. Eli Lilly & Co, unpublished data.

Copyright 2004 by Marcel Dekker, Inc. All Rights Reserved.

61. JA Rupley, G Careri. Adv Protein Chem 41:37–172, 1991.
62. DR Rigsbee, MJ Pikal. National AAPS Meeting, Orlando, Florida, Abstract #7418, 1993.
63. LN Bell, MJ Hageman, LM Muraoka. J Pharm Sci 84:707–712, 1995.
64. JL Green, J Fan, CA Angell. J Phys Chem 98:13780–13790, 1994.
65. IV Sochava, OI Smirnova. Food Hydrocolloids 6:513–524, 1993.
66. N-T Yu, BH Jo, CS Liu. J Am Chem Soc 94:7572–7575, 1972.
67. SJ Prestrelski, N Tedeschi, T Arakawa, JF Carpenter. Biophysical J 65: 661–671, 1993.
68. JF Carpenter, JH Crowe. Biochemistry 28:3916–3922, 1989.
69. SJ Prestrelski, T Arakawa, JF Carpenter. Arch Biochem Biophys 303:465–473, 1993.
70. RL Remmele, C Stushnoff. Biopolymers 34:365–370, 1994.
71. A Dong, P Huang, WS Caughey. Biochemistry 29:3303–3308, 1990.
72. SJ Prestrelski, KA Pikal, T Arakawa. Pharm Res 12:1250–1259, 1995.
73. BS Chang, NL Fischer. Colorado Protein Stability Symposium, Breckenridge, Colorado, July 17–20, 1994.
74. JC Lee, SN Timasheff. J Biol Chem 256:7193–7201, 1981.
75. T Arakawa, SN Timasheff. Biochemistry 21:6536–6544, 1982.
76. T Arakawa, SN Timasheff. Arch Biochem Biophys 224:169–177, 1983.
77. R Bhat, SN Timasheff. Protein Sci 1:1133–1143, 1992.
78. RA Robinson, RH Stokes. Electrolyte solutions. New York: Academic Press, 1959.
79. Handbook of Biochemistry and Molecular Biology. In: GD Fasman, ed. Physical and Chemical Data, Vol. 1, 3rd ed. Cleveland, OH: CRC Press, 1976, p 120.
80. BA Szkudlarek, GA Garcia, N Rodriguez-Hornedo. Pharm Res 13:S-85, 1996.
81. TJ Anchordoquy, JF Carpenter. Arch Biochem Biophys 332:231–238, 1996.
82. A Saleki-Gerhardt, G Zografi. Pharm Res 11:1166–1173, 1994.
83. EY Shalaev, F Franks. J Chem Soc Faraday Trans 91:1511–1517, 1995.

Copyright 2004 by Marcel Dekker, Inc. All Rights Reserved.

4

Freezing and Annealing Phenomena in Lyophilization

James A. Searles
Global Parenteral Products, Manufacturing Science and Technology, Eli Lilly and Company, Indianapolis, Indiana, U.S.A.

I. INTRODUCTION

The freezing step of lyophilization is of paramount importance. It is the principal dehydration step, and it determines the morphology and pore sizes of the ice and product phases. In general the desired attributes of a lyophilized product are: consistent, and if possible, high yield of active ingredient (e.g., activity) through lyophilization; appropriate crystallization (or not) of product and excipient(s); glass transition temperature higher than the desired storage temperature (related directly to residual moisture level); pharmaceutically elegant, mechanically strong cake; rapid reconstitution; fast and robust freeze-drying cycle; and stability of all product quality attributes through the intended shelf-life [1]. The means of freezing as well as any post-freezing temperature excursions above T_g' (the glass transition temperature at maximum freeze concentration) and/or the eutectic temperature influence many of the above attributes. This chapter will explain the freezing process, the most common freezing methods, and review how freezing can affect process and product quality parameters including primary and secondary drying rates, surface area, solute crystallization, product aggregation and denaturation, storage stability, reconstitution, and inter- and intra-batch consistency.

Copyright 2004 by Marcel Dekker, Inc. All Rights Reserved.

II. PROCESS PHYSICS—THE SUPPLEMENTED PHASE DIAGRAM

A discussion of freezing, annealing, and lyophilization is aided by viewing the process through the "supplemented phase diagram" first described by MacKenzie [2]. It is an equilibrium freezing point depression diagram supplemented with the glass transition curve (and solute crystallization and/or precipitation curve(s) as appropriate). Shown in Figure 1 is such a diagram for sucrose using data from Blond et al. [3] and Searles et al. [4]. The x axis is solute concentration in the non-ice phase, and the y axis is temperature. Sucrose does not crystallize during freeze concentration, so there is no eutectic point shown in Figure 1. If crystallizing solutes are being used (e.g., mannitol or glycine) then it would be important to add the appropriate eutectic points and phase lines for the crystallizing solute. The diagram will be explained in the context of freezing, annealing, and lyophilizing a 10% (w/w) sucrose solution.

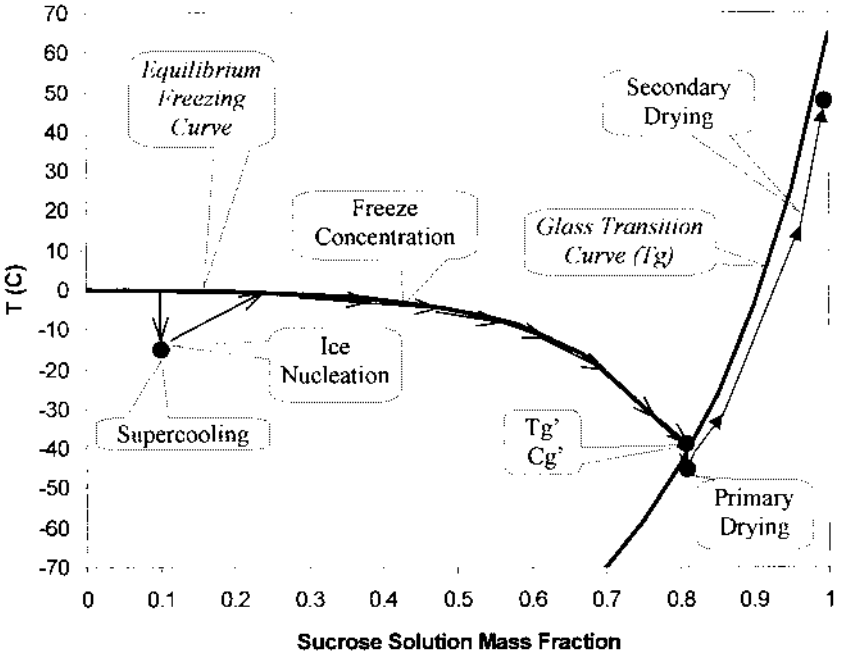

Figure 1 Supplemented phase diagram for sucrose. Arrows show freeze-drying process for a 10% sucrose solution.

Copyright 2004 by Marcel Dekker, Inc. All Rights Reserved.

In our example we will freeze vials containing the sucrose solution on the lyophilizer shelf as the shelf temperature is slowly reduced ("shelf-ramp" freezing). This method is undoubtedly the most prevalent in the pharmaceutical industry (not necessarily because it is the best method but because there are so few choices available—other freezing methods will be discussed in Section II). Figure 2 shows examples of the shelf and liquid temperatures through this process. For the present example we will assume that the liquid height in the vials and cooling rate are low enough such that the entire sample volume achieves a similar extent of supercooling before nucleation occurs. As discussed further below, this is termed "global supercooling," and the results of this type of freezing are naturally variable because nucleation is spontaneous and not under direct control. When freezing in this manner the nucleation temperature varies considerably from vial to vial [5].

When nucleation occurs in this sample, ice crystals grow to encompass the entire liquid volume because the entire liquid volume has nominally the same extent of supercooling. However, only a fraction of freezable water crystallizes during this initial nucleation event because crystallization is exothermic, and the supercooling is not sufficient to allow complete solidification. For a sample that nucleates at −15°C, about 20% of

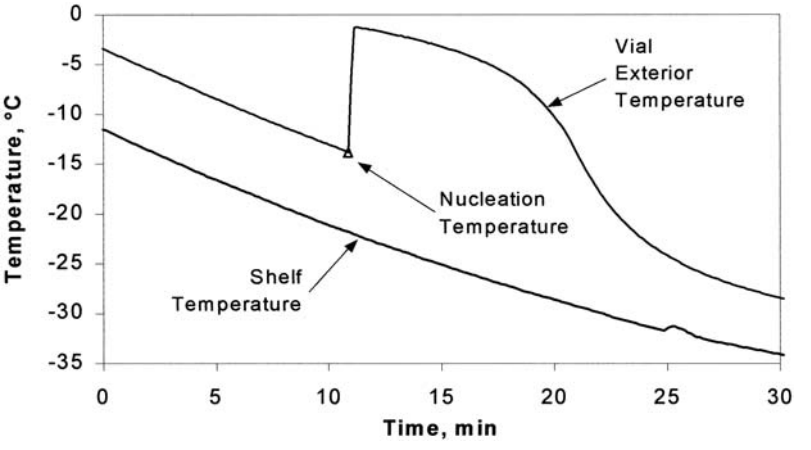

Figure 2 Shelf and vial temperature for shelf-ramp cooling: 2 mL of 10% hydroxyethyl starch (HES) in a 5 mL vial instrumented with a 36 gauge externally attached thermocouple. Nucleation occurs at −14°C, after which the supercooling is consumed by the latent heat of ice crystallization. The subsequent solidification of the nucleated volume occurs with a gradual temperature decrease (From Ref. 3).

Copyright 2004 by Marcel Dekker, Inc. All Rights Reserved.

freezable water crystallizes before the supercooling is extinguished [5] and the temperature reaches the equilibrium freezing temperature for the newly freeze-concentrated solution. For such a vial the sucrose solution concentration has risen to 24% and the solution temperature is near -1°C. However, the shelf temperature continues to decrease, and is now approximately -22°C. This provides a strong driving force for the completion of solidification, evidenced by the decreasing sample temperature.

Through the subsequent cooling as the shelf temperature continues to drop to -50°C, freeze concentration continues until the solution reaches the glass transition temperature at maximum freeze concentration, denoted as T'_g. The corresponding concentration is C'_g. This is shown on Figure 1, and is the intersection of the freezing point depression and glass transition curves. At this point any further thermodynamically favored freeze concentration is arrested by the high viscosity of the sucrose phase. The mobility of the water in this phase is too low to permit further migration of water to the ice interface for crystallization. The sucrose phase has reached a glassy state characterized by its high viscosity.

It is important to note at this point that the glass transition curve shown is actually one of a family of isoviscosity curves. The particular one shown corresponds to time scales relevant to our process, which for lyophilization is on the order of days. This means that if we hold a sample under these conditions for several days, we will not observe further freeze concentration. If we hold it for weeks, however, we might observe further freeze-concentration. The time scale of interest for the period from release to expiry is years. Therefore the T'_g determined using a rapid scanning technique like DSC is just a starting point for understanding the T'_g relevant to lyophilization and the final T_g appropriate for estimations of storage stability. Many have found that the faster the DSC scan rate, the higher the measured glass transition temperature. However, scan rates on the order of days are impractical because the intensity of the thermal transitions is too low to be measurable. Therefore for determining the sample temperature below which primary drying should be carried out to prevent collapse, T'_g should be a functional description of that temperature below which collapse is not observed. Searles et al. [4] and Ablett et al. [6] present methods to measure T'_g over time scales relevant to lyophilization. In addition, freeze-dry microscopy is commonly used to estimate collapse temperatures and observe other freezing and drying phenomena.

At T'_g the sucrose concentration in the amorphous phase is 81%, an eight-fold concentration increase. A material balance on the ice and amorphous phases reveals that at this point 88% of the water has frozen. The overall concentration of solutes during freeze concentration increases the potential for degradative processes. As stated by Felix Franks,

Copyright 2004 by Marcel Dekker, Inc. All Rights Reserved.

"chemical reaction rates in part-frozen solutions are substantially higher than in the original dilute solution at room temperature. The rate-enhancing effect of concentration far outweighs the rate-reducing effect of low temperature" [7]. Oxidation is a particular case. While the rate constant for an oxidation reaction will decrease with decreasing temperature, the overall rate of such a reaction can increase because the solubility of gasses in liquids is inversely proportional to temperature. It increases nearly two-fold between 25 and 0°C. In addition freeze concentration can combine with this effect to increase oxygen concentration to 1000 times that at 0°C [8] and increase oxidation rates [9].

Annealing is a hold step at a temperature above the glass transition temperature. Annealing can be carried out as a waypoint during the initial cooling, but more commonly it is a post-freezing warming and hold step, followed by recooling. For our present example the shelf temperature would be raised from −50°C to the annealing temperature (e.g., −20°C). The sucrose solution will follow the equilibrium freezing curve and equilibrate at 70% sucrose in the non-ice phase. This is the mechanism by which super-T_g' annealing results in *ice melting*: the ice fraction decreases to dilute the sucrose phase. The sample is now well above its glass transition temperature and a number of processes are free to take place. These include ice crystal maturation through Ostwald ripening, the crystallization of solutes, and possibly degradative reactions. These phenomena will be discussed further below.

The freezing step and any post-freezing temperature deviations above T_g' will determine the texture, or morphology of the product. As discussed in Section VI below, the morphology of the system has profound impacts upon drying rates, protein aggregation, and reconstitution. Figure 3 shows examples of product morphology before and after annealing.

We will now continue our tour of lyophilization using the supplemented phase diagram as our roadmap. Primary drying should take place at a temperature safely below T_g' and, although some secondary drying is know to occur during the primary drying phase of lyophilization, by definition primary drying includes only the sublimation of crystalline water from the system, and the solute phase concentration does not change. During secondary drying the shelf temperature is increased (and some practitioners also decrease the pressure set point for secondary drying). As the sample dries its T_g increases as shown on Figure 1. During an optimum secondary drying phase the sample temperature will be raised at a rate such that the product temperature always remains just below the glass transition temperature. As with primary drying, exceeding the glass transition temperature at any time during drying will lead to some extent of product collapse depending upon the duration of the event. In rare cases limited

Copyright 2004 by Marcel Dekker, Inc. All Rights Reserved.

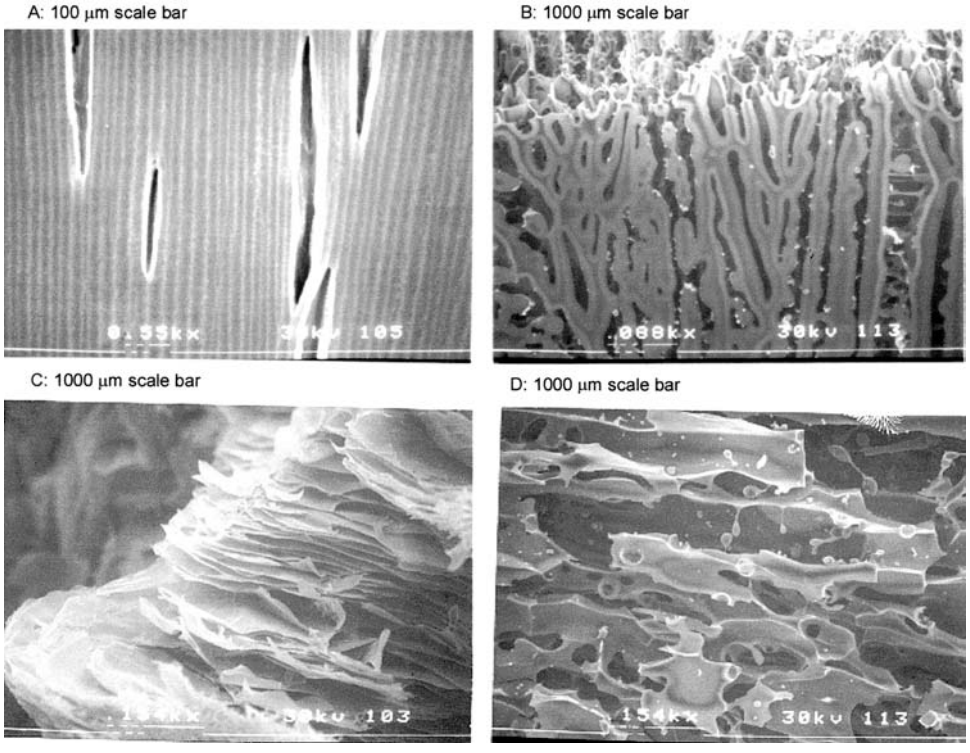

Figure 3 Scanning electron micrographs (SEMs) of 10% hydroxyethyl starch (HES) frozen in a vial by liquid nitrogen immersion. (A) and (B): top of the cake (A unannealed, B annealed); (C) and (D): interior of broken cake (C unannealed, D annealed) (From Ref. 4).

Copyright 2004 by Marcel Dekker, Inc. All Rights Reserved.

collapse is intentionally induced, but in general, collapse is cause for rejection of lyophilized pharmaceuticals.

The following sections will discuss specific product effects of different freezing methods and annealing steps. We will first review freezing methods and then explore how these methods, used in some cases with annealing, have been found to affect product quality and processing attributes.

III. FREEZING METHODS

Various freezing methods can be used, although some are not appropriate for full-scale GMP production of sterile pharmaceuticals. Principal methods are listed below in order of increasing cooling rate:

1. Slow directional solidification: creating ice nuclei on the bottom of a vial by contact with dry ice, followed by slow freezing on a pre-cooled shelf [10,11].
2. Placing vials on a shelf which is them ramped from above freezing temperature to below T'_g (''shelf-ramp'' freezing).
3. Placing vials in a freezer or on a lyophilizer shelf which is already below freezing temperature (''precooled shelf'' freezing).
4. Immersion in refrigerated heat transfer fluid (e.g., dry ice in alcohol).
5. Blast freezing via forced air and/or sprayed liquid nitrogen.
6. Liquid nitrogen immersion freezing (vial immersion).
7. Spraying of droplets into liquid nitrogen [12,13].

By far the most common method is the second one listed—shelf-ramp freezing. There are no issues with condensation on the shelves during loading, (other methods require freezing outside of the lyophilizer) and all lyophilizers can carry out this type of freezing without modification.

While many in the past have interchangeably used the terms ''cooling rate'' and ''freezing rate'' it is important to distinguish between them. The cooling rate is the rate at which the vial is cooled. This cooling rate may affect the temperature at which ice nucleates or, more precisely, the regions of the liquid volume over which nucleation occurs. The freezing rate only applies to the post-nucleation freezing which in some limited cases is irrelevant for determination of the final ice structure. A true freezing rate is in terms of either a linear front velocity for directional freezing, or mass per unit time for bulk freezing operations.

As discussed in Searles et al. the following terms are useful when discussing freezing for lyophilization. *Primary nucleation* is the initial ice nucleation event [5]. *Secondary nucleation* follows primary nucleation, and

Copyright 2004 by Marcel Dekker, Inc. All Rights Reserved.

moves with a velocity on the order of mm/s to encompass some portion of the liquid volume [14–16]. Subsequent to secondary nucleation, *solidification* is completed relatively slowly as the heat of crystallization is transferred from the solidification interface through the already-solidified layer and the vial bottom to the shelf. These terms pertain to freezing by *global supercooling* in which the entire liquid volume achieves a similar level of supercooling, and the secondary nucleation zone encompasses the entire liquid volume (as in the example in the previous section). Given the design of lyophilizer shelf temperature control systems, shelf-ramp freezing is by nature slow and it will, with typical vials and fill volumes, freeze by global supercooling, which yields a low surface area. In contrast, *directional solidification* occurs when a small portion of the volume is supercooled to the point of primary and secondary nucleation. The nucleation and solidification fronts are in close proximity in space and time with the front moving into non-nucleated liquid. Many write about liquid nitrogen immersion freezing inducing less supercooling than slower cooling methods, but more accurately faster cooling results in supercooling over a smaller *volume* before nucleation than slower cooling.

IV. MORPHOLOGY, SURFACE AREA, AND DRYING RATE

The freezing method and cooling rate during freezing have profound impacts upon the morphology and surface area of the final product. These parameters can be easily modified by any annealing steps (intentional or accidental), and the parameters in turn determine the resistance to vapor flow (affecting the primary drying rate and temperature during drying) as well as the secondary drying rate.

Reviews of early literature on lyophilization freezing and annealing phenomena appear in recent papers by Searles et al. [4,5] parts of which will be recapitulated here. In 1925 Tammann reported that the ice crystal morphology can be strongly influenced the nucleation temperature [17]. Samples frozen at ''low supercoolings'' yielded dendritic structures, whereas ''crystal filaments'' result from high supercoolings. In 1961 Rey described an annealing step for orange juice that resulted in a two-fold increase in the primary drying rate [18]. MacKenzie and Luyet in 1963 showed that annealing 30% gelatin gels resulted in slower primary drying [19]. It is likely that the extremely high solute concentration resulted in a low volume fraction of ice (<50%), in which case one would expect annealing to facilitate complete encasement of the ice crystals as the authors reported. Luyet and co-workers published several papers on ice morphology. Luyet and Rapatz identified hexagonal, dendritic, and dispersed spherulitic

Copyright 2004 by Marcel Dekker, Inc. All Rights Reserved.

morphologies in response to different freezing protocols and solutes in aqueous systems [20,21]. The morphology was dependent upon the freezing temperature, solute, and concentration. In one case the ice morphology in glycerol solutions shifted from hexagonal, to "irregular," to spherulitic with increasing supercooling [21].

Quast and Karel in 1968 published results on the effect of freezing method upon the subsequent dry layer resistance to gas flow [22]. They also provide a thorough review of earlier works on the subject. They studied concentrated coffee (20% and 30% solids) as well as a model food system (10% glucose, 10% microcrystalline cellulose, 2% starch). The samples were frozen in 25 mm diameter glass cylinders 20 mm long, which were frozen by liquid nitrogen immersion; or incubation in a freezer set at $-5^{\circ}C$, $-20^{\circ}C$, or $-40^{\circ}C$. In addition some samples frozen at $-40^{\circ}C$ were first seeded with ice crystals. Samples were frozen by the method being tested, freeze-dried, then placed in a gas flow cell for resistance measurement over a range of pressures. Higher solute concentrations led to greater resistance. Liquid nitrogen freezing yielded samples of the lowest resistance, after which, listed in order of increasing resistance, were the $-5^{\circ}C$, $-20^{\circ}C$, $-40^{\circ}C$ seeded, and $-40^{\circ}C$ methods. Therefore with the exception of liquid nitrogen immersion, the "faster" the freezing, the higher the resistance. All methods except the $-40^{\circ}C$ seeded method yielded a layer at the top of the sample of much greater resistance per unit length than the material making up the remainder of the sample. Liquid nitrogen frozen samples cracked extensively during drying.

Thijssen and Rulkens reported in 1969 that the freezing rate is an important determinant of pore size and drying rate in freeze-drying of liquid food products [23]. For a 20% dextran solution freeze-dried in slabs, a faster cooling rate during freezing resulted in smaller pores and therefore higher resistance and slower drying rates. In 1969 Blond et al. published results of solidification studies that show the dramatic effects of freezing rate upon surface area for polystyrene, starch, and silica gels [24,25]. Surface areas after sublimation increased dramatically with higher cooling rates during solidification.

Pikal et al. in 1983 found that annealing resulted in larger ice crystal sizes for small (5 μL) samples that were frozen rapidly between glass coverslips [26]. With sublimation studies in a 13 μL microbalance apparatus, Pikal et al. also showed that annealing resulted in an up to 50% decrease in the normalized dry product resistance during primary drying, but actual drying rates were not presented, and annealing was not tested on products frozen and dried in vials.

Nakamura et al. studied the effect of freezing conditions upon the sublimation rate of coffee extract [27]. The study was hindered by the

Copyright 2004 by Marcel Dekker, Inc. All Rights Reserved.

cracking of samples frozen with liquid nitrogen, which in their system also affected heat transfer to the sublimation interface. This prevented the authors from making any conclusions about the effect of freezing rate.

Roy and Pikal established an early linkage between the ice nucleation temperature and the subsequent primary drying rate [28]. They found that sample vials with internally placed thermocouples nucleated at higher temperatures and completed primary drying sooner than samples without thermocouples. Several have linked the nucleation temperature (extent of global supercooling) to ice crystal morphology [17,20,21].

In 1991 Kochs et al. reported on the effects of the directional solidification process parameters upon primary dendritic spacing for samples of 10% hydroxyethyl starch (HES) in a freeze-drying microscope fitted for controlled directional freezing and sublimation [29]. The samples were 0.3 mm in thickness, 1.2 mm wide, and 100 mm long. Cooling was applied at one end of the sample, and columnar ice crystals grew in the direction of heat transfer. Faster cooling rates resulted in decreased column spacing, leading to greater resistance and slower drying. The primary dendritic spacing was found to be proportional to the product $v^{-1/4}G^{-1/2}$ where v is the interface velocity and G is the temperature gradient at the interface. They also found a linear relationship between the diffusion coefficient for vapor transport through the dried layer, the lamellar spacing, and in turn the primary drying rate.

In a companion paper they examined effect of freezing conditions upon the primary drying rate for 23 mL samples and found higher primary drying rates for samples that had been frozen with slower post-nucleation cooling rates during solidification [30]. In addition they analyzed temperature and drying rate data for these samples and found product resistance at the top of the samples to be significantly higher than at the bottom. However, they did not report upon the microscopic appearance of the samples.

Dawson and Hockely demonstrated the effect of freezing conditions upon morphology for a variety of biological and carbohydrate formulations [31]. A 1% (w/v) trehalose formulation frozen by liquid nitrogen exhibited a fine filamentous directional network, whereas freezing by placement on a $-50^{\circ}C$ shelf yielded a leafy mixed-orientation appearance. The authors state that the rapidly frozen trehalose had less resistance to vapor flow during drying and reconstituted faster than the shelf-frozen samples.

Hsu et al. studied various freezing rates for shelf-ramp freezing, placement on a precooled shelf, and immersion into dry ice/isopropanol [32]. For shelf-ramp freezing they obtained lower cooling rates by using greater vial fill volumes in larger vials (keeping the vial:sample volume constant). Vials were instrumented with internal thermocouples near the

Copyright 2004 by Marcel Dekker, Inc. All Rights Reserved.

vial bottom, and the "freezing rate" was calculated as the post-nucleation cooling rate. The authors stated that for vials frozen by shelf-ramp nucleation appeared as a "sudden change in the appearance of the vial contents from a clear liquid to an opaque/translucent slush." This is indicative of global supercooling. Based upon the author's description of their observations of the freezing of vials in dry ice/isopropanol, freezing by that method yielded directional solidification. For samples frozen by shelf-ramp, the larger samples cooled slower before and after nucleation, achieved less supercooling, had lower surface areas, and better storage stability (discussed further in Section VI). The larger samples appear to nucleate at higher temperatures most likely because in a larger sample there would be less temperature homogeneity throughout the liquid volume at the time of nucleation. If when nucleation occurs at the bottom of the vial the temperature of the remaining volume is sufficiently low, the secondary nucleation front will propagate through the entire volume. Samples frozen by a pre-cooled shelf and those frozen by immersion in dry ice/isopropanol exhibited greater cooling rates, had larger surface areas, and poorer storage stability (see Section VI). When data from all vial sizes and cooling rates were plotted together, the surface area (ranging from 0.2 to 2 m^2/g) was a nonlinear function of the cooling rate, which ranged from 0.3 to 20°C/min.

Chemical composition can have a pronounced effect upon morphology. In particular one would think that surfactants have the potential to affect crystal structure and in fact they do. In studies of mannitol Haikala et al. found that polysorbate 80 concentrations even as low as 0.0001% resulted in altered morphology [33]. Increasing concentrations of the surfactant (from 0.0001% to 1%) resulted in generally coarser structure in which a fine, "lacy" structure gave way to large plates, longer reconstitution times, and greater mannitol crystallinity (particularly the δ form). Surfactants by definition preferentially populate the interface and thereby modify the thermodynamics of that interface. As discussed in Section VI below surfactants play a role in protecting active ingredients from interfacial damage during freezing.

Milton et al. demonstrated that partial collapse during primary drying could result in progressively decreasing resistance through primary drying itself [34]. Their findings were confirmed by direct observation of cake morphology. During drying of lactose near its collapse temperature small holes developed in the plate-like structures of the solid phase, lowering the resistance to vapor flow. Overcashier et al. studied the time course of product resistance to water vapor flow during the primary drying of recombinant humanized antibody and two placebo formulations over a range of pressures and shelf temperatures [35]. All samples were shelf-ramp frozen, product temperatures were measured via internal thermocouples,

Copyright 2004 by Marcel Dekker, Inc. All Rights Reserved.

and drying rates were determined gravimetrically by removing and weighing samples at intervals during the runs. Product resistances were calculated from the drying rate and temperature data, and the authors reported that in all cases resistance increased as the depth of dried sample increased. Although drying rates were constant (weight loss was linear with time), the calculated resistance increased due to the increase in measured product temperature through time. The resistance per unit thickness decreased from the top of the dried layer to the bottom. In addition they found, as had Milton et al. [34] that samples dried at higher temperatures had lower product resistance than their counterparts dried at lower product temperatures. This they attribute to localized collapse during primary drying at higher temperatures.

Franks in 1998 had suggested that the stochastic nature of nucleation results in heterogeneity among samples [36]. In a study published in 2001, Searles et al. confirmed this in their examination of the effect of nucleation temperature during shelf freezing upon the freezing mechanism, morphology and primary drying rate [5]. Using varying sample particulate content, vial scoring, and ice nucleating agents, they found the primary drying rate to correlate inversely with the extent of supercooling. To determine the nucleation temperature externally mounted thermocouples were used so as to not interfere with nucleation itself. Both global supercooling and directional solidification mechanisms were found to be possible for their system when frozen via shelf-ramp freezing, but that the latter only occurred with the aid of ice nucleating agents. Global supercooling freezing resulted in dispersed spherulitic morphology, and directional solidification was characterized by lamellar plate morphology. Ice crystal size is inversely correlated to the extent of supercooling; thereby the number of nuclei correlates directly with the extent of supercooling [37]. In cases where the supercooling exceeded 5°C, freezing took place via global supercooling. Sample cooling rates of 0.05 to 1°C/min had no effect upon nucleation temperatures and drying rate. Therefore within the "global supercooling" freezing regime the stochastic nucleation process is in control. Its stochastic nature is the cause of significant drying rate (and therefore temperature) heterogeneity for samples frozen by global supercooling [5]. Nucleation temperature heterogeneity may also result in variation in other morphology-related parameters such as surface area and secondary drying rate. Factors such as particulate content and vial condition, which influence ice nucleation temperature, must be carefully controlled to avoid, for example, lot-to-lot variability during cGMP production. The presence of operators has been found to be a significant source of particulates, [38] so the proximity of an operator during filling could result in atypically high particulate loading for a number of samples within a lot, and may lead to a subset of samples within

Copyright 2004 by Marcel Dekker, Inc. All Rights Reserved.

a lot nucleating earlier and drying faster. If the factors influencing nucleation temperature are not controlled and/or inadvertently changed during through-process development and scale-up a lyophilization cycle that was successful on the research scale may fail during large-scale production.

In a follow-on study, Searles et al. reported that post-freezing annealing can reduce freezing-induced heterogeneity in sublimation rates [4]. In addition they found annealing to result in several-fold drying rate increases. Aqueous solutions of hydroxyethyl starch (HES), sucrose, and HES:sucrose were frozen either by shelf-ramp or by liquid nitrogen immersion. Samples were then annealed for various durations over a range of temperatures and partially lyophilized to determine the primary drying rate. The drying rate results are shown in Figure 4. In some cases, annealing for only 30 min gave a substantial rate increase. Higher annealing temperatures and longer durations of annealing correlated with increased drying rates, but all drying rates appeared to be constrained by a maximum theoretical value. The cause was later identified to be a shift in control of the sublimation rate from mass transfer (water vapor transit through the dried layer of product) to energy transfer (energy from the shelf to the ice in the vial) due to the decreased mass transfer resistance of annealed samples [39].

The morphologies of fully dried liquid nitrogen-frozen samples were examined using scanning electron microscopy [4]. Figure 3 shows the morphologies of annealed and unannealed liquid nitrogen-frozen samples. Annealing resulted in the merging of the fine lamellar plate structures, reduction in surface area, larger pore sizes, and larger and more numerous holes on the cake surface of annealed samples. The mechanisms behind these changes are discussed in Section VIII. A wide range of post-annealing resolidification cooling rates did not affect the primary drying rate, and annealed HES samples dissolved slightly faster than their unannealed counterparts due to better wetting characteristics.

Annealing below T_g' did not result in increased drying rates. Based upon that finding the authors proposed a new annealing–lyophilization method of T_g' determination which can be carried out with only a balance and a freeze-dryer, measures T_g' over any time scale desired, and has the additional advantage that a large number of candidate formulations can be evaluated simultaneously [4].

Roth et al. used an in situ microbalance to measure the primary drying rate throughout primary drying for product in vials frozen by a variety of methods [40]. "Slow" freezing was by shelf-ramp from 10°C to −40°C at −0.14°C/min, "moderate" freezing was carried out in the same manner but cooling was at −1.7°C/min, and liquid nitrogen immersion was used as the "fast" freezing method. The microbalance enabled Roth et al. to observe changes in the drying rate through the entire period of

Copyright 2004 by Marcel Dekker, Inc. All Rights Reserved.

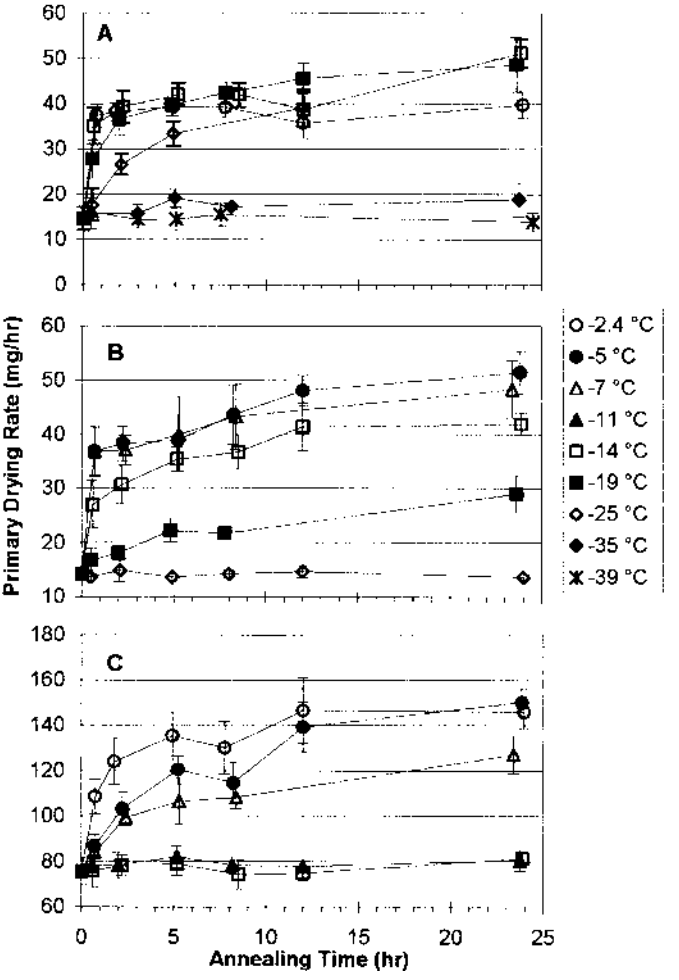

Figure 4 Primary drying rate as a function of annealing time and temperature for A 10% sucrose; B 5% sucrose, 5% hydroxyethyl starch (HES); C 10% HES. Groups A, B, and C were dried under different conditions (From Ref. 4).

primary drying. Drying rates through time for the slow and moderate freezing methods were virtually indistinguishable, but the fast freezing method resulted in samples that dried faster than the other methods.

Patapoff and Overcashier tested freezing methods and annealing upon primary drying rates, sample temperature during primary drying, dried product resistance, appearance of the freeze-dried cakes, and protein

Copyright 2004 by Marcel Dekker, Inc. All Rights Reserved.

aggregation [10]. Protein aggregation will be discussed in Section VI below. They tested a recombinant human antibody formulation. Cooling via immersion into a dry ice/ethanol bath resulted in the greatest product resistance and therefore slower sublimation rates and higher product temperatures. Shelf-ramp freezing and ice crystal seeded shelf-ramp freezing each resulted in successively less resistance. Samples frozen using the standard shelf-ramp method and annealed had the lowest resistance. The dry ice/ethanol and standard methods also formed a more resistive layer at the top of the sample. They also found that a placebo version of their formulation exhibited completely different freezing and drying characteristics than the active-containing formulation: the placebo dried significantly faster.

Vacuum-flask freeze-dryers are used in many laboratories for bulk lyophilization. They consist of a vacuum and condenser system to which glass flasks are attached externally. The liquid within the flasks is frozen by evaporative cooling. Kramer et al. used this principle to freeze solutions in vials within a freeze-dryer [41]. With vials loaded on a 10°C shelf, they reduced the pressure to 760 mT to induce the formation of a 1–3 mm thick layer of ice on the top of the solution within 5 min. The shelf temperature was then ramped down to −40°C to complete solidification and lyophilization was continued normally. The drying rates and morphologies of these samples were compared to those frozen by conventional shelf-ramp. In addition annealing was tested on samples frozen by both means. The evaporative nucleation method resulted in large "chimney-like" ice crystals, and the drying rates of some formulations were up to 20% faster. Annealing also resulted in increased drying rates. Shelf-ramp frozen sample morphology was spherulitic, and annealing of these samples increased the size of those spheroidal ice crystals.

Spray freeze-drying is a process in which fine droplets are sprayed through an ultrasonic nozzle directly into liquid nitrogen. The frozen droplets are then placed into vials and freeze-dried in a standard lyophilizer. They are of particular interest for pulmonary and epidermal delivery. Sonner et al. recently reported on the use of this technology using trypsinogen as a model protein [13]. They produced spherical particles with diameters from 20 to 90 μm that contain high internal porosity. Sonner et al. compared the properties of 20% trehalose samples that were spray freeze-dried and annealed during primary drying to those that were not annealed. Annealing caused the particles to shrivel. The authors tested the post-drying hygroscopicity of the particles by measuring moisture uptake rates. They found that the longer the particles were annealing during drying, the lower the subsequent moisture uptake rates. They theorized that annealing reduced the specific surface area of the particles, slowing water adsorption. Protein recovery results will be discussed in Section VI below.

Copyright 2004 by Marcel Dekker, Inc. All Rights Reserved.

Webb et al. studied several formulations of human interferon-γ, comparing liquid nitrogen immersion vial freezing with spray freezing [12]. Vial immersion resulted in a directional lamellar morphology, and the freeze-dried cakes were severely cracked. Spray freezing yielded spherical particles similar to Sonner et al [13]. Specific surface areas for the spray freeze-dried samples were 6.8–15 m^2/g, three to seven times those of their counterparts that were filled into vials and frozen by liquid nitrogen immersion. The liquid nitrogen immersion formulations contained more water at the end of freeze-drying than their spray freeze-dried counterparts, and reconstituted much more rapidly. The rapid reconstitution was a visually violent process with extensive bubble formation and some splattering of liquid onto the sides of the vials. Dissolution rates were not affected by the presence of 0.03% polysorbate 20. Annealing of the liquid nitrogen immersion frozen samples alleviated the cracking which occurred during drying, resulting in a more pharmaceutically elegant appearance. The internal microstructure of these samples was greatly simplified by annealing, leading to several-fold surface area reductions, faster primary drying, and slightly higher moisture levels after lyophilization. The annealed samples did not exhibit the bubbling and splattering during reconstitution, and reconstitution times were longer. Annealing also had profound impacts upon the spray freeze-dried samples. Surface areas of these samples were reduced by up to 30-fold. Regardless of the freezing method all samples tended toward a surface area of 0.5–1.0 m^2/g after annealing. After annealing the spray-frozen spheres appeared as agglomerated hollow shells, indicating that the spheres had collapsed outward toward their outer shells, and that some merging of adjacent shells had occurred. Annealing of these samples also resulted in faster primary drying and higher final moisture contents [12]. In 1990 Pikal et al. showed that for solutions of moxalactam disodium the *secondary* drying rate is proportional to the specific surface area (m^2/g) of the sample [42]. The fact that annealing decreases surface areas provides the linkage necessary to state that those of Pikal et al. corroborate the observation by Webb et al.

The stress relaxation and morphological changes that result from annealing can affect reconstitution. Those changes that allow more efficient water vapor transport during drying may also improve wetability of the porous matrix. For example, the holes formed in the ''skin'' layer on the surface of the cake may allow easier liquid penetration. However, simplification of the matrix morphology will increase the thickness of the matrix structures and reduce the surface area, which could slow dissolution. Webb et al. also found that annealed spray freeze-dried samples dissolved slightly faster than their unannealed counterparts during reconstitution [12]. Conversely, however, the annealed lyophilized samples dissolved more

Copyright 2004 by Marcel Dekker, Inc. All Rights Reserved.

slowly. This is in contrast to results of Searles et al. who found that the same formulation dissolved slightly faster after annealing, but the drying protocols for the two studies were different [4].

V. NON-AQUEOUS COSOLVENT SYSTEMS

As discussed above, the chemical makeup of a sample will play a large role in its freezing behavior. Non-aqueous cosolvent systems are no exception. Readers are referred to Teagarden and Baker for a comprehensive review of these systems in lyophilization [43]. Advantages of such systems include "increased drug wetting or solubility, increased sublimation rates, increased pre-dried bulk solution or dried product stability, decreased reconstitution time, and enhancement of sterility assurance of the pre-dried bulk solution" [43]. Disadvantages are requirements for additional manufacturing safety precautions, potential unique equipment modifications for solvent condensation, qualification of appropriate GMP purity, and increased regulatory scrutiny. This section will be confined to changes that cosolvents impart to freezing behavior.

Kasraian and DeLuca studied sucrose formulations with and without tertiary butyl alcohol (TBA). They found that inclusion of TBA resulted in the formation of large, columnar ice crystals [44] that appear characteristic of directional solidification. Sucrose with TBA was found to dry at one-tenth the rate, and the cake appearance indicated the presence of spheroidal ice crystals. Product resistance was dominated by a layer at the top of the cake for the sucrose-only formulation, whereas for the TBA-containing samples resistance was order of magnitude lower and appeared constant throughout the cake depth. Surface area measurements confirmed that the specific surface area of the TBA formulation was over 10 times that of the sucrose-only formulation (8.6 vs. $0.67\,m^2/g$) consistent with the high surface-to-volume ratio of columnar compared to spheroidal shapes. Others have found the addition of TBA to improve sublimation rates for their formulations [43].

In studies of sucrose lyophilization in a water/TBA cosolvent system Wittaya-Areekul and Nail found that the method of freezing affected the level of residual TBA after drying [45]. Freezing by shelf-ramp resulted in lower residual TBA levels than liquid nitrogen immersion freezing. The authors theorized that the slower cooling rate facilitated more complete crystallization of the TBA during freezing. It may be that these crystalline regions sublimate more rapidly than non-crystalline TBA can diffuse and desorb from the solid phase.

Copyright 2004 by Marcel Dekker, Inc. All Rights Reserved.

Wittaya-Areekul et al. found that annealing facilitated more complete crystallization of TBA in an aqueous solution of tobramycin, which resulted in lower levels of residual TBA after lyophilization [46]. While residual TBA was correlated with extent of TBA crystallization, residual isopropyl alcohol (IPA), which is an impurity in TBA, was highest with the annealed case. IPA does not crystallize, and the lower surface area and increased diffusion path length resulted in the annealed samples having the highest levels of residual IPA.

In two cited cases annealing was found to facilitate greater removal of *tert*-butanol, which the authors ascribed to crystallization of the cosolvent during annealing. Annealing also improved the uniformity of moisture levels among the samples.

VI. EFFECTS UPON ACTIVE INGREDIENTS

Freezing itself can adversely affect the active ingredient, and the freezing method can also affect the quality of the product through subsequent processing and until expiry. These impacts can result from the low temperature itself, acceleration of degradation reactions, crystallization of the product, product denaturation and aggregation, pH shifts, phase separation, and denaturation at the ice interface. Much of the literature on this subject concerns the stabilization of proteins. The interested reader is referred to comprehensive reviews of protein formulation and lyophilization [47–49]. This section will cover how freezing itself can have a major influence upon success of the formulation and the lyophilization process. Product crystallization will be covered in Section VII.

Proteins are prone to denaturation at both high and low temperatures. Although cold denaturation is frequently mistaken for freezing denaturation, it is known to occur in the absence of freeze concentration. For example, as early as 1930 it was reported that the rate of ovalbumin denaturation by urea is higher at 0°C than at 23°C [50]. Privalov provides a comprehensive review of the subject [51].

Several have found that faster freezing results in greater protein aggregation. In freeze–thaw studies Eckhardt et al. found that the formation of insoluble aggregates of recombinant human growth hormone during freezing increased sharply with increased cooling rates [52]. The authors stated possible causes to be surface denaturation, or recrystallization during thawing of rapidly frozen samples. Skrabanja et al. report on freezing method and formulation effects upon monoclonal antibody aggregation formation [53]. Rapid freezing by immersion in CO_2/acetone resulted in greater aggregation after freezing than slow freezing by placing vials into

Copyright 2004 by Marcel Dekker, Inc. All Rights Reserved.

a freezer at −20°C. In another study discussed in the same paper they report on recovery of a recombinant protein after lyophilization. The fast freeze yielded marginally higher yield than freezing by either shelf-ramp or a pre-cooled shelf. Chang et al. showed that denaturation of proteins during freezing is closely related to surface denaturation by quantifying both types of denaturation for a range of proteins [54]. A strong correlation ($r = 0.99$) was observed between the tendency of a protein to denature by freezing and its tendency to surface denature. Freezing by liquid nitrogen immersion caused more denaturation than shelf-ramp freezing. Small quantities of surfactant provided protection to the proteins against both types of inactivation (six surfactants were tested). A subsequent study from the same research group showed that surfactants stabilize against surface denaturation by competing with stress-induced soluble aggregates for interfaces, inhibiting subsequent transition to insoluble aggregates [55]. Jiang and Nail studied catalase, β-galactosidase, and LDH in phosphate buffers, and found that shelf-frozen samples retained more protein activity than those frozen by liquid nitrogen immersion [56]. Freezing by placement in a −40°C freezer yielded even better recovery. In all cases freeze/thaw as well as lyophilization protein activity retention was found to improve with protein concentration. This is possibly an artifact of constant loss of a given mass of protein. As the concentration is increased the fraction recovered increases but the same mass is lost. Jiang and Nail also found that the activity recovery increased with increasing residual moisture, suggesting that the drying process also contributed to loss.

The trend of greater protein losses via faster freezing continued with the finding by Sarciaux et al. that liquid nitrogen quench freezing of an antibody formulation resulted in more and larger insoluble aggregates than shelf-ramp freezing [57]. As discussed in detail above, Hsu et al. showed a clear correlation between surface area and cooling rate by using various cooling methods and vial sizes. They also found that poorer storage *stability* of their protein correlated inversely with the specific surface area, providing a linkage between the freezing method and rate and product stability through time after lyophilization [32]. Stability was even affected by the choice of vial and volume of fill through this linkage to the cooling rate for freezing–smaller fills in smaller vials resulted in greater product specific surface areas. No freeze/thaw protein loss was found. The authors stated that the phenomenon of lower stability for higher surface area samples might arise from possible lack of protection by the arginine excipient for those protein molecules at the surface of the amorphous phase. Citing preliminary results, Patapoff and Overcashier also found that annealing significantly reduced the rate of protein aggregation during storage stability studies [10].

Copyright 2004 by Marcel Dekker, Inc. All Rights Reserved.

Nema and Avis found contradictory evidence for protein denaturation in that fast freezing by liquid nitrogen resulted (88% recovery) in better retention of lactate dehydrogenase (LDH) activity than shelf-ramp freezing (68%) [58]. The authors did not identify a specific mode of action responsible. The protein was formulated neat with no buffers or cryopreservatives. They did test a number of cryoprotectants with self-ramp freezing, and found three formulations which afforded protection: 1% w/v bovine serum albumin, 1 M sucrose, and 0.05% w/v Brij 30. It is possible that during shelf-ramp freezing degradative reactions are taking place in the partially freeze-concentrated product phase during the slow solidification after ice nucleation. For this reason one would expect that a post-freezing annealing step would adversely affect any products for which shelf-ramp freezing yields are poorer than those for liquid nitrogen immersion.

Sarciaux et al. found that lyophilization resulted in insoluble aggregates of their bovine IgG formulations, but the damage was not observed after freeze/thaw [57]. Freezing by shelf-ramp resulted in less post-lyo aggregation than liquid nitrogen immersion freezing, and annealing reduced the damage further. The authors correlated the extent of aggregation with surface area, and found that aggregation progressed through the secondary drying step of lyophilization. Annealing reduced the percentage of aggregate in the final product from 33 to 12% [59]. The reduction was attributed to the lower surface area of the annealed samples. However, a new theory posits that these benefits may have been due to stress relaxation: the publication by Webb et al. reports that liquid nitrogen immersion and lyophilization resulted in greater yields of human interferon-γ then spray freeze-drying [12]. As discussed above, spray freezing yielded several times greater specific surface area than the immersion method. However, like Sarciaux et al. the authors did not find any freeze/thaw damage caused by spray freeze-drying, rather the damage was found to occur during the terminal stages of drying. The authors speculated that, instead of surface denaturation, which was ruled out by the ultrahigh cooling rates for spray freezing, residual stress retained within the solid matrix was responsible for the protein damage. Additional evidence to support their finding is provided by the fact that annealing relieves this stress and reduces the protein loss. Unfortunately Sonner et al. do not comment upon the effects of annealing upon protein recovery [13]. However, they did find that while spray freezing did not damage their protein, the subsequent freeze-drying step did. Shelf-ramp freezing and freeze-drying resulted in a similar level of damage, and polysorbate 80 in the formulation reduced the damage for both types of samples.

Freeze concentration may bring solutes into concentration ranges where they will phase separate, causing deleterious effects upon the product

Copyright 2004 by Marcel Dekker, Inc. All Rights Reserved.

[11,60–67]. Heller et al. demonstrated that the increased mobility during annealing facilitated phase separation in a PEG:Dextran formulation. The phase separation caused unfolding of recombinant hemoglobin, and they used formulation design strategies [63] and PEGylation of the protein [64] to avoid the damage. The freezing step has also been found to be critical in lyophilization of DNA for gene therapy [68,69].

VII. SOLUTE CRYSTALLIZATION

Many have found solute crystallinity to be strongly dependent upon the freezing method and annealing. This is understandable given the extreme freeze concentration that occurs through the freezing process. Supersaturation of some components can result if freezing is too rapid to allow complete crystallization. Dire consequences can result. If, for example, mannitol is not completely crystallized by the completion of lyophilization it may crystallize during subsequent storage, releasing waters of hydration and causing the lyophilized cake to seemingly spontaneously collapse. Mannitol is of great interest because it is widely used as a bulking agent for lyophilization, but it is only effective as a bulking agent when in the crystalline form. In addition to the dangers of incomplete crystallization, one must be aware of the fact that mannitol crystallization can cause vial breakage if the freezing step is not carried out appropriately [70,71]. Glycine is also used as a crystalline bulking agent [72]. These agents provide mechanical strength to the cake during drying and storage, and, if fully crystalline, provide excellent protection against collapse. A recent report cites a significant of crystalline mannitol—it can prevent collapse of a sucrose cake during drying at $-10^{\circ}C$ even though sucrose alone will collapse at $-40^{\circ}C$ [73].

Pikal-Cleland showed that the presence of glycine reduced the freeze concentration-induced pH drop in phosphate buffers depending upon the buffer and phosphate concentrations [74]. The greatest benefit was with 10 mM (rather than 100 mM) buffer, and glycine concentrations ≤ 50 mM. The authors found that the reduction in pH change was the result of decreased crystallization of disodium phosphate, and theorized that glycine hindered nucleation of the disodium phosphate by forming a glycine sodium salt. Interestingly for 10 mM phosphate buffer, the presence of glycine concentrations ≥ 100 mM resulted in greater pH drops than for no glycine at all. This was linked to more complete crystallization of disodium phosphate. Recovery of LDH activity after freeze/thaw was improved from ~80% to 100% by the use of intermediate glycine concentrations (75–250 mM) regardless of the pH shift during freezing.

Copyright 2004 by Marcel Dekker, Inc. All Rights Reserved.

Cannon and Trappler found that the freezing method affected the crystalline polymorph of 70 mM mannitol solutions [75]. Crystalline content was evaluated after lyophilization. Shelf-ramp freezing produced mostly the δ-form with a minor presence of the α polymorph, and freezing on a pre-cooled shelf led to mostly α with minor β content. Addition of a 4 h hold step at −20°C during the shelf-ramp protocol yielded a sample that contained only the δ polymorph. Annealing a shelf-ramp frozen sample at −20°C for 1 h resulted in only the β form.

A very important topic related to solute crystallization is the extreme pH drops that can occur when freezing solutions containing phosphate buffer systems. A recent publication by Gomez et al. provides a thorough characterization of the phenomenon [76]. The pH drop is caused by precipitation of the disodium salt during freeze concentration. They present dramatic time-course pH data through the freezing process, illustrating that for solutions with an initial pH of 7.4, the pH after freezing can be as low as 4. Sodium chloride also crystallizes during freeze concentration [77,78].

In some cases product crystallization can occur. Oguchi studied the freezing of methyl *p*-hydroxybenzoate (MPHB) and found that the freezing rate affected crystallization of the MPHB [79]. Rapid freezing resulted in amorphous MPHB while slow freezing caused crystalline inclusion complexes of the product. Slow freezing was by incubation at −13°C, and rapid freezing was by immersion in liquid nitrogen. Williams and Swhwinke reported on their efforts to produce crystalline pentamidine isethionate after lyophilization [80]. Normal shelf-ramp freezing and lyophilization of their 100 mg/mL formulation resulted in product crystallization within only about 20% of the samples. This was improved to 80% using a 15 h −5°C pre-freezing hold that exploited the fact that at 5°C the solubility of their product was only 39 mg/mL. Macroscopic appearance was markedly different as well. Those which were frozen subsequent to product crystallization were "fluffy and the particles clung together like a cotton ball," while the conventionally frozen sample cakes appeared hard and compact. Photostability of fully crystalline material was better as well. Chongprasert et al. used a similar method for pentamidine isethionate (PI) [81]. The product was held at 2°C prior to freezing to induce precipitation of a PI trihydrate that converted to an anhydrous crystal form during lyophilization. A different anhydrous crystal form was observed to result from liquid nitrogen immersion freezing. The authors found that when shelf-ramp frozen, the PI sometimes crystallized from solution before ice nucleation, and in the other cases crystallized as the other form subsequent to ice nucleation. In some cases both types were found within different regions of the same product cake. Therefore in this case the stochastic nature has been found to have a profound effect upon a product quality attribute.

Copyright 2004 by Marcel Dekker, Inc. All Rights Reserved.

Skrabanja et al. presented an interesting consequence of phosphate precipitation [53]. They studied a solution of sucrose in a buffer of citric acid and dibasic sodium phosphate. Non-enzymatic browning was observed after 1 month of storage at 60°C, caused by a pH drop resulting from the crystallization of sodium phosphate. The pH drop had caused hydrolization of sucrose into fructose and glucose. Glucose is a reducing sugar that could then bind to a protein product in the formulation via the Maillard ''browning'' reaction.

Izutsu et al. reported in 1993 that amorphous mannitol provides some protection to β galactosidase during freeze/thaw, but that crystallization during annealing reduced the protein stabilizing effects of the solute [82]. Greater activity of annealed samples remained after freeze/thaw than after lyophilization–reconstitution, confirming that damage also occurs throughout the process. In 1994 the same research group published results of a follow-on study in which they used annealing to crystallize mannitol in three different formulations, each containing a different protein [83]. In each case annealing led to mannitol crystallization, which caused protein inactivation to an extent proportional to the degree of mannitol crystallinity.

Pyne and Suryanarayanan found that glycine forms an amorphous freeze concentrate when quench cooled in liquid nitrogen, but crystallizes as the β-form when the solution is frozen by either rapid (20°C/min) or slow (2°C/min) cooling in a DSC [84]. When these pure glycine solutions were freeze-dried, the quench-cooled solutions formed γ-glycine during primary drying, and at the end of secondary drying both β- and γ-glycine were found. These measurements were made using novel in situ x-ray diffraction during lyophilization. Samples frozen by either the rapid or slow methods contained only the β-form after freeze-drying, a result that did not depend upon the choice of primary drying temperature used (from −35°C to −10°C). However, for quench-cooled solutions the β-glycine content did not change, but the γ-glycine crystalline content of the samples increased in samples dried at a higher primary drying temperature. It was found that the glycine concentration also affected the crystallization behavior for quench-cooled samples in that those dried at the lowest temperature of −35°C contained only β-glycine.

Pyne and Suryanarayanan also found the effect of annealing to depend upon freezing rate [84]. For solutions which had been frozen at 20°C/min or 2°C/min, annealing at −10°C led to an increase in the existing β-glycine content. As noted above quench-cooled glycine did not crystallize, but upon heating to −65°C an unidentified crystalline form appeared, which gave way to β-glycine at −55°C. Annealing at −10°C caused a transition from β-glycine to γ-glycine. However, annealing at −20°C only caused

Copyright 2004 by Marcel Dekker, Inc. All Rights Reserved.

increases in the β-glycine content, and −35°C annealing showed miniscule increases in β content with no detectable γ-glycine present.

VIII. MECHANISMS OF MORPHOLOGICAL CHANGE DURING ANNEALING

For amorphous solutes, annealing above T'_g will, by the definition of T'_g, result in melting of ice into neighboring non-ice regions (see Figure 1). The increased water content and higher temperature increase both the bulk mobility *of* the amorphous phase and diffusional mobility of all species in that phase. The increased bulk mobility of the amorphous phase during annealing allows it to relax into physical configurations of lower free energy. Surface free energy (also known as surface tension) (γ) is defined as free energy per unit area, and consequently has units of energy per unit area [85]. Therefore there will always be a driving force for a contiguous volume to reduce its surface area so long as it is not already a perfect sphere (the shape which possesses the minimum possible surface-to-volume ratio).

The structures in freeze-concentrated systems inevitably possess junctions, edges, and other departures from the perfect sphere. Each of these three-dimensional features has two principal radii of curvature. The *pressure* inside such a structure with positive radii of curvature can be shown to be

$$P = 2\gamma\left(\frac{1}{r_1} + \frac{1}{r_2}\right) + P_o$$

where γ is the surface free energy (energy/length^2), r_1 and r_2 are the radii of curvature, and P_o is the surrounding pressure. Consider a needle-shaped structure. The tip will have very small radii of curvature, and the radii of curvature for material in the body of the needle will be much greater. Using the equation above we can deduce that the pressure in the tip will be higher than the pressure in the body. Given sufficiently low viscosity, this pressure difference will (during our time scale of observation) cause *bulk flow* of material from the tip into the body, and the tip will actually retract: the needle will become more sphere-like in shape. Structures with negative internal radii, such as the concave surface at the junction of two spheres in contact, will have a *lower* pressure than the surroundings, leading to a flow of material to these areas. Sintering and accretion of high surface area ice particles into a single lower surface area structure are manifestations of this principle [86,87].

Copyright 2004 by Marcel Dekker, Inc. All Rights Reserved.

Another fundamental relationship of surface chemistry is the Kelvin equation, which states that smaller radii of curvature induce a higher vapor pressure:

$$\Delta G = RT \ln \frac{P_v}{P_v^0} = \gamma V \left(\frac{1}{r_1} + \frac{1}{r_2} \right)$$

In this equation ΔG is the increase in molar free energy, R is the universal gas constant, T is temperature, P_v^0 is the normal vapor pressure, P_v is the vapor pressure over a curved interface, V is the specific volume, and r is the radius of curvature. Ice crystal regions with samller radii will melt preferentially due to their higher free energy because smaller ice crystals have higher vapor pressures than larger ones. Searles et al. found that in some cases only a very short annealing period was required to achieve a maximum sublimation rate [4]. The authors believed this to be due to the preferential melting of the smallest ice crystals upon initial heating for annealing. Recooling did not result in new crystal growth because the volume was already nucleated. Rather upon recooling the fewer, larger remaining crystals simply grew. In that sense annealing can be thought of as a partial ''refreezing'' step.

Ostwald ripening (recrystallization) can also occur in these systems. It is a phenomenon by which dispersed crystals smaller than a critical size decrease in size as those larger than the critical size grow, and it can be either diffusion or surface-attachment limited. The food science literature contains several examples of diffusion-limited Ostwald ripening in aqueous carbohydrate solutions (model ice creams) [88–92]. A common feature of these reports is that no increase in ice crystal size is observed below T_g'.

Searles et al. observed that annealing opened up holes on the surface of the lyophilized cake [4]. This would occur via drainage of the amorphous film into adjacent junctions. Drainage of the surface film (''skin'') into the consolidated junctions is apparent in Figure 5. The thinnest area of the film between the junctions is most susceptible to instabilities, and rupture would be followed by film retraction from the edges with small positive curvature to the junctions due to their negative radii of curvature. Examining Figure 3, the lamellar plates can be seen as they join the surface film from below. From Figure 4B (note the difference in scale) it can be seen that some of the plates fused together, since the $\sim 5\,\mu m$ unannealed spacing has been consolidated into up to $100\,\mu m$ spacing, with the implication that up to 20 lamellae were fused. Shalaev and Franks show evidence of similar mechanisms in the formation of globular structures due to dendrite retraction due to partial collapse [93].

Copyright 2004 by Marcel Dekker, Inc. All Rights Reserved.

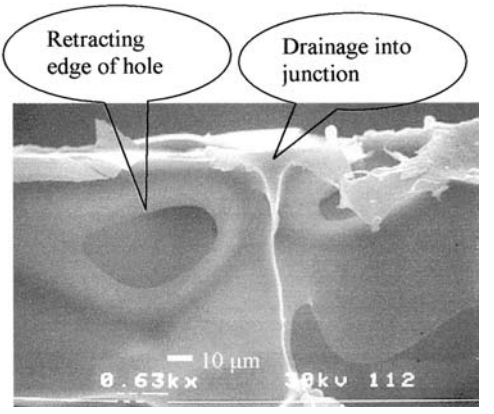

Figure 5 Evidence of drainage into a junction as a result of annealing: 10% hydroxyethyl starch which had been frozen by immersion into liquid nitrogen, annealed, then lyophilized. Retracting hole edges as well as a filling junction are evident.

IX. PRIMARY DRYING OPTIMIZATION THROUGH ANNEALING

Searles found that annealing decreased the resistance to vapor flow to such an extent that control of the process shifts from mass transfer to energy transfer [39]. Figure 6 shows predicted drying rate (panel A) and product temperature (panel B) as a function of product resistance for products lyophilized in vials. The heat transfer characteristics are particular for a specific vial and the chamber pressure (which in this case is 26.6 Pa). As product mass transfer resistance is increased the drying rate decreases and the product temperature increases. However, for products with a low product resistance (in this case less than approximately $1E+4$ Pa s m^2/kg) very slight drying rate decreases will be seen as product resistance is increased. That is because at low product resistance, the product resistance is not *controlling*. Rather the process is controlled by heat transfer. For high product resistance the drying rate is very sensitive to product resistance and mass transfer is controlling.

The product temperature trends shown in panel B are very interesting. Note that at high product resistance the product temperature tends toward that of the shelf. At low product resistance the product temperature tends toward the temperature at which the vapor pressure of ice equals the chamber pressure. In this case that temperature is $-33°C$. As shelf temperature is increased, drying rate increases and product temperature increases *if* the product resistance is high enough. Note that for low product

Copyright 2004 by Marcel Dekker, Inc. All Rights Reserved.

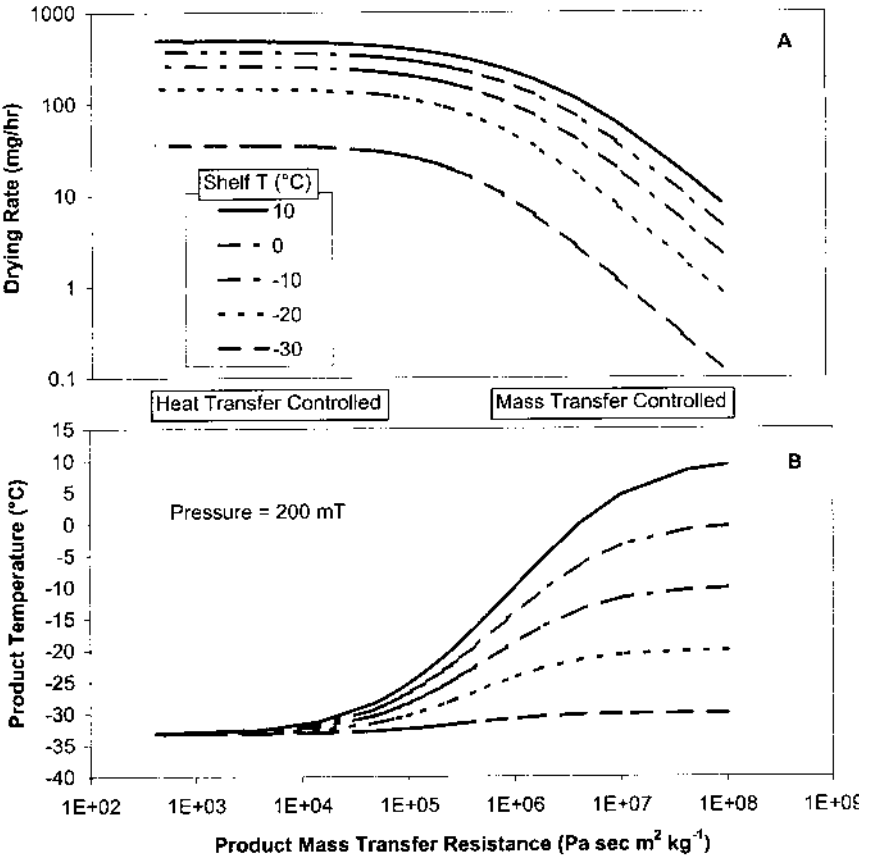

Figure 6 Simulations of (A) drying rate and (B) ice interface temperature as a function of the product mass transfer resistance and shelf temperature: 2 mL fill in a 5 mL vial, 26.6 Pa (200 mT) chamber pressure. Note the change from heat to mass transfer control over the drying rate and temperature.

resistance, shelf temperature increases yield higher drying rates but barely measurable product temperature increases. Similar to the boiling of water in a pot, additional heat input does not increase the temperature of the ice but merely increases the sublimation rate. Therefore low product resistance to mass transfer renders the product temperature insensitive to additional energy input.

The lyophilization of samples in vials on the shelf of a freeze-dryer presents a unique challenge in that the perimeter vials receive additional

Copyright 2004 by Marcel Dekker, Inc. All Rights Reserved.

energy during sublimation and dry at up to twice the rate as vials on the interior of the shelf [39]. Therefore the process development scientist/engineer must design the lyophilization cycle such that perimeter vials do not collapse due to the excessive energy input, but primary drying must be long enough to accommodate the vials in the center of the shelf (which can be drying at half the rate). However, if the vials were to have been sufficiently annealed, all would dry at the nearly same temperature (close to that dictated by the chamber pressure). Not only can the overall drying rate be increased to the maximum that the equipment can support, heterogeneity in product temperatures can be greatly reduced. Such a strategy will allow use of the maximum sublimation rate which the equipment can support and will improve product consistency.

X. THE FUTURE

While this chapter has summarized many examples of freezing and annealing effects upon the product and the lyophilization process (some of which are quite surprising), few of the citations in this chapter are for work devoted to better understanding the freezing process itself. Pharmaceutical active ingredients generally fall into one of two categories: characterized or uncharacterized. Can it be said that *lyophilized* dosage forms are fully characterized (even if the active ingredient is fully characterized)? When a fully characterized active ingredient is lyophilized we must be mindful of the limited extent to which we can characterize attributes of the final lyophilized product. For example, aspects of product cake structure and surface area are not well characterized and are part of what is accepted as the ''natural'' heterogeneity within a lyophilized batch. Do we understand how a shift in the freezing protocol will affect stability of the product? Without a better understanding of how freezing actually takes place, we cannot hope to fully characterize our lyophilized dosage forms. For example, how and why will cake morphology be affected by a change in vial? Why do cakes sometimes appear with a directional morphology in the bottom half of the cake and spherulitic in the top half? How do we correlate cake appearance (e.g., extent of collapse) with product quality for deviation investigations? What cooling rates during freezing will result in the ''same'' product? When freezing on a pre-cooled shelf, what conditions are necessary to achieve directional solidification? How will the cake morphology change with a slight change in the freezing protocol? Which forms of crystalline mannitol will arise from a slight change in the protocol? These questions are worth answering—failing to pursue them will lead to increased regulatory

Copyright 2004 by Marcel Dekker, Inc. All Rights Reserved.

scrutiny, occasional product development and manufacturing deviation failures, and inefficient use of our existing lyophilization infrastructure.

Better ways to control freezing are emerging. A good example is the evaporative nucleation concept recently demonstrated by Kramer et al. [41]. Searles et al. used ice nucleating agents *Pseudomonas syringae* and silver iodide to alter the freezing characteristics of 10% hydroxyethyl starch frozen by shelf-ramp in vials [5]. The agents increased the nucleation temperature of ice. The higher the nucleation temperature, the more directional the freeze and the resulting ice morphology. As discussed above, some products must be frozen with a directional solidification method [58]. Randolph and Searles suggest the possibility of incorporating ice nucleation chemistry into the vial interior [94].

Most other examples come from researchers working in the food science field—an industry in which lower financial margins place a premium upon innovative productivity improvements. Li and Sun reviewed novel methods for rapid freezing of food products [95]. These include high-pressure freezing and applications of antifreeze and ice nucleation protein. Ice nucleators are being pursued for better control of ice crystal size distributions and less costly food freezing [95–97]. High pressures can be used to assist freezing [95,98]. The freezing point of water is lower under high pressure, allowing more extreme supercooling. Nucleation can be induced by rapid release of pressure, ensuring larger numbers of small ice crystals and vial-to-vial consistency. The technology has been shown with meats to generate smaller ice crystals throughout, compared to conventional methods such as air and liquid nitrogen blast [99]. Nucleation can be induced by ultrasonic energy as well [100–102], raising the possibility of high-frequency vibration transmitted through the shelves to the vials, of through the gas phase acoustically. Lastly, ice nucleation has been found to occur through electrical discharge [103,104]. However, electrical discharge may not be required. If may be sufficient to use innocuous polar compounds appropriately arranged on the vial surface, as ice nucleation has been found to occur "between oppositely charged walls of narrow cracks, whatever their detailed atomic arrangement" [105,106].

XI. CONCLUSIONS

Freezing is the major dehydration step of lyophilization. It determines the texture of the final product. Changes to the freezing protocol, thermal history during freezing, vial, volume of fill, particulate levels, ice nucleation properties, or any post-freezing temperature excursions above T_g' (intentional or not) can result in morphological changes, phase separation,

Copyright 2004 by Marcel Dekker, Inc. All Rights Reserved.

product degradation, changes in the crystallization behavior of the solutes or the product, product stability, changes in drying rates (which can result in altered moisture levels or product collapse), and altered levels of residual cosolvent. Beware that many of the process factors affecting freezing can change through the scale-up/technical transfer process, leading to risk of failure at full scale if not adequately controlled.

Two fundamental types of freezing behavior have been identified: directional solidification and global supercooling. Directional solidification results in a directional lamellar morphology with connected pores, and global supercooling creates spherulitic ice crystals. The directional morphology has a higher specific surface area, and results in higher primary drying rates due to the connected, continuous nature of the pores.

Within a given type of freezing one can say that "faster freezing" leads to higher surface areas, smaller more numerous ice crystals, and slower primary drying rates. For directional solidification, freezing rate control equates to cooling rate control, but below a critical cooling rate one would expect a loss of directional solidification at least in some portion of the volume being frozen. For freezing by global supercooling Hsu et al. have altered the "freezing rate" by changing the vial sizes [32]. Searles et al. found that *within the global supercooling regime* the extent of supercooling and therefore "freezing rate" were independent of shelf cooling rate [5].

However, one *cannot* say that in general "faster freezing" means higher surface areas, smaller, more numerous ice crystals, and slower primary drying rates because liquid nitrogen immersion provides much faster cooling than shelf-ramp freezing. Liquid nitrogen immersion results in higher surface areas but faster primary drying rates due to the completely different type of morphology that results.

Different freezing methods and annealing steps are powerful tools to manipulate numerous product quality and productivity attributes. By understanding how freezing and annealing affect our products and processes, we can devise better freezing and annealing protocols to increase lyophilization plant capacity utilization and improve product quality and consistency. Do not blindly accept the results of your freezing method: investigate alternative freezing methods and test the effects of annealing steps.

REFERENCES

1. J Carpenter, BS Chang. Lyophilization of protein pharmaceuticals. In: KE Avis and V Wu, eds. Biotechnology and Biopharmaceutical Manufacturing, Processing, and Preservation, Buffalo Grove, IL: Interpharm Press, 1996.

Copyright 2004 by Marcel Dekker, Inc. All Rights Reserved.

2. AP MacKenzie. The physico-chemical environment during the freezing and thawing of biological materials. In: R Duckworth, ed. Water Relations of Foods, London: Academic Press, 1975.
3. G Blond, D Simatos, M Catte, C Gilles-Dussap, J Bernard-Gros. Modeling of the water-sucrose state diagram below 0 deg. C. Carbohydrate Research 298:139–145, 1997.
4. J Searles, J Carpenter, T Randolph. Annealing to optimize the primary drying rate, reduce freezing-induced drying rate heterogeneity, and determine T_g' in pharmaceutical lyophilization. Journal of Pharmaceutical Sciences 90:872–887, 2001.
5. J Searles, J Carpenter, T Randolph. The ice nucleation temperature determines the primary drying rate of lyophilization for samples frozen on a temperature-controlled shelf. Journal of Pharmaceutical Sciences 90:860–871, 2001.
6. S Ablett, MJ Izzard, PJ Lillford. Differential scanning calorimetric study of frozen sucrose and glycerol solutions. Journal of the Chemical Society Faraday Transactions 88:789–794, 1992.
7. F Franks. Freeze-drying: a combination of physics, chemistry, engineering, and economics. Japanese Journal of Freezing and Drying 38:5–16, 1992.
8. S Li, C Schoneich, R Borchardt. Chemical instability of protein pharmaceuticals: mechanisms of oxidation and strategies for stabilization. Biotechnology and Bioengineering 48:490–500, 1995.
9. F Franks. Freeze drying: from empiricism to predictability. Cryo-Letters 11:93, 1990.
10. T Patapoff, D Overcashier. The importance of freezing on lyophilization cycle development. BioPharm 15:16–21, 2002.
11. MC Heller. Causes and consequences of polymeric phase separations in protein formulations during lyophilization. Thesis/Dissertation, University of Colorado, 1998.
12. S Webb, J Cleland, J Carpenter, T Randolph. Effects of annealing lyophilized and spray-lyophilized formulations of recombinant human interferon-γ. Journal of Pharmaceutical Sciences 92:715–729, 2003.
13. C Sonner, Y Maa, G Lee. Spray-freeze-drying for protein powder preparation: particle characterization and a case study with trypsinogen stability. Journal of Pharmaceutical Sciences 91:2122–2139, 2002.
14. G Blond. Velocity of linear crystallization of ice in macromolecular systems. Cryobiology 25:61–66, 1988.
15. E Budiaman, O Fennema. Linear rate of water crystallization as influenced by temperature of hydrocolloid suspensions. Journal of Dairy Science 70:534–546, 1987.
16. A Muhr, J Blanshard. Effect of polysaccharide stabilizers on the rate of growth of ice. Journal of Food Technology 21:683–710, 1986.
17. C Knight. The Freezing of Supercooled Liquids. Princeton, NJ: Van Nostrand, 1967.
18. LR Rey, MC Bastien. Biophysical aspects of freeze-drying. In: F Fisher, ed. Freeze-Drying of Foods. Washington, DC: National Academy of Sciences, 1961.

Copyright 2004 by Marcel Dekker, Inc. All Rights Reserved.

19. AP MacKenzie, BJ Luyet. Effect of recrystallization upon the velocity of freeze-drying. Progress in Refrigeration Science and Technology 6:1573, 1963.
20. B Luyet, G Rapatz. Patterns of ice formation in some aqueous solutions. Biodynamica 8:1–68, 1958.
21. G Rapatz, B Luyet. Patterns of ice formation in aqueous solutions of glycerol. Biodynamica 10:69–80 1966.
22. D Quast, M Karel. Dry layer permeability and freeze-drying rates in concentrated fluid systems. Journal of Food Science 33:170, 1968.
23. H Thijssen, W Rulkens. Effect of freezing rate on rate of sublimation and flavour retention in freeze-drying. International Institute of Refrigeration Communications 10:99–113, 1969.
24. G Blond, M Medas, R Merle, M Fumanal, D Simatos, W Rulkens. Study of the porous texture resulting from the freeze-drying of certain aqueous and non-aqueous systems. International Institute of Refrigeration Communications 10:59–69, 1969.
25. D Simatos, G Blond. The porous texture of freeze dried products. In: S Goldblith, L Rey, W Rothmayr, eds. Freeze Drying and Advanced Food Technology. London: Academic Press, 1975.
26. MJ Pikal, S Shah, D Senior, JE Lang. Physical chemistry of freeze-drying: measurement of sublimation rates for frozen aqueous solutions by a microbalance technique. Journal of Pharmaceutical Sciences 72:635–650, 1983.
27. K Nakamura, H Kumagai, T Yano. Effect of freezing conditions on freeze drying rate of concentrated liquid foods. In: Food Engineering and Process Applications; Proceedings of the 4th International Congress on Engineering and Food, M Le Maguer, P Jelen, University of Alberta Faculty of Agriculture and Forestry. London: Elsevier, 1986.
28. ML Roy, MJ Pikal. Process control in freeze drying: determination of the end point of sublimation drying by an electronic moisture sensor. Journal of Parenteral Science and Technology 43:60–66, 1989.
29. M Kochs, C Korber, B Nunner, I Heschel. The influence of the freezing process on vapor transport during sublimation in vacuum-freeze-drying. International Journal of Heat and Mass Transfer 34:2395–2408, 1991.
30. M Kochs, C Korber, I Heschel, B Nunner. The influence of the freezing process on vapor transport during sublimation in vacuum freeze-drying of macroscopic samples. International Journal of Heat and Mass Transfer 36:1727–1738, 1993.
31. P Dawson, D Hockley. Scanning electron microscopy of freeze-dried preparations: relationship of morphology to freeze-drying parameters. Developments in Biological Standards 75:185, 1991.
32. C Hsu, H Nguyen, D Yeung, D Brooks, G Koe, T Bewley, R Pearlman. Surface denaturation at solid-void interface – a possible pathway by which opalescent particulates form during the storage of lyophilized tissue-type plasminogen-activator at high-temperatures. Pharmaceutical Research 12:69–77, 1995.
33. R Haikala, R Eerola, VP Tanninen, J Yliruusi. Polymorphic changes of mannitol during freeze-drying: effect of surface-active agents. PDA Journal of Pharmaceutical Science & Technology 51:96–101, 1997.

Copyright 2004 by Marcel Dekker, Inc. All Rights Reserved.

34. N Milton, M Pikal, M Roy, S Nail. Evaluation of manometric temperature measurement as a method of monitoring product temperature during lyophilization. PDA Journal of Pharmaceutical Science and Technology 51:7, 1997.
35. D Overcashier, T Patapoff, C Hsu. Lyophilization of protein formulation in vials: investigation of the relationship between resistance to vapor flow during primary drying and small-scale product collapse. Journal of Pharmaceutical Sciences 88:688, 1999.
36. F Franks. Freeze-drying of bioproducts: putting principles into practice. European Journal of Pharmaceutics and Biopharmaceutics 45:221, 1998.
37. O Fennema, W Powrie, E Marth. Low-Temperature Preservation of Foods and Living Matter. New York: Marcel Dekker, 1973.
38. S Chandler, L Trissel, L Wamsley, J Lajeunesse, R Anderson. Evaluation of air quality in a sterile-drug preparation area with an electronic particle counter. American Journal Hospital Pharmacy 50:2330–2334, 1993.
39. JA Searles. Heterogeneity Phenomena in Pharmaceutical Lyophilization Thesis/Dissertation, University of Colorado, 2000.
40. C Roth, G Winter, G Lee. Continuous measurement of drying rate of crystalline and amorphous systems during freeze-drying using an in situ microbalance technique. Journal of Pharmaceutical Sciences 90:1345–1355, 2001.
41. M Kramer, B Sennhenn, G Lee. Freeze-drying using vacuum-induced surface freezing. Journal of Pharmaceutical Sciences 91:433–443, 2002.
42. MJ Pikal, S Shah, ML Roy, R Putman. The secondary drying stage of freeze drying: drying kinetics as a function of temperature and chamber pressure. International Journal of Pharmaceutics 60:203–217, 1990.
43. D Teagarden, D Baker. Practical aspects of lyophilization using non-aqueous co-solvent systems. European Journal of Pharmaceutical Sciences 15:115–133, 2002.
44. K Kasraian, P DeLuca. Thermal analysis of the tertiary butyl alcohol-water system and its implications on freeze-drying. Pharmaceutical Research 12:484, 1995.
45. S Wittaya-Areekul, S Nail. Freeze-drying of tert-butyl alcohol/water cosolvent systems: effects of formulation and process variables on residual solvents. Journal of Pharmaceutical Sciences 87:491, 1998.
46. S Wittaya-Areekul, GF Needham, N Milton, ML Roy, SL Nail. Freeze-drying of *tert*-butanol/water cosolvent systems: a case report on formation of a friable freeze-dried powder of tobramycin sulfate. Journal of Pharmaceutical Sciences 91:1147–1155, 2002.
47. J Carpenter, S Prestrelski, T Anchordoguy, T Arakawa. Interations of stabilizers with proteins during freezing and drying. ACS Symposium Series 567:134, 1994.
48. J Carpenter, B Chang, W Garzon-Rodriguez, T Randolph. Rational design of stable lyophilized protein formulations: theory and practice. Pharmaceutical Biotechnology 13:109–133, 2002.

Copyright 2004 by Marcel Dekker, Inc. All Rights Reserved.

49. W Wang. Lyophilization and development of solid protein pharmaceuticals. International Journal Pharmaceutics 203:1–60, 2000.
50. F Hopkins. Denaturation of proteins by urea and related substances. Nature 126:383, 1930.
51. P Privalov. Cold denaturation of proteins. Critical Reviews in Biochemistry and Molecular Biology 25:281–305, 1990.
52. B Eckhardt, J Oeswein, T Bewley. Effect of freezing on aggregation of human growth hormone. Pharmaceutical Research 8:1360, 1991.
53. A Skrabanja, L De Meere, R De Ruiter, P Van Den Oetelaar. Lyophilization of biotechnology products. PDA Journal of Pharmaceutical Science and Technology 48:311, 1994.
54. BS Chang, BS Kendrick, JS Carpenter. Surface-induced denaturation of proteins during freezing and its inhibition by surfactants. Journal of Pharmaceutical Sciences 85:1326, 1996.
55. L Kreilgaard, L Jones, T Randolph, S Frokjaer, J Flink, M Manning, J Carpenter. Effect of tween 20 on freeze-thawing- and agitation-induced aggregation of recombinant human factor XIII. Journal of Pharmaceutical Sciences 87:1597, 1998.
56. S Jiang, S Nail. Effect of process conditions on recovery of protein activity after freezing and freeze-drying. European Journal of Pharmaceutics and Biopharmaceutics 45:249, 1998.
57. JM Sarciaux, S Mansour, MJ Hageman, SL Nail. Effects of buffer composition and processing conditions on aggregation of bovine IgG during freeze-drying. Journal of Pharmaceutical Sciences 88:1354–1361, 1999.
58. S Nema, K Avis. Freeze-thaw studies of a model protein, lactate dehydrogenase, in the presence of cryoprotectants. Journal of Parenteral Science and Technology 47:76–83, 1992.
59. JM Sarciaux, MJ Hageman. Effects of bovine somatotropin (rbSt) concentration at different moisture levels on the physical stability of sucrose in freeze-dried rbSt/sucrose mixtures. Journal of Pharmaceutical Sciences 86:365, 1997.
60. K Izutsu, S Kojima. Phase separation of polyelectrolytes and non-ionic polymers in frozen solutions. Physical Chemistry Chemical Physics 2:123, 2000.
61. K Izutsu, S Kojima. Freeze concentration separates proteins and polymer excipients into different amorphous phases. Pharmaceutical Biotechnology 17:1316–1322, 2000.
62. MC Heller, JF Carpenter, TW Randolph. Effects of phase-separating systems on lyophilized hemoglobin. Journal of Pharmaceutical Sciences 85:1358–1362, 1996.
63. MC Heller, JF Carpenter, TW Randolph. Manipulations of lypohilization-induced phase separation: implications for pharmaceutical proteins. Biotechnology Progress 13:590–596, 1997.
64. MC Heller, JF Carpenter, TW Randolph. Protein formulation and lyophilization cycle design: prevention of damage due to freeze concentration induced phase separation. Biotechnology and Bioengineering 63:166–174, 1999.

Copyright 2004 by Marcel Dekker, Inc. All Rights Reserved.

65. MC Heller, JF Carpenter, TW Randolph. Conformational stability of lyophilized PEGylated proteins in a phase-separating system. Journal of Pharmaceutical Science 88:58–64, 1999.
66. MC Heller. Causes and consequences of polymeric phase separations in protein formulations during lyophilization, Thesis/Dissertation, University of Colorado, 1998.
67. LM Her, M Deras, SL Nail. Electrolyte-induced changes in glass transition temperatures of freeze-concentrated solutes. Pharmaceutical Research 12:768, 1995.
68. M Molina, S Allison, T Anchordoquy. Maintenance of nonviral vector particle size during the freezing step of the lyophilization process is insufficient for preservation of activity: insight from other structural indicators. Journal of Pharmaceutical Sciences 90:1445–1455, 2001.
69. S Allison, MC Molina, T Anchordoquy. Stabilization of lipid/DNA complexes during the freezing step of the lyophilization process: the particle isolation hypothesis. Biochimica et Biophysica Acta 1468:127–138, 2000.
70. N Williams, T Dean. Vial breakage by frozen mannitol solutions: correlation with thermal characteristics and effect of stereoisomerism, additives, and vial configuration. Journal of Parenteral Science and Technology 45:94, 1991.
71. N Williams, Y Lee, G Polli, T Jennings. The effects of cooling rate on solid phase transitions and associated vial breakage occurring in frozen mannitol solutions. PDA Journal of Parenteral Science and Technology 40:135, 1986.
72. N Milton, M Akers, S Nail. The crystallization kinetics of glycine hydrochloride from ''frozen'' solution. Cryo-Letters 18:335–342, 1997.
73. R Johnson, C Kirchhoff, H Gaud. Mannitol-sucrose mixtures – versatile formulations for protein lyophilization. Journal of Pharmaceutical Sciences 91:914–922, 2002.
74. K Pikal-Cleland, J Cleland, T Anchordoquy, JF Carpenter. Effect of glycine on pH changes and protein stability during freeze-thawing in phosphate buffer systems. Journal of Pharmaceutical Sciences 91:1969–1979, 2002.
75. A Cannon, E Trappler. The influence of lyophilization on the polymorphic behavior of mannitol. PDA Journal of Pharmaceutical Science and Technology 54:13–22, 2000.
76. G Gomez, M Pikal, N Rodriguez-Hornedo. Effect of initial buffer composition on pH changes during far-from-equilibrium freezing of sodium phosphate buffer solutions. Pharmaceutical Research 18:90–97, 2001.
77. MJ Pikal. Freeze-drying of proteins part I: process design. BioPharm 3:18, 1990.
78. MJ Pikal. Freeze-drying of proteins – process, formulation, and stability. ACS Symposium Series 567:120–133, 1994.
79. T Oguchi, K Terada, K Yamamoto, Y Nakai. Freeze-drying of drug-additive binary systems. I. Effects of freezing condition on the crystallinity. Chemical and Pharmaceutical Bulletin 37:1881–1885, 1989.
80. N Williams, D Schwinke. Low temperature properties of lyophilized solutions and their influence on lyophilization cycle design: pentamidine isethionate. PDA Journal of Pharmaceutical Science and Technology 48:135–139, 1994.

Copyright 2004 by Marcel Dekker, Inc. All Rights Reserved.

81. S Chongprasert, U Griesser, A Bottorff, N Williams, S Byrn, S Nail. Effects of freeze-dry processing conditions on the crystallization of pentamidine isethionate. Journal of Pharmaceutical Sciences 87:1155, 1998.
82. K Izutsu, S Yoshioka, T Terao. Decreased protein stabilizing effects of cryoprotectants due to crystallization. Pharmacetical Research 10:1232–1237, 1993.
83. K Izutsu, S Yoshioka, T Terao. Effect of mannitol crystallinity on the stabilization of enzymes during freeze-drying. Chemical and Pharmaceutical Bulletin 42:5–8, 1994.
84. A Pyne, R Suryanarayanan. Phase transitions of glycine in frozen aqueous solutions and during freeze-drying. Pharmaceutical Research 18:1448–1454, 2001.
85. AW Adamson, AP Gast. Physical Chemistry of Surfaces. New York: John Wiley & Sons, 1997.
86. HHG Jellinek, Ibrahim SH. Sintering of powdered ice. Journal of Colloid and Interface Science 25:245–254, 1967.
87. K Itagaki. Some surface phenomena of ice. Journal of Colloid and Interface Science 25:218–227, 1967.
88. T Hagiwara, RW Hartel. Effect of sweetener, stabilizer, and storage temperature on ice recrystallization in ice cream. Journal of Dairy Science 79:735, 1996.
89. RL Sutton, RL Evans, JF Crilly. Modeling ice crystal coarsening in concentrated disperse food systems. Journal of Food Science 59:1227, 1994.
90. RL Sutton, A Lips, G Piccirillo. Recrystallization in aqueous fructose solutions as affected by locust bean gum. Journal of Food Science 61:746–748, 1996.
91. RL Sutton, A Lips, G Piccirillo, A Sztehlo. Kinetics of ice recrystallization in aqueous fructose solutions. Journal of Food Science 61:741, 1996.
92. RL Sutton, D Cooke, A Russel. Recrystallization in sugar/stabilizer solutions as affected by molecular structure. Journal of Food Science 62:1145, 1997.
93. E Shalaev, F Franks. Changes in the physical state of model mixtures during freezing and drying: impact on product quality. Cryobiology 33:14–26, 1996.
94. T Randolph, J Searles. Freezing and annealing phenomena in lyophilization: effects upon primary drying rate, morphology, and heterogeneity. American Pharmaceutical Review 5:40–46, 2002.
95. B Li, Sun DW. Novel methods for rapid freezing and thawing of foods – a review. Journal of Food Engineering 54:175–182, 2002.
96. J Li, T Lee. Bacterial ice nucleation and its potential in the food industry. Trends in Food Science and Technology 6:259–265, 1995.
97. J Li, M Izquierdo, T Lee. Effects of ice-nucleation active bacteria on the freezing of some model food systems. International Journal of Food Science and Technology 32:41–49, 1997.
98. P Sanz, LC Otero, J Carrasco. Freezing processes in high-pressure domains. International Journal of Refrigeration 20:301–307, 1997.
99. M Martino, L Otero, P Sanz, N Zaritzky. Size and location of ice crystals in pork frozen by high-pressure-assisted freezing as compared to classical methods. Meat Science 50:303–313, 1998.

Copyright 2004 by Marcel Dekker, Inc. All Rights Reserved.

100. T Inada, X Zhang, A Yabe, Y Kozawa. Active control of phase change from supercooled water to ice by ultrasonic vibration 1. Control of freezing temperature. International Journal of Heat and Mass Transfer 44:4523–4531, 2001.
101. X Zhang, T Inada, A Yabe, S Lu, Y Kozawa. Active control of phase change from supercooled water to ice by ultrasonic vibration 2. Generation of ice slurries and effect of bubble nuclei. International Journal of Heat and Mass Transfer 44:4533–4539, 2001.
102. X Zhang, T Inada, A Tezuka. Ultrasonic-induced nucleation of ice in water containing air bubbles. Ultrasonics Chemistry 10:71–76, 2003.
103. T Shichiri, Y Araki. Nucleation mechanisms of ice crystals under electrical effect. Journal of Crystal Growth 78:502–508, 1986.
104. G Mandal, P Kumar. A laboratory study of ice nucleation due to electrical discharge. Atmospheric Research 61:115–123, 2002.
105. J McBride. Crystal polarity: a window on ice nucleation. Science 256:814, 1992.
106. M Gavish, J Wang, M Eisenstein, M Lahav, L Leiserowitz. The role of crystal polarity in α-amino acid crystals for induced nucleation of ice. Science 256:815–818, 1992.

Copyright 2004 by Marcel Dekker, Inc. All Rights Reserved.

5

Freezing- and Drying-Induced Perturbations of Protein Structure and Mechanisms of Protein Protection by Stabilizing Additives

John F. Carpenter and Ken-ichi Izutsu
University of Colorado Health Sciences Center, Denver, Colorado, U.S.A.

Theodore W. Randolph
University of Colorado, Boulder, Colorado, U.S.A.

I. INTRODUCTION

There are numerous unique, critical applications for proteins in human healthcare [1–3]. However, even the most promising and effective protein therapeutic will not be of benefit if its stability cannot be maintained during packaging, shipping, long-term storage, and administration. For ease of preparation and cost containment by the manufacturer, and ease of handling by the end-user, an aqueous protein solution often is the preferred formulation. However, proteins are readily denatured (often irreversibly) by the numerous stresses arising is solution, e.g., heating, agitation, freezing, pH changes, and exposure to interfaces or denaturants [4]. The result is usually inactive protein molecules and aggregates, which compromise clinical efficacy and increase the risk of adverse side effects (e.g., [5]). Even if its physical stability is maintained, a protein can be degraded by chemical reactions (e.g., hydrolysis and deamidation), many of which are mediated by water. Thus, inherent protein instability and/or the logistics of product

Copyright 2004 by Marcel Dekker, Inc. All Rights Reserved.

handling often precludes development of aqueous, liquid formulations [6,7]. Also simply preparing stable frozen products, which is relatively straightforward, is not a practical alternative because the requisite shipping and storage conditions are not technically and/or economically feasible in many markets.

The practical solution to the protein stability dilemma is to remove the water. Lyophilization (freeze-drying) is most commonly used to prepare dehydrated proteins, which, theoretically, should have the desired long-term stability at ambient temperatures. However, as will be described in this review, recent infrared spectroscopic studies have documented that the acute freezing and dehydration stresses of lyophilization can induce protein unfolding [8–11]. Unfolding not only can lead to irreversible protein denaturation, even if the sample is rehydrated immediately, but can also reduce storage stability in the dried solid [12,13].

Moreover, simply obtaining a native protein in samples rehydrated immediately after lyophilization is not necessarily indicative of adequate stabilization during freeze-drying or predictive of storage stability. Many proteins unfold during lyophilization but readily refold if rehydrated immediately (cf. [8,11,14]). Without directly examining the structure in the dried solid, it is not possible to know whether an unfolded protein with poor storage stability is present or not.

To develop a protein formulation that minimizes protein unfolding during freezing and drying, it is crucial that the specific conditions (e.g., pH, specific stabilizing ligands) for optimum protein stability be established *and* the appropriate nonspecific stabilizing additives (i.e., those excipients that generally stabilize any protein) be incorporated into the formulation. Other physical factors—the glass transition temperature and the residual moisture of the dried solid—must also be optimized to assure storage stability in the dried solid (reviewed in [15]). These aspects of developing a lyophilized protein formulation will not be considered here because they are addressed in other chapters in this volume, as are the interplay between formulation, lyophilization cycle design, cake structure, and long-term stability of proteins (see [15]). Here we will describe how to design formulations that protect proteins during both freezing and drying and the mechanisms by which additives stabilize proteins and, also importantly, fail to do so. In addition, we will give an overview of the use of infrared spectroscopy to directly monitor protein conformation in frozen and dried samples. This structural information is crucial for the rational development of stable, lyophilized protein formulations.

We wish to emphasize that the principles and mechanisms to be discussed should be generally applicable to any protein. However, each protein has unique physicochemical characteristics, which often manifest

Copyright 2004 by Marcel Dekker, Inc. All Rights Reserved.

themselves as specific routes of chemical and physical degradation during storage. Although we will not address chemical degradation directly in this chapter (see earlier works in [15–17]), it is important to realize that minimizing unfolding during freezing and drying can reduce such degradation during lyophilization and subsequent storage (e.g., [13]). Currently, it is not possible to predict if degradation of a given protein will be inhibited by simply designing a formulation to maintain native structure, nor is it clear as to why the efficacy of "general" protein stabilizers often varies depending on the protein being studied. Thus, there is a great need to increase the fundamental understanding of the mechanisms by which protein stabilizers act and to document, by case studies, the applicability of the general rules to individual proteins. With sufficient effort by academic and industrial researchers, this can be an iterative process in which progress can be made toward developing a general strategy for protein formulation that can be rationally modified for the successful lyophilization of each new protein product.

II. PROTEIN STABILIZATION DURING LYOPHILIZATION/REHYDRATION

Much of the early research on protein stabilization during lyophilization was with labile enzymes, which were found to be irreversibly inactivated, presumably due to aggregation of nonnative molecules, to varying degrees after rehydration. As such, attempts at improving the recovery of activity were focused on the entire process of lyophilization and rehydration. It was not known at what point(s) during the process the damage arose and that stabilizers were operative. Also, usually these studies tested the capacity of nonspecific stabilizers (i.e., those that will generally protect any protein) to prevent irreversible protein denaturation (i.e., aggregation) and inactivation. However, for practical purposes, the first step in increasing the resistance of a given protein to lyophilization-induced damage is to choose the specific conditions that provide the greatest stability to that protein. In general, any factor that alters the free energy of unfolding in solution will tend to have the same qualitative effect during lyophilization. For example, the stability of many enzymes during freeze-thawing is altered by the presence of substrates, cofactors, and/or allosteric modifiers (e.g., [18]). Even for nonenzyme proteins, specific ligands can be important components of the formulation. For example, the stability of fibroblast growth factors is greatly increased in the presence of heparin or other polyanionic ligands (reviewed in [19]). The pH and specific ligands that

Copyright 2004 by Marcel Dekker, Inc. All Rights Reserved.

confer optimum stability often are known form purification protocols, preformulation studies, and/or earlier efforts at designing a liquid formulation.

However, most proteins are not adequately stabilized by specific solution conditions. Of the nonspecific stabilizers that have been tested, sugars have been shown to stabilize the most proteins during lyophilization and have been known to have this property for the longest time. To our knowledge, the first published report is the 1935 paper by Brosteaux and Eriksson-Quensel [20], in which they described the protection during dehydration/rehydration of several proteins by sucrose, glucose, and lactose. Subsequent detailed comparisons of sugars documented that usually disaccharides provide the greatest stabilization (e.g., [4,8,21,22]). For protection during the lyophilization cycle itself, both reducing and nonreducing disaccharides are effective. However, reducing sugars (e.g., lactose and maltose) can degrade proteins during storage via the Maillard reaction (protein browning), a process that can be accelerated at intermediate residual moisture contents [22,23]. Therefore, the choice of disaccharides is essentially limited to the nonreducing sugars, sucrose and trehalose. Since, as of early 1998, trehalose has not been used in any Food and Drug Administration (FDA) approved parenteral product, sucrose is usually the first choice for commercial protein drug formulations.

Although the data are much more limited, polyvinylpyrrolidone (PVP) and bovine serum albumin (BSA) have also been shown to protect a few tetrameric enzymes, i.e., asparaginase, lactate dehydrogenase (LDH) and phosphofructokinase (PFK), during lyophilization and rehydration [24,25]. Another class of compounds that has been found to be useful in freeze-dried formulations are nonionic surfactants. For example, sucrose fatty acid monoester, 3-[(3-cholamidopropyl)-dimethylammonio]-1-propanesulfonate (CHAPS), and Tweens have been found to increase recovery of β-galactosidase activity after freeze-drying and rehydration [26]. Various surfactants have been shown to protect LDH during freeze-drying and rehydration [27]. Hydroxypropyl-β-cyclodextrin, which is surface active [28,29], inhibited the inactivation of recombinant tumor necrosis factor [30], interleukin-2 [31,32], and LDH [27] during freeze-drying/rehydration.

III. MECHANISMS OF STABILIZATION OF PROTEINS BY SUGARS DURING DEHYDRATION

Most protein pharmaceuticals are multicomponent systems that contain the protein, buffer salts, bulking agents, and stabilizers. Each component has its intended role in the formulation. For example, often a crystallizing excipient

Copyright 2004 by Marcel Dekker, Inc. All Rights Reserved.

(e.g., mannitol or glycine) is chosen as a bulking agent (cf. [15]). In contrast, numerous studies have documented that stabilization of a protein during dehydration requires the presence of a compound that remains at least partially amorphous. When a protein formulation is frozen, the protein partitions into the non-ice phase with other amorphous components. The interaction between the protein and these amorphous components must be maintained during the entire freeze-drying process in order to assure recovery of a native protein in the dried solid and after rehydration (e.g., [8,9,33–36]).

Although most carbohydrates used for protein formulations remain amorphous in frozen solutions and during drying (e.g., sucrose and trehalose), some exhibit eutectic phase separation from frozen solutions [34–39]. For example, mannitol readily crystallizes during freeze-drying, but the degree of crystallization can be manipulated by altering processing conditions and formulation components [34–39]. In the concentration range where it remains mostly amorphous, mannitol has been shown to protect enzymes during freeze-drying in a concentration-dependent manner [35,36]. A relatively high mass ratio of protein to mannitol will serve to inhibit mannitol crystallization, whereas with excess mannitol crystallization and loss of stabilization arise. Similarly, substantial stabilization has been achieved with solutes (including buffer salts) that alone crystallize but in combination interfere with each other's crystallization. For example, Izutsu et al. [35] found that with a sufficiently high ratio of potassium phosphate to mannitol, mannitol remained amorphous and protected LDH during freeze-drying. However, when there was excess mannitol, its crystallization obviated protein protection. Similarly, Pikal et al. [40] found that appropriate ratio of mannitol and glycine resulted in a sufficiently large amorphous fraction to protect freeze-dried human growth hormone.

Although it is well established that an amorphous excipient is needed to protect proteins during dehydration, the nature of the protective interaction of amorphous solutes with the protein in the dried solid has been a subject of controversy in the literature. There are at least two nonexclusive mechanisms proposed. Before describing these mechanisms, we wish to emphasize that neither mechanism alone is sufficient to fully explain stabilization during lyophilization. Both mechanisms focus only on the effect of stabilizers during the terminal stress of dehydration and essentially ignore the freezing step. As documented below, no matter what the nature of the interaction of the additive with the dried protein, the most important factor is that the additive(s) prevent unfolding during *both* freezing and dehydration.

Proponents of one mechanism state that proteins are simply mechanically immobilized in the glassy, solid matrix during dehydration

Copyright 2004 by Marcel Dekker, Inc. All Rights Reserved.

(e.g., [41]). The restriction of translational and relaxation processes is thought to prevent protein unfolding, and spatial separation between protein molecules (i.e., ''dilution'' of protein molecules within the glassy matrix) is proposed to prevent aggregation. Although it is clear that protective additives must partition with the protein into the amorphous phase of the dried sample, simply forming a glassy solid does not assure protein stabilization. First, if all that were needed to prevent damage to a protein is the formation of a glass, then the protein by itself should be stable. Clearly, this is not the case because proteins themselves should form an amorphous phase in the dried solid [42]; however, most unprotected proteins are denatured during lyophilization [8–14]. In some cases adding another protein (e.g., BSA), which should simply add to the mass of the final protein glass, confers protection [25].

One might further qualify the mechanism by proposing that the requisite mechanical restriction to unfolding and aggregation can only be achieved if another amorphous compound is present to provide immobilization and spatial separation of the protein drug molecules. However, then the question becomes what amount of additive is sufficient to provide the desired physical properties of the dried solid, which are not achieved with the protein alone? This question has not been answered or addressed in the literature. However, it is expected that, in general, the capacity of an additive to protect a protein specifically during dehydration should depend on the final additive protein mass ratio. Increasing this ratio will favor spatial separation and immobilization of the protein within the glassy matrix. Also, the mass ratios between all compounds in the dried solid affect the influence of the compounds on each other's crystallization (e.g., with glycine and mannitol).

Several studies have shown that formation of a glassy phase by an additive, even when it is used in large excess relative to the protein, is not a sufficient condition for acute stabilization of proteins during lyophilization. For example, formulations of 100 mg/ml interleukin-1 receptor antagonist, prepared with sucrose concentrations ranging from 0 to 10% (wt/vol), all formed a glass during lyophilization and all had glass transition temperatures of $66 \pm 2^{\circ}C$ [13]. Yet only in formulations containing $\geq 5\%$ sucrose was lyophilization-induced unfolding prevented. Tanaka et al. [43] have found that the capacity of carbohydrates to protect freeze-dried catalase decreased with increased carbohydrate molecular weight. Dextrans were the largest and least effective of all of the carbohydrates tested, and the larger the dextran molecule the less it stabilized catalase. Although they did not determine whether their dried samples were amorphous, it is well known that as the molecular weight of the carbohydrate is increased, the glassy state is formed more readily [44–46]. In addition, more recent studies have

Copyright 2004 by Marcel Dekker, Inc. All Rights Reserved.

shown (T. Randolph, M. Zhang, S. Prestrelski, T. Arakawa, and J. Carpenter, unpublished data) that PFK was not protected, and LDH was inactivated further, by dextran during freeze-drying and rehydration. Differential scanning calorimetry documented that the dried samples were amorphous. The potential mechanistic bases for these observations will be described below. For now, it is important to stress the conclusion that it is necessary for stabilizing additives to remain amorphous to protect proteins during lyophilization, but glass formation alone appears not to be sufficient for stabilization of proteins against the severe stress of dehydration.

There are several studies supporting the other mechanism, which is often referred to as the water replacement hypothesis. According to this hypothesis, sugars, protect labile proteins during drying by hydrogen bonding to polar and charged groups as water is removed and, thus preventing drying-induced denaturation of the protein. For example, in early studies using solid state Fourier transform infrared (FTIR) spectroscopy, it was found that the band at $1583\,cm^{-1}$ in the spectrum for lysozyme, which is due to hydrogen bonding of water to carboxylate groups, is not present in the spectrum for the dried protein [33]. When lysozyme is dried in the presence of trehalose or lactose, the carboxylate band is retained in the dried sample, indicating that the sugar is hydrogen-bonding in the place of water. Similar results have been obtained with α-lactalbumin and sucrose [8]. More recently, it has been documented that the carboxylate band can be titrated back by freeze-drying lysozyme in the presence of increasing concentrations of either trehalose or sucrose. (S. Allison and J. Carpenter, unpublished observations). This effect correlates directly with an increased inhibition of protein unfolding in the presence of increasing amounts of sugar.

Three other recent studies on enzyme preservation provide further support for the water replacement mechanism. Tanaka et al. [43] have found that the capacity of a saccharide to protect catalase during freeze-drying is inversely related to the size of the saccharide molecule. They suggest that as the size of the saccharide increases, steric hindrance interferes with hydrogen bonding between the saccharide and the dried protein. In support of this contention, recent experiments have shown that the carboxylate band is only minimally detectable in the infrared spectrum of lysozyme freeze-dried in the presence of dextran (D. Barberi, T. Randolph, and J. Carpenter, unpublished observation). In addition, Tanaka et al. [43] found that the degree of stabilization was based on the saccharide sugar mass ratio, which is to be expected if protection is due to hydrogen bonding of the saccharide to the protein in the dried solid. More recently, by studying protein structure in the dried solid with FTIR spectroscopy,

Copyright 2004 by Marcel Dekker, Inc. All Rights Reserved.

Prestrelski et al. [12] found that as the molecular weight of the a carbohydrate additive was increased the capacity to inhibit unfolding of interleukin-2 during lyophilization decreased and the level of protein aggregation after rehydration increased. Also, it was clear that protection of the protein did not correlate directly with the formation of a glass (all samples were found to be amorphous) or with the glass transition temperature of the sample (the T_g increased as carbohydrate molecular weight increased). Rather, there was a negative correlation between stabilization and molecular weight, which is to be expected if protection during drying is due to the water replacement mechanism.

Some of the most compelling evidence for the water replacement hypothesis comes from studies on the effects of freeze-drying on a model polypeptide, poly-L-lysine [8]. This peptide assumes different conformations in solution, which have been well characterized with FTIR spectroscopy, depending on the pH and temperature. At neutral pH, poly-L-lysine exists as an unordered peptide. At pH 11.2, the peptide adopts an α-helical conformation. Poly-L-lysine assumes an intermolecular β-sheet conformation (cf. [11]) in the dried state, regardless of its initial conformation in aqueous solution. The preference for β-sheet in the dried state appears to be a compensation for the loss of hydrogen bonding interactions with water. The β-sheet allows for the highest degree of hydrogen bonding in the dried sample. If poly-L-lysine is freeze-dried in the presence of sucrose, the original solution structure is retained in the dried state because sucrose hydrogen bonds in place of water, obviating the need to form β-sheet.

IV. INFRARED SPECTROSCOPIC STUDIES OF LYOPHILIZATION-INDUCED STRUCTURAL CHANGES

Until recently, the only way to assess the capacity of an additive to stabilize a protein during lyophilization was to measure activity and/or structural parameters after rehydration. To confound matters further, it was proposed in the protein chemistry literature that dehydration did not alter a protein's conformation [47]. Such a claim was clearly counter to the known contributions of water to the formation of the native, folded protein [48,49]. Also, it was difficult to reconcile the finding that proteins could be irreversibly inactivated and aggregated after rehydration with the contention that protein structure was not perturbed by dehydration.

Reconciliation of this apparent dilemma was provided by FTIR spectroscopy, which can be used to study protein secondary structure in any state (i.e., aqueous, frozen, dried, or even as an insoluble aggregate). FTIR spectroscopy has long been used for quantitation of protein

Copyright 2004 by Marcel Dekker, Inc. All Rights Reserved.

secondary structure and for studies of stress-induced alterations in protein conformation (e.g., [50–52]). Structural information is obtained by analysis of the conformationally sensitive amide I band, which is located between 1600 and 1700 cm^{-1}. This band is due to the in-plane C=O stretching vibration, weakly coupled with C–N stretching and in-plane N–H bending [50,51,53]. Each type of secondary structure (i.e., α-helix, β-turn, and disordered) gives rise to a different C=O stretching frequency [50–54] and, hence, has a characteristic band position, which is designated by wavenumber, cm^{-1}. Band positions are used to determine the secondary structural types present in a protein. The relative band areas (determined by curve fitting) can then be used to quantitative the relative amount of each structural component. Therefore, an analysis of the infrared bands in the amide I region can provide quantitative as well as qualitative information about protein secondary structure [50–54].

To obtain this detailed structural information, it is necessary to enhance the resolution of the protein amide I band, which usually appears as a single broad absorbance contour (Figure 1). The widths of the overlapping component bands are often greater than the separation between the absorbance maxima of neighboring bands. Because the band overlapping is beyond instrumental resolution, several mathematical band-narrowing methods (i.e., resolution enhancement methods) have been developed to overcome this problem [11,50–52,54]. For studies of lyophilization-induced structural transitions, calculation of the second derivative spectrum is recommended [11]. This method is completely

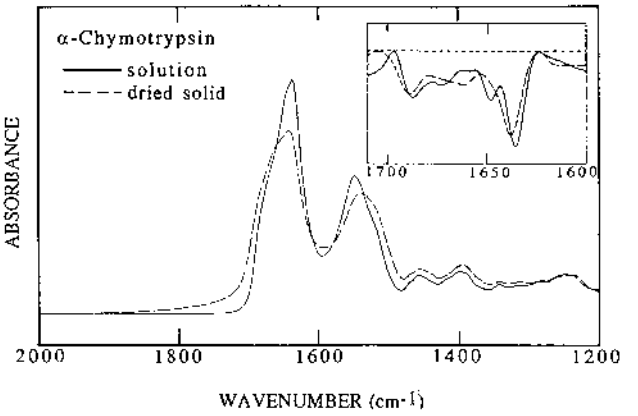

Figure 1 Comparison of infrared spectra of α-chymotrypsin in aqueous solution and dried solid state. The inset shows the second derivatives in the amide I region for the spectra in the main panel. (From Ref. 11.)

Copyright 2004 by Marcel Dekker, Inc. All Rights Reserved.

objective and alterations in component bandwidths, which are due to protein unfolding, are preserved in the second-derivative spectrum.

For most unprotected proteins (i.e., lyophilized in the presence of only buffer) the second-derivative spectra for the dried solid are greatly altered, relative to the respective spectra for the native proteins in aqueous solutions [8–14]. For example, Figure 1 compares the original and second-derivative spectra for α-chymotrypsin in solution and in the dried solid. Second-derivative spectra for aqueous and dried lactalbumin and lactate dehydrogenase, which are also greatly altered by lyophilization, and granulocyte colony-stimulating factor (GCSF), which is minimally perturbed, are shown in Figure 2. For dozens for proteins studied to date, lyophilization induces varying degrees of shifts in band positions, loss of bands, and broadening of bands.

The lyophilization-induced spectral alterations in the conformationally sensitive amide I region are due to protein unfolding and *not* simply to the loss of water from the protein. The intrinsic effects of water removal on the vibrational properties of the peptide bond, and hence protein infrared spectra, were found to be insignificant by Prestrelski et al. [8]. If the direct

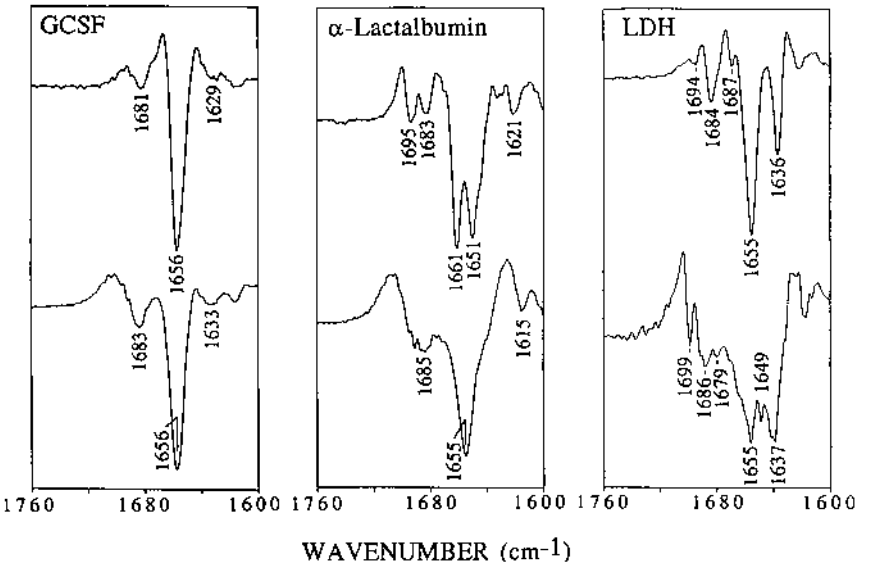

Figure 2 Second-derivative amide I spectra of granulocyte colony-stimulating factor (GCSF), α-lactalbumin, and lactate dehydrogenase (LDH) in aqueous solution (upper spectra) and dried solid (lower spectra) states. (From Ref. 11, employing data from Refs. 8 and 9.)

Copyright 2004 by Marcel Dekker, Inc. All Rights Reserved.

vibrational effects of water removal were responsible for drying-induced spectral changes, then the infrared spectra of all proteins should be altered to the same degree in the dried solid, which is not the case.

Two different behaviors of proteins unfolded in the dried solid are displayed during rehydration: (1) The protein regains the native conformation upon rehydration (reversible unfolding), as observed for α-lactalbumin, lysozyme, chymotrypsinogen, ribonuclease, β-lactoglobulins A and B, α-chymotrypsin, and subtilisin [8,10,11,13,14,55,56]. (2) A significant fraction of the protein molecules aggregate upon rehydration (irreversible unfolding), as noted for LDH, PFK, interferon-γ, basic fibroblast growth factor, and interleukin-2 [8–12]. It has been documented with several proteins in the latter class that prevention of aggregation and recovery of activity after rehydration correlate directly with retention of the native structure in the dried solid [8–12]. Thus, the mechanism by which stabilizing additives (e.g., sugars) minimize loss of activity and aggregation during lyophilization and rehydration is to prevent unfolding during freezing and drying [8–12].

For example, the spectrum for interferon-γ dried in the presence of 1 M sucrose is similar to that for the native aqueous protein, whereas that for the protein dried alone is greatly altered (Figure 3). For analysis of these data, a baseline was fitted to the second-derivative spectra and they have been normalized for total area (see [11,57]). This data presentation is useful because it allows visualization of the relative shifts of area from one component band to another, and, hence, the redistribution from native to nonnative secondary structural elements. For example, for the sample dried without sugar, there is a loss of α-helix as indicated by the decreased absorbance in the 1656 cm^{-1} band, which is compensated by increased absorbance in bands for β-sheet and turns (approximately 1640–1645 and 1665–1695 cm^{-1}). These changes are attenuated when the protein is lyophilized in the presence of sucrose, documenting an increased retention of native structure in the molecular population.

After rehydration, the spectra of both samples are very native-like, indicating that the majority of nonnative molecules have refolded (Figure 3). However, in the spectrum of the sample lyophilized without sucrose, the appearance of a new band near 1625 cm^{-1}, which is assignable to intermolecular β-sheet structure, and the decreased intensities in vibrational bands ascribed to α-helix (1656 cm^{-1}) and turn (1688–1665 cm^{-1}) structures, indicate the formation of protein aggregates upon rehydration (see [11] for a detailed review of the study of protein aggregation with infrared spectroscopy). In this sample, 18% of the protein formed insoluble aggregates. In contrast, in the sample lyophilized with sucrose, only 9% insoluble aggregate was noted after rehydration. This reduction in

Copyright 2004 by Marcel Dekker, Inc. All Rights Reserved.

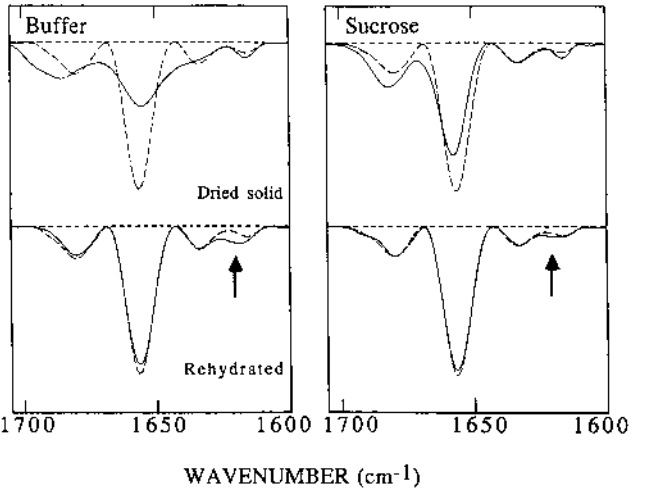

Figure 3 Comparisons of second-derivative spectra of interferon-γ in the dried solid and rehydrated states, with or without 1 M sucrose, with the spectrum of the native aqueous state. The spectrum of the native aqueous state is shown with the dashed line. The arrows indicate the band arising from nonnative intermolecular β-sheet. (From Ref. 11.)

aggregation is reflected in a much weaker 1625 cm^{-1} band in the spectrum of the rehydrated sample. In this case, 1 M sucrose does not provide complete protection during freeze-drying, presumably because it is inadequate at preserving the protein structure during the freezing step (see later).

Also, unfolding of proteins that refold if immediately rehydrated can be inhibited by stabilizing additives [8,10,12–14]. It appears crucial that even these proteins should be stabilized against lyophilization-induced unfolding in order to maintain stability during long-term storage in the dried solid [12,13,15]. Thus, an important criterion for a successful freeze-dried formulation of any protein is retention of the native protein structure in the dried solid, which can be readily documented with FTIR spectroscopy.

Although a qualitative visual comparison of second-derivative spectra can be useful to assess the influence of additives on protein structure during lyophilization, a quantitative comparison is often also desirable. For research on lyophilization-induced structural transitions two approaches can be employed. Occasionally, there is a need to know the secondary structural content. Then, the relative band areas can be determined with curve fitting (see [11,50–52,54]). For example, the percentage of

Copyright 2004 by Marcel Dekker, Inc. All Rights Reserved.

intermolecular β-sheet can be used to calculate the percentage of aggregated protein in dried samples [11,14].

However, for the general assessment of protein stabilization needed to evaluate formulations, it is usually more meaningful to make an overall global comparison between two spectra. For this analysis, Prestrelski et al. [8,9] originally developed a mathematical procedure to calculate the spectral correlation coefficient (similarity) between two second-derivative spectra. More recent analysis indicated that this method can provide misleading information [57]. If the spectra have offset baselines, then the correlation coefficient is much lower than that expected based on a visual assessment of spectral similarity (Figure 4, top). In contrast, if the spectra are dominated by a large band of high symmetry, the value is too great (Figure 4, middle). These shortcomings are avoided by simply normalizing the reference (e.g., aqueous native protein) second-derivative spectrum and that for the experimental sample (e.g., unfolded protein in the dried solid), and then determining the fractional area that the spectra share. The method of determining this area of overlap is described in detail in a paper by Kendrick et al. [57] and an example is presented in Figure 4 (bottom). It is important to note here that with some samples a visual impression is still important because band shifts, which are significant in terms of structure, may result in only a relatively small decrease in the area of overlap parameter. In such cases, the resolution between fully native and unfolded samples becomes so small that an incremental improvement in structure noted with a stabilizer is not resolved with the area of overlap analysis. Then, one most carefully make a qualitative assessment of the spectra to discern what stabilizer concentration and types afford the greatest retention of native-like features in the spectrum of the dried protein, e.g., relative intensity and positions of component bands that are most different between spectra for native and unfolded states.

In addition to the quantitating effect of lyophilization on protein structure, we have also used area-of-overlap analysis to quantitate protein unfolding by guanidine HCl (Figure 5). As can be seen in Figure 5, the changes in a protein's second-derivative spectrum induced by chemical denaturation are very similar to those noted after lyophilization. There are alterations in relative band absorbances, widths, and positions. Furthermore, the unfolding curve generated with infrared spectroscopic data is essentially identical to that based on circular dichroism spectroscopy (Figure 6). These results further support the contention that FTIR spectroscopy coupled with area-of-overlap analysis can be used to quantitatively assess protein unfolding.

It is obvious from the infrared studies to date that the effect of a given additive may vary depending on the protein (e.g., [8]), the presence of other

Copyright 2004 by Marcel Dekker, Inc. All Rights Reserved.

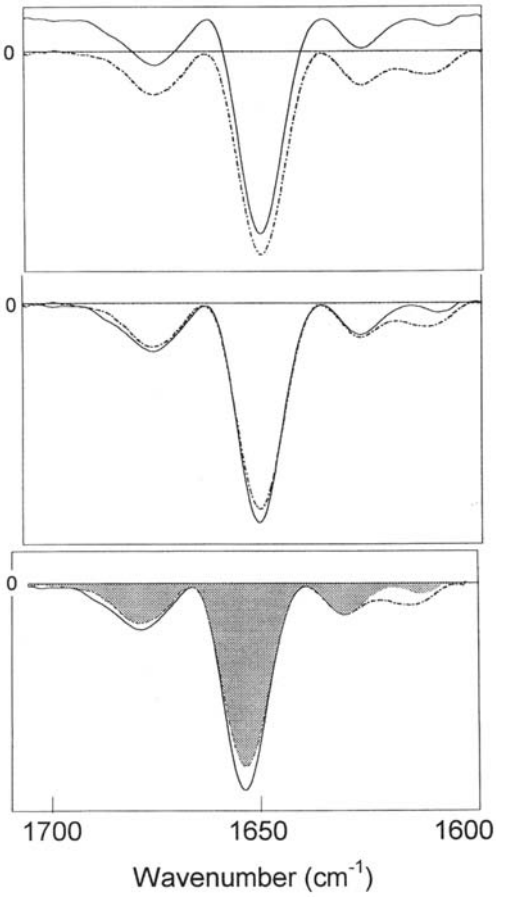

Figure 4 Second-derivative amide I spectra of interferon-γ: (top) uncorrected spectra, correlation coefficient = 0.80; (middle) baseline offset corrected, correlation coefficient = 0.995; (bottom) area-normalized spectra, area of overlap = 0.92. Solid lines indicated the native aqueous state, dashed lines indicate rehydrated aqueous state, and the gray fill (bottom panel) indicates the area of overlap. (From Ref. 57.)

additives, and other specific solution conditions, e.g., pH [12]. Therefore, the structure of each dried protein in each formulation should be studied with FTIR spectroscopy. Unfortunately, this will not be possible with certain formulations. If albumin is used, then, as is the case with any physical measurement, it will not be possible to separate the albumin contribution to the data from that of the protein drug. If other compounds (e.g., PVP, arginine, histidine, glycine) that absorb strongly in the amide I region

Copyright 2004 by Marcel Dekker, Inc. All Rights Reserved.

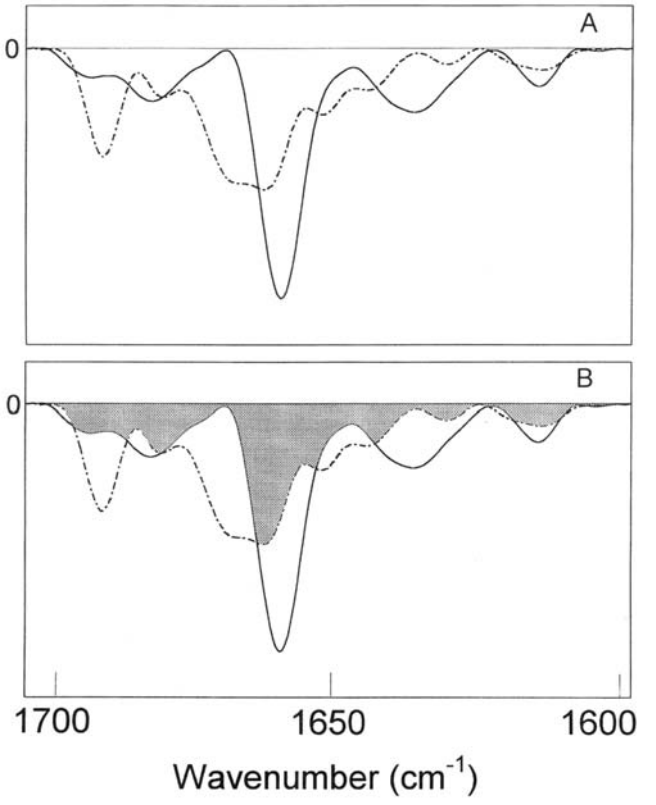

Figure 5 Second-derivative amide I spectra of wild-type iso-1-cytochrome c in aqueous solution in the presence and absence of guanidine HCl. (A) Baseline offset corrected and area normalized, correlation coefficient = 0.72. (B) Baseline offset corrected and area normalized, area of overlap = 0.63. Solid lines indicates zero guanidine HCl, dashed lines indicate 2.5 M guanidine HCl, and the gray fill (panel B) indicates the area of overlap. (From Ref. 57.)

are used in large excess relative to the protein, then they may interfere with the protein spectrum in the dried solid. However, if relatively low concentrations of such additives are used, it may be possible to substract quantitatively their specific absorbances from the protein spectra in both aqueous solutions and dried solids.

There should be few barriers to implementing infrared spectroscopic analysis, at least in industrial laboratories. The instrumentation is available commercially at relatively modest costs. Also, high-quality spectra can be acquired in less than 5 minutes and with minimal sample preparation.

Copyright 2004 by Marcel Dekker, Inc. All Rights Reserved.

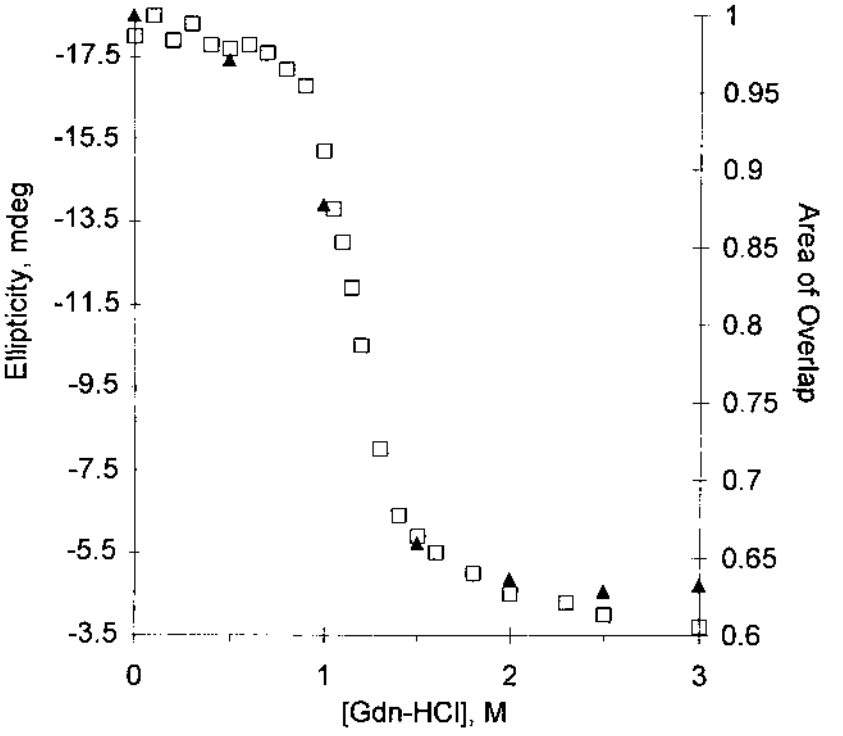

Figure 6 Guanidine HCl-induced unfolding of wild-type iso-1-cytochrome c. The unfolding transition is presented as a plot of ellipticity at 22 nm in millidegrees (open squares) and infrared spectral area of overlap (full triangles) as a function of guanidine HCl concentration. (From Ref. 57.)

The main disadvantage of the technique is that a minimum protein concentration of 3–5 mg/ml is needed to obtain quality spectra of proteins in H_2O solutions. The absolute mass of protein needed is not great because usually less than 50 μl of solution is required to load the sample cell. If solubility is limited, then the protein can be studied at much lower concentrations (around 1 mg/ml) in D_2O. However, the researcher must then be aware of the potential difficulties of data interpretation due to the direct effects of H–D exchange on the vibrational frequencies of amide I component bands (see [11,56]). In some cases, deuteration of the protein makes assignment of bands to different secondary structural types uncertain. This can be a problem if quantitation of secondary structural content is needed. However, if all that is required is a global comparison between a spectrum for an aqueous control sample and that for

Copyright 2004 by Marcel Dekker, Inc. All Rights Reserved.

a freeze-dried protein, then a protein can be studied reliably in D_2O. The only caveat is that sufficient time for H–D exchange must be allowed prior to lyophilization, so that additional exchange does not arise during freezing and drying.

V. MECHANISM FOR STABILIZATION OF MULTIMERIC ENZYMES BY POLYMERS

Hellman et al. [24] found that PVP protected the tetrameric enzyme, L-asparaginase, during freeze-drying and rehydration. In addition, it has been shown that PVP and BSA stabilize tetrameric LDH during freeze-drying [25]. Steric hindrance should minimize the ability of PVP or BSA to hydrogen-bond effectively to the charged and polar groups on the dried protein's surface. Also, as has already been described, polymer-induced stabilization cannot be ascribed just to the formation of a glassy phase with the proteins during the dehydration step.

To understand further how these polymers protect multimeric enzymes during lyophilization, stress-induced alterations in quaternary structure, especially during freezing, must be taken into consideration. First, simply reducing temperature can foster dissociation of many multimeric proteins. The chilling lability is due to disruption of hydrophobic interactions at the monomer–monomer contact sites, and/or an increase in enzyme protonation and the pK_a values of titratable histidines are increased during cooling (cf. [58]). Second, Chilson et al. [18] demonstrated that LDH dissociates during freeze-thawing and that stabilizers inhibit dissociation. The recovery of enzyme activity correlated directly with the degree to which dissociation was inhibited. We have extended this work and studied the effects of PVP and BSA on LDH dissociation during freeze-thawing and freeze-drying [25]. We found that the polymers protected LDH during both treatments by inhibiting dissociation in the frozen state. Dissociation was not induced by freezing itself but rather during an extended residency time in the frozen state (e.g., due to thawing with slow warming or during the early stages of primary drying) at a relatively high subzero temperature (e.g., $-20^{\circ}C$). The main factor causing dissociation appeared to be a decrease in the pH of the sodium phosphate buffer system from 7.5 at room temperature to 4.5 in the frozen solution at $-20^{\circ}C$. Dissociation did not occur when buffers that did not acidify were employed (e.g., Tris and potassium phosphate). PVP and BSA protected the enzyme during lyophilization, at least in part, by inhibiting the reduction in pH in the frozen state. These experiments provide direct evident that stabilization

Copyright 2004 by Marcel Dekker, Inc. All Rights Reserved.

during freezing is essential for inhibiting protein damage during lyophilization. Further examples are presented below.

VI. EVIDENCE FOR FREEZING-INDUCED UNFOLDING DURING LYOPHILIZATION

If a protein is not adequately protected during freezing, the protein will be unfolded in the final dried solid, no matter how effective the stabilization during the dehydration step (e.g., [9,36]). There is considerable evidence documenting freezing sensitivity of proteins. First, many proteins are irreversibly denatured by freeze-thawing (see [59]). Since this damage is due primarily to freezing, similar damage should also arise during the freezing step of lyophilization. Second, the capacity of an additive to protect during freeze-drying is often directly related to its initial bulk concentration and not to the final mass ratio of additive to protein [60]. For example, the data in Figure 7 show that the recovery of PFK activity after lyophilization and rehydration increases as the prefreeze concentration of trehalose increases, even though the same mass ratio of trehalose to protein

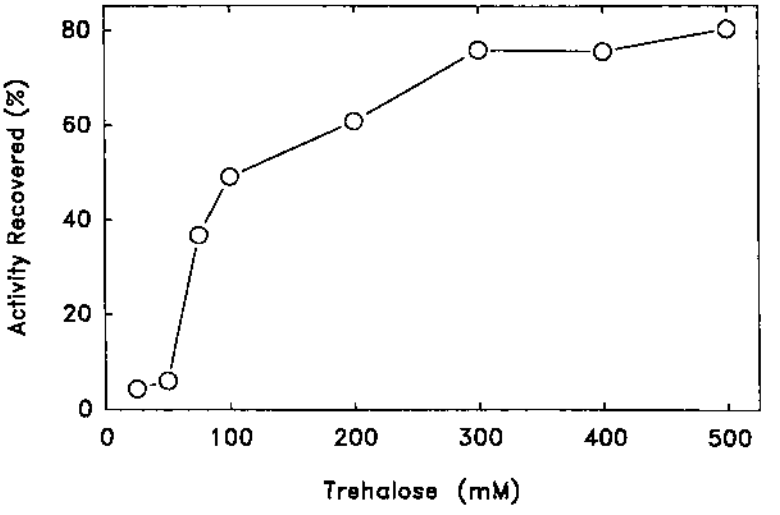

Figure 7 The effect of varying concentration of trehalose, while maintaining a constant sugar/protein mass ratio, on recovery of phosphofructokinase (PFK) activity after freeze-drying and rehydration. The protein concentration was adjusted concomitantly with the sugar concentration to maintain a constant sugar/protein mass ratio of 945. (Data taken from Ref. 59.)

Copyright 2004 by Marcel Dekker, Inc. All Rights Reserved.

was used for all the samples. As will be explained later, freezing protection by sugars is governed by initial concentration of the additive, whereas drying protection is related primarily to the mass ratio between the additive and protein.

Third, Carpenter et al. [36] recently documented more rigorously that freezing-induced denaturation can play an important role in the overall damage to a protein during lyophilization. The impetus for this research was the observation that the disaccharide trehalose was effective at protecting labile enzymes, whereas the constituent monosaccharide, glucose, was not. For example, when PFK is freeze-dried in the presence of 0.2–0.4 M trehalose, over 60% of the initial activity is recovered after rehydration [21]. In contrast, when similar amounts of glucose are used, the recovery is less than 5%. When considering only the effect of the sugar on the protein during dehydration, these results present a dilemma. This is because if hydrogen bonding of the sugar to dried protein in the place of water were all that was needed for stabilization, then mono- and disaccharides should provide similar protection. Glucose does not protect during freeze-drying because it provides minimal stabilization during freezing (based on freeze-thawing results), whereas similar concentrations of trehalose are effective at protecting the protein during both freezing and dehydration [21,61].

To examine the separate roles of protein damage and stabilization by freezing and dehydration. Carpenter et al. [36] developed a two-component system for stress-specific stabilization during lyophilization. In this stabilization scheme, polyethylene glycol (PEG) is used as a cryoprotectant and various carbohydrates can be used to protect during dehydration. PEG alone completely stabilizes either LDH or PFK during freeze-thawing. However, it provides little or no protection during dehydration because it crystallizes during lyophilization. When small amounts (e.g., 10–100 mM initial concentration) of trehalose or glucose are added, which alone at the concentrations tested are ineffective at protecting these enzymes during freeze-thawing or freeze-drying, excellent stabilization is noted during freeze-drying. Under conditions where cryoprotection is provided by PEG, glucose is almost as effective as trehalose in stabilizing dried enzymes (i.e., LDH and PFK).

In a complementary structural study of stress-specific stabilization using FTIR spectroscopy, Prestrelski et al. [9] found that the recovery of activity after rehydration correlated directly with the ability of the additives to preserve the native structure of the enzymes in the dried state. Full activity recovery and maintenance of essentially aqueous structure in dried samples were only noted when a combination of PEG and sugar was employed. Based on these results, Prestrelski et al. [9] have proposed a model of the conformational events during lyophilization and rehydration,

Copyright 2004 by Marcel Dekker, Inc. All Rights Reserved.

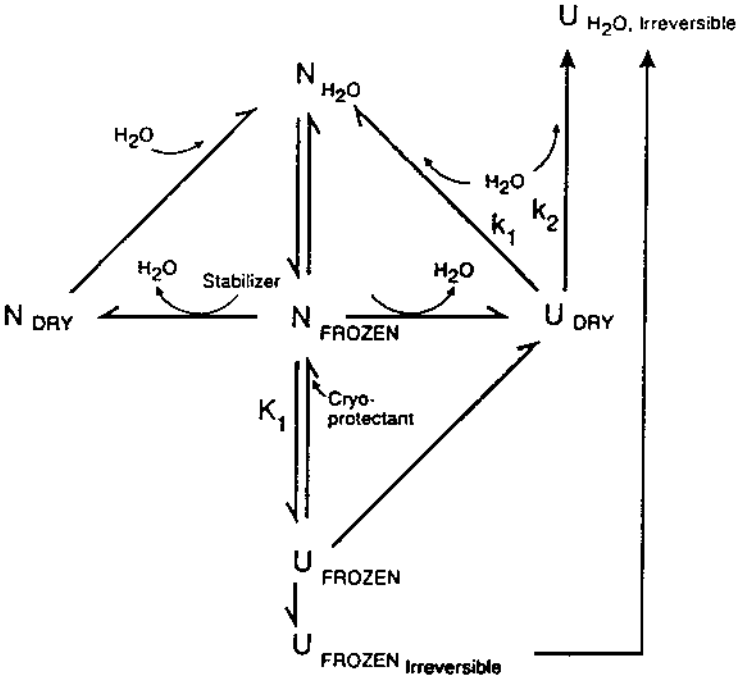

Figure 8 Schematic representation of model for conformational changes during freezing, drying, and rehydration. N, native; U, unfolded; K_1, conformation equilibrium upon freezing, which shifts toward the native state in the presence of a cryoprotectant; k_1, rate constant for refolding; k_2, rate constant for formation of irreversibly denatured (aggregated) forms. (From Ref. 9.)

which is shown in Figure 8. Briefly, this model proposes that in order to recover structure and function after rehydration, the native structure of labile proteins must be retained, both upon freezing and during subsequent dehydration. The appropriate cryoprotectant is required for the initial structural preservation and a specific stabilizer against drying is needed for the terminal stress during lyophilization. In some isntances (e.g., with disaccharides), a single additive can serve both protective functions.

More recently, there has been direct observation of protein structural perturbation in the frozen state using phosphorescence lifetime measurements [62]. Reductions in this parameter indicated that freezing perturbed the tertiary structure (at a protein concentration of 3–5 μM) of azurin, ribonuclease, alcohol dehydrogenase, alkaline phosphatase, glyceraldehyde 3-phosphate dehydrogenase, and LDH. The cryoprotectants sucrose and glycerol were tested and were found to inhibit the freezing-induced

Copyright 2004 by Marcel Dekker, Inc. All Rights Reserved.

structural perturbations, with almost complete protection noted at a 1 M concentration.

Finally, preliminary FTIR spectroscopic investigations have provided direct evidence for freezing-induced perturbation of protein secondary structure (B. Kendrick, A. Dong, L. Krielgard, and J. Carpenter, unpublished observations). For example, it was found that the structure of lactate dehydrogenase was slightly perturbed in the frozen state and that the protein refolded upon thawing. In contrast, recombinant Factor XIII dimer was irreversibly unfolded by freezing. In all cases, the degree of structural perturbation noted in the frozen state was intermediate to that noted in dried solid, indicating that freezing-induced unfolding contributes partly to the total protein damage noted during lyophilization. This FTIR method will be valuable for assessing the relative contributions of excipients to stabilzation during the freezing and drying steps and, hence, for testing the model presented in Figure 8. The only caveat is that at the concentrations necessary (i.e., about 5 mg/ml) to obtain high-quality protein infrared spectra in the frozen state, many proteins that are known to be denatured at lower concentrations (e.g., catalase) are not unfolded during freezing.

VII. PRACTICAL APPROACHES TO MINIMIZING FREEZING-INDUCED DAMAGE

The most damaging stresses to which a protein is exposed during freezing are low temperature and the formation of ice. Cold denaturation has been documented for many proteins and by itself may be sufficient to account for at least some of the damage noted during freezing [63–65]. Also, the protein, which partitions into the non-ice phase, is exposed to extremely high solute concentrations as the sample is frozen. If solutes that are destablizing to the protein are present, then this concentrating effect can contribute to protein denaturation. Finally, as noted above, there can be dramatic pH changes during freezing. For example, the dibasic form of sodium phosphate crystallizes in frozen solution, which results in a system that contains essentially solely the monobasic salt and has a very low pH [66,67]. Other components in a formulation may inhibit crystallization of dibasic sodium phosphate [25,39]. However, such inhibition is not predictable and must be investigated for each formulation with methods such as calorimetry [39] or direct pH measurements on the frozen systems [25]. To minimize problems associated with pH changes, whenever possible, sodium phosphate buffer should be avoided. Also, although somewhat obvious, it is important to realize that a sodium phosphate system will be present if one starts with

Copyright 2004 by Marcel Dekker, Inc. All Rights Reserved.

potassium phosphate buffer salts and NaCl, as is the case with phosphate-buffered saline.

Fortunately, to prevent freezing-induced damage to proteins, it is usually not necessary to discern which stresses are responsible for the damage or to target selectively each of these specific stresses. Rather, the most efficient approach is to design a formulation that provides the greatest overall resistance of the protein to denaturing forces. And as noted above, the first step in any stabilization process is to choose the specific conditions (pH or ligand) that maximize the stability of the given protein. These specific conditions, or adding a cryoprotectant solute such as sucrose, will protect the protein during freezing, whether the ultimate cause of denaturation is low temperature, high solute concentration, or some combination of stresses. This is because ultimately the stabilization of the protein derives from increasing the free energy barrier between the native and denatured states, which increases resistance to damage by any stress.

A wide variety of compounds have been found to provide nonspecific cryoprotection to proteins. These include sugars, amino acids, polyols, salting-out salts, methylamines, alcohols, other proteins, and synthetic polymers (e.g., [59,61,68–70]). During the initial screening of compounds as cryoprotectants, it is important that a relatively wide range of concentrations be tested for each compound. The range to be tested will be dictated by other formulation concerns (e.g., total excipient mass and tonicity of final rehydrated product) and the effectiveness of the cryoprotectant. Compared to sugars, polymers such as PEG and PVP and other proteins (e.g., albumins) are much more potent cryoprotectants [70]. Especially for proteins that must be formulated at low concentration, polymers can be useful as protectants and to minimize loss of active protein on the walls of the vial. Also, if high excipient mass in a concern, polymers are good candidates for cryoprotectants because they are effective at relatively low concentrations (i.e., less than 1% wt/vol). For some proteins, sufficient freezing protection can be obtained by using a disaccharide (e.g., sucrose), which has the added benefit of also protecting the protein during subsequent drying. However, often much higher concentrations (e.g., more than 30% wt/vol) of such low molecular weight solutes are needed to confer adequate protection during freezing.

Finally, at least one aspect of protein stability during freezing is qualitatively unique from that noted in aqueous solution. That is, with numerous proteins it has been found that increasing the initial protein concentration increases protein stability during freeze-thawing. This is usually not the case in unfrozen aqueous solution, except in the special instance in which increasing the concentration of a multimeric protein favors the more stable, fully assembled state. The direct correlation between

Copyright 2004 by Marcel Dekker, Inc. All Rights Reserved.

protein resistance to freezing and initial concentration appears to be related to other observations. First, it has been found with several proteins that increasing the rate of cooling leads to increased damage during freeze-thawing. This effect is attributed to the greater ice surface area associated with the smaller ice crystals that are generated with rapid cooling (e.g., [71]). Strambini and Gabierilli [62] directly documented with phosphorescence lifetimes studies that perturbation of protein tertiary structure in the frozen state was almost two-fold greater for protein frozen by cooling at 100°C/min than that for samples cooled at 1°C/min. They and others have interpreted such results to mean that the ice–water interface serves as a stress to protein during freezing. If this is the case, then increasing the initial protein concentration indeed should reduce the percentage of the total sample damaged, assuming that the surface involved will damage only a finite amount of protein. Accordingly, any level of protein exceeding this amount would be spared from damage by the ice–water interface. In addition, any factor that minimized the association of the protein with the interface should increase protein stability during freeze-thawing.

Consistent with this suggestion is the finding that many different nonionic surfactants, at very low concentration (less than 1% wt/vol), have been found to, provide complete protection to proteins during freeze-thawing (e.g., [71,72]). This protection has been attributed to the inhibition of damage at the ice–water interface [71]. However, it must be stressed that there has yet to be any published direct evidence that surfactants protect proteins during the *freezing* step. Even if surfactants are found to stabilize the native protein structure during freezing, the protection may not necessarily be manifested through competition of protein and surfactant for the ice–water interface. On the contrary, a strong case can be made that under most industrial lyophilization conditions, surfactants cannot be protecting in this manner because the ice–water interface is formed much faster than experimentally measured surfactant relaxation times at interfaces. Under typical industrial lyophilization conditions there is significant supercooling of the liquid before freezing. Once ice nucleates, freezing is nearly instantaneous (less than 0.1 s). Surfactant relaxation times at interfaces, in contrast, are on the order of minutes [73]. One alternative explanation for the freeze/thawing protection afforded by surfactants is that they may simply be serving to favor refolding over aggregation during thawing (see below). In addition, by binding to native protein, surfactants could inhibit interactions between protein molecules themselves and/or between protein molecules and the ice interface, which could be associated with freezing-induced denaturation (see below). Much more research is needed to document the role of this interface as a stress vector and to determine at what steps, and by what mechanisms, surfactants protect

Copyright 2004 by Marcel Dekker, Inc. All Rights Reserved.

proteins during freezing and thawing. Further considerations of the mechanisms by which surfactant protect proteins during freeze-drying and rehydration will be presented below.

VIII. MECHANISMS FOR PROTEIN PROTECTION BY SURFACTANTS DURING LYOPHILIZATION AND REHYDRATION

Surfactants have often been included in both liquid and lyophilized commercial formulations of pharmaceutical proteins. Most likely, this is because surfactants can protect proteins against surface-induced denaturation, which can arise at air–water interface during vial filling and other processing steps. In general, for lyophilized formulations it appears that, in addition to the benefits incurred prior to freezing, the presence of a surfactant in the formulation helps minimize the risk of the appearance of undesirable aggregates in the final rehydrated product. Despite the widespread use of surfactants in protein pharmaceuticals, the mechanism(s) by which surfactants protect proteins during lyophilization and rehydration, and even the steps at which this protection is operative, have not been determined. Based on the considerations of freezing damage given above, it seems that at least part of the benefit derived from surfactants might be due to inhibition or freezing-induced denaturation [74]. But recall that it is not known if the protective effects of surfactants during freeze-thawing are actually manifested during the freezing step. Direct examination of the effects of surfactants on the structure of labile proteins in the frozen state is needed to address this issue.

Surfactants could also serve to increase the resistance of the protein to damage during dehydration, but to date there is no direct evidence documenting improved structure in the solid state of proteins dried in the presence of surfactants. Alternatively, surfactants might only provide protection during rehydration, perhaps by acting as wetting agents and/or by fostering protein refolding. Clearly, there are numerous processing steps at which and mechanisms by which surfactants can be beneficial in freeze-dried formulations. For example, it is known that surfactants increase the resistance of human growth hormone to agitation-induced denaturation in aqueous solution by binding to the native protein and hindering the contact between protein molecules needed for aggregation [75]. An increase in protein concentration during both freezing and drying could foster such deleterious intermolecular interactions, which might be inhibited by surfactants. Also, interaction of protein molecules with the ice–water interface might be inhibited if a surfactant were bound to the protein

Copyright 2004 by Marcel Dekker, Inc. All Rights Reserved.

molecule. In addition, a surfactant could serve a ''chaparone'' function and foster refolding over aggregation during rehydration [76,77]. Alternatively, the surfactant, by binding to the native protein more favorably than the denatured state (see below), could simply increase the free energy of denaturation. Much more work is needed to sort out these possibilities and to determine the nature of the interaction of the surfactant with the protein that increases resistance of the protein to damage during freeze-drying and rehydration. And since very specific interactions between protein and surfactants might be important for some proteins but not others, it is clear that the mechanisms by which surfactants protect may vary depending on the specific properties of the protein. Understanding these matters is crucial if the benefits of using these compounds are to be fully exploited for formulation development.

IX. THERMODYNAMIC MECHANISM FOR CRYOPROTECTION OF PROTEINS

Numerous compounds can provide general cryoprotection to proteins, when used at concentrations of several hundred millimolar. These include sugars, polyols, amino acids, methylamines, and salting-out salts (e.g., ammonium sulfate) [59,61,68–70]. Based on the results of freeze-thawing experiments with LDH and PFK and a review of the literature on protein freezing, Carpenter and Crowe [59] have proposed that this cryoprotection can be explained by the same universal mechanism that Timasheff and Arakawa have defined for solute-induced protein stabilization in nonfrozen, aqueous solution (reviewed in [4,70,78,79]).

Prior to examining the specifics of the Timasheff mechanism, it is instructive to consider the general effects of ligand binding on protein stabilization. Here we will provide a simplified, qualitative description of the most salient aspects of this relationship, which is referred to as the Wyman linkage function (i.e., in this case, the link between ligand binding and stability of protein states binding the ligand). Rigorous explanations can be found in Wyman [80] and Wyman and Gill [81]. Here a two-state model will be considered, in which there is an equilibrium between native and denatured states of the protein ($N \leftrightarrow D$). At room temperature and in nonperturbing solvent environments, the native state is favored because it has a lower free energy than the denatured state. The magnitude of the difference in free energy between the two states (i.e., the free energy of denaturation) dictates the relative stability of the native state. Any alteration in a system that decreases this difference will reduce stability, e.g., reduce the

Copyright 2004 by Marcel Dekker, Inc. All Rights Reserved.

melting temperature of the protein. Conversely, increasing this free energy difference will increase stability of the native state.

Binding of a ligand to either state will reduce the free energy (chemical potential) of that state because thermodynamically binding can only occur if the free energy of the protein–ligand complex is lower than that for the protein alone. The effect of ligand binding on protein stability depends on the difference in binding between the two states. The state that binds the most ligand will have the greatest reduction in free energy. Consequently, if more ligand binds to the native state than to the denatured state, then the free energy denaturation will be increased, and the native state will be stabilized. The opposite will be seen if more ligand binds to the denatured state. If binding to the denatured state is sufficiently greater than that to the native state, then the denatured state will have the lowest free energy and will predominate.

Consider next how this general ligand binding argument relates specifically to the Timasheff mechanism for solute-induced protein stabilization and destabilization. Detailed, rigorous reviews of the Timasheff mechanism can be found elsewhere (e.g., [78,79]). For the purpose of the current review a brief summary, which purposely provides only a simplified explanation, will suffice. First, a descriptive overview will be given, followed by an examination in more detail of the most relevant thermodynamic equations.

In protein cryoprotection, and stabilization and denaturation in nonfrozen aqueous solution, by nonspecific compounds, relatively high concentrations (more than 0.2 M) of ligand (solute) are needed to affect protein stability. This is because the interactions of the solute with the protein are relatively weak. These weak interactions are determined by equilibrium dialysis experiments, in which ligand binding is determined by the difference in the ligand concentration in the dialysis bag with the protein and that outside the bag. Binding measured by this method is actually a measure of the relative affinities of the protein for water and ligand. Therefore, the ligand interaction is referred to as "preferential."

Ligand-induced destabilization by denaturants will be considered first because logically it is the easiest to understand in the context of the general ligand binding effects noted above. Timasheff and his colleagues have found that denaturants (e.g., urea and guanidine HCl) are bound preferentially to proteins and that the degree of binding is greatest for the denatured state. The free energy (chemical potential) of the denatured state is decreased more than that for the native state because more surface area for binding is exposed to solvent as the protein unfolds. Therefore, the free energy barrier between the two states is reduced. Consequently, the native state's resistance to stress is reduced (e.g., the melting point of the protein in

Copyright 2004 by Marcel Dekker, Inc. All Rights Reserved.

lowered). If this effect is great enough, the protein will be denatured at room temperature.

Conversely, Timasheff, Arakawa, and their colleagues have observed experimentally that there is a deficiency of stabilizing solutes (e.g., sugars and polyols) in the presence of the protein, relative to that seen outside the dialysis bag. That is, the solutes are preferentially excluded from contact with the surface of the protein. Preferential exclusion, in a thermodynamic sense, means that the solute (ligand) has negative binding to the protein. Thus, there is an increase in the free energy (chemical potential) of the protein. In the presence of preferentially excluded solutes, the native state is stabilized. This is because denaturation leads to a greater surface area of contact between the protein and the solvent and greater preferential solute exclusion. Thus, even though there is an increase in the free energy of the negative state, this effect is offset by the greater increase in the free energy of the denatured state.

Timasheff's preferential interaction mechanism also explains the influence of solutes on the degree of assembly of multimeric proteins. Preferentially excluded solutes tend to induce polymerization and stabilize oligomers since the formation of contact sites between constituent monomers serves to reduce the surface area of the protein exposed to the solvent. Polymerization reduces the thermodynamically unfavourable effect of preferential solute exclusion. Conversely, preferential binding of solute induces depolymerization because there is greater solute binding to monomers than to polymers.

Now, the key thermodynamic aspects of this mechanism (reviewed in [4,78,79]) will be examined in more detail. Setting component 1 = principal solvent (here water), component 2 = protein, and component 3 = solute (e.g., sucrose or PEG), the preferential interaction of component 3 with a protein is expressed, within close approximation, by the parameter $(\delta m_3/\delta m_2)_{\mu_1,\mu_3}$, at constant temperature and pressure, where μ_i and m_i are the chemical potential and molal concentration of component i, repsectively. A positive value of this interaction parameter indicates an excess of component 3 in the vicinity of the protein over the bulk concentration (i.e., preferential binding of the solute). A negative value for the parameter indicates a deficiency of component 3 in the protein domain. Component 3 (the solute) is preferentially excluded and component 1 (water) is in excess in the protein domain.

The preferential interaction parameter is a direct expression of changes in the free energy of the system induced by component 3 and has the relation:

$$(\delta\mu_2/\delta m_3)_{m_2} = -(\delta m_3/\delta m_2)_{\mu_1,\mu_3}(\delta\mu_3/\delta m_3)_{m_2} \tag{1}$$

Copyright 2004 by Marcel Dekker, Inc. All Rights Reserved.

The term on the left-hand side of the equation defines the change in protein chemical potential as a function of solute concentration. The first term on the right-hand side of the equation is the preferential interaction parameter, which was defined earlier. The second term is the solute self-interaction parameter, which will be described in detail later. Equation (1) indicates that those compounds that are excluded (i.e., $(\delta m_3/\delta m_2)_{\mu_1,\mu_3} < 0$) from the surface of the protein will have positive values of $(\delta\mu_2/\delta m_3)_{m_2}$; they will increase the chemical potential (free energy) of the protein, rendering the system more thermodynamically unfavorable. In the presence of excluded solutes, the exclusion will be greater for the denatured form of the protein than for the native form because the former has a larger surface area, as indicated by $(\delta m_3/\delta m_2)^{\mathrm{D}} < (\delta m_3/\delta m_2)^{\mathrm{N}} < 0$. Consequently, the increase in chemical potential is greater for the denatured form than for the native form in the presence of a preferentially excluded solute, as indicated by $(\delta\mu_2/\delta m_3)^{\mathrm{D}}_{m_2} > (\delta\mu_2/\delta m_3)^{\mathrm{N}}_{m_2} > 0$. There is an increase in the free energy difference between the native and denatured forms, thus stabilizing the native state.

The opposite is seen for potent protein denaturants such as urea and guanidine HCl. These solutes bind preferentially to both the native and the denatured form of the protein (reviewed in [4,78,79]) and hence decrease the chemical potential of the protein. Since the number of available binding sites is increased upon unfolding of the protein, an increase in preferential solute binding occurs as indicated by $(\delta m_3/\delta m_2)^{\mathrm{D}} > (\delta m_3/\delta m_2)^{\mathrm{N}} > 0$. There is a concomitant decrease in protein chemical potential, which is greater for the denatured state: $(\delta\mu_2/\delta m_3)^{\mathrm{D}}_{m_2} < (\delta\mu_2/\delta m_3)^{\mathrm{N}}_{m_2} < 0$. This serves to lower the free energy difference between the two states, and when the native state becomes the higher energy state, protein denaturation should result.

In more general terms, so long as $(\delta m_3/\delta m_2)^{\mathrm{D}} < (\delta m_3/\delta m_2)^{\mathrm{N}}$, the native state will be stabilized. Thus, stabilization could also arise if the solute bound preferentially to the native state was excluded from the denatured state, or if the solute was preferentially bound to both states but binding was less for the denatured state. Conversely in any situation in which $(\delta m_3/\delta m_2)^{\mathrm{D}} > (\delta m_3/\delta m_2)^{\mathrm{N}}$, the native state will be destabilized.

It is not possible to measure preferential interactions between solutes and proteins in frozen samples. Therefore, it is not known if cryoprotectants are actually preferentially excluded from frozen proteins. However, a recent study by Heller et al. [82] has provided direct evidence that the influence of a solute on protein chemical potential accounts for the solute's effect on protein stability during freezing. First, it was found with infrared spectroscopy that hemoglobin's secondary structure was perturbed in the frozen state. To test the effect of increasing the protein's chemical potential on inhibiting freezing-induced structural perturbation, hemoglobin was

Copyright 2004 by Marcel Dekker, Inc. All Rights Reserved.

prepared in a dextran/PEG mixture. This mixture forms two separate liquid phases, each enriched in one polymer, at room temperature. Hemoglobin partitions into both phases, and the protein's chemical potential will be increased by the presence of polymer in both phases. More importantly, since the system is in equilibrium, the protein's chemical potential is the same in both phases. When samples were removed from each phase and frozen, it was found that the infrared spectra of hemoglobin in the frozen state were identical and much more native-like than that seen in the absence of polymer. These results indicate that increasing protein chemical potential directly equates with increased protein stability during freezing. However, after freeze-drying the structure of hemoglobin in the dried state was more native-like in the sample taken from the PEG-rich phase than that from the dextran-rich phase. These results indicate that simply increasing protein chemical potential does not necessarily equate with stabilization of a protein during dehydration.

An important and often overlooked aspect of Timasheff's mechanism is the role of solid phase chemical potentials. Adding protective excipients to a protein solution increases the chemical potential of both the protein's native and denatured state. There is a limit to how high the chemical potential can be raised, however. This is because the *solid phase* chemical potentials of the protein are largely unaffected by the addition of excipients to the liquid solution. Thus, once the chemical potential of the native state is increased to a value greater than that of the solid state, precipitation of the protein will be favored. Protein precipitated will be at high concentration; this may pose problems due to aggregation upon drying and/or storage. Thus, there is a clear trade-off between conformational stability of the protein, which is increased with increasing cryoprotectant concentration, and stability against aggregation, which is decreased with increasing cryoprotectant concentration.

Finally, it is important to consider mechanistically how to explain the much greater potency of PEGs as cryoprotectants relative to other compounds such as sucrose. The data for one case, which are shown in Figure 9 and Table 1, illustrate this point. Figure 9 compares cryoprotection of LDH by PEG 8000, PEG 400, and sucrose (MW 342). LDH is completely protected during freeze-thawing by PEG 8000 at concentrations of $\geq$0.01% (wt/vol). In contrast, full protection in the presence of PEG 400 is not realized until the concentration is at least 2.5% (wt/vol). On a weight percentage basis, PEG 8000 is 250-fold more potent as a cryoprotectant. On a molar basis, the higher molecular weight PEG is 5000-fold more potent. Sucrose is much less effective than even PEG 400. Even at sucrose concentrations as high as 10% (wt/vol) the protein is not fully protected.

Copyright 2004 by Marcel Dekker, Inc. All Rights Reserved.

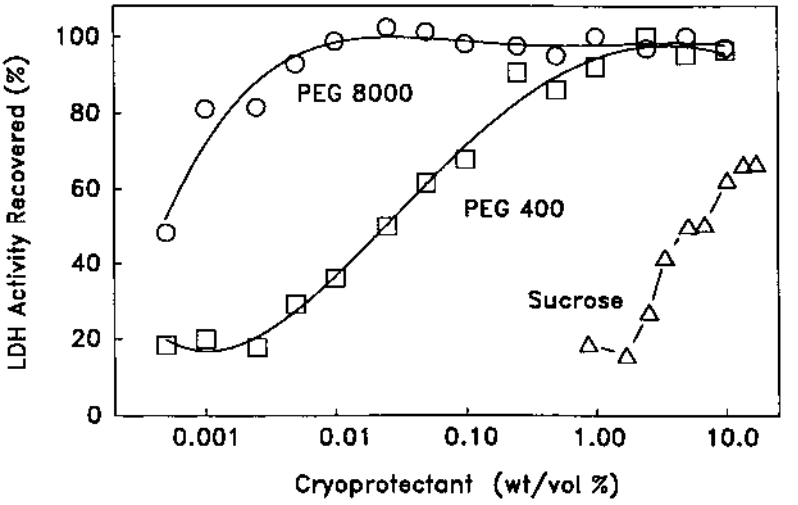

Figure 9 Effects of polyethylene glycols and sucrose on lactate dehydrogenase stability during freeze-thawing. (Data taken from Refs. 59 and 70.)

Table 1 Parameters for Solute Interactions with Chymotrypsinogen

Solute	Concentration	$(\delta m_3/\delta m_2)_{\mu_1,\mu_3}$	$(\delta\mu_3/\delta m_3)_{m_2}$ [a]	$(\delta\mu_2/\delta m_3)_m$ [b]
Sucrose[c]	1.27 m	−10.35	0.56	5.7
PEG 400[d] (0.27 m)	10% w/v	−6.87	2.42	16.6
PEG 6000[d] (0.0017 m)	1% w/v	−0.62	480.00	297.6

[a]kcal (mol of solute)$^{-1}$ (mol of solute in 1000 kg H_2O)$^{-1}$.
[b]kcal (mol of protein) $^{-1}$ (mol of solute) $^{-1}$.
[c]Data taken from Ref. 83.
[d]Data taken and calculated from Ref. 84.

In the past, we have ascribed these differences in protein stabilization to Timasheff's thermodynamic mechanism. The only protein for which the needed thermodynamic paramters have been measured in the presence of all three cryoprotectants is chymotrypsinogen [83,84]; Table 1. Although these data are not directly applicable to LDH, the general trends shown should be relevant to any protein. The increase in chymotrypsinogen chemical potential, $(\delta\mu_2/\delta m_3)_{m_2}$, in the presence of either of two different molecular weights of PEG (e.g., $M_r = 400$ or 6000) is greater than that noted in the presence of the sucrose, even though the PEGs are excluded to a lesser degree, on a per mole of solute basis. Comparing the two PEG

Copyright 2004 by Marcel Dekker, Inc. All Rights Reserved.

molecules indicates that the larger the PEG, the less it is excluded on a mole basis, but the more it increases protein chemical potential.

The basis for these observations can be explained by examining equation (20). The other major component in determining the effect of solute on protein chemical potential is the self-interaction parameter for the solute, $(\delta\mu_3/\delta m_3)_{m_2}$. The value for this parameter is several-fold greater for PEG 400 and almost three orders of magnitude greater for PEG 6000 than that for sucrose. The self-interaction parameter is given by:

$$(\delta\mu_3/\delta m_3)_{m_2} = [(RT/m_3) + RT(\delta \ln \gamma_3/\delta m_3)_{m_2}] \tag{3}$$

where γ_3 is the activity coefficient of the solute and R is the universal gas constant (reviewed in [4,78,79]). The molal concentrations needed for preferential exclusion of PEG are very small and the activity coefficient of PEG is quite large, relative to values for sucrose. Therefore, the self-interaction parameter for PEG is very large compared to that for sucrose. In addition, as the size of PEG increases there is a great increase in such nonideality (Table 1).

This argument does indeed support the contention that on a per-mole basis PEG is much more effective than sucrose at increasing protein chemical potential. And for cases where relatively high concentrations of PEG (e.g., >1% wt/vol) are needed to confer cryoprotection, the Timasheff mechanism may be applicable. However, it seems unlikely that a PEG concentration of 0.01% (wt/vol) would have a significant effect on the thermodynamics of the system. This is because the actual parameter of interest is the transfer free energy of the native versus denatured protein from water into cryoprotectant solution. The difference between the values for the two states determines the magnitude of the effect on the free energy of denaturation. The transfer free energy is obtained by integrating equation (1) from zero to the molal concentration of cryoprotectant of interest. With PEG 8000 at 0.01% wt/vol concentration, the molality is so low that the calculated transfer free energy would be extremely small. Thus, the effect on the free energy of denaturation would be trivial.

So, how can we account for the potent protection afforded by PEGs? The concentration range for cryoprotection is actually very similar to that seen with nonionic surfactants such as Tweens. PEGs have been shown to be surface-active and the magnitude of the decrease in water surface tension has been shown to correlate directly with PEG molecular weight [85]. Therefore, the most rational explanation for the results presented in Figure 9 is that PEGs are serving as such potent cryoprotectants because they are operating by the same mechanism(s) as more typical surfactants such as Tweens.

Copyright 2004 by Marcel Dekker, Inc. All Rights Reserved.

X. MECHANISMS FOR FAILURE OF DEXTRAN TO PROTECT LYOPHILIZED PROTEINS

In an idealized lyophilization cycle, a solution of proteins, buffers, and excipients is cooled to the solution's freezing point. At this point, it is thermodynamically favorable to form a new solid phase composed of pure ice. Once ice begins to form (not necessarily at the thermodynamic freezing point; substantial supercooling may occur), the remaining components of the solution in the nonfrozen phase become increasingly more concentrated, as shown in Figure 10. The combination of increased concentration and lower temperatures causes the viscosity of the non-ice phase to increase until, at a glass transition point termed T'_g, the solution becomes so viscous that further freezing of water is kinetically blocked.

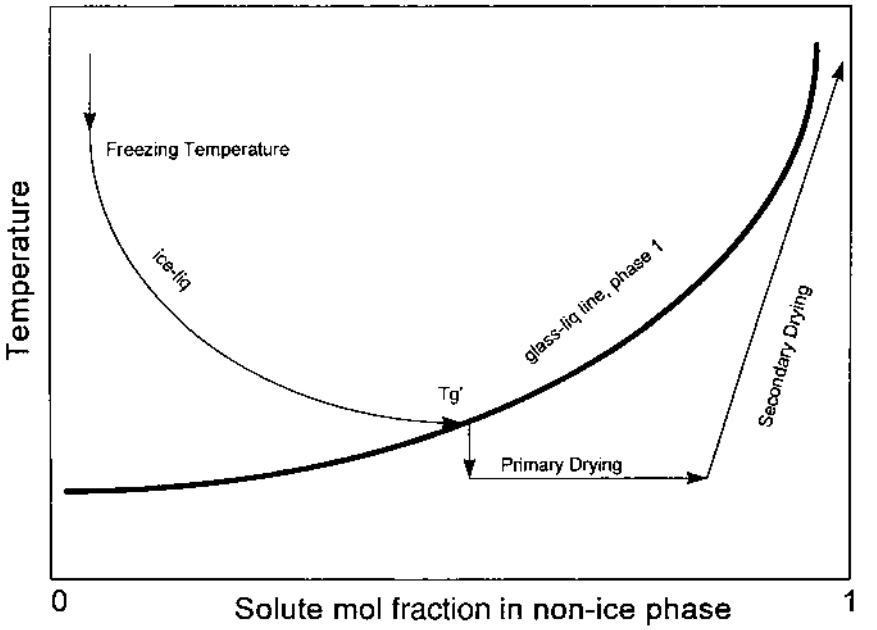

Figure 10 Phase diagram for an idealized, simple lyophilization cycle. A liquid sample first is cooled to the freezing temperature. As pure ice is formed, the solute remaining in the non-ice phase is concentrated until the ice–liquid line intersects the glass transition line at T'_g. No further concentration due to cooling occurs. Primary drying occurs under vaccum at a temperature below the glass transition temperature. After primary drying, the temperature is increased to effect secondary drying. Final storage temperature after secondary drying is below the glass transition line.

Copyright 2004 by Marcel Dekker, Inc. All Rights Reserved.

Further temperature decreases below T'_g have no additional concentrating effects.

It is important to realize that the preceding is a highly simplified description of the possible phase behaviors that can occur. In actual practice, phase behavior during freezing is rarely so simple. Instead, as the non-ice phase is concentrated, the chemical potentials of each solution component increase, until eventually a solubility point or a liquid–liquid miscibility point is reached. At this concentration it will be thermodynamically possible for an additional solid or liquid phase to be formed. Figure 11 shows one such diagram for a hypothetical system that undergoes

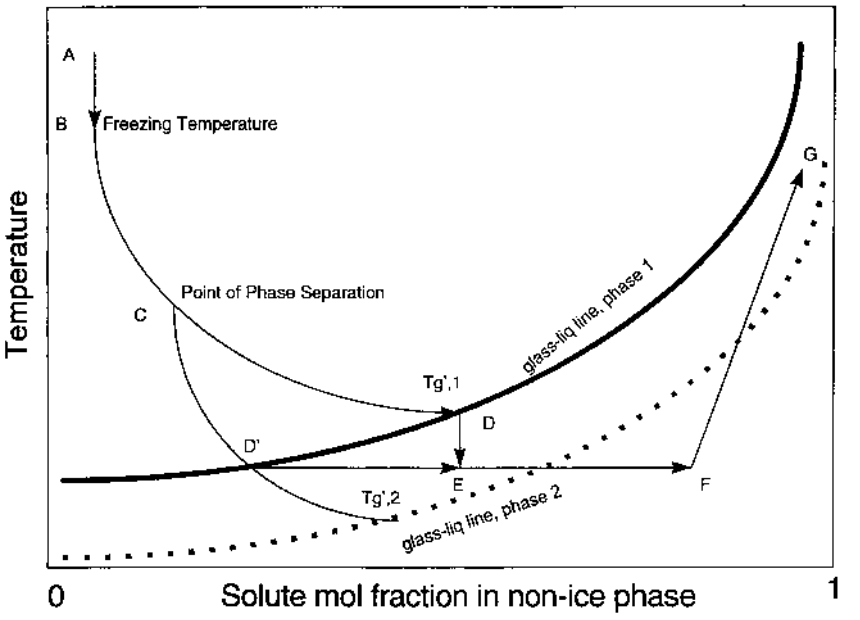

Figure 11 Phase diagram for a lyophilization cycle for a phase separation system. Starting with an aqueous solution at point A, the solution is cooled to the freezing point B. Further cooling results in concentration of solutes in the non-ice phase. At point C, the solutes are sufficiently concentrated that a phase split occurs. Additional cooling causes phase 1 to follows the path CDE, while phase 2 follows path CD′. Primary drying follows the path D′EF for phase 2 and EF for phase 1. Secondary drying for both phases begins at F, with the final dried condition at G. Note that for phase 2 the majority of both primary and secondary drying is conducted above its glass transition line, and final storage temperature is also above the glass transition line for phase 2.

Copyright 2004 by Marcel Dekker, Inc. All Rights Reserved.

a liquid-liquid phase split in the freeze-concentrated non-ice phase. That such a phase split can occur should not be surprising: many of the excipients that have been investigated as protein stabilizers (PEG, dextran, PVP, Ficoll) are well known to form two-phase aqueous systems when present at high concentration [86].

To achieve an optimally stabilized protein and maintain cake integrity, it is important to conduct primary and secondary drying steps at temperatures below the glass transition temperature. For systems that exhibit more complicated phase behavior, such as that shown in Figure 11, the preceding statement should be amended to state that drying steps should proceed at temperatures below *the lowest applicable glass transition temperature*. Systems that undergo liquid–liquid phase splits during freeze concentration will exhibit two or more characteristic glass transition temperatures. These glass transition temperatures may not be easily detected by conventional differential scanning calorimetry, especially if the phase volume of the second liquid phase is small. Electron paramagnetic resonance spectroscopic measurements have indicated the presence of multiple liquid phases in freeze-concentrated dextran/salt samples at $-15^{\circ}C$, under conditions where only one glass transition temperature could be detected by differential scanning calorimetry (C. Heinen and T.W. Randolph, unpublished observations).

It has been suggested that polymers such as dextran fail to protect proteins because they phase-separate from the protein during the freeze-drying process [87]. The dried solid could contain two or more amorphous phases. As Pikal [87] has stated, it is crucial that the stabilizing additive not only remain amorphous but also form a single phase *with the protein*.

Phase separation during freezing and/or drying may provide a possible reconciliation for the two competing hypotheses to explain protein stabilization by excipients during lyophilization. If a protein phase separates from an excipient on a microscopic scale, the excipient will not afford mechanical protection even if it forms a glass. Likewise, failure of an excipient to hydrogen-bond to a protein could be considered a manifestation of local phase separation. Indeed, the experiments of Carpenter et al. [36] showed that when PEG phase separates from PFK or LDH (by forming a solid crystalline phase), it fails to protect the proteins during drying. Thus, one could argue equally well from a "glass mechanics" point of view that because PEG phase separates it fails to envelop the protein in a competent glass. Or one could argue from the "water replacement" perspective that because PEG phase separates from the protein it cannot supply needed hydrogen bonds. In the end, both theories can be reduced to a single hypothesis: excipients must form a glass that intimately incorporates the protein if the native structure is to be maintained (cf. [87]).

Copyright 2004 by Marcel Dekker, Inc. All Rights Reserved.

Polymers such as dextrans could provide many desirable properties (e.g., high T_g' and T_g) to the freeze-dried formulation. Therefore, it is essential that future research address the theoretical and practical aspects of protein/polymer phase separation and develop the mechanistic insight to prevent this phenomenon during lyophilization. Also, as part of this effort, it is important to discern why other polymers (e.g., PVP and BSA) that protect labile proteins apparently do not phase separate from the protein during lyophilization.

ACKNOWLEDGMENTS

We gratefully acknowledge support by grants from the National Science Foundation (NSFBES9505301 and NSFBES9520288), the Whitaker Foundation, Boehringer Mannheim Therapeutics, Genentech, Inc., Genetics Institute, Inc., Genencor International, Amgen, Inc., and Zymogenetics, Inc. We also thank the National Science Foundation and American Foundation of Pharmaceutical Education, the American Pharmaceutical Manufacturing Association, and the Colorado Institute for Research in Biotechnology for providing predoctoral fellowships to our graduate students.

REFERENCES

1. MJ Geisow. Aching for approval, hoping for harmony—biotechnology product regulation. Trends Biotech 10(4):107–108, 1992.
2. YJ Wang, R Pearlman. Stability and Characterization of Protein and Peptide Drugs: Case Histories. New York, Pharmaceutical Biotechnology: Plenum Press, 1993, Volume 5.
3. JE Talmadge. The pharmaceutics and delivery of therapeutic polypeptides and proteins. Adv Drug Delivery Rev 10:247–299, 1993.
4. T Arakawa, SJ Prestrelski, W Kinney, JF Carpenter. Factors affecting short-term and long-term stabilities of proteins. Adv Drug Delivery Rev 10:1–28, 1993.
5. CA Thornton, M Ballow. Safety of intravenous immunoglobulin. Arch. Neurol. 50:135–136, 1993.
6. MJ Pikal. Freeze-drying of proteins. Part I: Process design. BioPharm 3(8):18–27, 1990.
7. MJ Pika, Freeze-drying of proteins. Part II: Formulation selection. BioPharm 3(9):26–30, 1990.
8. SJ Prestrelski, N Tedeschi, T Arakawa, JF Carpenter, Dehydration-induced conformational changes in proteins and their inhibition by stabilizers. Biophys J 65:661–671, 1993.

Copyright 2004 by Marcel Dekker, Inc. All Rights Reserved.

9. SJ Prestrelski, T Arakawa, JF Carpenter. Separation of freezing- and drying-induced denaturation of lyophilized proteins by stress-specific stabilization: II. Structural studies using infrared spectroscopy. Arch Biochem Biophys 303:465–473, 1993.
10. SJ Prestrelski, T Arakawa, JF Carpenter. The structure of proteins in lyophilized formulations using Fourier transform infrared spectroscopy. In: JL Cleland and R Langer, eds. Formulation and Delivery of Proteins and Peptides. American Chemical Society Symposium Series No. 567, 1994, pp 148–169.
11. A Dong, SJ Prestrelski, SD Allison, JF Carpenter. Infrared sepctroscopic studies of lyophilization- and temperature-induced protein aggregation. J Pharm Sci 84:415–424, 1995.
12. SJ Prestrelski, KA Pikal, T Arakawa. Optimization of lyophilization conditions for recombinant human interleukin-2 by dried-state conformational analysis using Fourier transform infrared spectroscopy. Pharm Res 12:1250–1259, 1995.
13. BS Chang, RM Beauvais, A Dong, JF Carpenter. Physical factors affecting the storage stability of freeze-dried interleukin-1 receptor antagonist: glass transition and protein conformation. Arch Biochem Biophys 331:249–258, 1996.
14. SD Allison, A Dong, JF Carpenter. Counteracting effects of thiocyanate and sucrose on chymotrypsinogen secondary structure and aggregation during freezing, drying and rehydration. Biophy J 71:2022–2032.
15. JF Carpenter and BS Chang. Lyophilization of protein pharmaceuticals. In: KE Avis, VL Wu, eds. Biotechnology and Biopharmaceutical Manufacturing, Processing and Preservation. Buffalo Grove, IL: Interpharm Press, 1996, pp 199–264.
16. TJ Ahern and MC Manning. Stability of Protein Pharmaceuticals: Part A. Chemical and Physical Pathways of Protein Degradation. New York: Plenum Press, 1992.
17. MC Manning, K Patel, RT Borchardt. Stability of protein pharmaceuticals. Pharm Res 6:903–908, 1989.
18. OP Chilson, LA Costello, NO Kaplan. Effects of freezing on enzymes. Fed Proc 24(2):S55–S65, 1965.
19. BL Chen, T Arakawa, E Hsu, L Narhi, TJ Tressel, SL Chen. Strategies to suppress aggregation of recombinant keratinocyte growth factor during liquid formulation development. J Pharm Sci 83:1657–1661, 1994.
20. J Brostreaux, IB Ericksson-Quensel. Etude sur la dessication des proteines. Arch Physique Biologique 23(4):209–226, 1935.
21. JF Carpenter, LM Crowe, JH Crowe. Stabilization of phosphofructokinase with sugars during freeze-drying: characterization of enhanced protection in the presence of divalent cations. Biochim Biophys Acta 923:109–115, 1987.
22. K Izutsu, S Yoshioka, Y Takeda. The effects of additives on the stability of freeze-dried β-galactosidase stored at elevated temperatures. Int J Pharm 71:137–146, 1991.

Copyright 2004 by Marcel Dekker, Inc. All Rights Reserved.

23. M Hageman. Water sorption and solid state stability of proteins. In: T Ahern, MC Manning, eds. Stability of Protein Pharmaceuticals. Part A. Chemical and Physical Pathways of Protein Degradation. New York: Plenum Press, 1992, pp 273–309.
24. K Hellman, DS Miller, RA Cammack. The effect of freeze-drying on the quaternary structure of L-asparaginase from *Erwinia carotovora*. Biochim Biophys Acta 749:133–142, 1983.
25. TJ Anchordoquy, JF Carpenter. Polymers protect lactate dehydrogenase during freeze-drying by inhibiting dissociation in the frozen state. Arch Biochem Biophys 332:231–238, 1996.
26. K Izutsu, S Yoshioka, T Terao. Stabilizing of β-galactosidase by amphiphilic additives during freeze-drying. Int J Pharm 90:187–194, 1993.
27. K Izutsu, S Yoshioka, T Terao. Stabilizing effect of amphiphilic excipients on the freeze-thawing and freeze-drying of lactate dehydrogenase. Biotechnol Bioeng 43:1102–1107, 1994.
28. T Imai, T Irie, M Otagiri, K Uekama, M Yamasaki. Comparative study of antiinflammatory drug fibroprofen with β-cyclodextrin and methylated β-cyclodextrins. J Inclusion Phenom 2:597–604, 1984.
29. A Yoshida, H Arima, K Uekama, J Pitha. Pharmaceutical evaluation of hydroxyalkyl ethers of β-cyclodextrins. Int J Pharm 46:217–222, 1988.
30. MS Hora, RK Rana, FW Smith. Lyophilized formulations of recombinant tumor necrosis factor. Pharm Res 9:33–36, 1992.
31. ME Brewster, MS Hora, JW Simpkins, N Bodor. Use of 2-hydroxypropyl-β-cyclodextrin as a solubilizing and stabilizing excipient for protein drugs. Pharm Res 8:792–795, 1991.
32. MS Hora, RK Rana, CL Wilcox, NV Katre, P Hirtzer, SN Wolfe, JW Thomson. Development of lyophilized formulation of interleukin-2. Dev Biol Stand 74:295–306, 1991.
33. JF Carpenter, JH Crowe. Infrared spectroscopic studies on the interaction of carbohydrates with dried protein. Biochemistry 28:3916–3922, 1989.
34. K Izutsu, S Yoshioka, T Teroa. Decreased protein-stabilizing effects of cryoprotectants due to crystallization. Pharm Res 10:1232–1237, 1993.
35. K Izutsu, S Yoshioka, T Terao. Effect of mannitol crystallinity on the stabilization of enzymes during freeze-drying. Chem Pharm Bull 42:5–8, 1994.
36. JF Carpenter, S Prestrelski, T Arakawa. Separation of freezing- and drying-induced denaturation of lyophilized proteins by stress-specific stabilization:I. Enzyme activity and calorimetric studies. Arch Biochem Biophys 303:456–464, 1993.
37. L Gatlin, P Deluca. A study of the phase separation in frozen antibiotic solutions by differential scanning calorimetry. J Parent Drug Assoc 34:398–408, 1980.
38. BJ Aldous, AD Auffret, F Franks. The crystallization of hydrates from amorphous carbohydrates. Cryo-Lett 16:181–186, 1995.
39. BS Chang, CS Randall. Use of subambient thermal analysis to optimize protein lyophilization. Cryobiology 29:632–656, 1992.

Copyright 2004 by Marcel Dekker, Inc. All Rights Reserved.

40. MJ Pikal, KM Dellerman, ML Roy, RM Riggin. The effects of formulation variables on the stability of freeze-dried human growth hormone. Pharm Res 8:427–436, 1991.
41. F Franks, RHM Hatley, SF Mathias. Materials science and the production of shelf stable biologicals. BioPharm 4(9):38–55, 1991.
42. CA Angell. Formation of glasses from liquids and biopolymers. Science 267:1924–1935, 1995.
43. T Tanaka, T Takeda, R Miyajama. Cryoprotective effect of sachharides on denaturation of catalase during freeze-drying. Chem Pharm Bull 39:1091–1094, 1991.
44. H Levine, L Slade. Principles of "cryostabilization" technology from structure/property relationships of carbohydrate/water systems—a review. Cryo-Lett 9:21–63, 1988.
45. H Levine, L Slade. Thermomechanical properties of small-carbohydrate-water glasses and "rubbers": kinetically metastable systems at sub-zero temperatures. J Chem Soc Faraday Trans 1 84:2619–2633, 1988.
46. H Levine, L Slade. Glass transitions in foods. In: HS Shartzberg and RW Hartel, eds. Physical Chemistry of Foods. New York: Marcel Dekker, 1992, pp 83–221.
47. JA Rupley, G Careri. Protein hydration and function. Adv Protein Chem 41:37–172, 1991.
48. ID Kuntz, W Kauzman. Hydration of proteins and polypeptides. Adv Protein Chem 28:239–345, 1974.
49. JT Edsall, HA McKenzie. Water and proteins II. The location and dynamics of water in protein systems and its relation to their stability and properties. Adv Biophys 16:53–183, 1983.
50. DM Byler, H Susi. Examination of the secondary structure of proteins by deconvoluted FTIR spectra. Biopolymers 25:469–487, 1986.
51. H Susi, DM Byler. Resolution enhanced Fourier transform infrared spectroscopy of enzymes. Meth Enzymol 130:290–311, 1986.
52. WK Surewicz, HH Mantsch. New insights into protein conformation from infrared spectroscopy. Biochim Biophys Acta 953:115–130, 1988.
53. S Krimm, J Bandekar. Vibrational spectroscopy and conformation of peptides, polypeptides and proteins. Adv Protein Chem 38:181–364, 1986.
54. A Dong, WS Caughey, Infrared methods for study of hemoglobin reactions and structures. Meth Enzymol 232:139–175, 1994.
55. A Dong, JD Meyer, BS Kendrick, MC Manning, JF Carpenter. Effect of secondary structure on the activity of enzymes suspended in organic solvents. Arch Biochem Biophys 334:406–414, 1996.
56. A Dong, J Matsuura, SD Allison, E Chrisman, MC Manning, JF Carpenter. Infrared and circular dichroism spectroscopic characterization of structural differences between β-lactoglobulin A and B. Biochemistry 35:1450–1457, 1996.
57. BS Kendrick, A Dong, SD Allison, MC Manning, JF Carpenter. Quantitation of the area of overlap between second-derivative amide I infrared spectra to

Copyright 2004 by Marcel Dekker, Inc. All Rights Reserved.

determine structural similarity of a protein in different states. J Pharm Sci 85:155–158, 1996.
58. PE Bock, C Frieden. Another look at the cold lability of enzymes. Trends Biochem Sci 3:100–103, 1978.
59. JF Carpenter, JH Crowe. The mechanism of cryoprotection of proteins by solutes. Cryobiology 25:244–255, 1988.
60. JF Carpenter, JH Crowe. Modes of stabilization of a protein by organic solutes during desiccation. Cryobiology 25:459–470, 1988.
61. JF Carpenter, SC Hand, LM Crowe, JH Crowe. Cryoprotection of phosphofructokinase with organic solutes: characterization of enhanced protection in the presence of divalent cations. Arch Biochem Biophys 250:505–512, 1986.
62. GB Strambini, E Gabellieri. Proteins in frozen solutions: evidence of ice-induced partial unfolding. Biophys J 70:971–976, 1996.
63. JF Brandts, J Fu, JF Nordin. The low temperature denaturation of chymotrypsinogen in aqueous solution and in frozen aqueous solution. In: GEW Wolstenholme, M O'Conner, eds. The Frozen Cell. London: Churchill, 1970, pp 189–212.
64. WJ Becktel, JA Schellman. Protein stability curves. Biopolymers 26:1859–1877, 1987.
65. PL Privalov. Cold denaturation of proteins. Crit Rev Biochem Mol Biol 25:281–305, 1990.
66. L van den Berg. The effect of addition of sodium and potassium chloride to the reciprocal system: KH_2-PO_4-Na_2HPO_4-H_2O on pH and composition during freezing. Arch Biochem Biophys 84:305–315, 1959.
67. L van den Berg, D Rose. The effect of freezing on the pH and composition of sodium and potassium solutions: the reciprocal system KH_2-PO_4-Na_2HPO_4-H_2O. Arch Biochem Biophy 81:319–329, 1959.
68. K Shikama, I Yamazaki. Denaturation of catalase by freezing and thawing. Nature 190:83–84, 1961.
69. SH Loomis, JF Carpenter, TJ Anchordoguy, JH Crowe, BR Branchini. Cryoprotective capacity of end products of anaerobic metabolism. J Exp Zool 252:9–15, 1989.
70. JF Carpenter, SJ Prestrelski, TJ Anchordoguy, T Arakawa. Interactions of stabilizers with proteins during freezing and drying. In: JL Cleland, R Lauger, eds. Formulation and Delivery of Proteins and Peptides. American Chemical Society Symposium Series No. 567, 1994, pp 134–147.
71. BS Chang, BS Kendrick, JF Carpenter. Surface-induced denaturation of proteins during freezing and its inhibition by surfactants. J Pharm Res 85:1325–1330, 1996.
72. S Nema, KE Avis. Freeze-thaw studies of a model protein, lactose dehydrogenase, in the presence of cryoprotectant. J Parent Sci Tech 47:76–83, 1993.
73. DO Johnson, KJ Stebe. Oscillating bubble tensiometry: A method for precisely measuring the kinetics of surfactant adsorptive-desorptive exchange. J Colloid Int Sci 168:526–538, 1994.

Copyright 2004 by Marcel Dekker, Inc. All Rights Reserved.

74. K Izutsu, S Yoshioka, S Kojima. Increased stabilizing effect of amphiphilic excipients on freeze-drying of lactate dehydrogenase (LDH) by dispersion into sugar matrices. Pharm Res 12:838–843, 1995.
75. NB Bam, TW Randolph, JL Cleland. Stability of protein formulations: investigation of surfactant effects by a novel EPR spectroscopic technique. Pharm Res 12:2–11, 1995.
76. JL Cleland, TW Randolph. Mechanism of polyethylene glycol interactions with molten globule folding intermediate of bovine carbonic B. J Biol Chem 267:3147–3153, 1992.
77. PM Horowitz. Kinetic control of protein folding by detergent micelles, liposomes, and chaperonins. In: JL Cleland, ed. Protein Folding. *In Vivo* and *In Vitro*. American Chemical Society Symposium Series No. 526, 1993, pp 156–163.
78. SN Timasheff. Stabilization of protein structure by solvent additives. In: T Ahern, MC Manning, eds. Stability of Protein Pharmaceuticals. Part B. Vivo Pathways of Degradation and Strategies for Protein Stabilization. New York: Plenum Press, 1992, pp 265–285.
79. SN Timasheff. Preferential interactions of water and cosolvents with proteins. In: RB: Gregory, ed. Protein-Solvent Interactions. New York: Marcel Dekker, 1995, pp 445–482.
80. J Wyman. Linked functions and reciprocal effects in hemoglobin: a second look. Adv Protein Chem 19:223–286, 1964.
81. J Wyman, SJ Gill. Binding and Linkage. Functional Chemistry of Biological Molecules. University Science Books, Mill Valley, CA, 1990.
82. M Heller, JF Carpenter, TW Randolph. Effect of phase separating systems on lyophilized hemoglobin. J Pharm Sci 85:1358–1362.
83. JC Lee, SN Timasheff. The stabilization of proteins by sucrose. J Biol Chem 259:7193–7201, 1981.
84. R Bhat, SN Timasheff. Steric exclusion is the principal source of the preferential hydration of proteins in the presence of polyethylene glycols. Protein Sci 1:1133–1143, 1992.
85. M Winterhalter, H Burner, S Marzinka, R Benz, JJ Kasianowicz. Interaction of poly(ethylene-glycols) with air–water interfaces and lipid monolayers: investigations of surface pressure and surface potential. Biophys J 69:1372–1381, 1995.
86. P-A, Albertsson. Partition of Cell Particles and Macromolecules. 3rd ed. New York: Wiley-Interscience, 1986.
87. MJ Pikal. Freeze-drying of proteins. In: JL Cleland, R Langer, eds. Formulation and Delivery of Proteins and Peptides. American Chemical Society Symposium Series No. 567, 1994, pp 120–133.

Copyright 2004 by Marcel Dekker, Inc. All Rights Reserved.

6

Molecular Mobility of Freeze-Dried Formulations as Determined by NMR Relaxation, and its Effect on Storage Stability

Sumie Yoshioka
National Institute of Health Sciences, Tokyo, Japan

I. INTRODUCTION

Freeze-drying is a useful method for preparing dosage forms of thermally unstable pharmaceuticals without the deleterious effect of heat. The method can also provide a dry product of pharmaceuticals with longer shelf-life than solutions or suspensions. Glassy state formulations obtained by freeze-drying are generally considered to exhibit sufficient storage stability for pharmaceuticals. However, degradation during storage has been observed in various freeze-dried formulations.

Many studies have demonstrated that storage stability of freeze-dried formulations is related to molecular mobility [1–15]. Chemical and physical degradation in amorphous pharmaceuticals of small molecular weight is enhanced by an increase in molecular mobility associated with moisture sorption. Degradation of freeze-dried protein formulations often increases as molecular mobility is increased by water sorption.

This chapter aims to provide an insight into the relationship between molecular mobility and storage stability of freeze-dried formulations.

Copyright 2004 by Marcel Dekker, Inc. All Rights Reserved.

First, methods for determining the molecular mobility of freeze-dried formulations are addressed. The effect of molecular mobility on storage stability is then discussed.

II. MOLECULAR MOBILITY OF FREEZE-DRIED FORMULATIONS

Various methods, including differential scanning calorimetry (DSC), dielectric relaxation spectrometry, and NMR, are known to be useful to determine molecular mobility of freeze-dried formulations [16,17]. The glass transition temperature (T_g) has been used as a measure of molecular mobility of lyophilized formulations, since it indicates the critical temperature of α-relaxation for amorphous polymer materials. Freeze-dried formulations containing polymer excipients can be considered to exhibit low molecular mobility without α-relaxation at temperatures below T_g.

NMR is another useful means of measuring molecular mobility of freeze-dried formulations. The spin–lattice relaxation time in the laboratory frame (T_1) and the spin–spin relaxation time (T_2) of ^{1}H, ^{2}H, ^{17}O, or ^{13}C have been used to represent the mobility of water and polymer molecules in freeze-dried cakes or aqueous polymer solutions [18–22]. In contract to DSC or dielectric relaxation spectrometry, NMR allows identification of the origin of molecular motion. Determining molecular mobility for each drug and excipient in a freeze-dried formulation is therefore possible when high-resolution solid-state NMR is used.

This section addresses the parameters of molecular motion that can be determined by T_1, T_2, and rotating frame spine–lattice relaxation time ($T_{1\rho}$) of protons and carbons in freeze-dried formulations measured using pulsed NMR and high-resolution solid-state NMR.

A. Molecular Mobility as Determined by Spin–Spin Relaxation Time of Protons

Spin–spin relaxation time (T_2) of protons present in freeze-dried formulations can be determined from free induction decay (FID). Figure 1 shows the FID of protons in a freeze-dried formulation containing γ-globulin as a model protein drug and dextran (molecular weight of 40 k) as a polymer excipient, measured by pulsed NMR using "solid echo" in the detection stage [23]. The FID shows two relaxation processes at 10°C at 60% relative humidity (Figure 1A); a slower decay described by the Lorentzian equation (equation (1)); and a faster decay described by a Gaussian-type equation

Copyright 2004 by Marcel Dekker, Inc. All Rights Reserved.

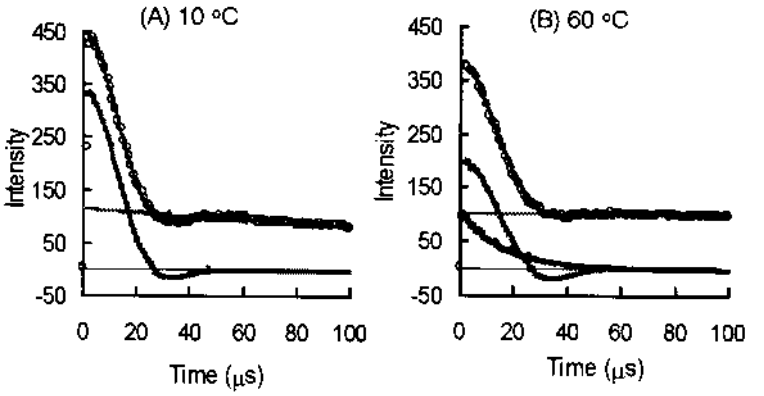

Figure 1 Free induction decay of protons in lyophilized γ-globulin formulation containing dextran at 10°C (A) and 60°C (B) at 60%RH.

(the Abragam equation, equation (2) with a constant c of 0.12). This slower decay can be attributed to protons with higher mobility, i.e., water protons, and the faster decay can be attributed to protons with lower mobility, i.e., protons of γ-globulin and dextran. The contribution of protein protons to the FID is not significant, because the content of protein was 50 times less than that of dextran. Therefore, the Abragam decay can be considered to be due to dextran protons. The FID of the freeze-dried formulation containing γ-globulin and dextran is describable by an equation representing the sum of the Abragam and Lorentzian equations (equation (3)). The T_2 of water protons can be calculated from the FID signals at the latter stage. Subsequently, the T_2 of dextran protons with lower mobility can be calculated from the FID signals at the former stage by inserting the calculated T_2 of water protons into equation (3):

$$F(t) = A\exp(-t/T_{2(\mathrm{hm})}) \tag{1}$$

$$F(t) = A\exp(-t^2/2T_{2(\mathrm{lm})}^2)\sin(ct)/ct \tag{2}$$

$$F(t) = (1 - P_{\mathrm{hm}})\exp(-t^2/2T_{2(\mathrm{lm})}^2)\sin(ct)/ct + P_{\mathrm{hm}}(\exp(-t/T_{2(\mathrm{hm})})) \tag{3}$$

where $T_{2(\mathrm{hm})}$ and $T_{2(\mathrm{lm})}$ are the spin–spin relaxation times of protons with higher mobility and slower mobility, respectively. P_{hm} is the proportion of proton with higher mobility.

As shown in Figure 1B, the decay due to dextran protons at 60°C cannot be described by a single Abragam equation, and therefore requires further solving by the Lorentzian equation. This indicates that at 60°C, the

Copyright 2004 by Marcel Dekker, Inc. All Rights Reserved.

dextran protons of the freeze-dried formulations exhibit a slower relaxation process due to higher mobility in addition to a faster relaxation process due to lower mobility. In other words, liquid-like dextran protons with higher mobility exist in the formulation at 60°C, in addition to solid-like dextran protons with lower mobility. Thus, the FID at 60°C is described by an equation representing the sum of the Abragam and Lorentzian equations for dextran protons as well as the Lorentzian equation for water protons. The proportion of liquid-like dextran protons can be calculated by fitting FID signals into equation (3) after subtracting signals due to water protons.

Lyophilized γ-globulin formulations containing poly(vinyl alcohol) (PVA) exhibited both Abragam and Lorentzian relaxation processes due to PVA protons, in addition to a Lorentzian relaxation process due to water protons even at 10°C, 60%RH, indicating that both solid-like and liquid-like PVA protons exist. However, the T_2 and proportion of liquid-like protons of PVA cannot be calculated by fitting FID signals into equation (3) after subtracting signals due to water protons, since decay due to water protons cannot be separated from that due to liquid-like PVA protons because of their close T_2 values. The FID of lyophilized formulations prepared with D_2O was needed to determine the proportion of liquid-like PVA protons.

Figure 2 shows the proportion of liquid-like dextran and PVA protons as a function of temperature [24]. Liquid-like polymer protons appear at

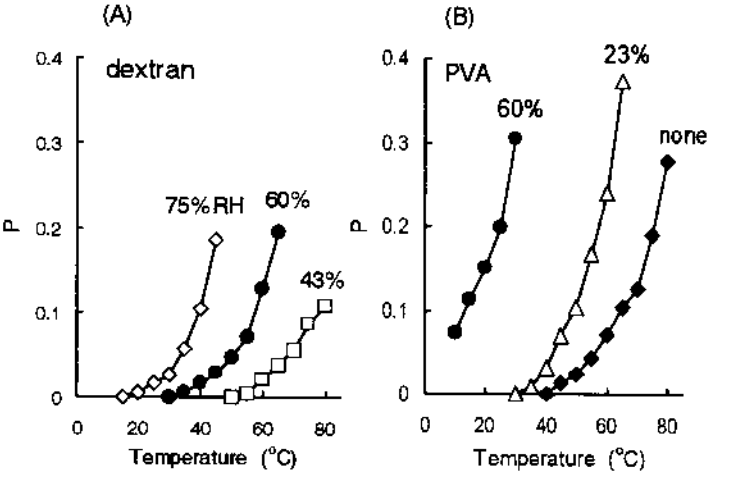

Figure 2 Proportion of liquid-like polymer protons in lyophilized γ-globulin formulations containing dextran (A) and PVA (B) at various humidities.

Copyright 2004 by Marcel Dekker, Inc. All Rights Reserved.

a certain temperature, and their proportion increases as temperature increases. This critical temperature of detection of liquid-like polymer protons shifts to a lower temperature as water content increases, indicating that the moleucular mobility of polymer excipients in the formulation is increased by the plasticizing effect of water. Liquid-like protons were detected even at 10°C/60%RH in formulations containing PVA, indicating that this formulation has a higher molecular mobility than the formulation containing dextran.

The temperature at which the spin–spin relaxation of protons begins to involve the Lorentzian relaxation process due to liquid-like polymer protons in addition to the Gaussian-type relaxation process due to solid-like polymer protons is considered to be a glass/rubber transition temperature. Basically, this is a critical temperature of molecular mobility as determined by NMR relaxation measurements, and is analogous to the glass transition temperature (T_g) determined by DSC. This critical mobility temperature is referred as T_{mc}.

The T_{mc} of formulations containing polymer excipients increases as the molecular weight of the polymers increases. Formulations containing dextran with a molecular weight of 510 k exhibited a T_{mc} 5°C higher than those containing dextran with a molecular weight of 40 k. Similarly, the T_{mc} of the MW 120 k PVA formulation was approximately 5°C higher than that of the MW 18 k PVA formulation. As shown in Figure 3, the T_2 of water protons calculated by the Lorentzian equation was not significantly affected by the molecular weight of dextran [25]. This indicates that the mobility of

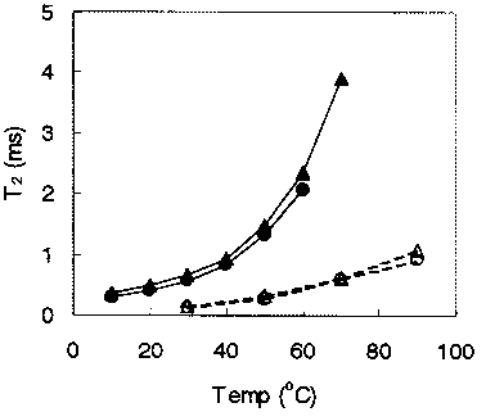

Figure 3 T_2 of water protons in lyophilized γ-globulin formulations containing dextran as a function of temperature: (●) MW 10 k dextran at 60%RH, (▲) MW 510 k at 60%RH, (○) MW 10 k at 12%RH, and (△) MW 510 k at 12%RH.

Copyright 2004 by Marcel Dekker, Inc. All Rights Reserved.

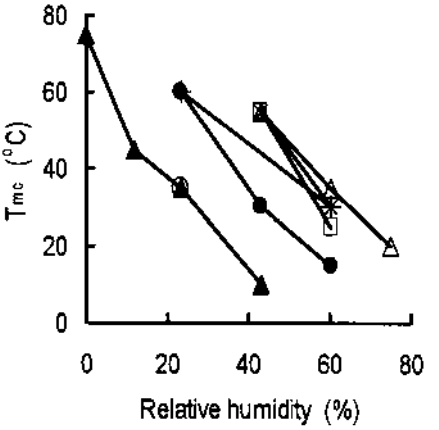

Figure 4 Critical mobility temperature (T_{mc}) of lyophilized γ-globulin formulations containing PVA (○) PHEA (▲), PVP (●), MC (+), HPMC (□), CMC-NA (∗), and dextran (△).

water molecules in the formulation is determined by the interaction between the glucose unit and water.

Figure 4 shows the T_{mc} of lyophilized formulations containing various polymer excipients as a function of relative humidity [26]. As relative hymidity increased, T_{mc} for each formulation decreased. Formulations containing α,β-poly (*N*-hydroxyethyl)-L-aspartamide (PHEA), methylcellulose (MC), and hydroxypropylmethylcellulose (HPMC) exhibited comparable T_{mc} values at lower humidities than formulations with dextran and carboxymethylcellulose sodium salt (CMC-Na). This indicates that the formulations containing PHEA, MC, and HPMC contain highly mobile protons at a lower temperature than the formulations containing dextran and CMC-Na at the same humidity.

The T_{mc} of lyophilized formulations containing polymer excipients is generally observed at a temperature 20 to 30°C lower than T_g determined by DSC (Figure 5) [26]. This indicates that these formulations have highly mobile protons even at temperatures below T_g. T_{mc} can be considered to be the temperature at which a certain region of the molecule, such as terminal units of polymer chains, begins to have greater mobility. T_{mc} is a glass/rubber transition temperature determined by spin–spin relaxation measurements, which can detect local changes in molecular mobility more sensitively than T_g determined by DSC. The T_g of lyophilized formulations containing polymer excipients with moisture is often difficult to determine because a change in heat capacity at T_g may be overlapped by the peaks of water evaporation and accompanying relaxation processes. Furthermore,

Copyright 2004 by Marcel Dekker, Inc. All Rights Reserved.

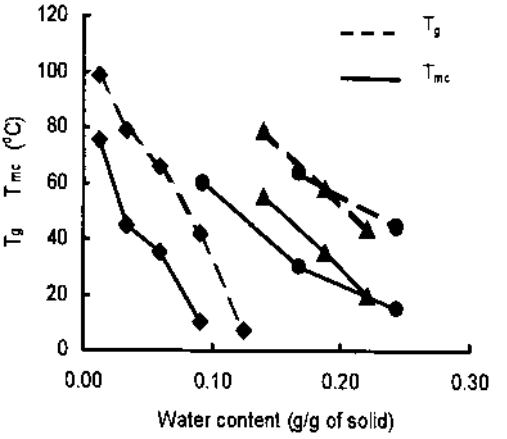

Figure 5 T_{mc} and glass transition temperature of lyophilized γ-globulin formulations containing PHEA (◆), dextran (▲), and PVP (●).

certain formulations, especially freeze-dried protein formulations, reveal unclear changes in heat capacity, causing a difficulty in the determination of T_g. In such cases, T_{mc} determined by spin–spin relaxation measurements can be a useful measure of molecular mobility.

B. Molecular Mobility as Determined by the Laboratory and Rotating Frame Spin–Lattice Relaxation Times of Protons

Spin–lattice relaxation times in laboratory and rotating frames (T_1 and $T_{1\rho}$) can also be used to measure the molecular mobility of lyophilized formulations. The rotational motion of protons with a certain value of correlation time (τ_c) is reflected by T_1 and $T_{1\rho}$. The relationship between τ_c and T_1 can be described as follows:

$$\frac{1}{T_1} = \frac{9}{8}\gamma^4\left(\frac{h}{2\pi}\right)^2\left[\frac{4\tau_c}{15r^6(1+\omega_0^2\tau_c^2)} + \frac{16\tau_c}{15r^6(1+4\omega_0^2\tau_c^2)}\right] \tag{4}$$

where γ is the gyromagnetic ratio of ^{1}H, h is Planck's constant, ω_0 is the ^{1}H resonance frequencies, and r is the H–H distance. On the other hand, $T_{1\rho}$ can be related to τ_c according to

$$\frac{1}{T_{1\rho}} = A\tau_c/(1+4\omega_1^2\tau_c^2) \tag{5}$$

Copyright 2004 by Marcel Dekker, Inc. All Rights Reserved.

where ω_1 is the frequency of precession generated by the spin locking field, and A is a constant. An example of the τ_c dependence of T_1 and $T_{1\rho}$ of protons is shown in Figure 6A. The temperature dependence of T_1 and $T_{1\rho}$ of protons calculated by assuming an Arrhenius behavior is shown in Figure 6B. $T_{1\rho}$ shows a minimum such that $T_{1\rho}$ decreases in a linear fashion with decreasing temperature at higher temperatures, but increases at lower temperatures. The temperature range below the $T_{1\rho}$ minimum corresponds to the slow motional regime in which an increase in molecular mobility brings about a decrease in $T_{1\rho}$, whereas the temperature range above the $T_{1\rho}$ minimum corresponds to the fast motional regime, in which an increase in molecular mobility brings about an increase in $T_{1\rho}$. The temperature dependence of T_1 also shows a minimum in a similar manner to $T_{1\rho}$. However, a minimum of T_1 is observed at a higher temperature than $T_{1\rho}$, since T_1 efficiently reflects faster motions compared to $T_{1\rho}$.

The $T_{1\rho}$ of all protons within a certain region of the molecule is averaged through spin diffusion, such that $T_{1\rho}$ preferentially reflects the motion of protons with the smallest relaxation time. If protons in lyophilized formulations have two different motions represented by τ_{c1} and τ_{c2} that are equally involved in the relaxation process, the relaxation rate (the reciprocal of T_1 and $T_{1\rho}$) can be calculated as the sum of the relaxation rates attributed to each τ_c (Figure 7). Thus, the observed values of T_1 and $T_{1\rho}$ closely approximate the smaller relaxation times of the two loci.

Figure 8 shows the time course of the laboratory and rotating frame spin–lattice relaxation of protons in lyophilized γ-globulin formulations containing dextran, determined at 55°C using a pulsed NMR spectrometer [26].

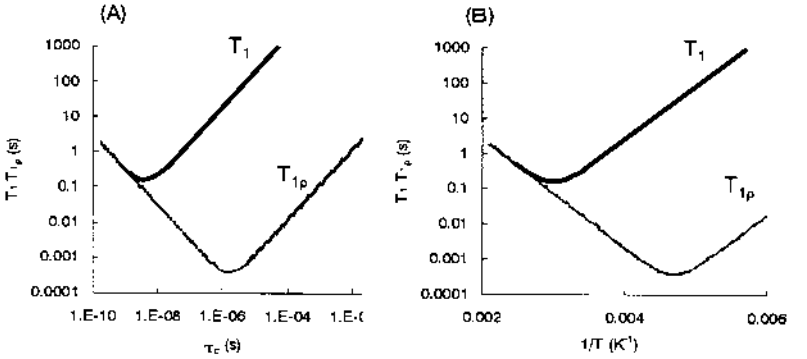

Figure 6 T_1(▬) and $T_{1\rho}$ (—) of protons as a function of correlation time (A) and temperature (B).

Copyright 2004 by Marcel Dekker, Inc. All Rights Reserved.

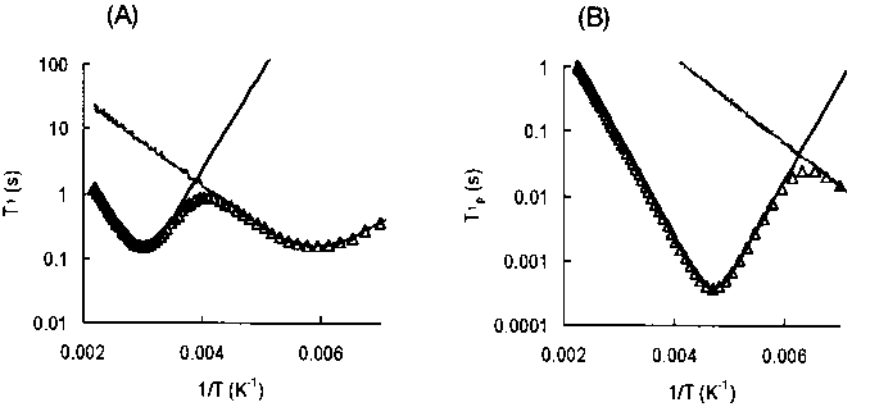

Figure 7 Temperature dependence of T_1 (A) and $T_{1\rho}$ (B) of protons with two correlation times.

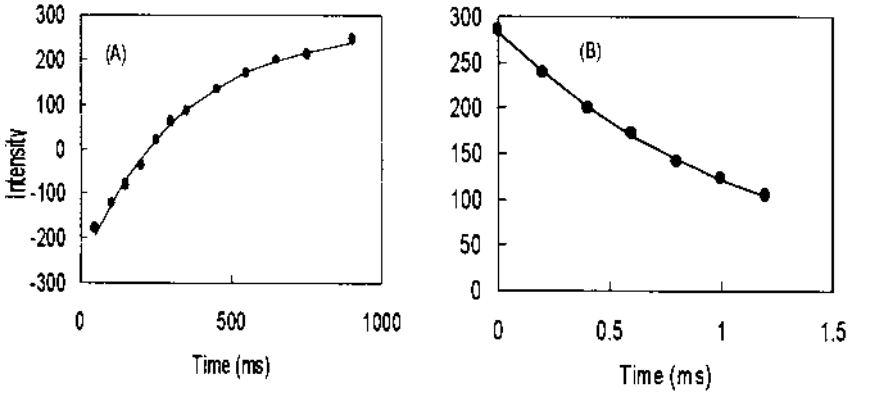

Figure 8 Time course of spin–lattice relaxation in laboratory (A) and rotating frames (B) of protons in lyophilized γ-globulin formulations containing dextran at 55°C.

T_1 and $T_{1\rho}$ can be determined from the corresponding signal decay, respectively, by a mono-exponential equation. The calculated T_1 and $T_{1\rho}$ represent the T_1 and $T_{1\rho}$ of unexchangeable protons (five methyne protons and two methylene protons in a repeating unit), since D_2O was used to prepare lyophilized samples. As shown in Figure 9, T_1 decreased with increasing temperature in the slow motional regime at 12–86%RH. As humidity increased, T_1 decreased, indicating an increase in the molecular mobility of the formulation.

Copyright 2004 by Marcel Dekker, Inc. All Rights Reserved.

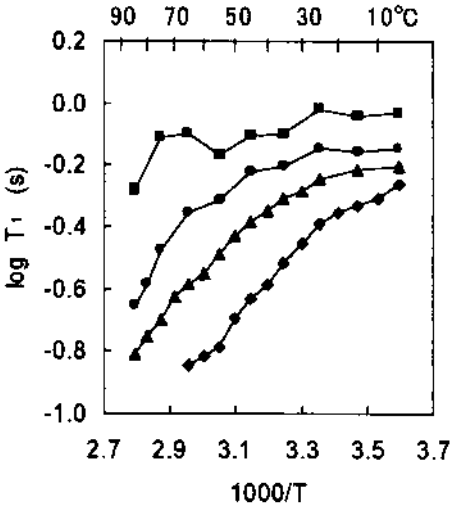

Figure 9 Temperature dependence of T_1 of protons in lyophilized γ-globulin formulations containing dextran at 12%RH (■), 60%RH (●), 75%RH (▲), and 86%RH (◆).

The temperature dependence of $T_{1\rho}$ exhibited a minimum at relatively high humidities (75%RH and 86%RH) (Figure 10). The temperature of the $T_{1\rho}$ minimum shifted to higher temperature as humidity decreased. At 60%RH, $T_{1\rho}$ similarly decreased with increasing temperature, but a minimum was not observed in the temperature range up to 80°C (it may be observed around 90°C). However, another minimum was observed at approximately −60°C at 60%RH, as shown in Figure 11. This minimum shifted to approximately 90°C in the dry state. Therefore, protons in the formulation appear to have two correlation times due to different motions.

The T_1 and $T_{1\rho}$ of protons observed at 60%RH (Figure 12) can be interpreted by the rotational motions of the methine and methylene groups in dextran. As shown in Figure 12B, the change in $T_{1\rho}$ with temperature can be described by two correlation times (τ_{c1} and τ_{c2}) with an activation energy of 8.0 and 2.5 kcal/mol, and with a pre-exponential factor of 2×10^{-10} and 5×10^{-9} s, respectively, at temperatures lower than 35°C ($1000/T$ of 3). The motion represented by τ_{c1} and τ_{c2} may be attributed to methine and methylene protons, respectively, on the basis of the values of activation energy. An activation energy of the same order as the calculated value of τ_{c2} has been reported for the methylene group of amorphous polyethylene (3.72 kcal/mol) [27]. $T_{1\rho}$ reflects the motion of methine groups at

Copyright 2004 by Marcel Dekker, Inc. All Rights Reserved.

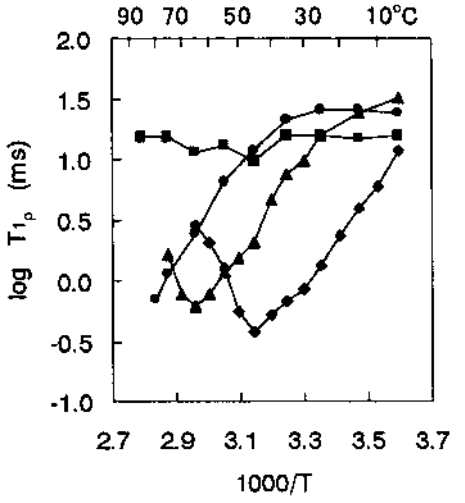

Figure 10 Temperature dependence of $T_{1\rho}$ of protons in lyophilized γ-globulin formulations containing dextran at 12%RH (■), 60%RH (●), 75%RH (▲), and 86%RH (◆).

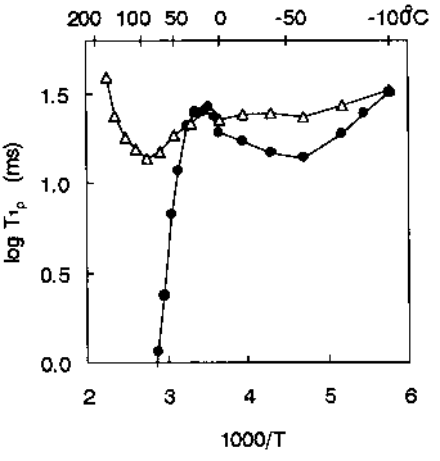

Figure 11 Temperature dependence of $T_{1\rho}$ of protons in lyophilized γ-globulin formulations containing dextran at 60%RH (●) and in the dry state (△).

temperatures between 35 and 10°C (1000/T of 3 and 3.5), but reflects the motion of methylene groups at temperatures lower than 10°C.

As shown in Figure 12A, the observed T_1 can be represented by the correlation time of methylene protons (τ_{c2}) at temperatures between 35 and

Copyright 2004 by Marcel Dekker, Inc. All Rights Reserved.

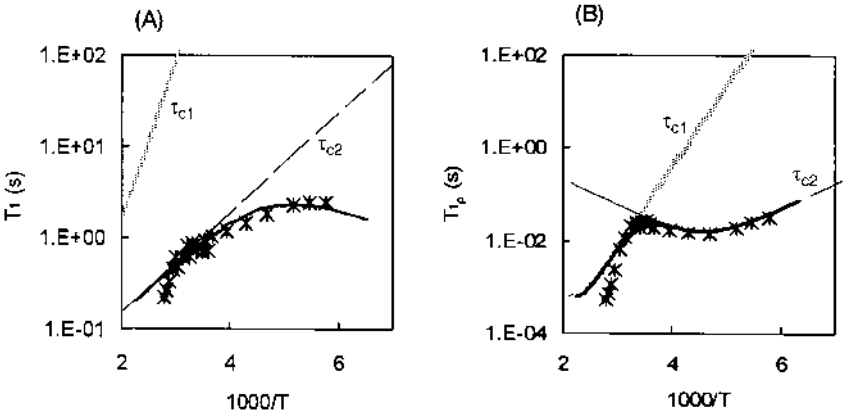

Figure 12 Curve fitting of T_1 and $T_{1\rho}$ observed at 60%RH using two correlation times.

$-20°C$ ($1000/T$ of 3 and 4). The observed values of T_1 are coincident with the values calculated using an r value of $1.8A$ in equation (4), corresponding to the distance between protons in a methylene group. This supports the interpretation that the motion represented by τ_{c2} is attributed to methylene protons. When the temperature decreased from $-20°C$, the observed T_1 diverged from the values calculated by τ_{c2}. This divergence of T_1 appears to be due to causes unrelated to molecular mobility.

In the temperature range shown in Figure 12, the motion of methine groups can be measured by $T_{1\rho}$ at higher temperatures. In contrast, the motion of methylene groups can be observed by $T_{1\rho}$ at lower temperatures and by T_1 at higher temperatures. The correlation times of methine and methylene protons were estimated to be on the orders of 10^{-4} s and 10^{-7} s, respectively, at 10°C. As shown in Figure 12A, the observed T_1 of methylene protons diverged from the values calculated from τ_{c2}, when the temperature increased past 35°C ($1000/T$ of 3). This indicates that the temperature dependence of τ_{c2} changes around 35°C, and the motion of methylene has a greater activation energy at temperatures above 35°C. The observed $T_{1\rho}$ of methine groups also diverged from the values calculated from τ_{c1} at temperatures above 35°C (Figure 12B), indicating that the temperature dependence of τ_{c1} changes around 35°C, and the motion of methine has a greater activation energy at temperatures above 35°C. The temperature at which a break is observed in the temperature dependence of the motions of methylene and methine is coincident with the critical temperature of molecular mobility (T_{mc}), described in Section II.A.

Copyright 2004 by Marcel Dekker, Inc. All Rights Reserved.

C. Molecular Mobility as Determined by Laboratory and Rotating Frame Spin–Lattice Relaxation Times of Carbons

Figure 13 shows the typical spectra of lyophilized γ-globulin formulation containing dextran (A), lyophilized γ-globulin (B), and lyophilized dextran (C), measured by high-resolution ^{13}C solid state NMR [28]. Peaks at 70 ppm and 180 ppm were assigned to the dextran methine carbon and γ-globulin carbonyl carbon, respectively. The T_1 of each carbon can be calculated from the signal decay due to laboratory frame spin–lattice relaxation, using a mono-exponential equation. The observed T_1 decreased with increasing temperature, indicating that relaxation occurs in the slow motional regime. The correlation time (τ_c) of dextran methine carbon then can be calculated from the observed T_1 according to equation (6), if the dipole–dipole interaction between the carbon and proton is predominant in the relaxation process, and if the relaxation time can be expressed by a single τ_c:

$$\frac{1}{T_1} = \frac{1}{10}\gamma_C^2\gamma_H^2 h^2 (2\pi)^{-2} r_{C-H}^{-6}\left[\frac{1}{(\omega_C - \omega_H)^2} + \frac{3}{\omega_C^2} + \frac{6}{(\omega_C + \omega_H)^2}\right]\frac{1}{\tau_c} \qquad (6)$$

where γ_C and γ_H are the gyromagnetic ratios of ^{13}C and ^{1}H, respectively, h is Planck's constant, and ω_C and ω_H are the ^{13}C and ^{1}H resonance

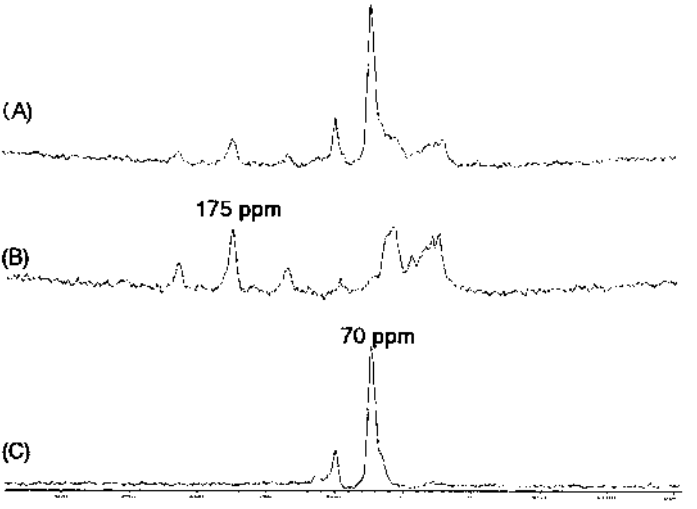

Figure 13 ^{13}C-NMR spectra of lyophilized γ-globulin formulations containing dextran (A), lyophilized γ-globulin (B), and lyophilized dextran (C).

Copyright 2004 by Marcel Dekker, Inc. All Rights Reserved.

frequencies, respectively. r_{C-H} is the C–H distance and the value of 1.2*A* was used for the calculation.

On the other hand, the τ_c of the γ-globulin carbonyl carbon can be calculated from the observed T_1 using equation (7) if the relaxation due to chemical shift anisotropy is predominant, and if the relaxation time in the slow motional regime can be expressed by a single τ_c:

$$\frac{1}{T_1} = \frac{6}{40}\gamma_C^2 B_0^2 \delta_z^2 \left(1 + \frac{\eta^2}{3}\right)\left(\frac{2}{\omega_0^2 \tau_C}\right) \tag{7}$$

where B_0, δ_Z, and η are the static field, the chemical shift anisotropy, and the asymmetric parameter, respectively. δ_z and η are defined in terms of three principal components (δ_{11}, δ_{22}, and δ_{33}):

$$\begin{aligned} &\delta_z = \delta_{11} - \delta_0, \qquad \eta = (\delta_{22} - \delta_{33})/(\delta_{11} - \delta_0) \\ &\qquad\qquad\qquad\qquad \text{when} \quad |\delta_{11} - \delta_0| \geq |\delta_{33} - \delta_0| \\ &\delta_Z = \delta_{33} - \delta_0, \qquad \eta = (\delta_{22} - \delta_{11})/(\delta_{33} - \delta_0) \\ &\qquad\qquad\qquad\qquad \text{when} \quad |\delta_{11} - \delta_0| < |\delta_{33} - \delta_0| \end{aligned} \tag{8}$$

where $\delta_0 = (\delta_{11} + \delta_{22} + \delta_{33})/3$.

Figure 14 shows the calculated τ_c of the γ-globulin carbonyl carbon in the lyophilized γ-globulin and the γ-globulin–dextran formulation. The τ_c of γ-globulin carbonyl carbon in the lyophilized γ-globulin exhibited

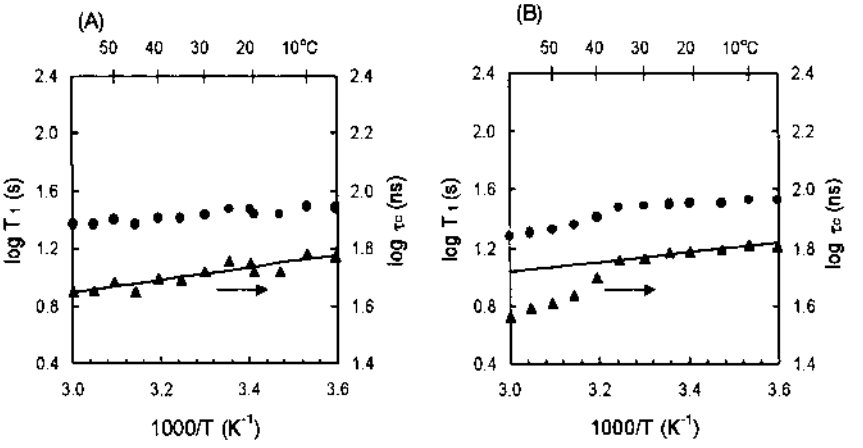

Figure 14 T_1 (●) and τ_c (▲) of γ-globulin carbonyl carbon in lyophilzed γ-globulin (A) and lyophilized formulation containing dextran (B), calculated from observed T_1

Copyright 2004 by Marcel Dekker, Inc. All Rights Reserved.

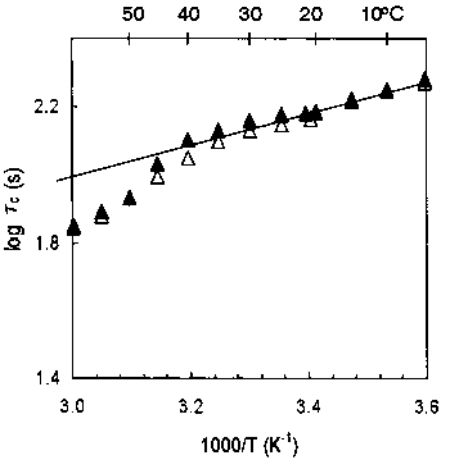

Figure 15 τ_c of dextran methine carbon in lyophilized dextran (▲) and lyophilized formulation containing dextran (△), calculated observed T_1.

linear Arrhenius-like temperature dependence. In contrast, the τ_c of γ-globulin carbonyl carbon in the γ-globulin–dextran formulation decreased significantly at temperatures above 35–40°C, resulting in discontinuous temperature dependence.

The τ_c of the dextran methine carbon revealed a similar discontinuous temperature dependence at 35–40°C in both the lyophilized dextran and the lyophilized γ-globulin–dextran formulation, as shown in Figure 15. At higher temperatures, the temperature dependence of the τ_c of dextran methine carbon appears to follow the Vogel–Tamman–Fulcher equation, which has generally been used to describe the temperature dependence of molecular mobility of amorphous materials at temperatures above T_g. At lower temperatures, in contrast, it appears to follow the Adam–Gibbs–Vogel equation, which has been used to describe the temperature dependence below T_g [17,29–32]. The temperature at which a break is observed in the temperature dependence of the τ_c of dextran methine carbon is coincident with the critical temperature of molecular mobility (T_{mc}), as determined by spin–spin relaxation (see Section II.A). The greater decrease in the τ_c of dextran methine carbon at temperatures above the T_{mc} indicates that the motion of methine groups in dextran is significantly enhanced, involving global segmental motion in addition to local segmental motion. This interpretation is supported by the greater decrease in the T_1 and $T_{1\rho}$ of dextran methine proton at temperatures above T_{mc}, as described in Section II.B.

As shown in Figure 14, the τ_c of γ-globulin carbonyl carbon in formulations containing dextran exhibited a discontinuous temperature

Copyright 2004 by Marcel Dekker, Inc. All Rights Reserved.

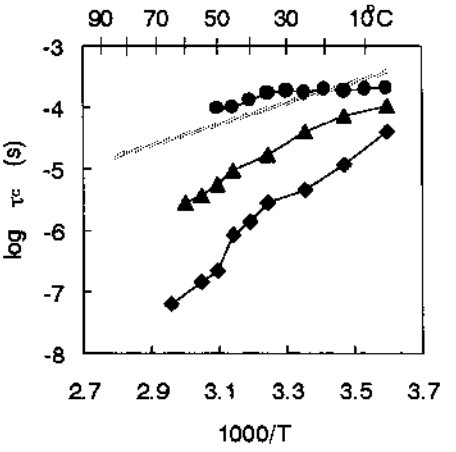

Figure 16 τ_c of dextran methine carbon in lyophilized formulation containing dextran, calculated from $T_{1\rho}$, at 60 (●), 75 (▲), and 86%RH (◆). Line represents the τ_{c1} of dextran protons calculated from $T_{1\rho}$ at 60%RH.

dependence at 35–40°C, similar to that observed for the τ_c of dextran methine carbon. This indicates that at temperatures above T_{mc}, the molecular motion of γ-globulin is enhanced in association with the increased motion of dextran above T_{mc}. This close linkage between the motions of dextran and protein molecules suggests that protein molecules are dispersed in the matrices of dextran.

As described above, the T_1 of carbons in protein and excipient molecules can provide important information on the molecular mobility of lyophilized formulations. Similarly, the $T_{1\rho}$ of carbons is useful as a measure of molecular mobility. Figure 16 shows the τ_c of methine carbons in a lyophilized formulation containing dextran, calculated from the observed $T_{1\rho}$ according to equation (5). The τ_c of methine carbon at 60%RH is of the same order as the τ_{c1} of methine protons described in Section II.B.

III. EFFECT OF MOLECULAR MOBILITY ON STORAGE STABILITY OF FREEZE-DRIED FORMULATIONS

The storage stability of pharmaceuticals in the solid state is largely affected by molecular mobility. Changes in the molecular mobility of amorphous

Copyright 2004 by Marcel Dekker, Inc. All Rights Reserved.

pharmaceuticals at T_g bring about changes in the temperature dependence of chemical and physical degradation rates. A distinct break in the temperature dependence of chemical degradation rates, which are associated with changes in molecular mobility at T_g, has been reported for several drugs of small molecular weight in lyophilized formulation [1–5]; hydrolysis of aspirin in lyophilized hydroxypropyl-β-cyclodextrin/aspirin complex [1], hydrolysis of peptides in lyophilized formulations containing cross-linked sucrose polymer [3], and deamidation of peptide in lyophilized formulations containing poly(vinylpyrrolidone) [4,5]. Physical degradation rates of pharmaceuticals, such as crystallization of amorphous compounds, are also related to molecular mobility.

In a similar manner to drugs of small molecular weight, degradation of protein pharmaceuticals is affected by molecular mobility [6–15]. An excellent correlation has been reported between T_g and chemical degradation of lyophilized antibody–vinca conjugate [8].

This chapter describes the dependence of the storage stability of lyophilized formulations on the molecular mobility as determined by NMR relaxation measurements, which was described in Section II, focusing on the degradation of small molecular weight drugs via bimolecular reaction and protein aggregation in lyophilized formulations.

A. Effect of Molecular Mobility on Bimolecular Reaction During Storage of Lyophilized Formulations

Acetyl transfer between aspirin and sulfadiazine is a bimolecular reaction in which the translational diffusion of reactant molecules becomes rate determining when molecular mobility is limited in the solid state [33]. Therefore, it can offer a useful reaction model for understanding the ways in which chemical degradation rates in lyophilized formulations are affected by molecular mobility. Figure 17A shows the temperature dependence of the rate constant of acetyl transfer in lyophilized formulations containing dextran. Figure 17B shows the pseudo rate constant of aspirin hydrolysis that occurs in parallel with acetyl transfer in the presence of water. The rate constant of acetyl transfer (k_T) and the pseudo rate constant of hydrolysis ($k_{H,\,pseudo}$) are described by following equations:

$$d[SD]dt = -k_T[SD][ASA] \tag{9}$$

$$d[ASA]dt = -k_T[SD][ASA] - k_{H,\,pseudo}[ASA] \tag{10}$$

The temperature dependence of acetyl transfer at 60%RH exhibited a distinct break at approximately 40°C, although it was linear at 12%RH

Copyright 2004 by Marcel Dekker, Inc. All Rights Reserved.

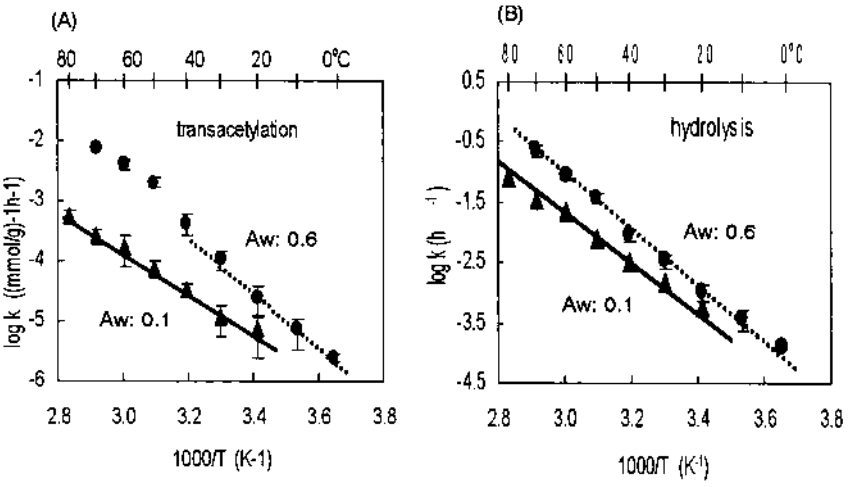

Figure 17 Temperature dependence of acetyl transfer between aspirin and sulfadiazine (A) and aspirin hydrolysis (B) in lyophilized formulations containing dextran at 12%RH (▲) and 60%RH (●).

(Figure 17A). The temperature of this distinct break observed at 60%RH is coincident with the critical mobility temperature (T_{mc}) as determined by spin–spin relaxation measurements, which was described in Section II. This indicates that the rate of acetyl transfer is affected by changes in the translational mobility of aspirin and sulfadiazine molecules at T_{mc}, resulting in a change in temperature dependence. The temperature dependence of acetyl transfer at 12%RH did not show any break, because T_{mc} at 12%RH was higher than the temperature range in which rate constants were determined.

Compared with acetyl transfer, hydrolysis of aspirin occurring in parallel with acetyl transfer did not show such a distinct break as acetyl transfer at T_{mc}, even though hydrolysis is also a bimolecular reaction (Figure 17B). Similarly, no distinct break was observed in the temperature dependence of hydrolysis of cephalothin in lyophilized formulations containing dextran, as shown in Figure 18.

The hydrolysis rate of cephalothin increased with increasing humidity because of the contribution of water to the rate-limiting step as a reactant. The temperature dependence of the apparent first-order rate constant was linear at all humidities in a manner similar to that of hydrolysis in aqueous solution, regardless of their T_{mc} indicated by arrows in the figure. The temperature dependence was also unaffected by the T_g of the formulations that are approximately 20 to 30°C higher than the T_{mc}. Since the

Copyright 2004 by Marcel Dekker, Inc. All Rights Reserved.

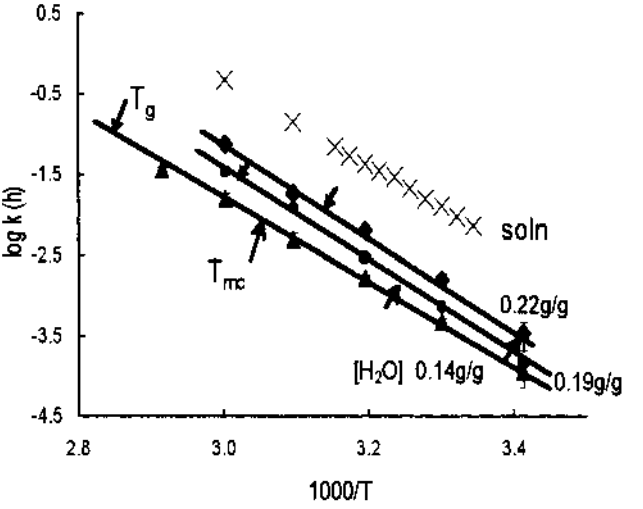

Figure 18 Temperature dependence of cephalothin hydrolysis in lyophilized formulation containing dextran at 23 (▲), 60 (●), and 75%RH (◆).

translational mobility of drug and water molecules in lyophilized formulations is affected by T_g and/or T_{mc}, the hydrolysis rate should be affected by T_g and/or T_{mc} if the translational diffusion of the drug and/or water molecules is rate limiting. The absence of a break in temperature dependence around T_g and T_{mc} suggests that the translational diffusion is not rate limiting. Since the translational diffusion of water can be considered to be much faster than that of the larger cephalothin molecule, the diffusion barrier of water molecules may be smaller than the activational barrier. This interpretation is supported by the finding that the activation energy for the hydrolysis of cephalothin in the lyophilized formulations containing dextran (between 23 and 26 kcal/mol) is close to the apparent activation energy obtained for hydrolysis in solution (24 kcal/mol). Because of the small diffusion barrier of water in lyophilized formulations compared to the activational barrier, the hydrolysis rate of cephalothin is not affected by T_g and/or T_{mc}, even if the translational mobility of water molecules changes around T_g and T_{mc}.

B. Effect of Molecular Mobility on Protein Aggregation during Storage of Lyophilized Formulations

Protein aggregation, one of the most common degradation pathways of lyophilized protein formulations, involves collisions between protein

Copyright 2004 by Marcel Dekker, Inc. All Rights Reserved.

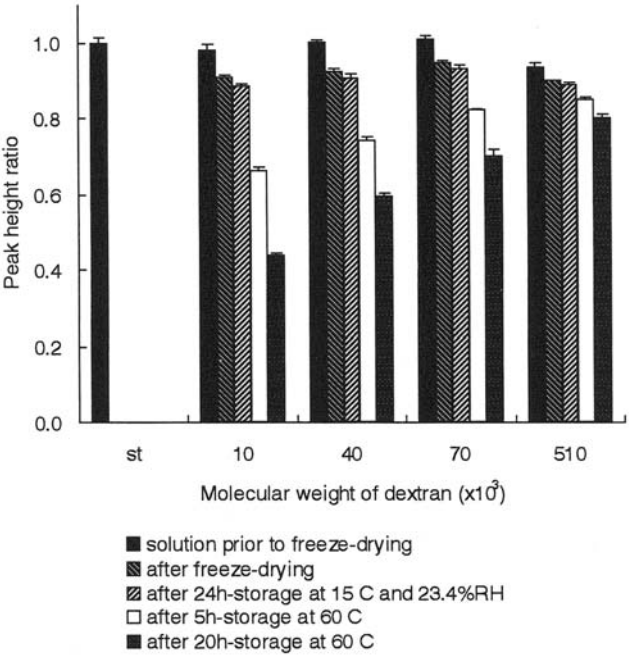

Figure 19 Decrease in amount of protein monomer through protein aggregation during various processes as a function of molecular weight of dextran.

molecules, and is closely related to molecular mobility. Therefore, the temperature dependence of protein aggregation may change with a change in molecular mobility at the glass/rubber transition.

Figure 19 shows changes in the amount of protein monomer after freeze-drying of γ-globulin solutions containing dextran of various molecular weights, and after water sorption and subsequent storage of the obtained freeze-dried cakes, determined by size exclusion chromatography [23]. The peak height ratio to the γ-globulin standard solution without dextran was decreased during freeze-drying and water sorption, indicating that protein aggregation occurs during these processes, although the effect of molecular weight was not significant. Storage at 60°C caused more marked aggregation, the degree of which depended largely on the molecular weight of dextran such that dextran of a smaller molecular weight demonstrated a higher degree of protein aggregation. Protein aggregation in the lyophilized formulations appears to be increased by increasing molecular mobility, since the T_g and T_{mc} of these lyophilized formulations are decreased (i.e., molecular mobility is increased) with decreasing

Copyright 2004 by Marcel Dekker, Inc. All Rights Reserved.

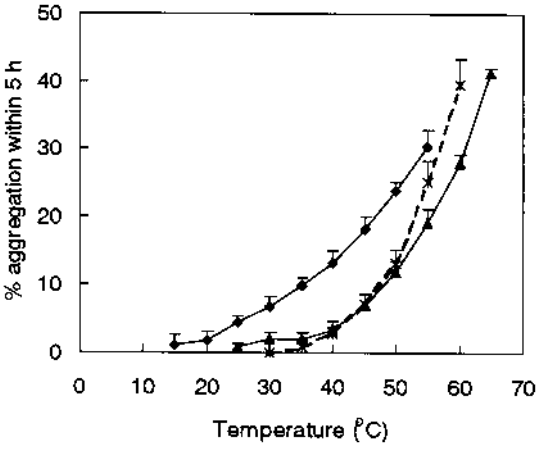

Figure 20 Protein aggregation observed after 5 h-storage of lyophilized γ-globulin formulations containing PVA at 23%RH (▲) and 60%RH (◆), and dextran at 60%RH (×).

molecular weight, as described in Section II.A. Similarly, γ-globulin aggregation in lyophilized formulations containing PVA depends on the molecular weight of PVA, such that PVA of a smaller molecular weight with lower T_{mc} exhibits larger protein aggregation [24].

As shown in Figure 20, protein aggregation in lyophilized formulation containing PVA at 60%RH is greater than that in lyophilized formulations containing dextran [24]. At temperatures below 30°C, significant degradation was observed in the PVA formulation, but not in the dextran formulation. The difference in T_{mc} between the two formulations (lower than 10°C for PVA vs. 35°C for the dextran formulations) appears to be one of the reasons for this difference in stability. The T_{mc} of the PVA formulation increases to 35°C at 23%RH, and protein aggregation is markedly enhanced when the temperature increases past T_{mc}. Thus, protein aggregation in lyophilized formulations is closely related to molecular mobility.

Lyophilized formulations containing protein molecules with a number of configurations that have been deformed to various degrees due to stresses created during the freeze-drying process, exhibit non-exponential protein aggregation through sequential high-order structure changes [34]. The time course of such protein aggregation can be described by the Kohlrausch–Williams–Watts stretched exponential function (KWW function), by assuming that during storage of the formulations, protein molecules having different degrees of deformation are assumed to aggregate at a

Copyright 2004 by Marcel Dekker, Inc. All Rights Reserved.

rate dependent on their degree of deformation (i.e., structure perturbation), and the time required for aggregation should exhibit a distribution: protein molecules that are only slightly deformed should aggregate via a number of sequential deformation steps, whereas protein molecules that are significantly deformed should aggregate through a fewer number of deformation steps. The KWW constants, τ and β, calculated according to equation (11), can be used as parameters representing the rate of protein aggregation:

$$f(t) = \exp(-(t/\tau)^{\beta}) \tag{11}$$

where $f(t)$ is the ratio of remaining protein monomer, and τ and β are constants representing "mean aggregation time" (i.e., the reciprocal of the aggregation rate constant) and "distribution of aggregation time", respectively.

Figure 21 shows the time course of protein aggregation in lyophilized γ-globulin formulations containing dextran, fitted by the KWW function. The parameter β obtained by the curve fitting changed abruptly at a temperature near T_{mc}, as exemplified by the β at 60%RH that is shown in Figure 22. A similar abrupt change in β around T_{mc} was observed with lyophilized formulations containing MC. The temperature dependence of paramter τ for both the dextran and MC formulations exhibited a distinct break around the temperature at which the abrupt change in β occurred, as shown in Figure 23. Both the dextran and MC formulations show a linear

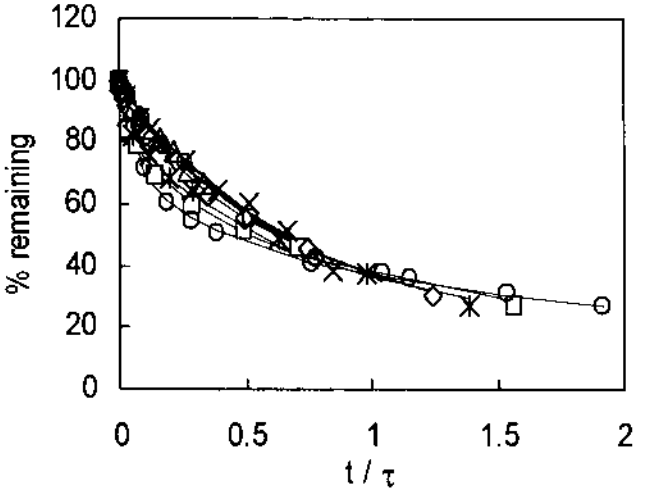

Figure 21 Protein aggregation in lyophilized γ-globulin formulation containing dextran at 20 (×), 30 (◇), 40 (–), 50 (●), 60 (∗), 70 (□), and 80°C (○) and 12%RH.

Copyright 2004 by Marcel Dekker, Inc. All Rights Reserved.

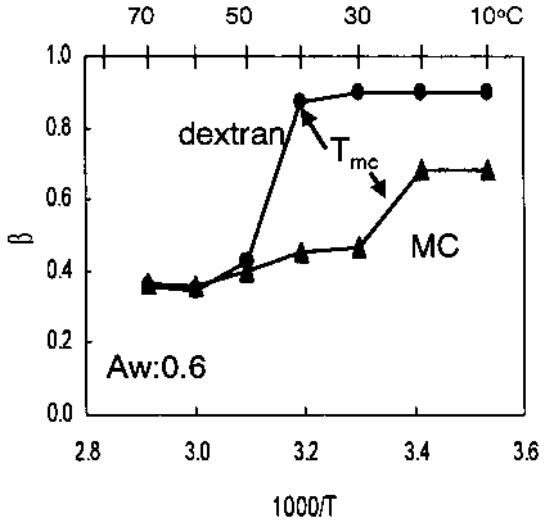

Figure 22 Temperature dependence of KWW parameter β for protein aggregation in lyophilized γ-globulin formulation containing dextran at 60%RH.

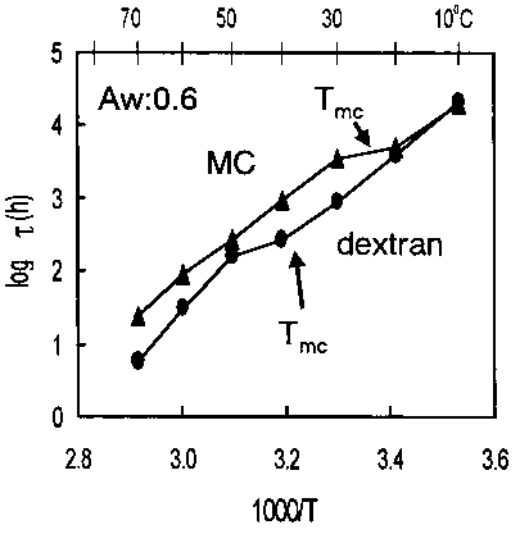

Figure 23 Temperature dependence of KWW parameter τ for protein aggregation in lyophilized γ-globulin formulation containing dextran (●) and MC (▲) at 60%RH.

Copyright 2004 by Marcel Dekker, Inc. All Rights Reserved.

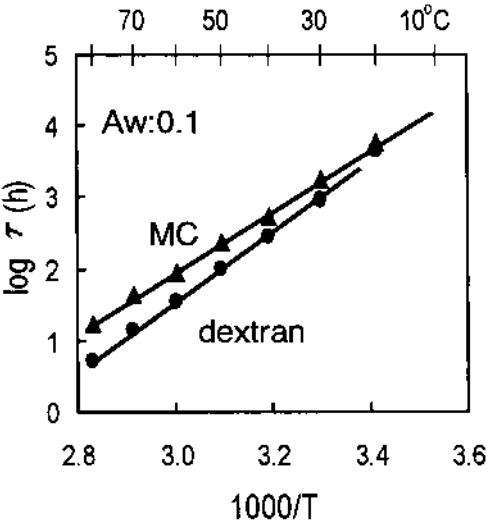

Figure 24 Temperature dependence of KWW parameter τ for protein aggregation in lyophilized γ-globulin formulation containing dextran (●) and MC (▲) at 12%RH.

temperature dependence of τ at 12%RH, since the T_{mc} of these formulations were higher than the temperatures at which τ was determined (Figure 24).

The abrupt changes at T_{mc} in the parameter τ representing "mean aggregation time" and the parameter β representing "distribution of aggregation time" indicate that protein aggregation is largely affected by a change in molecular mobility at T_{mc}.

REFERENCES

1. SP Duddu, K Weller. Importance of glass transition temperature in accelerated stability testing of amorphous solids: case study using a lyophilized aspirin formulation. J Pharm Sci 85:345–347, 1996.
2. BD Herman, BD Sinclair, N Milton, SL Nail. The effect of bulking agent on the solid-state stability of freeze-dried methylprednisolone sodium succinate. Pharm Res 11:1467–1473, 1994.
3. L Streefland, AD Auffret, F Franks. Bond cleavage reactions in solid aqueous carbohydrate solutions. Pharm Res 15:843–849, 1998.
4. MC Lai, MJ Hageman, RL Schowen, RT Borchardt, EM Topp. Chemical stability of peptides in polymers. 1. Effect of water on peptide deamidation in poly(vinly alcohol) and poly(vinyl pyrrolidone) matrixes. J Pharm Sci 88:1073–1080, 1999.

Copyright 2004 by Marcel Dekker, Inc. All Rights Reserved.

5. MC Lai, MJ Hageman, RL Schowen, RT Borchardt, EM Topp. Chemical stability of peptides in polymers. 2. Discriminating between solvent and plasticizing effects of water on peptide deamidatin in poly(vinylpyrrolidone). J Pharm Sci 88:1081–1089, 1999.
6. SP Duddu, G Zhang, PR Dal Monte. The relationship between protein aggregation and molecular mobility below the glass transition temperature of lyophilized formulations containing a monoclonal antibody. Pharm Res 14:596–600, 1997.
7. MJ Pikal, K Dellerman, ML Roy. Formulation and stability of freeze-dried proteins: effects of moisture and oxygen on the stability of freeze-dried formulations of human growth hormone. Dev Biol Stand 74:21–38, 1991.
8. ML Roy, MJ Pikal, EC Rickard, AM Maloney. The effects of formulation and moisture on the stability of a freeze-dried monoclonal antibody-vinca conjugate: a test of the WLF glass transition theory. Dev Biol Stand 74:323–340, 1991.
9. M Hageman. Water sorption and solid-state stability of proteins. In: Stability of Protein Pharmaceuticals, Part A: Chemical and Physical Pathways of Protein Degradation. New York: Plenum Press, 1992.
10. LN Bell, MJ Hageman, LM Muraoka. Thermally induced denaturation of lyophilized bovine somatotropin and lysozyme as impacted by moisture and excipients. J Pharm Sci 84:707–712, 1995.
11. F Franks. Freeze drying: A combination of physics, chemistry, engineering and economics. Jpn J Freezing Drying 38:5–16, 1992.
12. M Pikal. Freeze-drying of proteins. Biopharm 3:26–30, 1990.
13. SJ Prestrelski, KA Pikal, T Arakawa. Pharm Res 12:1250–1259, 1995.
14. SP Duddu, PR Dal Monte. Effect of glass transition temperature on the stability of lyophilized formulations containing a chimeric therapeutic monoclonal antibody. Pharm Res 14:591–595, 1997.
15. HR Costantino, R Langer, AM Klivanov. Aggregation of a lyophilized pharmaceutical protein, recombinant human albumin: Effect of moisture and stabilization by excipients. Bio/Technology 13:493–496, 1995.
16. SL Shamblin, X Tang, L Chang, BC Hancock, MJ Pikal. Characterization of the time scales of molecular motion in pharmaceutically important glasses. J Phys Chem 103:4113–4121, 1999.
17. V Andronis, G Zografi. The molecular mobility of supercooled amorphous indomethacin as a funciton of temperature and relative humidity. Pharm Res 15:835–842, 1998.
18. MT Kalichevsky, EM Jaroszkiewicz, S Ablett, JMV Blanshard, PJ Lillford. The glass transition of amylopectin measured by DSC, DMTA and NMR. Carbohyd Polym 18:77–88, 1992.
19. MT Kalichevsky, EM Jaroszkiewicz, JMV Blanshard. A study of the glass transition of amylopectin-sugar mixtures. Polymer 34:346–358, 1993.
20. CA Oksanen, G Zografi. Molecular mobility in mixtrures of absorbed water and solid poly(vinylpyrrolidone). Pharm Res 10:791–799, 1993.
21. S Yoshioka, Y Aso, T Otsuka, S Kojima, J Pharm Sci 84:1072–1077, 1995.

Copyright 2004 by Marcel Dekker, Inc. All Rights Reserved.

22. CA Rubin, JM Wasylyk, JG Baust. Investigation of vitrificaiton by nuclear magnetic resonance and differential scanning calorimetry in honey: a model carbohydrate system. J Agric Food Chem 38:1824–1827, 1990.
23. S Yoshioka, Y Aso, S Kojima. Dependence of the molecular mobility and protein stability of freeze-dried γ-globulin formulations on the molecular weight of dextran. Pharm Res 14:736–741, 1997.
24. S Yoshioka, Y Aso, Y Nakai, S Kojima. Effect of high molecular mobility of poly(vinyl alcohol) on protein stability of lyophilized γ-globulin formulations. J Pharm Sci 87:147–151, 1998.
25. S Yoshioka, Y Aso, S Kojima. The effect of excipients on the molecular mobility of lyophilized formulations, as measured by glass transition temperature and NMR relaxation-based critical mobility temperature. Pharm Res 16:135–140, 1999.
26. S Yoshioka, Y Aso, S Kojima. Different molecular motions in lyophilized protein formulations as determined by laboratory and rotating frame spin-lattice relaxation times. J Pharm Sci 91:2203–2210, 2002.
27. Q Chen, T Yamada, H Kurosu, I Ando, T Shiono, Y Doi. Dynamic study of the noncrystalline phase of ^{13}C-labeled polyethylene by variable-temperature ^{13}C CP/MAS NMR spectroscopy. J Polym Sci Part B 30:591–601, 1992.
28. S Yoshioka, Y Aso, S Kojima, S Sakurai, T Fujiwara, H Akutsu. Molecular mobility of protein in lyophilized formulations linked to the molecular mobility of polymer excipients, as determined by high resolution ^{13}C solid-state NMR. Pharm Res 16:1621–1625, 1999.
29. BC Hancock, G Zografi. Characteristics and significance of the amorphous state in pharmaceutical systems. J Pharm Sci 86:1–12, 1997.
30. IM Hodge. Physical aging in polymer glasses. Science 267:1945–1947, 1995.
31. BC Hancock, SL Shamblin, G Zografi. Molecular mobility of amorphous pharmaceutical solids below their glass transition temperatures. Pharm Res 12:799–806, 1995.
32. V Andronis, G Zografi. Molecular mobility of supercooled amorphous indomethacin, determined by dynamic mechanical analysis. Pharm Res 14:410–414, 1997.
33. S Yoshioka, Y Aso, S Kojima. Temperature dependence of biomolecular reactions associated with molecular mobility in lyophilized formulations. Pharm Res 17:923–927, 2000.
34. S Yoshioka, Y Aso, S Kojima. Usefulness of the Kohlrausch-Williams-Watts stretched exponential function to describe protein aggregation in lyophilized formulations and the temperature dependence near the glass transition temperature. Pharm Res 18:256–260, 2001.

Copyright 2004 by Marcel Dekker, Inc. All Rights Reserved.

7
Formulation Characterization

D. Q. Wang
Bayer Corporation, Berkeley, California, U.S.A.

I. INTRODUCTION

The first step, and the most important step in developing a lyophilization cycle, is to characterize the formulation. This cannot be overemphasized because understanding the formulation will allow us to develop a lyophylization cycle with a scientific rationale, instead of using trial and error [1]. Characterization of a lyophilization formulation is nothing new. In 1960, Rey reported the use of DTA and a freezing microscope to investigate freezing process of biological products [2]. In 1964, MacKenzie reported that the first model of a freeze-drying microscope that was constructed by R. J. Williams in 1962 enabled him to develop the model 2 as an improvement [3]. In 1972, MacKenzie discussed how the freeze-drying process could be affected by different formulations by measuring melting temperature (T_m), eutectic temperature (T_e), glass temperature (T_g), and glass transition temperature (T'_g) of a water/sucrose system and collapse temperatures (T_c) of NaCl/sucrose system [4]. In the 1990s, probably due to numerous publications about the glass transition theory and the wide use of freeze-drying in the biopharmaceutical industry, the importance of characterizing a lyophilized formulation became well recognized. Pikal reported that because eutectic and collapse temperatures vary over an enormous range, determining the maximum allowable product temperature is extremely important and is the first step in formulation and process development [5–7]. Franks pointed out that an understanding of a freeze-drying formulation can remove most of the empiricism from the freeze-drying cycle development [1,8].

Copyright 2004 by Marcel Dekker, Inc. All Rights Reserved.

In addition, the instrumentation used for characterizing formulation has also been improved significantly. Nail et al. developed a further improved model of a freeze-drying microscope that offered better temperature control, faster temperature responses, and sophisticated video recording and image capturing, among many others [9]. In the thermal analysis field, TA Instrument (New Castle, Delaware, U.S.A.) developed MDSC, which allows us to extend the thermal analysis to freeze-dried dry cakes in order to better understand and predict the stability of a lyophilized product. In this chapter, we will focus on techniques that have been used in recent years at Bayer Biotechnology in characterizing lyophilized formulation. Then we will discuss how to interpret data from these characterization studies to develop a lyophilization cycle.

A lyophilized formulation can consist of many different excipients. Sugars such as sucrose are usually used to stabilize protein conformation against denaturation caused by water removal. Polymers and other proteins such as human albumin serum (HAS) also function similarly. These excipients usually remain amorphous during and after lyophilization. A formulation consisting of mainly amorphous excipients is often called "amorphous formulation." On the other hand, bulking agents such as mannitol and glycine are commonly used for providing cake appearance. Such excipients are usually expected to be in crystalline structure after lyophilization. Totally crystalline cakes are not commonly used for protein lyophilization, since the crystallization of all excipients will tend to remove any stabilizing effect of the excipients on the protein [10–12]. For pharmaceutical protein products, a formulation termed "crystalline matrix" is widely used. In such a formulation, crystalline components are added at a relatively high level so that a crystalline matrix is formed for the amorphous components to collapse upon. In such a way, the crystalline component provides excellent cake appearance, good reconstitution characteristics, and ease in lyophilization. On the other hand, the amorphous component stabilizes proteins during processing and storage. Lyophilizing such a formulation allows partial collapse (also termed micro-collapse) without affecting cake appearance. As a result, the product can be lyophilized at a relatively higher product temperature if protein activity is not compromised. In this chapter, all of our discussion focuses on the crystalline matrix-type formulation.

A lyophilization process usually includes three steps. First, the aqueous solution, that has been filled into containers (such as vials and trays), is frozen to lower than $-40^{\circ}C$. Next, in the primary drying, the freeze-dryer chamber is evacuated and the shelf temperature is elevated to sublimate bulk water (also termed free water) out of the system. Finally, the shelf temperature is further increased to remove bound water by desorption.

Copyright 2004 by Marcel Dekker, Inc. All Rights Reserved.

This is called secondary drying. The principles of the lyophilization process have been well described by Pikal [5] and Franks [1].

At Bayer Biotechnology, we usually develop a freeze-drying cycle in five steps. First, the formulation is characterized. Second, based on the understanding of the formulation, the process is optimized. Third, the range of the critical process parameters is found. Fourth, the process is scaled up and transferred to production. Fifth, the process at the production scale is validated and qualified. Here, we focus only on the formulation characterization.

In summary, in this chapter we will discuss the freeze-drying formulation characterization, which is the first step and the most important step in developing a freeze-drying cycle. All of the characterization discussion will focus on a "crystalline matrix" type of formulation. In the discussion, we will follow the order given below:

Utilize DSC (Differential Scanning Calorimetry) to characterize the formulation for freezing and primary drying.
Confirm DSC results with a freeze-drying microscope and determine the maximum allowable product temperature during the primary drying.
Generate a water absorption/desorption curve for characterizing the secondary drying process.
Conduct a moisture optimization study to determine target moisture content for developing secondary drying.
Use MDSC to measure T_g in order to predict stability of the products.

II. UTILIZE DSC TO CHARACTERIZE FORMULATION

Basically, DSC measures heat flow as a function of temperature applied to a sample going through freezing, melting, crystallization, and glass transition. The thermal properties that can be measured by using DSC include eutectic crystallization temperature (T_x), eutectic melting temperature (T_e), glass transition temperature (T_g') and ice melting temperature (T_{im}). Among these critical temperatures, the glass transition temperature T_g', is one of the most important thermophysical properties of the formulation. For a formulation that forms an amorphous cake after being freeze-dried, the T_g' is also the collapse temperature, which is the most critical factor in ensuring the success of the primary drying. For example, MacKenzie measured the collapse temperature of the formulations with different ratios of sucrose:sodium chloride. He demonstrated that at a certain range of ratios, the lyophilization became impractical as the sodium chloride depressed the

Copyright 2004 by Marcel Dekker, Inc. All Rights Reserved.

collapse temperature to a point below −40°C [14–16]. Many other reports are available in determining T_g' by DSC [14,15].

In this chapter, as we have mentioned previously, we focus on the crystalline matrix formulation. The example formulation consists of 2.2% glycine, 1.0% of sucrose, 0.02 M of histidine, 0.03 M of sodium chloride (NaCl), and 0.0025 M of calcium chloride ($CaCl_2$). The concentration of therapeutic protein is in the range of 50–200 μg/mL, which is negligible.

Figure 1 shows a DSC thermogram of warming for the formulation. The sample was frozen to −60°C and then warmed up to 20°C. During the warming, the glass transition temperature (T_g') can be observed between −30 and −35°C. Under these conditions, the highest allowable product temperature during primary drying is about −35°C. In this case, we do not believe that the glycine crystallizes out and, as a result, we must freeze-dry the product below this maximum allowable temperature. The maximum allowable temperature here is also the collapse temperature. In other words, the cake will collapse if the product temperature is higher than this maximum allowable temperature during sublimation. Generally speaking, the lower the allowable product temperature, the less efficient the freeze-drying cycle.

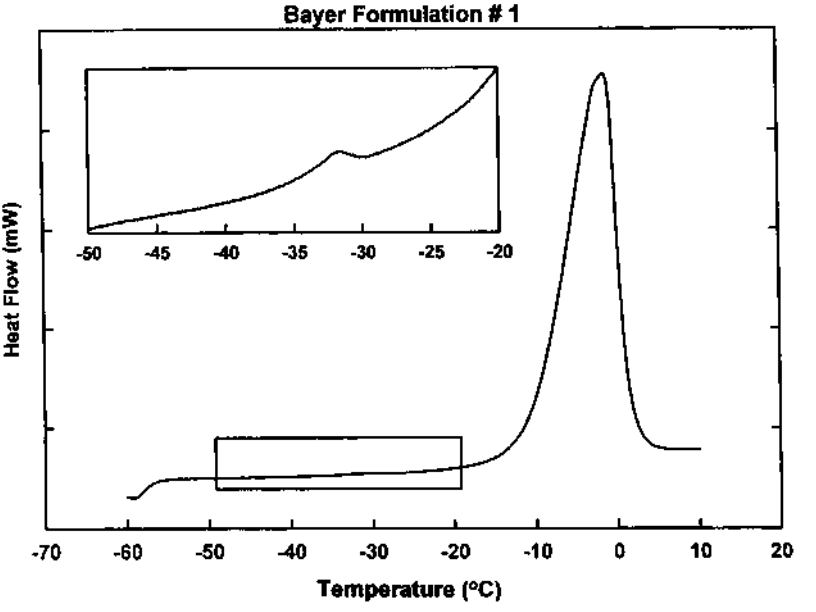

Figure 1 A DSC warming thermogram of a crystalline matrix formulation without annealing.

Copyright 2004 by Marcel Dekker, Inc. All Rights Reserved.

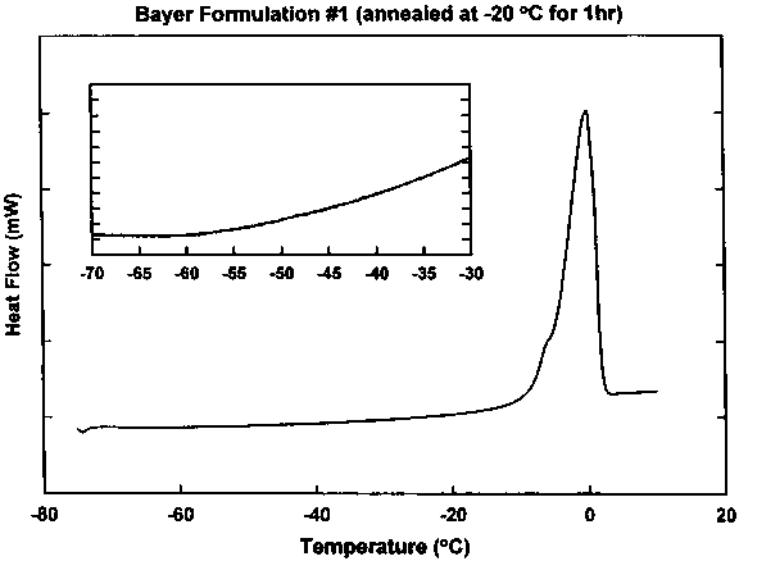

Figure 2 A DSC warming thermogram of a crystalline matrix formulation after annealing.

It may even become impractical for large-scale production if the highest allowable temperature approaches −40°C.

For the crystalline matrix-type formulation, however, adding an annealing step in freezing may make a significant difference in the freeze-drying process. Figure 2 shows a DSC thermogram of the same formulation described above, but it has been annealed during freezing. As before, the sample was first frozen to −60°C. Then the sample temperature was slowly increased to −20°C and held for 1 h at this temperature. We call this step annealing, or heat treatment. After holding at −20°C for 1 h, the sample was again slowly frozen down to −60°C to a fully frozen state. The sample was then warmed to 20°C. The thermogram shown in Figure 2 is from the last warming. As a result of the annealing, as shown in the thermogram, the thermal event observed between −30 and −35°C disappeared. Instead, there is a new thermal event, like a shoulder, which occurred at a temperature above −10°C. We believe the new thermal event is the eutectic melting of the glycine. It appears like a shoulder on the thermogram because the peak of glycine melting was quickly integrated into the peak of the ice melting. This also indicates that annealing has made glycine crystallize out as evidenced by the eutectic melting of glycine during the warming. The complete crystallization of the crystalline component makes the thermal transition

Copyright 2004 by Marcel Dekker, Inc. All Rights Reserved.

shift to −10°C. In other words, it is evident that annealing will allow primary drying to occur at a much higher product temperature because, for the crystalline matrix formulation, the eutectic melting temperature, T_e, is the collapse temperature. This is a clear advantage of the crystalline matrix-type formulation. However, care must be taken to prevent protein activity and stability from being compromised by annealing. We will discuss this in detail in a later section.

We stated in the previous paragraph that glycine was completely crystallized out as a result of annealing. The evidence was the eutectic melting of glycine shown in Figure 2. Another way to verify the crystallization of glycine is to conduct an x-ray powder diffraction study on the freeze-dried cake. Figure 3 is a diffractogram of the lyophilized crystalline matrix formulation. Figure 4 shows a diffractogram of a lyophilized glycine-only formulation. Comparing these two figures, we conclude that glycine was indeed crystallized when the annealing step was incorporated into the freezing cycle as observed by the sharp peaks in the diffractogram at the specific angles corresponding to standard crystalline glycine.

In addition to DSC, other instruments, such as differential thermal analysis (DTA) and electrical resistance analysis (ER), are also commonly used in determining the thermophysical properties of a lyophilized formulation, such as the glass transition temperature (T_g'), the collapse temperature, etc. One of the examples using DTA and ER has been recently reported by

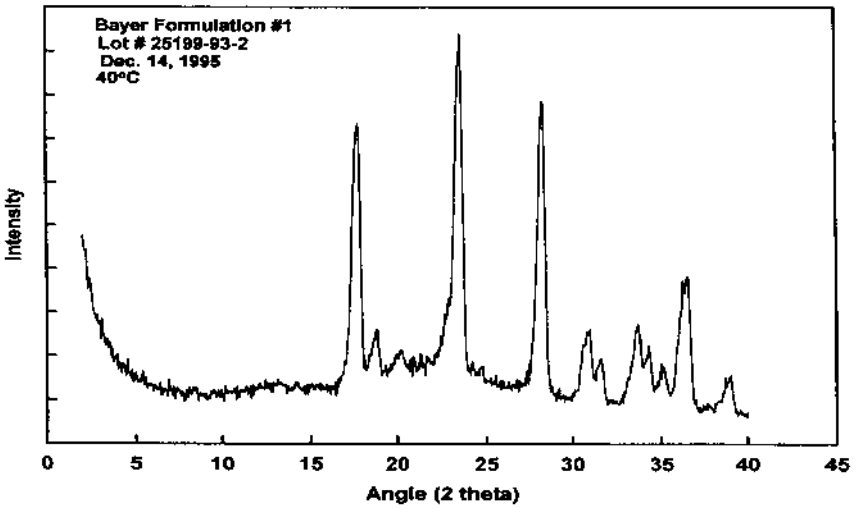

Figure 3 X-ray diffractogram of the crystalline matrix formulation.

Copyright 2004 by Marcel Dekker, Inc. All Rights Reserved.

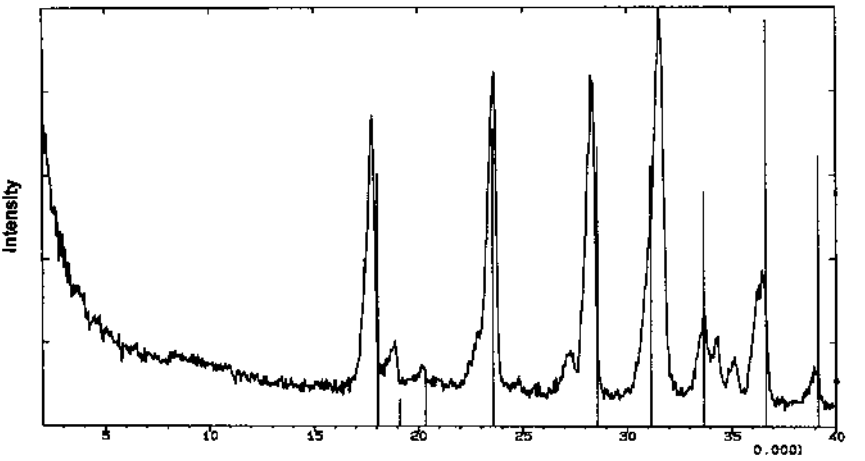

Figure 4 X-ray diffractogram of glycine.

Ma et al. on a similar crystalline matrix formulation [15]. Other literature on the application of DAT [18,19,22] and ER [3,17–21] in formulation characterization is also very informative. However, DSC is the most common and reliable means, and also the easiest.

III. CONFIRM DSC RESULTS WITH A FREEZE-DRIVING MICROSCOPE

A freeze-drying microscope provides real-time images of freezing, melting, crystallization, collapse, and melt-back during the freezing and lyophilization processes. A freeze-drying microscope that we have in our laboratory is shown in Figure 5, consisting of two major parts, an optical microscope with a Physitemp FDC-1 freeze-drying microscope stage. To investigate the freeze-drying behavior of the crystalline matrix formulation described previously, a small aliquot (10 μl) of formulation was frozen to −48°C between quartz coverslips in the freeze-drying stage, either with, or without, annealing. The behavior of the material during sublimation drying was then observed at temperatures between −48 and −11°C using an Olympus BX50P polarizing microscope. Micrographs were recorded using a Javelin Smartcam CCD video camera mounted on the microscope and a Data Translation DT3153 frame grabber card. The magnification used for observation of the freeze-drying front was 150X. More details about this type of freeze-drying microscope can be found in Nail [9].

Copyright 2004 by Marcel Dekker, Inc. All Rights Reserved.

Figure 5 A freeze-drying microscope.

Studies of freeze-drying microscopy have also been reported by others [3,4,13,22–24].

The freeze-drying microscope has become an excellent tool to confirm DSC results. The advantage of a freeze-drying microscope is that it provides real-time images, which can been seen by our own eyes, during freezing and freeze-drying. Figure 6 shows six freeze-drying microscopy images of the crystalline matrix formulation. Figure 6A shows the formulation was initially frozen at −48°C with no annealing. Figure 6B shows that the sample was then freeze-dried with a stepwise increase of drying temperature (i.e., the sample sublimation temperature) and we can see that significant amounts of structure are lost if samples are freeze-dried at temperatures as low as −42°C. Figure 6C shows that since the amorphous structure does not appear to be fully retained during freeze-drying even at −42°C, we stopped freeze-drying and froze the sample down to −48°C again. Then we slowly warmed the sample to −20°C and held it there for about 1 h for annealing. Figure 6D shows that after annealing some purple shadows appear between the ice crystals. We believe these purple shadows are crystallized glycine. Figure 6E shows that after annealing, freeze-drying restarted. The sample temperature was first set at −32°C and the cake structure is perfectly preserved. Figure 6F shows the retention of crystalline cake structure when lyophilization was performed at a sample temperature at −15°C. Clearly, the observation agrees with the DSC results described above, i.e., with an annealing step, glycine crystallizes out and freeze-drying can be done at a much higher temperature.

Copyright 2004 by Marcel Dekker, Inc. All Rights Reserved.

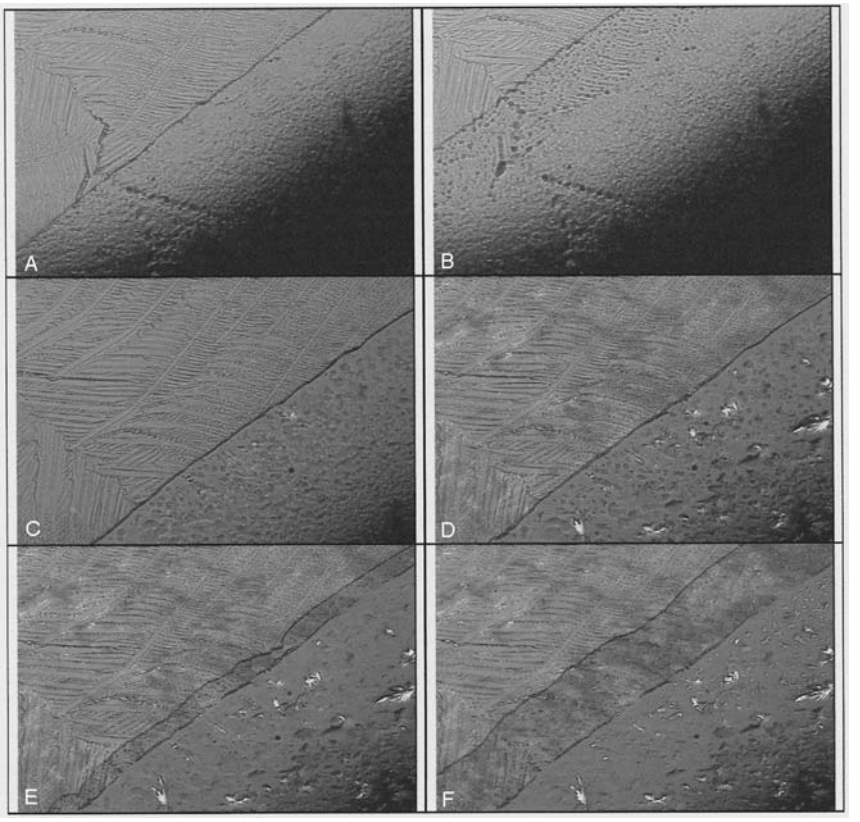

Figure 6 Freeze-drying microscope images.

So far we have described how to use DSC and a freeze-drying microscope to determine (1) the necessity of annealing in freezing; and (2) the highest allowable product temperature in primary drying. With these two different methods, we can confidently design the freezing cycle and primary drying cycles. For the crystalline matrix-type formulation discussed in this chapter it is clear that annealing is necessary to crystallize glycine. The annealing temperature should be at $-20^{\circ}C$. After the glycine crystallizes out, the highest allowable product temperature is elevated and, therefore, primary drying can be done with a much higher efficiency. Determining the highest allowable product temperature is the most critical factor in developing a primary drying cycle. During the primary drying the product temperature must be kept lower than the highest allowable temperature to avoid collapse and melt-back of the cake. The melt-back here includes both the melt-back

Copyright 2004 by Marcel Dekker, Inc. All Rights Reserved.

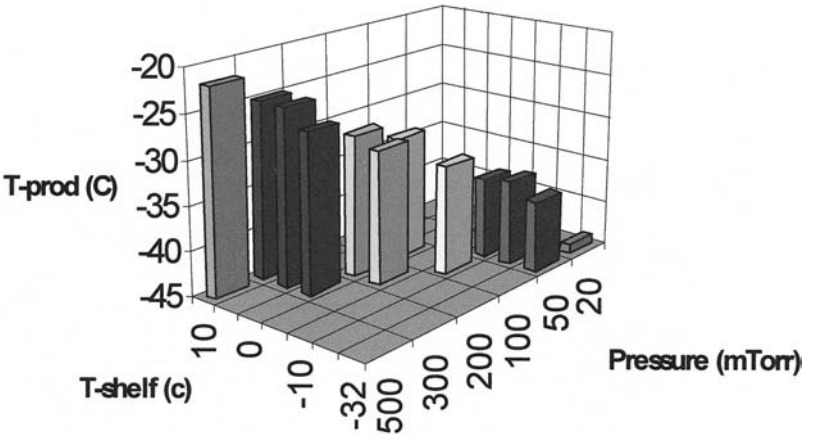

Figure 7 Relationship of product temperature as a function of shelf temperature and chamber pressure.

of a solid, such as glycine described above, and the melt-back of ice, which occurs at a much higher temperature than that of glycine. In addition, during primary drying, both heat transfer and mass transfer are important in affecting product temperature. In other words, we can achieve a product temperature lower than the highest allowable temperature by using many different combinations of shelf temperature and chamber pressure. Figure 7 demonstrates the possible combinations for the crystalline matrix-type formulation. This provides very important information not only for designing a primary drying process, but also for bracketing process parameters during validation. For example, if $-16^{\circ}C$ is the highest allowable temperature for the formulation, Figure 7 illustrates that all combinations of shelf temperature and chamber pressure resulting in a product temperature lower than $-16^{\circ}C$ would be acceptable process parameters. In practice, we usually take at least 2–5°C as a safety margin, and we always optimize the process by looking for the combinations that result in the highest sublimation rate and, consequently, the shortest drying time.

IV. STUDY WATER SORPTION

Water sorption, including desorption and adsorption, provides the degree of "hygroscopicity" of the formulation by plotting the increase in water content of a dry cake as a function of relative humidity to which the sample

Copyright 2004 by Marcel Dekker, Inc. All Rights Reserved.

has been exposed at a given temperature. The curve indicates water vapor sorption characteristics; in other words, the degree of ease in secondary drying. Although the desorption process is not a straightforward reversal of the adsorption, the trends are predictive. In general, the easier the water adsorption, the easier the water desorption.

To conduct a water sorption study, the product was stored in desiccators with solid salt or saturated salt solutions for 48 h of equilibration at an ambient temperature (Figure 8). The salts included phosphorus pentoxide, lithium chloride, potassium acetate, magnesium chloride, potassium carbonate, and sodium chloride, which generated relative humidities of, approximately, 0, 11, 23, 33, 43, and 75%, respectively. The vials were sealed immediately after equilibration. The moisture in the lyophilized product was determined by the Karl Fischer method.

Figure 9 shows a typical water adsorption curve for a typical crystalline matrix-type formulation. Such characteristics of a freeze-dried formulation provide information on the affinity of water for a dried product. It illustrates a progressive increase in water content as the relative humidity is increased. When samples were exposed to relative humidities from 6 to 75%, the resultant moisture content ranged from approximately 1.2 to 17%. This indicated that the lyophilized product was moderately hygroscopic in the relative humidity range of 6 to 43%, and more hygroscopic at relative humidities above 43%. The crystalline material is often "drying friendly" because only the surface of crystals is available for water vapor sorption. In addition, the degree of "hygroscopicity" of the formulation also provides

Figure 8 A demonstration of conducting a moisture sorption study with desiccators.

Copyright 2004 by Marcel Dekker, Inc. All Rights Reserved.

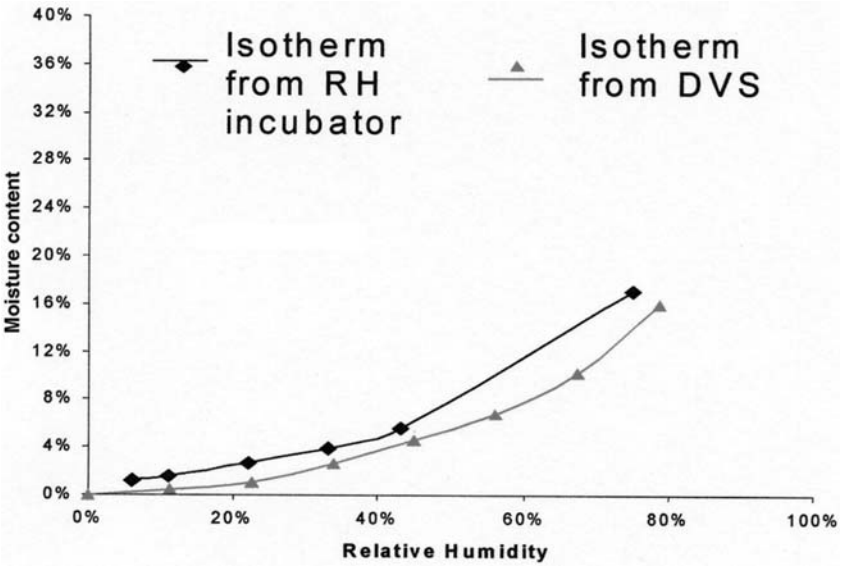

Figure 9 Water adsorption curves generated from desiccator method and DVC methods.

guidance for product handling, for example in the case of measuring moisture content for product release. Figure 9 also shows that in an environment where the relative humidity was greater than 75%, which is common under a non-controlled laboratory environment during a wet day, the moisture content could increase to as high as 17%. This suggests how important it is to control the environmental relative humidity during the moisture testing. Another tool for determining water sorption is Dynamic Vapor Sorption (DVS, Surface Measurement System, London). It measures weight changes due to moisture gain at different relative humidity conditions. This instrument also provides information on water sorption kinetics. Figure 9 also includes the results from the DVS method. The DVS data were comparable to those obtained by incubating the material in desiccators and indicate that moisture could be removed rapidly during secondary drying.

V. OPTIMIZE MOISTURE CONTENT

Lyophilization is a process to remove water so that the water activity, or the mobility of the water, in the dried product can be reduced to an optimal

Copyright 2004 by Marcel Dekker, Inc. All Rights Reserved.

level. This is achieved by using a secondary drying cycle. As a result, fully understanding the effects of the moisture content on product stability becomes the most important information necessary to develop a secondary drying. Generally speaking, for any formulation there is an optimal range of moisture content that would result in the best stability of the lyophilized product. Hsu et al. reported that there is an optimum residual moisture range for a lyophilized recombinant protein [25]. Overdrying may result in opalescence in the product upon reconstitution, while underdrying leads to a greater protein activity loss upon storage under temperature stress conditions. Greiff [26] and Liu et al. [27] revealed that aggregation or insoluble proteins can be induced by a moisture content that was higher than the optimal range.

Samples for a moisture optimization study are usually generated in the same desiccators that incubate samples for the water adsorption study. That is, samples were exposed to different relative humidities for 48 h to allow them to adsorb various amounts of moisture. An accelerated stability program was then conducted at 40°C storage temperature. For a crystalline matrix-type formulation, Figure 10 shows how protein activities are affected by moisture levels. It clearly demonstrates that as moisture increased,

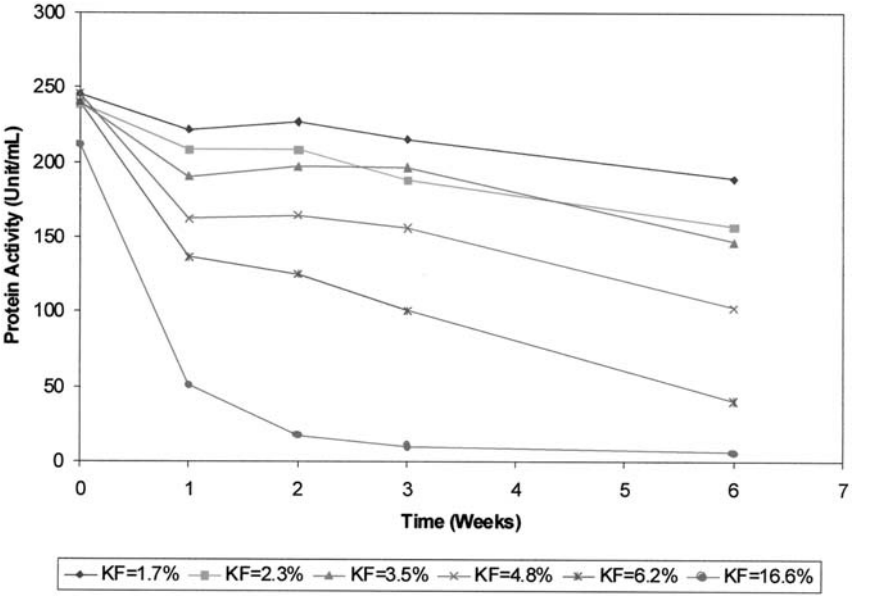

Figure 10 Protein activity as a function of storage time and moisture content when samples are stored at 40°C.

Copyright 2004 by Marcel Dekker, Inc. All Rights Reserved.

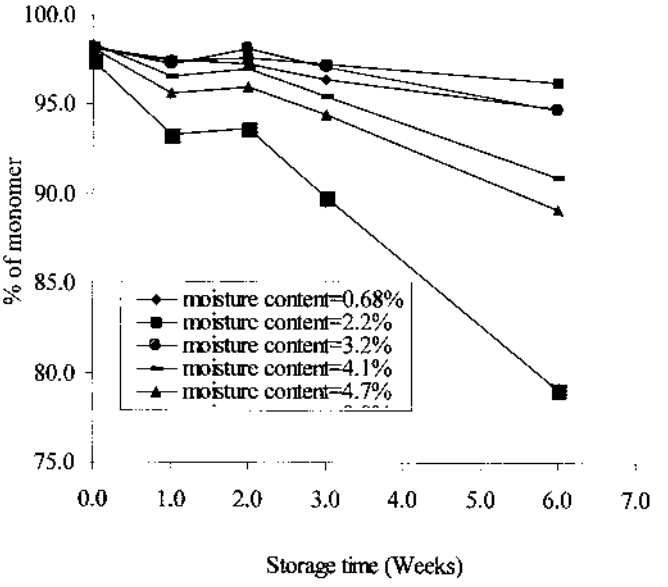

Figure 11 Percentage monomer measured by HPLC for product samples stored at 40°C.

protein activity decreased accordingly. It should also be noted that the greatest loss occurred in the first week, particularly for the high moisture content samples. The percentage monomer of another protein product, shown in Figure 11, was measured by the HPLC–SEC method. Data stored for only 6 weeks had already shown a clear trend: as moisture increased, percentage monomer dropped rapidly, meaning protein aggregation increased drastically. The data demonstrate a trend of "the dryer, the better," which suggests having a long secondary drying cycle that can make a "bone-dry" product. In addition, partial production loads can be comfortably bracketed in the validation because "overdrying" is not a concern for such a formulation.

It should be pointed out that Greiff proposed that the thermostability of freeze-dried protein products could be a bell-shape function of the residual moisture content [26]. In other words, both overdrying and underdrying are detrimental. Hsu et al. also concluded that the generally accepted concept "the drier, the better" is not necessarily appropriate for their product [27]. It is noted that their data were generated from excipient-free proteins. In this study, however, our results did not demonstrate a bell-shape function for the crystalline matrix formulation,

Copyright 2004 by Marcel Dekker, Inc. All Rights Reserved.

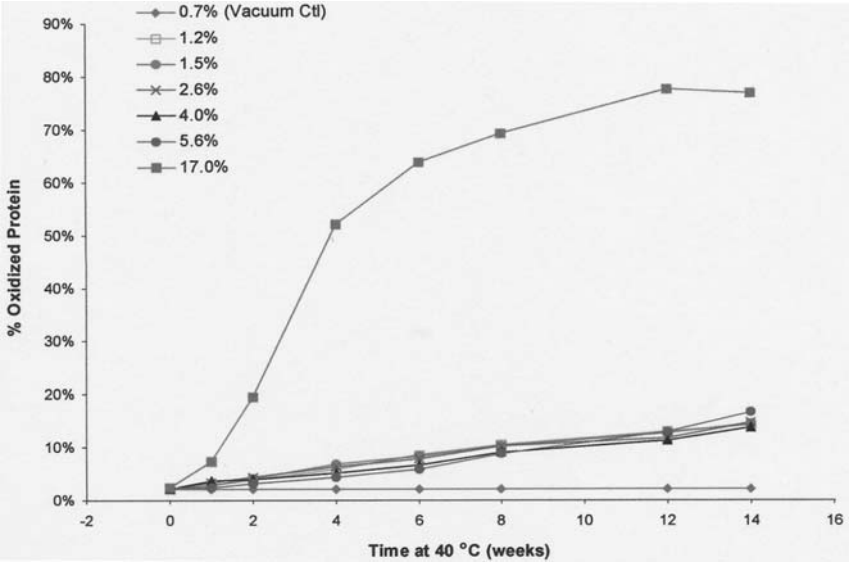

Figure 12 Result from another moisture optimization study for a different protein. Oxidation of the protein was studied.

but a trend of "the drier, the better." In another study on the same protein but in a different formulation, we found that overdrying was indeed detrimental and resulted in an increase of insoluble aggregates and a decrease of protein activity. Therefore, the range of optimal moisture content and the shape of the curve are formulation dependent.

Figure 12 shows results from a moisture optimization for a different protein product but with a similar crystalline matrix-type formulation. However, as oxidation is one of the instability mechanisms, this figure shows the percentage of oxidized protein versus storage time and moisture content. The assay of oxidation used here is reversed phase HPLC. The percentage of oxidation was calculated as the area under the peak for oxidized protein divided by the sum of the areas under the oxidized and non-oxidized peaks. The percentage of oxidized protein increased dramatically at a moisture content of 17%. However, the oxidation rate was comparable for moisture contents of 1.2 to 5.6%. Note that the percentage oxidation is lowest for the vacuum control because of the headspace vacuum. Unsealing the other vials and exposing the contents to atmospheric pressure when samples were incubated in the desiccators increased the percentage of oxidation.

Copyright 2004 by Marcel Dekker, Inc. All Rights Reserved.

VI. MEASURE T_g OF DRY CAKES

Another way to determine the optimal moisture content for stability is to develop a relationship between moisture content and glass transition temperature (T_g) of lyophilized dry cakes. T_g can be measured using either DSC or MDSC (Modulated Differential Scanning Clorimetry). T_g is a measure of the molecular motion of water, which is a major factor in denaturing proteins [28,29]. In order to increase the long-term storage stability of a pharmaceutical protein, the motion of water can be limited (frozen storage) or water can be removed (lyophilization). However, even for a lyophilized biopharmaceutical product, residual moisture in the dry cake could be mobile depending on the level of the residual moisture content and storage temperature. High residual moisture content and high storage temperature may result in more mobility of water [29], and as a consequence may damage the product protein significantly as well as harm the cosmetic properties of the lyophilized cake. The glass transition temperature of a freeze-dried cake (T_g) marks an increase in the mobility of the remaining water [28]. Freeze-dried products stored below their T_g will exhibit much greater stability and structural integrity than those stored above T_g. Due to the cost of storing a product at low temperatures, it is economically more desirable for the T_g of a lyophilized product to be relatively high. Each product formulation will have a different relationship between moisture content and glass transition [29]. MDSC can be used to characterize the glass transition of a dry cake [30,31]. By analyzing cakes of different moisture contents the relationship between T_g and moisture content can be quantified. In the following paragraphs, the relationship between dry cake moisture content and T_g is reported for the crystalline matrix-type formulation.

Again, samples for T_g measurement are prepared similarly to those for adsorption study using desiccators. Each desiccator maintained a different relative humidity by using different saturate salts as described previously in the water adsorption study. As a result, different levels of moisture content were achieved for the samples in different desiccators. The driest samples were obtained by keeping them sealed after freeze-drying until sample preparation. The moisture content of each sample was determined by near-infrared content analysis. The near-infrared (NIR) used here is provided by a FOSS Model 5000 Rapid Content Analyzer.

All sample preparation for T_g measurement using MDSC took place within a glove box. The relative humidity of the glove box was matched to that of the desiccator each vial had been stored in. This was done to avoid any change in the moisture content of the sample. Approximately 5 to 10 mg of each freeze-dried cake were sealed into a hermetic aluminum DSC sample

Copyright 2004 by Marcel Dekker, Inc. All Rights Reserved.

pan. All DSC work was performed on a TA Instruments 2920 Differential Scanning Calorimeter in MDSC mode. Thermogram analysis was carried out with TA Instruments Universal Analysis software. Helium was used as the purging gas. A typical thermogram and testing conditions are given in Figure 13. The scanning rate was 2°C/min, from –40 to 120°C, modulated at ±0.6°C every 100 s. Glass transition values were determined from the reversing heat flow and then corrected to the total heat flow. The relationship of T_g and moisture content for the crystalline matrix formulation is given in Figure 14. It shows if the relationship between T_g and the moisture content of a dry cake is known, an optimum moisture content can be chosen based upon the desired storage conditions. Product stability at a higher storage temperature can be achieved by lowering the moisture content of the cake as much as possible. For example, to achieve a product stability at room temperature storage, we have to keep moisture content lower than 2%. In the pharmaceutical industry, it is common practice to use 40°C storage as an accelerated stability test to predict product stability using Arrhenius kinetics. Figure 14 also shows that for this formulation such practice may not be appropriate because it is hardly possible to have T_g

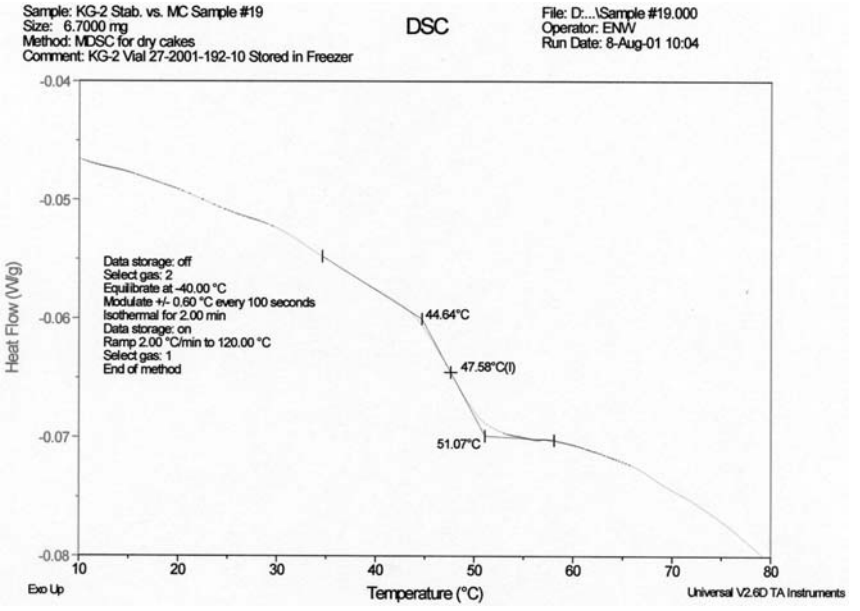

Figure 13 A typical thermogram of T_g measurement using MDSC.

Copyright 2004 by Marcel Dekker, Inc. All Rights Reserved.

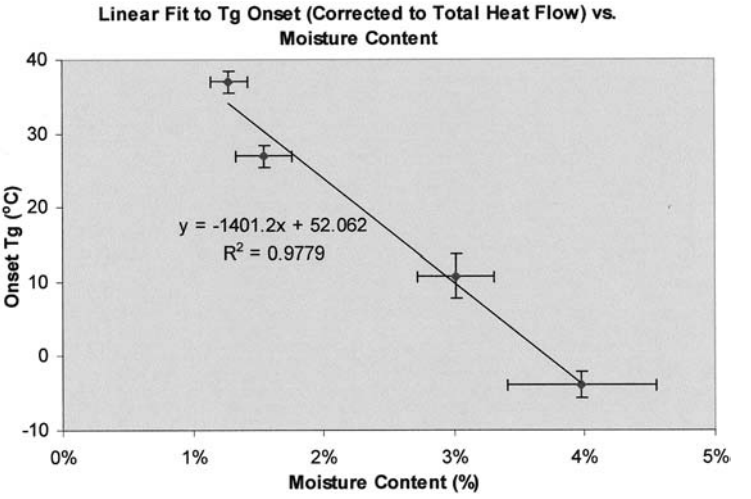

Figure 14 T_g of dry cakes as a function of moisture content.

above 40°C with a reasonable moisture content. Instead, WLF kinetics may better predict the stability as suggested by Franks [1].

VII. INTERPRET DATA FOR CYCLE DEVELOPMENT

With a thorough understanding of the formulation, we can reduce the amount of trial and error in cycle development. Results from DSC and the freeze-drying microscope, as we described in previous sections, indicate an annealing step is necessary to crystallize glycine in the formulation. Consequently, this allows us not only to conduct the primary drying aggressively at a relatively high product temperature, but also to obtain a good cake appearance. In addition, it also provides a scientific rationale to determine freezing temperature, annealing temperature, primary drying shelf temperature, and primary drying pressure. Data from the adsorption study and moisture optimization studies, on the other hand, demonstrate a characteristic of "the drier, the better" for this formulation. As a result, it guides us to confidently design secondary drying processes such as determining optimal drying temperature, pressure, and time in order to provide uniform moisture content in the final containers. The information from the formulation characterization studies also assists in the validation of the cycle, particularly in bracketing the process parameters.

Copyright 2004 by Marcel Dekker, Inc. All Rights Reserved.

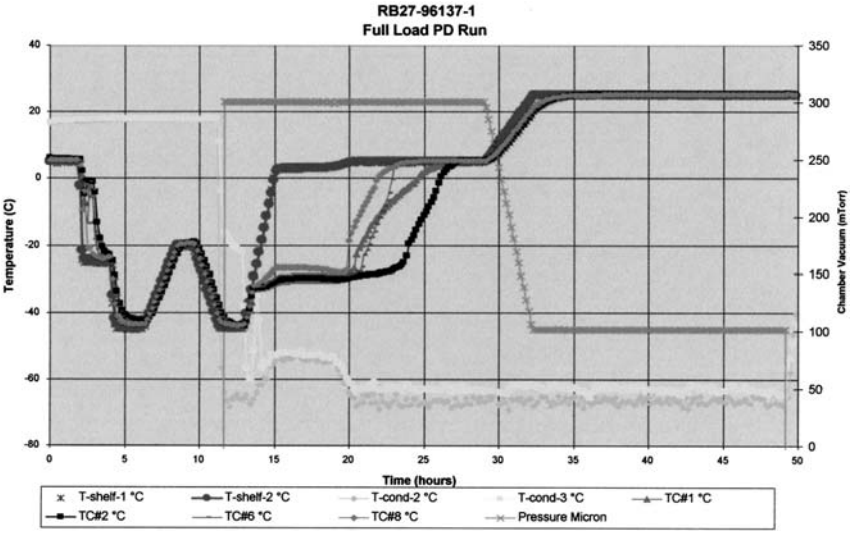

Figure 15 A typical freeze-drying cycle.

A typical lyophilization cycle for a crystalline matrix-type formulation, such as the one discussed here, is illustrated in Figure 15. The cycle includes:

1. An annealing step in freezing to slowly warm the product to −20°C and then hold for 1 h.
2. An aggressive primary drying with a shelf temperature of 5°C and a chamber pressure of 300 m Torr.
3. An ''overdrying'' secondary drying with a ramped shelf temperature of 25°C and a chamber pressure of 100 m Torr for a total of 24 h.

VIII. CONFIRM THE HYPOTHESIS

As described previously, lyophilizing a ''crystalline matrix'' type of formulation allows ''micro-collapse'' of the amorphous components. This allows primary drying to be performed at a relatively high product temperature without loss of the cake structure. The hypothesis we made is that the micro-collapse would not compromise product quality, particularly in stability. Here we discuss this issue and particularly a study that we performed to confirm the hypothesis.

Copyright 2004 by Marcel Dekker, Inc. All Rights Reserved.

In the case of pharmaceuticals, collapse of the cake structure during freeze-drying results in a pharmaceutically unacceptable product. There are several obvious potentially detrimental effects of collapse on the stability and desirability of a freeze-dried product. The collapse of a system during freeze-drying will reduce the surface area of the cake and so will prevent efficient secondary drying. Also, the collapse may remove the pores or channels left by the sublimated ice, and so may increase the resistance to water vapor moving out of the product, thereby inhibiting primary drying to a greater extent. Since the secondary drying is less efficient the final product may contain higher levels of moisture than is optimal and the higher moisture content of the cake can then lead to increased levels of instability of the protein being lyophilized. The collapse of the cake may also promote protein aggregation [29]. A further complication brought about by collapse is that the reconstitution step may take longer to complete, since the surface area of the cake is greatly reduced. Although some investigations [10,29–36] have been published on the effects of collapse on freeze-dried materials, little has been published on the effects of collapse on the long-term storage stability of freeze-dried proteins. Therefore, it is necessary to conduct an investigation of the long-term storage stability. The previously described protein in the crystalline matrix formulation was freeze-dried using three different freeze-drying protocols. These protocols were chosen to produce a collapsed cake, a micro-collapsed cake, and a non-collapsed cake. This investigation aims to test the impact of the micro-collapsed cake on the protein stability.

The three freeze-drying cycles were selected to produce cakes with different physical properties. The first, ''no collapse'' (NC), was a very gentle cycle, in which the samples were annealed to allow crystallization of the glycine eutectic to occur and the primary drying temperature was very low. The second cycle, ''micro-collapse'' (MC), also included an annealing step, but the primary drying temperature was much higher. The third cycle, ''collapse'' (C), did not include an annealing step, and the temperature during primary drying was also kept low to inhibit the crystallization of the glycine eutectic. Following freeze-drying, the products were placed in stability chambers at 5, 25, and 40°C in order to assess their long-term stability during storage at each of these temperatures. Sample vials were removed from the stability chambers periodically and assayed for protein activity, moisture content, and aggregate by size-exclusion high-performance liquid chromatography (SEC–HPLC).

Figure 16 is a photograph of samples freeze-dried by each of the three methods, and shows the level of physical, macroscopic collapse that typically resulted from using the ''collapse'' freeze-drying method.

Copyright 2004 by Marcel Dekker, Inc. All Rights Reserved.

Figure 16 Photograph of non-collapsed (NC), micro-collapsed (MC), and collapsed (C) α-amylase samples after freeze-drying.

Scanning electron microscopy (SEM) showed that the "C" cakes are significantly different on a microscopic scale from the other cakes, as shown in Figure 17. The magnification of these pictures is 760X. The "C" cake shows much less structure than is observed for the "NC" or "MC" cakes, which at this magnification are indistinguishable. No evidence was detected by SEM for any level of collapse in the "MC" samples.

Figure 18 shows the average protein activity measurements for each freeze-drying protocol up to the 18-month time point of the stability study. This plot shows data from each of the storage temperatures, 5, 25, and 40°C, as well as for liquid samples that were taken immediately prior to freeze-drying, and zero time point (T_0) samples taken immediately after freeze-drying. The protein activity is calculated as the percentage of the T_0 activity. As expected, the activity decreases most rapidly at the higher storage temperatures. However, this loss of activity at 40°C appears to be slightly greater for the "NC" and "MC" samples than for the "C" samples. At the lower storage temperatures, the loss of activity appears to be slightly greater in the "C" samples than in the "MC" or "NC" samples after the 18 month storage time point.

The results of this study suggest that collapse is not necessarily detrimental to either the activity or stability of freeze-dried protein.

Copyright 2004 by Marcel Dekker, Inc. All Rights Reserved.

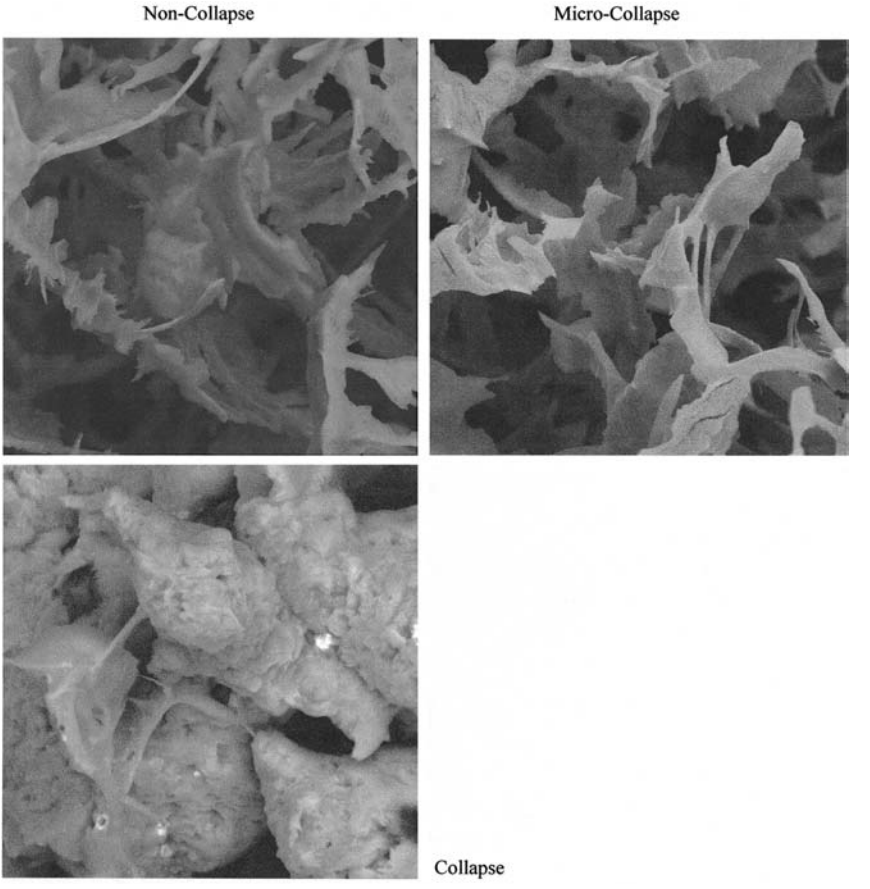

Figure 17 Scanning electron micrograph of each of the freeze-dried cakes, non-collapsed (NC), micro-collapsed (MC), and collapsed (C). Magnification is 760X.

Particularly, data support the hypothesis that the more aggressive, shorter primary drying cycle permitted by the MC cycle does not compromise the stability of the protein product. The similarity between the results of the stabilities of the samples lyophilized by the "NC" and "MC" cycles indicates that using the more aggressive cycle is not harmful to the protein. This is important because it permits a more efficient freeze-drying cycle to be used, without decreasing the stability of the protein. However, it is important to point out that such a conclusion may only apply to the protein and formulation studied here. For other proteins and formulations, the behavior may be totally different.

Copyright 2004 by Marcel Dekker, Inc. All Rights Reserved.

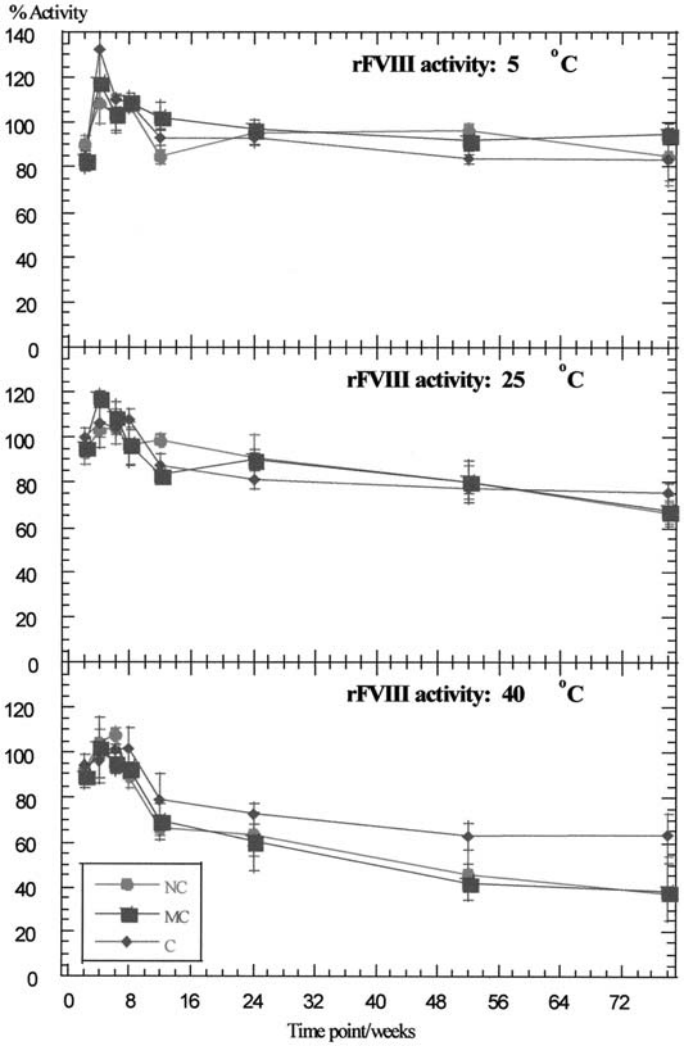

Figure 18 Protein activity versus storage time.

IX. CONCLUSIONS

This chapter described how to characterize a crystalline matrix-type formulation in order to successfully develop a lyophilization cycle. Techniques used for characterizing the formulation include differential

Copyright 2004 by Marcel Dekker, Inc. All Rights Reserved.

scanning calorimetry (DSC), lyo-microscopy, water adsorption study, and moisture optimization. We found that DSC and lyo-microscopy are excellent tools to determine the thermophysical properties of a formulation such as freezing, melting, crystallization, and glass transition temperatures. This information allows us to precisely design freezing and primary drying parameters, such as annealing temperature, shelf temperature, and pressure. We also described how to generate a water adsorption curve and how to conduct a moisture optimization study. We demonstrated that this information is critical for optimizing the secondary drying process, such as drying temperature, pressure, and time. In addition, we also reported a confirmation study that demonstrated after annealing, that we could lyophilize protein product at a high temperature without compromising protein activity and stability. The techniques and methods used can be used in other protein formulation characterization studies. In summary, we have demonstrated that a better understanding of formulation characteristics allows us to develop an optimal lyophilization cycle with a scientific rationale.

ACKNOWLEDGMENTS

The author wants to thank Dr. Jeff Hey, Dr. Xinghang Ma, and Bruce Gardner from Bayer Corporation for their hard work in generating some of the data reported in this chapter. The author also wants to thank Dr. Steve Nail from Purdue University for his work on some of the DSC and x-ray diffraction data.

REFERENCES

1. F Franks. Freeze-drying: from empiricism to predictability. The significance of glass transitions. In: J May, Brown eds. Developments in Biological Standardization. Basel: Karger, 1991, Vol. 74, pp 9–38.
2. L Rey. Thermal analysis of eutectics in freezing solutions. Ann NY Acad Sci 85 (part 2):510–534, 1960.
3. AP MacKenzie. Apparatus for microscopic observations during freeze-drying. Biodynamica 9(186):213–222, 1964.
4. AP MacKenzie. Freezing, freeze-drying and freeze-substitution. Proceedings of the Workshop on Biological Specimen Preparation Techniques for Scanning Electron Microscopy, IIT Research Institute, April, 1972.
5. MJ Pikal. Freeze-drying of proteins. Part I: process design. BioPharm, 3(8): 18–27, 1990.

Copyright 2004 by Marcel Dekker, Inc. All Rights Reserved.

6. MJ Pikal. Freeze-drying of proteins. Part II: formulation selection. BioPharm, 10:26–30, 1990.
7. M Pikal, S Shah. The collapse temperature in freeze-drying: dependence on measurement methodology and rate of water removal from the glassy phase. Int J Pharm, 62:165–186, 1990.
8. F Franks. Improved freeze-drying: an analysis of the basic scientific principles. Proc Biochem 2:iii–vii, 1989.
9. SL Nail, LM Her, PB Christopher, LL Nail. An improved microscope stage for direct observation of freezing and freeze drying. Pharm Res, 11(8): 1098–1100, 1994.
10. K Izutsu, S Yoshioka, S Kojima. Physical stability and protein stability of freeze-dried cakes during storage at elevated temperatures. Pharm Res, 11(7): 995–999, 1994.
11. T Arkawa, SJ Prestrelski, WC Kenney, JF Carpenter. Factors affecting short-term and long-term stabilities of proteins. Adv Drug Delivery Rev 10:1–128, 1993.
12. JF Carpenter, SJ Prestrelski, T Arkawa. Separation of freezing- and drying-induced denaturation of lyophilized proteins using stress-specific stabilization. Arch Biochem Biophys 303(2): 456–644, 1993.
13. AP MacKenzie. A current understanding of the freeze-drying of representative aqueous solutions. In: Refrigeration Science and Technology, IIF-IIR Commission C Tokyo, 1985, pp 21–34.
14. LM Her, SL Nail. Measurement of glass transition temperatures of freeze-concentrated solutes by differential scanning calorimetry. Pharm Res 11(1): 54–59, 1994.
15. X Ma, DQ Wang, R Bouffard, A MacKenzie. Characterization of murine monoclonal anitbody to tumor necrosis factor (TNF-MAb) formulation for freeze-drying cycle development. Pharm Res 18(2):196–202, 2001.
16. RHM Hatley. The effective use of differential scanning calorimetry in the optimization of freeze-drying processes and formulations. In: Developments in Biol. Standard. 74:105–122 (Karger, Basel, 1991).
17. T Jennings. Thermal-analysis instrumentation for lyophilization. Medical Devices Diagnostics & Instrumentation 11: 49–57, 1980.
18. LR Rey. Thermal analysis of eutectic in freezing solution. International Institute of Refrigeration and Laboratoire de Physiologie, Ecole Normale, Paris, France, 1975, pp 510–534.
19. L Rey. Study of the freezing and drying of tissues at very low temperatures. In: A Parkes, A Smith eds. Recent research in freezing and drying. Oxford: Blackwell, 1960, pp 40–620.
20. P DeLuca, L Lachman. Lyophilization of pharmaceuticals, I: effect of certain physical-chemical properties. J Pharm Sci 54:617–624, 1965.
21. AP MacKenzie. Changes in electrical resistance during freezing and their application to the control of the freeze-drying process. In: Refrigeration Science and Technology, IIF-IIR Commission C Tokyo, 1985, pp 155–163.

Copyright 2004 by Marcel Dekker, Inc. All Rights Reserved.

22. AP MacKenzie. Factors affecting the transformation of ice into water vapor in the freeze-drying process. Ann NY Acad Sci 125:522–547, 1965.
23. AP MacKenzie. Collapse during freeze-drying – qualitative and quantitative aspects. In: S Goldblith, L Rey, W Rothmayr eds. Freeze-drying and advanced food technology. New York: Academic Press, 1975, pp 277–307.
24. L Rey, Dispositif pour l'examen microscopique aux basses temperatures. Experientia XIII:201–202, 1957.
25. CC Hsu, CA Ward, R Pearlman, HM Nguyen, DA Yeung, JG Curley. Determining the optimum residual moisture in lyophilized protein pharmaceuticals. Dev Biol Stand 74:257–271, 1991.
26. D. Greiff. Protein structure and freeze-drying effects of residual moisture and gases. Cryobiology 8:145–152, 1971.
27. WR Liu, R Langer, AM Klibanov. Moisture-induced aggregation of lyophilized protein in the solid state. Biotechnol Bioeng 37:177–184, 1991.
28. S Yoshioka, Y Aso, S Kojima. The effect of excipients on the molecular mobility of lyophilized formulations, as measured by glass transition temperature and NMR relaxation-based critical mobility temperature. Pharm Res 16(1):135–140, 1999.
29. B Hancock, G Zografi. The relationship between the glass transition temperature and the water content of amorphous pharmaceutical solids. Pharm Res 11(4):471–477, 1994.
30. D Miller, J de Pablo, H Corti. Thermophysical properties of trehalose and its concentrated aqueous solutions. Pharm Res 14(5):135–140, 1997.
31. P Royal, D Craig, C Doherty. Characterisation of the glass transition of an amorphous drug using modulated DSC. Pharm Res 15(7):578–595, 1998.
32. B Lueckel, B Helk, D Bodmer, H Leuenberger. Effects of formulation and process variables on the aggregation of freeze-dried Interleukin-6 (IL-6) after lyophilization and on storage. Pharm Dev Technol 3(3):337–346, 1998.
33. GDJ Adams, JR Ramsay. Optimizing the lyophilization cycle and the consequences of collapse on the pharmaceutical acceptability of Erwinia L-Asparaginase. J Pharm Sci 8606(12):1301–1305, 1996.
34. GDJ Adams, LI Irons. Some implications of structural collapse during freeze-drying using Erwinia Caratovora L-Asparaginase as a model. J Chem Biotechnol 58:71–76, 1993.
35. B Lueckel, D Bodmer, B Helk, H Leuenberger. Formulations of sugars with amino acids or mannitol – influence of concentration ratio on the properties of the freeze-concentrate and the lyophilizate. Pharm Dev Technol 3(3):325–36, 1998.
36. S Jiang, SL Nail. Effect of process conditions on recovery of protein activity after freezing and freeze-drying. Eur J Pharm Biopharm 45(3):249–257, 1998.

Copyright 2004 by Marcel Dekker, Inc. All Rights Reserved.

8

Practical Aspects of Freeze-Drying of Pharmaceutical and Biological Products Using Non-Aqueous Co-Solvent Systems

Dirk L. Teagarden and David S. Baker
Pfizer Corporation, Kalamazoo, Michigan, U.S.A.

I. INTRODUCTION

Freeze-drying of pharmaceutical and biological solutions to produce an elegant stable powder has been a standard practice employed to manufacture many marketed pharmaceutical and biological products for over 50 years. The vast majority of these products are lyophilized from simple aqueous solutions. Water is typically the only solvent of significant quantity that is present which must be removed from the solution via the freeze-drying process. However, frozen water (ice) is not the only frozen liquid which can sublime under reduced pressures. Numerous organic and mineral solvents have been shown to possess this property [1]. It is also noteworthy that during the freeze-drying of pharmaceutical or biological products it is not unusual for small quantities of organic solvents to be present in either the active pharmaceutical ingredient or one of the excipients. These low levels of organic solvent are commonly found because they may be carried through as part of the manufacture of these individual components since the ingredient may be precipitated, crystallized, or spray dried from organic solvents. Therefore, many freeze-dried products may be dried from solutions

Copyright 2004 by Marcel Dekker, Inc. All Rights Reserved.

which contain low levels of a variety of organic solvents. Additionally, there may be instances where freeze-drying from substantial quantities of organic solvents or mixtures of water and organic solvent may offer the formulation scientist advantages over simply drying from an aqueous solution. An example of at least one pharmaceutical product on the market which has utilized an organic co-solvent system during freeze-drying is CAVERJECT® Sterile Powder [2,3]. This particular product has been successfully manufactured by freeze-drying from a 20% v/v tert-butanol/water co-solvent system.

There are many reasons why it may be beneficial to both product quality and process optimization to select a lyophilization process which employs a strictly organic or organic/water co-solvent system. A list of some of these potential advantages is summarized Table 1. However, the development scientist must be aware that use of these organic/water co-solvent systems causes a variety of issues which must be properly addressed. A list of some of these potential disadvantages is summarized in Table 2.

Table 1 Potential Advantages of Use of Co-Solvents in Freeze-Drying

Increases rate of sublimation and decreases drying time
Increases chemical stability of the pre-dried bulk solution
Increases chemical stability of the dried product
Facilitates manufacture of bulk solution by increasing drug wettability and solubility in solution
Improves reconstitution characteristics (e.g., decreases reconstitution time)
Offers potential alternative to manufacture of products requiring powder filling
Enhances sterility assurance for pre-dried bulk solution

Table 2 Potential Disadvantages of Use of Co-Solvents in Freeze-Drying

Toxicity concerns
Operator safety concerns due to high degree of flammability or explosion potential
Lack of compendia grades or monographs
May require special manufacturing facilities/equipment or storage areas
Possess difficult handling properties
Require high-purity solvent with known impurities at low levels
Must reach acceptable residual solvent in final product
High cost to use
Potential for splash/spattering of product in vial neck
Lack of regulatory familiarity
Potential adverse environmental impact

Copyright 2004 by Marcel Dekker, Inc. All Rights Reserved.

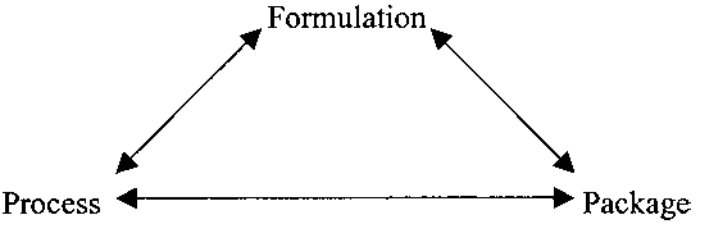

Figure 1 Interrelationships between formulation, process, and package.

When developing a new freeze-dried product it is critical to evaluate and gain a proper understanding of the fundamental interrelationships between the formulation, the process, and the package (Figure 1) since all must work in unison for a successful product to be developed. The knowledge gained from the interrelationships enables optimization of the formulation which can be successfully manufactured and packaged in a production-scale setting. These same principles apply to the use of organic solvents in freeze-drying. The advantages and disadvantages for a particular organic co-solvent system must be carefully weighed before they are selected for use in the manufacture of a pharmaceutical or biological product, especially one that is an injectable dosage form.

A list of some of the solvents which have been evaluated in one form or another in freeze-drying studies is provided in Table 3. Included in this table is a summary of some of the critical physical/chemical properties for each of these solvents. Several pharmaceutical and biological products or drugs in various stages of formulation and/or clinical development have been manufactured via a process which required freeze-drying from organic co-solvent systems. These types of solvent systems were chosen for one or more of the advantages described earlier. Table 4 contains a list of examples of a few drug preparations which have been evaluated.

Additional uses for the technique of freeze-drying from organic co-solvent systems, other than in the manufacture of pharmaceuticals and/or biologicals, includes the preparation of biological specimens or the preparative isolation of excipients such as lecithin. The biological specimens can be prepared by lyophilization from organic co-solvent systems in order to improve specimen preservation for scanning electron microscopy examinations [4–6]. Tert-butanol appears to be the major organic solvent selected for this use. The surface structure of the specimen remains intact when employing rapid freezing followed by freeze-drying from an appropriate organic solvent such as tert-butanol [7]. The phospholipid, lecithin, has been shown to be readily prepared in a solvent-free from via lyophilization from cyclohexane [8].

Copyright 2004 by Marcel Dekker, Inc. All Rights Reserved.

Table 3 Properties of Organic Solvent Evaluated in Freeze-Drying

Solvent	Solubility in water (%)[a]	Vapor pressure (mm Hg at 20°C)	Freezing point (°C)	Boiling point (°C)	Flammability			
					Flash point (°F/°C)	Autoignition temperature (°F/°C)	Lower flamm. limit (in air vol. %)	Upper flamm. limit (in air vol. %)
Tert-butanol	100	26.8	24.0	82	52/11	892/478	2.4	8.0
Ethanol	100	41.0	−114	78.5	62/16	793/423	3.3	19
n-propanol	100	14.5	−127	97.1	59/15	760/404	2.1	13.5
n-butanol	7.7	5.6	−90	117.5	95/35	689/365	1.4	11.2
Isopropanol	100	31.0	−89.5	81	53.6/12	750/398	2.5	12
Ethyl acetate	8.7	64.7	−84	77.1	24/−4	800/426	2.2	11.5
Dimethyl carbonate	9.5	72	2	90	65/18	—	4.2	12.9
Acetonitrile	100	69.8	−48	80.1	45/8	975/524	4.4	16.0
Dichloromethane	1.3	343.9	−97	40	none	1033/556	14	22
Methyl ethyl ketone	27	76.2	−87	79.6	26/−3	885/474	1.7	10.1
Methyl isobutyl ketone	2.0	5.1	−80	117	56/13	860/460	1.2	8

Copyright 2004 by Marcel Dekker, Inc. All Rights Reserved.

Acetone	100	160.5	−94	56.2	1/−7	1000/538	2.6	12.8
1-pentanol	2.7	1.8	−78	138	120/49	572/300	1.2	10
Methyl acetate	25	148.7	−98	57	15/−9	935/502	3.1	16
Methanol	100	87.9	−98	65	52/11	835/446	6.0	36
Carbon tetrachloride	0.08	78.9	−23	76	none	none	none	none
Dimethyl sulfoxide	100	0.5	18.4	189	188/87	572/300	3.5	42
Hexafluoroacetone	100	5.0[b]	−129	−26	none	none	none	none
Chlorobutanol	0.8	—	97	167	>212/>100	—	—	—
Dimethyl sulfone	100	—	107	248	290/143	—	—	—
Acetic acid	100	11.6	16.2	118.5	103/39	960/516	6.6	19.3
Cyclohexane	0.008	66.4	6.5	81	−1/−18	500/260	1	9

[a]100% = miscible.
[b]25°C.

Copyright 2004 by Marcel Dekker, Inc. All Rights Reserved.

Table 4 Examples of Drug Preparations Freeze-Dried from Co-Solvents

Drug	Co-solvent system	Ref.
Alprostadil (CAVERJECT S.Po.)	20% v/v tert-butanol/water	[2]
Aplidine	40% v/v tert-butanol/water	[10]
Amoxicillin sodium	20% v/v tert-butanol/water	[65]
Tobramycin sulfate	Tert-butanol/water	[42]
Gentamicin sulfate	Tert-butanol/water	[39]
N-cyhclodexyl-*N*-methyl-4-(2-oxo-1,2,3,5-tetrahydroimidazo-[2,1-b]quinazolin-7-yl)oxybutyramide with ascorbic acid	50% v/v tert-butanol/water	[9]
Cyclohexane-1,2-diamine Pt(II) complex	Tert-butanol	[66]
Annamycin	Tert-butanol/dimethyl sulfoxide/water	[67]
Cephalothin sodium	5% w/w isopropyl alcohol/water	[19]
Cephalothin sodium	4% ethanol, 4% methanol, or 4% acetone/water	[40]
Prednisolone acetate/ polyglycolic acid	Carbon tetrachloride/ hexafluoroacetone sesquihydrate	[64]
Gabexate mesylate	Ethanol/water	[68]
Piraubidin hydrochloride	Ethanol/water	[69]
Progesterone, coronene, fluasterone, phenytoin	Chlorobutanol hemihydrate/ dimethyl sulfone	[32]
Fructose-1,6-diphosphate	Tert-butanol/water	[70]
Poly(lactide-co-glycolide)	Acetic acid	[71]
Dioleoylphosphatidylcholine and dioleoylphophatidylglycerol	Cyclohexane	[72]
Vecuroniumbromide	Acetonitrile	[73]
Bovine pancreatic trypsin inhibitor	Dimethyl sulfoxide/ 1% water	[43]

II. FACILITATING MANUFACTURE OF BULK SOLUTION

The first step in the manufacture of almost all freeze-dried products is the formation of a solution of the ingredients to be dried. Typically these solutions are sterile filtered, aseptically filled into containers, and freeze-dried. Some hydrophobic ingredients (e.g., the bulk drug or excipients) may

Copyright 2004 by Marcel Dekker, Inc. All Rights Reserved.

be difficult to wet or may require large amounts of water to adequately solubilize. The use of organic co-solvents can greatly facilitate the wetting of the hydrophobic substance, decrease the time to achieve a solution or uniform dispersion, and decrease the amount of solvent which needs to be removed during the drying process. All of these attributes can potentially have a positive effect on the consistency and ease of product manufacture. Several examples of this increased drug solubility in the presence of organic co-solvents targeted for lyophilization include: (1) alprostadil formulated in a tert-butanol/water solution [2] and (2) cardiotonic phosphodiesterase inhibitors complexed with vitamins formulated in a tert-butanol/water solution (however, other alcohols such as ethanol n-propanol, or isopropyl alcohol are also claimed to provide further increases in solubility [9]) and (3) aplidine formulated in tert-butanol/water solution [10]. The actual tert-butanol concentration (i.e., 40% v/v in water) selected for aplidine produced a greater than 40-fold increase in solubility compared to that in pure water. However, one must be aware of the possible negative impact of organic co-solvents on the solubility of hydrophilic excipients. The precipitation potential must be evaluated to determine whether the organic level chosen will allow the solution components to remain in solution throughout the processing steps, especially as temperature changes occur or nucleation sites become available.

III. STABILIZATION OF BULK SOLUTION

A major challenge in developing a sterile injectable product can be its instability in solution. Most freeze-dried products are developed as this dosage form in order to circumvent poor stability whether it be chemical or physical instability. The manufacture of a freeze-dried product necessitates that the product is usually first manufactured as a solution, filtered to sterilize, aseptically filled, and finally lyophilized to remove the solvents. All of these unit operations require that the product be held in the solution state for a defined period of time. However, as the product is held in the solution phase it can experience various levels of degradation which are dependent on the kinetics of the degradation mechanism. The presence of the various levels of organic solvent can have a profound effect on the chemical stability. Those drug candidates which are very labile in aqueous solutions may require the added stability to achieve an acceptable level of degradation during manufacture. Early efforts to freeze-dry an anti-neoplastic agent (1,3-Bis(2-chloroethyl)-1-nitroso-urea) from an ethanol/water solution were initiated because of the rapid degradation in aqueous solution and improved solution stability in ethanol/water solutions [11].

Copyright 2004 by Marcel Dekker, Inc. All Rights Reserved.

Unfortunately freeze-drying this product in the ethanol/water co-solvent system proved to be unsuccessful due to potency losses and unacceptable clarity. Flamberg et al. [11] suggested that an alternative process to freeze-drying solvent systems containing ethanol would be to use low-temperature vacuum drying. However, alprostadil has been successfully freeze-dried from a tert-butanol/water solution. The first order degradation rate constant of alprostadil in 20% v/v tert-butanol/water ($k = 0.0011$ day^{-1} at 25°C) was significantly reduced compared to water buffered at the same pH value ($k = 0.0041$ day^{-1} at 25°C). These data are consistent with the claims of extraordinary stability of prostaglandins in tert-butanol [12]. This decreased degradation rate enables the manufacturing unit operations to be performed at ambient conditions without requiring cooling of the solution during manufacture. Additionally, it adds flexibility in scheduling these various operations because the solution degradation has been minimized.

The formulation of trecetilide fumarate, a sterile injectable in clinical development for the treatment of arrhythmias, also involved freeze-drying from a tert-butanol/water mixture [13]. Kinetic analysis showed solution degradation occurred by a process of defluorination through SN_1 substitution and E_1 elimination, both proceeding through the same carbonium ion intermediate. Since factors such as ionic strength, buffer type, solution pH, and drug and buffer concentrations did not significantly affect degradation rate, destabilization of the fluoride leaving group was one of the few methods left to control this reaction. Use of tertiary butyl alcohol as a co-solvent slowed solution state degradation by a factor of approximately 4–5. This significantly increased the probability of being able to scale up the manufacturing process while maintaining tight control of the level of degradation. The rate constant (k) for drug degradation was decreased substantially as the tert-butanol content was increased. The work required to separate two charges to infinite distance is related to the function $(1 - 1/E_r)$ where E_r is the relative permittivity of the medium. The linear relationship observed between log k and this function (Figure 2) indicates that the decreased relative permittivity of the solvent system (i.e., the increased work required to remove the fluoride group) was the major effect for the improved solution state stability of trecetilide fumarate. The decreased ability of tert-butanol (relative to water) to solvate and stabilize the two ions appeared to be less of a factor. The use of tert-butanol allowed formulation and filling on a production scale over a 24 h period for this compound. The resulting freeze-dried product was predicted to have an acceptable shelf-life of at least 2 years at ambient temperature. This was a dramatic improvement compared to a frozen aqueous solution which had to be stored at −80°C and required use within 3 h of thawing and admixture preparation. This type of effect would be

Copyright 2004 by Marcel Dekker, Inc. All Rights Reserved.

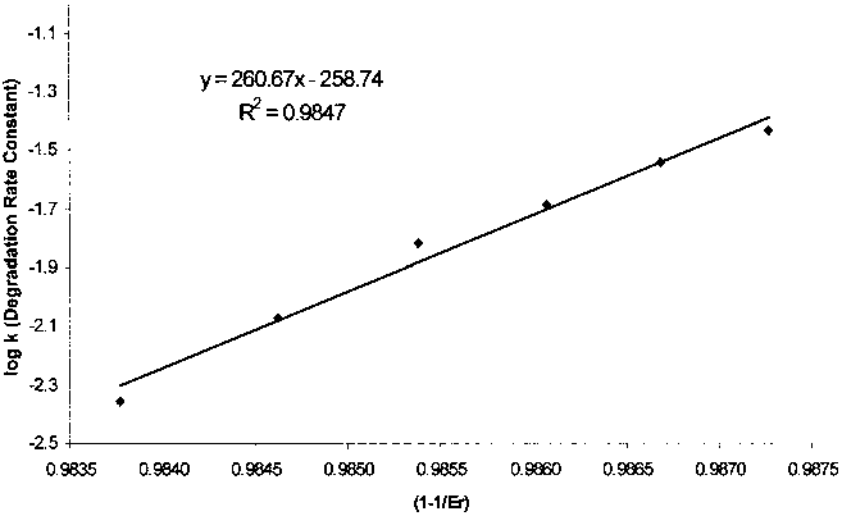

Figure 2 Effect of relative permittivity (E_r) on the solution degradation rate constant for trecetilide fumarate, a compound undergoing SN_1 substitution and E_1 elimination through the same carbonium ion intermediate.

expected to be observed for many other drug products which are degraded in the presence of water.

IV. IMPACT ON THE FREEZE-DRYING PROCESS

A. Effect on Freezing

The first stage of freeze-drying involves freezing the solution to remove solvent (typically water) from the drug and excipients through the formation of ice. The resulting semi-frozen system is cooled further to transform all components into a frozen state. A selected time/temperature profile is achieved by placing the solution, which is commonly held in glass vials or syringes, onto cooled shelves. Suspended impurities in the solution or imperfections in the walls of the container initiate heterogeneous nucleation during freezing. This event almost always involves supercooling whereupon crystallization occurs below the equilibrium freezing point of the solution. Consequently, when freezing does occur, crystal growth tends to be rapid and results in a complex mixture of crystalline, amorphous, and metastable materials. The impact of the presence of organic solvents on the various phases of freeze-drying has been discussed in detail [14–18].

Copyright 2004 by Marcel Dekker, Inc. All Rights Reserved.

Not surprisingly, the type and concentration of the organic solvent present affects the freezing characteristics of the solution prior to initiation of drying. The resulting frozen or semi-frozen solution significantly impacts the crystal habit of the ice, the drying rates, the collapse temperatures, the appearance of the dried cake, the surface area of the dried cake, and the reconstitution properties, etc. The choice of solvent can also affect the degree of crystallinity of the drug. It has been demonstrated that incorporation of isopropyl alcohol readily results in highly crystalline cefazolin sodium [19]. Scaling up this process required incorporation of a heat treatment step to insure complete crystallization of the drug. Conversely, use of co-solvents can sometimes have deleterious effects during freezing. The use of volatile organic solvents has been reported to result in drug precipitation in the latter parts of freezing due to solvent evaporation. This can lead to an increase in drug concentration above its saturation level [17]. Care should be taken to select excipient concentrations such as buffer salts so that they do not exceed their saturation solubility. This is particularly important for phosphate buffers since they have very low-solubility products with certain cations such as aluminum, calcium, or iron [20–23]. As a result, salt precipitation can produce a haze upon reconstitution. Additionally, the preferential precipitation of one the forms of phosphate can also cause a significant pH shift for the frozen solution. Therefore, it is critical to select buffer components that can maintain pH in both the solution and frozen state. These precipitation problems can be exacerbated in co-solvent systems due to the decreased solubility and higher association constants for such systems.

The size and shape of the ice crystals has been found to vary with different organic solvents. Trace impurities of isobutyl alcohol have been shown to significantly alter the crystal habit of ice crystals [24]. The presence of small levels of organic solvents (e.g., DMSO, ethanol, dichloromethane, or acetone) in an aqueous solution has been shown to influence the nucleation of ice crystals and their subsequent growth [25]. These organic impurities can also potentially reduce the collapse temperature for the frozen solution [26,27]. The presence of high melting point solvents, such as tert-butanol, results in solvent crystallizing between the ice matrix as the temperature is decreased. The presence of the tert-butanol altered the crystal habit of the ice as it formed. The size of the ice crystals (i.e., large versus fine) changed depending on the quantity of tert-butanol present in the system. Thermal analysis studies (via DSC (Differential Scanning Calorimetry) and freeze-dry microscopy) have been used to evaluate the various stable and metastable states which form for tert-butanol/water systems during freezing [28]. The DSC warming thermograms for the tert-butanol/water mixtures are illustrated in Figure 3. The authors were

Copyright 2004 by Marcel Dekker, Inc. All Rights Reserved.

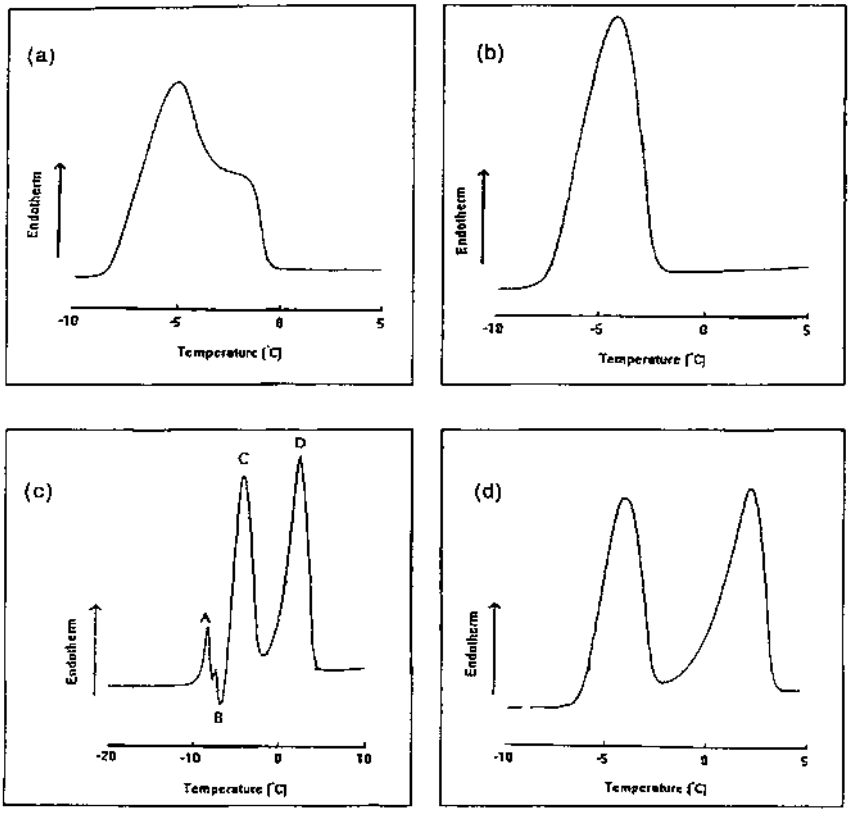

Figure 3 DSC warming thermograms for tert-butanol/water mixtures: (a) 15% w/w tert-butanol; (b) 20% w/w tert-butanol; (c) 50% w/w tert-butanol (Endotherm A: melting of metastable eutectic; Exotherm B: recrystallization of metastable eutectic form to stable form; Endotherm C: melting of eutectic; Exotherm D: melting of tert-butanol hydrate); (d) thermal treatment of 50% w/w solution at −7°C to eliminate metastable states [28].

able to apply various annealing techniques to eliminate the metastable states and were able to construct the true phase diagram (Figure 4). Although this phase diagram agreed well with other tert-butanol/water phase diagrams reported in the literature [29,30], it was claimed that the slight differences could be explained by the presence of metastable events which thermal treatments eliminated. These data suggested that tert-butanol levels in the range of 3–19% caused the ice to form needle-shaped crystals. As these large needle-shaped crystals sublimed they created a more porous, less resistant

Copyright 2004 by Marcel Dekker, Inc. All Rights Reserved.

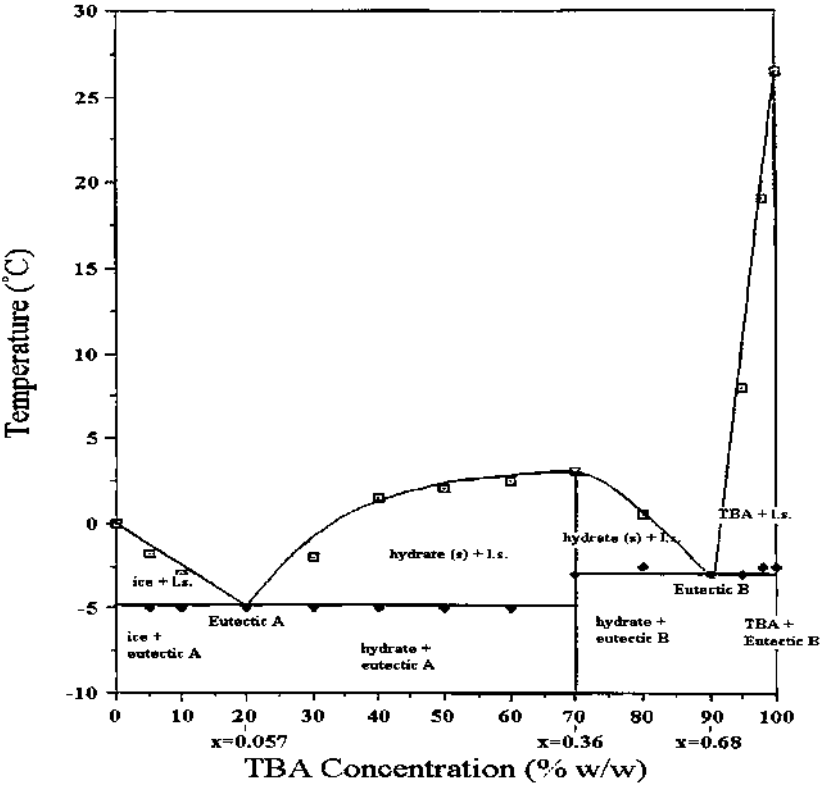

Figure 4 Phase diagram of the tert-butanol (TBA)/water system plotted on % (w/w) basis. Mole fractions are listed for eutectic A and B and the pure hydrate; x is tert-butanol concentration on mole fraction basis [28].

matrix, which facilitates drying. Other solvents such as acetic acid, formic acid, or dimethyl carbonate also appear to freeze under production freeze-dryer conditions and can be adequately lyophilized. However, most of the organic solvents investigated [18] such as methanol, ethanol, n-propanol, n-butanol, acetonitrile, methyl ethyl ketone, dichloromethane, and methyl isobutyl ketone do not freeze in typical commercial freeze-dryers but remain as liquid residues within the frozen matrix. The following appears to occur when using conventional freeze-dry equipment: (1) solutions containing 8% ethyl acetate, 10% dimethyl carbonate, or 10% n-butanol appeared to dry rapidly; (2) solutions containing 10% ethanol, 10% n-propanol, or 10% methanol appeared to dry slowly; (3) solutions containing up to 20% ethanol experienced collapsed cakes and were near impossible to dry [18].

Copyright 2004 by Marcel Dekker, Inc. All Rights Reserved.

Some of the more hydrophilic solvents such as ethanol and methanol retained significant amounts of associated water which only partially froze as the temperature decreased. Samples dried with organic solvents which do not completely freeze may produce a product which is heterogeneous with respect to residual solvent. Use of appreciable levels of solvents which do not freeze usually result in unacceptable cake appearance. However, in those products which produce a resistant surface skin during the drying process, a small level of unfrozen organic can cause discontinuities in the skin sufficiently to potentially facilitate the removal of the frozen water vapor [31].

In those system which completely froze (e.g., tert-butanol) the ice and frozen solvent grew upwards until reaching the solid surface and formed a eutectic skin. Hydrophilic solvents which retained large volumes of water formed thick liquid skins containing ice whereas less hydrophilic solvents containing less water formed thinner skins with less ice. It should also be noted that the time between filling the co-solvent solution and the freezing of this solution should be carefully controlled. The volatility of the organic portion of the solution can be such that a significant portion of the organic solvent can be lost due to evaporation. One should be aware of the potential for a reflux-type phenomenon when using highly volatile solvents such as tert-butanol. This situation can happen when the evaporating tert-butanol condenses near the top of the vial and forms a stream of solvent returning to the solution. The dissolved substances in the solution can diffuse in this stream. After freeze-drying has been completed, the vial can contain spots of powder near the neck of the vial. The presence of dried powder near the neck of a vial is not desired because of both a poor appearance and the possibility of negatively impacting the seal with the rubber closure. This problem can be decreased by shortening the time period between the filling and the freezing of the solution.

An interesting study was performed [32] to investigate the feasibility of using organic solvents which are solid at room temperature to lyophilize drug products without the use of conventional freeze-drying equipment. These organic solvents were selected based on their ability to solubilize hydrophobic drugs, increase the solution stability of water-sensitive drug molecules, be readily removed via vacuum drying, and produce elegant dried cakes which were easily reconstituted with acceptable solvents. It was found that the chlorobutanol hemihydrate-dimethyl sulfone eutectic was an optimum solvent system based on its low toxicity, excellent solubilizing capability, and ease of removal via sublimation under vacuum. Lyophilization was accomplished without refrigeration and only required modest heating under vacuum. The resulting dried cakes contained less than 1% residual solvent. Use of this method should be undertaken with caution since the practicalities of heating potentially flammable solvents and keeping

Copyright 2004 by Marcel Dekker, Inc. All Rights Reserved.

the solutions in the liquid phase during filtration, filling, etc., may require additional development time and cost to make this work at a production scale.

B. Acceleration of Sublimation Rate

The freeze-drying process is a unit operation which typically involves a long and expensive process. Improvements in the rate of mass transfer of solvent through the partially dried cake layer will increase the rate of sublimation and hence decrease the time for the primary drying phase of the freeze-dry cycle. Mathematically it has been shown that:

$$\text{Sublimation rate} = \text{pressure difference/resistance}$$

The resistance term is an additive term which reflects the sum of the dried product resistance, the vial/stopper resistance, and the chamber resistance. However, the predominant resistance of the three terms is typically the product resistance which usually accounts for about 90% of the total resistance [33]. The mass transfer in the dry layer occurs via two general mechanisms: bulk flow (the movement of material in the direction of a pressure gradient, which may be molecular or viscous) or diffusive flow (the movement of material by molecular motion from higher concentration to lower concentration or partial pressure) [34]. Typically the resistance to mass transfer increases with cake depth. What happens during the freezing phase can have a profound impact on the resistance of the dried cake to mass transfer during primary drying. Those co-solvents which can alter the ice crystal habit and size of the ice crystals, such as promoting the formation of large needle crystals, can dramatically increase the rate of bulk flow. This is because the permeability of the dried layer would increase proportionally (to the third power for molecular flow and to the fourth power for viscous flow) to the average diameter of the pore created by the sublimation process [34]. Many of the co-solvents selected for freeze-drying increase sublimation rate because they have higher vapor pressures than water and hence an expected larger driving force for sublimation because the latter depends on this vapor pressure difference [35].

The potential acceleration of the freeze-drying rates of aqueous solutions of lactose and sucrose with 5 and 10% aqueous solutions of tert-butanol has been studied [36]. It was found that both lactose and sucrose solutions could be successfully freeze-dried in the presence of tert-butanol at considerably higher shelf temperatures than corresponding aqueous solutions of either lactose or sucrose. The drying rates were significantly

Copyright 2004 by Marcel Dekker, Inc. All Rights Reserved.

increased when using the tert-butanol as a co-solvent. The drying times were decreased to approximately half the time when drying sucrose in the presence of tert-butanol. The collapse temperature for the frozen solutions appeared to increase when tert-butanol was present. The tert-butanol readily froze and remained frozen during the primary drying phase. The tert-butanol sublimed during primary drying and created a porous structure which facilitated the mass transfer of water vapor due to decreased cake resistance. The resulting dried cakes exhibited significantly increased surface areas. Freeze-drying of a similar amorphous carbohydrate such as a lactose base formulation from a tert-butanol/water co-solvent (e.g., CAVERJECT Sterile Powder) also produces a very porous cake structure as illustrated by the SEM picture shown in Figure 5. Alternatively, it was demonstrated that using other organic co-solvents at a 5% level (e.g., methanol, ethanol, isopropanol, acetone, n-butanol, or dioxane) that do not freeze under operating conditions for conventional commercial freeze-dryers produced unacceptable freeze-dried cakes of either lactose or sucrose due to boiling of solvent and cake collapse.

A more in-depth study was later completed evaluating the use of tert-butanol as a mass transfer accelerator during the freeze-drying of a 5% w/v sucrose solution [37,38]. Again it was demonstrated that the primary drying phase (i.e., sublimation) proceeded more rapidly when 5% w/w

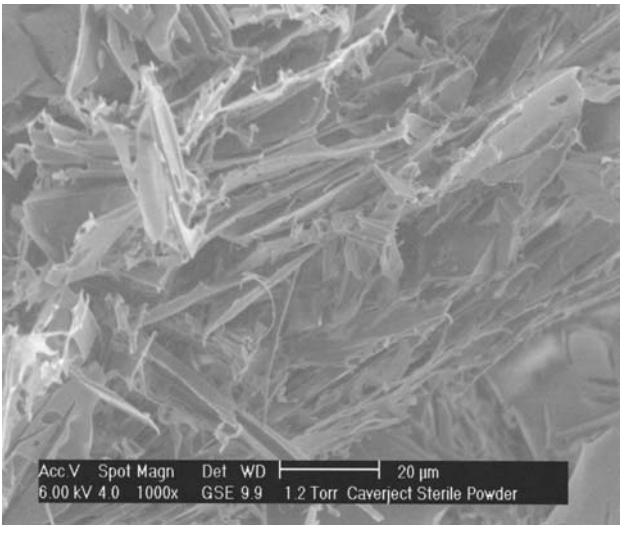

Figure 5 SEM picture of CAVERJECT Sterile Powder which has been lyophilized from a 20% v/v tert-butanol/water solution.

Copyright 2004 by Marcel Dekker, Inc. All Rights Reserved.

tert-butanol was present, thereby resulting in an approximately 10-fold reduction in drying time. This increased drying rate was caused by the formation of needle-shaped ice crystals which dramatically lowered the product resistance of the dried cake. The resulting surface area of the dried cake increased by approximately 13-fold when the 5% tert-butanol was used. The presence of the tert-butanol did not impact the collapse temperature, but the rapid sublimation prevented the product from reaching the collapse temperature. The rationale for this was postulated to be because the water content in the partially dried layer decreased faster in the presence of the tert-butanol, which resulted in an increased viscosity and thereby prevented collapse. The rate of sublimation of both the water and the tert-butanol was impacted by the ratio of the two solvents. Water appeared to sublime faster at ratios of less than 20% w/w tert-butanol/water. Tert-butanol appeared to sublime faster at ratios of greater than 20% w/w tert-butanol/water. Both solvents sublimed at equal rates at 20% w/w tert-butanol/water. The latter data suggested a strong association at this concentration. These data are consistent with the sublimation of water and tert-butanol from the frozen matrix of CAVERJECT Sterile Powder during freeze-drying as illustrated in Figure 6.

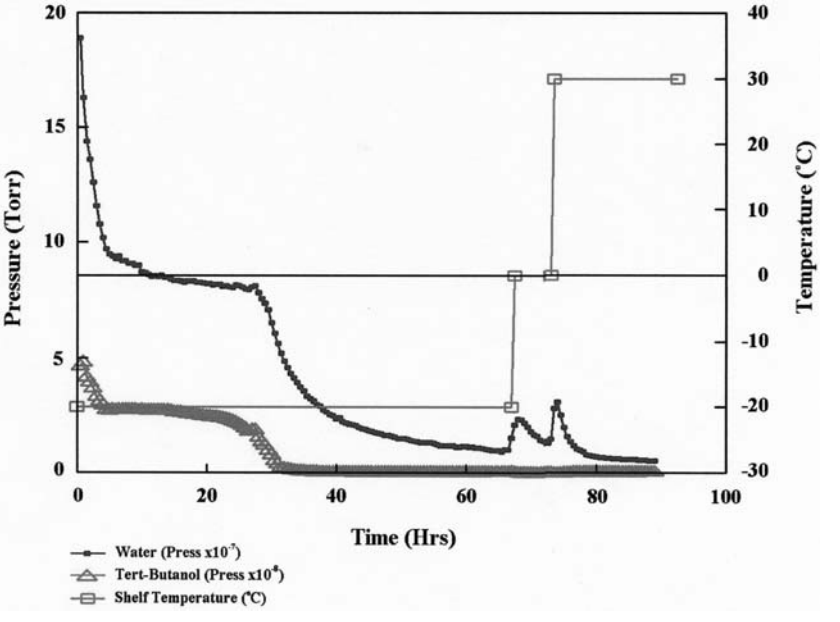

Figure 6 Sublimation data (via Turboquad mass spectrometer) for CAVERJECT Sterile Powder (freeze-dried from 20% v/v tert-butanol/water).

Copyright 2004 by Marcel Dekker, Inc. All Rights Reserved.

Mixtures of tert-butanol/water were also used to increase the rate of freeze-drying for solutions for a model drug, gentamicin sulfate [39]. Simple freeze-drying of the gentamicin with the co-solvent system was not sufficient to produce an acceptable cake. The investigators had to apply a statistical experimental design to achieve the final formulation. All components of the formulation studied, i.e., the active ingredient, tert-butanol/water ratio, and the amount of the maltose bulking agent, were optimized in order to achieve a reduction in drying time by approximately 40% and yet produce a freeze-dried cake of acceptable porosity. The addition of the maltose was a key component for this particular formulation and process. It should be readily apparent that optimization of the formulation and process parameters is necessary in order to maximize the impact of the co-solvent system on drying rates.

V. IMPACT ON STABILITY OF FREEZE-DRIED PRODUCT

A. Positive Impact on Stability

It is also noteworthy that the chemical stability of the freeze-dried product can be positively impacted by the type of solvent system from which it is lyophilized. The product, CAVERJECT Sterile Powder, is significantly more stable when it is freeze-dried from a 20% v/v tert-butanol/water co-solvent system compared to a simple aqueous solution. The reason for the improved stability appears to be related to the marked increase in dried cake surface area (approximately five-fold) which is produced when using this solvent system. Figure 7 illustrates that the degradation rate constant for this product is related to the reciprocal of the dried cake surface area. Since the degradation kinetics of the active ingredient, alprostadil, appear to fit an apparent second-order mechanism with respect to the alprostadil concentration (i.e., the rate of formation of the major degradation product, PGA_1, increases by the square of the alprostadil concentration), the improved chemical stability is consistent with a larger cake surface area which might increase the distance between the alprostadil molecules.

Another example of improved chemical stability for the lyophilized product includes the use of isopropyl alcohol in the freeze-drying of cefazolin sodium [19]. The presence of the isopropyl alcohol helped induce crystallization of the amorphous cefazolin sodium during the freezing phase. Use of the isopropyl alcohol with a thermal treatment phase enabled a freeze-dried crystalline form of the drug to be produced which possessed superior stability. Use of this co-solvent system also enabled the product to be more effectively processed with shorter

Copyright 2004 by Marcel Dekker, Inc. All Rights Reserved.

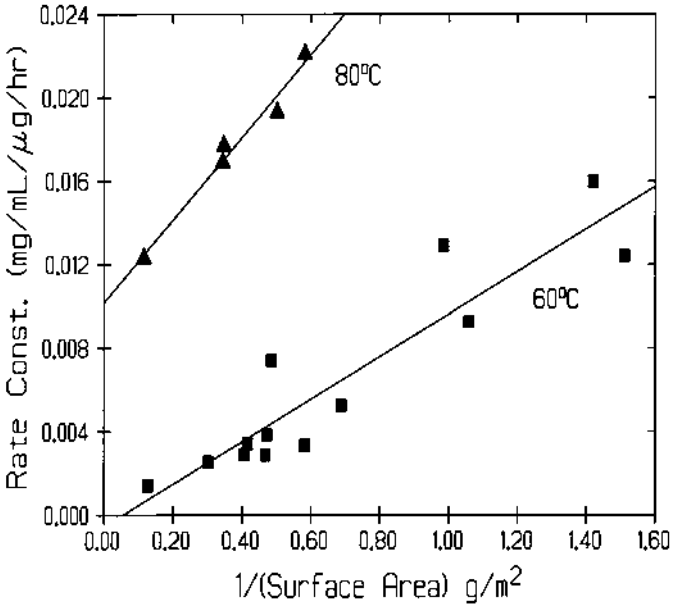

Figure 7 Impact of surface area of CAVERJECT Sterile Powder on degradation rate constant.

lyophilization times and fewer instances of cake collapse. Other short-chain alcohols, e.g., methanol, ethanol, and n-propanol, or acetone are also claimed to provide similar improvements to freeze-drying cefazolin sodium [40]. Freeze-drying of sucrose solutions with isopropanol has been shown to produce a cohesive cake which is more physically stable at higher temperatures [41]. Heating of the dried amorphous sucrose under the right conditions can induce the sucrose to become crystalline as the residual alcohol evaporates.

A very unique technique was employed in stabilizing tobramycin sulfate by use of freeze-drying from a 20% tert-butanol/water system [42]. Initially the product is freeze-dried using this co-solvent system. The resulting cakes contain amorphous tobramycin sulfate. However, prior to unloading the dryer, humidified nitrogen is pumped into the freeze-dry chamber. The increasing moisture level causes the glass transition temperature of the tobramycin sulfate to sufficiently decrease and allow crystallization to occur. This is followed by rapid release of the residual tert-butanol. The resulting product is an in situ crystallized form of tobramycin sulfate with very low level of residual tert-butanol (0.008%).

Copyright 2004 by Marcel Dekker, Inc. All Rights Reserved.

B. Negative Impact on Stability

Conversely, there are cases where the lyophilization from co-solvents can produce a less stable system. An example of this occurrence is illustrated by the lyophilization of the protein, bovine pancreatic trypsin inhibitor, from 1% water/dimethyl sulfoxide [43]. The data appear to support the premise that the protein-dissolving dimethyl sulfoxide denatures the protein sufficiently to reduce its enzymatic activity after reconstitution. Additionally, it is important to evaluate the impact of residual organic solvent remaining at the end of primary drying since the combination of the solvent and higher product temperatures during secondary drying may lead to undesirable chemical reactions [31].

VI. IMPACT ON RECONSTITUTION PROPERTIES

The ability of the freeze-dried cake to readily reconstitute upon addition of an appropriate pharmaceutical solvent is dependent on several factors. The structure of the dried product, the degree of cake collapse or melt-back that has occurred during drying, the surface area of the cake, the presence of hydrophobic coatings, and the homogeneity of the dry matrix are all factors which can influence the reconstitution properties of the dried product. Depending on the organic co-solvent selected and processing conditions used to freeze-dry, the product may or may not readily reconstitute. Therefore, one will need to evaluate this property on a case-by-case basis. However, there are examples of freeze-drying sucrose and lactose solutions from tert-butanol/water solutions with the proper drying cycle where amorphous cakes with large surface areas were produced [2,36]. These cakes tended to reconstitute extremely rapidly upon addition of the reconstitution vehicle. Proper freeze-drying of tobramycin sulfate from tert-butanol/water systems produced a friable easily reconstitutable cake; however, freeze-drying the same drug with less than 10% ethanol or isopropanol produced a hard and difficult to reconstitute cake [42].

It is also important to recognize the importance of extractables from the filling line and package system (i.e., the glass vial and rubber closure or the filter and tubing) used to filter, fill, and hold the solution being lyophilized. In particular the use of siliconized vials or stoppers can cause problems when organic co-solvents are used because the organic solvent can solubilize or extract silicone oil from the package component. This same problem can also occur if silicone tubing is used to transfer solution during filtration, filling, etc. The extracted silicone oil can impede the wetting of the affected portions of the cake, result in the cake being difficult to reconstitute,

Copyright 2004 by Marcel Dekker, Inc. All Rights Reserved.

cause the reconstituted solution to become hazy, or exceed the particulate matter and/or clarity specification limits. A high organic content also requires a judicious choice of sterilizing filters. Fortunately there is now a reasonable choice of high-quality solvent-resistant filters available. However, it is recommended that the filter manufacturer be consulted on their selection and that appropriate compatibility studies be performed.

VII. ENHANCEMENT OF STERILITY ASSURANCE

Since many freeze-dried products tend to be injectable formulations, they are required to be manufactured under sterile conditions. The growth promotive properties of the bulk solution prior to freeze-drying can impact the facilities and processes required to manufacture the sterile freeze-dried product (e.g., conventional aseptic manufacturing versus advanced aseptic manufacturing such as barrier-type suites). Many of the potential organic co-solvents proposed for lyophilization possess some form of microbicidal properties [44]. Ethanol and isopropanol at concentrations of greater than 20% exhibit excellent antimicrobial activity against both gram-positive and gram-negative bacteria, fungi, yeasts, and molds [45]. However, neat ethanol is less bactericidal than mixtures with water because the combination of alcohol plus water promotes the loss of cell proteins through a solvent-damaged cell membrane. Neat tert-butanol exhibits excellent bactericidal properties against *P. aeruginosa*, *E. coli*, *S. areus*, and *S. epidermidis*. There are also reports of several organic solvent-resistant organisms [46,47]. The presence of an organic solvent, therefore, does not guarantee that the bulk solution will have adequate microbicidal properties. Each formulation must be evaluated as to its growth promotive nature to determine the appropriate aseptic manufacturing requirements. If the solution is sterilized by filtration then the prefiltration bioburden must be evaluated and an appropriate holding time for the unfiltered solution qualified.

VIII. CONTROL OF RESIDUAL SOLVENT LEVELS

The retention of volatile components such as organic solvents during freeze-drying has been well described in the literature [48–57]. Many of the organic compounds in the food aroma have a vapor pressure higher than water. However, a significant number of these compounds remain with the freeze-dried cake after lyophilization. Two theories which are used to explain this phenomenon have been described as "selective diffusion" [57] and

Copyright 2004 by Marcel Dekker, Inc. All Rights Reserved.

Table 5 Retention of Volatiles in Freeze-Dried Model Systems[a] [54]

Organic volatile	Vapor Pressure of volatile at −22°F (mmHg)	Volatile retention in systems containing specified carbohydrate (g volatile per 100 g solid)		
		Maltose	Sucrose	Lactose
Acetone	11.0	2.01	2.30	1.83
Methyl acetate	9.40	2.29	2.51	2.20
Ethanol	1.10	1.76	—	—
n-propanol	0.26	2.41	—	—
Isopropanol	0.70	2.71	3.02	2.71
n-butanol	0.10	2.27	2.83	2.50
tert-butanol	0.44	3.10	3.28	3.15
1-pentanol	< 0.10	1.37	—	—

[a]All systems had the initial composition (% by weight): carbohydrate, 18.8; organic volatile, 0.75; water, 80.45.

"microregion entrapment" [54]. The retentive behavior for model amorphous carbohydrate systems which were freeze-dried from various volatile organic solvents is illustrated in Table 5. The retention levels were similar for volatiles of different vapor pressures. The "microregion entrapment" theory postulates that the retention is not due to adsorption of the dried material. The solvent retention appears to occur in localized regions where the volatile was initially frozen. These regions occur on a microscale. Increases in the secondary drying conditions of temperature or reduced pressure do little to decrease the volatile retention level. The volatile retention shows no competition with water vapor for sorption sites, which might be indicative of different modes of interaction with the amorphous carbohydrate. The previous statement appears to be true up to a point as long as the samples are kept dry. Upon humidification of the dried carbohydrate containing the entrapped volatile organic there appears to be a critical humidity condition which results in a corresponding moisture level where the volatile organic is rapidly released. An example of this effect is illustrated by the humidification of maltose which had been freeze-dried from either isopropanol/water or tert-butanol/water. Both exhibited a trend whereby, as the moisture content reached approximately 8–9%, the residual alcohol content dropped significantly [52]. Structural changes in the cake due to moisture absorption, especially during cake collapse, can result in rapid loss of the entrapped volatile. The volatile retention appears to be related to hydrogen bonding to the amorphous carbohydrates.

Copyright 2004 by Marcel Dekker, Inc. All Rights Reserved.

As the hydrogen bonds are broken, such as at certain moisture levels, the volatile loss accelerates. The "selective diffusion" model predicts that as the water content for carbohydrate systems decreases the ratio of the diffusion coefficient of the volatile organic to the diffusion coefficient of water decreases. This ratio becomes so small for low water/organic concentrations in dry amorphous carbohydrates that the system is only permeable to water [57,58].

The impact of formulation and process variables on residual solvent levels for formulations which were freeze-dried from tert-butanol/water co-solvent systems has been critically evaluated [59]. The physical state of solute (i.e., amorphous versus crystalline), the initial tert-butanol concentration, freezing rate, cake thickness, and temperature during secondary drying were examined. It was noted that when a crystalline matrix was used (e.g., glycine) the residual tert-butanol was very low (0.01–0.03%) regardless of freezing rate or initial tert-butanol concentration. Interestingly the residual tert-butanol data reported when a D-mannitol matrix was used were approximately 0.8% [10]. Although the authors claimed to have produced crystalline mannitol via annealing at −20°C it is possible that the thermal treatment was only annealing some unfrozen tert-butanol hydrate and that part of the mannitol remained uncrystallized. This may explain the higher than expected residual tert-butanol levels for a totally crystalline matrix. Considerably higher residual tert-butanol levels were noted when freeze-drying an amorphous sugar such as sucrose from tert-butanol/water systems. However, processing conditions had a profound impact on the residual solvent level present at the end of drying. Low levels of tert-butanol/water (1–2% w/w) resulted in high levels of tert-butanol residuals in the dried sucrose amorphous cake (≈10–18%). Higher levels of tert-butanol (3–5% w/w of an aqueous solution) resulted in lower residual tert-butanol levels in the dried amorphous cake (≈2%). Freeze-drying tobramycin sulfate from various levels of tert-butanol (5–9%) produced residual solvent levels ranging from 0.6 to 1.0% [42]. Similar results (1–2% residual levels) were obtained when freeze-drying lactose solutions from 20% v/v tert-butanol/water mixtures [2]. This latter matrix would also be expected to produce an amorphous cake. It was postulated that, when using tert-butanol levels above the threshold concentration required for eutectic crystallization of the solvent, lower residual tert-butanol levels in the freeze-dried cake are obtained. The reverse is true when the starting tert-butanol concentration is below this threshold. Freezing rate appeared to impact the residual tert-butanol level for amorphous systems in that fast freezing (e.g., with liquid nitrogen) produced cakes with higher residual tert-butanol. Examples of the latter observation were supported by the higher residual alcohol levels when flash freezing tert-butanol solutions of tobramycin

Copyright 2004 by Marcel Dekker, Inc. All Rights Reserved.

sulfate or sucrose [42,59] or liquid nitrogen freezing of aqueous solutions of n-butanol [56]. These data appeared to contradict the data reported for isopropanol retention in freeze-dried maltose or dextran [54] and other n-alcohols in malto-dextrin [57]. They also contradict data for residual tert-butanol retention in freeze-dried lactose. It would, therefore, appear that the impact of freezing rate on residual solvent content requires evaluation on a case-by-case basis. Increases in both time and temperature for the secondary drying phase did not significantly reduce the residual tert-butanol level in the freeze-dried sucrose cakes. Similar results for lactose dried from tert-butanol/water have been observed.

A. Thermal Treatment (Impact of Annealing)

It is noteworthy that the level of residual solvent remaining at the end of the freeze-dry cycle can be significantly impacted by use of thermal treatments (e.g., annealing) of the frozen solution prior to initiation of the drying phase. This effect is illustrated by studying the impact that process conditions had on the residual tert-butanol levels remaining in the CAVERJECT Sterile Powder. This product contains a predominantly lactose base and is lyophilized from a 20% v/v tert-butanol/water solution. Normal freezing by loading on precooled (i.e., -40°C) shelves followed by lyophilization produced a bimodal distribution of residual tert-butanol levels (Figure 8). The majority (94–97%) of a typical lot contained residual tert-butanol levels in the range of 1–2%. However, the remaining 3–6% of the lot contained tert-butanol levels ranging from 3.4 to 5.5%. A tighter control of the residual alcohol level was achieved for this product through the addition of a thermal treatment step (i.e., annealing) during the freezing phase in order to control metastable forms of solvents which might form. The DSC thermogram of the CAVERJECT frozen solution (unannealed and annealed) is illustrated in Figure 9. The annealing likely enabled any remaining unfrozen tert-butanol hydrate to crystallize and produce a more uniform frozen product. The effect of this thermal treatment on the residual tert-butanol was rather dramatic (Figure 8). The resulting tert-butanol levels were on average slightly lower (0.8–1.1%), much tighter, and no values exceeded 1.3%. A similar annealing technique was employed during the freezing phase for aplidine in a 40% v/v tert-butanol/water system and for tobramycin sulfate in a 5% tert-butanol/water system prior to lyophilization [10,42]. It is clear from the above discussion that the formulation scientist must evaluate the impact of the process conditions on the developing freeze-dried formulation in order to adequately control the residual volatile organic present at the end of freeze-drying.

Copyright 2004 by Marcel Dekker, Inc. All Rights Reserved.

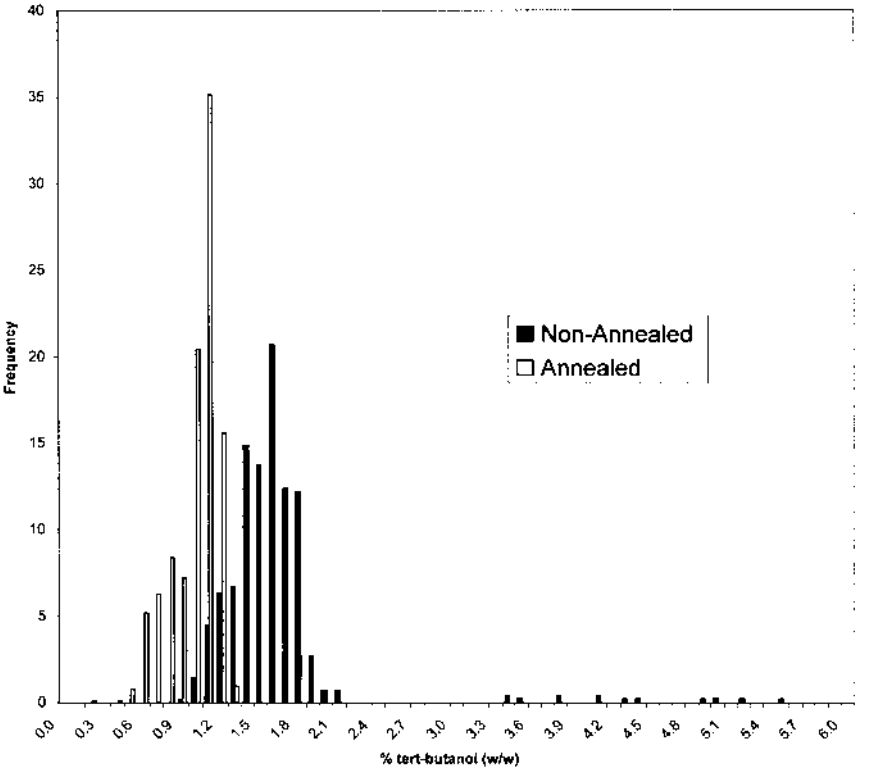

Figure 8 Residual tert-butanol levels in annealed versus non-annealed CAVERJECT Sterile Powder.

B. Purity of Solvent (Impact of Impurities, etc.)

A critical component in the selection of an organic co-solvent is the evaluation of the purity of the solvent which is intended for use. Since many of the organic solvent impurities may not freeze or sublime they can be retained in the freeze-dried cake. Typically they are either not removed or are only partially removed during the freeze-drying process. Therefore, it is possible that the impurities can become concentrated in the freeze-dried cake. Knowing the type and level of impurities in the selected organic solvent is critical to determining whether the grade or supplier is acceptable. A list of the significant organic impurities found in a lot of tert-butanol is summarized in Table 6. The organic impurities retained in a lactose cake prepared from freeze-drying from a 20% v/v tert-butanol/water co-solvent

Copyright 2004 by Marcel Dekker, Inc. All Rights Reserved.

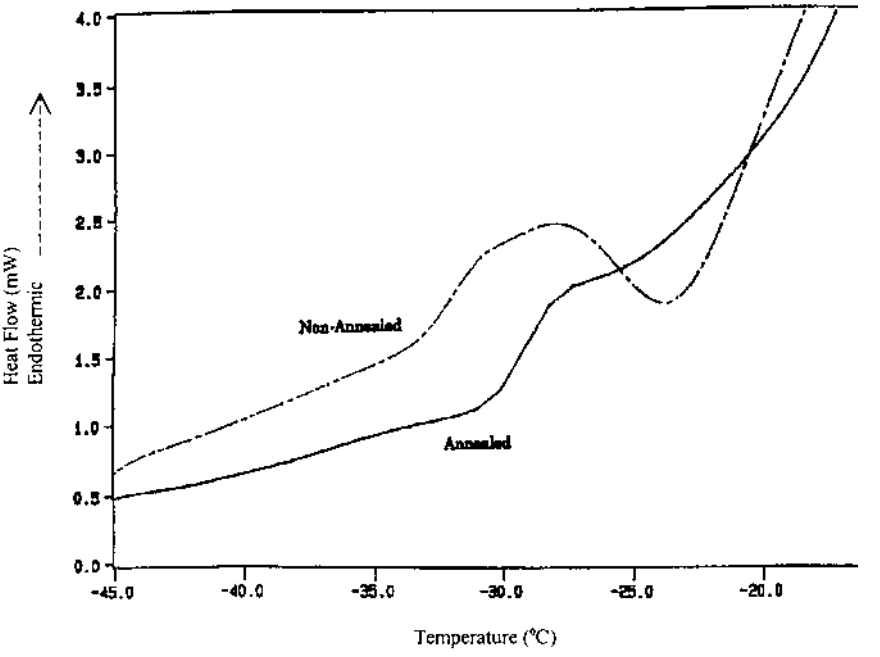

Figure 9 Differential scanning calorimetry thermograms for annealed versus non-annealed bulk solution used in CAVERJECT sterile powder.

Table 6 Organic Impurities Found in Tert-Butanol

Impurity	Concentrations (% w/w)
Methanol	0.02
Ethanol	0.01
Isopropanol	0.26
2-butanol	0.02
2-methyl-1-propanol	0.04
t-butyl peroxide	<0.01
t-butyl ether	0.01

system are summarized in Table 7. It is readily apparent that many of the organic impurities in the parent solvent are only partially removed via the lyophilization process. It is therefore critical that proper quality control specifications are established for the selected organic solvent.

Copyright 2004 by Marcel Dekker, Inc. All Rights Reserved.

Table 7 Residual Organic Impurities in Lactose Freeze-Dried from 20% v/v Tert-Butanol/Water

Impurity	Concentration (% w/w)
Tert-butanol	1.1–2.0
Ethanol	0.01
Isopropanol	0.12–0.24
2-butanol	0.01
2-methyl-1-propanol	0.03–0.04

Table 8 Potential Specification Assays for Organic Solvents Used in Freeze-Drying

Description
Identification
GC impurities
Non-volatile residue
Potency
Water
Specific gravity
Acidity
Alkalinity
Refractive index
Microcount
Pathogens

Table 8 contains a list of potential specification assays which one might use to determine raw material quality. Once specifications are established, each lot of organic solvent used for freeze-drying should be tested to confirm acceptable purity.

IX. ULTRA-LOW-TEMPERATURE FREEZE-DRYING

Rey [60] pioneered the use of ultra-low-temperature freeze-drying by evaluating solvents such as benzene and solid ammonia to lyophilize unstable compounds such as phospholipids. Ammonia is described as an exceptional solvent, based on its remarkable properties which are somewhat analogous to water. It is easily frozen by liquid nitrogen and can be lyophilized by sublimation between -130 and $-110^{\circ}C$. Liquid ammonia is

Copyright 2004 by Marcel Dekker, Inc. All Rights Reserved.

also a reaction medium which will allow the study of new chemical entities and include the storage of unstable and reactive elements containing free radicals. Liquid ammonia allows the lyophilization of tissues since it completely dissolves the glycerol used to coat and protect the tissue during freezing. Truly freeze-drying low-freezing solvents (i.e., those with freezing points ranging from -50 to $-120^{\circ}C$) would require very specialized freeze-dry equipment. A description of the specialized equipment required to achieve these ultra-low-temperature freeze-drying conditions has been provided by various authors [26,27]. Since these solvents, like water, will supercool prior to freezing, a shelf which can reach very low temperatures such as that achieved with liquid nitrogen would be required to enable the solvent to properly freeze. Additionally, external radiation would need to be controlled to achieve uniform drying [26]. Rey [60] also describes the use of liquid carbon dioxide to extract organic compounds. Subsequent lyophilization is achieved at low temperature ($-78.8^{\circ}C$) and atmospheric pressure. Solidification of the CO_2 is achieved either by using liquid nitrogen, or by releasing some of the CO_2 as gas, with subsequent cooling and freezing of the remaining CO_2. Carbon tetrachloride is also described as a good solvent for lipids, with the use of glycol distearate to modify its solubilizing characteristics. Other solvents used include dioxane and chloroform. Ultra-low-temperature freeze-drying was found to mimic that of aqueous systems such that with a suitable choice of the drying temperature and pressure, sublimation of the crystallized solvent resulted in preservation of the structure of the frozen interstitial phase [61]. Freeze-drying more complex systems was studied by depositing and freezing thin films of two immiscible solvent systems. Two sets of solvents were studied, water/dioxane and benzene/chloroform/carbon tetrachloride/cyclohexane. Freeze-drying was described as stepwise if the vapor of one of the solvents is eliminated preferentially and complex if the vapors of both solvents are eliminated together at comparative rates.

X. TOXICITY ISSUES

As discussed in the previous section, the volatile organic solvent component will be retained to a certain extent by the freeze-dried cake. The amount retained will be governed by the solvent used, the formulation which is lyophilized, and the processing conditions selected. Because most residual solvents offer no therapeutic benefit, they should be removed to low levels to meet product specifications, good manufacturing practices, and other quality-based requirements. A major concern which must be addressed is whether the residual solvent present is at an acceptable level

Copyright 2004 by Marcel Dekker, Inc. All Rights Reserved.

based on safety considerations. The acute toxicity (i.e., the LD_{50} for several species) for many of the potential solvents investigated as a freeze-dry solvent has been summarized previously [62]. These data, plus other toxicity data which reside in the literature, provide some level of assurance on the relative safety of the solvent. However, an additional resource to use to gauge the acceptability of a particular solvent and its acceptable residual level has been provided in the International Conference on Harmonization guidance document on impurities: residual solvents [63]. The guidance ranks various solvents into classes based on a safety risk assessment. Class 1 solvents should be avoided since they can be known carcinogens, possess a high toxicity potential, or pose an environmental hazard. An example of a Class 1 solvent investigated in freeze-drying is carbon tetrachloride [64]. Class 2 solvents are those solvents which cause reversible toxicity. They can also be non-genotoxic animal carcinogens or possible causative agents of other irreversible toxicity. Their content should be limited. Examples of Class 2 solvents found in pharmaceutical products are illustrated in Table 9 along with their permitted daily exposure and concentration limits. Several of the Class 2 solvents listed in Table 9 have been used in freeze-drying investigations. The residual content of all of these Class 2 solvents should be limited in pharmaceutical products because of their inherent toxicity. The allowable residual level should be less than the permitted daily exposure limit. Class 3 solvents exhibit low-toxicity potential to humans. Examples of Class 3 solvents found in pharmaceutical products are illustrated in Table 10. Several of these Class 3 solvents have been used in freeze-drying investigations. Permitted daily exposure limits of 50 mg/day or less would be acceptable for these solvents without additional justification. The most used organic solvent in freeze-drying, i.e., tert-butanol, is not listed in the guidance document. However, it is likely to fall in the category of a Class 3 solvent based on the similarity of acute LD_{50} toxicity data for other Class 3 solvents. It should be noted that the ICH guidance does not apply either to potential new drug substances, excipients, and drug products used during the clinical research stages of development, or to products marketed prior to July 1997. The guidance also notes that higher levels of residual solvent may be acceptable in cases such as short-term exposure (30 days or less). However, this would require justification on a case-by-case basis.

XI. HANDLING, SAFETY, AND STORAGE ISSUES

After an appropriate organic solvent has been selected for use in the freeze-drying process it is important to consider how the solvent can be

Copyright 2004 by Marcel Dekker, Inc. All Rights Reserved.

Table 9 Class 2 Solvents in Pharmaceutical Products

Solvent	Permitted daily exposure (mg/day)	Concentration limit (ppm)
Acetonitrile[a]	4.1	410
Chlorobenzene	3.6	360
Chloroform	0.6	60
Cyclohexane[a]	38.8	3880
1,2-dichloroethene	18.7	1870
Dichloromethane[a]	6.0	600
1,2-dimethoxyethane	1.0	100
N,N-dimethylacetamide	10.9	1090
N,N-dimethylformamide	8.8	880
1,4-dioxane	3.8	380
2-ethoxyethanol	1.6	160
Ethylene glycol	6.2	620
Formamide	2.2	220
Hexane	2.9	290
Methanol[a]	30.0	3000
2-methoxyethanol	0.5	50
Methylbutyl ketone	0.5	50
Methylcyclohexane	11.8	1180
N-methylpyrrolidone	48.4	4840
Nitromethane	0.5	50
Pyridine	2.0	200
Sulfolane	1.6	160
Tetralin	1.0	100
Toluene	8.9	890
1,1,2-trichloroethene	0.8	80
Xylene	21.7	2170

[a]Organic solvents evaluated in freeze-drying.

safely handled and properly stored. The package in which the solvent is received must be inert and not provide any additional extractables which may contaminate the freeze-dried product. Usually stainless steel or glass containers are preferred to minimize contaminants. Most of the organic solvents are highly flammable so proper care must be exercised when handling and storing to prevent fires or explosions. Manufacture of the bulk solution may need to take place in an explosion-proof manufacturing module. Use of electrical mixers should be avoided. Equipment should be appropriately grounded to make intrinsically

Copyright 2004 by Marcel Dekker, Inc. All Rights Reserved.

Table 10 Class 3 Solvents Which Should Be Limited by GMP or Other Quality-Based Requirements

Acetic acid[a]	Heptane
Acetone[a]	Isobutyl acetate
Anisole	Isopropyl acetate
1-butanol[a]	Methyl acetate[a]
2-butanol[a]	3-methyl-1-butanol
Butyl acetate	Methylethyl ketone[a]
Tert-butylmethyl ether	Methylisobutyl ketone[a]
Cumene	2-methyl-1-propanol
Dimethyl sulfoxide[a]	Pentane
Ethanol[a]	1-pentanol[a]
Ethyl acetate[a]	1-propanol[a]
Ethyl ether	2-propanol[a]
Ethyl formate	Propyl acetate
Formic acid	Tetrahydrofuran

[a]Organic solvents evaluated in freeze-drying.

safe where possible. Transport of the manufactured solution should occur in sealed tanks (preferably stainless steel vessels). Use of a nitrogen blanket above the solution headspace is recommended as an additional safety feature. The tanks must have a pressure relief valve and there must be a shut-off valve on the tank to turn off liquid flow should there be an emergency. If pressure filtration is employed, nitrogen as opposed to air should be used. Hard piping of the transfers is recommended as opposed to use of flexible tubing. Appropriate care must occur during the filling and loading of the freeze-dryer. Distance of electrical equipment used during the filling operation from the manufacturing tank must comply with appropriate national electrical and fire safety codes for flammable materials. Local ventilation should be used near vessel connection points to prevent vapor buildup should a leak occur. The vacuum sensors for the freeze-dryer that are hot-wire resistance variety (thermal conductivity-type gauge, Pirani, etc.) should be replaced with capacitance manometer-type diaphragm gauges to minimize the hazards associated with these volatile organics [31]. It may even be necessary to work in explosion-proof environments or at least to explosion-proof the electric motors on the vacuum pumps. Depending on the type of organic solvent used it may be necessary to add a liquid nitrogen cold trap in front of the vacuum pumps if the condensers are not cold enough to remove the migrating vapors. The freeze-drying of ethanol containing products has been such that it is sufficient to install a tube which is in thermal contact

Copyright 2004 by Marcel Dekker, Inc. All Rights Reserved.

with the condenser coils and which can be drained at the end of drying [25]. One must be aware that contamination of the vacuum pump oil with organic solvents may decrease pump efficiency and lead to the inability to adequately control the vacuum in the drying chamber. The proper disposal of the solvent and its environment impact must be appropriately assessed.

The most commonly used organic solvent in freeze-drying, tert-butanol, presents an additional unusual handling requirement. This solvent freezes close to room temperature with the pure solvent creating a negative volume change on freezing. The pure material may be completely liquid, a solid, or a mixture of both at room temperature. In order to use this solvent any solid material must be liquified by warming, taking care to not break the container as the solution expands. The total container should be mixed after warming to produce a uniform solution since the unfrozen impurities typically tend to concentrate in the liquid portion because they possess lower freezing points. This solvent is flammable so caution must be used to warm it.

However, an alternative method to use this key freeze-drying solvent is to have the supplier provide the tert-butanol as a slightly diluted mixture with water (e.g., 95% v/v tert-butanol/water). The appropriate quality of water (e.g., water for injection) should be selected to make the dilution if the solvent mixture is destined for use in the manufacture of an injectable product. This addition of water lowers the freezing point from room temperature to approximately 2°C. This mixture is much easier to handle because it remains liquid at room temperature. The tert-butanol is commonly used as a mixture with water anyway during freeze-drying so the additional water will not have any negative impact on the drying process.

XII. SUPPLIER SELECTION AND QUALIFICATION

As discussed previously, the purity of the organic co-solvent must be closely monitored since the freeze-drying process may not remove unwanted impurities which can be retained in the freeze-dried cake. It is wise to select a supplier which has a drug master file established for the manufacture, packaging, and storage of GMP-grade organic solvent. If a drug master file is not available the supplier needs to work to establish one. It is recommended to audit the supplier to confirm that appropriate documentation of the production process is in place to satisfy GMP requirements. This would especially include verification of cleaning validation and records to ensure that manufacturing equipment, packages used, transport tankers, etc., do not add unwanted contaminants. A sufficient number of lots should be evaluated

Copyright 2004 by Marcel Dekker, Inc. All Rights Reserved.

to confirm that the quality will consistently meet targeted specifications and enable the manufacture of reproducible freeze-dried product lots.

XIII. COST

All factors impacting the cost of goods need to be assessed before one should choose to use organic solvents in freeze-drying. Those parameters such as potentially increased drying rates, increased solution stability, ease of drug wetting, increased product stability, etc., can have a positive influence in reducing manufacturing costs. However, there are numerous factors which can add significantly to the cost. First, there are several one-time development costs which must be factored into the expense estimates. Typically a new solvent supplier may need to be located, qualified, and materials tested/evaluated. Additional safety studies may need to be completed to satisfy potential regulatory concerns of residual solvents in the product. The manufacturing facilities may require modification to handle the storage and use of flammable solvents in a safe manner. The continual fixed cost of high-purity GMP-grade solvents must be evaluated. It is not unusual for the GMP-grade solvent expense to exceed 10–20 times the cost of the same corresponding analytical-grade solvent. The cost of disposal of the used solvent and its environmental impact must also be taken into consideration. The positive and negative influences of the use of organic co-solvents on the cost to manufacture product must be weighed together to determine the overall cost acceptability.

XIV. REGULATORY CONCERNS

The majority of the pharmaceutical regulatory agencies throughout the world have limited experience with the review or approval of freeze-dry processes using organic co-solvents. Therefore, increased scrutiny of the regulatory file should be expected. However, there has been some recent precedence with the worldwide regulatory approval of CAVERJECT Sterile Powder. Additionally, since it is quite common for most active pharmaceutical ingredients and some excipients to be precipitated and/or dried from organic solvents, the same type of safety evaluation and/or justification for the residual organic solvent levels should be employed. It is important to demonstrate that the product has been carefully evaluated for all possible residual solvents since it is quite possible that impurities in the starting solvent can concentrate during the drying process. Appropriate qualification of the solvent vendor (ideally with a drug master file), the solvent storage

Copyright 2004 by Marcel Dekker, Inc. All Rights Reserved.

package, and conditions would appear a prudent course. This is especially critical when using non-compendia grades of solvents. The ICH guidelines on residual solvents discussed earlier should be used to justify the proposed specification limits.

XV. CONCLUSIONS

Non-aqueous co-solvent systems have been used in the freeze-drying of pharmaceutical and biological products, preparation of biological specimens, or preparative isolation of excipients. The reasons for freeze-drying from these non-aqueous solvent systems for pharmaceutical products include: increased drug wetting or solubility, increased sublimation rates and hence decreased drying time, increased pre-dried bulk solution or dried product stability, decreased reconstitution time, potential alternatives to powder filling, and possible enhancement of sterility assurance of the pre-dried bulk solution. However, the practicalities of use of these co-solvent systems must be properly assessed before they should be considered for use. This especially applies when using them in the manufacture of a pharmaceutical or biological product. The issues which must be evaluated include: the proper safe handling and storage of flammable and/or explosive solvents, the special facilities or equipment which may be required, the determination and control of residual solvent levels, the toxicity of the remaining solvent, qualification of an appropriate GMP purity and supplier, the overall cost benefit to use of the solvent, a possible adverse environmental impact, and the potential increased regulatory scrutiny when used in pharmaceutical or biological products.

The co-solvent system that has been most extensively evaluated was the tert-butanol/water combination. The tert-butanol possesses a high vapor pressure, freezes completely in most commercial freeze-dryers, readily sublimes during primary drying, can increase sublimation rates, and has low toxicity. This co-solvent system is being used in the manufacture of a marketed injectable pharmaceutical product. When using this solvent system, both formulation and process control required optimization to maximize drying rates and to minimize residual solvent levels at the end of drying.

Other co-solvent systems which do not freeze completely in commercial freeze-dryers were more difficult to use, do not sublime but rather boil during the evacuation process, often resulted in unacceptable freeze-dried cakes, and may bypass condensers and contaminate vacuum pumps. Their use appears limited. Many of these types of solvents were near impossible to dry when levels used exceed 10%.

Copyright 2004 by Marcel Dekker, Inc. All Rights Reserved.

REFERENCES

1. L Rey. Potential prospects in freeze-drying. In: L Rey, JC May, eds. Freeze-drying/lyophilization of Pharmaceuticals and Biological Products. New York: Marcel Dekker, 1999, pp 470–471.
2. DL Teagarden, WJ Petre, PM Gold. Stabilized prostaglandin E_1. United States Patnent 5,741,523, April 21, 1998.
3. DL Teagarden, WJ Petre, PM Gold. Method for preparing stabilized prostaglandin E_1. United States Patent 5,770,230, June 23, 1998.
4. T Inoue, H Osatake. A new drying method of biological specimens for scanning electron microscopy: the t-butyl alcohol freeze-drying method. Arch Histol Cytol 51:53–59, 1998.
5. H Akahori, H Ishii, I Nonaka, H Yoshida. A simple freeze-drying device using tert-butyl alcohol for SEM (scanning electron microscopy) specimens. J Electron Microsc 37(6):351–352, 1988.
6. T Hojo. Specimen preparation of the human cerebellar cortex for scanning electron microscopy using a t-butyl alcohol freeze-drying device. Scanning Microsc, Suppl 10 (Science of Biological Specimen Preparation for Microscopy):345–348, 1996.
7. R Herman, M Müller. Limits in high-resolution scanning electron microscopy: natural surfaces? Scanning 19:337–342, 1997.
8. Norman S Radin. The preparative isolation of lecithin. J Lipid Res 19(7): 922–924, 1978.
9. EJ Benjamin, GC Visor. Cardiotonic phosphodiesterase inhibitors complexed with water soluble vitamins. United States Patent 4,837,239, June 6, 1989.
10. B Nuijen, M Bouma, REC Henrar, P Floriano, JM Jimeno, H Talsma, JJ Kettenes-van den Bosch, AJR Heck, A Bult, JH Beijnen. Pharmaceutical development of a parenteral lyophilized formulation of the novel antitumor agent aplidine. PDA J Pharm Sci Technol 54(3):193–208, 2000.
11. DW Flamberg, DL Francis, SL Morgan, GF Wickes. Low temperature vacuum drying of sterile parenterals from ethanol. Bull Parent Drug Assoc. 24(5):209–216, 1970.
12. DC Monkhouse. Tertiary alcohol stabilized E-series prostaglandins. United States Patent 3,927,197, December, 16, 1975.
13. DS Baker. Unpublished results.
14. H Seager, CB Taskis, M Syrop, TJ Lee. Freeze drying parenterals containing organic solvent – Part 1. Manuf Chem Aerosol News 49(11):43–44, 47–48, 1978.
15. H Seager. Freeze drying parenterals containing organic solvent – Part 2. Manuf Chem Aerosol News 49(12):59–60, 64, 1978.
16. H Seager. Freeze drying parenterals containing organic solvent – Part 3. Manuf Chem Aerosol News 50(1):40, 42–45, 1979.
17. H Seager. Freeze drying parenterals containing organic solvent – Part 4. Manuf Chem Aerosol News 50(2):41–42, 44–45, 48, 1979.

Copyright 2004 by Marcel Dekker, Inc. All Rights Reserved.

18. H Seager, CB Taskis, M Syrop, TJ Lee. Structure of products prepared by freeze-drying solutions containing organic solvents. J Parenter Sci Technol 39(4):161–179, 1985.
19. Y Koyama, M Kamat, RJ De Angelis, R Srinivasan, PP DeLuca. Effect of solvent addition and thermal treatment on freeze drying of cefazolin sodium. J Parenter Sci Technol 42(2):47–52, 1988.
20. K Hasegawa, K Hashi, R Okada. Physiochemical stability of pharmaceutical phosphate buffer solutions I – complexation behaviour of Ca(II) with additives in phosphate buffer solutions. J Parenter Sci Technol 36:128–133, 1982.
21. K Hasegawa, K Hashi, R Okada. Physiochemical stability of pharmaceutical phosphate buffer solutions II – complexation behaviour of Al(III) with additives in phosphate buffer solutions. J Parenter Sci Technol 36:168–173, 1982.
22. K Hasegawa, K Hashi, R Okada. Physiochemical stability of pharmaceutical phosphate buffer solutions IV – prevention of precipitation in parenteral phosphate buffer solutions. J Parenter Sci Technol 36:210–215, 1982.
23. K Hasegawa, K Hashi, R Okada. Physiochemical stability of pharmaceutical phosphate buffer solutions V – precipitation behaviour in phosphate buffer solution. J Parenter Sci Technol 37:38–45, 1983.
24. J Hallet. Nucleation and growth of ice crystals. In: L Rey, ed. Advances in Freeze-drying Lyophilisation. Paris: Hermann, 1966, p 33.
25. H Willemer, Experimental freeze-drying. In: L Rey, JC May, eds. Freeze-drying/lyophilization of Pharmaceuticals and Biological Products. NewYork: Marcel Dekker, 1999, pp 79–119.
26. H Willemer. Low temperature freeze drying of aqueous and non-aqueous solutions using liquid nitrogen. In: SA Goldblith, L Rey, WW Rothmayr, eds. Freeze Drying and Advance Food Technology. New York: Academic Press, 1975, pp 461–477.
27. L Rey. Orientations nouvelles de la lyophilisation. In: L Rey, ed. Research and Development in Freeze-Drying. Paris: Hermann, 1964, pp 630–643.
28. K Kasraian, PP DeLuca. Thermal analysis of the tertiary butyl alcohol-water system and its implications on freeze-drying. Pharm Res 12(4):484–490, 1995.
29. JB Ott, JR Goates, BA Waite. (Solid + liquid) phase equilibria and solid-hydrate formation in water + methyl, + ethyl, + isopropyl, + tertiary butyl alcohols. J Chem Thermodyn 11:739–746, 1979.
30. M Woznyj, HD Lüdemann. The pressure dependence of the phase diagram t-butanol/water. Z Naturforsch 40a:693–698, 1985.
31. K Murgatroyd. The freeze drying process. In: P Cameron, ed. Good Pharmaceutical Freeze-Drying Practice. Buffalo Grove, IL: Interpharm Press, 1997, pp 55–57.
32. MS Tesconi, K Sepassi, SH Yalkowsky. Freeze-drying above room temperature. J Pharm Sci 88(5):501–506, 1999.
33. M Pikal. Freeze-drying of proteins. Part I: Process design. Biopharm. 3 (September):18–27, 1990.

Copyright 2004 by Marcel Dekker, Inc. All Rights Reserved.

34. SL Nail, LA Gatlin. Freeze-drying: principles and practice. In: KE Avis, HA Lieberman, L Lachman, eds. Pharmaceutical Dosage Forms: Parenteral Medications Volume 2. New York: Marcel Dekker, 1993, pp 163–233.
35. S Wittaya-areekul. Freeze-drying from nonaqueous solutions. Mahidol Uni J Pharm Sci 26(1–4):33–43, 1999.
36. PP DeLuca, MS Kamat, Y Koida. Acceleration of freeze-drying cycles of aqueous solutions of lactose and sucrose with tertiary butyl alcohol. Congr Int Technol Pharm, 5th 1:439–447, 1989.
37. K Kasraian. The utilization of tertiary butyl alcohol (TBA) as a mass transfer accelarator in lyophilization. Diss Abstr Int B 54(7):3570, 1994.
38. K Kasraian, PP DeLuca. Effect of tert-butyl alcohol on the resistance of the dry product layer during primary drying. Pharm Res 12(4):491–495, 1995.
39. G Baldi, M Gasco, F Pattarino. Statistical procedures for optimizing the freeze-drying of a model drug in tert-butyl alcohol-water mixtures. Eur J Pharm Biopharm 40(3):138–141, 1994.
40. MD Cise, ML Roy. Improvements in or relating to freeze-drying cephalothin sodium. British Patent 1,589,317, May 13, 1981.
41. MPWM te Booy, RA de Ruiter, ALJ de Meere. Evaluation of the physical stability of freeze-dried sucrose-containing formulations by differential scanning calorimetry. Pharm Res 9(1):109–114, 1992.
42. G Needham. Formulation and processing factor affecting residual solvent levels in TBA/water formulations. Freeze-Drying of Pharmaceuticals and Biologicals, Breckenridge, CO, August 1–4, 2001.
43. UR Desai, AM Klibanov. Assessing the structural integrity of lyophilized protein in organic solvents. J Am Chem Soc 117(14):3940–3945, 1995.
44. WP Olsen. Volatile solvents for drying and microbial kill in the final container – a proposal and a review, with emphasis on t-butanol. Pharm Eng July/August:112–117, 1997.
45. KH Wallhausser. Appendix B. Antimicrobial preservation used by the cosmetic industry. In: JJ Kabara, ed. Cosmetic and Drug Preservation. New York: Marcel Dekker, 1984, pp 605–745.
46. A Inoue, K Horikoshi. A Pseudomonas thrives in high concentrations of toluene. Nature 338:264–266, 1989.
47. A Pinazo, L Puigjamer, L Coderch, M Vinas. Butanol resistant mutants of Clostridium acetylbutylicum: isolation and partial characterization. Microbios 73:93–104, 1993.
48. JM Flink. Loss of organic volatiles in freeze-dried carbohydrate solutions. Ph.D. thesis, Massachuetts Institute of Technology, 1970.
49. J Flink, F Gejl-Hansen. Retention of organic volatiles in freeze-dried carbohydrate solutions: macroscopic observations. J Agr Food Chem 20(3): 691–694, 1972.
50. JM Flink, M Karel. Retention of organic volatiles in freeze-dried solutions of carbohydrates. J Agr Food Chem 18(2):295–297, 1970.
51. JM Flink, M Karel. Effects of process variables on retention of volatiles in freeze-drying. J Food Sci 35:444–447, 1970.

Copyright 2004 by Marcel Dekker, Inc. All Rights Reserved.

52. JM Flink, M Karel. Mechanisms of retention of organic volatiles in freeze-dried systems. J Food Technol 7:199–211, 1972.
53. JM Flink, TP Labuza. Retention of 2-propanol at low concentrations by freeze-drying carbohydrate solutions. J Food Sci 37:617–618, 1972.
54. JM Flink. The retention of volatile components during freeze-drying: a structurally based mechanism. In: SA Goldblith, L Rey, WW Rothmayr, eds. Freeze Drying and Advance Food Technology. New York: Academic Press, 1975, pp 351–372.
55. D Lambert, J Flink, M Karel. Volatile transport in frozen aqueous solutions I: development of a mechanism. Cryobiology 10:41–45, 1973.
56. D Lambert, J Flink, M Karel. Volatile transport in frozen aqueous solutions II: influence of system parameters. Cryobiology 10:52–55, 1973.
57. HAC Thijssen. Effect of process conditions in freeze drying retention of volatile components. In: SA Goldblith, L Rey, WW Rothmayr, eds. Freeze Drying and Advance Food Technology. New York: Academic Press, 1975, pp 373–400.
58. WH Rulkens, HAC Thijssen. Retention of volatile compounds in freeze-drying slabs of malto-dextrin. J Food Technol 7(1):79–93, 1972.
59. S Wittaya-areekul, SL Nail. Freeze-drying of tert-butyl alcohol/water cosolvent systems: effects of formulations and process variables on residual solvents. J Pharm Sci 87(4):491–495, 1998.
60. L Rey, Un dévelopment nouveau de la lyophilisation: la cryodessication des systèmes non-aqueux. EXPERIENTIA 21:241–246, 1965.
61. L Rey, F Chauffard, M Dousset. Les lyophilisations complexes. In: L Rey, ed. Advances in Freeze Drying Lyophilisation Recherches et Applications Nouvelles. Paris: Hermann, 1996, pp 89–94.
62. DL Teagarden, DS Baker. Practical aspects of lyophilization using non-aqueous co-solvent systems. Eur J Pharm Sci 15:115–133, 2002.
63. WK Hubbard. International Conference on Harmonization; guidance on impurities: residual solvents. Federal Register 62(247):67377–67388, December 24, 1997.
64. PP DeLuca, M Kanke, T Sato, HG Schroeder. Porous microspheres for drug delivery and methods for make same. United States Patent 4,818,542, April 4, 1989.
65. JR Tica Grau, A Del Pozo Carrascosa, R Salazar Macian, S Alonso Ciriza. Determinacion de disolventes residuals en materias primas farmaceuticas: aplicacion en amoxicilinas sodicas liofilzadas. Cienc Ind Farm 7(11):325–330, 1988.
66. N Tanno, N Ae, K Ishizumi. Freeze-dried pharmaceuticals of fat-soluble platinum(II) complexes. Japanese Patent 03255025, March 2, 1990.
67. Y Zou, W Priebe, R Perez-soler. Submicron liposome suspensions obtained from preliposome lyophilizates. United States Patent 5,902,604, May 11, 1999.
68. S Kamijo, A Imai, H Kodaira. Preparation of crystalline lyophilized gabexate mesilate with high stability. Japanese Patent 63270623, April 30, 1987.

Copyright 2004 by Marcel Dekker, Inc. All Rights Reserved.

69. S Kaneko, M Kishikawa, T Sato, K Maeda. Manufacture of freeze-dried anthracycline glycoside preparations with improved solubility. Japanese Patent 07076515, June 30, 1993.
70. BW Sullivan, PJ Marangos. Partially lyophilized fructose-1,6-diphosphate (FDP) for injection into humans. United States Patent 5,731,291, March 24, 1998.
71. P Meredith, AM Donald, RS Payne. Freeze-drying: in situ observations using cryoenvironmental scanning electron microscopy and differential scanning calorimetry. J Pharm Sci 85:631–637, 1996.
72. PL Felgner, DA Eppstein. Stable liposomes with aqueous-soluble medicaments. European Patent 0172007B1, May 22, 1991.
73. FHJ Jansen. Process to prepare pharmaceutical compositions containing vecuronium bromide. United States Patent 5,681,573, October 28, 1997.

Copyright 2004 by Marcel Dekker, Inc. All Rights Reserved.

9
Closure and Container Considerations in Lyophilization

Frances L. DeGrazio
West Pharmaceutical Services, Inc., Lionville, Pennsylvania, U.S.A.

I. INTRODUCTION

Lyophilization as a parenteral process began in the early twentieth century as a way to prepare pharmaceutical products that are unstable in liquid form. In the 1980s and with the birth of biopharmaceutical development, the need to store products that were not stable in a liquid format increased. The process of freeze-drying these types of products became much more common. Currently there are more than 100 lyophilized products in the market in the United States alone.

Although over the years there was much development on understanding the equipment and the processes used for lyophilization, one critical factor leading to a successful final drug product was minimally investigated. This factor is the container/closure system that holds the drug product and aids in the effectiveness of the final freeze-drying process.

With the advent of biopharmaceutical products, selection of container/closure systems has become even more critical. Frequently lyophilized products are more sensitive compared with traditionally derived pharmaceutical products. For instance, protein and peptide-based products may have a greater tendency to adsorb to the surface of their container/closure system. Additionally, these products are typically smaller in final cake weight; therefore, they are much more sensitive to moisture. In any case, the performance of the lyophilization process and the quality of the final product can be directly related to the container/closure system.

Copyright 2004 by Marcel Dekker, Inc. All Rights Reserved.

II. OVERVIEW

The container/closure system, which consists of the elastomeric stopper and the glass vial, impacts the effectiveness of the lyophilization process in two fundamental ways:

1. Resistance to heat transfer
2. Reduction in throughput

The container/closure system can impact final product quality and pharmaceutical elegance in a number of ways:

1. General Chemical Compatibility
2. Extractables/leachables
3. Moisture ingress
4. Surface adsorption
5. Silicone contamination
6. Seal integrity
7. Functionality in the field

III. PROCESS EFFECTS

A. Resistance to Heat Transfer [1]

The limiting factors relating to heat transfer are the contact between the product and the chamber shelf and their thermal conductivity. The limit to the heat transfer is principally due to the lack of intimate contact between the product and the shelf and, to a lesser degree, to the lower thermal conductivity of the container and the frozen product. These resistances need to be compensated for in the process of getting heat to the sublimation front. The greatest impact upon the level of quality for batch uniformity is the efficiency and the effectiveness of the heat transfer system; therefore, the container is a critical component of the entire heat transfer system in the lyophilization chamber.

B. Reduction in Throughput

The volume of production over a period of time is defined as throughput. Throughput can be affected by problems with the container/closure system such as vial breakage, incomplete stoppering, extended drying times for closures, or poor sublimation rate due to a poor package design.

Copyright 2004 by Marcel Dekker, Inc. All Rights Reserved.

In choosing an appropriate container/closure system, it is important to address all of these considerations, in addition to issues such as chemical compatibility and stability.

If all of these needs are identified early in the process of choosing a primary package for lyophilization, a container/closure system that is optimal for all critical factors will need to be investigated for development.

IV. VIAL CONSIDERATIONS FOR LYOPHILIZATION [1]

The process of lyophilization is affected by the vial's dimensions, physical characteristics, chemical properties, and interactions with both the drug product contained and the chamber shelf on which the vial rests. The text that follows will detail various key characteristics that can be either an advantage or disadvantage to the lyophilization process.

A. Physical Properties of Vials

In the pharmaceutical and biotechnology industries, Type I tubing vials are typically used for the primary container for lyophilized drugs. One of the key reasons tubing vials are used over molded vials is dimensional tolerance consistency. The capability of tubing vials to meet tight dimensional tolerance is superior to molded vials. Because of mold-to-mold variations that occur in the manufacture of the vials, wall weight, outside diameter, and bottom thickness may vary. The lower the coefficient of expansion for a glass type, the better it is for use in the lyophilization process. Because of these reasons, the discussion below will focus on tubing vials.

B. Bottom Thickness

The bottom thickness of a tubing vial is not normally the same as the wall thickness, because of the characteristics in the manufacturing process. As a general rule, the bottom thickness is 55 to 65% of the wall thickness. For example, in a tubing vial with a standard wall of 1.20 mm, the minimum bottom thickness would be in the range of 0.66 to 0.78 mm. The uniformity of glass distribution in the bottom is also important to prevent or minimize vial bottom breakage. If the bottom thickness is too thin, ''ring-out,'' or bottom breakage, becomes a problem and lyophilization chamber throughput can be greatly reduced. Conversely, if the bottom becomes too thick, the lyophilization process is affected by an increase in the resistance to heat transfer, again impacting chamber throughput.

Copyright 2004 by Marcel Dekker, Inc. All Rights Reserved.

C. Bottom Flatness or Concavity

The relative flatness of the bottom of a tubing vial is essential to limiting the resistance to heat transfer. The greater the concavity of the bottom, the further away the product in the tubing vial is from the shelf, which is the source of the energy for the lyophilization process (Figure 1). Excessive concavity also allows more air underneath the tubing vial, adding insulation and further increasing resistance to the heat transfer from the shelf to the product. In both tubing and molded vials, bottoms that have a very concave structure can create angles where the wall and bottom meet that can act as stress points, potentially causing the bottom of the vial to break away from the sides, as well as creating cracks in the wall. Chamber throughput can be severely lessened as a result.

D. Bottom Inside Radius

This dimension is controlled by the formation of vial bottoms with a minimum of concavity. The greater the concavity, the sharper the angle

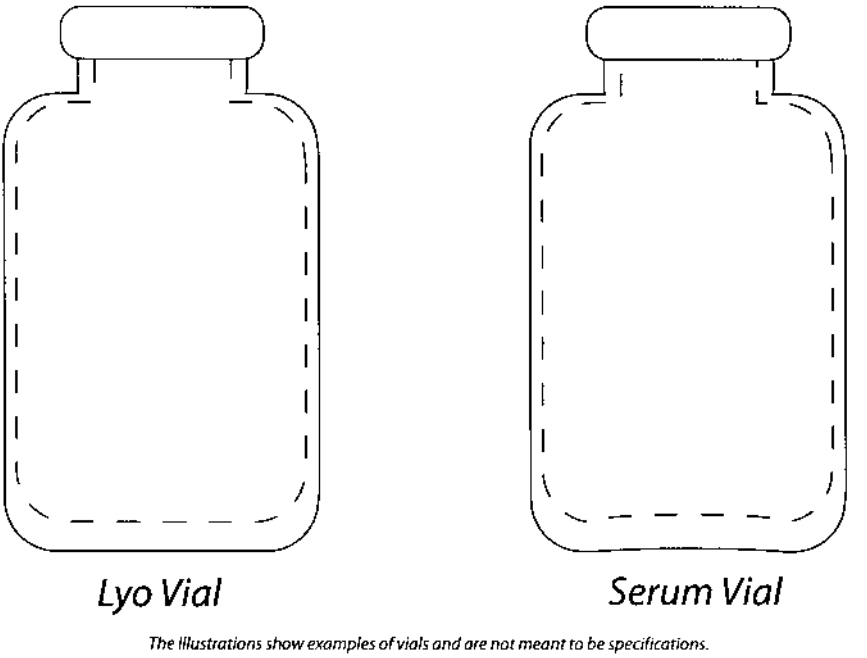

Figure 1 Flat bottom vial vs. concave bottom vial.

Copyright 2004 by Marcel Dekker, Inc. All Rights Reserved.

inside. If this angle is too sharp, the resulting radius may become a stress point. As a result, when the product is frozen, the ice crystals will expand into the area available, pushing on the bottom inside radii. This force will create a weakness that can lead to "lens-out" of the bottom of the vial.

E. Bottom Outside Radius

This angle is critical for maximizing the surface area of the tubing vial on the lyophilization chamber shelf. It is also necessary for the elimination of stress points on the outside radius where the vial contacts the chamber shelf. While independent of the inside radius, the effects of a sharp outside radius are essentially the same. It is important to have the optimal radii that will lead to minimization of stress in the glass, yet lead to a reduction in the resistance to heat transfer. The optimal rounded diameter will help to absorb and alleviate the stress build-up that occurs during the lyophilization cycle.

F. Amount of Fill in the Container

The amount of internal pressure generated during the lyophilization cycle is directly related to the amount of fill in the vial. Fill level of product up to a maximum of 35% of the vial's capacity are generally recommended as these proportions seem to create the fewest processing problems.

V. LEACHING AND DISSOLUTION OF GLASS

Several studies of glass vials have identified the potential of the glass to react in different ways with liquid products stored in the vials over time. A dissolution or a leaching reaction between the liquid and the glass is very probable and is dependent on various specifics of the drug product and its processing in the vial. For instance, basic or high pH products can lead to dissolution of the glass surface.

The lyophilization process minimizes the potential for interactions between the glass and the drug product. In some circumstances, a pharmaceutical manufacturer may decide that lyophilization is the best alternative for extended product shelf-life because a compatible glass container for the liquid product cannot be found. An example of this may be a strongly alkaline solution. For this reason, this chapter will briefly explain the concepts of leaching and dissolution as they relate to the glass vial; there will be more focus on the potential of the rubber closures to have extractables that may leach into the lyophilized drug product since this process is more likely to occur.

Copyright 2004 by Marcel Dekker, Inc. All Rights Reserved.

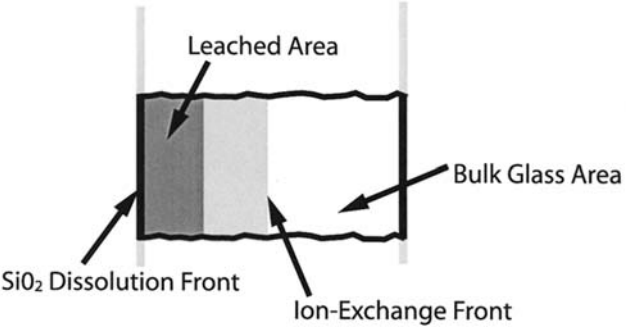

Figure 2 Schematic illustration of the leaching process.

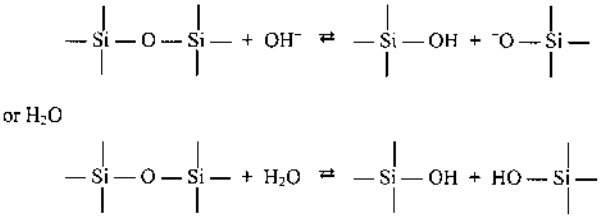

Figure 3 Dissolution schematic.

Glass leaching is a selective process. It is primarily an ion exchange process for glass modifiers such as Li^+, Na^+, K^+, Mg^{++}, Ca^{++}, and Mg^{+++}[2,3]:

$$Na^+(\text{glass}) + H^+(\text{solution}) \rightarrow H^+(\text{glass}) + Na^+(\text{solution})$$

A schematic view of the general glass leaching process is given in Figure 2. There is an exchange of the metal ions with the hydrogen ions from water. This is typical of an acidic solution [4].

The other predominant reaction of water with glass is dissolution. This typically occurs with basic solutions. Glass dissolution reactions result in the release of metal ions and other inorganic materials [2] (see Figure 3).

VI. ELASTOMERIC CLOSURES FOR LYOPHILIZATION

A. Composition and Manufacturing Process

Elastomeric closures for lyophilization are composed primarily of proprietary rubber formulations based on butyl polymer. Rubber is used because of

Copyright 2004 by Marcel Dekker, Inc. All Rights Reserved.

Table 1 Considerations in Developing and Choosing a Closure for Freeze-Drying

Low moisture permeation
Low moisture absorption
Low headspace volatiles
Low extractables
Low absorption and adsorption characteristics
Low oxygen transmission
Low coring/fragmentation
Good reseal
Low surface tackiness during processing
Capability to have good seal integrity with gas or vacuum
Good handling properties during initial and final stoppering

its capacity to seal well against the surface of a glass vial. Non-halogenated and halogenated butyl rubbers have been used for years in these types of applications for two primary reasons: low moisture vapor transmission rate and low extractability. Each of these characteristics will be covered in detail in this chapter.

There are many considerations in developing and choosing a closure for freeze-drying. These are identified in Table 1.

A rubber closure, although predominately rubber polymer, is typically composed of 6 to 12 materials. Each material gives the finished rubber formulation its chemical and functional characteristics. The typical rubber composition is composed of the following ingredients:

Polymer
Filler
Primary curative
Accelerator
Activator
Plasticizer
Pigment
Antioxidants/stabilizers

There may be a combination of inert mineral fillers used in the rubber formulation to reinforce the rubber. Additionally, the primary cure, accelerator, and activator would be considered the ''cure system'' for the formulation.

The raw materials are weighed according to a formulation card, which is specific for the type and amount of each ingredient. The raw materials are then blended together in a mixer. A final blending step is typically completed on an open mill to assure that adequate dispersion has occurred. The rubber

Copyright 2004 by Marcel Dekker, Inc. All Rights Reserved.

batch is then calendered or extruded in preparation for molding. Typically, compression molding technology is used to produce the stoppers. Compression molding takes sheet of precisely weighed uncured rubber and puts them into a tool that has two molding surfaces, one for the top of the stopper and one for the plug, or drug contact side.

The mold is then closed and a specified amount of heat, pressure, and time are applied, forming chemical cross-links within the rubber matrix. This is the phenomenon of curing rubber. The web of stoppers is removed from the mold and then trimmed into individual closures using an appropriate die. These stoppers are then ready for washing, siliconization, sterilization, and any other processing that is needed.

One important point to remember about traditional thermoset rubber closures, such as those explained above, is that the raw materials undergo a chemical reaction. The application of various types of energy, such as heat, will continue that reaction. At some point, the energy input can begin to break down the cross-links within the rubber matrix, leading to the beginning of degradation of the rubber. This is an important consideration when identifying the drying and sterilization cycles for closures. Too much energy input can lead to issues such as surface rubber degradation. This phenomenon can be evidenced by the tackiness of the closures. Additionally, butyl rubber, by nature, is tacky. The addition of other ingredients and coatings are used to help to minimize this tendency.

B. Physical Properties

Each raw material can have an effect on the various characteristics necessary for an optimal lyophilization closure formulation.

One key physical characteristic of the stopper that relates to its ability to handle well in the stoppering process is the hardness of the vial closure. Typically, a durometer between 45 and 55 (Shore A Durometer Units) will permit good handling during stopper insertion, yet will not have a negative effect on features such as needle penetration, coring, and reseal. An elastomeric closure that is too hard will have detrimental effects on some of the key functional characteristics that will be important when the final drug product is in the market.

Since a needle will penetrate the lyophilization stopper at least twice, the characteristic of reseal is very important. Reseal is the ability of the rubber to close the hole made by penetration of a needle once it is removed.

The optimal lyophilization formulation will have the correct hardness and reinforcement materials, which will balance the need for good seal integrity (softer, low compression set) and good machinability (harder, higher durometer). The compression set of an elastomeric formulation is

Copyright 2004 by Marcel Dekker, Inc. All Rights Reserved.

important as it will dictate the formulation's ability to keep its rubber characteristics—specifically its ability to bounce back after deformation. The ability of a rubber closure to seal properly is extremely important for several reasons. Typically, in a liquid parenteral application the secondary seal (aluminum crimp) will be applied shortly after stoppering the vial and while it is still in the sterile suite. In the case of lyophilized product, the stoppers are pressed into the vials at the end of the cycle; the stoppered vials are then removed from the chamber. They may then sit for a period of several hours before the aluminum seal is put onto the vial. In some cases, in addition to the concern of microbial ingress, there is also a need to keep a vacuum or gas in the vial. The subject of container/closure system integrity will be discussed in great detail later in the chapter.

Another interesting physical characteristic of the rubber is glass transition temperature. This feature is important because many lyophilized products are stored at temperatures below ambient. The need for the rubber formulation to be able to keep its rubber characteristics under those conditions is extremely important. The glass transition of uncured butyl rubber is typically in the range -75 to -67°C [5]. Finished rubber formulations have typically been found to have glass transition temperatures in the range of -65 to -55°C [6]. Quite often frozen products are shipped under dry-ice conditions. These temperatures are below the glass transition temperature for rubber, so special precautions may need to be taken. The glass transition point is the temperature at which rubber becomes more plastic-like. If this occurs, it loses its elastic characteristics.

C. Closure Configuration Considerations [1]

Drug or biological drying time is critical to the efficiency of the overall lyophilization process. Closure vent design plays a direct role in allowing the efficient sublimation of water that occurs during the primary drying stages of lyophilization. A theoretical mathematical model for the conductance of water vapor through the stopper vent was developed in order to aid in the optimization of stopper design. If moisture vapor is considered a gas, the enhancement of its flow depends on flow rate, the properties of the gas, and the geometry of the stopper vent. Two properties can be calculated from this information. These are the mean free path, which is the average distance a molecule will travel before colliding with another molecule, and the effective vent diameter, which is the diameter of the largest circle that can be inscribed in the cross-section of the vent. Based on these properties the flow can be characterized as viscous, molecular, or mixed. Through experimentation the flow of water vapor through a lyophilization stopper vent was determined to be a mixed flow. This means the diameter of the vent is several

Copyright 2004 by Marcel Dekker, Inc. All Rights Reserved.

$$C = \frac{ab^3}{1000\mu LK}\,\bar{P}\text{-}9.71\sqrt{\frac{T}{M}}\,\frac{a^2b^2}{(a+b)L+(8/3)\,ab}$$

a = Width (cm)
b = Height (cm)
μ = Viscosity $\frac{\text{dynes}\cdot\text{sec}}{\text{cm}^2}$
L = Length (cm)
K = Constant based on a/b
$\bar{P}$ = Average pressure across vent (dynes cm^2)
T = Temp (K)
M = MW

Figure 4 Calculation of conductance.

times greater than the mean free path. The mathematical model for mixed gas flow is shown in Figure 4.

The important conclusions that can be derived from this model are as follows:

Conductance is a function of the geometry as well as the area of the vents.

Conductance is greater for a vent when the width and height are equal.

Overall stopper conductance is computed by calculating the conductance of each individual vent area and summing the results. A small number of large vents are more efficient than a large number of small vents, even if the total vent areas are equal. Variations in vent areas are illustrated in Figure 5.

Traditionally there are two styles of lyophilization closure configurations, namely, the two-legged style (double vent) and the igloo style (single vent). These styles are illustrated in Figure 6.

It is important when choosing a closure configuration to understand the washing, sterilization, and stoppering process, the amount of lubricant on the closure, and the glass vial type and dimensions. A combination of these factors can have an effect on the insertion of the stopper into the vial.

Incomplete stoppering can occur as a result of stoppers sticking together or if the stopper–container interference fit is not optimal. This is an important factor in giving the freeze-drying process as good start. When the stopper is inserted into the filled container it needs to be at the proper position. It cannot be angled or misplaced prior to chamber loading. Also, when the lyophilization chamber shelves are lowered after completion of the lyophilization cycle, the stopper must be able to be pushed into the vial and fit snuggly. The stopper cannot be pulled out because of tackiness nor can it

Copyright 2004 by Marcel Dekker, Inc. All Rights Reserved.

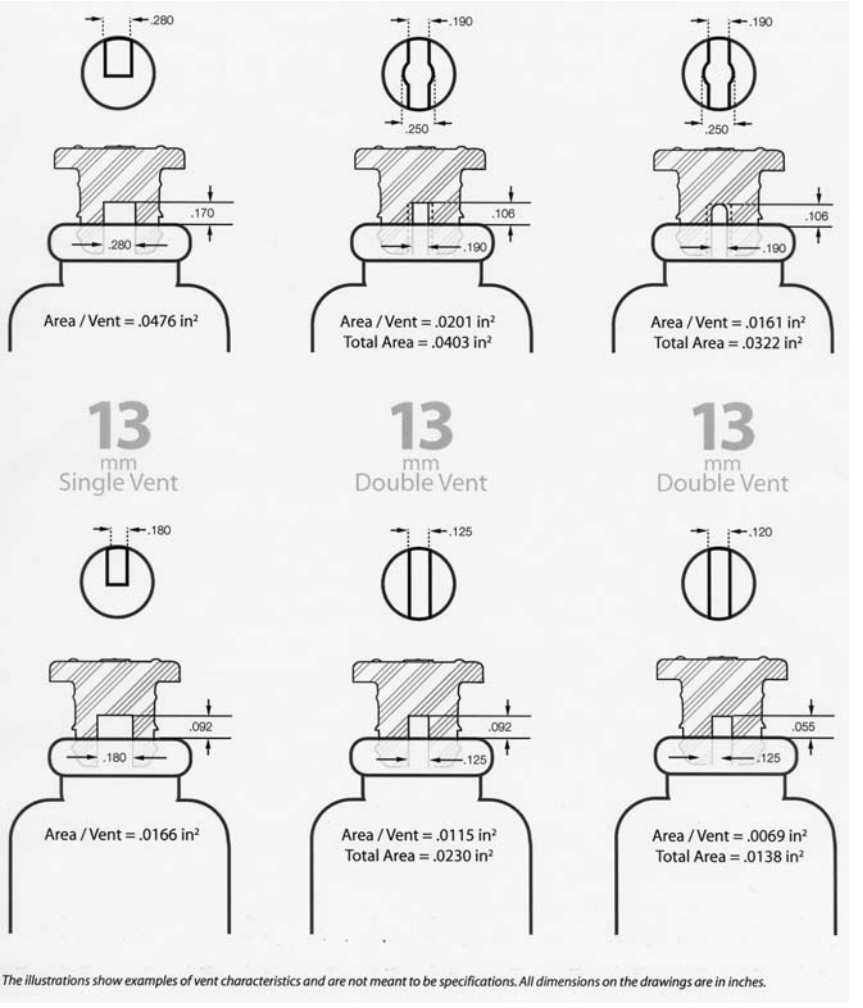

Figure 5 Various vent geometries.

pop out of the vial because of inappropriate interference fit between the stopper and the glass or because of over-lubriciousness. A common mistake is to apply too much silicone oil to lyophilization closures to ensure that they do not stick to the chamber shelves. This may cause a pop-out problem during stopper insertion because of the excessive lubricity provided by the silicone oil. Issues with lyophilization and siliconization will be discussed to a greater depth later in this chapter.

Copyright 2004 by Marcel Dekker, Inc. All Rights Reserved.

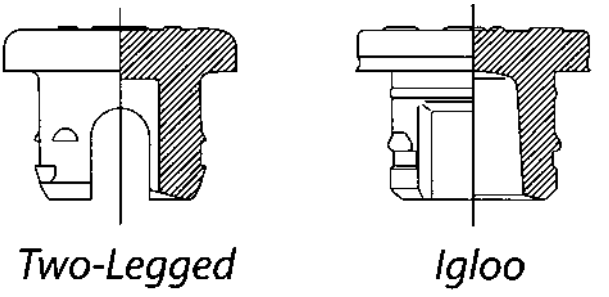

Figure 6 Two-legged stopper vs. igloo stopper.

D. Chemical Properties

The chemical properties of any drug primary container/closure system are very important. These properties bear a direct relationship to compatibility, stability, and leachables in the final dosage form.

Chemical properties are an important consideration when choosing a primary closure. Each lyophilization cycle and drug product will have its own characteristics and processes, so understanding the closure formulation that will be used for each independent application is critical.

E. Extractables/Leachables

In the Guidance for Industry entitled "Container Closure Systems for Packaging Human Drugs and Biologics," released by the Center for Drug Evaluation and Research (CDER) and Center for Biologics Evaluation and Research (CBER) divisions of the U.S. Food and Drug Administration (FDA), there is information to help the manufacturer better prepare for New Drug Application (NDA) submissions. One of the newer areas of interest discussed in the guidance is extractables and leachables. Extractables are species that can extract from the packaging component under stressed conditions with various solvents. Leachables are the container/closure extractables that are found in the drug product. There is concern with liquid drug products that the potential to extract is greater because of direct solvent vehicle interaction and refluxing of solvent into the component over time. However, the issue of volatile extractables plays a major role in lyophilized products. Extractables from a rubber compound are important to consider even with freeze-dried products because they may alter the composition of the reconstituted drug product either directly, by interaction, or indirectly by changing a formulation parameter such as pH.

Copyright 2004 by Marcel Dekker, Inc. All Rights Reserved.

There have been several fully documented cases of ingredients from a rubber closure migrating from the closure to the lyophilized drug product, quite often resulting in haze of the reconstituted solution. Pikal and Lang [7] concluded that at the low-pressure characteristics of the environment in the freeze-dryer, vapor phase diffusion is fast enough to allow significant quantities of sulfur and wax, two raw material components of a specific stopper formulation, to transfer from the closure to the product surface where absorption occurs. The lyophilization cycle and the elastomeric closure formulation are two critical variables in this type of occurrence which can lead to unsatisfactory product elegance in the market.

Low molecular weight materials such as oils, waxes, and polymer fragments may become absorbed on the surface of the freeze-dried products and this may prevent complete dissolution upon reconstitution.

The absorption of other volatiles from the stopper may not lead directly to a solubility issue but are still leachables in the drug. Examples of this are breakdown products of a peroxide-cured rubber formulation. Alcohols and ketones are examples of some of these resultant leachables.

Depending upon the uniqueness of the situation, these extractables may also leave deposits within the lyophilization chamber—another issue to consider.

These examples show the importance of selecting the appropriate testing of leachables for the drug products. Volatilization can continue over the drug product's shelf-life; therefore, it is important to evaluate leachables over the shelf-life of the product to make sure that the closure, process, and drug product are optimal.

VII. MOISTURE

There are at least three sources of moisture in a lyophilized drug. The first is residual moisture in the drug following the lyophilization cycle. The second is moisture from the environment that may pass through the closure or the seal. The third is moisture from the stopper itself. If the stopper contains moisture when applied to the vial, the cake has the potential to absorb this moisture.

A. Moisture Vapor Transmission

The permeation of moisture through the stopper is by moisture vapor transmission (MVT). Typically lyophilization closure recommendations are for stoppers that contain non-halogenated butyl or halogenated butyl rubber. The MVT rate of these polymers is low in comparison to alternative polymers. Table 2 lists a comparison of typical MVT rates.

Copyright 2004 by Marcel Dekker, Inc. All Rights Reserved.

Table 2 Comparison of Typical Moisture Vapor Transmission Rates

Formulation type	Moisture vapor transmission (g/m^2 per day)
Natural rubber	9.0
Synthetic isoprene	13.7
Ethylene propylene diene monomer (EPDM)	1.8
Non-halogenated butyl	0.2
Bromobutyl	0.3
Chlorobutyl	0.1

B. Moisture Absorption

As discussed earlier, a finished rubber formulation is composed of many different materials. These materials bring a certain amount of retained moisture to the rubber batch; additionally, each may have its own implications in the formulation's capacity to absorb water. This can occur directly from the environment, but more often occurs during the sterilization cycle. Most closures are steam sterilized through an autoclave process. This process pushed steam into the matrices of the rubber. The composition of the rubber will have a direct impact on the amount of moisture which is absorbed and retained.

Under normal conditions, the closures should be put through a drying cycle to remove residual water. This cycle should be designed not only to remove the water on the surface of the stopper, but also to dry the internal moisture.

The final cake weight for biotechnology-derived drugs may be smaller than that of a traditional pharmaceutical product. The same amount of moisture that may have been acceptable with a larger cake weight product may cause problems for biotech products.

Research [8] has found that MVT at equilibrium bears no relationship to the moisture absorption capacity of a rubber formulation. This was a critical determination because, previously, it was assumed that MVT rate was the only real characteristic of concern in relationship to a rubber closure and its use for lyophilization. Table 3 lists both MVT and percentage weight gain for several rubber formulations. Weight gain can be used to understand the capacity of an individual stopper to absorb moisture after an autoclave cycle or some other environmental conditioning.

It is also important to understand how a stopper formulation will "dry" or rid itself of moisture. Weight loss methods are not satisfactory for

Copyright 2004 by Marcel Dekker, Inc. All Rights Reserved.

Table 3 Moisture Vapor Transmission vs. Moisture Absorption Comparison

Stopper formulation	Moisture vapor transmission (g/m^2 per day)	Weight gain (%)
EPDM 1	2.15	0.48
Butyl 4	0.65	0.87
Butyl 5	0.50	1.95
Butyl 2	0.40	1.39
Butyl 1	0.35	0.27
Butyl 3	0.10	1.31

this characteristic [8]. These methods will count not only moisture loss but also the loss of other volatiles from the rubber. To quantify moisture in rubber closures accurately, it is recommended that Karl Fischer coulometric titration be used. A drying oven is used to drive moisture out of closures that have been cut into small pieces to facilitate the drying. Dry nitrogen is used to carry the moisture from the oven to the titrator. Methods have been developed and validated to assure accuracy of measurement. These methods can be used to help develop and validate drying cycles used in production for processing lyophilization stoppers.

Another important fact is that closures must be dried before the lyophilization cycle. The drug lyophilization process does not dry the rubber closure because the stopper does not experience the same cooling and heating cycle as the drug. Typically a two-step process is used to optimize the drying cycle for a load of closures. Again, it is important to realize that the validation of this drying cycle is specific for the rubber formulation, its configuration, the amount of closures in a container, the type of container holding the closures, and the equipment being used to dry the closures.

The first phase of designing the appropriate drying cycle is to understand, under normal processing conditions, the effect extended drying has on the residual moisture in the closure. This can be understood by plotting the amount of moisture in the closures by the amount of time they were dried. The drying time should be extended until the amount of moisture found in the closures has leveled off. This value can then be used as a target to understand process consistency. Multiple samples should be taken from multiple process runs in order to validate that the designed drying process does routinely get the closure moisture load to an acceptable level. It is important to take samples from different areas of the container holding the stoppers—for instance, the sterilizable bag or the stainless steel vessel—to ensure that sufficient drying has occurred in all areas of the container.

Copyright 2004 by Marcel Dekker, Inc. All Rights Reserved.

Table 4 Milligrams of Water Absorbed by Sucrose After Lyophilization Compared to Moisture Load in 20 mm Lyo Closure (per Karl Fischer testing)

Stopper formulation	Amount of water in 20 mm closure when vials were sealed[a]	Amount of water gain by sucrose in 3 months[b]
Butyl Y	10.9	3.6
Butyl Z	9.5	2.5
Butyl X	6.3	1.7
Butyl W	2.8	1.4

[a]Average milligrams of water per triplicate testing.
[b]Average milligrams of water per quadruplicate testing.

The other consideration in designing extended drying cycles is to understand the implication of temperature and time on the rubber formulation for characteristics other than moisture content. For instance, does surface tackiness of the closures increase or does coring of the closure change because of additional heat input?

C. Moisture Transfer from Closure Product

Studies have shown [9] that the amount of moisture in a stopper bears a direct relationship to the amount that may be transferred to the freeze-dried product (see Table 4).

In this study, the average percentage of moisture initially after freeze-drying compared with three-month storage gives an indication of the amount of moisture gained by sucrose that had been lyophilized using closures containing varying levels of moisture. Initial testing of the sucrose showed it contained approximately 2 to 2.5% moisture immediately after freeze-drying. If 3% was a maximum specification for stability of the product, only the sucrose packaged with one of the closure formulations would be within specification after three months of storage. See Table 5.

The study demonstrated that the larger the amount of initial water held by a closure, the more moisture is passed to the dry product. The product, however, will reach a maximum amount of moisture as an equilibrium develops between the closure and the dry product.

VIII. SILICONIZATION OF CLOSURES

Another area where problems may be encountered in processing and use of closures for lyophilization is siliconization. Siliconization is the process of

Copyright 2004 by Marcel Dekker, Inc. All Rights Reserved.

Table 5 Percentage of Moisture in Sucrose After Lyophilization vs. Three-Month Storage (per Karl Fischer testing)

Name	Percentage of water in sucrose immediately after lyophilization[a]	Percentage of water in sucrose after 3 months storage at room temperature[a]
Butyl Y	2.25	3.91
Butyl Z	2.45	3.62
Butyl X	2.34	3.12
Butyl W	1.95	2.65

[a]Average percentage of water per triplicate testing.

applying silicone oil to the surface of a rubber closure to give the surface adequate lubricity. Lubricity aids in processing, or machinability. This is critical in relation to several specific areas, such as the application of the stopper to the vial. Typically a stopper moves down a chute and is applied to the mouth of the vial, which is then placed in the lyophilization chamber. The stoppers are seated in a position that allows sublimation of the water to occur. After sublimation, a vacuum or nitrogen may be used to backfill the vial headspace. The shelves of the lyophilization chamber move to press the stopper into the vial in a closed position, sealing the vacuum or inert gas inside the vial. The seal between the rubber and glass vial must hold for a period of time before the secondary aluminum seal is applied. The application of silicone at an optimized level is important for several reasons. In applying the stopper to the vial, the closures are typically placed in high-speed sealing equipment. Any hesitation of the rubber closures can cause a problem with this system. Siliconization is critical to the closures when they are in the lyophilization chamber to prevent the closures from sticking to the shelves after they are pressed into the vials so they cannot be pulled out of the vial when the shelving is raised. Additionally, insertion into the vial needs to be smooth to facilitate the entire process; too much or too little silicone may cause problems with friction during insertion and may cause pop-up of the stopper after it is inserted if there is too much lubricity.

A. Process for Siliconization

Typically silicone oil is applied to closures during one of the final rinses in the wash process prior to sterilization. A mechanical emulsion of the silicone oil (e.g., Dow Corning 360 Medical Fluid) and water should be made. This is then applied to the rinse water in the washer. The wash cycle should

Copyright 2004 by Marcel Dekker, Inc. All Rights Reserved.

be optimized to assure adequate distribution of the silicone throughout all of the closures.

Some companies may use a pre-made emulsion such as Dow Corning 365 Medical Grade emulsion; however, these types of emulsions contain materials other than silicone oil and water to keep them in the emulsion phase.

B. Problems with Silicone

Excess silicone may cause various problems with injectable products. These range from droplets in solution to hazing of lyophilized product.

A documented study [10] conducted by Preston et al. showed the potential for the lyophilization cycle with an aqueous solvent vehicle to create a residue, found to be sodium bicarbonate from the Type I vial and silicone oil from the rubber closure. This caused hazing in the vials.

In addition to the silicone oil itself being found as droplets, there are also documented examples of the silicone oil particles acting as a nucleus to attract other materials, such as proteins. An example of this phenomenon is documented in a study of particle generation of siliconized stoppers and tumor necrosis factor formulations [11]. One of the conclusions drawn from the study was that oil droplets promoted the growth of particles by absorbing to them, thus producing sites for additional particle growth.

C. Testing for Silicone Oil

The presence of silicone oil on closures can be easily identified qualitatively through infrared (IR) spectroscopy. Typically, strong bands are found in the 1200–1000 cm^{-1} region, and near 2900 cm^{-1} with additional sharp bands in the 1270–1250 cm^{-1} and 874–740 cm^{-1} regions. A quantitative method for understanding the amount of silicone oil applied to the closures is required to determine the optimization of silicone oil application. This can be conducted through a quantitative IR method or through atomic absorption methods. In both cases, the silicone oil is removed from the stoppers with an organic solvent. The amount of silicone oil is then quantified in the solution by comparing the samples to predetermined standards and calibration curves.

These methods can be used to assist in silicone-level and application optimization.

Methods have also been developed to quantify the amount of silicone oil in some drug products or placebos. Typically, atomic absorption is used following a liquid/liquid extraction of the drug solution. These methods are valuable in helping to analyze the cause of a hazing or leaching problem.

Copyright 2004 by Marcel Dekker, Inc. All Rights Reserved.

D. Alternatives to Silicone

For many years silicone oil was the only material added to closures for lubricity purposes.

Closure manufactures have developed several alternatives to the traditional silicone oil that can be used in a similar function. The alternatives range from a cured silicone that is retained on the closure surface better than traditional silicone oil, to films that are based on fluoroelastomer polymers. Each of these alternatives can be beneficial. Their use helps avoid the need to optimize silicone application by the drug manufacturer and, in some cases, such as with the film coatings, additional benefits in areas such as reduction of extractables are typical.

IX. CONTAINER CLOSURE SYSTEMS

One extremely important feature of the entire package is its need to keep a seal after the lyophilization process. Many features have to come together to achieve this in a satisfactory manner. This is more of a challenge for a lyophilized product than a liquid injectable because the seal must be maintained for several hours without the application of the aluminum overseal. The elastomeric formulation, the closure shape, any closure coating, and the glass vial all must fit together perfectly to achieve the required sealing characteristics. The fit between the rubber and the glass is critical. The use of, for instance, a rubber formulation that is too hard may cause a problem because harder formulations become less elastic. Closures with coatings must be evaluated carefully. The addition of a coating may increase surface hardness or may, depending on its area of application, become a barrier between the glass and the rubber. This barrier or increase in hardness prevents the rubber from sealing adequately, especially where there may be nicks or lines in the surface of the glass vial finish. If the rubber does not seal these areas, they create routes for the ingress of contamination or egress of gases.

X. SEAL INTEGRITY METHODS

Many methods have been used by industry to evaluate seal integrity. These range from very insensitive methods such as bubble testers to extremely sensitive methods such as helium leak detection.

Methylene blue testing is a common method used to ensure seal integrity. Methylene blue, however, tests that the product meets sealing

Copyright 2004 by Marcel Dekker, Inc. All Rights Reserved.

requirements for liquid transfer or product loss. In many cases, lyophilized products actually hold an inert gas or vacuum. Methylene blue methods or other more traditional procedures are not sensitive enough to evaluate a package for loss of these gases. Neither are they sensitive enough to optimize or validate a sealing process for a package that is designed to hold a gas. The best alternative in this case is a method that uses a gas such as helium. Additionally, a method such as helium leak detection can give quantitative data on the package and its leak rate, thus giving better information which allows for improved problem solving and optimization.

XI. ALUMINUM CRIMP ALTERNATIVES

Injectable products, including lyophilized products, are typically sealed with aluminum seals with plastic buttons on top that must be removed to access the medicament. The plastic buttons are typically made of polypropylene material. In some cases, certain lyophilized products may be held at extreme conditions during shipment or storage. The plastic buttons may not be able to withstand these conditions because of their composition. In these cases, specially designed buttons manufactured from materials that can withstand extreme temperature and shipping conditions are used.

XII. CONCLUSION

Many facets of the container/closure system should be taken into consideration to expedite the development, scale-up, and production processes for lyophilized materials. It is important to remember that just as every drug product is unique, so is its packaging requirements. A thorough evaluation early in the development process will help to avoid problems later in the cycle.

REFERENCES

1. The West LyoTec™ System Manual, Technology to Optimize Your Cost Effective Lyophilization Process. West Pharmaceutical Services Inc. (formerly the West Company, Inc.), 1990.
2. Steven J Borchert, Michele M Ryan, Richard L Davison, William Speed. Accelerated extractable studies of borosilicate glass containers. Journal of Parenteral Science & Technology 43(2):67–79, 1989.
3. Y John Wang, Yie W Chien. Sterile pharmaceutical packaging: compatibility and stability. Parenteral Drug Association, Inc., Technical Report No. 5, 1984.

Copyright 2004 by Marcel Dekker, Inc. All Rights Reserved.

4. RH Doremus. Chemical durability of glass. In: M Tomozawa, RH Doremus, eds. Treatise on Materials Science and Technology, Vol. 17: Glass II. New York: Academic Press, 1979, pp 41–69.
5. WJ Roff, JR Scott, J Pacitti. Handbook of Common Polymers. Fibres, Films, Plastics and Rubber. Cleveland, OH: CRC Press, 1971.
6. B Alexander. West Pharmaceutical Services Inc. (formerly The West Company, Inc.), Inter-Office Correspondence Reference Project#WUTS950821TS, August 21, 1995.
7. MJ Pikal, JE Lang. Rubber closures as a source of haze in freeze dried parenterals: test methodology for closure evaluation. Journal of Parenteral Science & Technology, 32(4):162–173, 1978.
8. Frances L DeGrazio, Edward J Smith. Moisture content of lyophilization stoppers. Parenteral Drug Association Summer Meeting, Rosemont, IL, June 7–8, 1990.
9. Frances L DeGrazio, Karen Flynn. Lyophilization closures for protein based drugs. Journal of Parenteral Science & Technology 46(2):54–61, 1992.
10. Wendy A Preston, John Baldoni, Bruce E Haeger, David B Paul, Stephen P Simmons. Residue in vials after lyophilization. Journal of Parenteral Science & Technology 41(1):40–41, 1987.
11. MS Hora, RK Rana, FW Smith. Lyophilized formulations of recombinant tumor necrosis factor. Pharmaceutical Research 9:33–36, 1992.

Copyright 2004 by Marcel Dekker, Inc. All Rights Reserved.

10
Advanced Glassware for Freeze-Drying

Jürgen Thürk and Peter Knaus
Forma Vitrum, Schott Pharmaceutical Packaging, St. Gallen, Switzerland

I. THE CHALLENGE

Glass is unique in that it provides an optimum combination of important characteristics for primary packaging: it is durable, inert, clean, and offers the pharmaceutical drug sterile integrity protection with optimal transparency.

Many special features are achievable by composition or processing of the glass as follows:

- for parenterals the chemical durability of the glass is adapted to the special need of low alkalinity and reduced leaching of other ions by the chemical composition, e.g., borosilicate glasses like DURAN®, Fiolax®;
- for special applications the chemical durability of glass is increased greatly by coating, e.g., Type I plus® container with SiO_2 coating (PICVD)*;
- for highly diluted substances the adsorption at the glass wall can be influenced by specially designed coatings (by PICVD processing [2]);
- for sterilization of glass containers by gamma, electron-beam, or x-ray irradiation the resulting browning can be reduced by doping the glass

*Plasma Impulse Chemical Vapour Deposition, a coating process applied by Schott Glass [1].

Copyright 2004 by Marcel Dekker, Inc. All Rights Reserved.

with cerium [3]; additional increased hydrolytical stability can be reached by PICVD [4].

One drawback which remains is its fragility: in everyday life we have learned to live with this characteristic of glass and have developed safety precautions and appropriate handling methods to reduce the risk of breakage.

In the pharmaceutical industry, particularly those manufacturing and filling parenterals, a breakage of or crack in the glass container is unacceptable, and not simply due to economic reasons. Even small microcracks in the glass vial may lead to a non-sterile condition in the filled package. It must then be judged as a critical defect which could endanger human life and health. It is therefore justified to ask for "zero defects" in the final product in this regard, and this is the challenge to be mastered at every level of production including the supply and processing chain.

A still more special case is the freeze-drying process: this process is expensive and therefore worthy of a total cost optimization. Parameters influenced by the properties of the glass container and to be improved are:

process cycle (heat transfer conditions, product stability, freezing and drying properties of the product, crystal size, structure);
energy costs (cooling/heating power);
breakage rate (lost material, toxicity, loss of sterile integrity).

To reduce the risk of breakage and cracking, glass containers with thicker walls (e.g., molded glass) were used—with the disadvantage of poorer heat transfer and consequently increased cycle times.

So the problem of the pharmaceutical industry with glass containers in the freeze-drying process was either the risk that glass breakage was too high (thin glass containers, suboptimal geometry) or the heat transfer was too slow (glass container with thick wall/bottom).

The challenge now was to develop and make available glass containers which are optimized for the freeze-drying process, i.e., optimization of mechanical resistance against breakage in combination with good heat transfer of the glass container in the freeze-drying process.

II. THE APPROACH

The task was to fulfill the special requirements of the freeze-drying process for glass containers and to reduce the total costs by optimizing the

Copyright 2004 by Marcel Dekker, Inc. All Rights Reserved.

parameters, i.e.:

No breakage or cracking by the thermal differentials and the high inner pressure in the container induced by the freeze-drying process (to avoid critical contamination of the production line and the sterile surroundings and to reduce the risk of non-sterility).

Fast heat transfer from the cooling pan to the drug inside the glass container (to reduce energy costs and cycle time).

To meet these requirements a new design of the glass container was necessary. To optimize the design with regard to strength/stress *and* heat transfer it was necessary to understand the stress behaviour of the glass container and the heat transfer in the freeze-drying process.

To explain the background for the measures taken, let us first introduce some basics:

1. Strength/stress/breakage: Breakage or cracking will occur if the stress (thermally or mechanically induced) is higher than the actual strength of the glass (which in practical use is not a material constant but mainly a function of its surface condition [5]), i.e.:

if the strength of the glass container is reduced (e.g., surface failures) and/or

if the applied stress is too high.

So the problem of glass breakage is solved ideally from both sides:

by reducing the stress and

by conserving most of the initial high materials strength* of the container.

2. Heat transfer in the freeze-drying process: The heat for the sublimation is transferred from the pan/shelf and the chamber walls of the freeze-dryer to the glass vial and the drug mainly by conduction and radiation [7] (Figure 1).

Unfortunately the conduction from the cooling shelf to the container is low due to the small contact area (ring shaped), and in addition concavity of the bottom is needed for increased mechanical resistance (as we show later). Pharmaceutical products also show very low values in the dried state and the glass wall adds to the resistance too.

*Increase of strength is possible by chemical or thermal toughening, but it is a rather expensive step and in contradiction to the pharmaceutical requirement of delivering stress-free glass [6]. Nevertheless in special applications it might be useful.

Copyright 2004 by Marcel Dekker, Inc. All Rights Reserved.

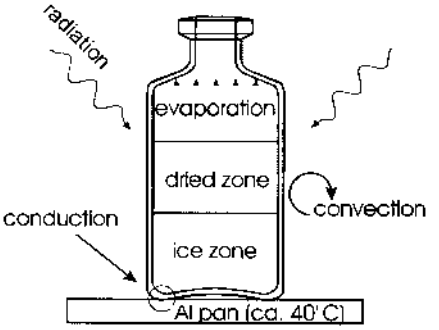

Figure 1 Heat transfer during the primary drying stage.

Convective heat transfer is important but decreases greatly with low pressures (vacuum [8]).
Heat radiation is on the same order of magnitude as conduction, i.e., rather low [9]. Improvements may be made by adapting the chamber/wall surface or material.

So the problem of heat transfer has to be solved by improving conduction from the shelf to the glass vial through

a big contact area and
a thin bottom wall.

Thus the task was to improve the mechanical resistance of the glass against breakage by reducing the stress, in combination with thinner walls and a flat bottom to improve the heat transfer (Section A–C below).

A. Reduction of Stress in the Freeze-Drying Process

Stress in the glass container is mainly due to:

temperature differentials in the heating up and cooling down procedures;
volume increase of the freezing agent;
geometry of the crystals; and
geometric constrictions of the container.

To measure those stresses and their effect on the breakage rate of glass containers freeze-drying crash tests were performed in a LYOVAC GT3 small-scale lyophilizer with 10% mannitol solution (most critical, i.e., a high breakage and cracking rate, because of its extreme expansion [10] (see Figure 2)).

Copyright 2004 by Marcel Dekker, Inc. All Rights Reserved.

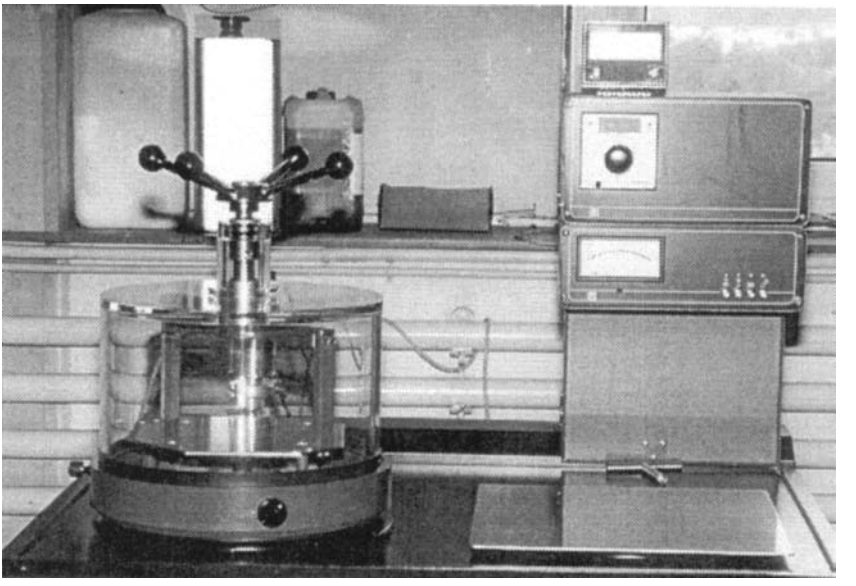

Figure 2 Apparatus.

The highest number of cracks was generated during the vacuum phase following the freezing stage (highest static pressure difference between the inside and outside of the vial, up to 30 bars). Additional stress was induced by temperature differentials in the glass container. In a typical freeze-drying process the temperature difference between the pan surface and the product in the bottom of the vial can reach values up to 30°C (Figure 3).

On the basis of these experiments FEM*, the calculations, burst test, the simulations (vials under inner pressure, the best simulation), and crack analysis (breakage cause and origin) were performed [11]. These data were the input of the optimization shown in Figure 4. In this example of geometrical optimization the axial stress at the critical points was reduced by more than 50%!

The burst tests for determining the maximum applicable inner pressure for differently shaped vials are illustrated in Figure 5.

The results of the FEM calculations and burst tests were in accordance with the freeze-drying tests and gave clear evidence for the optimization of freeze-drying vials.

*Finite Element Method.

Copyright 2004 by Marcel Dekker, Inc. All Rights Reserved.

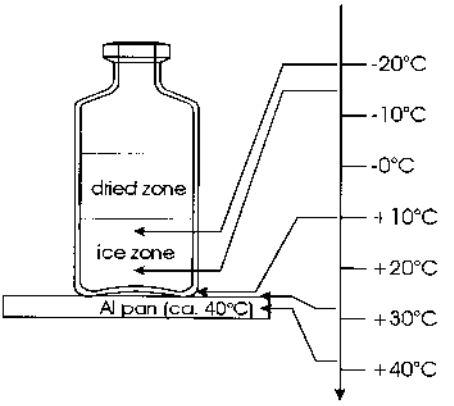

Figure 3 Typical temperature profile during primary drying stage.

The following parameters were evaluated as essential for the mechanical resistance:

1. Essential for the bottom strength:

   bottom radius
   bottom thickness
   bottom concavity.

2. Essential for the cylindrical body strength:

   ratio of wall thickness to body diameter.

These parameters were the basis for optimizing the shape to reduce stresses in the freeze-drying process.

B. Improvement of Heat Transfer

As conductive heat transfer is the predominant mechanism for the heat transfer from the shelf to the vial, shape and thickness of the bottom are most important. For the best heat transfer thin walls and high contact area are ideal, so optimization of the container implies achieving the thinnest and flattest bottom with the required strength.

C. Optimizing Heat Transfer *and* Stress of the Glass Container in Freeze-Drying

With this knowledge from Section A and B vials were designed according to the results of the FEM calculations with the optimized geometric shape

Copyright 2004 by Marcel Dekker, Inc. All Rights Reserved.

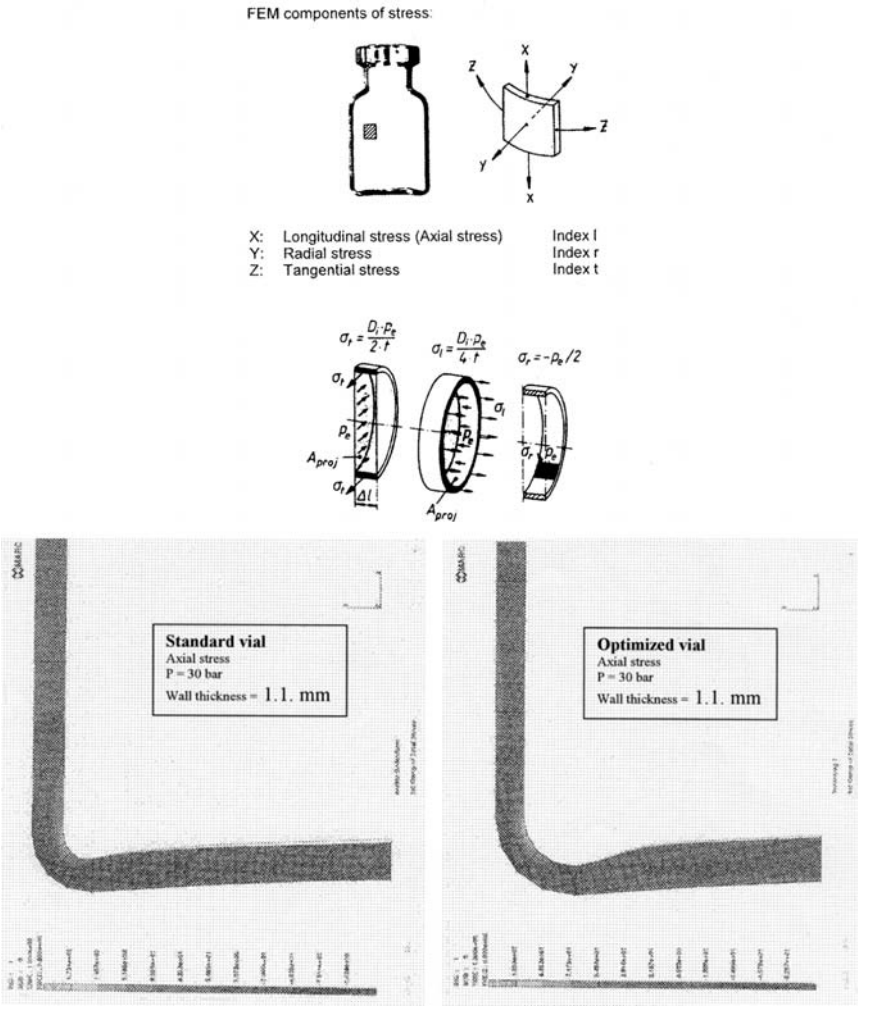

Figure 4 FEM calculation with regard to axial, radial, and tangential stress.

and minimum bottom wall thickness and concavity (indeed, a slight concavity is necessary for the best mechanical resistivity).

The mechanical tests with these optimized containers in the lyophilizer and under inner pressure showed the expected result: namely no more breakages under freeze-drying conditions and improved heat transfer through the thin and flat bottom.

Copyright 2004 by Marcel Dekker, Inc. All Rights Reserved.

Figure 5 Burst test equipment and vials.

As the strength of glass is high in statu nascendi and in practical use depends mainly upon its surface quality, it was very important to prevent damage to the surface of these optimized vials. So additionally the manufacturing process of freeze-drying vials was optimized through:

careful handling of the tubes, from which the glass containers are made;
coated glass tubes (to avoid surface damage);
flame setting;
transport and handling systems (friction, soft material, temperature), avoiding hot glass–glass and hot glass–metal contacts;
soft packaging.

Copyright 2004 by Marcel Dekker, Inc. All Rights Reserved.

Also optional (as prevention is imperative but not for all purposes sufficient) is a 100% inspection by highly sophisticated camera systems to eliminate any remaining cracks, microcracks, etc., e.g., TopLine® vials by Forma Vitrum.

III. RESULTS

These vials, specially designed for freeze-drying, have shown their reliability over years and satisfied our clients. Their outstanding performance was reached by a targeted optimization and the fact that they are manufactured from tubular glass. The advantages of such a tubular glass vial for freeze-drying are really convincing namely:

high dimensional precision;
less weight for same filling volume;
better hydrolytic resistance without treatment;
even wall thickness distribution;
defined bottom thickness;
increased heat transfer in freeze-drying cycle;
optimal for camera inspection (automated surface and particle inspections);
smooth surface quality;
high cosmetic standard;
negligible tooling costs.

In addition some recommendations for the handling of these optimized vials in the pharmaceutical filling and freeze-drying process were made to conserve the high strength of the delivered glass vials:

Reduce the sterilization temperature to the minimum needed as glass is most sensitive after hot air sterilization (high T $\rightarrow$ higher friction coefficient $\rightarrow$ more mechanical stress on the glass).
Avoid immediate change from a heating zone to a cooling zone (i.e., design of tunnel, critical for thick glass walls).
Stop tunnel transport if transport pressure gets too high.
Use feed-in screws, often a critical process step. A turntable as a buffer zone avoids tailbacks under pressure.
Ensure the filling height in the freeze-drying process is less than 50% of the cyclindrical part of the vial (the higher the filling height, the more breakages).

Copyright 2004 by Marcel Dekker, Inc. All Rights Reserved.

REFERENCES

1. M Walther. Schott type I Plus^{TM} containers for pharmaceutical packaing. In: H Bach, D Krause, eds. Thin Film on Glass. Berlin: Springer, 1977, pp 370–377.
2. A Schrattenholz. Wirkstoffverlust durch Adsorption eines nikotinischen Acetylcholinrezeptors in Schott Type I plus and Standardfläschchen. Gemany: Brochure Schott Glaskontor, 1999.
3. B Speit. Irradiation Energy Dependence of Discoloration in Radiation Shielding Glasses, SPIE Conference, San Diego, CA, 1990.
4. M Spallek, W Marten, A Geiger. Sterilisierbarer Glasbehälter für medizinische Zwecke, insbesondere zur Aufbewahrung pharmazeutischer oder diagnostischer Produkte. Patent pending, DE 197 06 255 A1, 1997.
5. H Scholze. Glas: Natur Struktur und Eigenschaften. Berlin: Springer, pp 238–259, 1988.
6. FR Rimkus. Defect evaluation list for containers made of tubular glass, Vol. 19. Aulendorf: Eitio Cantor Verlag, 2000.
7. R Taylor, S Zhai. http://www.chemsoc.org/exemplarchem/entries/2002 (Department of Chemical Engineering, University Cambridge, 2002).
8. D Esig, R Oschmann. Lyophilisation. Stuttgart: Wissenschaftliche-Verlag, 1993.
9. U Fotheringham. Priv communication, Schott Glas Mainz, 2002.
10. TA Jennings, NA Williams, Y Lee, GP Polli. J Parent Sci Technol 40:135, 1986.
11. R Egli. Festigkeitsuntersuchungen an Glasfläschchen für die Gefriertrocknung von Flüssigkeiten. Diplomarbeit, 1994.

Copyright 2004 by Marcel Dekker, Inc. All Rights Reserved.

11

Critical Steps in the Preparation of Elastomeric Closures for Biopharmaceutical Freeze-Dried Products

Maninder S. Hora and Sidney N. Wolfe
Chiron Corporation, Emeryville, California, U.S.A.

I. INTRODUCTION

Over the past two decades, biotechnology has progressed from a laboratory science to a viable industrial technology with advances that have led to the development and commercialization of new medications for a variety of diseases. The U.S. Food and Drug Administration (FDA) has approved at least two dozen biopharmaceutical proteins or antibodies for cancers, immunological disorders, and infectious, neurological, cardiac, and other diseases. In the early years of biotechnology, manufacturers realized that protein products would require special care in the final formulation because of two conflicting properties. Proteins are potent medicines, with only small amounts per dose necessary for biological efficacy. This would indicate formulation in a dilute solution. On the other hand, proteins are generally unstable in solution. The dilemma was resolved by lyophilizing dilute solutions of proteins, and this became the leading strategy in the 1980s. Although the number of solution dosage forms for proteins has increased considerably in the present decade, lyophilization is still the only practicable stabilizing method for some proteins.

Lyophilization technology, adapted from existing practices in formulating chemically synthesized drugs, was at first applied directly to proteins.

Copyright 2004 by Marcel Dekker, Inc. All Rights Reserved.

However, research into refining the process for proteins was undertaken, and problems associated with protein stabilization and dosage form lyophilization cycle development received a great deal of attention. In contrast, issues relating to the container closure system were largely neglected. Yet without an adequate and compatible closure, the advantages of lyophilizing a biopharmaceutical product cannot be fully realized. In this chapter, we discuss the use of elastomeric closures for biopharmaceutical freeze-dried products and offer some explanations and solutions based on our own experience in this field.

II. DESIRED PROPERTIES OF CLOSURES FOR FREEZE-DRIED PRODUCTS

A. General Requirements for Therapeutic Product Container Closures

The first set of requirements that closures for lyophilized product containers must meet are those described for stoppers used in containers for parenteral drugs. They must serve as a barrier to microbial contamination, be compatible with the formulated drug product, and not leach out toxic materials. They must be tested in the prescribed manner for seal integrity and product capability. The reader is referred to sections in the U.S., European, and Japanese pharmacopoeias for appropriate test methods for evaluating extractables.

B. Drying Properties of Lyophilization Closures

Lyophilization stoppers must not allow moisture from the atmosphere into the container or be a significant source of moisture themselves. Stoppers are principally composed of synthetic and/or natural rubbers, fillers to strengthen the stoppers, and curing agents to cross-link the rubber formulation. The selection of these components affects the moisture uptake and drying properties of the stopper [1]. Due to proprietary reasons, the stopper manufacturers do not disclose the composition of stoppers to the pharmaceutical companies. Therefore, establishment of a clear relationship between stopper components and their moisture gain property is not possible. Consequently, we need to develop efficient procedures for achievement of the required level of drying of the stoppers.

The most common method of sterilization for stoppers is steam sterilization. To prevent a product from regaining moisture during storage, stoppers must be dried after steam sterilization; those that absorb relatively high amounts of water may need to be dried more thoroughly than those

Copyright 2004 by Marcel Dekker, Inc. All Rights Reserved.

that absorb less. How to assess and control moisture in stoppers is discussed at length in Section III.C, below.

C. Slots in Lyophilization Closures

Lyophilization stoppers are designed to allow the passage of moisture from the vial during lyophilization. One or more slots run part way down the plug of the stopper, which is only partially inserted into the filled product container during the lyophilization process. This leaves an opening or openings through which large volumes of water vapor must pass during the primary drying cycle of lyophilization. The size and depth of the slot determines the stoppers' resistance to the flow of vapor for a given pressure differential between the vial and the chamber. Pikal et al. [2] demonstrated that even though the resistance of 13 mm stoppers (slot diameter 0.2 cm) was five times greater than the resistance of 20 mm stoppers (slot diameter 0.4 cm), the total resistance of the 13 mm stopper is less than 12% of the total resistance of the flow of water vapor with sublimation rates of about 0.5 g/h. Most of the resistance to the flow of water vapor is from the dried product. Thus the slot size of the stopper should not significantly affect the rate of lyophilization unless a stopper has a slot diameter of less than 0.2 cm or the rate of lyophilization is greater than 0.5 g/h.

Our experience is that single-slotted stoppers, also known as igloo closures, perform similarly during primary drying to two-legged design stoppers with similar cross-sectional area. The advantage of the single-slotted stoppers is that they are easier to set in the correct position during filling operations on a commercial scale.

III. COMMON PROBLEMS ENCOUNTERED WITH LYOPHILIZATION CLOSURES

A. Siliconization

Siliconization, or application of silicone oil to elastomeric closures, is usually necessary to ease their insertion into container openings via high-speed automatic filling and sealing equipment. Without this treatment, shingling or jam-up of stoppers in feed chutes may occur because of the high friction of the untreated rubber. Additionally, during high-speed stoppering operations by automatic machines, the lubrication imparted by siliconization helps to compensate for slight misalignment between the vial and the stopper positions and allows for easy insertion. Two methods are used for siliconization of elastomeric closures. In the first method, a small quantity of silicone oil (e.g., Dow Corning 360 Medical Fluid) is added to a large

Copyright 2004 by Marcel Dekker, Inc. All Rights Reserved.

number of stoppers in a vat and coated by mild agitation of the vat. In the second method, a silicone oil emulsion (e.g., Dow Corning 365 Medical Grade Emulsion) is added during the rinse cycle of the stopper washing procedure. The emulsion method provides a more uniform application of silicone oil to the stopper surfaces than the agitation method does and is generally preferred.

1. Silicone Oil Particulates

Residual silicone oil is immiscible with water and disperses in aqueous solutions, appearing as a haze or a suspension of fine particles. Therefore, excess silicone oil present on stoppers could contaminate a pharmaceutical product. In lyophilized products, only the prelyophilization and the reconstituted solutions are subject to contact with the stopper. However, components of the container closure system have been shown to create a residue in the container when water for injection only was lyophilized [3]. Silicone oil was one component of the residue.

In experiments conducted in our laboratories, we evaluated the particulate generation potential of siliconized stoppers with lyophilized tumor necrosis factor (TNF) formulations [4]. Vials of TNF solution and its corresponding placebo were inverted to allow liquid contact with siliconized stoppers for 5 min, after which aliquots of the solutions were examined under a light microscope. As shown in Table 1, oil droplets migrated into TNF and the placebo after the 5 min incubation step and were detected as

Table 1 Microscopic Examination of Tumor Necrosis Factor (TNF) of Placebo Solutions After Equilibration with Stoppers

Experiment	Observation
Placebo freshly equilibrated with siliconized stoppers for 5 min. Aliquot withdrawn for examination	Oil droplets (10–20 μm) seen floating in the solution
Placebo equilibrated with siliconized stoppers for 5 min. Stoppers removed and the placebo solution allowed to stand at room temperature overnight. Aliquot withdrawn for examination	No oil droplets seen
Freshly formulated TNF equilibrated with stoppers for 5 min. Aliquot withdrawn for examination	Oil droplets (10–20 μm) seen. Some oil droplets associating with other particles (total size 30–40 μm) seen

Copyright 2004 by Marcel Dekker, Inc. All Rights Reserved.

Table 2 Role of Siliconization on Particulate Generation in an Experimental TNF Lyophilized Formulation[a]

		Number of particles per ml		
Stopper	Treatment	7 μm	10 μm	25 μm
Siliconized	After reconstitution	30	8	0
	Shaken for 10 s	1296	364	2
Unsiliconized	After reconstitution	32	8	0
	Shaken for 10 s	368	60	2

[a] 0.25 mg TNF, 2% dextran, 1% mannitol in 10 mM sodium citrate (pH 6.5) was lyophilized in 3 cm^3 type I glass vials with West 890 gray butyl lyophilized closures.

10 to 20 μm droplets. When the same placebo solution was allowed to stand overnight at room temperature, the droplets were no longer seen. It is possible that the migrated silicone oil was present in such small quantities that it self-emulsified in the solution in this period. In the TNF solution, larger globules (30–40 μm) were seen in addition to the 10 to 20 μm droplets. Further investigation of the larger globules showed they were soluble in 1% sodium dodecyl sulfate solution. The inference was that these were conglomerate oil and protein-aceous particles. It is possible that oil droplets promoted the growth of small protein particles by adsorbing to them, thus providing more adsorption sites for other particles.

The TNF formulations described above were lyophilized in containers closed with siliconized and unsiliconized stoppers and hand-crimped. Following reconstitution of TNF, equivalent particulate loads were seen in the two solutions. Table 2 presents particle counts taken at 7, 10, and 25 μm settings. The same containers were then shaken for 10 min, so that the solution made contact with the stopper. The containers closed with the siliconized stoppers had about four times more particles in the 7 to 10 μm sizes than the ones closed with unsiliconized stoppers.

Based on these studies, we concluded that the amount of silicone oil applied to stoppers should be minimized. This amount is determined by the minimum level of siliconization required for adequate machinability of stoppers during the filling process. This example clearly emphasizes the need for careful selection of siliconization conditions for preparation of lyophilization stoppers.

B. Volatile Substances

Lyophilization stoppers can be a source of volatile substances that may contaminate the product during during lyophilization or during its shelf-life.

Copyright 2004 by Marcel Dekker, Inc. All Rights Reserved.

Pikal and Lang [5] found that paraffin wax-like materials and sulfur from stoppers were a source of haziness in reconstituted antibiotics and that lower pressures during lyophilization exacerbated the problem. Further research determined that unsaturated and aromatic hydrocarbons from halobutyl stoppers were mainly responsible for the formation of the haze [6]. The amount of haziness caused by volatiles varies greatly with the type of stopper used [7]. The investigators [6] showed that Teflon-coated stoppers produced the least amount of haze. However, the data on most of the stoppers tested were not quantitative. Coated stoppers are considerably more expensive and may not seal with the vial well if the coating surface is on the upper flange of the vial [8].

Drug manufacturers go to great lengths to avoid contamination of product in gas, air, and water systems. It is the authors' opinion that stopper manufacturers should identify and quantify the volatile components in their products to help the users determine which stoppers are most suitable for their product. Similar information is routinely available for such product contact items as tubing and filters used for filling and sterilization operations.

C. Moisture

The literature suggests that stopper permeability could be an issue for product used in hot and humid environments. Two groups of authors independently [9,10] evaluated the permeability of stoppers to moisture. Both determined that products gained moisture after storage at 40°C, 90% relative humidity with stoppers that were well dried. The gain in moisture had a lag time and was rate dependent on the type of stopper used. Stoppers containing natural rubber [10] were more permeable than stoppers containing only halobutyl rubber. Both studies chose storage conditions more extreme than those recommended in the International Conference on Harmonization (ICH) guidelines [11] for accelerated stability studies for products used in tropical climates. Neither study looked at the permeability of stoppers under more temperate storage conditions.

All stoppers absorb and retain some moisture during the stopper preparation procedures of washing and autoclaving. This retained water is often termed *occluded* or *trapped moisture*. Stoppers gain moisture during sterilization as hot steam is supplied at high pressure during the cycle. The stoppers thus absorb considerably more water than is present after the washing process. After lyophilization, some of the occluded moisture effuses out of the stopper into the product during storage and raises the residual moisture of the product.

Copyright 2004 by Marcel Dekker, Inc. All Rights Reserved.

The presence of occluded moisture in lyophilization stoppers was first noted by Grieff in 1978 [12]. For conventional drugs, the amount of occluded moisture does not represent a significant quantity compared to the total amount of solids present. For biologicals and biopharmaceuticals, the solid content of the lyophilized plug is frequently in the range of 30–100 mg. Occluded moisture, therefore, is a critical issue for preservation of these products in the lyophilized state. In a 1990 symposium cosponsored by the National Institute of Biological Standards and the FDA, several workers reported this problem in some detail [13]. In the remaining sections, we intend to discuss the measurement and control of occluded moisture from stoppers for lyophilized products.

1. Methods for Assessing Occluded Moisture

We have developed a method for extracting moisture retained in stoppers. In this method, stoppers are cut into eight pieces with a sharp razor blade and loaded into screw-cap glass tubes containing anhydrous methanol. The tubes have been previously equilibrated with anhydrous methanol to rid them of any environmental moisture. Simultaneously, a suitable number of blank tubes are also prepared by opening glass tubes containing methanol for about the same time as the tubes that contain cut stoppers at room temperature. An aliquot (1 ml) of methanol is withdrawn from each tube and immediately injected into the Karl Fischer coulometric moisture analyzer. The moisture content of stoppers is calculated as the difference between the readings for tubes containing stoppers and those of the blanks.

The methanol extraction method in our hands has the difficulty that 1–5% of samples and blanks have very high values. We attribute the high values to contamination of the methanol with atmospheric moisture during sample preparation. Because of this problem and the need for a rapid and more reproducible method, we developed an alternative procedure for measuring the moisture content of stoppers using a drying oven purged into a Karl Fischer coulometric instrument.

In the oven drying method we cut five stoppers into eight pieces. An oven is first purged for several hours with dry nitrogen at 250°C to eliminate background, which may drift, and then heated at the appropriate temperature. This is usually in the range of 150–180°C but varies with the type of stopper. Excessive temperatures may cause changes in the stopper that prevent the removal of occluded moisture. The cut-up stoppers are placed into the oven and heated for 1–2 h or until the rate of water removal is minimal. The resulting vaporized water is continuously evacuated with a nitrogen stream at about 100 ml/min via a heated Teflon-lined tube to the Karl Fischer coulometric titration cell. The data in Table 3 show that

Copyright 2004 by Marcel Dekker, Inc. All Rights Reserved.

Table 3 Water Vaporized from West 890 13 mm Gray Stoppers in 1 h at Different Oven Temperatures

Oven temp. (°C)	Amount of water vaporized in 1 h (μg/stopper)
150	1274
165	1689
170	565

Table 4 Water Vaporized from Stelmi 6720 13 mm Gray Stoppers in 1.5 h at Different Oven Temperatures

Oven temp. (°C)	Amount of water vaporized in 1.5 h (μg/stopper)
150	1311
160	1511
170	1940
180	2219

the amount of water released by West 890 stoppers in 1 h increases with temperature up to 165°C but decreases beyond that point. In contrast, Stelmi 6720 stoppers (Table 4) can be heated in the oven at temperatures as high as 180°C without a drop-off in the amount of water released.

The oven drying and methanol extraction methods for determining stopper moisture are not intended for determining the total amount of water present in the stopper because neither method extracts all water. These methods instead can help to determine the relative amount of water present in a stopper, which is useful for developing a stopper drying cycle.

2. Methods for Removal of Occluded Moisture

Application of heat, vacuum, or a combination of both can accomplish removal of occluded moisture from stoppers. Vacuum drying is a simple procedure, i.e., merely the drying of stoppers in the autoclave following stream sterilization. Alternately, sterilized stoppers could be transferred to a dry-heat oven and dried at an appropriate temperature.

In our experience, the choice of a method is greatly dependent on the type of stopper. A pharmaceutical company must determine the moisture removal and retention properties of a given stopper on an individual

Copyright 2004 by Marcel Dekker, Inc. All Rights Reserved.

basis since the exact composition of the stopper (polymer, filler, binding agent, etc.) is not disclosed to them. We tested four different stoppers from three different manufacturers: two from the West Company (formulations 890 gray and 4416/50), one from Tompkins Rubber Company (B1119C56C), and one from Helvoet Pharma (HP002). The West 890 gray is a blend of natural and synthetic butyl rubbers. The West 4416/50, Tompkins B1119C56C, and Helvoet HP002 all consist of a synthetic butyl rubber formulation. Natural rubber is relatively hydrophilic; synthetic butyl rubber is hydrophobic. This experiment was designed to evaluate differences in the residual moisture retention properties of the different stoppers.

Three stopper drying procedures were applied to samples of all four stopper types: vacuum drying in the autoclave for 4 or 12 h, dry-heat treatment for 4 h 110°C, and a 4 h drying in the autoclave followed by a 5 h dry-heat treatment. Results presented in Table 5 indicate that no single drying procedure was suitable for removing the maximum moisture from all stoppers. For West 890 gray and Tompkins B1119C56C stoppers, 12 h drying in the autoclave was best; for the Helvoet HP002, a combination of 4 h of vacuum and 5 h at 95°C was needed. For the West 4416/50, several methods gave roughly equivalent results.

In the above experiment, we note that a relatively smaller fraction (40–60%) of the total moisture associated with bromobutyl stoppers was extractable while about 75% of the total moisture was extracted from the stopper containing a blend of natural and synthetic rubbers. We postulate that stoppers made from synthetic elastomers have a higher amount of bound water than those made from a blend of natural and synthetic rubbers. The natural rubber component in the blend presumably imbibes more

Table 5 Effect of Stopper Treatment on Drying of Several Stoppers

	Stopper moisture (μg)				
Stopper type	Initial (post autoclaving)	Post 4 h vacuum drying	Post 12 h vacuum drying	Post 4 h heat treatment at 110°C	Post 4 h vacuum + 5 h heat treatment at 95°C
West 890	6828	2600	1940	2900	1780
West 4416/50	4829	2940	3280	3750	2800
Tompkins B1119C56C	6993	4446	2216	6387	3395
Helvoet 6213 HP002	7026	4730	5243	4312	3071

Copyright 2004 by Marcel Dekker, Inc. All Rights Reserved.

moisture that is relatively free and consequently more easily extractable upon drying. Moreover, bound water is less likely to effuse into the lyophilized product than free water.

3. Kinetics of Moisture Removal from Stoppers

To understand the moisture removal process, we prepared several batches of stoppers and vacuum dried each batch for a different time duration in the autoclave following the sterilization cycle. In this experiment, the stoppers were left in the autoclave and the temperature was allowed to gradually decrease on its own. The temperature fell from 121°C at the time of sterilization to about 60°C after 12 h during a typical drying run. At least 10 stoppers from each batch were analyzed for their occluded moisture content. The average moisture per stopper is plotted as a function of the drying time in Figure 1. The process of sterilization, in which hot steam is introduced into the autoclaving chamber under pressure, increased the moisture within stoppers nearly two-fold. In the evacuation phase, free water remaining in the pore structure was first removed, as shown by the steep decline in readings in the first 2 h of drying. The bound water was removed more

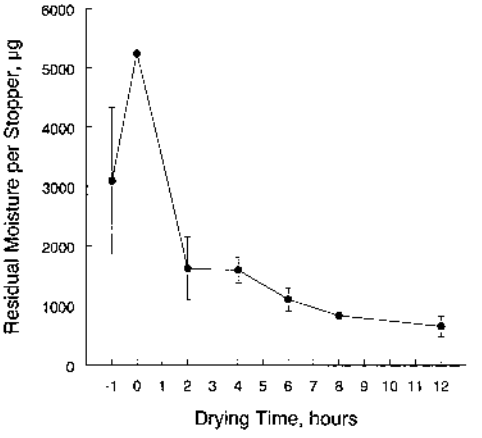

Figure 1 Kinetics of moisture removal from West 890 gray stoppers by application of vacuum in the autoclave post sterilization. Each point represents a separate experiment and at least 10 stoppers were analyzed for the residual moisture content in each experiment. The −1 time point on the *x* axis represents the washed stopper prior to autoclaving. The 0 time point on the *x* axis corresponds to sterilized stoppers that were subjected to no drying at all. The later time points represent stoppers treated for various amounts of vacuum drying post sterilization.

Copyright 2004 by Marcel Dekker, Inc. All Rights Reserved.

slowly, as shown by the later time points. The moisture value reaches a plateau after which no significant moisture removal is obtained through further drying. These results indicate that the vacuum drying procedure is capable of removing moisture present in the stopper gained during washing and autoclaving.

4. Validation of Moisture Removal from Closures

The drying processes for removing water from stoppers, whether by dry heat or vacuum, do not remove all moisture from the stoppers. The validation strategy we have used consisted of two parts. The first part was to do a series of runs with progressively longer drying times until the amount of water removed was minimal with longer drying times. The data from the first part were used to establish an acceptance criterion. The second part was to test the level of moisture from three runs and determine whether the runs consistently met the acceptance criterion. This type of validation approach is limited in that it establishes the drying procedure for only one given stopper (size, shape, and formulation), in a specific autoclave, with the maximum load of stoppers.

Data were collected from a single series of runs to establish the run time required for adequate drying. Repeating runs in order to establish a meaningful acceptance criterion is recommended, but can be expensive and time consuming, since these runs must be done at full scale. In order to save time and money, we modeled the data from the drying process single runs with a range of five time points, using a nonlinear regression model of the form:

$$\text{Occluded moisture} = A \times \exp(B \times \text{drying time}) + C$$

The coefficients A, B, and C are fitted using a least-squares approach. Results from this approach are given in Table 6. Each data point for the occluded moisture at a given time is a mean value of at least six assays from samples sterilized and dried in different locations within the autoclave. The model predicts mean moisture values within the 95% confidence interval of the measured mean moisture values. Using the data in Table 6 we selected 12 h as the time required to adequately dry the stoppers, since 16 h did not offer a significant decrease in moisture over the 12 h results.

In the second part of the validation we used the predicted values from the model at 12 h for the acceptance criterion for three reproducibility runs. The model predictions were used since they take into account all of the data generated in the first part of the validation. The acceptance criterion for the mean level of stopper moisture was the 99% confidence interval determined

Copyright 2004 by Marcel Dekker, Inc. All Rights Reserved.

Table 6 Measured Occluded Moisture in Stoppers as a Function of Drying Time[a]

Drying time (h)	Occluded moisture mean value (μg/stopper)	Standard error of the mean (μg/stopper)	Upper 95% confidence interval (μg/stopper)	Lower 95% confidence interval (μg/stopper)	Predicted value (μg/stopper)
6	1822	86	2032	1612	1887
8	1606	71	1780	1432	1459
10	1129	71	1293	965	1165
12	882	45	986	778	963
16	778	28	841	715	723

[a] Moisture values are a mean of at least six measurements of samples taken from different locations in the drying chamber. The predicted values are from the model equation in the text.

Table 7 Results of Drying Stoppers for 12 h Post Autoclaving in Three Different Runs[a]

Run number	Occluded moisture mean value	Upper 95% confidence interval of the mean	Lower 95% confidence interval of the mean
1	909	982	836
2	1076	1216	936
3	1000	1104	896

[a] Ten samples were assayed from each run. Values are in the μg water/stopper.

from the model. The calculated 99% confidence interval for the mean value after 12 h of drying was 963 ± 213 μg/stopper. Results from validation runs in Table 7 show that the modeling approach accurately predicted the mean moisture content of the stoppers. The moisture content of the stoppers was consistent from run to run as can be seen in the overlapping 95% confidence intervals for the mean values.

5. Uptake of Occluded Moisture During Product Storage

The effect of moisture on the stability of proteins has been reviewed in the literature [13]. The conventional view that the residual amount of water in the lyophilized plug should be minimized to as low a level as possible has been challenged by many in the field. It is believed that protein molecules need at least a monolayer of water molecules to maintain their native structure in the dried state [14]. Whatever the water requirement of a particular protein formulation, it is still important to maintain the residual

Copyright 2004 by Marcel Dekker, Inc. All Rights Reserved.

moisture content of a pharmaceutical product within its stability specifications to maintain its quality.

Moisture retained within the stopper could effuse out and enter the lyophilized plug, thus increasing its residual moisture over time. It is reasonable to suppose that the temperature of storage might influence the rate of effusion. As mentioned in Section III.C, elevated temperatures are often used to screen formulations and predict their shelf lives based on potency and other physicochemical stability parameters. It is therefore important to know whether the residual moisture of the lyophilized product stored at higher tempertures is comparable to that for the same product under regular storage conditions.

We monitored the residual moisture of a protein product at different temperatures to evaluate its dependence on the temperature of storage. The stoppers were prepared by our normal manufacturing process, which had previously been optimized for occluded water removal. The product was placed at 5°C, the normal storage condition, and 25°C, an accelerated stability condition. Residual moisture in the 5°C samples was monitored for 36 months; in the 25°C samples, for 12 months. The data are plotted in Figure 2. Residual moisture increased slowly in the 5°C samples from the initial value of 0.5% to about 1.0% in 36 months. In contrast, residual moisture rose much more rapidly at 25°C, attaining a value of 1.8% in 12 months. The data were fitted to a straight line and the slopes of the curves

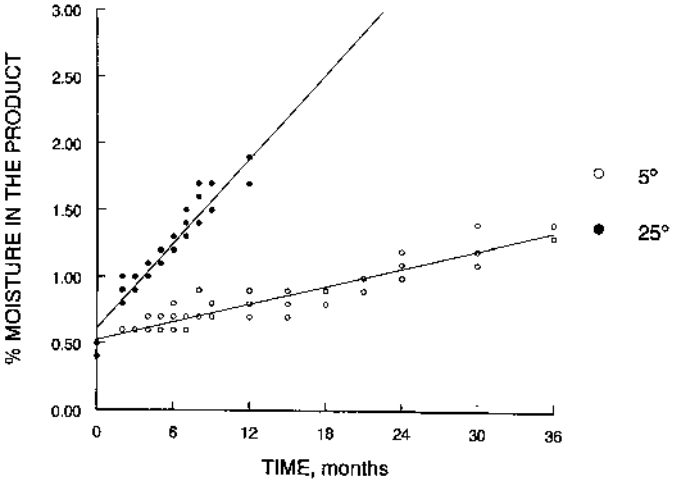

Figure 2 Moisture increase in a lyophilized protein product at 5 and 25°C as indicated.

Copyright 2004 by Marcel Dekker, Inc. All Rights Reserved.

were calculated. Whereas the slope of moisture uptake at 5°C was only 0.02% per month, that at 25°C was 0.11% per month. In other experiments (data not shown), we have found that moisture is gained at an even faster rate at 37°C (approximately 0.50% per month).

The data clearly demonstrate that higher temperatures extract much greater moisture from stoppers and that accelerated temperature conditions are poor predictors of long-term moisture uptake at lower temperatures. In contrast to our observations, Pikal and Shah [13] reported that the total moisture gain by a lyophilized plug during storage was independent of temperature. We believe that regain of moisture by a lyophilized product depends on factors such as product and stopper formulations and a general statement regarding this cannot be made.

IV. CONCLUSION

In this chapter, we have reviewed some critical aspects of stoppers that are used for packaging of lyophilized biopharmaceuticals. We have listed the desirable attributes for lyophilization closures for use with protein formulations. We have discussed issues relating to preparation of stoppers. Two issues, siliconization and occluded water, have been dealt with in detail. Siliconization can be a cause of particulate generation and aggregation, as shown by our experience with recombinant tumor necrosis factor formulations. We have described methods of measurement of stopper-occluded moisture and discussed their relative merits and demerits. We further studied the kinetics of moisture removal from stoppers under selected conditions. Our approach to validation of moisture removal from stoppers has also been presented. Finally, we have discussed the usefulness of occluded moisture measurement for determination of moisture uptake by protein products under real-time and accelerated storage conditions. We hope that readers have gained some useful knowledge in this important area, too long overlooked, that would help them to better protect the biopharmaceutical freeze-dried product from deleterious effects of improper or inadequate closure preparation.

REFERENCES

1. F Degrazio, K Flynn. Closures for protein based drugs. J Parenter Sci Technol 46(2):54–61, 1991.
2. MJ Pikal, ML Roy, S Shah. Mass and heat transfer in vial freeze-drying of pharmaceuticals: role of the vial. J Pharm Sci 73(9):1224–1237, 1984.

Copyright 2004 by Marcel Dekker, Inc. All Rights Reserved.

3. WA Preston, J Baldoni, BE Haeger, DB Paul, SP Simmons. Residue in vials after lyophilization. J Parenter Sci Technol 41:40–41, 1987.
4. MS Hora, RK Rana, FW Smith. Lyophilized formulations of recombinant tumor necrosis factor. Pharm Res 9:33–36, 1992.
5. MJ Pikal, JE Lang. Rubber closures as a source of haze in freeze dried parenterals: test methodology for closure evaluation. J Parenter Drug Assoc 32(4):162–173. 1978.
6. H Franke, P Hencken, G Ross, J Krueter. Influence of volatile rubber stopper components on the clearness of parenteral antibiotics stored in multiple or single dose containers after reconstitution with water. Eur J Pharm Biopharm 40(6):379–387, 1994.
7. JB Portnoff, MW Henley, FA Restaino. The development of sodium cefoxitin as a dosage form. J Parenter Sci Tech 37(5):180–185, 1983.
8. DK Morton, NG Lordi, TJ Ambrosio. Quantitative and mechanistic measurements of parenteral vial container/closure integrity. Leakage quantitation. J Parenter Sci Technol 43:88–97 (1989).
9. S Caorveleyn, S De Smedt, JP Remon. Moisture absorption and desorption of different rubber lyophilisation closures. Int J Pharm 159:57–65, 1997.
10. H Vromans, JAH van Laarhoven. A study on water permeation through rubber closures of injection vials. Int J Pharm 79:301–308, 1992.
11. W Grimm. Extension of the international conference on harmonization tripartite guideline for stability testing of new drug substances and products to countries of climatic zones III and IV. Drug Dev Ind Pharm 24(4):313–325, 1988.
12. GH Hopkins. Rubber closures for freeze-dried products. Dev Biol Stand 36:139–144, 1977.
13. MJ Pikal, S Shah. Moisture transfer from stopper to product and resulting stability implications. Dev Biol Stand 74:165–179, 1991.
14. LN Bell, MJ Hageman, LM Muraoka. Thermally induced denaturation of lyophilized bovine somatotropin and lysozyme as impacted by moisture and excipients. J Pharm Sci 84:707–712, 1995.

Copyright 2004 by Marcel Dekker, Inc. All Rights Reserved.

12

Development of a New Concept for Bulk Freeze-Drying: LYOGUARD® Freeze-Dry Packaging

Meagan Gassler
W. L. Gore & Associates, Inc., Elkton, Maryland, U.S.A.

Louis Rey
Cabinet d'Etudes, Lausanne, Switzerland

As discussed throughout this text, freeze-drying, or lyophilization, is the most effective technique for the long-term preservation of sensitive products, including biologicals, pharmaceuticals, cosmetics, and food. Indeed, the low-temperature sublimation of ice from previously frozen specimens allows a progressive and careful dehydration of materials which, most often, cannot be stored and distributed at ambient temperatures. Antibiotics, blood derivatives, vaccines, natural extracts from bacterial, vegetable, or animal origin, sensitive carbohydrates, proteins, or dyes are among the many different products which are still, today, processed by freeze-drying.

However, dramatic advancements in biochemistry and genetic engineering, as well as the rising interest in pristine natural active substances, has again pushed freeze-drying into the limelight. Most of these materials are fairly unstable in solution and/or at elevated temperatures, are difficult to filtrate, and need to be sterile if they are to be used for human parenteral injection. Accordingly, they have to be processed under strict aseptic conditions and be protected from outside contamination. Conversely, as is the case for antimitotic drugs used in cancer therapy, some of them are highly toxic and should not be released into the environment.

Copyright 2004 by Marcel Dekker, Inc. All Rights Reserved.

Given these characteristics, freeze-drying/lyophilization provides the ideal means of preparing many biopharmaceutical materials for transport and/or processing. However, their treatment by freeze-drying is best done within a controlled, confined container that, in turn, does not hinder processing. This is even more important if these products are in relatively large amounts and in a rather diluted state. Indeed, in this particular case, bulk lyophilization should be carried out in such a way that, at decent speeds of drying, they do not fly off in the water vapor stream emerging from the frozen matrix, which needs to escape freely from the container.

For a long time, no satisfactory solutions were offered to that end, and many freeze-drying cycles were either seriously impeded time-wise, or else substantial amounts of product were lost by direct transport. Common lyophilization practices involved utilizing flasks or vials to contain the material to be treated. While containment could be shown to be acceptable with this technique, processors were severely limited in the amount of material that could be freeze-dried at one time. The most widely used method of large-scale bulk freeze-drying today calls for open stainless steel trays. While the trays provide excellent durability, the obvious result is undesirable—and sometimes risky—contamination of the equipment (mainly the chamber) and a substantial financial loss through product flyoff and the necessary cleaning time required after processing individual product batches.

This is the reason why a sustained interest is presently devoted to a new development made in the field by W. L. Gore & Associates—the LYOGUARD® Freeze-Dry Tray (see Picture 1).

This unique product, which has roughly the dimensions of a conventional stainless steel tray used for freeze-drying (400×270 mm), is a lightweight "box" made of a rigid frame (50 mm high) in polypropylene (homo polymer). It is sealed on its bottom by a thin, transparent, flexible film with a polypropylene product contact surface. The upper side of the tray is closed by a permeable GORE-TEX® expanded polytetrafluoroethylene (ePTFE) laminate developed specifically for lyophilization. The unique microporous membrane structure allows LYOGUARD Freeze-Dry Trays to effectively contain and protect product, while also featuring a high vapor transfer rate, which minimizes the lyophilization cycle time.

On the upper side of the tray, a 30 mm fill port, secured during processing by a liquid-tight screw-tight cap, allows easy filling and unloading of the tray. The whole product, placed thusly in the tray, remains, over the course of freeze-drying, perfectly secluded in this controlled and confined environment. In fact, the most interesting feature is that this structure allows both an easy heat transfer through the bottom film and an equally good mass transfer throughout the upper ePTFE membrane.

Copyright 2004 by Marcel Dekker, Inc. All Rights Reserved.

Picture 1 LYOGUARD Freeze-dry tray.

I. TESTING OF CLOSED-CONTAINMENT LYOPHILIZATION TRAYS

We have carefully checked these two properties using not only distilled water, but also mannitol solutions (quite common in freeze-drying) and compared the drying cycles of LYOGUARD trays to those of open stainless steel trays and found that LYOGUARD trays performed equally well and sometimes better. We have also challenged the upper PTFE membrane, drying previously frozen suspensions of 1 μm latex particles in distilled water and demonstrated that all particles were stopped by the membrane while water vapor *alone* could escape easily toward the chamber and the condenser. We do believe, then, that the LYOGUARD tray concept gives an excellent answer to the everlasting question of the bulk freeze-drying of sensitive solutions or materials that need to be carefully maintained within a controlled environment.

To assess industrial applicability, we evaluated three items in comparing the performance of open steel trays vs. closed-containment lyophilization (LYOGUARD) trays:

Part 1—the freezing and heating temperature profiles of a closed-containment tray.
Part 2—the impact of the upper barrier membrane on the time for primary drying.
Part 3—the effectiveness of the upper membrane as a barrier.

Copyright 2004 by Marcel Dekker, Inc. All Rights Reserved.

A. Summary of Testing Results

Our testing has shown that the heat transfer is faster and more uniform for the LYOGUARD trays compared to open steel trays. While the upper barrier membrane does contribute some mass transfer resistance for the subliming water vapor, this resistance becomes insignificant relative to the mass transfer resistance of the drying product cake layer. With a cake thickness of >10 mm, heat transfer and thermal characteristics of the closed lyophilization tray can result in faster freezing and primary drying cycle times than for open steel trays. Finally, the upper membrane is an effective barrier to 1 μm spherical particles that may escape from drying product.

1. Part 1: Heat Transfer

From Figures 1 and 2, we see that the open stainless steel tray (the medium line) has a more gradual temperature drop during freezing and a longer time for the ice to crystallize. The steel tray takes 20–30% longer to freeze than the LYOGUARD tray. This shows that the LYOGUARD tray has a higher rate of heat transfer because the flexible bottom membrane creates less of an air layer between the shelf and the bottom of the LYOGUARD tray and because of lower thermal inertia compared to the

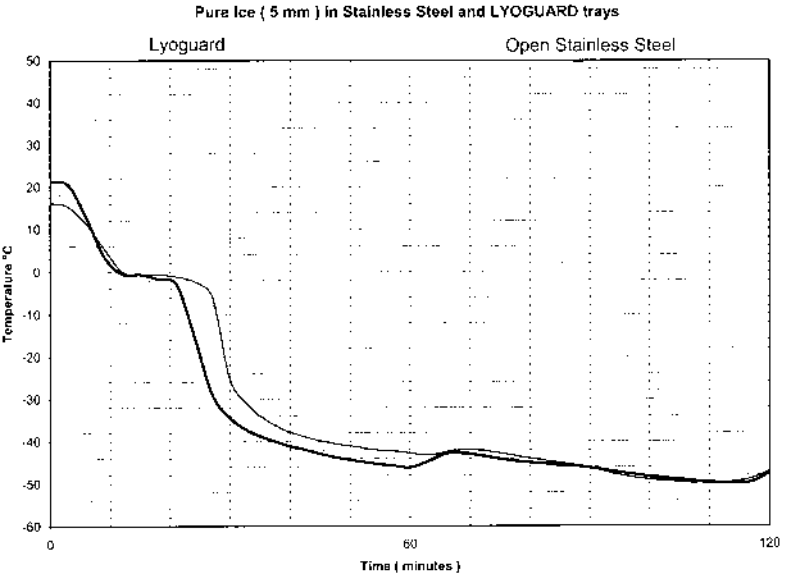

Figure 1 Cooling curve for pure water in trays.

Copyright 2004 by Marcel Dekker, Inc. All Rights Reserved.

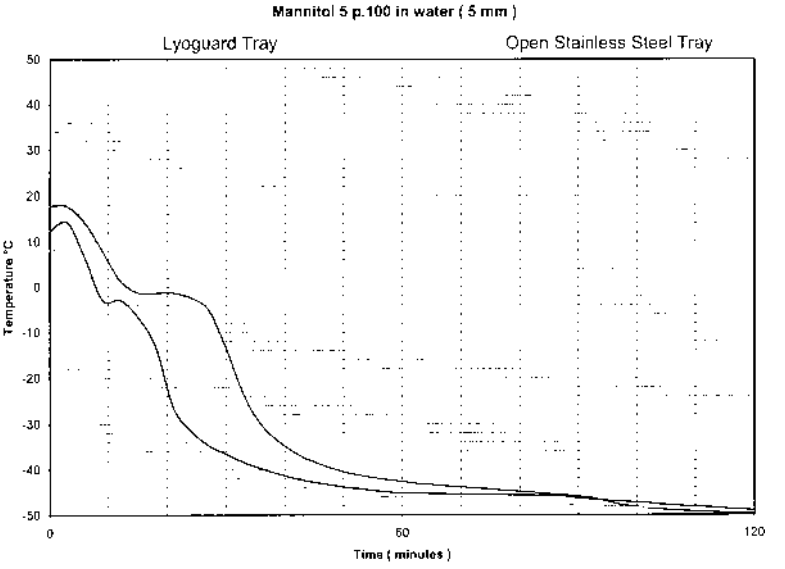

Figure 2 Cooling curve for 5% mannitol in water with 5 mm liquid thickness.

1.5 mm thick, 960 g steel tray. In a production operation, this difference will be more exaggerated if the steel tray is warped.

2. Part 2: Mass Transfer Resistance

From an examination of Figure 3, showing the freeze-drying of pure water, it is clear that the temperature profile of both of the open trays turn upward at the same time, indicating completion of sublimation (primary drying), at about 320 min. The LYOGUARD tray takes 10–15% longer with an upturn around 360–370 min. So, the GORE-TEX membrane does add slightly to the mass transfer resistance.

However, when bulking agent is added to the water (5% mannitol), the porous structure of the cake begins to contribute mass transfer resistance for the subliming water vapor. Figure 4, with the product height very small (only 5 mm), shows this porous cake structure beginning to influence the sublimation mass transfer with less difference between the open and closed trays. When the product thickness is increased to 10 mm (see Figure 5) the porous mannitol cake resistance becomes significant and in fact the sublimation period in the open steel tray is actually longer than with the closed LYOGUARD tray. If we were to extrapolate this trend to 20 mm of product thickness (about 1.9 L fill) we would expect to find a significant cycle-time saving for the LYOGUARD tray over open steel trays. Each

Copyright 2004 by Marcel Dekker, Inc. All Rights Reserved.

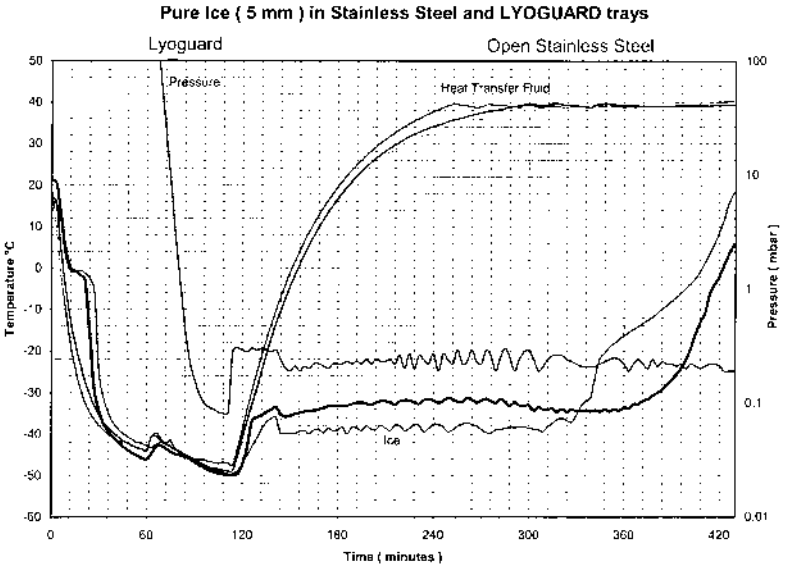

Figure 3 Temperature and pressure curves for freeze-drying of pure water at 5 mm.

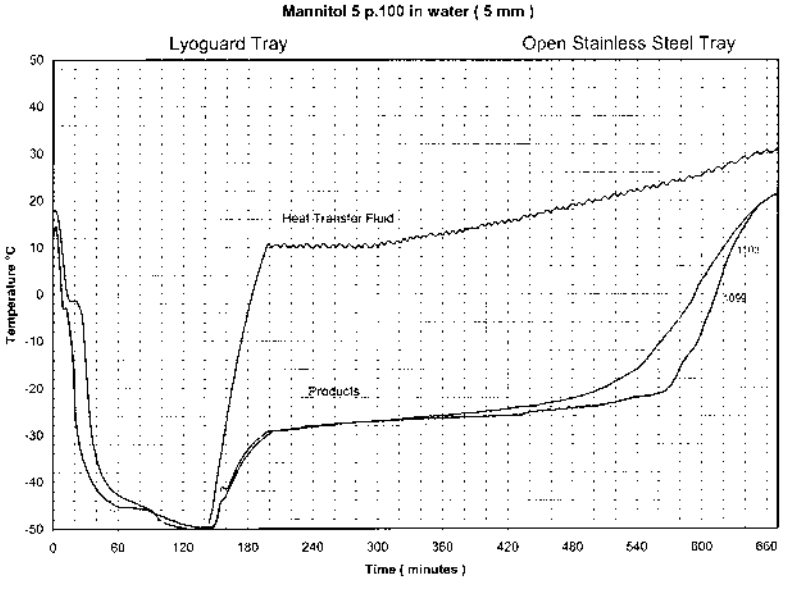

Figure 4 Temperature curves for freeze-drying of 5% mannitol in water with 5 mm thickness.

Copyright 2004 by Marcel Dekker, Inc. All Rights Reserved.

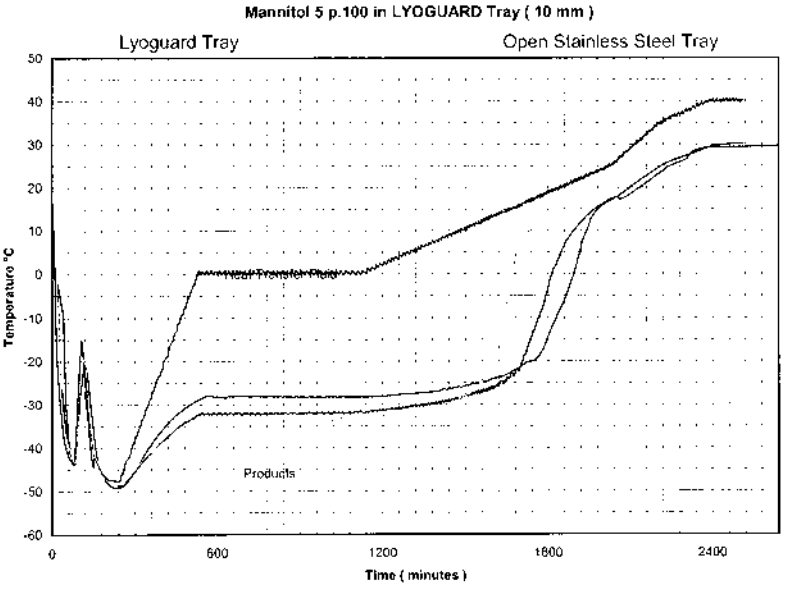

Figure 5 Temperature curves for freeze-drying of 5% mannitol in water with 10 mm thickness.

tray user will have to evaluate this in his/her particular process, but several biopharmaceutical companies drying peptide and protein solutions have reported 20–30% faster cycle times with the LYOGUARD trays.

3. Part 3: Effective Barrier of the Gore-Tex Membrane

To test the filtration effectiveness of the upper membrane, we fabricated the test apparatus shown in Figure 6. Latex particles of 1 μm diameter and concentration of $1.5 \times 10^7\,\mathrm{cm}^{-3}$ were dispersed in water. This suspension was added to glass vials with a 10 mm product depth. By testing membrane exposure during an actual freeze-drying cycle, we could observe whether the sonic velocity of the subliming water vapor could carry the particles through the membrane. After a freeze-dry cycle, SEM photomicrographs were taken of the underside of the membrane exposed to the drying product. Figures 7 and 8 respectively show the particles seen on the bottom (ePTFE side) of the GORE-TEX membrane from the LYOGUARD tray and a 0.2 μm PC membrane respectively.

Finally, a test was run with the ePTFE membrane exposed to the drying latex suspension together with a 0.2 μm PC membrane backing up the ePTFE membrane. Figure 9 shows that no particles made it through the

Copyright 2004 by Marcel Dekker, Inc. All Rights Reserved.

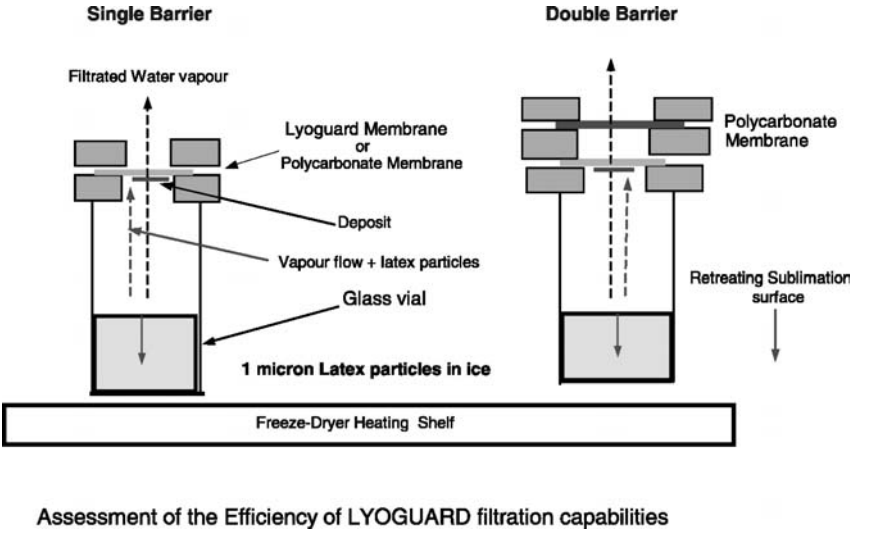

Figure 6 Test setup for trapping particles on membrane.

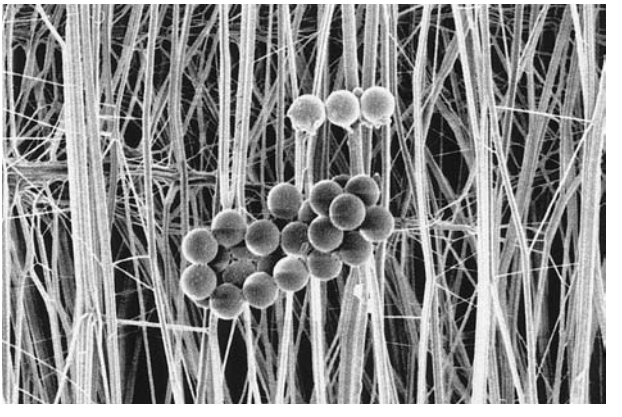

Figure 7 1 μm particles trapped on underside of LYOGUARD tray membrane.

ePTFE membrane to become captured on the 0.2 μm backup membrane. Thus the ePTFE membrane effectively prevented all of the 1 μm latex particles from escaping into the freeze-dryer chamber. This study supports auxiliary studies performed at the American Type Culture Collection

Copyright 2004 by Marcel Dekker, Inc. All Rights Reserved.

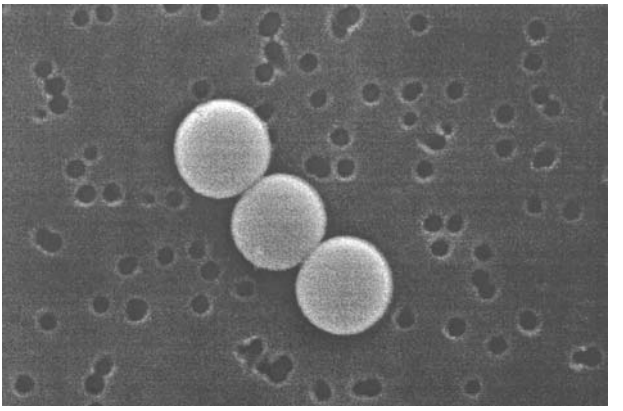

Figure 8 1 μm particles trapped on underside of 0.2 μm PC membrane.

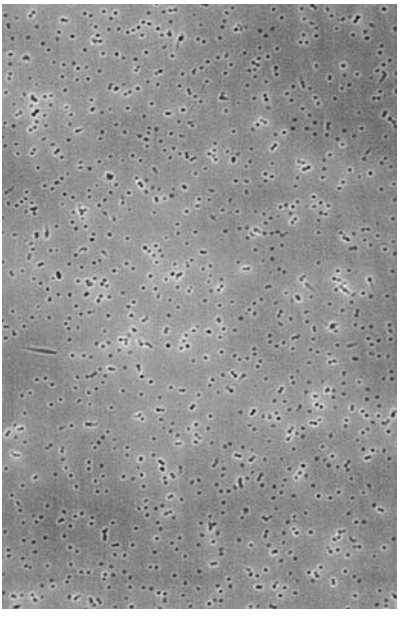

Figure 9 Clear 0.2 μm PC membrane showing no particles passing through the LYOGUARD tray membrane.

Copyright 2004 by Marcel Dekker, Inc. All Rights Reserved.

Laboratory (ATCC) at the request of Gore which showed the membrane was impervious to 0.2 μm *B. diminuta* and 0.45 μm *S. marcesens* bacteria spiked in skimmed milk that was freeze-dried.

II. VALIDATION OF LYOGUARD TRAYS

A. General Reference

1. Controlled Environment Statement

LYOGUARD trays are manufactured in a controlled environment to assure that they do not introduce unacceptable levels of contamination to the user's process.

2. FDA-Regulated Status of LYOGUARD Trays

The LYOGUARD tray is intended for use as a processing aid in the production of materials that are frequently subject to FDA regulation. The regulatory status of the end product resulting from a manufacturing process, such as a pharmaceutical, does not transform a manufacturing apparatus into a medical device. The LYOGUARD Tray is neither classified nor regulated as a medical device, and thus is not subject to FDA regulation.

3. Material Master File Statement

Although LYOGUARD trays are not subject to FDA regulation, a Type II material master file has been submitted to the FDA to be referenced as needed for new drug manufacturing submissions. Upon request, W. L. Gore & Associates, Inc. may provide written permission to reference the material master file with the FDA.

4. Chemical Compatibility

All product contact surfaces are composed of polytetrafluoroethylene or polypropylene. Both polymers are highly chemically inert and have a high degree of compatibility with a variety of fluids. As with other processing aids, the user, who is most knowledgeable about the formulation of the product, is responsible for ensuring the compatibility of his/her formulation with LYOGUARD trays.

Copyright 2004 by Marcel Dekker, Inc. All Rights Reserved.

B. Quality Testing

1. Visual Inspection

LYOGUARD trays are 100% inspected for defects in manufacture and visible contamination.

2. Manufacturing Integrity Testing—Leak Test Method

A representative sample of each lot of LYOGUARD trays is integrity tested using a leak test method developed by W. L. Gore and Associates, Inc. The leak test challenges LYOGUARD trays with water filled to a head pressure of 0.5 PSI. After the LYOGUARD tray is filled, it is inspected for leaks. Since this test is destructive in nature, LYOGUARD trays are sampled according to ANSI/ASQC Z1.4.

3. Correlation of Leak Test to Aerosol Challenge Test

A correlation study was performed to prove that the manufacturing integrity test for LYOGUARD trays could accurately detect small flaws and to verify that the leak test could predict the results of the aerosol challenge test.

To perform the correlation study, a total of 90 sister pairs of LYOGUARD trays were manufactured with the normal manufacturing process. Flaws were induced in 60 of those pairs to represent typical possible failure modes. Table 1 shows the breakdown of the pairs.

One of the samples from each pair was subjected the leak test. The other sample from each pair was subject to the aerosol challenge test, as follows.

4. Summary of Results

These are given in Table 2.

As expected, the good parts all passed both the leak integrity test and the aerosol challenge test.

Table 1 Correlation Study Sample Description

# of sister parts	Sample type	Flaw description
30 pairs	Good (no flaw induced)	Manufactured under normal manufacturing conditions
30 pairs	Pinhole (pinhole flaw induced)	350 μm hole through membrane barrier
30 pairs	Poor seal (seal flaw induced)	0.009 inch opening in heat seal

Copyright 2004 by Marcel Dekker, Inc. All Rights Reserved.

Table 2 Correlation Study Results

	Leak test		Aerosol challenge test	
Sample type	Pass	Fail	Pass	Fail
Good	30	0	30	0
Pinhole	1	29	26	4
Poor seal	0	30	30	0

The pinhole samples demonstrated leak failures in 29 of the 30 samples; leak failures were expected in all 30 pinhole samples. After investigation, it was discovered that a hole was not induced in the membrane barrier for the sample that passed the test. Of the 30 pinhole samples subjected to the aerosol challenge test, four samples failed, as they demonstrated growth of the indicator organism. It was expected that all 30 pinhole samples would fail the aerosol challenge test.

All 30 of the poor seal samples failed the leak integrity test, as expected. None of the 30 poor seal samples failed the aerosol challenge test. Failure of all 30 poor seal samples was expected in the aerosol challenge test.

The results of this correlation study demonstrate that the leak integrity test is more challenging test than the aerosol integrity test, a standard industry package integrity test, as it was more sensitive at detecting flaws in LYOGUARD trays.

C. USP Biological Testing

1. Biological Reactivity Tests In Vitro, USP 25 <87>

Using the USP elution test, LYOGUARD trays were tested to determine the potential for cytotoxicity. Under the conditions of the test, LYOGUARD trays were determined to be not toxic.

2. Biological Reactivity Tests In Vivo, USP 25 <88>

LYOGUARD trays were subjected to USP Class VI Plastics testing. Systemic toxicity and intracutaneous toxicity Studies used saline, alcohol in saline, polyethylene glycol, and cottonseed oil as extracting media. In both studies, the extracts did not produce a significantly greater reaction than the corresponding control extracts. The muscle implantation study was conducted on all components of LYOGUARD trays. In all cases, the microscopic cellular reaction was not significant, as compared to the negative control. LYOGUARD trays therefore meet the requirements of USP Class VI Plastics testing.

Copyright 2004 by Marcel Dekker, Inc. All Rights Reserved.

3. Bacterial Endotoxin Test, USP 25 <85>

LYOGUARD trays were tested using the Limulus Amebocyte Lysate (LAL) Kinetic–Turbidimetric Method to determine the level of USP bacterial endotoxin contamination. The test was conducted using the lysate to rinse the product contact surfaces of LYOGUARD trays. The limit of bacterial endotoxin contamination is based on the USP monograph *Transfusion and Infusion Assemblies – Implants*, USP 25 <161>. Per this monograph, the endotoxin limit is not to exceed 20 USP endotoxin units (eu) per device. LYOGUARD trays demonstrated a level of endotoxin contamination less than 20 eu per device. LYOGUARD trays meet the bacterial endotoxin limits of USP transfusion and infusion assemblies for implants.

D. USP Container Testing

1. Physicochemical Tests, Plastics, USP 25 <661>

Water Extracts. Physicochemical tests were conducted on LYOGUARD trays (see Table 3). The extracting conditions were 70°C for 24 h using USP purified water.

Under the conditions of this test, LYOGUARD trays comply with the requirements of USP physicochemical tests for plastic containers.

Expanded Extracts. There are a wide variety of solvents, with very different properties, used in pharmaceutical processing. LYOGUARD trays were tested with selected, commonly used processing solvents (Table 4).

The expanded extract study was conducted using a modified version of the USP containers, physicochemical tests for non-volatile residue and residue on ignition (Table 5).

The results of this test demonstrate levels of non-volatile residue and residue on ignition well below the limits set forth in the above USP tests, which use water as the extracting medium.

Table 3 Physicochemical Test — Water Extracts

Test	Result	USP limits
Non-volatile residue	< 1 mg	15 mg
Residue on ignition	< 1 mg[a]	5 mg
Heavy metals	< 1 ppm	1 ppm
Buffering capacity	< 1 mL	10 mL

[a]Based on non-volatile residue results.

Copyright 2004 by Marcel Dekker, Inc. All Rights Reserved.

Table 4 Physicochemical Tests — Expanded Extracts Extracting Conditions

Expanded extracts	Extracting conditions
70% isopropanol in USP purified water	50°C for 72 h
40% acetonitrile in USP purified water	50°C for 72 h
Hydrochloric acid adjusted to pH 2	50°C for 72 h
Ammonium hydroxide adjusted to pH 10	50°C for 72 h

Table 5 Physicochemical Tests — Expanded Extracts Results

Extracting medium	Non-volatile residue	Residue on ignition
USP limits	15 mg	5 mg
70% isopropanol in USP purified water	4 mg	1 mg[a]
40% acetonitrile in USP purified water	2 mg	1 mg[a]
Hydrochloric acid adjusted to pH 2	2 mg	< 1 mg[a]
Ammonium hydroxide adjusted to pH 10	4 mg	1 mg[a]

[a]Based on non-volatile residue results.

E. USP Physical Testing

1. Particulate Matter In Injections, USP 25 <778>

Microscope Particle Count Test. Particulate tests were conducted on LYOGUARD trays. Based on actual use fill volumes, testing was conducted using a rinse volume of 1.8 L of water. Since LYOGUARD trays are intended for lyophilization of bulk formulations, the results are subject to the Large-volume Injections Guidelines (Table 6).

Under the conditions of this test, LYOGUARD trays comply with its requirements.

Table 6 Particulate Test Results

	Lot #	LGT2000-091400		LGT2000-091500		LGT2000-091600	
Particle size	USP LVP limits	Average	Maximum individual	Average	Maximum individual	Average	Maximum individual
10 μm	12	< 1	1	< 1	1	< 1	< 1
25 μm	2	< 1	1	< 1	1	< 1	< 1

Units are in particles/mL.

Copyright 2004 by Marcel Dekker, Inc. All Rights Reserved.

F. Package Integrity Testing

1. Aerosol Challenge Test

The aerosol challenge test is a standard industry test used to evaluate the adequacy of packaging in maintaining a sterile barrier. An aerosolized microbial challenge with *Bacillus subtilis* var. *niger* (strain globigii) was used as the organism in testing LYOGUARD trays.

Autoclaved LYOGUARD trays were aseptically filled with 1 L of USP soybean case in digest broth (SCDB) and incubated. Samples exhibiting growth originating from the filling process were removed from the study. The samples were placed flat in the chamber ensuring that the SCDB was not in contact with the membrane barrier. A positive control was compromised and placed in the chamber. A negative control was withheld from chamber exposure.

The LYOGUARD trays were exposed to the *B. subtilis* var. *niger*. After removing the trays from the chamber, the external surfaces were decontaminated, and the trays were incubated at 37°C for 7 days. After the incubation period, the trays were inspected for turbidity, an indicator of challenge organism growth. If turbidity was noted, the organism was subjected to identification procedures.

LYOGUARD trays were challenged at a level of 2500 CFU/cm^2 to 23,800 CFU/cm^2, with the average particle size ranging from 2.1 to 2.7 μm. No growth of the indicator organism was found in any of the LYOGUARD tray samples. The positive control exhibited growth of the indicator organism but the negative control did not. The LYOGUARD trays demonstrated 100% sterile barrier properties.

2. Talc Challenge Test

The talc challenge test is a standard industry test used to evaluate the adequacy of packaging in maintaining a sterile barrier. Talc, seeded with a high concentration of *B. licheniformis* spores, was used to challenge LYOGUARD trays in a dust chamber.

Autoclaved LYOGUARD trays were aseptically filled with molten trypticase soy agar (TSA). After the media hardened, the trays were incubated to look for growth. Samples exhibiting growth, confirmed to be from the filling process, were removed from the study. The remaining samples were then placed flat in the dust chamber. The TSA was verified as not in contact with the membrane barrier during the test procedure. A positive control was compromised and placed in the chamber. A negative control was withheld from chamber exposure.

Copyright 2004 by Marcel Dekker, Inc. All Rights Reserved.

In the chamber, the LYOGUARD trays were exposed to the *B. licheniformis* contaminated talc. After removing the trays from the chamber, the exterior surfaces were decontaminated, and the trays were incubated at 35°C for 7 days. After incubation, the trays were inspected for turbidity, an indicator of challenge organism growth. If turbidity was noted, the organism was subjected to identification procedures.

The LYOGUARD trays were challenged at a level of 8.4×10^{-6} CFU/cm^2. No growth of the indicator organism was found in any of the tray samples. The positive control exhibited growth of the indicator organism but the negative control did not. The LYOGUARD trays demonstrated 100% sterile barrier properties.

III. REDUCING MANUFACTURING COSTS WITH LYOGUARD TRAYS

It is well established that product lyophilized in open trays routinely escapes into the production environment during processing. While this lost product reduces yields, it also creates a potential contamination and exposure hazard when it comes in contact with equipment surfaces and workers. In order to minimize the possibility of worker exposure and product contamination from this material, extensive decontamination measures must be taken to remove all traces of escaped product from all area surfaces between production runs, adding to the time and cost of production.

LYOGUARD trays are designed to minimize the costs of open tray lyophilization through product containment (see Picture 2). These enclosed trays utilize an ePTFE membrane vent, which blocks the migration of liquids and solids. Because product is effectively contained throughout the process, yields are increased and cleanup effort is reduced. This combination of yield increase and cleanup reduction can have a significantly beneficial impact on operating costs.

A. Variable Cost Savings from Product Containment

During the drying phase, the same forces that drive the sublimation process also blow dried product out of the open trays. Product losses of 3–5% are not uncommon and typically increase with more dilute solutions due to the greater friability of their cake structures.

During the product recovery phase, dried product can be lost due to air currents as well as due to adhesion to containers when it is transferred between tray and storage containers. These loss rates typically fall in the 3–5% range, but also can increase depending on the dried product

Copyright 2004 by Marcel Dekker, Inc. All Rights Reserved.

Picture 2 LYOGUARD trays offer many manufacturing benefits over open trays.

characteristics. Generally speaking, the lighter and more friable the dried product is, the greater the amount lost during processing.

Based on these ranges, 6–10% of a product is unrecoverable due to the open tray lyophilization process. By effectively containing product throughout the drying process, LYOGUARD trays prevent product loss, increasing yields and profitability as illustrated by the following examples.

Example 1. 100 L batch of 5% solution
Total product: 5000 g
Product value: \$5/g
Drying loss from open trays: 5%
Recovery loss from open trays: 4%

	Open tray process	LYOGUARD tray process
Drying loss	250 g	0 g
Recovery loss	200 g	50 g[a]
Total loss	450 g	50 g
Value of loss	\$2250	\$250

[a]Assumes 1% product adhesion to containers.

Per run variable cost savings due to product containment: \$2000.

Copyright 2004 by Marcel Dekker, Inc. All Rights Reserved.

Example 2. 100 L batch of 5% solution
Total product: 5000 g
Product value: \$25/g
Drying loss from open trays: 5%
Recovery loss from open trays: 4%

	Open tray process	LYOGUARD tray process
Drying loss	250 g	0 g
Recovery loss	200 g	50 g[a]
Total loss	450 g	50 g
Value of loss	\$11,250	\$1250

[a]Assumes 1% product adhesion to containers.

Per run variable cost savings due to product containment: \$10,000.

Obviously, the higher the value of the product, the greater the value of the savings. This does not mean, however, that products at the lower end of the value spectrum cannot realize significant cost reductions. In these instances, we can find reductions in fixed costs.

B. Fixed Cost Savings from Product Containment

Significant fixed cost savings are possible during the product recovery and cleanup stages of the lyophilization process. At this time, open trays are gently removed from the dryer and the dried product carefully transferred to intermediate storage containers. After transfer is completed, the trays and all facility surfaces must be carefully cleaned to ensure that all traces of product residue are removed to avoid contaminating the next production run.

1. Recovery Savings

Unlike open trays, it is possible to store dried product within LYOGUARD trays. Upon termination of the drying cycle, LYOGUARD trays filled with product can quickly be removed from the dryer, sampled, and sealed into moisture-proof overwraps for long-term storage. This option eliminates a full process step and significantly shortens the time required to empty the dryer and prepare the product for storage anywhere from 50 to 75%.

Copyright 2004 by Marcel Dekker, Inc. All Rights Reserved.

2. Cleanup Savings

As a single-use product, LYOGUARD trays eliminate the entire tray cleaning process. Additionally, the amount of time and effort required for facility cleaning is greatly reduced because product no longer comes in contact with the production area, cutting the cleanup time by roughly 50%.

3. Other Comparisons

During the filling operation, the fixed cost comparison between LYOGUARD trays and open trays is typically the same.

Generalized fixed cost comparisons of drying times are difficult as they are subject to individual product drying profiles. When LYOGUARD packaging is used, some drying cycles may be slightly extended, while others may be unaffected or even shortened. It should be noted, however, that drying cycle extensions that are encountered in a LYOGUARD tray process are usually offset by reductions in the recovery and cleanup steps so that the overall process is still shorter, or at least comparable to an open tray process.

Example 1. Allocated costs @ \$75/h/worker
Fill time: 6 h*
Dry time: 48 h
Recovery time: 8 h*
Cleanup time: 14 h*
No drying cycle extension
(*Denotes steps with three workers allocated.)

	Open tray process	LYOGUARD tray process
Filling	\$1350	\$1350
Drying	\$3600	\$3600
Product recovery	\$1800	\$900
Cleanup	\$3150	\$1575
Total allocated costs	\$9900	\$7425
Actual process time	76	63

Example 2. Allocated costs @ \$75/h
Fill time: 6 h*
Dry time: 48 h
Recovery time: 8 h*
Cleanup time: 14 h*

Copyright 2004 by Marcel Dekker, Inc. All Rights Reserved.

20% drying cycle extension
(*Denotes steps with three workers allocated.)

	Open tray process	LYOGUARD tray process
Filling	$1350	$1350
Drying	$3600	$4320
Product recovery	$1800	$900
Cleanup	$3150	$1575
Total costs	$9900	$8145
Actual process time	76	72.6

C. Additional Cost Savings

There are a number of other ways in which LYOGUARD trays can deliver additional cost savings that will vary based on individual process requirements. The following are some examples:

Product Protection: Reduced incidence of out-of-specification product due to contamination—less lost product.

Worker Protection: Reduced incidence of worker exposure to product—fewer injuries, lost workdays, and compensation claims.

Capital Avoidance: Eliminate need for use of barrier isolators.

Reduced Shipping Costs: Ship product between facilities in lightweight LYOGUARD trays rather than in heavy, breakable glass containers.

Shortened Time to Market: LYOGUARD trays are sized to fit in both development *and* production-scale dryers, simplifying process scale-up.

More Flexible Production Scheduling: By minimizing cleanup requirements and product carryover concerns, production schedules for busy equipment can be optimized.

IV. PROCESS IMPROVEMENTS RESULTING FROM LYOGUARD TRAYS

The unique design of LYOGUARD trays makes them much more than a cost-effective replacement for open trays. LYOGUARD trays also provide process options that are simply not possible with open trays. These can range from simple operator convenience to advanced processing schemes.

Copyright 2004 by Marcel Dekker, Inc. All Rights Reserved.

The following are some noteworthy examples of process improvements categorized by industry segment:

1. Diagnostics manufacturing:

   Protection and storage of high-value peptide conjugates.

2. Contract manufacturing:

   Drying, storage, and transport of customer products within same container.
   Product protection in multi-product dryers.

3. Vaccine manufacturing:

   Enable bulk drying in existing vial dryers.
   Enable formulation optimization for new delivery method.

4. Pharmaceutical R&D:

   Eliminate need for use of barrier isolator in potent product suite.
   Reduced need for specialized remediation of rinse water.

5. Biologics manufacturing:

   Product protection in multi-product dryers.

6. Pharmaceutical manufacturing:

   Stabilization and transport of product in lightweight bulk lyophilized form rather than as frozen liquid in cryogenic tanks.
   Enable multi-use of currently dedicated dryers.

While LYOGUARD trays provide benefits that can be realized by the entire industry, there are certain types of facilities and product categories where the containment and performance capabilities are especially valuable. Facility types include:

Potent and cytotoxic product facilities
Contract manufacturing facilities
Bulk oligonucleotide manufacturing facilities
Bulk peptide manufacturing facilities
Human source biologicals facilities

Product categories include:

Chemotherapeutic agents
Cytotoxics
Steroids
Hormones
Vaccines
Growth factors
Blood and plasma components

Copyright 2004 by Marcel Dekker, Inc. All Rights Reserved.

Albumins
Collagens
Peptides
Antisense oligonucleotides

A. Storing and Transporting Product in LYOGUARD trays

Long-term storage of product in open trays has never been a practical consideration in bulk drying operations. Due to the exposed design of the trays, the product must be immediately removed and transferred into intermediate containers for storage and transport, resulting in increased processing time, product loss, and opportunity for product contamination or rehydration. Because LYOGUARD trays offer a totally enclosed design that is constructed from product-friendly materials, it is now possible to eliminate this costly transfer step and store product directly inside the original drying container. This processing breakthrough is made possible by the use of simple foil pouches.

Once the drying cycle is completed, LYOGUARD trays can be removed from the lyophilizer, sampled, and quickly sealed within a preformed foil pouch. The foil pouch blocks any further vapor passage through the tray's ePTFE membrane barrier, making the trays suitable for use as storage and shipping containers. Additionally, product can be reconstituted within the trays at point of use.

This storage option has a number of advantages:

1. Reduction of the amount of time and labor required to empty the dryer and recover the dried product.
2. Reduction of the amount of product lost during post-drying transfer steps.
3. Minimization of the amount of time hygroscopic products are exposed to ambient moisture.
4. Enables product to be shipped within lightweight, shatter-proof containers rather than traditional glass containers.
5. Enables product to be maintained within the same environment throughout the entire manufacturing process, minimizing potential product contamination routes and worker and equipment exposure.

B. Throughput Improvements from LYOGUARD Trays

The following is a summary of various ways that LYOGUARD trays can boost facility throughput:

1. Elimination of product loss:

Copyright 2004 by Marcel Dekker, Inc. All Rights Reserved.

By preventing product escape during processing, yields can be increased an average of 3–5% per run.

2. Reduced cleanup enables faster dryer turnaround:

Post-drying cleanup requirements are reduced by over 50% because product no longer escapes into the dryer and processing area.

Single-use design of the trays totally eliminates open tray cleaning requirements.

Product can be stored and transported within the trays, eliminating the time-consuming transfer of dried product from trays to sealed containers. Dryers can be unloaded 75% faster.

C. Optimized Processes

Many open tray drying cycles are deliberately dried at a slow rate in order to cut down on product loss due to flyout. Because LYOGUARD trays eliminate the possibility of product flyout, users may be able to dry at a faster rate, enabling further reductions in processing times. The improved heat transfer qualities of LYOGUARD trays may make it practical to dry thicker cakes. This can boost the amount of product dried per run. Because product is safely contained, existing vial dryers can be also be used for bulk processes without risk of contamination.

V. SUMMARY: BENEFITS OF UTILIZING CLOSED-CONTAINMENT TRAYS IN LYOPHILIZATION

Given the superior performance of Gore's LYOGUARD® Freeze-Dry Trays over standard open stainless steel trays in lyophilization of pharmaceuticals, processors throughout the industry can realize significant improvements in freeze-drying results and major savings in overall processing costs by utilizing such a product. Specifically, companies can boost facility throughput by the elimination of product loss, the reduction in cleanup, and in the optimization of their overall lyophilization processes.

Just by the physical process of freeze-drying a product in a closed container, companies can easily realize an average increase in yield of 3–5% per run simply by preventing product escape during processing. This elimination of product loss also results in significantly reduced cleanup times, enabling much faster dryer turnaround. Post-drying cleanup requirements are reduced by more than 50% because product no longer

Copyright 2004 by Marcel Dekker, Inc. All Rights Reserved.

escapes into the dryer and processing area, and the single-use design of LYOGUARD trays totally eliminates open tray cleaning requirements. Further, product can be stored and transported within the trays which are subsequently sealed in high moisture barrier foil pouches, thus eliminating the time-consuming transfer of dried product from trays to sealed containers.

Our testing also showed that use of the LYOGUARD trays can result in an optimized lyophilization process. Many open tray drying cycles are deliberately done at a slow rate to cut down on product loss due to flyout. Because closed freeze-dry trays eliminate the possibility of product flyout, users may be able to dry at a faster rate, enabling further reductions in processing times. And the improved heat transfer qualities of LYOGUARD trays may make it practical to dry thicker cakes, boosting the amount of product dried per run. Additionally, because product is safely contained, existing vial dryers can also be used for bulk processes without the risk of contamination.

LYOGUARD trays can be used throughout the drug manufacturing process, from formulation R&D and clinical manufacturing to full-scale production. In addition, the multifunctional package design provides convenient handling, storage, and transport and permits sterilization by steam autoclave or vaporous hydrogen peroxide (VHP). LYOGUARD trays are compatible with most lyophilization processes, and require no modification of existing equipment.

A. About the Manufacturer

W. L. Gore & Associates, Inc. is global solutions provider, specializing in the application of fluoropolymer technologies. Best known for its GORE-TEX® fabric and GLIDE® dental floss, Gore also leads technical innovation in the fields of chemical processing, medical implants, and microfiltration. The company posts $1.4 billion in annual sales from its 45 worldwide offices, with headquarters in Newark, Delaware, USA.

W. L. Gore & Associates
401 Airport Road
P.O. Box 1550
Elkton, MD 21922-1550, USA
Phone: 1-800-368-4673

Copyright 2004 by Marcel Dekker, Inc. All Rights Reserved.

13

Regulatory Control of Freeze-Dried Products: Importance and Evaluation of Residual Moisture*

Joan C. May
Center for Biologics Evaluation and Research, Food and Drug Administration, Rockville, Maryland, U.S.A.

I. INTRODUCTION

The residual moisture content of the freeze-dried biological product is usually near 1.0% (wt/wt) to 3.0% (wt/wt). Optimum residual moisture limits are set for each freeze-dried biological product on a case-by-case basis. Residual moisture limits for the freeze-dried product are supported with stability data that demonstrate that at the recommended moisture level the safety, purity, and potency of the product is maintained throughout the product's dating period. The Center for Biologics Evaluation and Research of the U.S. Food and Drug Administration (FDA) regulates freeze-dried biological products in its section pertaining to residual moisture as published in Title 21 of the Code of Federal Regulations for Food and Drugs. The regulation requires that each lot of dried product be tested for residual moisture and meet and not exceed established limits as specified by an approved method on file in the product license application. Specific information about test methods and illustrative residual moisture limits for

*This chapter was done in the author's professional capacity but does not necessarily express the opinion of the U.S. Food and Drug Administration.

Copyright 2004 by Marcel Dekker, Inc. All Rights Reserved.

vaccines and biological product is addressed in the Center for Biologics Evaluation and Research Guideline for the Determination of Residual Moisture in Dried Biological Products. Many recent articles report studies that have focused on residual moisture as it relates to potency, formulation, aggregation, and container closure and stopper considerations. Methods used for the measurement of residual moisture in the freeze-dried final container include the traditional loss on drying, Karl Fischer, and gas chromatographic methods as well as recent advances in coulometric Karl Fischer methods, thermogravimetry, and thermogravimetry/mass spectrometry. Special applications for near-infrared reflectance spectroscopy and tritium isotope methods are described. Recent advances in vial headspace moisture methodology (vapor pressure moisture) research have the potential to shed light on moisture and processes occurring within the freeze-dried vial over time, e.g., redistribution of moisture between container closure, container headspace, and freeze-dried cake. In addition, there is the redistribution of moisture between surface moisture and bound water in the various chemical constituents such as protein and hydrated salts in the freeze-dried cake.

A. Residual Moisture

Residual moisture is the low level of water, usually in the range of less than 1–3% (wt/wt), remaining in a freeze-dried product after the freeze-drying (vacuum sublimation) process [1–5] is complete. Nail and Johnson [6] have described in-process methods to monitor the endpoint of freeze-drying using residual gas analysis, pressure rise, comparative pressure measurement, and product temperature measurement. Roy and Pikal [7] used and electronic moisture sensor inside the lyophilization chamber. Residual moisture [8] content is important in the final freeze-dried product because it affects the potency of the product, its long-term stability, and the official shelf-life of the product.

Examples of freeze-dried biological products (Figure 1) include yellow fever vaccine, thrombin, BCG vaccine, intravenous immune globulin, α-interferon, measles virus vaccine live, antihemophilic factor (human), honey bee venom allergenic extract, streptokinase, and meningococcal polysaccharide vaccine groups A and C combined. These freeze-dried products could contain live bacteria, attenuated virus, or therapeutic proteins. The final container could be a single-dose or multidose glass vial with a rubber container closure or a flame-sealed glass ampoule.

The freeze-dried product contains the freeze-dried biological material, residuals of the manufacture of the product such as buffer, and any excipient such as lactose, sucrose, mannitol, sodium chloride, or sorbitol that has been

Copyright 2004 by Marcel Dekker, Inc. All Rights Reserved.

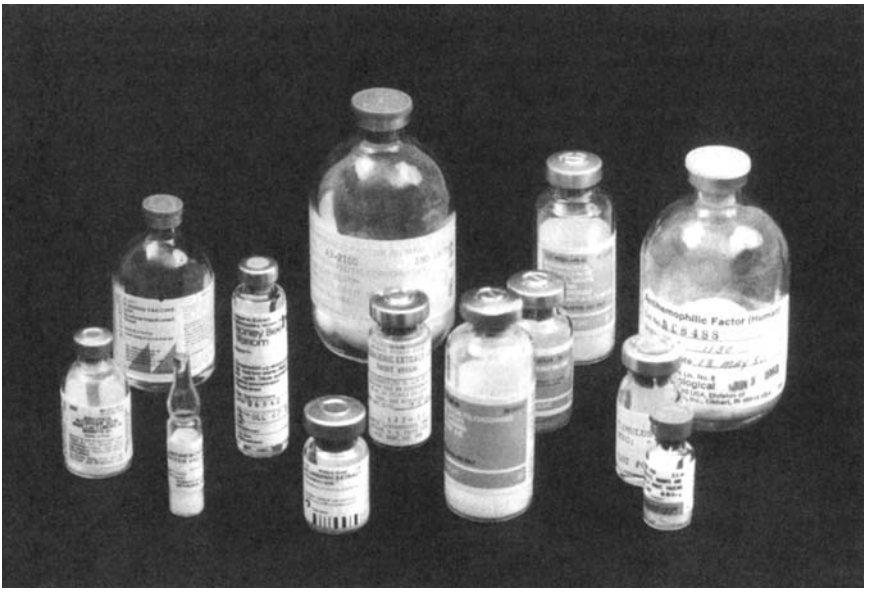

Figure 1 The variety found in freeze-dried final containers includes flame-sealed glass ampoules and many sizes of glass vials with container closures.

added to the product to optimize the freeze-drying process and protect product potency. The types of water present in the freeze-dried product cake may be different for each product depending on the residuals of manufacture and the excipients present; the water could be surface water, bound water, or trapped water.

The levels of residual moisture in the biological products should be low and optimized so that, depending on the type of biological product, properties such as the viability, immunological potency, and integrity of the product are retained over time. Final overdrying could kill living cells [9–12]. If the level of water remaining in the freeze-dried product is not enough, the excess water may promote structural changes in protein molecules which in turn may alter the product's immunological properties or foster heat instability. Optimum residual moisture limits are set for each freeze-dried biological product on a case-by-case basis. Residual moisture limits for the freeze-dried product are supported with stability data that demonstrate that at a certain moisture value the safety, purity, and potency of the product are maintained throughout the product's dating period. Potency and residual moisture are monitored when freeze-dried product stability is being determined.

Copyright 2004 by Marcel Dekker, Inc. All Rights Reserved.

B. Regulations

Freeze-dried biological products are regulated by the specification for residual moisture that is contained in the Code of Federal Regulations [13] revised in 1990. The specification states that:

> 21 CFR 610.13 (a) Purity
> "Each lot of dried product shall be tested for residual moisture by an approved method on file in the product license application."

A guideline [14] is available that summarizes pertinent technical considerations. Prior to 1990, in the previous regulation [15], the gravimetric or loss-on-drying moisture method was described and specified as the method to be used with limits obtained by the gravimetric method listed for several products. The regulation was very specific. It stated:

> 21 CFR 610.13 Purity
> "Products shall be tested as provided in paragraphs (a) of this section
> (a) Test for residual moisture. Each lot of dried product shall be tested for residual moisture and other volatile substances.
> (1) Procedure. The test for dried products shall consist of measuring the maximum loss of weight in a weighed sample equilibrated over anhydrous phosphorus pentoxide at a pressure of not more than 1 mm of mercury, and at a temperature of 20° to 30°C for as long as it has been established is sufficient to result in a constant weight.
> (2) Test results, standards to be met. The residual moisture and other volatile substances shall not exceed 1.0 percent except that, (i) they shall not exceed 1.5 percent for BCG Vaccine, (ii) they shall not exceed 2.0 percent for Measles Virus Vaccine Live, Measles Live and Smallpox Vaccine, Rubella Virus Vaccine Live, and Antihemophilic Factor (Human); (iii) they shall not exceed 3.0 percent for Thrombin and Streptokinase, and (iv) they shall not exceed 4.5 percent for Antibody to Hepatitis B Surface Antigen for the Reverse Passive Hemaglutination Test."

Alternate methods [16] to the gravimetric moisture method could be used if appropriate comparative data were submitted to the FDA showing the alternate method to be equal or superior to the gravimetric method.

The gravimetric method most accurately measures surface moisture and loosely bound waters of hydration. Changes in technology prompted the change in the FDA regulation. The Karl Fischer, gas chromatographic, and thermogravimetric moisture methods are rapid tests and are preferred by testing laboratories. Evaluation is required as these methods may measure not only surface moisture but bound water. This fact has led to different moisture limits by different moisture methods [17].

Copyright 2004 by Marcel Dekker, Inc. All Rights Reserved.

C. Recently Reported Studies Focused on Residual Moisture and Its Relation to Potency, Formulation, Aggregation, and Container Closure/Stopper Considerations

1. Product Potency and Residual Moisture

Evidence continues to accumulate in the literature attesting to loss in product potency or activity associated with elevated moisture content in freeze-dried products.

Of particular interest is work by Pitombo et al. [18]. They studied the effect of moisture content on the invertase activity of freeze-dried *S. cerevisiae* with respect to monolayer moisture content. Samples with water activity above the monolayer moisture content lost at least 60% of their invertase activity; samples with water activity at about the monolayer moisture content retained at least 85% of their original invertase activity.

Ford and Dawson [19] used alkaline phosphatase as a model and found that alkaline phosphatase activity decreased with increasing moisture content. The study involved treated stoppers, flame-sealed glass ampoules, and untreated rubber stoppers. The lowest alkaline phosphatase activity was found in vials with untreated stoppers and relatively high moisture content. The moisture appeared to have originated from the stopper.

Bell et al. [20] found, via differential scanning calorimetry, that the denaturation temperature of lyophilized bovine somatotropin and lysozyme decreased, and therefore stability decreased, with increasing moisture content. The denaturation temperature decreased with increasing moisture irrespective of the excipient. The magnitude of the decrease in denaturation temperature was, however, dependent on the type of excipient.

Herman et al. [21] found that increased water content in the microenvironment of freeze-dried methylprednisone sodium succinate decreased the glass transition temperature of the amorphous phase, resulting in an increased rate of decomposition reaction.

Other articles have stressed the importance of residual moisture content. Oliyai et al. [22] evaluated the chemical stability of an Asp-hexapeptide (Val-Tyr-Pro-Asp-Gly-Ala) in lyophilized formulations as a function of multiple formulation variables, including pH, temperature, moisture content, and amorphous or crystalline bulking agent. Analysis-of-variance (ANOVA) calculations of the main effects indicated that while the influence of pH of the starting solution was not statistically significant, residual moisture level, temperature, and, especially, type of bulking agent had a significant impact on the solid state chemical reactivity of the hexapeptide. Furthermore, residual moisture level and temperature could be important stability variables depending on the type of excipient used.

Copyright 2004 by Marcel Dekker, Inc. All Rights Reserved.

Oliyai et al. [23] studied an Asn-hexapeptide (Val-Tyr-Pro-Asn-Gly-Ala) in lyophilized formulation as a function of pH of the bulk solution, temperature, and residual moisture content in a factorial study. A statistically significant two-factor interaction indicated that the pH of formulation solution determined the extent to which this peptide stability depends on moisture level and temperature.

Chang and Fischer [24] developed an efficient single-step freeze-drying cycle for protein formulations, namely, human interleukin-1 receptor antagonist (rhIL-1ra) formulations. The process resulted in successful drying of 1 ml of rhIL-1ra formulation to 0.4% moisture content within 6 h.

Adams and Irons [25] freeze-dried the enzyme *Erwinia caratovora* L-asparaginase assessing criteria of dried cake appearance, moisture content, or ease of reconstitution.

Baffi and Garnick [26]

> considered 'the most common modes of degradation to evaluate the stability of'' proteins... to be ''oxidation, deamidation, aggregation, disulfide rupture and rearrangement, and fragmentation'' ...caused by exposing candidate lyophile to ''heat, light, agitation or freeze-thaw'' cycle... ''Oxidation may be detected by reversed-phase high-performance liquid chromatography (RP-HPLC), hydrophobic interaction chromatography (HIC), or peptide mapping. Deamidation ...detected by isoelectric focusing (IEF) or high-performance ion-exchange chromatography (HPIEC). Aggregation and fragmentation may be detected by sodium dodecylsulfate polyacrylamide gel electrophoresis (SDS-Page) or high-performance size-exclusion chromatography (HPSEC).... These methods'' are ''integrated into stability-monitoring protocols used to evaluate multiple batches of product.'' The residual moisture in the cake must be defined and controlled. ''The desired moisture level can be obtained by the development and validation of a reproducible lyophilization cycle. If the moisture level is too high, the cake'' might collapse.... ''Degradation by deamidation may continue in the presence of small traces of residual moisture. Overdrying of the protein is yet another concern. If the residual moisture is too low aggregation, inadequate reconstitution, and/or loss of activity may occur.''

Lai et al. [27] studied the mechanistic role of water in the deamidation of a model asparagine-containing hexapeptide (Val-Tyr-Pro-Asn-Gly-Ala) in freeze-dried formulations containing poly(vinylpyrrolidine) (PVP) and glycerol. Glycerol was used to vary glass transition temperature (T_g) of the formulation without any significant changing water content or activity. Residual water appeared to assist deamidation in the solid PVP formulations investigated by promoting molecular mobility, solvent/medium

Copyright 2004 by Marcel Dekker, Inc. All Rights Reserved.

interaction, and by acting as a chemical reactant in the breakdown of the cyclic imide.

2. Formulation and Residual Moisture

Pikal et al. [28] studied effects of formulation variables on the in-process and shelf-life stability of freeze-dried human growth hormone at low moisture levels. A combination of mannitol and glycine, where the glycine remains amorphous, provided the greatest protection against decomposition via methionine oxidations and asparagines deamidation and aggregation. Severe aggregation was observed at high pH.

Skrabanja et al. [29] reviewed the lyophilization of biotechnology products and emphasized that the final quality of a protein product is determined by an interplay between the proper choice of excipients and the freeze-drying process; the glass temperature that defines that state of the freeze-dried cake can be influenced by the moisture content and the choice of the excipient.

Mattern et al. [30] investigated sugar-free L-amino acid systems as stabilizers in protein formulations. Increase in moisture content during storage reduced the glass transition temperature (T_g) enhancing crystallization and decreasing protein stability.

3. Aggregation and Residual Moisture

Katakam and Banga [31] studied moisture-induced aggregation of solid state albumin and gamma globulin. Moisture-induced (2–10 μl added to 10 mg) aggregation of solid state albumin and gamma globulin was investigated by incubation at 37°C for 24 h. Aggregation was observed with increasing moisture content and was especially prominent for bovine serum albumin. When mixed with carbohydrate excipients in a 1:1 ratio, aggregation was reduced for both bovine serum albumin and gamma globulin by Emdex, dextrose, trehalose, and hydroxypropyl β-cyclodextrin excipients. The mechanism of the aggregation was indicated to be covalent linkages formed due to intermolecular thiol disulfide interchange.

Bell et al. [32] studied lyophilized recombinant bovine somatotropin (rbSt) and found an increasingly significant contribution of exothermic aggregation at higher moisture contents. In the presence of moisture they identified hydrophobic aggregation as being most prominent. In the dry state covalent modifications including polymerization into compounds of higher molecular weight were more prominent, whereas in the presence of moisture, hydrophobic aggregation was most prominent. This can be explained by the increasingly significant contribution of the exothermic aggregation at higher moisture contents.

Copyright 2004 by Marcel Dekker, Inc. All Rights Reserved.

Hekman et al. [33] linked elevated moisture content to the formation of aggregates for a conjugated IgG lyophilized with maltose and citrate buffer. The increase in molecular size was a function of both the moisture content in the vial and the amount of time for which the sample was stressed thermally. The data suggest that the increase in molecular size as a function of thermal stress is due to attachment of maltase, which is a glucose disaccharide present in the lyophile as an excipient. This degradation pathway was only observed in the lyophile.

Prestrelski et al. [34] using Fourier transform infrared spectroscopy (FTIR) and accelerated stability studies examined interleukin-2 (IL-2) with respect to pH and stabilizers that provide optimal storage stability for the lyophilized product. IL-2 prepared at pH 5 is approximately an order of magnitude more stable than at pH 7 with regard to formation of soluble and insoluble aggregates.

Pikal et al. [35] also looked at effects of moisture and oxygen on the formulation and stability of freeze-dried human growth hormone evaluating the formation of irreversible aggregates.

Prestrelski et al. [36] demonstrated that FTIR is a rapid and useful method for studying protein conformation in the dried state and can aid in determining the optimum conditions for stabilization of proteins during freeze-drying.

Dong et al. [37] indicated that a successful lyophilized protein formulation is the preservation of the native conformation in the dried solid. They used FTIR as a tool to study lyophilized-induced unfolding and aggregation of proteins, namely, through the bands at $1620\,cm^{-1}$ to $1685\,cm^{-1}$, common IR spectral features indicative of lyophilization- and temperature-induced protein aggregation, used to monitor and quantify aggregation even in the dried solid.

Lueckel et al. [38] assessed the residual moisture, glass transition temperature (T_g), and excipient physical state of different formulations in relation to the in-process and shelf-life stability of freeze-dried unterleukin-6 (IL-6). The amorphous state of the excipients and a high T_g can be considered necessary condition for preventing aggregation of freeze-dried IL-6. Sarciaux et al. [39] compared effects of buffer composition and processing conditions on aggregation of bovine IgG during freeze-drying. The data were supportive of a mechanism of aggregation formation involving denaturation of the IgG at the ice/freeze concentrate interface which is reversible upon freeze-thawing, but becomes irreversible after freeze-drying and reconstitution. Breen et al. [40] studied the effect of residual moisture in the range of 1% to 8% on the stability of a lyophilized humanized monoclonal antibody formulation. They found that high-moisture cakes had higher aggregation rates than drier samples if stored above their T_g

Copyright 2004 by Marcel Dekker, Inc. All Rights Reserved.

values. Intermediate moisture-containing cakes were more stable to aggregation than low moisture-containing cakes.

4. Container Closure/Stoppers and Residual Moisture

Pikal and Shah [41] studied moisture transfer from stopper to product and the resulting stability implications. They found that the product moisture content increases with time and reaches an apparent equilibrium value characteristic of the product, the amount of product, and the stopper treatment method.

Crist [42] studied lyophilized pharmaceuticals sealed under reduced pressure and demonstrated that vial pressure is primarily due to desorption of water vapor from the stopper into the headspace of the vial. The presence of a hydrophilic product decreases the rate of pressure rise, and pressure increases more rapidly in smaller vials. Results are discussed in terms of testing for seal integrity and for stopper effects on moisture in the product.

Pikal and Shah [43] studied intravial distribution of residual moisture in dextran, human serum albumin, and bovine somatotropin. In general, the residual moisture in the top of a core sample of the freeze-dried product was less than the moisture content in the bottom core section of the product. The section closest to the vial wall was consistently found to be lowest in moisture content.

II. RESIDUAL MOISTURE MEASUREMENT IN THE FREEZE-DRIED FINAL CONTAINER

A. Current Methods

The methods for the determination of residual moisture currently used at the Center for Biologics Evaluation and Research at the FDA are the gravimetric (loss on drying) method, the Karl Fischer method, and the thermogravimetric and thermogravimetric/mass spectrometric method. Current work in progress involves the use of vapor pressure moisture measurements to provide additional information about residual moisture content and its interaction with the components to the freeze-dried final container and its contents.

1. Gravimetric Method (Loss on Drying)

The gravimetric method measures surface moisture and loosely bound water of hydration [17]. The gravimetric method was described in the U.S. Code of Federal Regulations [15] before 1990. In the CBER/FDA laboratory the gravimetric (loss on drying) test [2,44] is performed in a humidity- and

Copyright 2004 by Marcel Dekker, Inc. All Rights Reserved.

temperature-controlled room. In actuality the room is a walk-in incubator converted to maintain the 20–25% relative humidity range and 20–25°C temperature range required by the test. The room contains a five-place analytical balance on a marble balance table, vacuum pump, Pirani vacuum gauge, hygrometer, desiccators, and sulfuric acid scrubbers for the air used to release desiccator vacuum (Figures 2 and 3). Figure 4 shows the typical dry box configuration of weighing bottle, sample vials, hygrometer, Petri dishes containing anhydrous phosphorus pentoxide to maintain a low humidity, spatula, and pliers. This equipment is necessary to perform the transfer (and pooling if necessary) of the freeze-dried sample from the vials. The dry box and its contents equilibrate for over 3 h to ensure that the phosphorus pentoxide has absorbed excess moisture and dried the box as indicated by the portable hygrometer in box. Sample is transferred from the vials to the preweighed weighing bottles. The weighing bottles plus sample are capped, removed from the dry box, weighed on the five-place Mettler balance, and placed in a desiccator containing anhydrous phosphorus pentoxide. The weighing bottle tops are opened and the desiccator is closed. A vacuum of less than 1 mm Hg measured by the Pirani gauge is drawn on the desiccator by the vacuum pump. The desiccator is sealed and remains in the controlled room for 3 days. At that time the desiccator vacuum is released by allowing air to enter after passing through three gas-washing bottles filled with concentrated sulfuric acid, which removes water from the air. This process takes approximately 1.5 h. The desiccator is then reopened, and the weighing bottles are capped and reweighed. The loss in sample weight divided by the initial sample weight and multiplied by 100 yields the percent moisture (wt/wt) in the original sample.

2. Karl Fischer Method

Iodine in the presence of pyridine, sulfur dioxide, and methanol reacts quantitatively with water, Karl Fischer [45] developed this quantitative method for water determination [46] in 1935. In the coulometric method iodine is electrically generated at the surface of the electrode emersed in pyridine, sulfur dioxide, and methanol to react with water. Coulometric Karl Fischer measurements [47] are conducted in a Plexiglas glove box that is located in a chemical fume hood. A low relative humidity is maintained in the glove box with anhydrous phosphorus pentoxide. The relative humidity is monitored by a portable hygrometer. The Karl Fischer instrument (Aquatest 8 Coulometric Moisture Analysis System, Photovolt, Indianapolis, Indiana) is placed on top of the dry box (Figure 5) to minimize corrosion of the electrical wiring. Custom elongated wires (Photovolt) connect the titration

Copyright 2004 by Marcel Dekker, Inc. All Rights Reserved.

Figure 2 Vacuum pump, Pirani vacuum gauge, and hygrometer in low-humidity room for gravimetric moisture test.

Copyright 2004 by Marcel Dekker, Inc. All Rights Reserved.

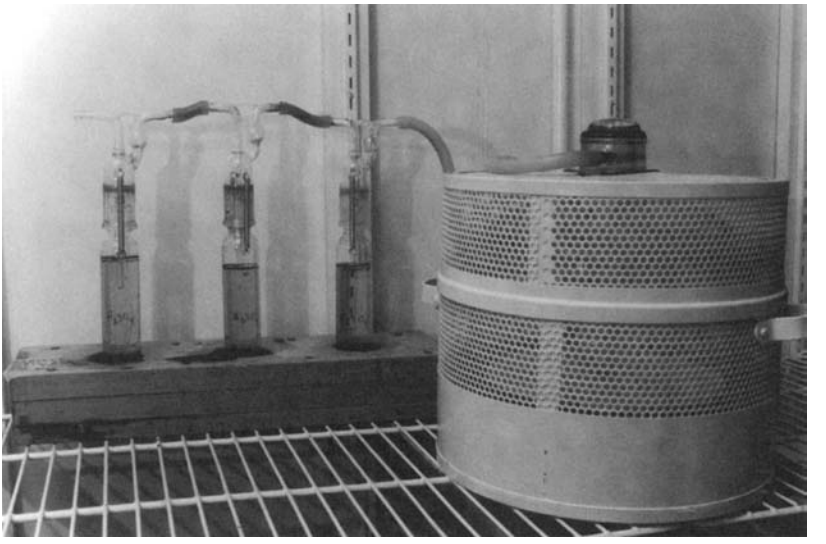

Figure 3 Desiccator in desiccator guard and sulfuric acid scrubbers to remove water from air used to release vacuum in desiccator in gravimetric moisture test.

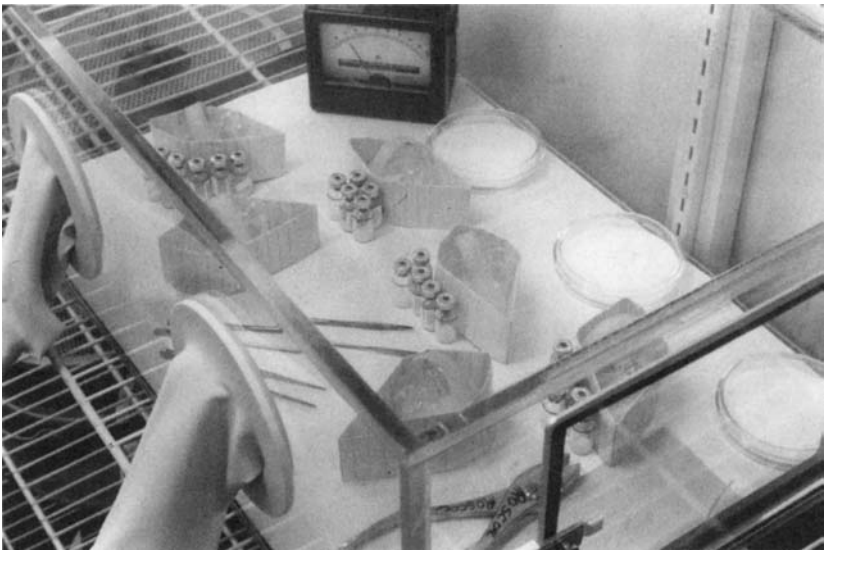

Figure 4 Dry box with sample vials, weighing bottles, hygrometer, and Petri dishes filled with anhydrous phosphorus pentoxide for sample preparation for gravimetric moisture test.

Copyright 2004 by Marcel Dekker, Inc. All Rights Reserved.

Figure 5 Karl Fischer dry box configuration with coulometric processing unit outside and titration vessels inside the dry box. Elongated wires connect the instrument to electrodes in the titration vessel in the dry box. Unit on the right uses pyridine solvent; unit on the left uses pyridine-free solvent.

vessel inside the dry box to the instrument outside through rubber-stoppered ports in the Plexiglas. Samples are vortexed to render the freeze-dried cake into a powder; vials are scraped free of labels and glue. The vial is placed inside the dry box at approximately 15–20% relative humidity and the vial's vacuum, if present, is released by quickly opening and then closing the stopper. Not releasing the vacuum could cause a significant erroneous weight due to buoyancy when the vial or ampoule contains vacuum instead of air. The vial's weight is derternined to four decimal places with a Mettler balance and then the vial is place back into the dry box. Approximately 20–30 mg of sample is poured into the pyridine-containing vessel (Figure 6) for titration after a zero microgram of water background reading is obtained by the instrument. After the sample is stirred in the vessel for 1.5 min (or another optimized time) the sample is titrated for moisture content. The instrument readout indicates the micrograms of water in the sample. The vial is reweighed to determine the exact amount of sample delivered for titration. The micrograms of water (converted to milligrams) determined by the coulometric titrator divided by the milligrams of sample multiplied by 100

Copyright 2004 by Marcel Dekker, Inc. All Rights Reserved.

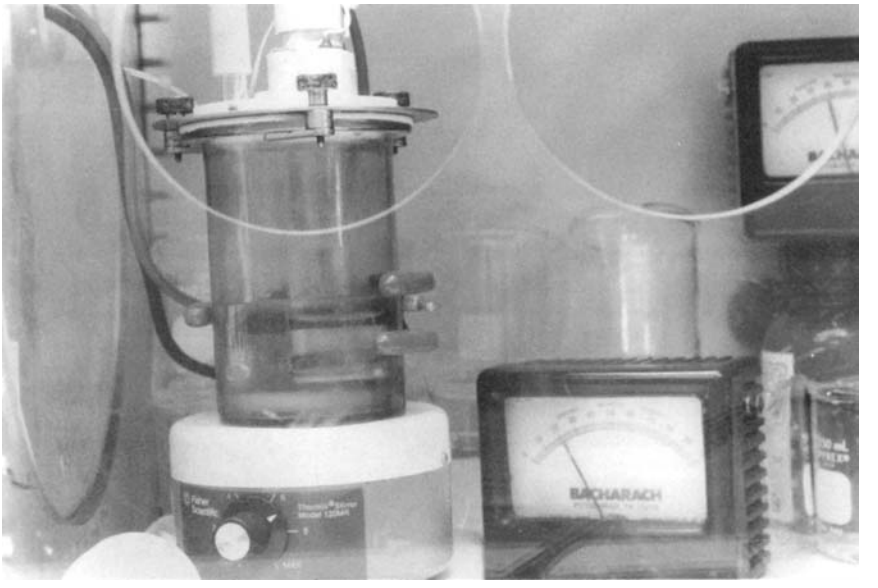

Figure 6 Close-up of Karl Fischer titration vessel containing Karl Fischer reagent, electrodes, automatic stirrer, and portable hygrometer.

yields the percent water in the sample. Standards used for this method included sodium tartrate dihydrate or known amounts of water carefully and accurately delivered into the titration solution with a microsyringe.

3. Thermogravimetry

Thermogravimetric (TG) analysis is described in the U.S. Pharmacopeia [48] as a method for the determination of the weight of a substance as a function of temperature. TG measurements for biological products [47] are carried out with the electrobalance (with furnace) (Thermal Analyst A51, TA Instruments, Wilmington, Delaware) in a Plexiglas glove box (Figure 7) at a low humidity maintained by phosphorus pentoxide and monitored by a portable hygrometer. The quartz tubes surrounding the samples and balance counter weights are painted with gold paint [17] to minimize the effect of static electricity on sample handling and the balance in the dry box. Wires connect the gold layer to the electrobalance ground (Figure 8). Pulverized samples ranging from 5 to 11 mg are placed on the TG pan for analysis. Thermograms are collected by the Thermal Analyst 2220

Copyright 2004 by Marcel Dekker, Inc. All Rights Reserved.

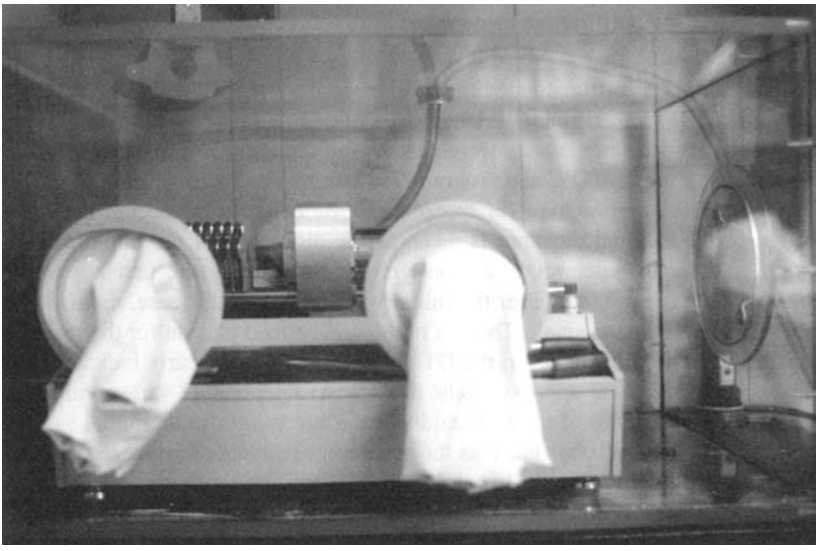

Figure 7 TG electrobalance (with furnace) enclosed in dry box/glove box maintained at low humidity by anhydrous phosphorus pentoxide.

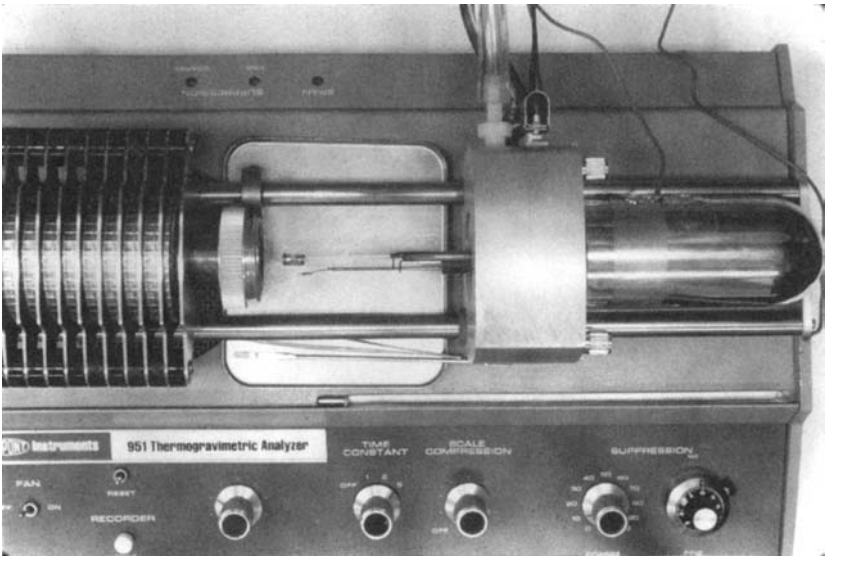

Figure 8 Close-up of electrobalance showing sample pan, gold-coated quartz tubes, thermocouple, and furnace before sample is placed on pan.

Copyright 2004 by Marcel Dekker, Inc. All Rights Reserved.

Figure 9 TG data processor displaying thermogram of sodium tartrate dihydrate standard.

(TA Instruments) with IBM Personal System 12 color display (Figure 9). The IBM LaserPrinter 10 by LexMark prints out the thermograms. In the TG profile method sample loses weight as the furnace temperature increases from room temperature to 400°C at a programmed heating rate of 20°C/min. Figure 10 shows a typical thermogram for freeze-dried varicella virus vaccine live. The weight of the residual moisture is taken as the difference of the initial sample weight and the sample weight at constant weight, usually the first horizontal plateau of the thermogram after the initial weight loss. In this case, the residual moisture weight loss is small. There is not a well-defined plateau for the residual moisture weight loss. However, the DT curve (dashed line) clearly indicates that the weight loss ends at approximately 140°C. The temperature varies with each product type. The ratio of the lost residual moisture weight to the initial sample weight multiplied by 100 is taken as the percentage residual moisture in the sample. For varicella virus vaccine live, lot A, the TG moisture result was calculated to be 0.92% (Table 1). The Karl Fischer moisture result for this lot was 0.95%. Sodium tartrate dihydrate is used as a standard. The waters of hydration, shown by well-defined plateaus, are

Copyright 2004 by Marcel Dekker, Inc. All Rights Reserved.

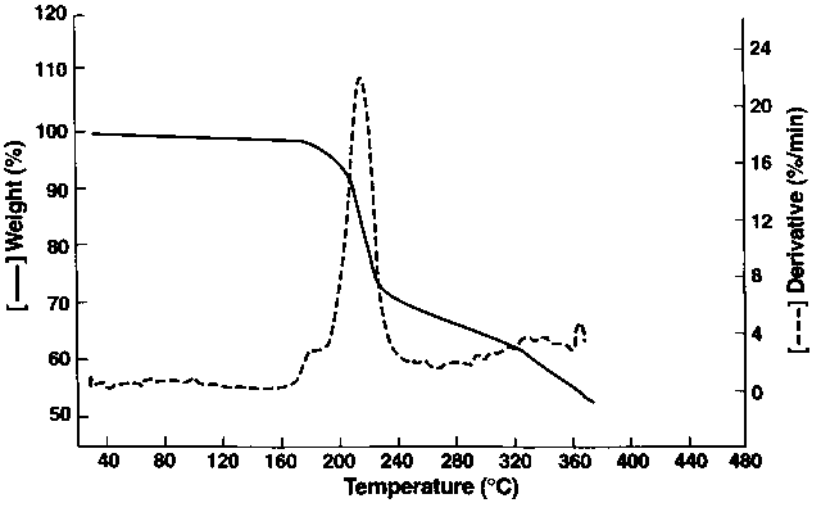

Figure 10 TG of varicella virus vaccine live.

Table 1 Thermogravimetric (TG) and Karl Fischer Residual Moisture Data for Varicella Virus Vaccine Live and Limulus Amoebocyte Lysate

	Residual moisture (%)[a]			
Sample	TG method	TG/MS method	Karl Fischer method	Relative error (%)[a]
Varicella virus vaccine live lot A	0.92 ± 0.03	—	0.95 ± 0.18	3.3
Limulus amoebocyte lysate lot A[c]	—	7.84 ± 0.22	7.97 ± 0.33[d]	1.6

[a]Arithmetic mean and standard deviation of two determinations unless otherwise indicated.
[b]Relative error from the Karl Fischer value.
[c]Moisture results are both over the 5.0% limit for this product.
[d]Arithmetic mean and standard deviation of three determinations.

measured thermogravimetrically and are accurately determined as shown in Figure 11.

4. Thermogravimetry/Mass Spectrometry (TG/MS)

When a clearly defined plateau is not in evidence for the residual moisture TG transition as is shown in the data for a limulus amoebocyte lysate (LAL)

Copyright 2004 by Marcel Dekker, Inc. All Rights Reserved.

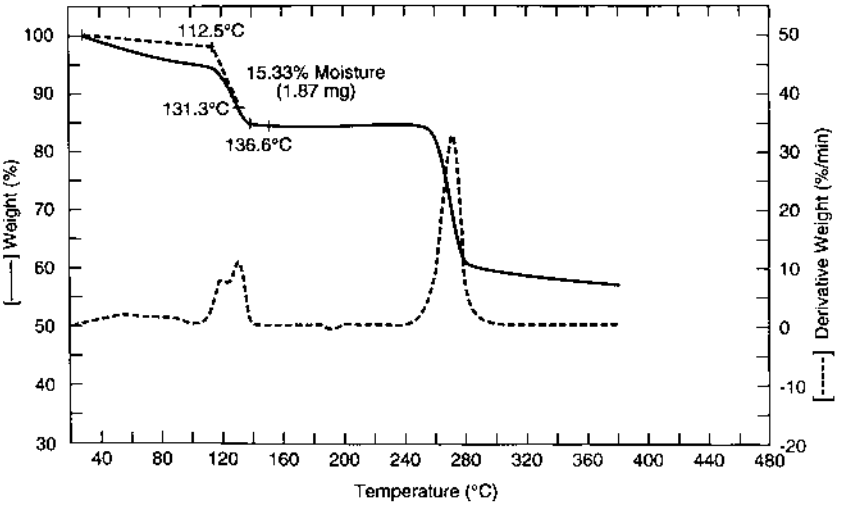

Figure 11 TG of standard sodium tartrate dihydrate.

illustrated in Figure 12, TG/MS is employed to determine the endpoint of the evolution of the residual moisture. TG/MS has been shown to elucidate the TG transitions attributable to residual moisture in freeze-dried biological products [17,47,49,50]. The combination of TG and MS has proven to be effective by providing precise TG heating conditions and weight loss information along with mass spectral identification of volatiles evolved during the weight loss process. As shown in the Figure 12 composite of TG and MS data for LAL, mass spectra are taken of the TG off-gases continuously while the weight loss and rate of weight loss (differential thermogram, or DTG) scans are recorded. The ion intensities of mass peaks 18 and 44 are monitored to show the changes in the amounts of water and carbon dioxide, respectively, in the TG off-gases. When superimposed on the respective TG data, the mass spectral ion intensities verify the transition caused by moisture in the sample by differentiating between the water content of the sample and the water evolved from thermal decomposition of the sample, which coincides with the evolution of carbon dioxide [17].

In the TG/MS data obtained for the LAL the TG curve does not display a clearly defined weight loss transition that could be attributed to residual moisture (Figure 12). The presence of carbon dioxide (shown by the ion abundance of $m/e = 44$) coinciding with the evolution of water after 260°C would indicate that the water evolved (after 260°C) resulted from

Copyright 2004 by Marcel Dekker, Inc. All Rights Reserved.

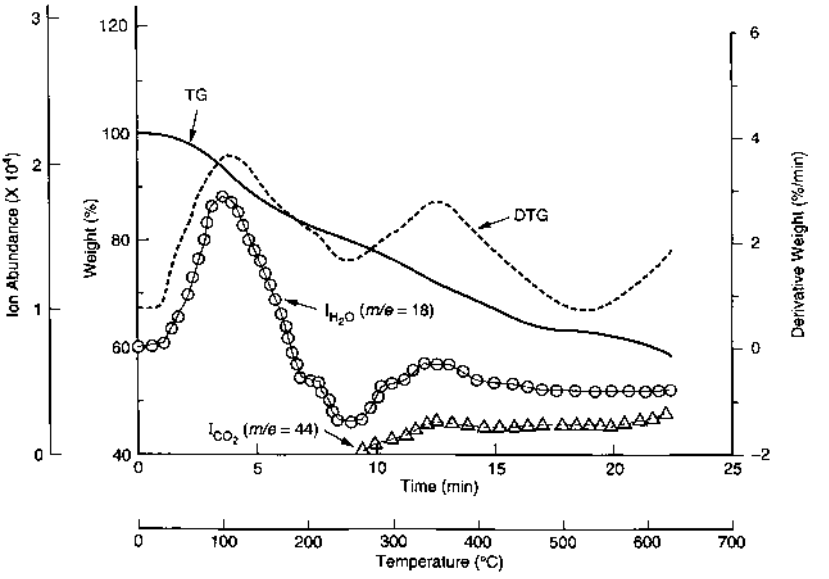

Figure 12 Plot of TG/MS data for limulus amoebocyte lysate (LAL).

sample decomposition. Since carbon dioxide is not evolved during the evolution of the first water peak, the TG weight loss attributed to residual moisture is indicated by the ion abundance for water ending at approximately 260°C. The loss in weight of LAL to 260°C is 7.84%. The LAL TG/MS residual moisture result is in close agreement with the residual moisture results obtained by the Karl Fischer method (7.97%) (Table 1). This particular lot of LAL has test results that are outside the acceptable limit of 5.0% for LAL residual moisture by both the Karl Fischer and TG methods.

Figure 13 displays the TG/MS data for U.S. standard pertussis vaccine lot 8. The TG has a well-defined plateau for the weight loss attributable to residual moisture. The DTG curve clearly indicates the end of the residual moisture evolution at approximately 160°C. The ion intensity for carbon dioxide also begins at approximately 160°C indicating that the moisture before this temperature is residual moisture, not moisture resulting from product decomposition.

Earlier TG/MS data for residual moisture in freeze-dried biological products were obtained by the continuous monitoring method of Chiu and Beattie using a DuPont 990 thermal analysis system interfaced with a glass tee to a DuPont 21-104 mass spectrometer and the methodology

Copyright 2004 by Marcel Dekker, Inc. All Rights Reserved.

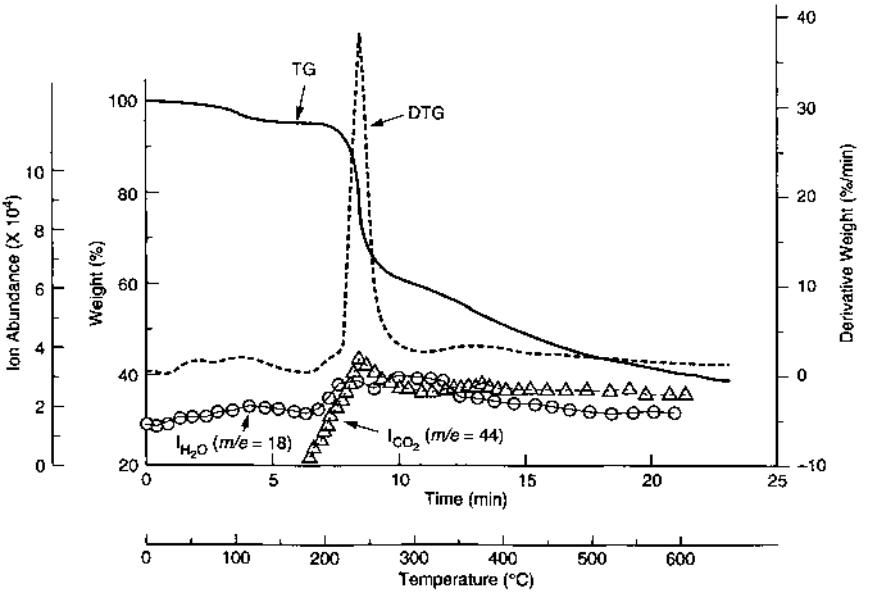

Figure 13 Plot of TG/MS data for U.S. standard pertussis vaccine lot 8.

of May et al. [49] in which a DuPont 1090 thermal analysis system was interfaced to a Hewlett-Packard 5995B quadrupole mass spectrometer. Figure 14 shows the DuPont 1090 TG analyzer (Wilmington, Delaware) and Hewlett-Packard 5995B quadrupole mass spectrometer (Rockville, Maryland) configuration in the laboratory. The TG/MS interface consists of a glass tube of 1/4 in. outer diameter that is 10 in. in length. One end connects to the TG. Swagelock connections are used in both cases. This straightforward TG/MS interface utilizes the characteristics of the jet separator to reduce TG effluent pressure) about 1 atm) to the low pressure necessary for MS operation (10^{-6} Torr). While discriminating against lower molecular weight species (helium) and therefore eliminating helium carrier gas, the jet separator increases the relative concentration of thermal decomposition products in the flow.

In current work the TA Instruments thermal analyst 220 was interfaced [46] to the Hewlett-Packard 5972 series mass selective detector (Figure 15) equipped with a hyperbolic quadrupole mass filter and vapor diffusion high-vacuum pump used in conjunction with a LaserJet 4 Plus printer. The TG analyzer's effluent tube was modified to terminate in a straight 1/4 in. OD glass tube. A 1/4 to 1/6 in. tube reducing union

Copyright 2004 by Marcel Dekker, Inc. All Rights Reserved.

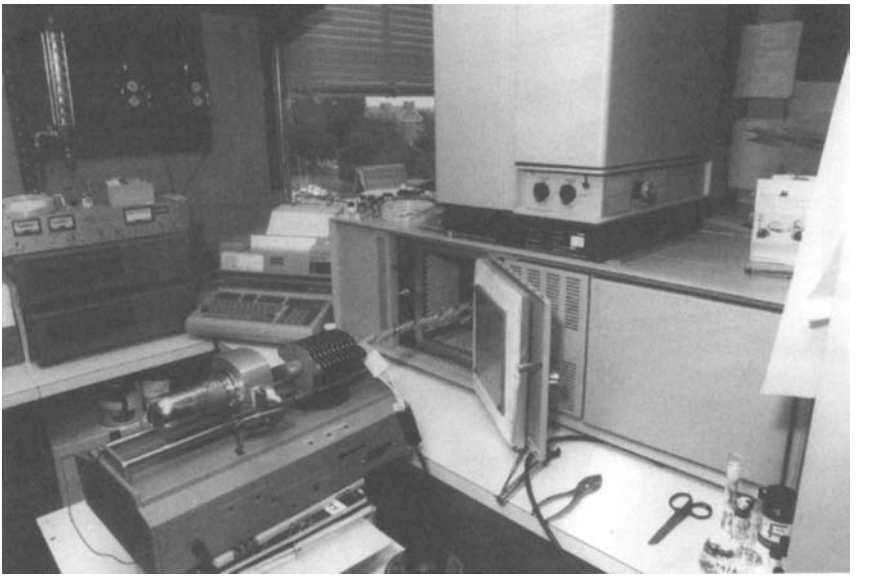

Figure 14 TG/MS-jet separator interface.

(Swagelok) was used to connect the TG effluent tube to a 0.53 mm ID fused silica capillary tube (Figure 16). An OSS-2 variable outlet splitter (Scientific Glass Engineering Pty. Ltd., Ringwood, Australia) (Figure 17) was plumbed between the TG and the mass spectrometer (Figure 18). This effluent splitter reduces the flow into the mass selective detector by venting a portion of the flow to the atmosphere. All of the O rings and connections in the TG balance were tightened so that excessive amounts of oxygen and nitrogen did not enter the system. This capillary interface allows continuous monitoring of the ion intensities of mass peaks $m/e = 18$ (water) and $m/e = 44$ (carbon dioxide). Comparable results for TG/MS plots were obtained with both interfaces indicating continuity.

5. Prevention of Sample Contamination by Ambient Humidity

The sample must be protected from contamination by ambient humidity in both the Karl Fischer and TG moisture methods as well as in the gravimetric method. This is necessary for every sample analyzed. Normally the sample is manipulated in the Karl Fischer dry box maintained at a low

Copyright 2004 by Marcel Dekker, Inc. All Rights Reserved.

Figure 15 TG/MS–capillary interface.

humidity (approximately 15–20% relative humidity) monitored by a protable hygrometer. If the sample appears to take on or give up water rapidly, the relative humidity in the dry box is lowered or raised, respectively, for the analysis. Lowering the relative humidity involves adding sufficient phosphorus pentoxide to the dry box to have the hygrometer read less than 5% relative humidity and working quickly to transfer the sample from the vial to the Karl Fischer solution to minimize its exposure. At this point the sample in question is analyzed for moisture content by the Karl Fischer method (at lower dry box relative humidity) and by the TG

Copyright 2004 by Marcel Dekker, Inc. All Rights Reserved.

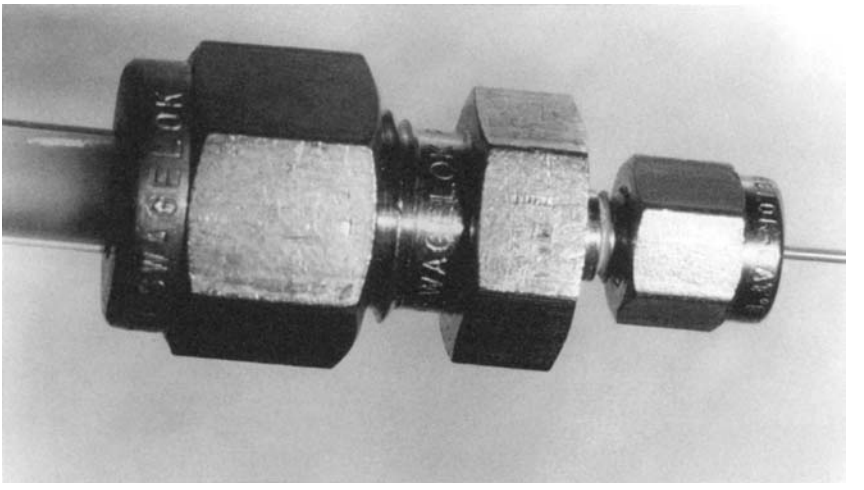

Figure 16 Capillary interface: Swagelock adapter connecting TG effluent to capillary tubing.

method. The moisture results should be in good agreement if the adjustment to the relative humidity in the dry box has successfully dealt with preventing sample contamination.

Samples with lactose as the excipient are usually run at between 0% and 5% relative humidity in the dry box. Single-dose vials containing approximately 5 mg or less per vial are pooled by consecutive delivery into the vessel solution of the contents of four or five vials.

In order to increase the accuracy and reliability or results, Karl Fischer results are usually compared to TG results. The moisture results should be nearly equivalent from these two methods since they are both measures of total bound and surface moisture in the sample cake [17]. Vial-to-vial moisture variability in the samples is usually inherent in freeze-dried samples since each vial is unique with respect to freeze-drier shelf and position on the shelf. Both the Karl Fischer and TG methods are frequently capable of measuring the moisture content of one vial and therefore vial-to-vial variability for one lot since one test requires either 20 or 5 mg of sample, respectively. For these two methods also the relative standard deviation is near 10%. Low vial-to-vial variability is produced by a well-controlled sample lyophilization process. After the freeze-drying of U.S. National Reference Preparation for α-Fetoprotein in Mid-Pregnancy Maternal Serum [51], 85 samples were chosen at random. The mean residual moisture content of the 85 samples was 0.55% with a standard deviation of $\pm 0.19\%$.

Copyright 2004 by Marcel Dekker, Inc. All Rights Reserved.

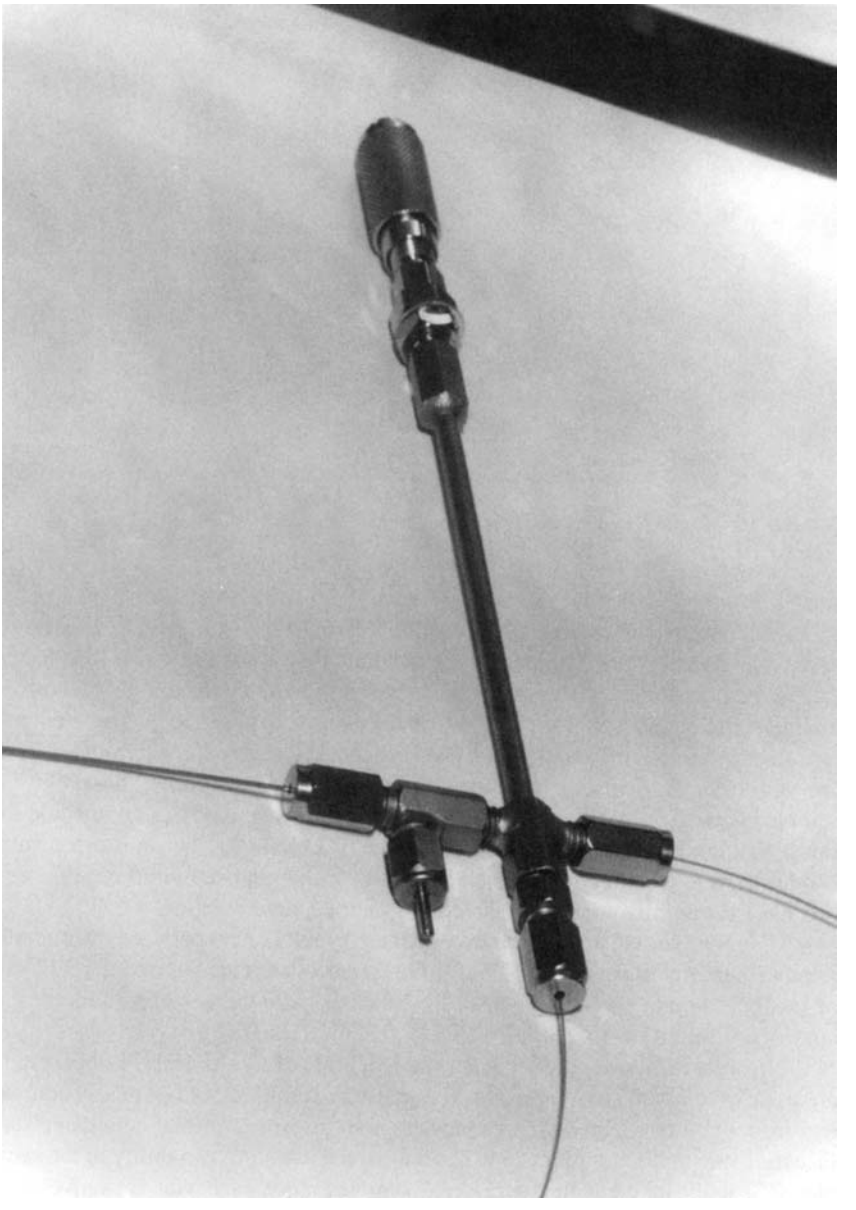

Figure 17 Capillary interface: variable outlet splitter.

Copyright 2004 by Marcel Dekker, Inc. All Rights Reserved.

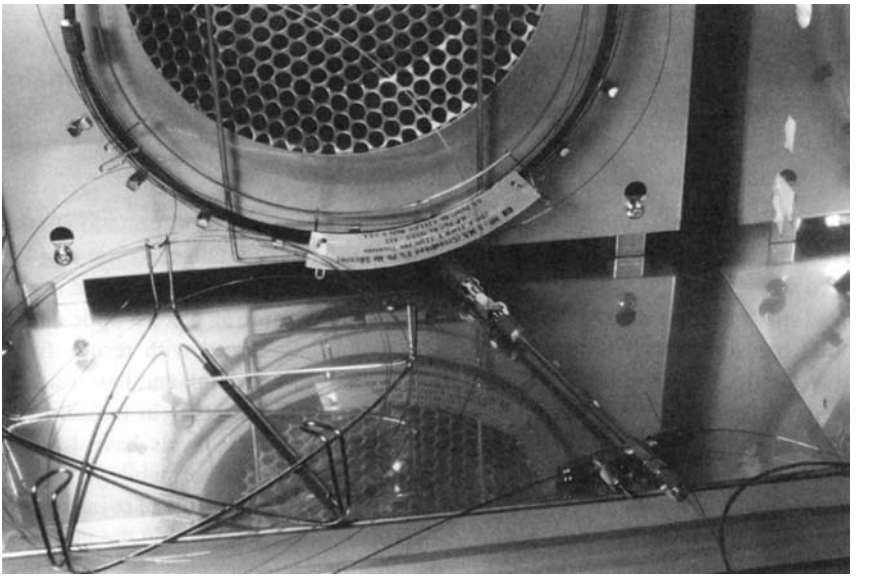

Figure 18 Capillary interface: variable outlet splitter in place in spectrometer.

These residual moisture results are illustrative of an excellently freeze-dried product with relatively low vial-to-vial residual moisture variability as determined by the Karl Fischer test method.

6. Comparative Results

Evaluation is required as the gravimetric, Karl Fischer, and TG methods may measure not only surface moisture but bound water. This fact has led to different moisture limits by different moisture methods. For example, measles virus vaccine has a limit of 3.0% by the Karl Fischer method and 2.0% by the gravimetric method. This was set by correlating the data collected from both assay methods on the some lots [17].

Gravimetric and Karl Fischer results are in excellent agreement for certain manufacturers' anistreplase, mite allergenic extract, fibrinolysin and desoxyri-bonuclease combined, and digoxin immune FAB (ovine) [14] with results in the 0.48–2.13% moisture range.

Karl Fischer and TG/MS results have been shown to be in good agreement for certain manufacturers' typhoid vaccine, meningococcal polysaccharide vaccine groups A and C combined, honey bee venom allergenic

Copyright 2004 by Marcel Dekker, Inc. All Rights Reserved.

extract, measles virus vaccine live attenuated [52], antibody to hepatitis B surface antigen, Anti-Jk[a] blood grouping serum [50], antihemophilic factor (human), and BCG TheraCys [47] in the range of 0.65–3.18% residual moisture.

7. Vapor Pressure Moisture Methodology

Vapor pressure moisture methodology has added a new piece of information to the evaluation of residual moisture in the freeze-dried final container. Rey [53] used water vapor pressure methodology to determine the moisture content of the headspace in several freeze-dried biological products using and electro-optical dew point measurement instrument (Figure 19). This information has agreed with results from gravimetric, Karl Fischer, TG, and TG/MS testing for both high and low residual moisture levels in vials. Verifying high residual moisture levels in freeze-dried biologicals

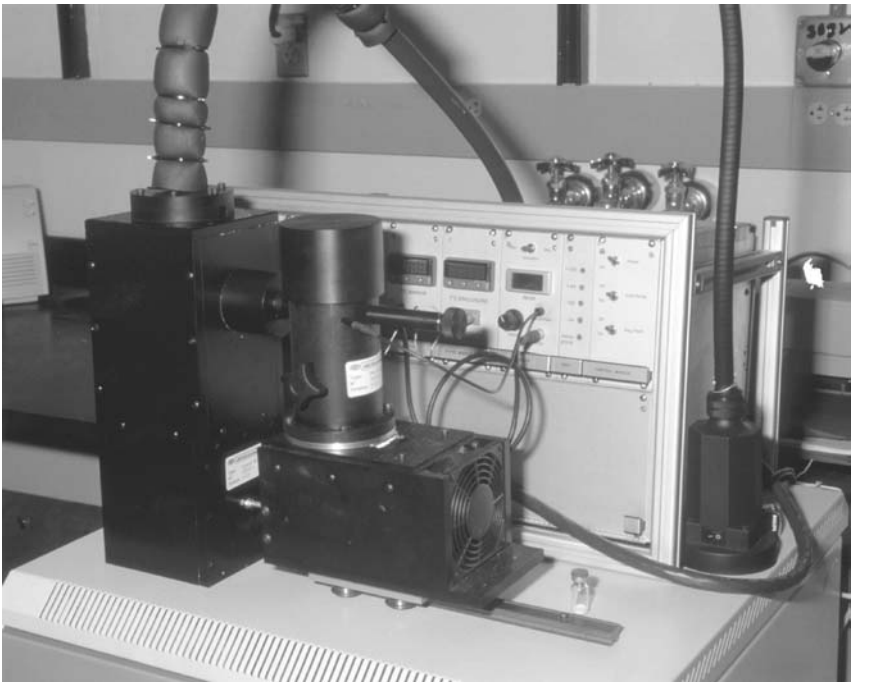

Figure 19 Instrument for the measurement of vapor pressure moisture within sealed vials (JMD Electronique, Montelier, France).

Copyright 2004 by Marcel Dekker, Inc. All Rights Reserved.

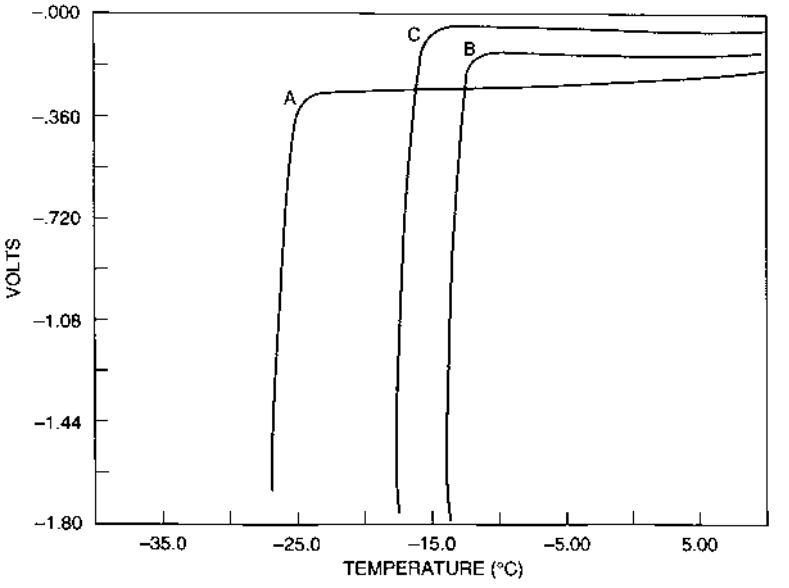

Figure 20 Vapor pressure moisture condensation temperature curves for three lots (A, B, and C) of α-interferon.

is important since excessive residual moisture levels have led to decreases in product potency and therefore decreases in product stability.

Figure 20 shows the condensation temperatures for three lots of α-interferon with residual moisture values near 1.0% (Table 2), which are within the moisture limit for the product (3.0%). The condensation temperatures are very low (between $-11.8°C$ and $-24.3°C$) and are relatively close to one another. The corresponding water vapor pressure moisture values are low, between 2.05 and 6.67 μg of water per vial, indicative of only small amounts of moisture in the vial headspace. Antihemophilic factor (Table 2) similarly has a low residual moisture (1.05%), a condensation temperature of $-42°C$, and a very low vapor pressure moisture within the vial headspace (0.2 μg water/vial). In contrast, the condensation temperature graphs for the sequence of U.S. pertussis vaccines, lots 8, 9, and 10 shown in Figure 21, show condensation temperatures near $-6°C$ and $-7°C$ for lot 8 and lot 10 and a condensation temperature near $+4.5°C$ for lot 9. This corresponds to vapor pressure moisture values of 9.5 and 10.2 μg watrer/vial for lots 8 and 10, respectively. Lot 9 has a vapor pressure moisture value of 26 μg water/vial, indicating high headspace water vapor and therefore moisture content. This agrees with the higher cake residual moisture value

Copyright 2004 by Marcel Dekker, Inc. All Rights Reserved.

Table 2 Freeze-Dried Cake Residual Moisture Values Compared to Corresponding Vapor Pressure Moisture Values and Whether the Product Met Its Dating Period Stability Requirement

Sample	Residual moisture TG method (%)	Vapor pressure moisture (μg/vial)	Stability
α-Interferon lot A	1.19	2.05	+
α-Interferon lot B	0.98	6.67	+
α-Interferon lot C	1.28	4.76	+
AHF	1.05	0.20	+
Pertussis vaccine lot 8	2.44	9.5	+
Pertussis vaccine lot 9	4.75	26	−
Pertussis vaccine lot 10	2.14	10.2	+

+, Product meets dating period requirement. −, Product does not meet dating period requirement.

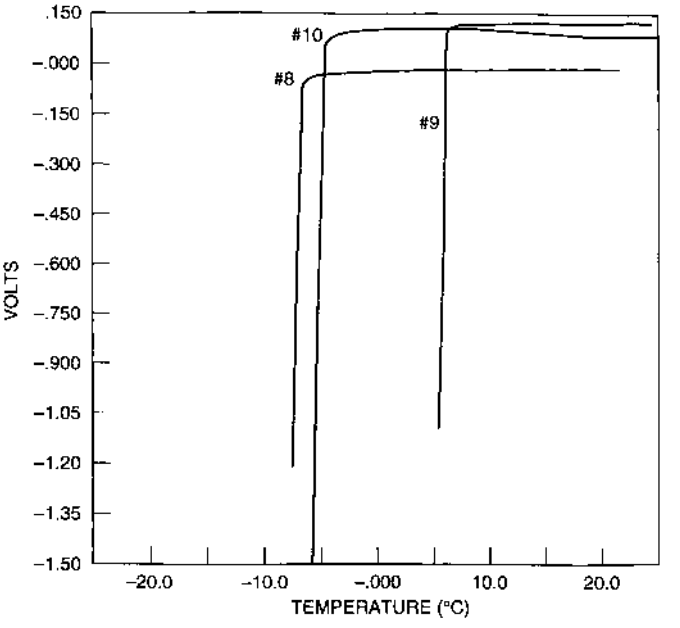

Figure 21 Vapor pressure moisture condensation temperature curves for three lots (8, 9, and 10) of U.S. standard pertussis vaccine.

Copyright 2004 by Marcel Dekker, Inc. All Rights Reserved.

of 4.75% for lot 9 compared to 2.44% and 2.14% of lots 8 and 10, respectively. These are high moisture values for both cake and headspace for lot 9. Lot 9 failed the product stability requirement. This is illustrative of high moisture values in a freeze-dried product leading to loss of product potency and therefore stability over time. This vapor pressure moisture methodology is being applied to the study of vial-to-vial variability within one lot and redistribution of moisture between cake, headspace, and stopper or headspace and cake over time.

B. Methodology in Use by Manufacturers of Biological Products

The methods approved for analyzing residual moisture in freeze-dried biological products licensed by the FDA are the gravimetric (loss on drying) method, many variations of the Karl Fischer method, thermogravimetry, gas chromatography, and a modification of the moisture evolution analyzer.

1. Gravimetric Methods

Flosdorf [1] described the gravimetric method in 1949. There are several variations on the basic gravimetric method in use. The test may be carried out in a relatively large dry box rather than in the humidity-controlled room. The sample may be heated in a drying oven. The Abderhalden method uses a small sample size and heat is provided by a refluxing solvent. The sample is dried in the Abderhalden apparatus over refluxing liquid that boils near room temperature. There are other variations in terms of time, temperature, and vacuum that have been licensed for a particular product since, on a case-by-case basis, data demonstrated that at a chosen temperature a constant weight loss was obtained without decomposing the product.

2. Karl Fischer Methods

The approved variations [14] in the Karl Fischer method include volumetric titration methods to either a visual (excess iodine or addition of an indicator) or voltametric endpoint detection method. The visual or voltametric endpoint methods usually require 30–40 mg of sample for analysis for freeze-dried biological products containing from 1.0% to 3.0% residual moisture. Coulometric Karl Fischer instruments generate the iodine from potassium iodide for water titration at the electrodes. Only 10–20 mg of freeze-dried sample is required for accurate analysis.

Methods of sample addition include the direct addition of pulverized (vortexed) freeze-dried cake to the Karl Fischer vessel solution using a

Copyright 2004 by Marcel Dekker, Inc. All Rights Reserved.

four-place analytical balance to determine the weight of the sample delivered. This is the most accurate sample addition method.

A second method involves the delivery of an aliquot of the suspension of the freeze-dried cake in a methanol solvent. The methanol solvent is usually added to the sample vial by a syringe through the stopper. The test aliquot is usually withdrawn from the stoppered vial with the syringe and delivered into the vessel solution through a stopper on the top of the vessel solution cover. This type of procedure has been operated on the open laboratory bench with the intent that the syringe and rubber closure system keeps out moisture contamination. However, the syringe volumetric delivery of a portion of the solvent-suspended cake has not yet been demonstrated to be as accurate as a four-place analytical balance determination of sample weight delivered to the Karl Fischer titration vessel for analysis. The methanol solvent that is usually used is volatile and its evaporation increases the delivery error. In addition, methanol picks up water from its surroundings. It is difficult to accurately compensate for this moisture contamination in the blank. In a similar variation the sample is titrated inside the vial using burettes with needle tips that pierce the freeze-dried final container rubber closure.

In a third variation of the Karl Fischer method a sample is heated and the evolved moisture is taken by a carrier gas from the sample to the vessel solution for titration. Careful validation data must be collected that ensure that the heating temperature does not decompose the biological material in the sample. This decomposition would evolve carbon dioxide and water. The water of decomposition would be mislabeled as residual moisture.

In order to prevent contamination of the sample and reagents by moisture in the surrounding air, the Karl Fischer apparatus is enclosed in a dry box or other apparatus. Anhydrous phosphorus pentoxide is placed in the box as a desiccant. A portable hygrometer monitors humidity in the dry box.

Both pyridine and nonpyridine Karl Fischer solvent systems are approved for licensed biological products. The major advantage of the nonpyridine solvent is that its use eliminates the hazard of pyridine fumes. The solubility properties of the two different Karl Fischer reagents are not always the same.

For a very limited number of biological product sample types the Karl Fischer method cannot be used. There may be a substance present in the product that interferes chemically with the Karl Fischer reaction such as a substance that binds iodine, or the sample may not dissolve adequately into the Karl Fischer reagent, or the sample moisture may not adequately extract into the Karl Fischer solvent.

Copyright 2004 by Marcel Dekker, Inc. All Rights Reserved.

3. Thermogravimetric Methods

Thermogravimetry has been used for measuring residual moisture in freeze-dried viral and bacterial vaccines.

4. Gas Chromatographic Methods

Robinson [54] described a gas chromatographic method for measuring residual water in freeze-dried smallpox vaccine in 1972. The method was developed to optimize quality control of a tissue-culture smallpox vaccine. Water is extracted from the sample with benzene and determined by gas chromatography with thermal conductivity (hot wire) detection and columns packed with Chromosorb 102.

5. Moisture Evolution Analyzer

The TA Instruments moisture evolution analyzer (MEA) has been adapted for use for determining residual moisture in freeze-dried allergenic extracts. Jewell et al. [55] applied the method to several allergenic extracts including freeze-dried mold, ragweed, and house dust allergenic extracts. All determinations were performed at low humidity in a controlled humidity dry box using phosphorus pentoxide as desiccant. In the MEA the sample is heated in a controlled oven. The moisture driven off by the heat applied is carried by a dry nitrogen purge gas to an electrolytic cell where it reacts with phosphorus pentoxide. The current required to regenerate the phosphorous pentoxide is converted to micrograms of water and is identified as the amount of water evolved from the sample.

III. OTHER METHODOLOGY

A tritium isotope technique and a near-infrared reflectance (NIR) technique have been reported in the literature but have not been formally approved for use a moisture methods for freeze-dried biological products.

A. Tritium Isotope

In 1973 Kassai and Sikos [56] described the determination of moisture content in freeze-dried products by tritium isotope. This method involves adding tritium oxide to 5–10 ampoules of the dissolved product in experimental lots containing 2000–8000 ampoules prior to lyophilization.

Copyright 2004 by Marcel Dekker, Inc. All Rights Reserved.

After lyophilization, the dry material is assayed for radioactivity using liquid scintillation counting and the water content is calculated. A comparison was made between the tritium method and the gravimetric method. The sensitivity of the tritium method was stated to be 1 μg of water; it measures the water content of 1 mg of dry material with an accuracy of $\pm 0.1\%$. It was noted that small amounts of tritium were found in the nontest ampoules after lyophilization. In addition, tritium oxide was used to measure the exchange of water molecules between stopper and material. Kassai and Sikos stated that "the product distributed into the vial takes up water from the stopper until a state of equilibrium ensues."

B. Near-Infrared Reflectance Spectroscopy

Last and Prebble [57] developed a near-infrared reflectance (NIR) method for the determination of moisture in an experimental freeze-dried injection product. NIR spectra were collected through the bases of unopened product vials using a horizontal instrument accessory. The samples in these vials were then used for Karl Fischer analysis to generate a standard curve for the analysis. The NIR data must be correlated with an accepted residual moisture technique in order to yield a meaningful result. This article states that NIR accuracy and precision in this application are not consistent with allowing the use of the current method in anything but a screening role.

Lin and Hsu [58] assessed the value of using NIR spectroscopy to analyze residual moisture in lyophilized protein pharmaceuticals sealed in glass vials. They found that doubling or halving the concentration of a disaccharide used as a lyoprotectant caused significant deviation between NIR and Karl Fischer data because the NIR absorbance of the disaccharide overlapped with the moisture signal.

IV. FUTURE DEVELOPMENT

The current challenges to moisture measurement include devising methods to deal with smaller and smaller sample sizes in single-dose final containers, working with samples that are very sensitive to ambient humidity even in the dry box, and understanding the interaction between water in the freeze-dried cake, the vial headspace, and the container closure, and the changes that occur over time.

Copyright 2004 by Marcel Dekker, Inc. All Rights Reserved.

REFERENCES

1. EW Flosdorf. Freeze-Drying. New York: Reinhold, 1949.
2. EB Seligmann, Jr., JF Farber. Freeze-drying and residual moisture. Cryobiology 8:138–144, 1971.
3. MJ Pikal. Freeze-drying of proteins, Part I: Process Design. BioPharm 3:18–27, 1990.
4. MJ Pikal. Freeze-drying of proteins, Part II: Formulation selection. BioPharm 4:26–30, 1990.
5. LR Rey. Basic aspects and future trends in the freeze-drying of pharmaceuticals. Developments in Biological Standardization. In: Int. Assoc. Biol. Stand. ed. Basel: Karger, 1992, pp 3–8.
6. SL Nail, W Johnson. Methodology for in-process determination of residual water in freeze-dried products. In: Developments in Biological Standards, Int. Assoc. Biol. Stand. ed. Vol. 74. Basel: Karger, 1992, pp 137–151.
7. ML Roy, MJ Pikal. Process control in freeze-drying: determination of the end point of sublimation drying by an electronic moisture sensor. J Parent Sci Technol 43(2):60–66, 1989.
8. D Greiff. Protein structure and freeze-drying: the effects of residual moisture and gases. Cryobiology 8:145–152, 1971.
9. T Nei, T Araki, H Souzu. Studies of the effect of drying conditions on residual moisture content and cell viability in the freeze-drying of microorganisms. Cryobiology 2:68–73, 1965.
10. T. Nei, H Souzu, T Araki. Effect of residual moisture content on the survival of freeze-dried bacteria during storage under various conditions. Cryobiology 2:276–279, 1966.
11. D Greiff. Stabilities of suspensions of influenza virus dried by sublimation of ice in vacuo to different contents of residual moisture and sealed under different gases. Appl Microbiol 20:935–938, 1970.
12. JD Sparkes, P Fenje. The effect of residual moisture in lyophilized smallpox vaccine on its stability at different temperatures. Bull WHO 46:729–734, 1972.
13. Code of Federal Regulations. Test for residual moisture, 21CFR610.13(a). Washington, DC: U.S. Government Printing Office 1996:56–57, 1996.
14. JC May, RM Wheeler, N Etz, A Del Grosso. Measurement of final container residual moisture in freeze-dried biological products. Dev Boil Stand 74:153–164, 1992.
15. Code of Federal Regulations. Test for Residual Moisture, 21CFR610.13(a). Washington, DC: U.S. Government Printing Office 1988:52, 1988.
16. Code of Federal Regulations. Equivalent methods and processes, 21CFR610.9. Washington, DC: U.S. Government Printing Office 1988:45, 1988.
17. JC May, E Grim, RM Wheeler, J West. Determination of residual moisture in freeze-dried vial vaccines: Karl Fischer, gravimetric and thermogravimetric methodologies. J Biol Stand 10:249–259, 1982.

Copyright 2004 by Marcel Dekker, Inc. All Rights Reserved.

18. RN Pitombo, C Spring, RF Passos, M Tonato, M Vitolo. Effect of moisture content on the invertase activity of freeze-dried S. cerrevisiae. Cryobiology 31:383–392, 1994.
19. AW Ford, PJ Dawson. Effect of type of container; storage temperature and humidity on the biological activity of freeze-dried alkaline phosphatase. Biologicals 22:191–197, 1994.
20. LN Bell, MJ Hageman, LM Muraoka. Thermally induced denaturation of lyophilized bovine somatotropin and lysozyme as impacted by moisture and excipients. J Pharm Sci 84:707–712, 1995.
21. BD Herman, BD Sinclair, N Milton, SL Nail. The effect of bulking agent on the solid-state stability of freeze-dried methylprednisolone sodium succinate. Pharm Res 11:1467–1473, 1994.
22. C Oliyai, JP Patel, L Carr, RT Borchardt. Chemical pathways of peptide degradation. VII. Solid state chemical instability of an aspartyl residue in a model hexapeptide. Pharm Res 11:901–908, 1994.
23. C Oliyai, JP Patel, L Carr, RT Borchardt. Solid state chemical instability of an asparaginyl residue in a model hexapeptide. J Pharm Sci Technol 48:167–173, 1994.
24. BS Chang, NL Fischer. Development of an efficient single-step freeze-drying cycle for protein formulations. Pharm Res 12:831–837, 1995.
25. GD Adams, LI Irons. Some implications of structural collapse during freeze-drying using Erwinia caratovora L-asparaginase as a model. J Chem Technol Biotechnol 58:71–76, 1993.
26. RA Baffi, RL Garnick. Quality control issues in the analysis of lyophilized proteins. Dev Biol Stand 74:181–184, 1992.
27. MC Lai, MJ Hageman, RL Schawen RT, Borchardt, BB Laird, EM Topp. Chemical stability of peptides in polymers. 2. Discriminating between solvent and plasticizing effects of water on peptide deamidation in poly (vinylpyrrolidone), J Pharm Sci 88:1081–1089, 1999.
28. MJ Pikal, RM Dellerman, ML Roy, RM Riggin. The effects of formulation variables on the stability of freeze-dried human growth hormone. Pharm Res 8:427–436, 1991.
29. AI Skrabanja, AL de Meere, RA de Ruiter, PJ van den Oetelaar. Lyophilization of biotechnology products. J Pharm Sci Technol 48:311–317, 1994.
30. M Mattern, G Winter, U Kohnert, G Lee. Formulation of proteins in vacuum-dried glasses. II. Process and storage stability in sugar-free amino acid system. Pharm Dev Technol 4:199–208, 1999.
31. M Katakam, KA Banga. Aggregation of proteins and its prevention by carbohydrate excipients: albumins and gamma-globulin. J Pharm Pharmacol 47:103–107, 1995.
32. LN Bell, MJ Hageman, JM Bauer. Impact of moisture on thermally induced denaturation and decomposition of lyophilized bovine somatotropin. Biopolymers 35:201–209, 1995.
33. C Hekman, S Park, WY Ten, NA Guzman, T Rossi. Degradation of lyophilized and reconstituted Macroscint. J Pharm Biomed Anal 13:1249–1261, 1995.

Copyright 2004 by Marcel Dekker, Inc. All Rights Reserved.

34. SJ Prestrelski, KA Pikal, T Arakawa. Optimization of lyophilization conditions for recombinant human interleukin-2 by dried-state conformational analysis using Fourier-transform infrared spectroscopy. Pharm Res 12:1250–1259, 1995.
35. MJ Pikal, K Dellerman, ML Roy. Formulation and stability of freeze-dried proteins: effects of moisture and oxygen on the stability of freeze-dried formulations of human growth hormone. Dev Biol Stand 74:22–38, 1992.
36. SJ Prestrelski, T Arakawa, JF Carpenter. Separation of freezing- and drying-induced denaturation of lyophilized proteins using stress-specific stabilization. Arch Biochem Biophys 303:465–473, 1993.
37. A Dong, SJ Prestrelski, SD Allison, JF Carpenter. Infrared spectroscopic studies of lyophilization- and temperature-induced protein aggregation. J Pharm Sci 84:415–424, 1995.
38. B Lueckel, B Helk, D Bodmer, H Leuenberger. Effects of formulation and process variables on the aggregation of freeze-dried interleuking-6 (IL-6) after lyophilization and on storage. Pharm Dev Technol 3:337–346, 1998.
39. JM Sarciaux, S Mansour, MJ Hageman, SL Nail. Effects of buffer composition and processing conditions on aggregation of bovine IgG during freeze-drying. J Pharm Sci 88:1354–1361, 1999.
40. ED Breen, JG Curley, DE Overeashier, CC Hsu, SJ Shire. Effect of moisture on the stability of a lyophilized humanized monoclonal antibody formulation. Pharm Res 18:1345–1353, 2001.
41. MJ Pikal S Shah. Moisture transfer from stopper to product and resulting stability implications. Dev Biol Stand 74:165–177, 1992.
42. B Crist. Time-dependence of pressure in lyophilization vials. J Pharm Sci Technol 48:189–196, 1994.
43. MJ Pikal, S Shah. Intravial distribution of moisture during the secondary drying stage of freeze drying. PDA J Pharm Sci Technol 51:17–24, 1997.
44. JC May, RM Wheeler, E Grim. The gravimetric method for the determination of residual moisture in freeze-dried biological products. Cryobiology 26: 277–284, 1990.
45. E Scholz. Karl Fischer Titration: Determination of Water Chemical Laboratory Practice. Berlin: Springer-Verlag, 1984.
46. United States Pharmacopeia/National Formulary (USP 23/NF 18) 1995. Water Determination. Rockville, MD: U.S. Pharmacopeial Convention, Inc., 1995, pp 1840–1842.
47. JC May, AV Del Grosso, RM Wheeler, N Etz. TG/MS capillary interface: applications to determination of residual moisture in BCG vaccine and other freeze-dried biological products. J Thermal Anal 49:929–936, 1997.
48. U.S. Pharmacopeia/National Formulary (USP 23/NF 18) 1995. Thermal Analysis. Rockville, MD: U.S. Pharmacopeial Convention, Inc., 1995, pp 1837–1838.
49. JC May, A Del Grosso, R. Wheeler. TG/MS interface: applications to the determination of moisture in polysaccharides and freeze-dried biological products. Thermochim Acta 115:289–295, 1987.

Copyright 2004 by Marcel Dekker, Inc. All Rights Reserved.

50. JC May, RM Wheeler, A Del Grosso. Compositional analysis of drugs and injectable biological products by thermogravimetry. In: ASTM Special Technical Publication 997. Philadelphia: American Society for Testing and Materials, 1988, pp 48–56.
51. CB Reimer, SJ Smith, TW Wells. The U.S. National Reference Preparation for Alpha-Fetoprotein in Mid-Pregnancy Maternal Serum. Clin Chem 28:709–716, 1982.
52. JC May, RM Wheeler, E Grim. The determination of residual moisture in several freeze-dried vaccines and a honey bee venom allergenic extract by TG/MS. J Thermal Anal 31:643–651, 1986.
53. L Rey. Personal communication.
54. LC Robinson. A gas chromatographic method of measuring residual water in freeze-dried smallpox vaccine. Bull WHO 47:7–11, 1972.
55. JE Jewell, R Workman, LD Zelenznick. Moisture analysis of lyophilized allergenic extracts. Dev Biol Stand 36:182–189, 1977.
56. L Kassai, K Sikos. Determination of moisture content of freeze-dried products by tritium isotope. Ann Immunol Hung 17:259–264, 1973.
57. IR Last, KA Prebble. Suitability of near-infrared methods for the determination of moisture in a freeze-dried injection product containing different amounts of the active ingredient. J Pharm Biomed Anal 2:1071–1076, 1993.
58. TP Lin, CC Hsu. Determination of residual moisture in lyophilized protein pharmaceuticals using a rapid and non-invasive method: near infrared spectroscopy. PDA J Pharm Sci Technol 56:196–205, 2002.

Copyright 2004 by Marcel Dekker, Inc. All Rights Reserved.

14

Freeze-Drying of Biological Standards

Paul Matejtschuk, Michelle Andersen, and Peter Phillips
Standards Division, National Institute for Biological Standards & Control (NIBSC), Hertfordshire, England

I. INTRODUCTION

A. Biological Medicines and Biological Standards

Biological medicines cannot be adequately characterized by physical or chemical means alone. They include bacterial and viral vaccines, blood and serum products, and other immunological, endocrinological, and cell-based medicines. Biologicals play a significant role in medicine and public health, as well as featuring in transplantation and cell therapy programs.

Many national regulatory authorities make special provisions for the control of biological medicines, reflecting their complex nature and production processes. The functional activity of biologicals in most cases cannot be determined in absolute units; it has to be measured against some reference preparation (standard) of the same material. Usually, the standard is a single large batch of well-characterized biological material dispensed into suitable containers with minimal between-container variation, stored under stable conditions prior to use. The large majority of biological standards are freeze-dried for long-term stability and ease of distribution.

The definitive reference materials for most biological medicines are World Health Organization (WHO) International Biological Standards. These international standards are the primary benchmark for the relevant biological and thus are the biological equivalent of the kilogram or meter. They were established by WHO after extensive international collaborative

Copyright 2004 by Marcel Dekker, Inc. All Rights Reserved.

studies and meet demanding requirements for consistency and stability. WHO International Biological Standards are generally assigned potency values expressed in terms of international units of biological activity. WHO International Reference Reagents are biological materials usually selected for their qualitative value and have been studied less extensively than International Biological Standards.

The WHO Expert Committee for Biological Standards (ECBS) assesses and if "appropriate" approves proposals for materials to be recognized as WHO International Biological Standards or Reference Reagents. The criteria reflect the suitability for purpose of the material, stability, reproducibility, and, if freeze-dried, the residual moisture (see Section II for details). There is no requirement for sterility but any microbial contamination should not cause interference in the assay system in which the reference material is to be used, which may include cell culture or *in vivo* assays.

The National Institute for Biological Standards and Control (NIBSC) is a UK public body reporting to the UK Department of Health. Its mission is to safeguard and enhance public health through the standardization and control of biological medicines. The provision of these standards is a central feature of the work of NIBSC [1,2].

B. Candidate Biological Standards and Reference Materials Processed at NIBSC

Most of the materials are single-batch products; indeed that particular combination of biological material and formulation may not be encountered again until the reference material is replaced. Typically, a batch comprises a 1 g fill weight of material in some 100 to 10,000 containers, usually heat-sealed, type I neutral glass ampoules, although glass vials may be used for some reference materials. In general, we process to a residual moisture of less than 1% weight of the dry weight and dispense with a coefficient of variation for dispensing of 1% or less for formulations with a plasma-like viscosity or 0.25% or less for aqueous-type materials. Table 1 shows some of the biological materials developed at NIBSC and established by WHO ECBS as International Biological Standards and International Reference Materials during the year 1999/2000 [3].

Typical biological standards are shown in Figure 1.

Typically, NIBSC distributes some 50,000 individual reference materials per year. Table 2a shows the distribution of biological reference materials across the world and Table 2b the distribution by type.

NIBSC distributes biological standards and reference materials with a "handling" charge to part-cover the costs of storage and distribution by general mail. For materials which have to be shipped by other means,

Copyright 2004 by Marcel Dekker, Inc. All Rights Reserved.

e.g., infectious materials via special carrier, this is at the cost of the requestor. Current charges and the catalog of reference materials are available from NIBSC's web site (http://www.nibsc.ac.uk).

C. Quality Management System

NIBSC processing facilities operate under a quality management system independently certified to the international standard ISO 9001. This quality system is a visible sign of NIBSC's commitment to quality for the preparation of reference materials, as is NIBSC's independent accreditation to ISO 17025 for its regulatory batch release testing of biological medicines and other related testing activities.

II. PROCESSING OF BIOLOGICAL STANDARDS

A. Requirements for Processing—Acceptance Criteria

The particular requirements for processing (e.g., batch size, fill volume, container) are agreed between the Standards Division and the responsible scientists for individual fills, prior to processing requests being accepted. The fundamental criterion is that data submitted to the ECBS demonstrate fitness for intended use. In addition, every container (ampoule or vial) should be identical, in terms of quantity, potency, composition, and stability.

The general criteria set by WHO have been published [11] although they are applied on a case-by-case basis. These criteria have been incorporated by the Standards Division into its Quality Management System (ISO 9001) and are a routine requirement for all fills undertaken. The criteria can be reduced for individual fills where they are not deemed necessary. Some examples of how these criteria are met are shown below.

WHO Criteria: "the coefficient of variation (CV) of the fill weights should be less than 0.25% for aqueous materials". Control of the variation of fill is important since a defined volume of typically water is normally used to reconstitute the freeze-dried material irrespective of the volume of material originally dispensed into that particular container. The between-container variation in fill weight must be insignificant compared to the uncertainty of the assay in which it will be used.

Within the Quality Management System, the target for variability of fill weight for a 1 ml fill of aqueous (or similar viscosity) material in ampoules is a CV of 0.25% or less; for a 1 ml fill of non-aqueous material it is 1% or less. In addition, material filled into vials has a target CV of 1%,

Copyright 2004 by Marcel Dekker, Inc. All Rights Reserved.

Table 1 Some of the Biological Materials Developed at NIBSC and Established by WHO as International Biological Standards and International Reference Materials, During the Year 1999/2000 [3]

Preparation	WHO status	Formulation	Stability (loss in activity)
Anti-pertussis serum, mouse	1st Reference Reagent 97/642	0.5 ml part purified Ig in 10% normal mouse serum in PBS	Not available
Prostate specific antigen (PSA), free	1st International Standard 96/668	2 ml fill 500 μg/l PSA 10 g/l BSA, 20 mM PBS pH 7.4	0.042% p.a. at −20°C [4]
Prostate specific antigen (PSA) (bound:free 90:10)	1st International Standard 96/670	2 ml fill 500 μg/l PSA 10 g/l BSA, 20 mM PBS pH 7.4	0.027% p.a. at −20°C [4]
Diphtheria toxoid, adsorbed	3rd International Standard 98/560	70Lf diphtheria toxoid in 1 mg aluminum salts, 10 mg trehalose, in PBS pH 6–6.5	No significant loss after 2 years at 4°C [4].
Hepatitis A vaccine, inactivated	1st International Standard 95/500	1 ml liquid containing hepatitis A antigen, medium 199, host cell protein, neomycin, formaldehyde, 2-phenoxyethanol.	Not available
Blood coagulation Factors II and X, concentrate, human	3rd International Standard 98/590	50 mM tris,10 mM trisodium citrate, 120 mM NaCl pH 7.3	0.024% p.a. at −20°C[a]
Blood coagulation Factor IXa concentrate, human, recombinant	1st International Standard 97/562	50 mM tris-HCl, 0.15 M NaCl, 5 mg/ml trehalose, 1.25% HSA pH 7.4	No loss in activity after 10 months at 37°C compared to control at −70°C[a]

Copyright 2004 by Marcel Dekker, Inc. All Rights Reserved.

Fibrinogen, plasma, human	2nd International Standard 98/612	Plasma	Not available
Tissue plasminogen activator (tPA), recombinant	3rd International Standard 98/714	20 μg/ml tPA in 5 mg/ml HSA, 60 mM sodium phosphate buffer pH 7.4	Not available
Hepatitis B virus DNA	1st International Standard 97/746	Plasma	18 months at +20°C compared to control at −20°C [6]
Insulin-like growth factor II, human, recombinant	1st Reference Reagent 96/538	4.5 mg/ml NaCl, 4 mg/ml sodium phosphate, 0.1 mg/ml Tween 20, 30 mg/ml trehalose	No significant loss after 8 months at 45°C compared to reference (−20°C) [8]
Hepatocyte growth factor/scatter factor	1st International Standard 96/564	4.5 mg/ml NaCl, 4 mg/ml sodium phosphate, 0.1 mg/ml Tween 20, 30 mg/ml trehalose	No loss in activity after 8 months at 45°C compared to reference (−20°C) [8]
Hepatocyte growth factor/scatter factor (precursor)	1st International Standard 96/556	4.5 mg/ml NaCl, 4 mg/ml sodium phosphate, 0.1 mg/ml Tween 20, 30 mg/ml trehalose	No loss in activity after 8 months at 45°C compared to reference (−20°C) [8]
Leptin, human	1st International Standard 97/594	5 μg/ml leptin in 2 mg/ml trehalose, 5 mg/ml HSA, 10 mM sodium citrate pH 5.2	No loss in activity after 349 days at 45°C compared to control at −20°C [9].
Leptin, mouse	1st International Standard 97/626	4 μg/ml leptin in 2 mg/ml trehalose, 5 mg/ml HSA,10 mM sodium citrate pH 5.2	No loss in activity after 349 days at 45°C compared to control at −20°C [9].

(*continued*)

Copyright 2004 by Marcel Dekker, Inc. All Rights Reserved.

Table 1 Continued

Preparation	WHO status	Formulation	Stability (loss in activity)
Calcitonin, salmon	3rd International Standard 98/586	30 μg/ml calcitonin 2 mg/ml mannitol, 1 mM acetic acid	No loss in activity after 8 months at 45°C compared to reference (−20°C) [10]
Interferon alpha, human leukocyte	1st International Standard 94/784	220 ng in 6-salt PBS pH 7, 6 mg HSA	No significant loss after 1.7 years at elevated temperature compared to −150°C reference[b]
Interferon omega, human	1st International Standard 94/754	165 ng in 6-salt PBS pH 7, 6 mg HSA	No significant loss after 1.7 years at elevated temperature compared to −150°C reference[b]
Interferon alpha 2a, human	2nd International Standard 95/650	250 ng in 6-salt PBS pH 7, 6 mg HSA	No significant loss after 1.7 years at elevated temperature compared to −150°C reference[b]
Interferon alpha 2c, human	1st International Standard 95/580	250 ng in 6-salt PBS pH 7, 6 mg HSA	No significant loss after 1.7 years at elevated temperature compared to −150°C reference[b]
Interferon alpha 2b, human	2nd International Standard 95/566	500 ng in 6-salt PBS pH 7, 6 mg HSA	No significant loss after 1.7 years at elevated temperature compared to −150°C reference[b]

Copyright 2004 by Marcel Dekker, Inc. All Rights Reserved.

Interferon alpha consensus, human	1st International Standard 94/786	100 ng in 6-salt PBS pH 7, 6 mg HSA	No significant loss after 1.7 years at elevated temperature compared to −150°C reference[b]
Interferon alpha lymphoblastoid n1, human	2nd International Standard 95/568	250 ng in 6-salt PBS pH 7, 6 mg HSA	No significant loss after 1.7 years at elevated temperature compared to −150°C reference[b]
Interferon alpha (leukocyte n3), human	1st International Standard 95/574	250 ng in 6-salt PBS pH 7, 6 mg HSA	No significant loss after 1.7 years at elevated temperature compared to −150°C reference[b]
Interferon alpha 1/8, human	1st International Standard 95/572	250 ng in 6-salt PBS p 7, 6 mg HSA	No significant loss after 1.7 years at elevated temperature compared to −150°C reference[b]
Chorionic gonadotrophin	4th International Standard 75/589	70 μg CG in 0.5 ml with 5 mg HSA, 445 μg NaCl, 300 μg acetic acid	No loss of activity at 4, 20, or 37°C after 23.2 years compared to −20°C reference[c]

HSA = human serum albumin, PBS = phosphate buffered saline, BSA = Bovine serum albumin, Ig = immunoglobulin, Lf = lethal units.
Unpublished data kindly supplied by [a]Elaine Gray, [b]Tony Meager, and [c]Patrick Storring, NIBSC.

Copyright 2004 by Marcel Dekker, Inc. All Rights Reserved.

Figure 1 Typical biological standards produced at NIBSC.

Table 2a Distribution of Biological Reference Materials by Geographical Area (April 1998 to March 1999)

	Reference materials distributed	
Geographical destination	Number	Percent
Europe	39,497	72.2
America	9,979	18.2
Asia	4,019	7.3
Western Pacific	764	1.4
Africa	422	0.8
Total	**54,681**	**100**

due to the lesser precision of the peristaltic pump on the vial-filling machine compared with the piston dispenser used for ampoules.

During any filling run at least 1% to 2% of the containers filled are selected at intervals for ''check weighing,'' as a measure of the variability of the material dispensed over the period of the fill. This is a limitation imposed by the practicalities of check weighing on our automated filling equipment. Table 3 shows the CV of fill weights for some of the materials established by ECBS in the year 2000.

Copyright 2004 by Marcel Dekker, Inc. All Rights Reserved.

Table 2b Distribution of Biological Reference Materials by Work Area (April 1998 to March 1999)

	Reference materials distributed	
Work area	Number	Percent
Virology, including influenza	26,603	48.7
Miscellaneous, including allergens and various sera.	14,803	27.1
Bacteriological	5,897	10.8
Endocrinological	3,540	6.4
Hematological	2,267	4.1
Antibiotics	815	1.5
Immunological	756	1.4
Total	**54,681**	**100**

WHO Criteria: "standards must be stable, it is WHO policy not to set expiry dates for International Biological Standards and Reference Reagents". Stability is determined by various factors including the intrinsic properties of the material, the moisture content of the freeze-dried material, and the oxygen and moisture content of the headspace within the container.

Since, in general, WHO standards are designed to be usable for a period of a decade or more, they are processed using heat-sealed glass ampoules (in preference to rubber-stoppered vials). These containers currently offer the most secure method of preventing ingress of moisture and oxygen. In addition, to maintain stability over long periods of time, freeze-dried materials are normally stored in the dark at $-20^{\circ}C$ until shipped.

Candidate WHO materials are subjected to accelerated degradation tests (see Section IV for further details) to predict the stability of the material at the temperature of storage. This prediction supplements real-time measurements.

WHO Criteria: "the oxygen level within the container should be less than 40 μmol/liter". Since the presence of oxygen may result in loss of activity, air must be excluded from ampoules and vials at the end of processing (after freeze-drying or further desiccation).

Vials are stoppered under vacuum or dry nitrogen to preserve the internal environment and then capped. For ampoules, flame-sealing will cause failures due to the increase in internal pressure caused by the heat from the flame. For this reason, during processing, the ampoules are fitted with a capillary labyrinth [12] and a freeze-drying stopper. The capillary labyrinth reduces the rate of uptake of air and water as the ampoules

Copyright 2004 by Marcel Dekker, Inc. All Rights Reserved.

Table 3 Residual Moisture Levels and Coefficient of Variation of Fill for Some Recently Enobled Standards

Preparation	WHO status	CV of fill weight (%)	Residual moisture content (% w/w)
Islet cell antibodies	1st Reference Reagent 97/550	0.44	1.09
Antipertussis serum, mouse	1st Reference Reagent 97/642	0.24	1.56
Diphtheria toxoid, adsorbed	3rd International Standard 98/560	0.13	1.41
Hepatitis A vaccine, inactivated	1st International Standard 95/500	Not relevant	Liquid fill
Blood coagulation factors II and X, concentrate, human	3rd International Standard 98/590	0.38	0.07 (f.d.)
Blood coagulation factor IXa concentrate, human, recombinant	1st International Standard 97/562	0.15	0.03 (f.d.)
Fibrinogen, plasma, human	2nd International Standard 98/612	0.07	0.30 (f.d.)
Tissue plasminogen activator, recombinant	3rd International Standard 98/714	0.09	1.00 (f.d.)
Hepatitis B virus DNA	1st International Standard 97/746	Not relevant	Liquid fill
Insulin-like growth factor II, human, recombinant	1st Reference Reagent 96/538	0.11	3.19
Hepatocyte growth factor/scatter factor	1st International Standard 96/564	0.18	2.92
Hepatocyte growth factor/scatter factor (precursor)	1st International Standard 96/556	0.14	2.93

Copyright 2004 by Marcel Dekker, Inc. All Rights Reserved.

Leptin, human	1st International Standard 97/594	0.08	0.33
Leptin, mouse	1st International Standard 97/626	0.11	0.36
Calcitonin, salmon	3rd International Standard 98/586	0.10	0.45
Interferon alpha, human leukocyte	1st International Standard 94/784	0.16	0.21 (f.d.)
Interferon omega, human	1st International Standard 94/754	0.21	0.18 (f.d.)
Interferon alpha 2a, human	2nd International Standard 95/650	0.12	0.17 (f.d.)
Interferon alpha 2c, human	1st International Standard 95/580	0.17	0.19 (f.d.)
Interferon alpha 2b, human	2nd International Standard 95/566	0.35	0.19 (f.d.)
Interferon alpha consensus, human	1st International Standard 94/786	0.17	0.28 (f.d.)
Interferon alpha lymphoblastoid n1, human	2nd International Standard 95/568	0.17	0.16 (f.d.)
Interferon alpha (leukocyte n3), human	1st International Standard 95/574	0.12	0.19 (f.d.)
Interferon alpha 1/8, human	1st International Standard 95/572	0.15	0.20 (f.d.)

f.d.: Processing included further desiccation.

Copyright 2004 by Marcel Dekker, Inc. All Rights Reserved.

await sealing. In addition the capillary labyrinth allows venting of the internal pressure, as the ampoule is flame sealed.

WHO Criteria: "the moisture content of the material shall be determined in order to verify that drying is adequate". If the formulation has been freeze-dried previously, the conditions required and achievable residual moisture level will be known. However, for formulations not previously freeze-dried, a series of laboratory tests and pilot studies are performed (see Section III) on the formulation. Results of these tests and trials are used to determine the most suitable freeze-drying conditions, in order to achieve the desired product including optimum residual moisture level.

As part of this development work, residual moisture is routinely measured by the Karl Fischer method (in a dry box as recommended by May et al. [13], see Section III.B), with control liquid samples of known moisture, to determine the residual moisture in the freeze-dried material. See Table 3 which shows residual moistures of some of the materials established by ECBS in the year 1999/2000, and Figure 2 which shows the reproducibility and variability of the control liquid of known moisture.

WHO Criteria: "potency tests are essential to confirm there has been no undue loss of activity/potency during processing". Following processing of the candidate materials, the responsible scientist assays the material for activity/potency. In addition, at the end of the dispensing and before freeze-drying, 'frozen baseline" samples of the material are sealed and stored at $-150^{\circ}C$ to allow comparative testing between finished freeze-dried material and frozen material, to indicate any loss of potency attributable to freeze-drying.

WHO Criteria: "full records should be kept of all procedures and tests used during processing". All materials processed are assigned a unique code used to identify the material throughout its existence. All information, including the original request, agreed criteria, documentation, anomalies in processing, and any tests undertaken, is included in a batch record referred to as the Product Record. Product Records are stored for at least the lifetime of the material.

Additional Measurements/Criteria Carried Out at NIBSC. Processing is carried out in a controlled environment with respect to temperature and environmental cleanliness. Although there is no formal specification for a maximum microbial content or sterility (materials distributed by NIBSC are not for administration to humans), a high microbial content could interfere with the final assay procedure in which the material is to be used, or cause increased degradation of the active material.

The microbial content of the bulk material is determined on arrival for processing, on samples removed during processing, and on the final product.

Copyright 2004 by Marcel Dekker, Inc. All Rights Reserved.

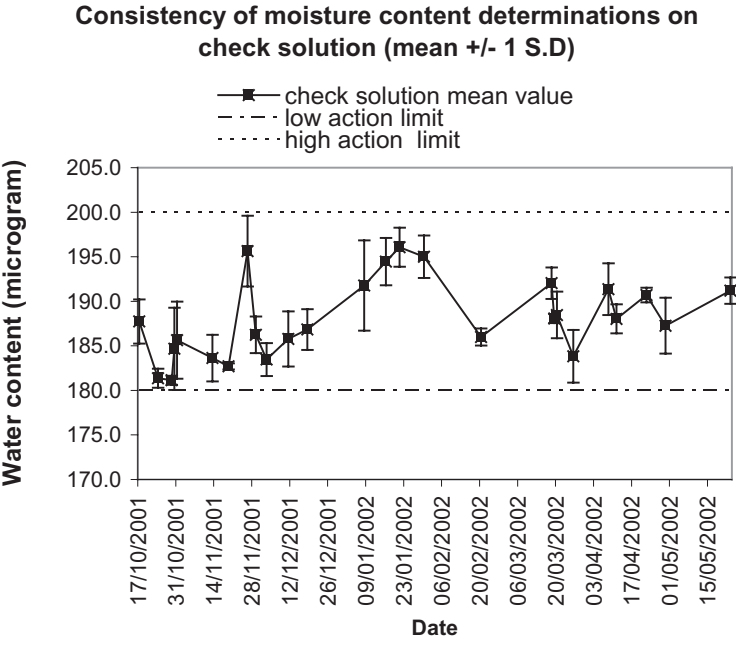

Figure 2 Consistency of moisture determination of commercially available check solution by Karl Fischer coulometric assay.

The dry weight of the freeze-dried material is measured and is compared with the expected dry weight of the material in the formulation.

The final freeze-dried material must completely reconstitute within a reasonable period (typically less than 2 min) with occasional gentle agitation.

B. Process Description

1. Equipment Used*

NIBSC has two pharmaceutical grade filling machines for different uses, a Bausch and Strobel AVF10/10 ampoule dispensing/sealing machine, and a Schubert Paxal vial dispensing/capping machine. There is also other small-scale filing equipment used for pilot studies and laboratory work.

*Note: Details of any equipment used should not be taken as a recommendation for use.

Copyright 2004 by Marcel Dekker, Inc. All Rights Reserved.

Currently, we use two production freeze-dryers, both manufactured by Serail, a CS100 (usable capacity 20,000 ampoules or 10,000 vials) and a CS15 (capacity 4000 ampoules or 1000 vials). For development work we have a laboratory-scale Virtis Genesis. We can then further dry materials at room temperature by exposure to phosphorus pentoxide under vacuum using either an Edwards Lyomax 5 freeze-dryer or a holding tank system.

We have various measuring and monitoring equipment, including balances, and temperature and vacuum measuring devices, which are used during processing to monitor the various stages of the process. All equipment has a defined maintenance and where necessary calibration program (traceable to national standards) within the Division's formal Quality Management System. In addition all critical equipment has alarms to indicate malfunction and where possible automatic reversion to conditions "safe" for the product.

2. Consumables Used

For candidate WHO standards, 5 ml, type I neutral glass, DIN ampoules are used for freeze-drying, fitted with a two part capillary labyrinth to reduce the rate of air/moisture ingress as the ampoules await sealing and to facilitate effective glass fusion, as previously described.

In addition to 5 ml DIN ampoules, various vials are also used, ranging from 5 to 20 ml with crimped, tear-off, aluminum caps.

3. Processing Environment

The environment in which materials are processed is tightly controlled in terms of temperature and microbial contamination. The microbial contamination of the environment is monitored on a weekly basis to ensure that low bio-burden conditions are maintained.

Figure 3 shows trends of results of microbial contamination testing with action and warning limits, these are used to ensure microbial contamination does not rise above the defined limits.

4. Pilot-Scale Work (see Section III)

In most cases, small-scale trials are carried out well in advance of the large-scale batch to determine the best processing conditions; this is not always necessary where past experience can be used as noted earlier.

In all cases, the results of the pilot studies and any previous batches of the same formulation are reviewed and recorded well in advance of processing the definitive batch in order to allow time for any problems or potential problems to be identified and minimized.

Copyright 2004 by Marcel Dekker, Inc. All Rights Reserved.

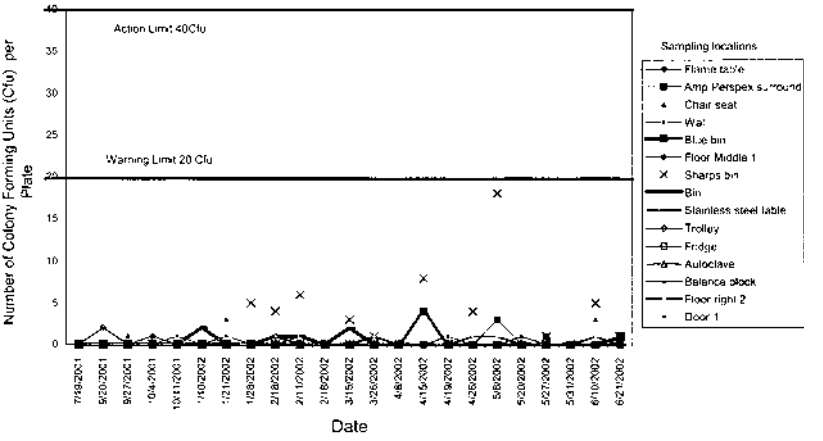

Figure 3 Environmental monitoring of filling suite showing warning and action limits (Data: J Charlton, Standards Division, NIBSC).

5. Preparation

All consumables are cleaned in a non-detergent system. Normally dilute hydrochloric or acetic acid is used for glassware and ethanol for cleaning of rubber/plastics. Freeze-drying stoppers for use with vials are subjected to a drying process to remove absorbed moisture. Prior to use, all filling vessels, tubing, and needles are autoclaved after cleaning. After washing, ampoules and vials are labeled (by ink jetting) with the unique batch code and baked in an oven. This enables them to be identified at all stages of processing prior to application of the final label. Prior to processing the bulk material is stored at the appropriate temperature using controlled, calibrated, and monitored storage facilities.

6. Dispensing

Dispensing is carried out under controlled, monitored conditions, as demanded by the material, typically 2 to 8°C, with gentle stirring. The dispensing machine is adjusted and verified to give the nominal fill weight required.

After dispensing, ampoules are individually fitted with the capillary labyrinth and freeze-drying stopper (vials are fitted with freeze-drying stoppers only) and packed into aluminum tins. They are then stored at the same temperature as required by the bulk product until the entire batch has been filled.

Copyright 2004 by Marcel Dekker, Inc. All Rights Reserved.

7. Monitoring of the Dispensing Process

The temperature of the bulk product is monitored and recorded in the Product Record during dispensing. The fill weight is monitored over the dispensing process (check weighing). Typically, the net fill weight of every 50th ampoule or vial is determined. An example of monitoring of fill weights during dispensing is shown in Figure 4.

A minimum of six of the ampoules/vials used for check weighing are marked and numbered at intervals throughout the fill to determine the dry weight (by weighing before filling and after freeze drying and/or further desiccation) of the final material. These samples are used to determine the percentage residual moisture content of the freeze-dried material by the Karl Fischer method.

Other samples are also taken during/after filling, for assessing the microbial contamination, and for conductivity or thermal analysis, to confirm results obtained in any trial/pilot studies (see Section III).

8. Freeze-Drying

The appropriate freeze-drying cycle (see Figure 7 of typical cycle), as determined previously, is selected or constructed and the freeze-dryer

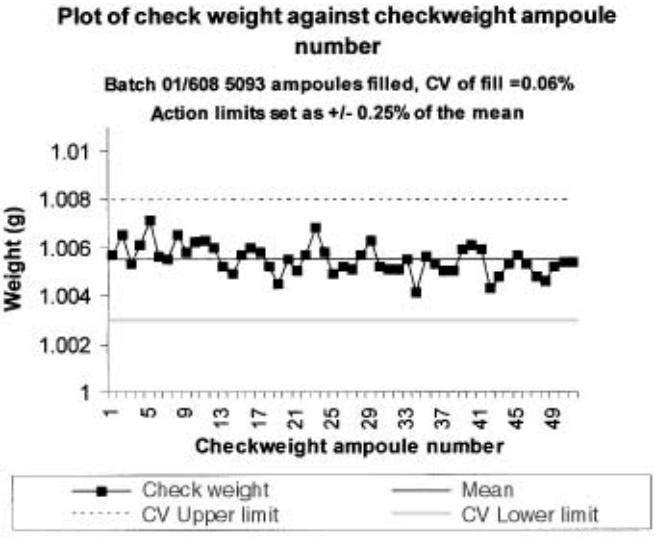

Figure 4 Consistency of fill weight across the filling process (Bausch and Strobel filling machine).

Copyright 2004 by Marcel Dekker, Inc. All Rights Reserved.

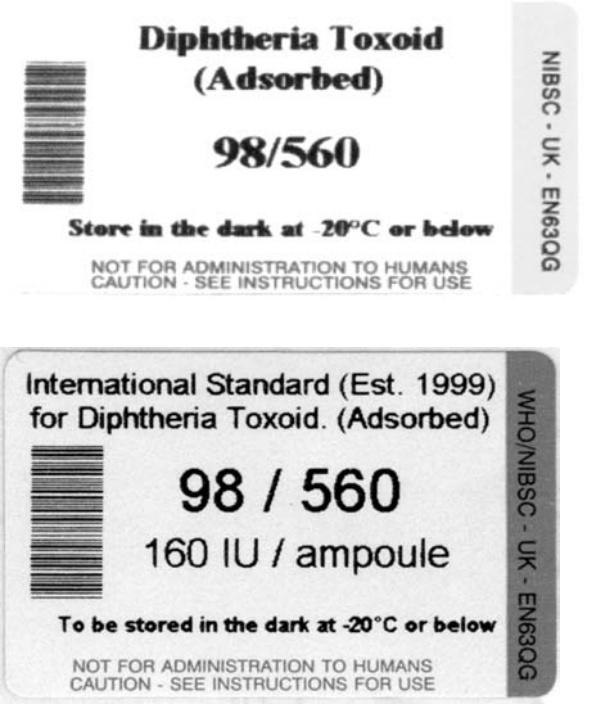
Diphtheria Toxoid
(Adsorbed)
98/560
Store in the dark at -20°C or below
NOT FOR ADMINISTRATION TO HUMANS
CAUTION - SEE INSTRUCTIONS FOR USE
NIBSC - UK - EN63QG
International Standard (Est. 1999)
for Diphtheria Toxoid. (Adsorbed)
98 / 560
160 IU / ampoule
To be stored in the dark at -20°C or below
NOT FOR ADMINISTRATION TO HUMANS
CAUTION - SEE INSTRUCTIONS FOR USE
WHO/NIBSC - UK - EN63QG

Figure 5 (a) Typical NIBSC label for a candidate reference material; (b) Typical WHO label for an endorsed International Reference material.

started. When the shelves reach the set temperature (typically either $+4^{\circ}C$ or $-50^{\circ}C$) and filling is complete, the entire batch of steel tins containing the filled ampoules/vials are loaded onto the shelves and the bases of the tins removed. The position of each tin within the freeze-dryer is recorded on the Product Record.

Resistance thermometers are inserted in one to six of the ampoules/vials (depending on the specified need) and the location of each is recorded on the Product Record. Once the temperature of the thermometers in the ampoules/vials reaches the shelf temperature, the freeze-drying cycle is started. The information gained from these thermometers is used in comparisons between batches and sometimes as an indicator as to the speed of freeze-drying, in the knowledge that the containers with the probes are not typical of the batch.

The freeze-drying parameters are continuously monitored and recorded by the freeze-dryer control system, and are checked and recorded

Copyright 2004 by Marcel Dekker, Inc. All Rights Reserved.

twice daily by the processing team to detect and deal with any deviations or potential problems. Typical parameters measured are shelf temperature, product temperature, condenser temperature, condenser and chamber vacuum; these are compared to the set points in the freeze-drying cycle used. All recordings are attached to the Product Record.

At the end of freeze-drying, the chamber is restored to atmospheric pressure with pure, dry nitrogen and the ampoules/vials are removed. The ampoules/vials are then stoppered and sealed/capped (see Section II.B.10), or if required further desiccated over phosphorus pentoxide (see Section II.B.9).

9. Further Desiccation

For materials where a very low residual moisture level is required which is not achievable by secondary drying during freeze-drying, further desiccation may be required. If this is so, the ampoules/vials are held at room temperature either in a series of tanks, or within the freeze-dryer, under vacuum with trays of phosphorus pentoxide for a period of 4 to 7 days.

10. Sealing/Capping

Ampoules and vials are stoppered, either in the freeze dryer or by hand, to preserve the internal environment prior to sealing or capping. The chamber or tank is backfilled with pure, dry nitrogen and the ampoules/vials removed for sealing/capping. It takes approximately 10–15 min to seal all ampoules from one tin, and during this time the capillary device reduces the ingress of air and moisture.

11. Leak Testing of Containers

Prior to the introduction of DIN ampoules, bespoke "test-tube" types of ampoules were used with a diameter of 10 mm. The large diameter caused some problems in sealing and therefore each batch of ampoules was tested for leaks by immersion in a dye. With the introduction of industry standard DIN ampoules, this practice continued until a review of one year's production showed no leaks had been found and the practice was no longer necessary.

12. Labeling

Generally ampoules/vials are labeled to indicate the unique batch identifier, product name, manufacturer, and storage conditions. An example of a typical label is shown in Figure 5a.

Copyright 2004 by Marcel Dekker, Inc. All Rights Reserved.

On establishment by WHO, the ampoules/vials are overlabeled to indicate their new international status; the new label has opaque backing to occlude the previous label, as in Fig. 5b. Overlabeling is preferred to removal of the previous label for quality assurance reasons.

13. Test and Inspection

Visual inspection and monitoring of product quality is carried out by the processing team at all stages of the process. This is to detect any potential problems: for example, splashing during dispensing, broken or damaged ampoules, poor freeze-drying (collapse), poor sealing or capping. All comments are noted in the Product Record. In addition, the following are recorded/tested:

Fill weight and coefficient of variation.
Dry weight and coefficient of variation.
Residual moisture and coefficient of variation.
Visual appearance of the freeze dried plug.

All of the above are recorded in the Product Record, which is reviewed by a team consisting of production, processing, and scientific personnel, prior to release of the batch. In addition, reconstitution time, biological activity/potency, and stability are determined subsequently by the relevant scientist

The whole process is reviewed to ensure it has been carried out in accordance with the agreed criteria and the freeze-drying is reviewed to determine if the chosen conditions were satisfactory.

C. Storage and Dispatch

Biological standards and reference materials are stored at the appropriate temperature in controlled, calibrated, monitored, and alarmed storage facilities. The freeze-dried materials are normally stored at $-20^{\circ}C$ to maintain stability over the period of the materials' availability, which may be a decade or more. Freeze-dried materials should be sufficiently stable to withstand short-term shipping at ambient temperatures without deterioration to their intended use.

The ampoules/vials are removed from storage on the day of dispatch and packed in accordance with national/international regulations. Shipment is typically by mail (post) except for countries where import via the post is a known problem or the shipment is urgent when couriers are used.

Infectious standards, e.g., Hepatitis B Surface Antigen, and frozen materials which require solid carbon dioxide (dry ice), are shipped via

Copyright 2004 by Marcel Dekker, Inc. All Rights Reserved.

specialized carriers and according to IATA and air security regulations, using UN certified packaging. Shipments sent with solid carbon dioxide include a "tell-tale" monitor to indicate thawing of the contents (even if refrozen). Special training and certification is required for staff involved in shipping these substances.

Biological standards and reference materials are supplied for immediate use and prior to use should be stored at the temperature indicated on the label. Once freeze-dried material is reconstituted, users must determine the stability of the material according to their own methods of preparation, storage, and use. In general, NIBSC follows the WHO policy in not setting expiry dates for freeze-dried biological standards and reference materials.

III. PROCESS DESIGN AND TROUBLESHOOTING

A. Cycle Design

The cycle design process used at NIBSC has resulted from different priorities than those facing most users of freeze-drying in the pharmaceutical or food industries. Unlike these sectors there is little requirement for repeat batches of the same material. The normal constraints, such as the number of batches which have to be processed per week and the cost of the freeze-drying process per batch, are not considered as the highest priority. Unlike most pharmaceutical freeze-drying, our control programs must take into account that active processing occurs in a "9 to 5" weekday-only environment.

The key factors in determining successful freeze-drying are long-term stability, preservation of sufficient activity, and rapid facile reconstitution. The product residual moisture content and atmospheric composition (in terms of oxygen content) are adjuncts to this. In the WHO guidelines, there are no set limits for minimal moisture level. We have an in-house limit of $<1\%$ to reduce the likelihood of water catalyzed hydrolytic and other degradative processes. However, in practice the level of residual moisture is usually well below this for most of our materials.

In common with most freeze-drying operations there are three basic stages in the process: freezing, primary drying, and secondary drying.

1. Freezing

All constituent water needs to be totally immobilized before a vacuum is drawn and freeze-drying can commence, either by crystallization to ice or by

Copyright 2004 by Marcel Dekker, Inc. All Rights Reserved.

incorporation into a glass of the superconcentrated biological. The product must be maintained at a sufficiently low temperature to be below the eutectic point(s) of the major crystallizing electrolyte present and the glass transition temperature (T'_g) of the protein/carbohydrate glass for sufficient time to ensure this. As freeze-drying commences the products must be held below these temperatures to avoid collapse as drying commences and a visually unacceptable cake, or, worse still, loss of functional activity. NIBSC is unusual in facing different freeze-drying challenges in terms of disparate formulations with almost every fill. The start material may be any of a wide range of biologicals, by nature protein, carbohydrate, glycoprotein, nucleic acids, or a complex mixture of several different components. Indeed, we are now encountering whole cell and whole virus preparations where integrity is required after reconstitution. There may be a wide variety of excipients required for the preservation of the biological activity following reconstitution but which may help or hinder the freeze-drying process.

It is best to know the composition of the material to be freeze-dried so as to determine the suitable freezing conditions. Some salts such as tris, hepes, or calcium chloride with low T'_g values may lower the glass transition to such an extent that the freezing temperature may be below the operational capabilities of the freeze-dryer; the lowest practical temperature achievable with our production-scale freeze-dryers is $-50^{\circ}C$.

The freezing process may also be important; snap freezing by placing product on pre-cooled shelves can result in heterogeneous crystal formation and final product appearance [14]. This has been particularly apparent to us when freeze-drying plasma where shelf freezing on precooled shelves ($-50^{\circ}C$) resulted in up to 60% of ampoules having freeze-dried cakes with a markedly striated appearance and some having a heterogeneous appearance, partially uniform (non-crystalline) and partially striated (see Figure 6).

For plasma, to prevent this heterogeneity we routinely use shelf freezing from $4^{\circ}C$ down to $-50^{\circ}C$ at a modest rate of cooling ($0.2^{\circ}C$/min) and then perform primary drying from shelf temperatures of -30 to $-40^{\circ}C$. This controlled freezing results in a homogeneous cake without marked crystalline appearance. However, if there is a tendency for freeze-induced damage in a biological then there may be no alternative to rapid freezing, achieved by loading product onto precooled shelves at $-50^{\circ}C$. Historically, snap freezing in liquid nitrogen was used, but this is neither safe nor practical at the scale of current manufacture, often resulting in a high proportion of ampoules breaking and leading to the crystalline problems described above.

Copyright 2004 by Marcel Dekker, Inc. All Rights Reserved.

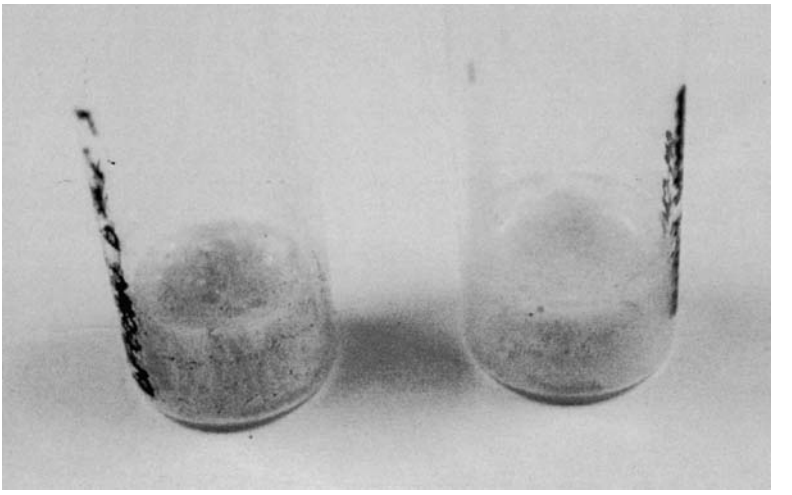

Figure 6 Comparison of freeze-dried plasma placed directly on precooled shelf (left) or controlled frozen on shelf (right).

2. Primary Drying

The aim of primary drying is to remove the crystalline water ice. The initial product temperature during primary drying must not exceed the glass transition (T'_g) or eutectic (T_e) points while not being so low that the sublimation rate is too slow. Product temperatures 5–10°C below the T'_g or T_e are chosen and maintained for sufficient time for an inflexion in the temperature profile to be evident and the product temperature to rise to be equal or above that of the shelf (see Figure 7). During the early stages of freeze-drying the product temperature is at a temperature lower than the shelves due to evaporative cooling; the heat loss from the product exceeds the heat flow into the product, primarily from the shelf. The inflexion in the product temperature profile represents the stage at which this cooling loss finishes and the product temperature rises, at least for the ampoules being monitored.

During primary drying, should a processing equipment failure occur, it is important that the shelf temperature and therefore the product temperature be rapidly lowered to ensure that the product retains biological activity. Routinely, low shelf temperatures have been used at NIBSC, with prolonged primary drying periods. Under such conditions, although sublimation rates are slow, the likelihood of product temperature exceeding the product T'_g is low. This, although not optimal in terms of the duration of the freeze-drying process, does allow the processing of a wide variety of

Copyright 2004 by Marcel Dekker, Inc. All Rights Reserved.

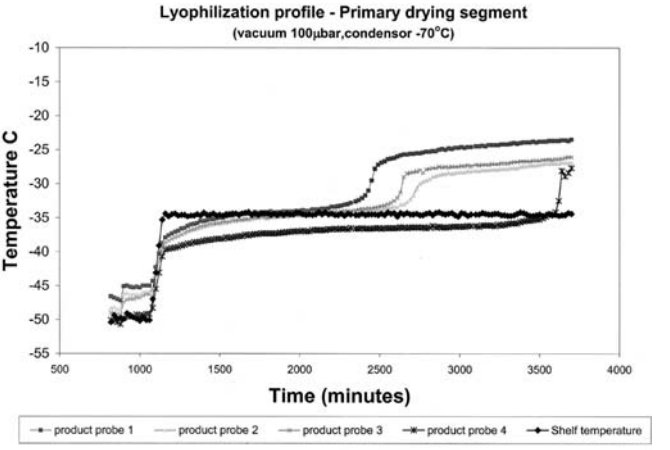

Figure 7 Primary drying profile for a biological reference material prepared at NIBSC.

formulations with minimal cycle development. Chamber vacuum is maintained typically at 100 μbar during the primary drying process in most of our operations.

It is well demonstrated in the literature that probe-containing vials undergo process changes more rapidly than those containers without probes [15]. It has been our practice to extend the length of the process stages well beyond the minimum time indicated from the probe-containing ampoules/vials during development studies; a 20% extra time has been suggested in the literature [16]. Pressure rise testing, where the chamber pressure rises on brief closure of the isolator valve between condenser and chamber is monitored, is a useful tool for the assessment of completion of primary drying in laboratory scale freeze dryers. However, we do not normally use it in the production of definitive materials.

3. Secondary Drying and Further Desiccation

Following primary drying, secondary drying is used to remove most of the amorphous water component of the glass. The shelf temperature used is as high as can be applied to the biologicals to promote rapid drying without loss of functional activity. Given that some of our standards are labile biological factors there might well be loss of activity if too high a secondary drying temperature is used. We typically use 25°C with a 30 μbar chamber pressure across a range of biological materials. The product does not quite attain the shelf temperature in our experience even after prolonged secondary drying periods (Figure 7).

Copyright 2004 by Marcel Dekker, Inc. All Rights Reserved.

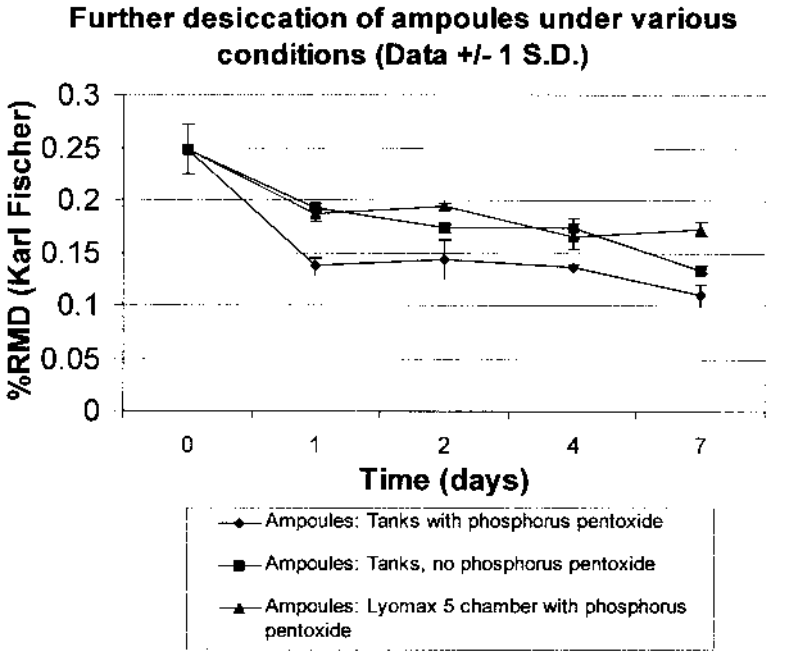

Figure 8 Comparison of further desiccation performed in freeze-dryer or desiccation tank over phosphorus pentoxide.

Residual moisture is a particular concern for biological standards due to the requirement for a prolonged shelf-life. Levels of moisture which would be typical for freeze-dried products, such as 2–5%, are not satisfactory for our use. Routinely, we dry to 0.5% or less residual moisture. To attain such levels of dryness we use ''further desiccation'' under vacuum in the presence of phosphorus pentoxide following secondary drying in the freeze-dryer. Ampoules, fitted with the capillary labyrinth, are removed from the freeze-dryer to drying tanks with the products stoppered but unsealed, with a constricted air path still present to allow further moisture loss during desiccation. Further desiccation periods of up to 6 days have been used mainly as a matter of operational convenience; however, it has been shown that in fact most of the further drying occurs rapidly over 1–3 days. The level of residual moisture achievable in further desiccation cannot be achieved in our experience by secondary drying alone (see Figure 8). This is because the product dryness attainable by further desiccation is not limited by the saturated vapor pressure of ice at the given condenser temperature as is the case for secondary drying within the freeze-dryer.

Copyright 2004 by Marcel Dekker, Inc. All Rights Reserved.

Table 4 Predicted Degradation Rates for Porcine Insulin (With and Without Further Desiccation) at −20°C (adapted from Ref. 17)

Preparation method	Predicted degradation rate (% p.a)	Residual moisture (%)
Freeze-dried only	0.105	0.46
Freeze-dried and further desiccated 7 days over phosphorus pentoxide	0.475	< 0.1

Degradation rates based on Arrhenius calculations from degradation at elevated temperatures, assayed by reverse phase HPLC.

There is evidence to support the view that products can be overdried. Some water may be needed to maintain the structural stability of the biological and removal of this may lead to destabilization. Extended drying of insulin resulted in a rise in the level of degradation products detected by reverse phase HPLC analysis, as shown in Table 4 [17]. Other researchers have noted loss of activity in influenza virus with excessive drying [18]. The optimum level of dryness should be determined for each material to be dried [19], where feasible, given the number of formulations to be dried.

B. Use of Product Temperature Probes

It is well accepted that containers housing product temperature probes are uncharacteristic of the containers that do not have probes; nucleation is enhanced by the heterogeneous surface introduced by the probe [20] and the probe leads present a heat source. Probes in containers cannot be used as an absolute indication of the conditions occurring in those containers without a probe during a freeze-drying run and should be regarded as a source of information and not used to control the system. For the processing of infectious materials probes are not included due to decontamination concerns.

Given this proviso, temperature probes and vacuum probes can and do provide a useful means of monitoring the progress of the freeze-drying process and to some degree indicate the consistency of process changes within and across the shelves of the freeze-drying chamber. Probes are also useful indicators of equipment non-compliance and system failures—for instance, in terms of pressure leakages, inadequate heating, or cooling steps, etc.

Copyright 2004 by Marcel Dekker, Inc. All Rights Reserved.

Evidence of ice crystallization (and the degree of supercooling) and the crystallization of excipients can be observed (for the probe-containing ampoules at least) from the temperature profile as inflexions during the progress of the freezing step (see Figure 9).

Most commercial freeze-dryers allow for a number of product temperature probes which are usually distributed so as to provide details of temperature profiles across the shelves and between shelves. Even then there may be only six probes (in the case of the Serail CS-100), for instance, to monitor the freeze-drying of 10,000 ampoules/vials. Of the types of probes available simple K-type or T-type thermocouples are small, convenient, and inexpensive. We use resistance thermometers, although these are larger (3–4 mm in length and 2 mm wide), as they give more accurate readings with a more linear response than thermocouples. Typically we would aim to place at least one probe in product on each shelf of a run covering multiple shelves.

We are investigating the use of externally located probes. Initial data have suggested that probes can detect ice crystallization isotherms in both the container to which the probe is attached and adjacent touching containers. The primary concern with the location of probes is the reproducibility in terms of the location within the container (centrally or

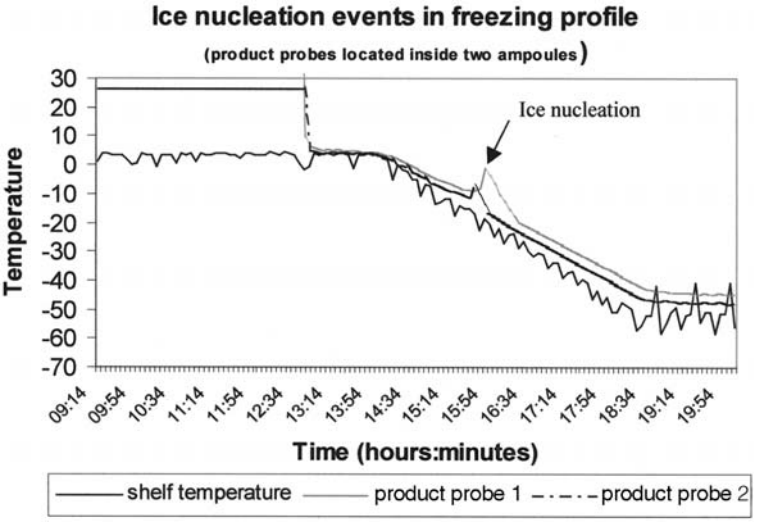

Figure 9 Freeze-drying profile showing product probe signal response due to the occurrence of ice nucleation compared to shelf temperature.

Copyright 2004 by Marcel Dekker, Inc. All Rights Reserved.

to the side), and the degree to which contact is made with the material to be freeze-dried.

Although the drying process progresses on the basis of the preprogrammed profile of shelf temperature and chamber pressure with time, there can be variation in terms of temperature within a shelf and across the chamber itself. The mapping of the variation in temperature across the freeze-dryer is an important part of the qualification of a new plant and should be repeated periodically, especially if problems are suspected in coolant flow path etc.

C. Formulation and Freeze-Drying Conditions

Ideally a product for freeze-drying might contain only water as the solvent and the biological to be dried as the solute. The establishment of suitable freezing conditions would be straightforward and once the water had been eliminated by sublimation the product would be stable and remain active. However, in reality a variety of non-volatile excipients will be present either to stabilize the product during the drying process or to ensure activity once the product is reconstituted. Other excipients may supply bulk, as often the quantity of the biological standard is minute and to ensure good cake formation at least 2% w/w solids should be maintained. These excipients will themselves influence the freeze-drying conditions and may influence the activity and stability of the product as they are concentrated on sublimation of the water ice. For instance, buffers may be added to preserve biological activity, but the pH range created by these buffer components may vary due to differential crystallization during freezing.

Typically we would avoid high levels of salts, such as sodium chloride and buffers (such as phosphate-based systems), which might shift pH on freezing [21]. Preferred excipients would be lyoprotectants such as non-reducing sugars, especially trehalose [22], and albumin or glycine as bulking agents [23].

In order to determine the freeze-drying parameters a number of critical parameters are required. The eutectic point of formulation components which crystallize on freezing and the glass transition of those which form an amorphous state should be determined in order to set the maximum safe product temperature for primary drying. This can be ascertained by one of a number of methods, as follows.

1. Differential Scanning Calorimetry (DSC)

The determination of T'_g of frozen liquids and the T_g of freeze-dried solids have been widely reported [24]. We have recently used modulated DSC

Copyright 2004 by Marcel Dekker, Inc. All Rights Reserved.

(for a review of m-DSC see [25]) as a routine primary tool in determining the freeze-drying conditions to apply to standards being processed. The glass transition is observed as an inflexion in the modulated reversed heating profile and the T'_g is derived by application of the manufacturer's software. In our experience the use of large (100 μL) sample pans has helped to enhance what can be very weak signals. In addition, clearer glass transitions can be observed at high concentrations of sample. For some samples at least, the determined T'_g at a high concentration holds true also at the lower concentrations being freeze-dried. For example, low molecular weight heparin analyzed at concentrations of 200, 50, and 10 mg/ml (the last one being the concentration at which freeze-drying was to be performed) all gave a similar T'_g value. However, the inflexion in the DSC signal was far less distinct at the concentration at which freeze-drying was to occur (see Figure 10).

The limitations of this methodology are that some samples (e.g., plasma and albumin) appear to give no glass transition, even at high concentration (10–20% w/v protein) and often the standards to be dried are only available in small quantities and dilute concentration making T'_g

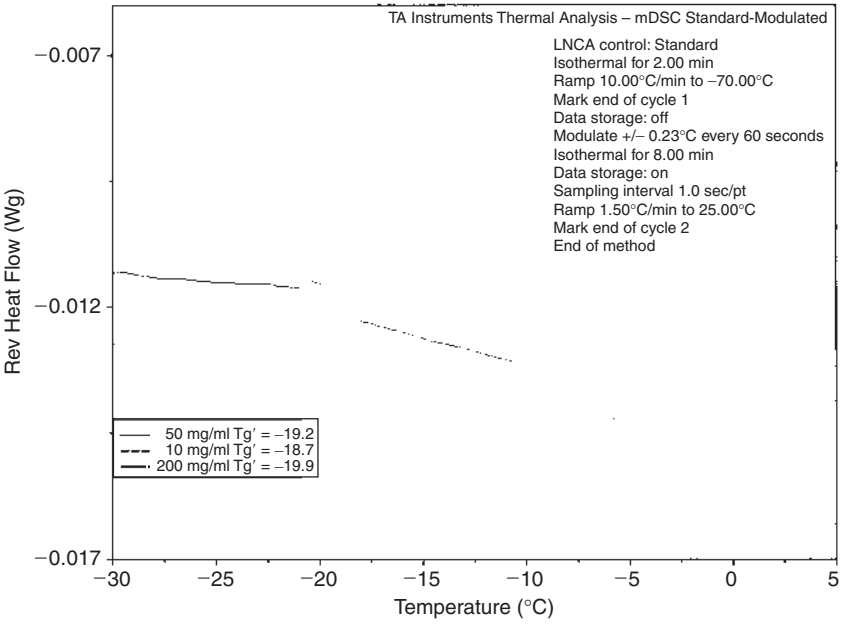

Figure 10 mDSC analysis of heparin at three concentrations showing impact of concentration on resultant signal for glass transition point (T'_g).

Copyright 2004 by Marcel Dekker, Inc. All Rights Reserved.

determination by m-DSC difficult. For example, in our experience no specific T'_g was detectable by DSC for a preparation of tRNA at 1 mg/ml. In the literature a value for modified RNA was reported using DSC [26] but with analysis on a sample at 100 mg/ml concentration—conditions which would unlikely be available for most nucleic acid samples we encounter. In other samples containing sodium chloride the eutectic event dominates the profile and weak T'_g may be missed or masked.

In summary, DSC is a rapid technique and can be automated but requires a significant financial outlay for the equipment and does not provide T'_g values for all samples under consideration for freeze-drying.

2. Electrical Resistance

The changes in electrical resistance which occur as a sample undergoes incipient melting can be followed by a number of methods (see [16] for a review). At NIBSC the SLTT (Solid Liquid Transition Temperature) was measured using an in-house technique, performed with equipment developed in the 1980s in conjunction with Brunel University, London, based upon the design of Lachman et al. [27]. This technique was used for many years to indicate the temperature at which the electrical conductivity of a sample varies during controlled heating after snap freezing in liquid nitrogen to equal or be below $-60^{\circ}C$. Values obtained were derived from extrapolation of the tangent to the conductivity curve at the water mobilization point. The values obtained were not identical to those derived from DSC (see Table 5)—for instance the SLTT value for sodium chloride solution was $-35^{\circ}C$ whereas the eutectic temperature is $-21.5^{\circ}C$. Commercial devices for resistivity measurement are now available, for instance, the Lyotherm from Biopharma, which combine both resistivity and differential thermal analysis.

Differential thermal analysis permits more detailed analysis of thermal events and can be used to determine equilibrium freezing temperature, phase changes, and onset temperature for ice melting. An advantage is that analysis can be performed in the same containers in which lyophilization will occur.

3. Freeze-Drying Microscopy (FDM)

FDM mimics the freezing and thawing process under the microscope by means of a controlled temperature microscope stage with a sample mounted under vacuum in a thin film [28,29]. It yields a collapse temperature based on visual inspection of collapse of crystal structure as the sample is gradually warmed from frozen. Although initially a home-built technology, the technology is less expensive than DSC; cryostages are available from

Copyright 2004 by Marcel Dekker, Inc. All Rights Reserved.

Table 5 Comparison of mDSC and SLTT Data for Some Formulations Encountered in Biological Standards

Standard for which formulation used	Formulation details	T_g' or T_e (°C) (mDSC)	SLTT °C (mean of two estimates)
Plasma	None	n.d.	−23
Plasma hepes	40 mM hepes	n.d.	−31
Anti Factor VIII antibody	12.5% albumin, 50 mM tris HCl pH 7.5 5 mg/ml trehalose	−21, −25	−43
Interleukin –17	1 mg/ml trehalose 0.9% NaCl 2 mg/ml HSA	−21 and −23	−26
Heparin	Water	−19	−4
Anti-D Immunoglobulin	0.25 M glycine 0.4% NaCl pH 6.7	−22 to −25	−44

n.d. = not detected

microscopy suppliers (such as Linkam) and an integrated freeze-drying microscope is also available (Lyostat, Biopharma).

Although FDM should generate T collapse values for all samples, these figures are derived from the collapse in a 1–2 mm section in the slide, whereas freeze-drying will be of containers filled to a height of several centimeters. For this reason broad margins for error are applied. It has been suggested to perform freezing at temperatures 2–5°C below the T_g' value [16,30].

In conclusion, it is necessary to have an array of techniques available to get the most accurate temperature for use during freeze-drying.

D. Residual Moisture Determination

The Karl Fischer solutions are methanolic and in some cases the reconstitution of samples—plasma in particular—can be problematic. We overcome solubility problems by the injection of entire vial/ampoule contents (redissolved in 1–4 ml of anolyte) into the electrolytic cell. Also we perform coulometric Karl Fischer determinations within a dry box [13] to avoid interference from atmospheric moisture.

There is a practical limit to the number of samples which can be measured before the electrode solutions are replaced. The limit of detection in our hands is 2–3 μg of water, i.e., 0.02% in a 1 g sample. In theory, it is possible to pool multiple samples and perform analysis on the pool but we have not needed to resort to this in practice. Moisture determination by

Copyright 2004 by Marcel Dekker, Inc. All Rights Reserved.

non-destructive infrared methods is popular in some pharmaceutical situations but difficult to apply in our situation as calibration of the IR output against a standard curve of known moistures is required for each product and presentation size. This is attractive where there are repeated batches of a few products but would not be easy for NIBSC where the standards differ so much from preparation to preparation and the generation of standard curves is time consuming to perform.

E. Product Stability

Of prime importance as a test of the success of the freeze-drying of standards is the retention of good reactivity after reconstitution. In practice, some loss of activity may be acceptable on freeze-drying but the resultant product should maintain its activity once dried. Within NIBSC this assessment is often by specialist functional assays, some of which may have confidence limits that are wider than others. However, we offer the option of laying down snap-frozen sample stored in liquid nitrogen (frozen baselines) as a means of checking whether it is the freezing or the drying process which is causing the deterioration. Activity of the standards after freeze-drying is generally well preserved as can be seen from the illustrations of three biologicals in Table 6.

Vials may be readily stoppered within the freeze-dryer and so do not pose the same degree of problem in maintaining the internal environment during sealing. However, these rubber stoppers may prove less suitable in terms of long-term storage, particularly at subzero temperatures, compared with flame-sealed ampoules which are impervious to gas exchange.

Table 6 Preservation of Functional Activity of Some Biological Materials During Freeze-Drying (iu = International Units)

Biological activity	Activity pre-freeze drying (defined as 100%)	Activity post-freeze drying	
		Activity	Percent
Heparin 01/592[a]	1312 iu/ml	1270 iu/ml	96
Factor VIII (in plasma) 01-037-MA[b]	0.5 iu/ml	0.46 iu/ml	92
Thrombin 01/586[c]	24 iu/ml	22.3 iu/ml	93

[a]Measuring Factor Xa activity.
[b]Pre-freeze-dried samples were baseline samples held at −70°C.
[c]Measured by chromogenic substrate assay.
Data kindly provided by Drs Elaine Gray, Anthony Hubbard, and Colin Longstaff, Division of Haematology, NIBSC.

Copyright 2004 by Marcel Dekker, Inc. All Rights Reserved.

IV. ACCELERATED DEGRADATION STUDIES

A. Overview

Degradation at the selected temperature of storage often is too slow for real-time studies to be practical before determining whether a material can be used, although real-time studies can continue in parallel with the initial use of the materials.

In principle, material is stored at a range of elevated temperatures and also at some reference temperature at which degradation is assumed to be insignificant. The activity of these samples is determined at known time intervals relative to the activity of the reference material stored for the same duration. It is important always to include a sample from the reference temperature at every testing and sufficient material should be placed in storage for this purpose.

The reference temperature should be less than the intended temperature of storage. These studies yield no direct information on the stability of the material at the reference temperature, although some indirect information can be obtained from the magnitude of the assay response of the reference material over time.

B. Typical Testing Protocol

At first, samples from the higher temperature storage sites (e.g., 56°C) are removed periodically and tested against samples from the reference storage temperature until significant degradation (20% to 30%) is observed. It is important not to use samples from the lower temperature storage sites early in the study. Such samples probably would show no significant degradation and would waste irreplaceable material.

Attention is then focused on the next highest temperature storage sites (e.g., 45°C and 37°C). These are removed periodically and tested until significant degradation (15% to 25%) is observed. The study proceeds for a suitable period until degradation (5% to 10%) is observed at the lower storage temperatures (e.g., 20°C and 4°C). Subsequently, samples are assayed from all the available storage temperatures against samples from the reference storage temperature.

The frequency of testing will depend on the rate of degradation observed at the higher storage temperatures. Initially, in the absence of any prior knowledge of the degradation rate, a suggested protocol is 1 month, 2 months, 3 months, 6 months, and 1 year. On removal from storage temperature, if the material cannot be assayed without delay, it should be stored at the reference temperature.

Copyright 2004 by Marcel Dekker, Inc. All Rights Reserved.

C. Models

It is usual to model the degradation of materials using the Arrhenius equation:

$$\ln(K\{t\}) = A + B/T$$

or the Heyring equation:

$$\ln(K\{t\}) = A + B/T + \ln(T)$$

where $K\{t\}$ is the degradation rate at the absolute temperature T (kelvin), relative to that at the reference temperature, and A and B are constants.

The Heyring equation is said to have a slightly stronger theoretical basis. Both models assume a unimolecular, single mechanism of degradation of first-order kinetics.

By determining the relationship between the degradation rate and temperature using samples stored at a range of higher temperatures of storage, the degradation rate at lower, i.e., conventional, storage temperature can be predicted using these models. For the computational methods used refer to the work of Kirkwood [31,32].

D. Confidence Limits of Prediction

The random error in potency estimates is assumed to be log-normally distributed.

The upper 95% confidence limit is derived from the equation:

$$K\{t\}'' = K\{t\} + (C \operatorname{se} K\{t\})$$

where $K\{t\}''$ is the upper 95% confidence limit of the degradation rate $K\{t\}$, C is a constant, and, $\operatorname{se} K\{t\}$ is the standard error of $K\{t\}$.

It is not possible to determine a value of C to be used in all cases. The value of C depends on the total statistical weight of the study (the reciprocal of the variance of $\log_{10}$ estimates of relative potency, from which the mean relative potency is obtained), i.e.:

For a total statistical weight of 30,000 or more, and at least 25% degradation has occurred at temperatures of 37°C or greater, a value for C of 4 (with three elevated temperatures) or of 3 (with four elevated temperatures) or of 2 (with five elevated temperatures).

For a total statistical weight of less than 30,000, a value for C of 5 should be used.

Copyright 2004 by Marcel Dekker, Inc. All Rights Reserved.

The precision of estimates of degradation rate from accelerated degradation tests is much improved by:

increasing the range of temperatures at which the samples are stored, even if the total statistical weight is kept constant;
increasing the total statistical weight by having replicate samples tested;
increasing the duration of the study.

A separate analysis of the measured response from the reference samples (e.g., if a radial diffusion assay, the ring diameter; or if an ELISA assay, the absorbance; or if an HPLC assay, the peak height) will indicate the between-assay variation. The analysis of duplicate samples of the reference samples will indicate the within-assay variation.

E. Common Problems Seen with Accelerated Degradation Studies

1. Reduction in Degradation Rate with Time

This may be seen with freeze-dried preparations and is be likely to be caused by an irreversible consumption of residual oxygen or moisture present as a contaminant of the atmosphere within the container or within the freeze-dried material itself.

2. Discontinuity in the Relationship Between Degradation Rate and Temperature

The analytical models assume that the rate of molecular diffusion (i.e., viscosity) in the stored samples does not significantly alter over the range of temperatures studied.

A significant change in viscosity can occur in the accelerated degradation testing of freeze-dried preparations containing a large proportion of substances that do not crystallize on freezing but form a glass, e.g., some proteins and carbohydrates as bulking materials or cryoprotectants. If, during subsequent storage, the temperature of the freeze-dried material exceeds the glass transition temperature of the glassy matrix, e.g., by storage at some elevated degradation storage temperature, there is progressive collapse of the previously stable glass by the water released from the glass. Subject to the magnitude of the water released, the glass progressively collapses into a deformable rubber, a viscous syrup fluid, and finally to a mobile fluid.

Over the temperature range where this progressive transformation occurs, there will be a marked change in the rate of diffusion and the

Copyright 2004 by Marcel Dekker, Inc. All Rights Reserved.

Arrhenius/Heyring equations are not valid over this point of discontinuity. This may be revealed by a discontinuity in the relationship between ln(relative potency), or degradation rate, and the reciprocal of absolute temperature.

For information, at temperatures near the glassy transformation point, the kinetics is said to be better described by the William–Ferry–Landle equation:

$$\log(k) = [C_1(T - T_g)]/[C_2 + (T - T_g)]$$

where k is the rate constant, T the absolute temperature (kelvin), T_g the glass transition absolute temperature (kelvin), and C_1 and C_2 are constants.

3. Additional Degradation Processes at Higher Temperatures

At higher storage temperatures additional degradation processes can become significant that are irrelevant at lower, conventional, temperatures of storage. These additional degradation processes can include Amadori products arising from reactions between protein and carbohydrates and often result in a discoloration of the material stored at elevated temperatures. If statistically significant, these additional processes can prevent the experimental data from being fitted to the degradation equation since there is no longer a linear relationship between ln(degradation rate) and the reciprocal of absolute temperature.

When not statistically significant, such additional processes can lead to an overestimation of the rate of degradation at conventional storage temperatures by using the combined degradation at the higher temperatures. This is particularly the case if the degradation study has not continued long enough for significant degradation to occur at the lower storage temperatures, when undue weight is placed on the data from the higher temperatures.

4. Temperature Effects on the Integrity of the Container

If vials are used as the container of the material, high or low temperatures may affect the physical properties of the stopper and thus the integrity of the seal it makes with the neck of the container. This should be investigated prior to their use [33].

Copyright 2004 by Marcel Dekker, Inc. All Rights Reserved.

F. Example of Accelerated Degradation Studies on a Biological Standard

The use of accelerated degradation studies is illustrated in Table 7 by reference to Factor VIII concentrate stored at −20°C: potency was tested using the Ph Eur chromogenic assay

Data were fitted using the Arrhenius equation: $\ln(K_{\{T\}}) = A + B/T$, where $K_{\{T\}}$ is the degradation rate at the absolute temperature T, relative to the rate at the reference temperature, and A and B are constants.

Maximum likelihood estimates of the constants A and B are:

A	24.24
Asymptotic error of A	1.61
B	−7244.98
Asymptotic error of B	502.27
Asymptotic covariance of A and B	−810.90

The chi-square test statistic for the predicted versus observed activity remaining at the various time points is 4.41 for 5 degrees of freedom. At the 5% level, the predicted remaining activities are not significantly different from the observed remaining activities. The predicted potency loss is shown in Figure 11, indicating that at a storage temperature of −20°C the standard had good stability with low degradation rate.

Table 7 Typical Testing Protocol for Accelerated Degradation Studies.

Elapsed time	Reference temperature	Temperature of storage site				
		4°C	20°C	37°C	45°C	56°C
1 month	×			×	×	×
2 months	×			×	×	×
3 months	×		×	×	×	(×)
6 months	×		×	×	(×)	
12 months	×	×	×	×		
n months	×	×	×	×		

×: sample is taken for analysis.
(×): sample may be taken depending on whether significant degradation has occurred in the previous sample.

Copyright 2004 by Marcel Dekker, Inc. All Rights Reserved.

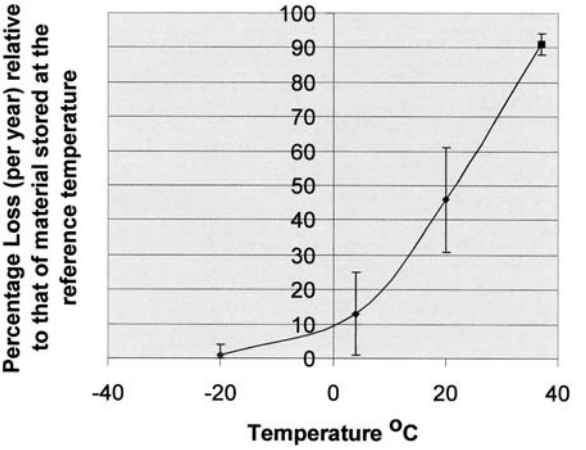

Figure 11 Plot of degradation against storage temperature for a preparation of Factor VIII.

V. FUTURE DEVELOPMENTS

At the time of writing, NIBSC has a new production unit being commissioned. This facility will include the following:

The capability to freeze-dry up to 10 l of containment level 3 materials using a freeze-dryer interfaced with a negatively pressured pharmaceutical-grade isolator containing vial filling/capping equipment. This should significantly increase the availability and ease of supply of these key reference materials which currently are available only as liquid preparations.

A new labeling machine to allow the possibility for labeling with self-laminating labels to allow labeling of ampoules/vials prior to processing.

A new ampoule/vial washer, to allow cleaning as a single automated process.

A stopper washer to remove the need for manual washing of stoppers.

Two new autoclaves; one for the sterilization of consumables prior to processing, the other for decontamination of waste materials.

Over the next decade a range of new recombinant medicines will reach the market and this will necessitate the need for new and replacement international standards to control them. In addition the advent of gene

Copyright 2004 by Marcel Dekker, Inc. All Rights Reserved.

therapy and the growing interest in the use of stem cell technology will present new areas in which quality reference preparations will be required. The first international standards in the area of PCR have been certified and the use of this and related technologies will doubtless increase, requiring further standards to be developed. To produce these new reference materials will require continually improving lyophilization techniques with which to yield robust stable reference material.

ACKNOWLEDGMENTS

We thank our colleagues at NIBSC, especially Drs Gray, Hubbard, Longstaff, and Bristow, for providing functional assay and storage stability data.

REFERENCES

1. Campbell PJ. International biological standards and reference preparations II. Procedure used for the production of biological standards and reference preparations. J Biol Stand 2:255–267, 1974.
2. Phillips P. The preparation of international biological standards. Fresenius J Anal Chem 360:473–475, 1998.
3. WHO Expert Committee on Biological Standards 50th Report. WHO Technical Report Series 904, 2002.
4. Rafferty B, Rigsby P, Rose M, Stamey T, Gaines Das R. Reference reagents for prostate-specific antigen (PSA): establishment of the first international standards for free PSA and PSA (90:10). Clin Chem 46(9):1310–1317, 2000.
5. Sesardic D, Wisnes R, Rigsby P, Gaines-Das R. Calibration of replacement first international standard and EP biological reference preparation for diphtheria toxoid adsorbed. Biologicals 29:107–112, 2001.
6. Saldanha J, Gerlich W, Lelie N, Dawson P, Heerman K, Heath A. An international collaborative study to establish WHO international standard for Hepatitis B virus DNA nucleic acid amplification techniques. Vox sang 80:63–71, 2001.
7. Rafferty B, Rigsby P, Gaines Das RE. Multicentre collaborative study to calibrate IGF-II by bioassay and immunoassay: establishment of the First WHO Reference Reagent. Growth Hormones & IGF Research 11:18–23, 2001.
8. Rafferty B, Maille P, Rigsby P, Gaines Das RE, Robinson CJ. International standards for hepatocyte growth factor/scatter factor: initial assessment of candidate materials and their evaluation by multicentre collaborative study. J Immunol Methods 258:1–11, 2001.
9. Robinson CJ, Gaines Das R, Woolacott D. First international standard for human leptin and first international standard for mouse leptin. J Mol Endocrinol 27:69–76, 2001.

Copyright 2004 by Marcel Dekker, Inc. All Rights Reserved.

10. Rafferty B, Corran P, Bristow A. Multicentre collaborative study to calibrate salmon calcitonin by bioassay and HPLC: establishment of the Third International Standard. Bone 29(1):84–89, 2001.
11. WHO guidelines for the preparation, characterization and establishment of international and other standards and reference reagents for biological standardization. WHO Tech Rep Ser 800:181–214, 1990.
12. Phillips PK, Dawson PJ, Delderfield A. The use of DIN glass ampoules to freeze-dry biological materials with a low residual moisture and oxygen content. Biologicals 19:219–221, 1991.
13. May JC, Wheeler RM, Elz N, DelGrons A. Measurement of final container residual moisture in freeze dried biological products. Dev Biol Stand 74:153–164, 1992.
14. Jennings TA. Guidelines for validation of the freeze drying process. J Validation Technol 3:386–391, 1997.
15. Murgatroyd K. The freezing process. In: Cameron P ed. Good Pharamaceutical Freeze Drying Practice, Interpharm Press, 1997.
16. Jennings TA. Lyophilization: An Introduction to Basic Principles. Interpharm Press, 1999.
17. Bristow AF, Dunn D, Tarelli E. Additives to biological substances IV. Lyophilization conditions in the preparation of International Standards: an analysis by high performance liquid chromatography of the effects of secondary desiccation. J Biol Stand 16:55–61, 1988.
18. Cammack KA, Adams GDJ. Formulation and storage. Animal Cell Biotechnol 2:252–288, 1985.
19. Hsu CC, Ward CA, Pearlman R, Nguyen HM, Yeung DA, Curley JG. Determining the optimum residual moisture in lyophilised protein pharmaceuticals. Dev Biol Stand 74:255–271, 1992.
20. Jiang S, Nail SL. Effect of processing conditions on recovery of protein activity after freezing and freeze drying. Eur J Pharm Biopharm 45:245–257, 1998.
21. Carpenter JF, Chang BS, Garzon-Rodrigues W, Randolph TW. Rational design of stable lyophilized product formulation theory and practice. Pharm Res 14:969–975, 1997.
22. Ford AW, Dawson PJ. The effect of carbohydrate additives in the freeze drying of alkaline phosphatase. J Pharm Pharmacol 45:86–93,1993.
23. Wang W. Lyophilization and development of solid protein pharmaceuticals. Int J Pharm 203:1–60, 2000.
24. Martini A, Kume S, Rivaldelo M, Arito R. Use of sub ambient differential scanning calorimetry to monitor the frozen state behaviour of blends of excipients for freeze drying. PDA J Pharm Sci Technol 51:62–67, 1997.
25. Kett V. Modulated temperature differential scanning calorimetry and its application to freeze-drying. Eur J Parenter Sci 6:95–99, 2001.
26. Jameel F, Amsberry KC, Pikal MJ. Freeze dried preparations of some oligonucleotides. Pharm Dev Technol 65:151–157, 2001.

Copyright 2004 by Marcel Dekker, Inc. All Rights Reserved.

27. Lachman L, Deluca PP, Withnell R. Lyophilisation of pharmaceuticals II. High sensitivity resistance bridge for low conductance measurements at eutectic temperatures. J Pharm Sci 54:1342–1347, 1965.
28. MacKenzie AP. Physicochemical basis for the freeze drying process. Dev Biol Stand 36:51–67, 1977.
29. Nail SL, Mer LM, Proffitt C, Nail L. An improved microscope stage for direct observation of freezing and freeze drying. Pharm Res 11:1098–1100, 1994.
30. Murgatroyd K. Freeze drying - a review. Eur J Parenter Sci 6:21–25, 2001.
31. Kirkwood, TBL. Predicted stability of biological standards and products. Biometrics 33:736–742, 1977.
32. Kirkwood, TBL. Design and analysis of accelerated degradation tests for the stability of biological standards III. Principles of design. J Biol. Stand 12:215–224, 1984.
33. Ford AW, Dawson PJ. Effect of type of container, storage temperature and humidity on the biological activity of freeze-dried alkaline phosphatase. Biologicals 22:191–197, 1994.

Copyright 2004 by Marcel Dekker, Inc. All Rights Reserved.

15

Industrial Freeze-Drying for Pharmaceutical Applications

Georg-Wilhelm Oetjen
Lübeck, Germany

I. INTRODUCTION

This chapter concentrates on (1) the process engineering for the production of two model products and (2) the engineering of an automated production plant for the two model products.

The two model products are used to develop the process engineering for the production of these products, to show how these processes could be automated and to specify production equipment for the two processes and products.

The two products are named PA and PB. Their qualities have been defined by the product development and the process data were developed by pilot plant [1] runs as described.

Some relevant information on the two products is summarized in Table 1.

The data used in the following sections are not all from the same two runs, but are selected from various experiments to demonstrate some extreme situations.

Copyright 2004 by Marcel Dekker, Inc. All Rights Reserved.

Table 1 Qualities of the Two Products PA and PB, Production Requirements

Qualities	PA	PB
Type of vials and stoppers	app.1	app.2
K_{tot} (kJ/°C m^2 h)	80	60
Product thickness (mm)	15	10
Loading time (h)/temperature (°C)	1/5	2/5
Rate/end temperature of cooling (°C/min)/(°C)	>1.5/<−55	>0.8/−50
Subcooling range (°C)	0 to −3	0 to −7
Time (h), temperature of heat treatment (TT) (°C)	none	2, −35
Maximum T_{ice} during MD	−43	−35
Change MD/SD at dT_{ice} (°C)	2.0	1.5
Temperature (°C), pressure (mbar) SD	30, 0.005	45, 0.01
Termination of SD at dW (%)	0.5 +0/−0.5	0.1 +0.01/−0.02
Gas type, pressure at closing stoppers (bar)	N_2, 1	N_2, 0.8
Production requirements		
Vials per charge	12,000	40,000
Water content (kg)	92.7	326
Shelf area approx. (m^2)	10	18
Solid content (g)	2867	36,280
Leak testing time (h)	1	2
Loading/freezing time (h/h)	1/2	2/5
p_c (mbar)	0.035	0.08
$T_{sh,MD}$ (°C)	−5	0
$T_{co,MD}$ (°C)	<−60	<−50
t_{MD} (h)	~11	~9
$p_{perm.gas,MD}$ (mbar)	<0.005	<0.01
$T_{sh,SD}$ (°C)	30	45
$T_{co,SD}$ (°C)	<−65	<−60
t_{SD} (h)	~6	~7
$p_{pem.gas,SD}$ (mbar)	$<10^{-3}$	$<2\times10^{-3}$
Closing/unloading time (h)	0.5/2	0.5/4
Total loading, freezing, drying, unloading time (h)	~24.5	~33

II. PROCESS ENGINEERING FOR PRODUCTION OF TWO MODEL PRODUCTS

A. Leak Test

Leak testing is done by measuring the rate of pressure rise in the evacuated parts of the plant after they are sealed off from the vacuum system.

Copyright 2004 by Marcel Dekker, Inc. All Rights Reserved.

The prerequisite of the pressure rise measurement is a sufficiently long evacuation of the areas to be tested. For details see pp 274–278 in [2] or pp 161–163 in [3]. As a routine test the end pressure (e.g., 0.01 mbar) and the time to reach it (e.g., 12 min) can be used, if the history of the plant before the test is the same as in the test to be compared with.

B. Loading and Freezing

The loading of a production plant with some 10,000 vials will be done automatically with a limited capacity, e.g., 10,000 to 30,000 vials per hour. The process has to take into account three considerations:

1. If the loading is possible at room temperature and this temperature can be applied for several hours, only the water content of the chamber volume can freeze, at 25°C and 60% relative humidity (rh) approximately, 25 g per m^3 of chamber volume.
2. If the product has to be kept and loaded at, for example, 5°C, the shelves at 5°C will freeze some water out of the atmospheric air, depending on its rh. At 5°C and 60% rh_2, $p_{H_2O} \sim 5$ mbar, the freezing of water will be limited to ~ 7 g/m^3 of chamber volume. These data can be reduced by running a positive pressure of dry nitrogen in the plant.
3. If the freezing of the product has to be carried out on precooled shelves at approximately −50°C, the flow of nitrogen would be difficult to operate with the large door open. Small loading doors are recommended as shown in Figure 1(a) and (b). If the loading is enclosed in an isolator as shown in Figure 2(a) and (b) filled with a dry gas, the problem of water condensation on the shelves is excluded.

The fact remains that the first vials loaded will be at −50°C longer for the loading time than the last ones. The pilot runs will have to show how important this resting time is for the product structure: ice crystals will grow in this time; this may be neglected for one product but may be critical for another. (Different crystal sizes and freeze-concentrated inclusions can produce different structures in the first and the last loaded vials behaving differently during main drying, MD and secondary drying, SD.) In many cases a thermal treatment almost to the onset of melting and a second freezing may substantially reduce the non-homogeneous behavior. If thermal treatment is a not sufficient remedy, the addition of a structure-building substance can be recommended, but this should have been decided during product development or pilot plant tests. The

Copyright 2004 by Marcel Dekker, Inc. All Rights Reserved.

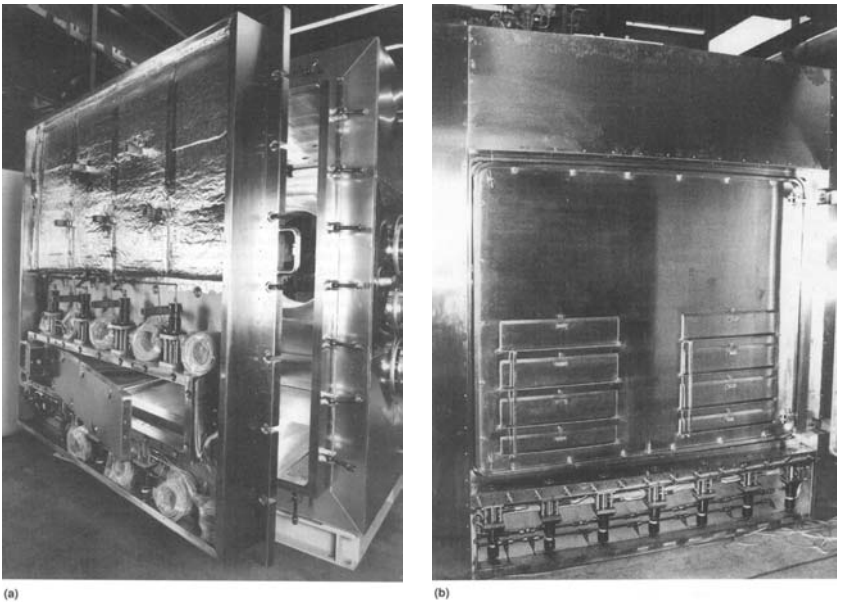

Figure 1 (a) Door of a freeze-dryer with a small loading door (Photograph: Steris GmbH, D-50354 Hürth, Germany). (b) Freeze-drying chamber with open main door and flaps for loading and unloading (Photograph: Steris GmbH, D-50354 Hürth, Germany).

structure behavior during resting at different low temperatures can be an important product quality to be studied during development.

For the freezing engineering of 15,000 vials in PA and 40,000 vials in PB, 1 and 2 h are calculated as the loading time. A shelf temperature of 5°C is acceptable. Production has to ensure a maximum humidity in summertime, and as a precaution the raising of T_{sh} to −5°C and 0°C should be done in two steps, first for PA to −43°C and −35°C for PB; if the pressure of 0.035 mbar (resp. 0.08 mbar) can be kept, the temperature can be raised further. The temperature treatment for PB is a relative straightforward process: 20 min from −50°C to −37°C of T_{sh}, kept at −36°C ±1°C for 120 min ±1 min, cool in 20 min from −35°C to −50°C, keep for 30 min before starting MD. The freezing rate in PA at 1.5°C is critical in the range 5 to −30°C where the main part in crystallization occurs:

$$t_f = (\Delta J/\Delta T)\rho_g(d^2/2\lambda_g + d/K_{su}) \quad (1)$$

Copyright 2004 by Marcel Dekker, Inc. All Rights Reserved.

(a)

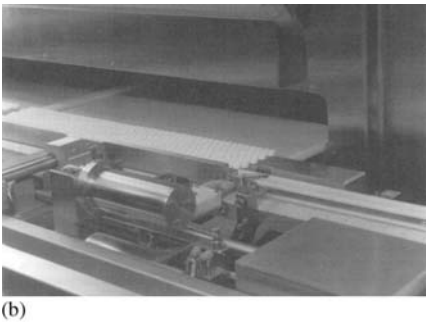

(b)

Figure 2 (a) Automatic loading of freeze-drying plant completely enclosed in an isolator (Photograph: Steris GmbH, D-50354 Hürth, Germany). (b) Loading of vials inside the isolator (Photograph: Steris GmbH, D-50354 Hürth, Germany).

where:

t_f = freezing time
ΔJ = enthalpy difference between the initial freezing point and the final temperature
ΔT = difference of temperature between the freezing point and the cooling medium
d = thickness parallel to the direction of prevailing heat transfer
ρ_g = density of the frozen product
λ_g = heat conductivity of the frozen product
K_{su} = surface heat transfer coefficient

A rate of 1.5°C/min in PA or 30/1.5 = 20 min or 0.33 h would only be possible with $K_{su} \sim 450\,kJ/m^2h°C$ and $dT = 40°C$ or by lowering T_{sh} to −80°C and raising ΔT to 65°C.

Production should check the tolerances of the freezing rate with product development and K_{su} data with the pilot plant department. K_{su} will

Copyright 2004 by Marcel Dekker, Inc. All Rights Reserved.

be difficult to enlarge in the production plant but if the liquid nitrogen method of cooling is chosen and $T_{sh} = -80°C$ are possible in the production plant, the freezing rate could be close to 1.5°C/min. For PB the required freezing rate 0.8°C/min can be achieved by $T_{sh} - T_{ice} = 35°C$ and $K_{su} = 200\,kJ/m^2\,h\,°C$, which gives the estimate of 0.9°C/min.

C. Main Drying

The main drying (MD) is, with some simplifications, governed by controlled operation pressure p_c, T_{ice} and T_{sh}, or by p_c and the temperature difference $T_{sh} - T_{ice}$, called T_{to} here:

$$t_{MD} = (\rho_g \xi_w \text{ LS } \Delta m\, d)/T_{to}[(1/K_{to}) + (d/2\lambda_g) + (d/2\,\text{LS}\,b/\mu)] \qquad (2)$$

where:

ρ_g = density of the frozen product (kg/m^3)
ξ_w = part of water (kg/kg)
LS = sublimation energy (2805 kJ/kg)
T_{to} = temperature difference ($T_{sh} - T_{ice}$)
K_{to} = total heat transmisson coefficient from the shelf to the sublimation front of the ice (kJ/m^2 h °C)
λ_g = thermal conductivity of the frozen product (kJ/m h °C)
d = thickness of the layer (m)
Δm = content of frozen water = 0.9
b/μ = permeability (kg/m h mbar) for water vapor through the dried product

The simplifications are as follows. The layer is endless, energy is only transmitted from the shelf to one side of the layer parallel to d, the vapor is only transported from the ice front through the dried layer. With a given product and its configuration in vials, t_{MD} can only be minimized by making T_{to} as large as possible. The maximum T_{ice} is given in Table 1. It is mainly controlled by p_c and T_{sh}. The control of T_{sh} is slow because the heat capacity of the shelves and the heat transfer medium are large. It is much easier to control the operation pressure as shown in Figure 3. With equation (2) the main drying process can be analyzed and possible improvements discussed. In this equation all data are well known, including ρ_g and b/μ [3], with the exception of K_{to} and T_{ice}. K_{to} can be measured for one type of vial on one design of heating shelf. It is pressure dependent as shown in fig. 16 in [2], e.g., 60 kJ/h m^2 °C at 0.08 mbar and 150 kJ/h m^2 °C at 0.65 mbar. K_{to} depends strongly on the bottom form of the vial: it can change K_{to} by a factor of 2 or more. The type of vial and the reproducibility of its bottom form have to be determined during product development and checked

Copyright 2004 by Marcel Dekker, Inc. All Rights Reserved.

during the following stages before manufacturing. T_{ice} cannot be measured by sensors as shown in fig.1.76 in [3]. Figure 4 shows the pressure rise after the valve between the chamber and condenser has been closed and the first derivation of it. The maximum in the derivation indicates the saturation pressure of the ice. The short time (e.g., 2.14 s) to measure T_{ice} requires 50 to 100 pressure measurements per second. The standard deviation of T_{ice} as a function of t_{MD} and the plots of T_{ice} (Figure 5) offer some indication of the homogeneity of the frozen product (freeze concentration) or collapses in microregions or collapse during MD. From equation (2) one can estimate the main drying time with the data of Table 1 as PA ~ 11 h, PB ~ 9 h. The requested T_{ice} can be very closely adjusted by selecting p_c as shown in Figure 3. T_{ice} is the temperature at which the transport of energy to the sublimation front and the consumption of energy by the sublimation of ice are in equilibrium. From this statement it is evident that T_{ice} depends on many factors, such as the heat transfer from the brine to the shelf, and the heat conductivity of the frozen product, to name two of the not so obvious ones, and obviously the number of vials in the charge, the uniformity of the sublimation front, and, last but not least, the flow resistance of the system from the sublimation surface in the container, to the chamber and to the

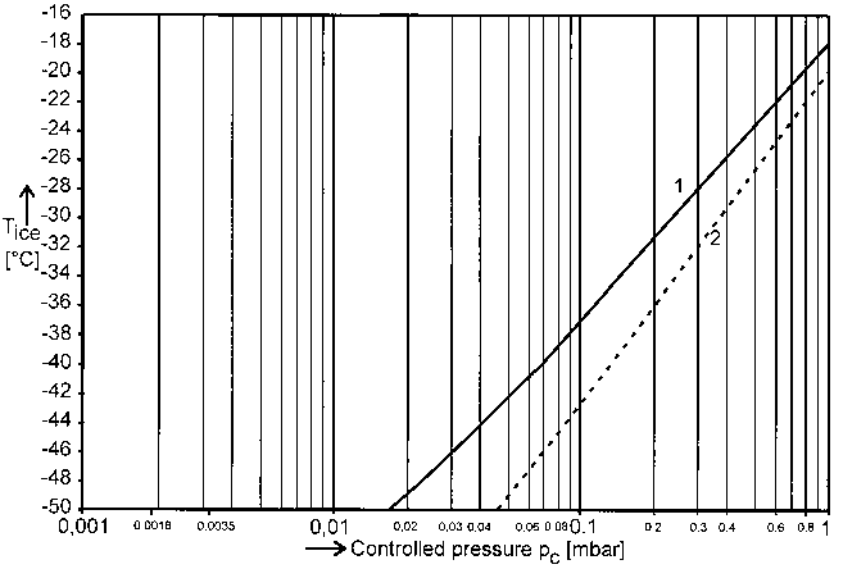

Figure 3 T_{ice} as a function of p_c. The plot is only valid for one type of product, in the same vials, in the same plant, and one T_{sh}. 1, T_{ice} as a function of p_c; 2, saturation vapor pressure of ice (from Ref. 4).

Copyright 2004 by Marcel Dekker, Inc. All Rights Reserved.

condenser surface. From Figure 3 the operation pressures for PA are determined as 0.035 mbar and for PB as 0.08 mbar. During MD the pump sets have to keep the pressure of permanent gases small compared with these data; they must have a final pressure in the range of $5\,10^{-3}$ mbar.

Figure 6 permits flow rates in plants from the chamber to the condenser to be estimated, where the chamber and the condenser are directly connected (by short tubes without bends). The influence of valves in this connection depends on the valve design. With mushroom valves (D in fig. 18 and 7 in fig. 25) and the chamber and condenser directly flanged together (fig. 25) one can expect an "effective" $l/d \sim 1.6$. The important general information of Figure 6 is the fact that the flow does not decrease in proportion to the pressure but decreases more strongly with lower pressure (e.g., for $l/d = 1.6$): at 0.6 mbar it is 22 g/h cm^2, at 0.06 mbar it is 1 g/h cm^2, and at 0.02 mbar it is 0.2 g/h cm^2. The vapor flow in production plants frequently limits the estimated t_{MD} in equation (2). To engineer the MD for the two model substances, the vapor transport has to be checked: for PA, 92.7 kg water in 11 h at 0.035 mbar; PB, 326 kg water in 9 h at 0.08 mbar. As per Figure 6 the vapor flow density at 0.035 mbar is 0.5 to 0.7 g/h cm^2, and at 0.08 mbar the vapor flow density is 1.8 to 2.0 g/h cm^2, depending on l/d. For PA the connecting diameter is calculated as ~120 cm or ~140 cm, for PB it is ~150 cm or ~160 cm.

The consequences of the vapor flow estimations are important in both cases. Valves with a diameter of 120 cm are technically possible and have been realized. For PA there are two possibilities: in an optimum designed

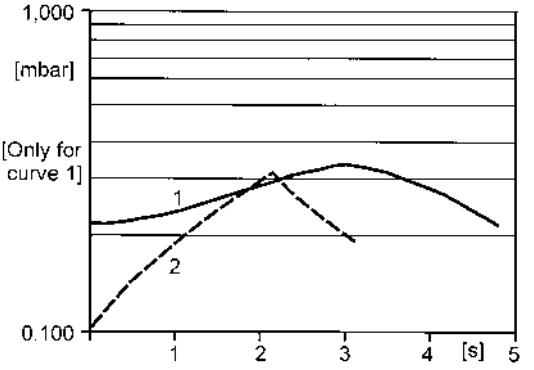

Figure 4 Pressure rise as a function of time: 1, pressure rise in the chamber after the valve is closed; 2, first derivation of 1. The maximum of 2 is reached at 2.14 s, the related equilibrium vapor pressure is $p_s = 0.286$ mbar corresponding to $T_{ice} = -32.7$ °C (from Ref. 12).

Copyright 2004 by Marcel Dekker, Inc. All Rights Reserved.

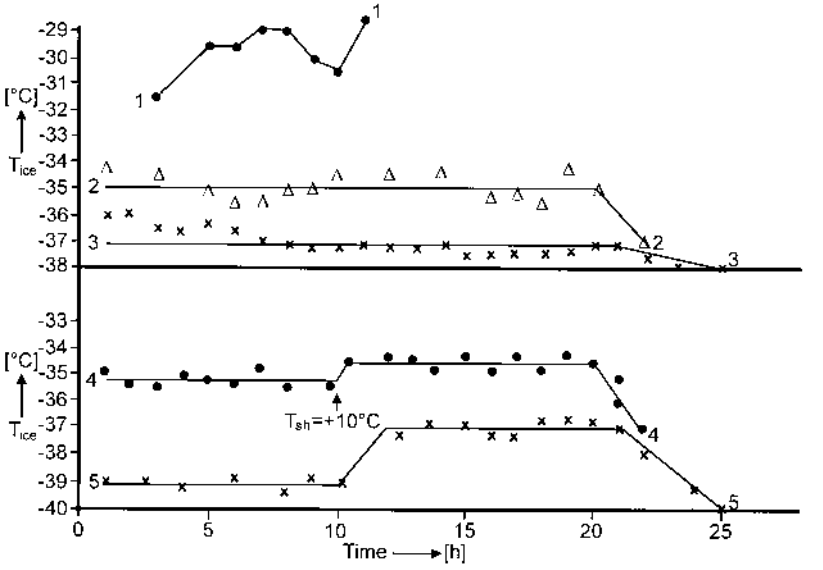

Figure 5 T_{ice} as indicator of the frozen structure of a 10% mannitol solution, $d = 10$ mm. Runs 1–3, product frozen in vials on the shelves down to $<-45°C$. Run 1, sublimation rate too high for the possible water vapor transportation, T_{ice} rises, product collapses, T_{ice} is irregular. Run 2, T_{sh} 0°C, p_c 0.15 mbar, av. T_{ice} −34.9°C, sd 0.65°C, product contains high concentrated inclusions between ice crystals; depending of the position of the sublimation front T_{ice} changes abruptly with the amount of concentrates being dried. Run 3, T_{sh} −5°C, p_c 0.08 mbar, av. T_{ice} −37.2°C, SA 0.7 °C, due to lower T_{sh} and p_c the mobility of water molecules in the concentrate is reduced; in the first ~6 h T_{ice} is a little higher than average, inclusions near the surface from freeze concentration are dried, thereafter the structure becomes more uniformly represented by a lower temperature of the ice. Runs 4–5, product frozen in liquid nitrogen and loaded on to shelves at −45°C, T_{sh} is raised at 10 h to +10°C. Run 4, T_{sh} and p_c as in run 2, av. T_{ice} −35.1°C, sd 0.50°C, after 11 h −34.5°C, sd 0.6°C. Run 5, T_{sh} and p_c as in run 3, av. T_{ice} −39.1°C, sd 0.22°C, after 12 h −37.0°C, sd 0.33°C (from Ref. 4).

plant the vapor transportation may just be possible with a valve of 120 cm diameter; and it is possible to prolong the drying time (e.g., from 11 h to 12.5 h) by reducing T_{sh} from −5 to ~−10°C. For PB two valves are necessary, of 1.1 m diameter each.

D. Change from MD to SD

The decrease of T_{ice} can be used to define t_{MD} in an objective and reproducible way. As an example Figure 7 shows T_{ice} data in the three runs

Copyright 2004 by Marcel Dekker, Inc. All Rights Reserved.

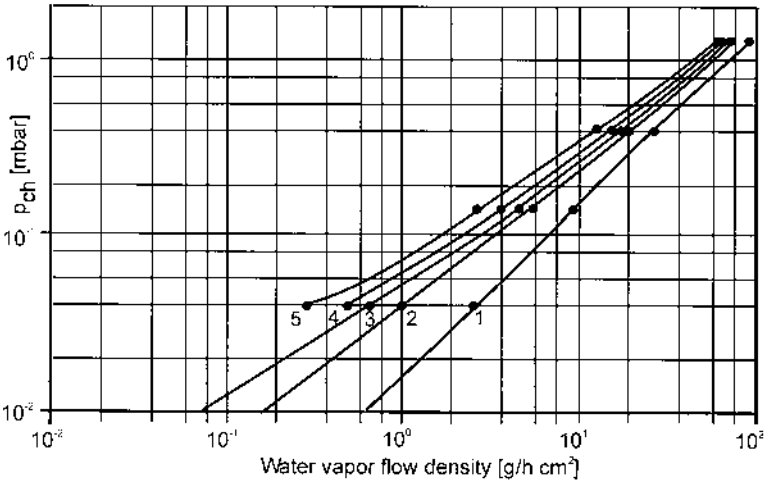

Figure 6 Density of water vapor flow (g/cm^2 h) as function of p_{ch} with jet flow (1) and length (l)/diameter (d) of the connection: l/d of 1 (2), 1.6 (3), 2.5 (4), 5 (5) as parameter; (4) and (5) are not plotted below 4×10^{-2} mbar; these data depend much on design details of the plant. They should be measured if needed.

that have a standard deviation between 0.55 and 0.33°C and the maximum average T_{ice} called max. $T_{ice/n}$. After 6 or 7 h MD, T_{ice} becomes measurable at less than max. $T_{ice/n}$, e.g., 1, 2, or 3°C, indicated in Figure 7 as 4, 4′, and 5. This decrease is the control function to change from MD to SD (see also Section III.D). In the two examples the process PA may be changed from MD to SD as follows: max. $T_{ice/n}$ was −34.9°C; change T_{sh} from −5°C to 30°C at $-34.9 - 1°C = -35.9°C$, and stop pressure control of 0.08 mbar at $-34.9 - 3°C = -37.9°C$.

E. Secondary Drying and In-Process Moisture Determination

On p 298 of [2] several methods for following SD are described. By quantifying the pressure rise method, the desorption rate (DR) is defined by equation (3) where DR is measured by pressure rises over 1 to 2 min (as T_{ice} over a few seconds):

$$DR = -2.89 \times 10^2 \ (V_{ch}/m_{fest}) \ (dp/dt) \text{ (desorption of water vapor in \% of solids per h)} \quad (3)$$

where:

V_{ch} = volume of chamber (L)
dp = pressure increase during dt (mbar)

Copyright 2004 by Marcel Dekker, Inc. All Rights Reserved.

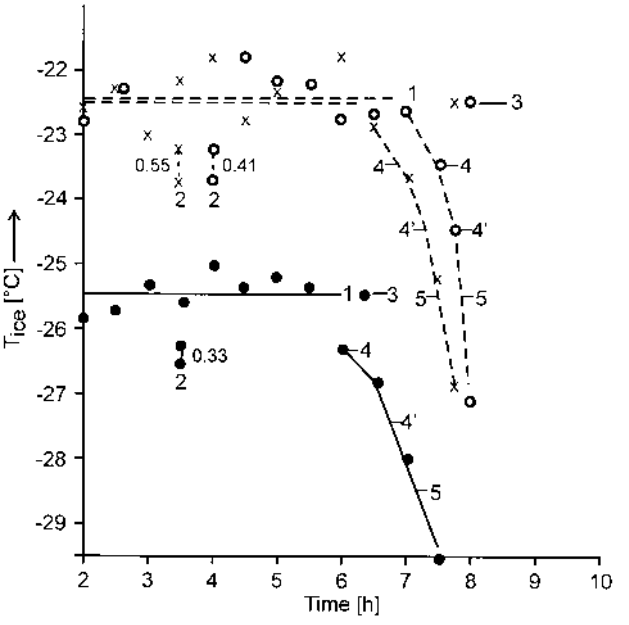

Figure 7 T_{ice} as a function of drying time. ○—○, ×—×, measurements and repetition with the same product and the same process data, ●—● another product with other process data. 1, average T_{ice}; 2, standard deviation of T_{ice}, 3, maximum $T_{ice/n}$ for ○ and × identical, −22.53°C; 4, maximum $T_{ice/n}$ −1°C; 4′, maximum $T_{ice/n}$ −2°C; 5, maximum $T_{ice/n}$ −3 °C (from Ref. [12]).

$\mathrm{d}t$ = time of pressure increase (s)
m_{fest} = mass of solids (g)

From DR data the desorbable water ($\mathrm{d}W$) is calculated as an indicator of the residual moisture content (RM) during SD:

$$\mathrm{d}W_t = \int_0^t DR\,\mathrm{d}t \tag{4}$$

i.e., $\mathrm{d}W$ is the integral from 0 to t over DR $\mathrm{d}t$ (residual water in % of solids).

The selected process data during SD are the maximum tolerable temperature 30°C (resp. 40°C), the required pressure ~0.008 mbar (resp. ~0.0035 mbar), and the final RM as $0.5+0/-0.5\%$ (resp. $0.1+0.1/-0.02\%$) measured by the Karl Fischer method. The $\mathrm{d}W$ data corresponding to these data have to be determined experimentally as shown

Copyright 2004 by Marcel Dekker, Inc. All Rights Reserved.

in Section III.D. The required pressure during SD is a function of the applicable T_{sh} and the desorption isotherm at this temperature. The desorption isotherm is in most cases not measured, but one can expect empirically that p_{SD} should in the end phase reach 0.1 to $0.2p_c$. If p_{SD} is too low, it does not shorten t_{SD}; if it is too high (compared with the isotherm data) it will prolong t_{SD}; and if p_{SD} becomes equal to the vapor pressure at the given temperature, the desorption will stop.

To achieve these pressures, the ice condenser has to have a temperature for with the two model substances of $T_{co} < -65°C$ and $< -70°C$ respectively. The permanent gas pressure should be small compared with the total pressure of ~0.1 to $0.2p_c$, e.g., in the region of 10^{-3} mbar.

Figure 8 sums up the additional product and process information gained during the engineering of the main drying, the change from MD to SD, and during secondary drying, as follows:

Product collapse in run 1: Large number of vials, high T_{sh}, too much vapor to be transported, product collapses.

Influence of crystal growth during resting: Runs 3 and 4 could be more uniform, but the details show that run 3 has been frozen in liquid nitrogen, but the freeze-drying started only 2 h after the end of liquid nitrogen freezing, time for the crystals to grow, resulting in a little higher T_{ice}, a little lower t_{MD}.

Influence of loading: Runs 5, 2, and 6 are for 100, 300, and 400 vials with $T_{ice} = -34.5$, -33.2, and $32.3°C$ respectively. More vapor transport needs a little higher pressure in the chamber, i.e., 0.23, 0.27, and 0.29 mbar.

Influence of t_{MD} on t_{SD}: Run 6 has, compared with run 5, a short SD, but a prolonged MD. The total drying time down to dW of 1% is similar, but run 6 needs a longer time to reach a low DR of 0.3%.

In conclusion, the engineering of the process and the discussion of the various pilot plant runs not only result in MD and SD data for production, but also provide information on possible structural changes during freezing and MD as well as consequences for SD.

F. Packing and Storage

The influence of the water content of the venting gas on the RM is described on p 308 in [2]. The influence of the water content of the stoppers on the RM during storage is more complex: stoppers are normally sterilized by steam, which is partially bound to the stopper material (order of magnitude 1% of

Copyright 2004 by Marcel Dekker, Inc. All Rights Reserved.

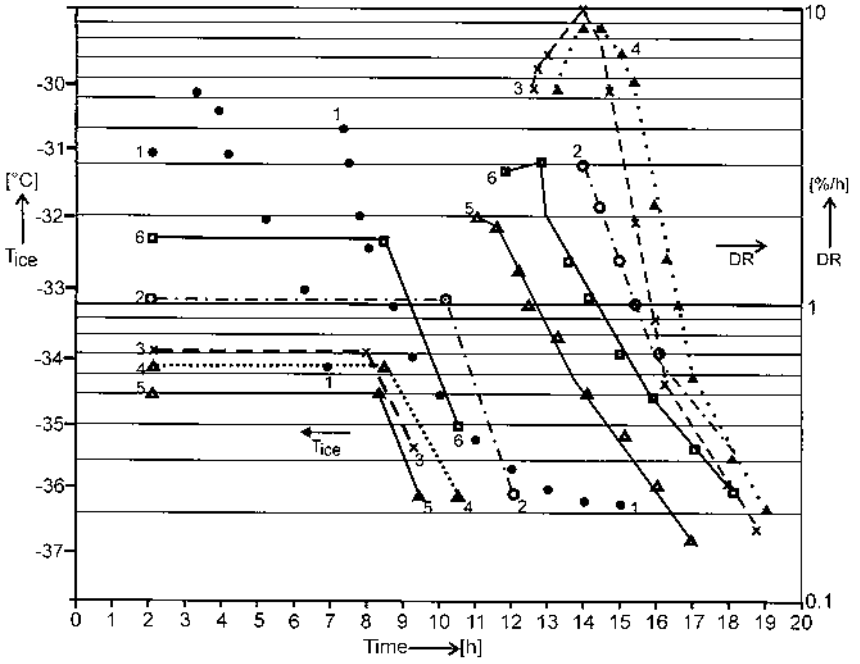

Figure 8 T_{ice} and DR as a function of drying time for six different freezing and freeze-drying runs, 10% saccharose solution, $d = 10$ mm, $p_c = 0.15$ mbar.

Plot no.	Vial no.	FM[a]	T_{sh}[b] (°C)	T_{ice} (°C)	t_{MD}[c] (h)	DR (%/h)[d] 1.0	DR (%/h)[d] 0.3	dW 1 (%)[e]	$T_{sh/20}$[f] (°C/min)	t_{SD}[g] (h)
1	300	W	30	–	–					
2	300	W	−5	−33.2	11.1	15.6	18.8	18.0	0.10	6.9
3	100	LN_2	0	−33.8	9.1	15.9	17.6	15.6	0.06	6.5
4	100	LN_2	0	−34.1	9.3	16.4	18.2	16.1	0.07	6.8
5	100	W	0	−34.5	9.15	12.5	13.9	15.0	0.10	5.85
6	400	W	0	−32.3	10.15	14.3	17.6	14.6	0.12	4.45

[a]FM, freezing method; W, vials charged on shelves of room temperature and cooled with the shelf; LN_2, product frozen in vials cooled by LN_2.
[b]T_{sh} shelf temperature during main drying.
[c]t_{MD}, main drying time, $T_{ice} = \max T_{ice}/m - 1.5$°C
[d]DR (%/h), time in h in which 1.0 or 0.3 %/h have been reached.
[e]dW 1(%), time (h) in which the desorbable water content has reached 1 %.
[f]$T_{sh/20}$, heating rate to reach 20°C in the product.
[g]t_{SD} to reach 1% dW.

Copyright 2004 by Marcel Dekker, Inc. All Rights Reserved.

stopper weight) and can only be removed by either temperature or vacuum, or both. The influence of this bound water on RM during storage depends on the binding energy of the water to the material of the stopper, the storage temperature, the amount of dry product in the vial, and the absorption behavior of the dry product. Corveleyn et al. [5] measured the water take-up of five chlorobutyl and three bromobutyl stoppers after their storage in an atmosphere of 95% rh and after sterilization. Wang et al. [6] differentiated between free and bound water in stoppers. The differentiation permits use of relatively short test times (1 week) to determine the necessary treatment for stoppers, instead of observing the RM of products over a long time, e.g., many months or some years.

III. PROCESS AUTOMATION

A. Prerequisites

This chapter does not deal with the electronic soft- and hardware to document the data, to calculate the desired results, and to monitor failures. The hardware is available in different configurations and the software can be bought or developed to fit into the software used in production. The prerequisites discussed are those for the methods of measurements and the plant layout to permit automation. The general prerequisite is the use of the same freeze-drying "methods" from product development through pilot plant studies to production: for example, the same principle of temperature and pressure measurements, identical definitions of tolerances, and similar criteria for statistical evaluations. If this prerequisite is not observed, the development steps may have to be repeated to permit later automation.

B. Measuring Methods and Tolerances

In an automated loading and unloading freeze-drying system no temperature sensors can be used in the product. One method to document the freezing process is shown in Figure 9. The temperature difference of the brine inlet and outlet at the shelves is recorded (1) with empty vials and (2) with filled vials. The difference between plots 1 and 2 is proportional to the energy used for cooling and freezing the product; plot 3 is the amount of energy removed as a percentage of the total energy. Plot 3′ shows this for a different product in a different plant. In the upper part of the figure are the maximum and minimum temperatures of four thermocouples given for comparison. The $T_i - T_o$ data characterize the freezing process in more detail than the thermocouples: between 10°C and the first 0°C

Copyright 2004 by Marcel Dekker, Inc. All Rights Reserved.

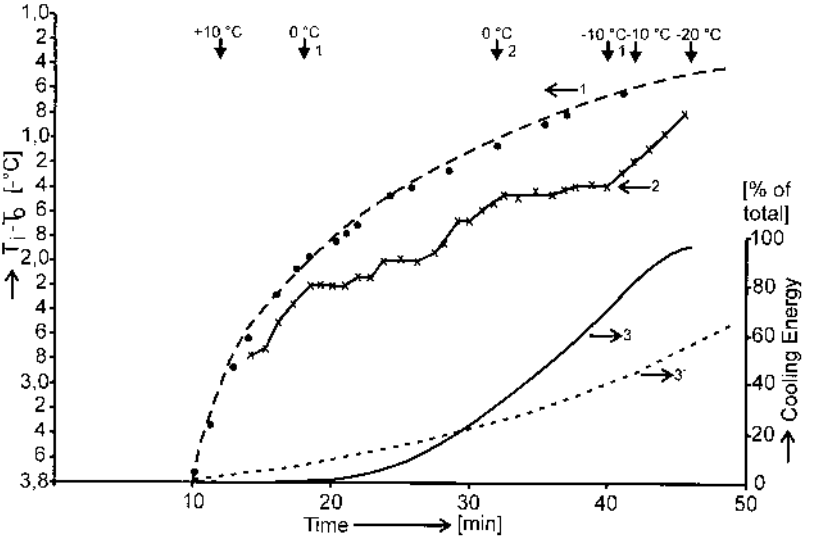

Figure 9 Thermodynamic data as a function of freezing time: 1, difference between temperature of brine inlet and outlet with empty vials; 2, same temperature difference with filled vials; 3, energy removed during cooling and freezing as % of total energy; 3′, energy removed in a different plant with different vials and a different product.

only cooling of the product occurs; the freezing of the main part takes place between $0°C_1$ and $-10°C_1$; at $-20°C$ most part of the crystallization is finished, and all four couples show the same temperature. The product in plot 3′ freezes at a much lower temperature, at $-20°C$; only $\sim 60\%$ of total energy is removed. In three measurements with the same product the standard deviations of the data in plot 1 were 0.07°C and in plot 2 they varied between 0.07 and 0.14°C.

During MD the measurement of T_{ice} is most important: p_s can be expected to be between 1.0 mbar ($\approx -20°C$) and 0.12 mbar ($\approx -40°C$). In this pressure range 1°C corresponds to a pressure difference of 0.07 mbar to 0.02 mbar. A vacuum gauge having a reproducibility of ± 0.002 mbar can differentiate $\pm 0.1°C$ or, with a reproducibility of ± 0.005 mbar, $\pm 0.25°C$. The standard deviations presented in this chapter fall in that range. To avoid temperature changes in the product, the time of measurement dt has to be not longer than ≈ 3 s as shown on p 89 in [3].

The requirements and limits for DR measurements during SD are as follows. A vacuum gauge as mentioned above can measure a pressure rise from 30×10^{-3} mbar to 60×10^{-3} mbar with an error of about $\pm 10\%$. In a chamber of 100 L the pressure rise of 30×10^{-3} is produced in 120 s, if

Copyright 2004 by Marcel Dekker, Inc. All Rights Reserved.

2.4×10^{-3} g water are desorbed in this time or 7.2×10^{-2} g/h. If the chamber contains 100 g dry material a DR value of 7.2×10^{-2} %/h can be measured with an error of $\pm 10\%$. This is only correct if the ratio of V_{ch}/m_s (L/g) ≈ 1. If the volume is larger or the mass smaller the error will increase. At a ratio of 0.1 the error can become 100% under the conditions mentioned. To measure a $dp = 30 \times 10^{-3}$ mbar in 120 s $= 0.25 \times 10^{-3}$ mbar/s in a volume of 100 L, this corresponds to 2.5×10^{-2} mbar L/s. The leak rate should be small compared with this value, e.g., 2.5×10^{-3} mbar L/s, to avoid the leak rate influencing the pressure rise measurement for DR.

C. Loading, Heat Treatment, and Freezing

The mechanical solutions of automatic loading and unloading are given in Section IV. The process problems are at least as severe as the mechanical one, discussed in Section II. The problems with the temperature treatment (TT) of products in large automated plants are the same as if the process was controlled by hand. Maintaining a uniform temperature in the whole plant as a function of time and location is the crucial task. Generally it is recommended to use longer time scales and lower treatment temperatures instead of short time scales and higher temperatures. The influence of time and temperatures during TT on the secondary drying and the residual moisture is shown in Figure 10. Plot 9 and 10 vary only by TT: respectively 480 min at -40°C and 20 min at -24°C; both have the same plots and T_{ice} is identical. In runs 5, 6, and 7 TT time is 18 min at -23.5, -26, and -24.5°C. Only in plot 7 is the dW plot a straight line, while plots 5 and 6 show a different slop below $\sim 1\%$ dW. In only 18 min at -24.5°C all unfrozen water was crystallized, and a uniform structure was obtained during TT. The 1 h longer drying time in plot 7 is due to the later change to SD from MD. At -23.5°C and 18 min (plot 5) the temperature is a little too high (or the time a little too long) and some product may sinter or collapse in micro areas. The drying of this product structure takes ~ 2.5 h longer to reach dW of 0.4%. In plot 6 at -26°C the crystals grew less during TT (MD is ~ 1.5 h longer), and the unfrozen part of the water is more pronounced (the slop at $\sim 1\%$ becomes flatter). In plot 8, 18 min and -24°C are used, but MD is at a lower pressure, lower T_{sh}, and therefore ~ 4°C lower T_{ice}. This delays MD by ~ 5 h, but the dW plot is straight: at the higher viscosity (whereas several decades) concentrated inclusions act mechanically like solids. This behavior may be generally used if some water cannot be crystallized and low dW data are required, but it is paid for by a longer drying time.

The main problem of automation of the freezing step in large production plants is the same as during TT: the uniformity of temperature

Copyright 2004 by Marcel Dekker, Inc. All Rights Reserved.

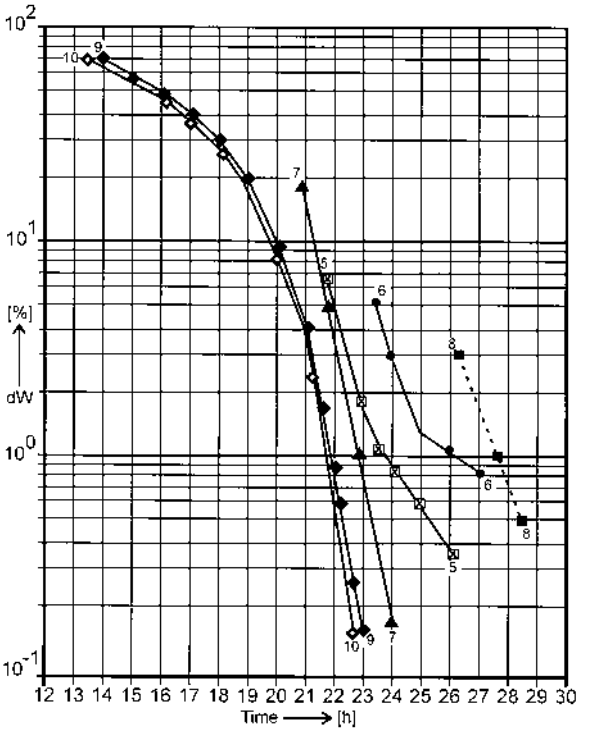

Figure 10 Desorption rate (DR), desorbable water (dW), and thermal treatment as a function of time of five runs with 10% mannitol solution, filling height 10 mm, T_{sh} 0°C during first/T_{sh} +10°C during second part of MD, $T_{sh,SD}$[c] +30°C, p_c[d] 0.15 mbar, frozen in LN_2, run 8 T_{sh} −5°C, and p_c 0.08 mbar (from Ref. 13).

Plot	T_{ice}[e] (°C)	SD[f] (h)	DR[g] 0.8%/h (h)	dW[h] 1% (h)	TT[i] Time (min)	TT[i] Temp. (°C)
5	−34.88/−34.38	21.9	23.5	23.7	18	−23.5
6	−35.12/−34.43	23.4	24.8	25.1	18	−26
7	−34.94/−34.43	20.6	23.5	23.0	18	−24.5
8	−39.13/−37.09	26.4	28.1	27.7	18	−24
9	−34.93/−33.85	13.6	22.3	22.1	480	−40
10	−34.66/−33.98	13.6	22.2	21.9	20	−24

[a] $T_{sh\,1}$, shelf temperature during the first 11 h of MD; [b] $T_{sh\,2}$, shelf temperature from 11 h to end of MD; [c] $T_{sh,SD}$, shelf temperature during SD; [d] p_c, controlled operation pressure during MD; [e] T,9 ice temperature during first/second part of MD; [f] SD, beginning of SD; [g] DR, time when DR 0.8% is reached; [h] dW, time when dW 1% is reached; [i] TT, thermal treatment: duration (min), temperature (°C).

Copyright 2004 by Marcel Dekker, Inc. All Rights Reserved.

as a function of time and location. If a certain freezing rate is required, e.g., $> 0.8°C/min$, the uniformity cannot be achieved by a different temperature–time profile (as with TT); the desired process data can only be achieved by specification of the equipment (see Section IV.G).

D. Main Drying, Secondary Drying, and Residual Moisture Content

A freeze-drying production process should always be engineered with the possibility to automate it. In Section II the measuring and control steps of the process were discussed. Table 2 shows a possible automated program for the freeze-drying of product PB. The plant and the process are operated and controlled by the thermodynamic data of the process itself. This method is called thermodynamic lyophilization control (TLC). In the complete program the tolerances are given, but are omitted here for brevity. This program is an example of how sections, steps, and criteria can be chosen differently. For some steps the reasons are listed in the following as examples:

Step 01/02: Depending on the accuracy of calibration and sensor reproducibility one may request $dT < 1°C \pm 0.2°C$. This would ease operation (less nodes of failure), but it limits information on the end of freezing.

Step 01/04: The difference between T_{sh} and T_{pr} is assumed to be 2°C.

Step 01/08: All pressure data in this program are measured by a capacitive gauge.

Step 02/03: Maximum T_{ice} is given in the product specification as −35°C. As a safety margin T_{ice} in the program is limited to −37.5°C. Depending on accepted tolerances one may choose −36°C.

Step 02/04: The T_{ice} decrease to change from MD to SD could be 1°C and 2°C.

Steps 03/01 to 03/04: It is assumed that $T_{pr} = 45°C$ is achieved by $T_{sh} = 47°C$, the decrease in pressure during SD and the related DR could be substantially different, depending on the desorption isotherms of the product at temperatures between 5 and 45°C. dW calculated from DR will change accordingly.

The automatic calculation of dW from DR determines only the water which desorbs from the solid at the given temperature. If the data calculated from DR are compared with data produced by different methods, one has to remember that water molecules are bound to the solids in various states, represented by the respective binding energy. Generally each method

Copyright 2004 by Marcel Dekker, Inc. All Rights Reserved.

Table 2 Program for the Automated Thermodynamic Lyophilization Control (TLC) Process with Product PB

Section	Step	Start[a]	End[b]	T_{co}^{a}/T_{co}^{e} [c] (°C)	T_{sh}^{a}/T_{sh}^{e} (°C)	p_e^a/p_c^e (mbar)	T_{ice} (°C)	sd (°C)	$T_{ice,max}$ [d] (°C)
01 Freezing	01		T_{sh}^{e} −50°C	—	20/<−50	—	—	—	—
	02	T_{sh} −50°C	A^e	—	<−50	—	—	—	—
	03	A^e	A^e +30min	—	<−50	—	—	—	—
	04	A +30min	T_{sh} −33°C	—	−50/−33	—	—	—	—
	05	T_{sh} −33°C	2 h	—	−33	—	—	—	—
	06	after 2 h	T_{sh} −50°C A[f]	—	−33/−50	—	—	—	—
	07	A^f +30min	T_{co} <−50°C	20/<−50	<−50	—	—	—	—
	08	T_{co} <−50°C	p < 0.08 mbar	<−50	<−50	—	—	—	—
02 MD	01	p_c < 0.0008 mbar	T_{sh} 5°C	<−50	<−50/5	1000/0.08			
	02	T_{sh} 5°C	+1 h = D^h	<−50	5	0.08	−88.0	—	—
	03	D^h	Y[i]	<−50	5	0.08	−37.5	0.3	−37.5
	04	(−37.5°C −1.5°C)[j]	(−87.5°C −3.0°C)[k]	<−50	5/47	0.08	−39.0	0.7	−37.5
	05	−40.5°C[k]	< 0.008 mbar	−50/−70	47		DR (%/h)	dW(%)	
03 SD	01	0.05 mbar	< 0.04 mbar	<−70	47	0.08/<0.04	1.2	2.2	
	02	0.04 mbar	< 0.02 mbar	<−70	47	0.02	0.5	1.0	
	03	0.02 mbar	< 0.01 mbar	<−70	47	0.01	0.2	0.5	
	04	0.02 mbar	< 0.008 mbar	<−70	47	0.008	0.02	0.09	
	05	end of SD, dW < 0.1%							
04 Vial closing	01	0.008 mbar	400 mbar N_2		20°C	—	—	—	
05 Vial unloading	01	400 mbar	atm. N_2				—	—	

[a]Start citerion for the start of a step; [b]End citerion for the end of a step; [c]T_{co}^{a}/T_{co}^{e}, T_{sh}^{a}/T_{sh}^{e}, P_c^a/p_c^e data at the beginning and at the end of one step; [d]$T_{ice,max}$ highest av. T_{ice} during one run; [e]A, time at which dT between brine inlet and outlet < 0.2°C, for example; [f]A, end time of TT; [g]X, time at which T_{ice} measurements start after T_{sh} = 5°C; [h]D, time of first T_{ice} data; [i]Y, time at which $T_{ice,max}$ is measured; [j](−37.5°C − 1.5°C), time at which T_{ice} = $T_{ice,max}$ −1.5°C; [k](−37.5°C − 3 °C), time at which $T_{ice,max}$ −3°C is reached.

Copyright 2004 by Marcel Dekker, Inc. All Rights Reserved.

will count only water molecules that are less bound to the solids than the method can overcome. The determination of the residual moisture content in proteins by near infrared (NIR) spectroscopy is described by Lin and Hsu [15]. Mathematical tools were used to quantify the complex, overlapping peaks from different components. NIR data are specific for a given formulation and product dimension changes are only tolerated under certain conditions.

By using the automatic dW calculation one has to consider the difference between permanent measurement of the average DR of the whole charge and the measurement of a product in a single vial taken from the charge at given intervals. Figure 11(c) shows the dW data calculated from DR measurements (Figure 11(b)) in three (called 1, 2, 3) different runs (10% sucrose solution, 10 mm cake thickness), which have been controlled by identical data as closely as possible process data in Figure 11(a); the data determined by the thermogravimetric method (RG) are from product in vials that have been closed as indicated by the drying time. The RG data

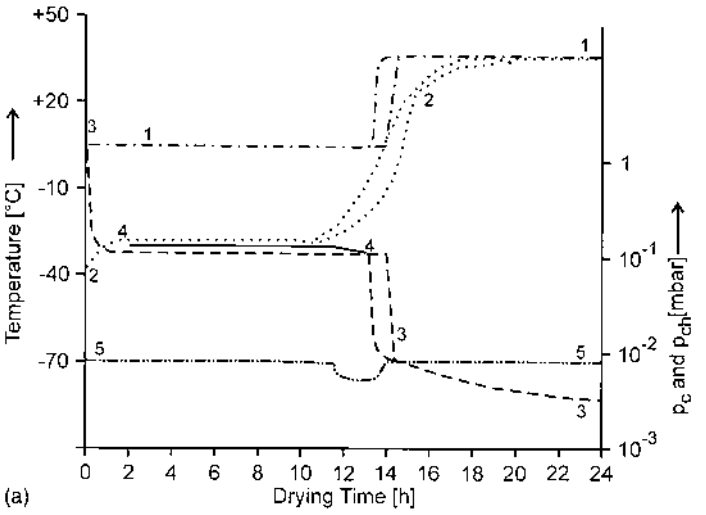

Figure 11(a) Process data of the three freeze-drying runs (from Ref. 14): 1, shelf temperature T_{sh}; 2, product temperature by sensors; 3, chamber pressure; 4, T_{ice} by BTM; 5, condenser temperature. Double lines of the same data indicate the maximum and minimum values measured. T_{ice} for the three runs are: −34.99°C, −35.02°C, and −34.81°C, average T_{ice} of the three runs is −34.94°C, standard deviation 0.11°C. The calculated freezing rate are: run 1,0.7°C/min; run 2,0.65°C/min; run 3,0.75 °C/min, average 0.7°C/min, sd 0.05°C.

Copyright 2004 by Marcel Dekker, Inc. All Rights Reserved.

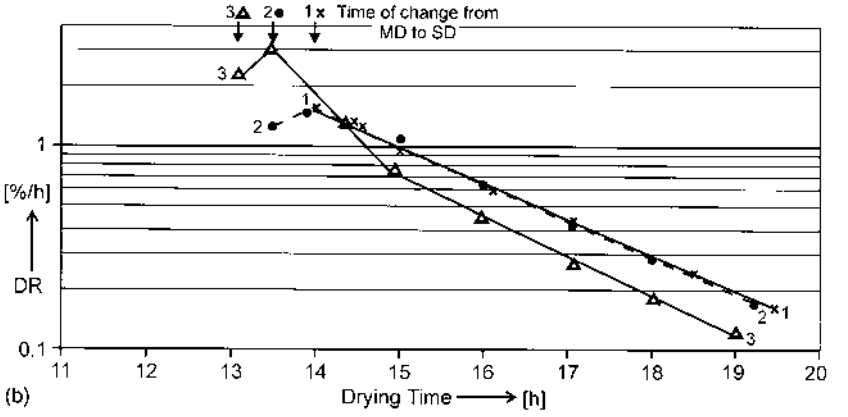

Figure 11(b) DR as a function of drying time of the process data given in Figure 11(a) (from Ref. 14).

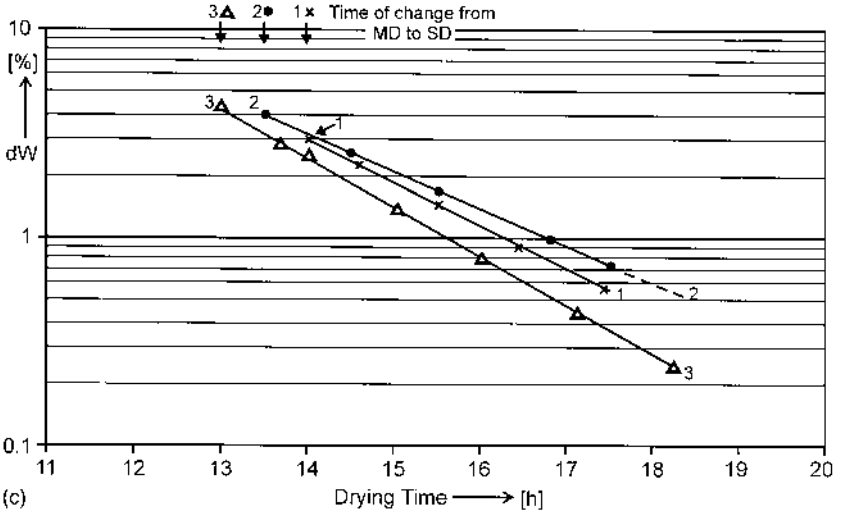

Figure 11(c) dW plots of three runs calculated from DR data in Figure 11(b) by equation (6) in [2, pp 303–304], (from Ref. 14). RG Scale = dW Scale

marked by $\Delta, \bullet, \times$ were obtained at the end of drying by weighing or thermogravimetric analysis at a constant temperature of 55°C. The automatic change from MD to SD occurred within 1 h. The last run changed from MD to SD is not the latest at dW = 1% nor at 0.3%. Average

Copyright 2004 by Marcel Dekker, Inc. All Rights Reserved.

T_{ice} during MD was −34.94°C, with a standard deviation (sd) of 0.11°C. The RG data above 1% vary, mostly lower than dW.

This behavior at the end of MD and the beginning of SD was determined by Pikal and Sham [7], Table 3. The dW data can be expected on the higher (safe) side, since the pressure rise results mainly from the product with the highest water content. At RG lower than 1% it will be difficult to differentiate between the three runs, but the dW data will permit this if required. A comparison between dW, RG, and data measured by Karl Fischer (RF) is given in Table 4.

In the Karl Fischer method water molecules are detected which are not desorbed at 45°C, while the gravimetric methods at 40°C desorb less water molecules than the desorption during SD.

E. Uniformity Within One Charge and Between Charges

The uniformity of the quality of a product in different vials in one charge and the reproducibility between charges are the criteria for efficient production. This section deals therefore with the uniformity of one charge and the reproducibility of different charges in automated processes. The uniform freezing and freeze-drying are mainly influenced by: (1) the correct situation of the stopper in the filled vial, (2) the bottom form of the vial (not the glass thickness), (3) the heat transfer from the brine in the shelves to the

Table 3 Mean Water Content in a 1 cm Cake Thickness of Bovine Somatotropin Varies Substantially at the End of MD and the Beginning of SD (from Ref. 7)

At 7% the standard error is from 4% to 10%	(±3%)
At 3.2% the standard error is from 2.2% to 4.2%	(±1%)
At 2% the standard error is from 1.5% to 2.5%	(±0.5%)
At 1% the standard error is within drawing accuracy	(<0.1%)

Table 4 Residual Water Content in Three Freeze-Dried Products Measured by Different Methods

Product	dW (%) at 45°C	RF (%)	RG (%) at 40°C
10% egg albumin solution	0.2 (±0.02)	0.7 (sd 0.12)	0.17 (sd 0.02)
10% mannitol solution	0.2 (±0.02)	0.8 (sd 0.23)	0.13 (one measurement)
20% human blood derivate	0.3 (±0.02)	0.7–1.1	—

sd = standard deviation.

Copyright 2004 by Marcel Dekker, Inc. All Rights Reserved.

product, (4) the situation of one vial in relation to its neighboring vials, and (5) the temperatures of the chamber walls and doors. The influences exist of course not just in automated operations, but they become particularly severe with increasing number of vials, e.g., several tens of thousands, which have to be more and more automatically handled. Note that, in (1), with automated filling and stopper positioning of vials and optically checked stopper position, a part of the stopper may slide into the vials during cooling, especially if the end temperature is very low, e.g., $< -50^{\circ}C$, or the coating of the stoppers not uniform. This effect can be found during product development by measuring the closing force for the stoppers as a function of temperature. Production should make sure that this dependence is known. If accidental closing happens only rarely, one may conclude that the coating of the stoppers is not uniform. A wide variation of drying performance with uniform frozen product structure often indicates a variation of stopper position. In (2) the effect is mainly observed if vials from different manufactures are used in one charge. Besides, with different forms of bottom the freezing behavior can be influenced by the different histories of the vials. The time and temperature of vials after sterilization can lead to different water layers on the walls of the glass vials and thereby to a different frozen structure. In (3) the effect is characterized by the repetition of its locations: the brine flow may be different near the inlet and outlet of a shelf, near the borders of the shelf, and in shelves of different size and with different flow pattern. The transfer of freezing data from a pilot to a production plant has to be carefully checked.

To measure the uniform temperature distribution of the empty shelf is not sufficient to ensure a uniform heat transfer. There are several ways to check the heat transfer under load. If the shelves are of equal design, one shelf, for example, may be loaded automatically with vials as used in the pilot plant. The vials are filled with water to 15 mm height; 25 vials are filled the same way but through the stoppers a thermocouple or another temperature sensor is fixed approximately in the middle of the water layer. These 25 vials are exchanged with vials on the shelf by hand in such a way that 15 vials are placed on the border of the shelf as widely distributed as mechanically possible. The other 10 vials are placed in different positions (again as widely distributed as mechanically possible) in between the center part of the vials. The positions of the vials are marked. The temperature in the product of the vials is recorded as a function of time. The temperature of the brine inlet and outlet is also recorded approximately every 30 s. The freezing behavior in the product of the vials will not be identical (see plot 2 in Figure 9), but if the temperature difference between the brine inlet and outlet are $< 0.2^{\circ}C$, the temperatures in the product should be very similar with a standard deviation of $< 2^{\circ}C$. If the temperature plots

Copyright 2004 by Marcel Dekker, Inc. All Rights Reserved.

of vials at the border of the shelf or in other positions decrease much slower, the test should be repeated with test vials at the same position. A similar deviation indicates that the shelf design has to be checked, because the heat transfer can be a reason for non-uniform freezing. (Note: During freezing the required heat transfer is normally larger than during main drying. Therefore it is easier to check the heat transfer from the shelf during freezing).

Regarding (4), a large number of vials automatically loaded on the shelves are normally placed statistically in relation to their neighbors, but they should not be pressed against each other nor should the space between them be larger than millimeters. If the vials are pressed together the problems may be three-fold: the bottoms may lose contact with the shelf, vials may stick together and are difficult to move in and out, and the pressure during closing of the stoppers may not be strictly vertical, so vials may brake. A little space between the vials does not usually hurt: there will always be some minor vibration in the shelves which moves the vials statistically.

In (5) the influence of the temperature of the chamber walls and door(s) is the most common reason for non-uniform freezing and drying. Fig. 2(b), p 272 in [2] shows that the temperatures at the walls and the door of the chamber remain between 10°C and 0°C even if the shelves are cooled to −40°C for 4 h. The temperature differences may look less important during SD, but this impression is incorrect: the temperature difference between product and shelf can be 50°C during the heating of the product from T_{ice} during MD to T_{pr} during SD, while the difference between walls (door) and product can be 20–30°C; the heating of the outer vials can take twice as high as the inner vials. The influence on the residual moisture content of no or different shielding is shown in Figure 12. For each run (a), (b), and (c), six groups of vials (168 vials in each group), filled with 2.8 cm^3 (9 mm thickness) human albumin product, containing 6% solids, were used. The rows 4, 5, and 6 were close to the door, and 1, 2, and 3 close to the back wall; the condenser connection was in the bottom of the chamber. The RM was determined by the Karl Fischer method. In run (a) no shield was used; in (b) shielding was provided by aluminum sheet metal, standing on the shelves, surrounding all vials, and with a height the same as the cylindrical part of the vials; in (c) the shielding is as described in Section IV, fig. 25. (The results are given below the figure). The results should be looked at as an example: they are also influenced by the factors mentioned above on the uniformity of the product. If the amount of product is small the influence of wall temperatures is relatively large (radiation and gas conductivity depend on the wall and vial surfaces and on the temperatures).

Copyright 2004 by Marcel Dekker, Inc. All Rights Reserved.

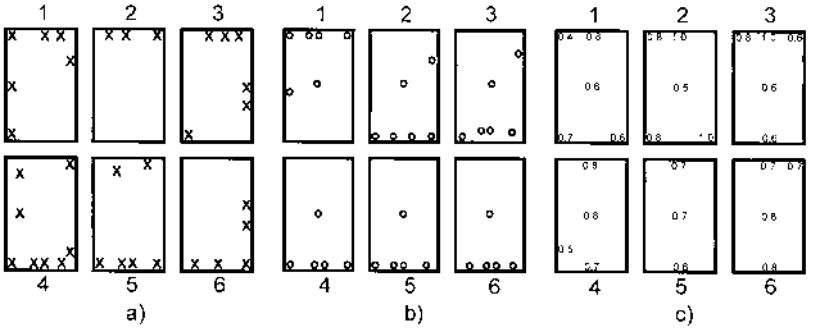

Figure 12 Residual moisture content in three identical runs with different shielding between vials and walls and door(s) (from Ref. 4). In each run six groups of vials were formed (168 vials each). The rows 4, 5, and 6 were close to the door, rows 1, 2, and 3 to the back wall. (a) No shielding; (b) shielding by aluminum sheet metal, standing on the shelves, surrounding all vials, height as the cylindrical part of the vials; (c) shielding as described in Section IV, Figure 25. Residual moisture content distribution in the three runs:

Run	a	b	c
Shrunk product:			
row 1–3	10	0	0
4–6	13	0	0
RM:			
in shrunk product	7/21% av. 15%, sd 6.2%	–	–
product in center vials	0.9/1.1% av. 1%, sd 1%	0.6%/1.0% av. 0.85, sd 0.15	–
product row 1–6	–	0.9%/4.5% av. 1.9%, sd 1.6%	
all vials	–	–	0.4%/1.0% av. 0.72%, sd 0.15%

The reproducibility of an automated freezing and freeze-drying process depends on the reproducibility of the instruments and the control systems used. Other influences are an inherent part of the process: A certain variation in subcooling and freeze concentration resulted in some differences in heat conductivity of the ice and the dried product and in the desorption behavior of the solid. Figures 11(a–c) give a practical example of the reproducibility of three repeated runs with an automated freezing and freeze-drying process. Figure 11(a) presents the process data of the three

Copyright 2004 by Marcel Dekker, Inc. All Rights Reserved.

runs in the same plant with a 10% sucrose solution of 10 mm thickness. The average T_{ice} in the three runs is $-34.94°C$, sd $0.11°C$; the calculated freezing rates are $0.7°C$/min, $0.65°C$/min, and $0.75°C$/min, average $0.7°C$, sd $0.05°C$. Double lines of the same data indicate the maximum and minimum values measured. The results of the three runs are summarized in Figure 11(b) and 11(c). The automatic change from MD to SD occurs within 1 h. The rules for the change were: DR measurement every 15 min, change when $T_{ice} = \max.T_{ice/n} - 1.5°C$ has been measured a second time. This could for example lead to: $\max.T_{ice/n} = -35.0°C$, $T_{ice,13.00h} = -35.9°C$, $T_{ice,13.25\,h} - 35.7°C$, $T_{ice,13.5\,h} = -36.5°C$, $T_{ice,13.75} = -36.7°C$, change starting at 13.75 h. If the DR measurement at the end of SD is taken every 5 min, the time difference could be a minimum of 10 min. The extrapolation of the dW plots to 12 h shows that MD until 11.5 or 12 h is practically identical (average 7% dW after 12 h); this is confirmed by the very similar T_{ice} data. It is the change from MD to SD and SD itself which produce some inherent variations: the rest ice in the product at a given time is not identical and the desorption behavior, the binding of water molecules to the solid, varies a little with the above-mentioned subcooling and freeze concentration. This is confirmed by the dW plots which are not parallel, but deviate with decreasing residual moisture content. If the final dW is requested to be $< 0.5\%$, the three runs could be terminated at ~ 16.5 h, 17.5 h, and 18.5 h, at $dW = 1\%$, the time difference will be ~ 1 h.

In consequence, production runs with low RM should be monitored by DR measurements, especially if the RM data are critical—time control only may be not accurate enough.

IV. SPECIFICATION OF THE PRODUCTION EQUIPMENT FOR AN AUTOMATED PROCESS DEVELOPED IN SECTIONS II AND III

Besides the automatic loading and unloading of the vials four main decisions have to be taken:

1. What kind of cleaning process should be applied?
2. How will the plant be sterilized: by steam or by vapor hydrogen peroxide (VHP®)?
3. Must it be possible to load the plant at shelf temperatures below $0°C$?
4. Should the loading and unloading be done in an isolator?

All four decisions influence the design specifications in general. Since the process should be as much automated as possible for the safety of personnel,

Copyright 2004 by Marcel Dekker, Inc. All Rights Reserved.

for sterility of the product, and for the efficiency of the production, the decisions used here will be:

1. The cleaning process should be automated, documented, and validated.
2. The freeze-drying plant should be sterilized by steam. Such a decision can be very controversial. All logical arguments are in favor of the Vaporized Hydrogen Peroxide VHP process, i.e., no pressure, but a vacuum process; no high temperatures (e.g., 121°C for 30 min), therefore less stress and shorter cycle times (the difference can be many hours); smaller investments; fewer problems with seals, bellows, and thermal expansion; no special steam required; the requirements for VHP (see below) are relative simple. In spite of theses arguments, steam sterilization is still mostly used for new freeze-drying plants. The retrofit of older plants which are not designed for pressure or the isolators, which can hardly be made for pressure, are sterilized by VHP.
3. In the two examples PA and PB the loading of vials is only necessary at 5°C.
4. In this example ice condensation during loading will not exist, since the loading will be done in isolators.

After these basic decisions the specifications can be written as follows.

A. Loading and Unloading of Vials, Drying Chamber, Stoppering of Vials

The decision to load and unload the vials in isolators excludes the method of automated guided vehicles as shown in fig. 27(a) [2]. It requires a "push and pull" system, in which the vials are transported by conveyors from the filling machines to a platform before the drying chamber, Figure 13 (in this plant no isolators are used), pushed from there onto the shelves and pulled from the shelves after drying to the table and then transported from there to the capping installation. The capacity for both plants should be specified as 10,000 vials/h to have the same system twice. (In an isolator it will be very difficult to move a loading system from one plant to another.)

A freeze-drying chamber is a pressure vessel built to the regulations of the country of operation, with many sophisticated details which need to be specified as follows:

1. The total mass of chamber and door is to be selected as a function of cost and the time and energy needed to heat and cool the mass

Copyright 2004 by Marcel Dekker, Inc. All Rights Reserved.

Figure 13 Loading system (push and pull) with a partially open small door, called a slot door (Photograph: Steris GmbH, D-50354 Hürth, Germany).

during sterilization. It will be necessary to heat the whole chamber to sterilization temperature (relatively quick by steam), but the time for cooling back to loading temperature may be substantially shortened by a separate cooling system with water. The gain in time is of special interest, if short cycle times are expected: in the two examples with 24.5 and 33 h cycle time the cooling time after sterilization may decide the possible number of runs per week. In view of the temperatures during freezing and drying in the two examples thermal shielding is recommended for the reasons demonstrated in Figure 12. With thermal shielding of the shelf temperature additional time can be gained, since the loading could start at a much higher wall and door temperature without risk to the product.

2. The surface quality of all material in the chamber, the inclination of the chamber floor, and the minimum radius of the corners of the chamber are further examples.
3. The insulation of the chamber and the door, partly under sterile room conditions, is another critical part of the specification.

Copyright 2004 by Marcel Dekker, Inc. All Rights Reserved.

4. The "stoppering" of vials, pushing the stoppers from their position during drying into the fully closed position, will need ~ 1 kg force per stopper, e.g., 10,000 vials per shelf require 10 tonnes of force. The problems during stoppering can be two-fold: rubber stoppers may stick to the shelf above, fall down during unloading and break, or disturb the unloading; and vials may be pressed together during loading, losing partially contact with the shelf and may not stand strictly vertical. The first event can be substantially reduced if the rubber ring on top of the stopper, marking the needle entrance, is interrupted, e.g., in four sections, or in general there are no closed forms on the top of the stopper which can be compressed by the closing pressure to a closed evacuated area, not filled with gas during venting. The number of vials not "vertical" during loading can be reduced by a slow, continuous movement of the vials over the full width of the shelf and suitable guidance at the edge of the shelves.
5. The sterilization of the piston rod is shown in fig. 26 in [2]. To avoid the additional space (length of the rod), a bellows system can be used as shown in Figure 14.

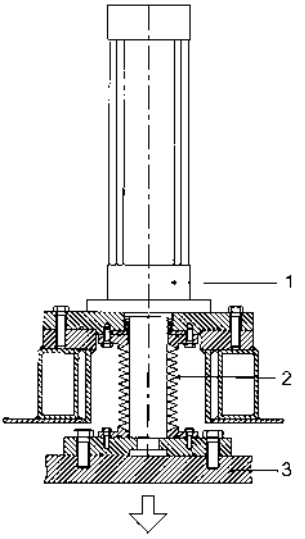

Figure 14 Closing system for stoppers sealed by a bellows from the chamber: 1, piston rod, hydraulic-operated; 2, stainless steel bellows; 3, pressure plate for stoppering vials (from Ref. 4 and Steris GmbH, D-50354 Hürth, Germany).

Copyright 2004 by Marcel Dekker, Inc. All Rights Reserved.

B. Ice Condenser

The four main criteria for the specification of a condenser are given on pp 311–316 of [2], here summarized as:

1. The ice thickness on the condenser surface at the end of drying should not exceed 1–1.5 cm; if the permanent gas pressure is not small compared with the water vapor pressure the ice has a snow-like structure with a thermal conductivity upto 10 times smaller than solid ice.
2. The temperature difference between differently controlled condenser coils or plates should be $< 1°C$.
3. The water vapor should condense completely, the water vapor pressure before the vacuum pump should correspond closely to the condenser temperature, e.g., the ice surface has a temperature of $\sim -55°C$, and the vapor pressure should be ~ 0.02 mbar.
4. Permanent gases have to be pumped off at the lowest point in the condenser to avoid gases filling the condenser and reducing condensation surface. A condenser cooled by liquid nitrogen is schematically shown in Figure 15(a) and as a photograph (partially finished) in Figure 15(b).

C. Cooling Systems for Condensers and Shelves

Today most condensers in freeze-drying plants are directly cooled by injection of a refrigerant compressed by mechanical compressors, while the shelves are temperature controlled by brine which is cooled in heat exchangers by a refrigerant and heated electrically or by steam. Most compressors are double-stage piston compressors. As shown in Figure 16 and Figure 17 the cooling efficiency E_c = compressor capacity C_c/electrical power consumption P_c of a screw compressor is only above $-55°C$ more favorable than a piston compressor. The data in Table 1 show T_{co} mostly in the region of $-60°C$; economically both types can be specified. The screw compressors have a smaller noise level (< 75 dBA), and are expected to have smaller maintenance cost, but the investment costs are mostly higher. The specification should ask for the preference of the supplier and the reason. The refrigerant in the cooling system will be specified by the supplier, but in a new plant it must belong to the group mentioned in Table 6. (Refrigerants listed in Table 5 can only be used temporarily after January 1, 2000 in existing plants.) The alternative to compressors and refrigerants is the use of liquid nitrogen (LN_2). A condenser for LN_2 is schematically shown in Figure 15. To specify LN_2 could be due to two reasons in the two examples: (1) the freezing rate in PA (1.5°C/min) could be reached, if T_{sh} during

Copyright 2004 by Marcel Dekker, Inc. All Rights Reserved.

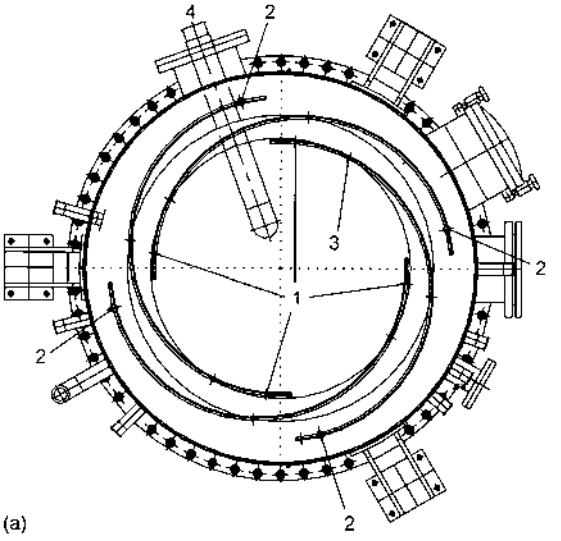

(a)

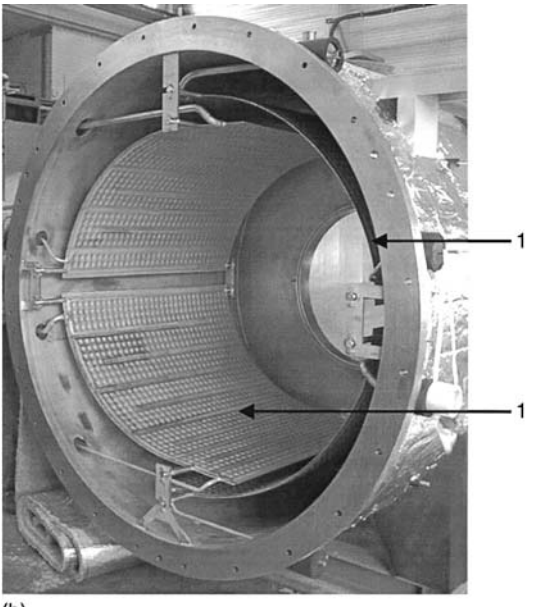

(b)

Figure 15 (a) Schema of an LN_2-cooled condenser: 1, LN_2 inlets; 2, LN_2 outlets, 3, temperature sensors: 4, vacuum pump set connection (Steris GmbH, D-50354 Hürth, Germany). (b) LN_2 condenser, partially finished: 1, condensing surfaces (Photograph: Steris GmbH, D-50354 Hürth, Germany).

Copyright 2004 by Marcel Dekker, Inc. All Rights Reserved.

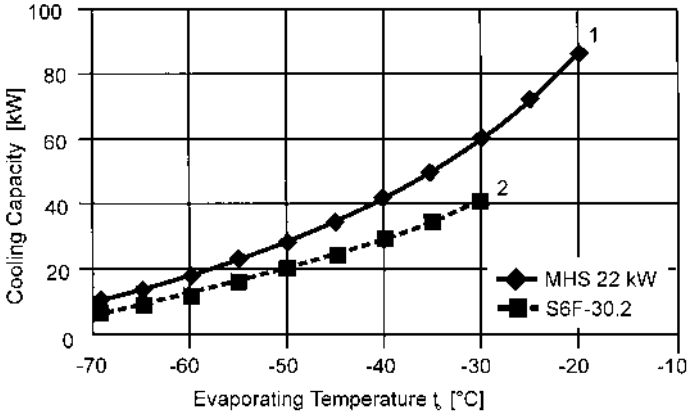

Figure 16 Cooling capacity (kW) of (1) screw compressor (MHS 22 kW) and (2) piston compressor (S6F-30.2) as a function of evaporating temperature (from Ref. 4).

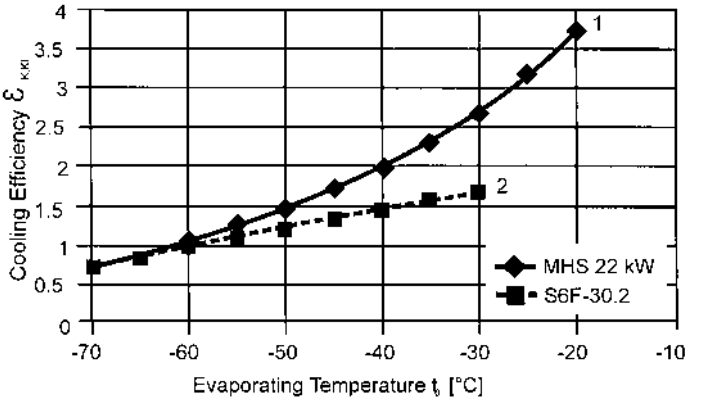

Figure 17 Cooling efficiency $\varepsilon_{k,kl}$ = compressor capacity C_c/electrical power consumption P_c for 1 and 2 of Figure 14 as a function of evaporation temperature (liquefying temperature 30°C) (from Ref. 4).

freezing is not −55°C but −75°C; and (2) the two plants would need four sets of double-stage compressors: in each plant one set for the cooling of the brine in the shelves and one set for the condenser cooling. The four compressor systems contain many moving and control parts, which have to be maintained; they need cooling water and substantial electrical energy. As a rule of thumb, one can assume that to freeze and sublimate 1 kg of ice 20 kg of LN_2 are needed or ~ 2,000 kg for one cycle of PA and ~ 7,000 kg

Copyright 2004 by Marcel Dekker, Inc. All Rights Reserved.

Table 5 Alternative Temporary Refrigerants, No Longer Permitted for New Systems After January 1, 2000 (Table 2.1 from Ref. 4)

Type	Manufacturer	Mixture	ODP	GWP	Oil
HP 80 (R402A)	DuPont	R125/R290/R22	0.03	2570	Alkyl benzol mineral oil
HP 81 (R402B)	DuPont	R125/R290/R22	0.02	2240	Alkyl benzol mineral oil
Isceon 69 L (R403B)	Rhone-Poulenc	R290/R218/R22	0.03	3680	Alkyl benzol mineral oil
Isceon 69 S (R403A)	Rhone-Poulenc	R290/R218/R22	0.04	2670	Alkyl benzol mineral oil
FX 10 (R408A)	Elf Atochem	R22/R125/R143a	0.03	3050	Polyolester

for one cycle of PB. For safety reasons two LN_2 storage tanks should be specified. Cully [9] estimates that LN_2 cooling of a 30 m^2 plant starts in the third year to become more economic than compressor operation (in his estimate mainly due to the maintenance cost of compressors). If lower shelf and condenser temperatures are required in future, as in the two examples, the specification should ask alternatively for compressor and LN_2 cooling.

D. Water Vapor Transport from the Vials to the Condenser

The water vapor flow from the chamber to the condenser is described by Figure 6. The Y plot represents the flow, if the connection is designed as an ideal yet, with a flow velocity equal to that of sound. Details can be found in Diels and Jaeckel [16] and on pp100–103 in [3]. Neither the Y plot nor the plot $l/d = 1$ will be technically possible. l/d is the ratio between the length and diameter of the connection between the chamber and condenser. In an optimum design plant (Figure 18) one can expect to achieve $l/d = 1.6$. This ratio is not the geometrical ratio of the measured dimensions; it also reflects the deviation of the flow by a valve and other changes of the flow direction. A test is described in [2] pp 318–319 to measure the flow in a given plant at desired pressures and estimate the l/d value of the plant. Figure 18 shows the critical dimensions between the chamber, the valve, and the condenser. The optimum combination between chamber, valve, and condenser is a condenser directly flanged to the chamber and the areas B and C each are large (~3–5 times) compared with A. With a plant design in accordance with Figure 18 the l/d parameter equals 1.6 or a little better. With more conventional configurations, e.g., B and C ~ A, or longer connection

Copyright 2004 by Marcel Dekker, Inc. All Rights Reserved.

Table 6 Long-Term Refrigerants (Table 2.2 from Ref. 4)

Type	Manufacturer	Mixture	ODP	GWP	Availability	Oil
HP 62 (R404A)	Diverse	R125/R134a/R143a	0	3750	Unlimited	Polyolester
Genetron AZ 50 (R507A)	Allied Signal	R125/R143a	0	3800	Unlimited	Polyolester
R507A	Diverse	R125/R143a	0	3800	Unlimited	Polyolester
FX 70 (R404A)	Elf Atochem	R125/R134a/R143a	0	3750	Unlimited	Polyolester
KLEA 60 (R407A)	ICI	R32/R125/R134a	0	1920	Unlimited	Polyolester
R410A	Solvay	R32/R125	0	1890	Unlimited	Polyolester

ODP = Ozone Depletion Potential.
GWP = Global Warming Potential.

Copyright 2004 by Marcel Dekker, Inc. All Rights Reserved.

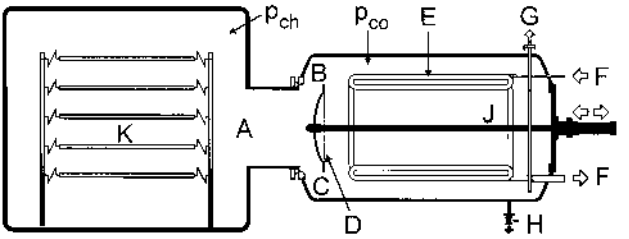

Figure 18 Schema of optimized flow conditions from the chamber to the condenser: A, free diameter of the valve; B and C, free areas to the condenser coils (E); D, mushroom valve with conical displacement piston J; F, inlet and outlet of refrigerant; G, vacuum pump connection; H, water drain; K, shelves; p_{ch}, chamber pressure; p_{co}, condenser pressure.

between the chamber and condenser (l) the parameter may change to 2.5. The consequences for the two examples PA and PB are as follows:

Product	PA	PB
Main drying time calculated from heat transfer data (h)	11	9
90% of water in MD (g/h)	7.600	32.600
Operation pressure p_c (MD) (mbar)	0.035	0.08
Water flow density $l/d = 1.6$ (g/h cm^2)	~0.7	~3
Water flow density $l/d = 2.5$ (g/h cm^2)	~0.5	~1.7
Required free valve area, if $l/d = 1.6$ (m^2)	~1	~1
Required free valve area, if $l/d = 2.5$ (m^2)	~1.5	~2

With a valve of 1.1 m diameter ~1 m^2, a valve of ~1 m diameter ~0.75 m^2, and a valve of 0.8 m diameter ~0.5 m^2, the valve specifications may require two different solutions for PA and PB

a. One valve with a free diameter (m)	1.1	1.1
b. Two valves with a free diameter (m)	1.0	1.1

Solution a will be the most economical. But one must accept that the vapor transport may be somewhat smaller in the plants than the estimated 0.7 g/h cm^2 or 3 g/h cm^2. If the measured transport data are, say, 0.6, resp. 2.5 g/h cm^2 (15% smaller), the main drying time has to be prolonged to 13 h, resp. 11 h. In view of the total freeze-drying cycle time (without cleaning and sterilization) this prolongation seems acceptable. Solution b will require two valves of almost the same diameter (for PA one should not consider two valves of different diameter). The two-valve solution can be preferable if future products are expected to need even lower T_{ice} and lower p_c. In view of the trends observed today T_{ice} down to -50°C may be required.

Copyright 2004 by Marcel Dekker, Inc. All Rights Reserved.

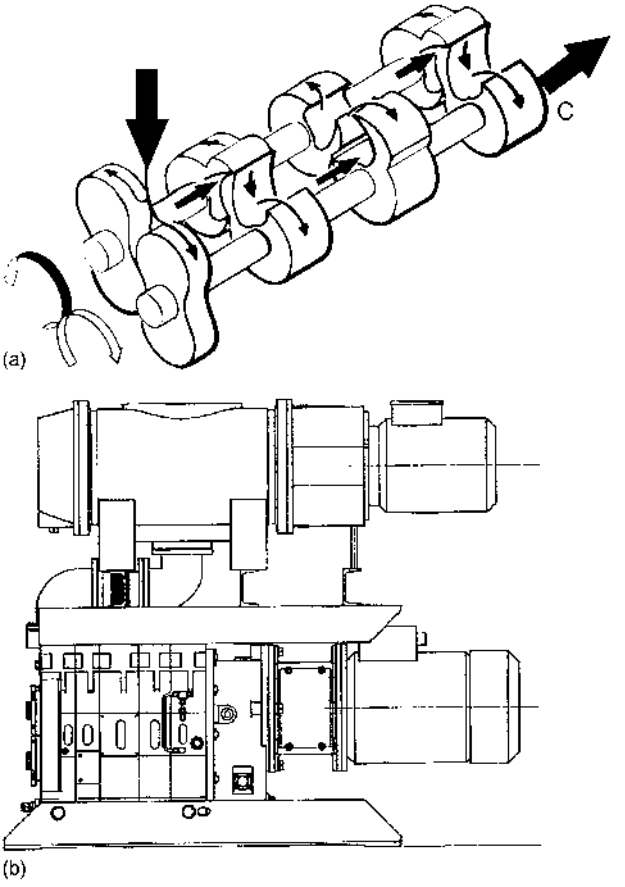

Figure 19 (a)–(c) Oil free vacuum pump sets. (a) Schema of a dry vacuum pump working on the claw principle. The short gas path through the pump prevents condensation between stages. (b) Dry vacuum pump combination with a dry roots pump for fast evacuation, and a high pumping speed in the range 0.02 to 1 mbar. (c) Pumping speed of a three-stage pump set: two dry roots blowers EH 500 plus EH 250, and one dry vacuum pump GV 80 with a high pumping speed from 0.001 to 40 mbar, end pressure $\sim 10^{-4}$ mbar (BOC Edwards GmbH, D-85551 Kirchheim/München, Germany).

Besides the connection between the chamber and condenser two more flow resistances are to be considered: (1) the flow resistance through the stopper and (2) the resistance from the stopper to the connection between the chamber and condenser. The flow resistance of the stopper can be measured in a pilot plant as described in the contribution by Willemer in this

Copyright 2004 by Marcel Dekker, Inc. All Rights Reserved.

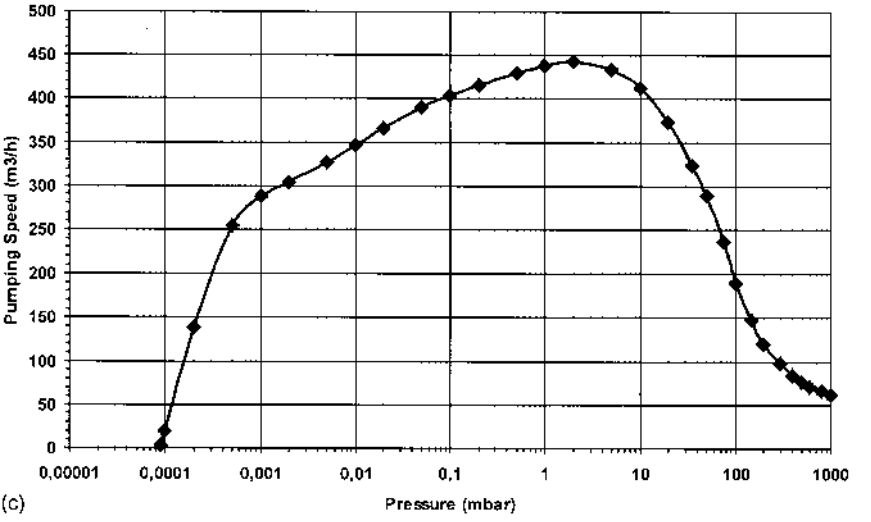

Figure 19 Continued.

book (Chapter 16). In a production plant with stopper closing, CIP and SIP (see Section IV.F), the areas between walls and shelves are normally large compared with the area A. If the flow is measured as described in the test above, all resistances are included, represented by a value of l/d larger than that given by the physical dimensions. With the one-valve solution a, discussed above, it might become difficult to design areas B and C large enough compared with A without running into disproportional dimensions. In such a case the two-valve solution mentioned above might be the trend-setting and more promising specification.

E. Vacuum Pumps, Venting System

The layout of pumping systems for production freeze-drying plants is calculated according to two requirements: (1) the evacuation time of the plant should be between 10 and 20 min and (2) the pump set has to pump the permanent gases during MD and SD. During MD the dissolved gases in the product (usually 10^{-4} to 10^{-3} g/g, exceptionally up to 10^{-2} g/g) have to be pumped at pressures small compared with p_c in Table 1, e.g., 0.005 mbar and 0.01 mbar. During SD the permanent gases are desorped from the product, the stoppers, the vials, the walls of the chamber, and all surfaces in the plant. There is no rule of thumb for the amount of these gases, but an end pressure of the pump set with the empty plant in the two examples

Copyright 2004 by Marcel Dekker, Inc. All Rights Reserved.

$< 10^{-3}$ mbar should be sufficient. If the back streaming of oil from oil-sealed pumps has to be completely excluded, pumps without oil seals have to be used in series. A multistage claw pump (the principal gas flow is shown in Figure 19(a)), followed by a roots pump (schematically shown in Figure 19(b)) provide an end pressure of a few times 10^{-3} mbar. Two roots blowers and one multistage claw pump have a pumping speed as shown in Figure 19(c) with an end pressure below 10^{-4} mbar.

The sterilization efficiency of the inlet venting filters has to be assured by regular integrity tests. The filter integrity test should be performed automatically with the relevant data documented by the control system; the principle is shown in Figure 20. The criteria for an integrity test given by the Parenteral Society [10] are summarized as:

The test should be reproducible within specified error margins.

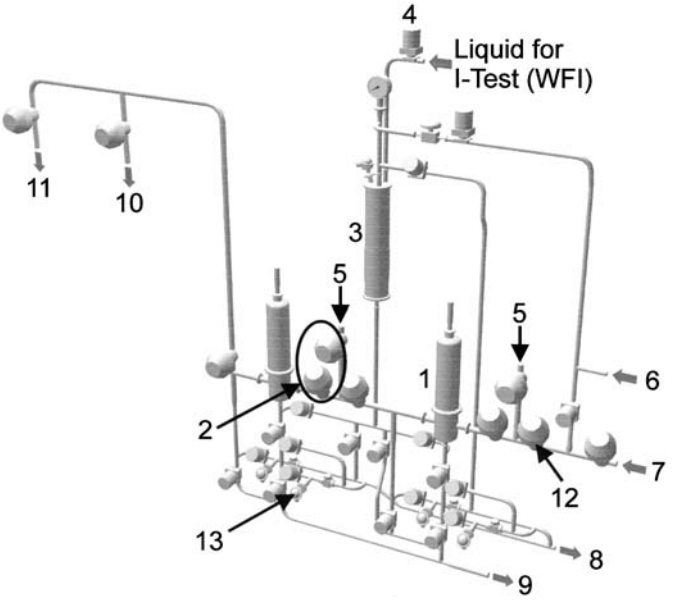

Figure 20 Principle of a venting filter for in situ integrity tests. The integrity tests are carried out following the water intrusion method: 1, primary filter with an 0.22 μm cartridge; 2, secondary filter with an 0.22 μm cartridge installed as a backup filter, sterilized independently of the filter 1; 3, test liquid reservoir (WFI) with heater; 4, inlet valve for test liquid (WFI); 5, pure steam inlet; 6, filtered air (5 bar absolute); 7, venting gas (1060 mbar); 8, drain line with valves; 9, to water ring pump (WRP); 10, to condenser; 11, to chamber; 12, sanitary valves; 13, temperature sensors.

Copyright 2004 by Marcel Dekker, Inc. All Rights Reserved.

The test should be correlated to a bacterial challenge test in which a sterile filtrate has to be produced when the filter is challenged with 10 *Pseudomonas diminuta* per cm^2 of filter surface.

The test should be carried out without removing the filter or the housing from the system.

The test should be performed after steam sterilization before freeze-drying the next batch.

F. Process Control, Vacuum Measuring, Leak Testing Systems

The process control in automated manufacturing surroundings should control, monitor, and document the process, must comply with GPM or GAMP (Good Automation Manufacturing Practice), and has to be validated. An example of a hardware architecture is shown in Figure 21.

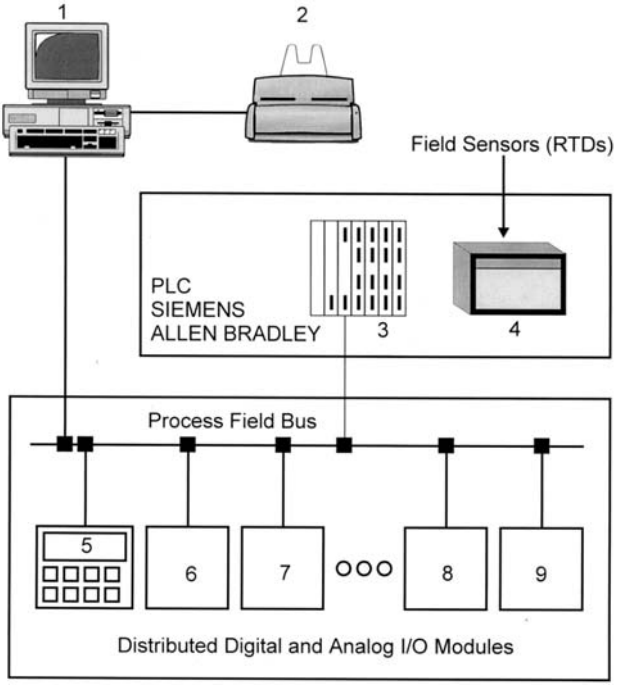

Figure 21 Architecture of the control systems hardware: 1, PC; 2, color printer; 3, CPU: 4, recorder; 5, control panel sterile room; 6, compressor; 7, vacuum pumps; 8, venting filter; 9, condenser (Steris GmbH, D-50354 Hürth, Germany).

Copyright 2004 by Marcel Dekker, Inc. All Rights Reserved.

It is recommended to use programmable logic controllers (PLCs) for the design of the machine control separately to avoid interference between machine failures and the data management. Furthermore the control system should be SCADA (Supervisory Control and Data Acquisition) compatible; an example of a hardware configuration is shown in Figure 22.

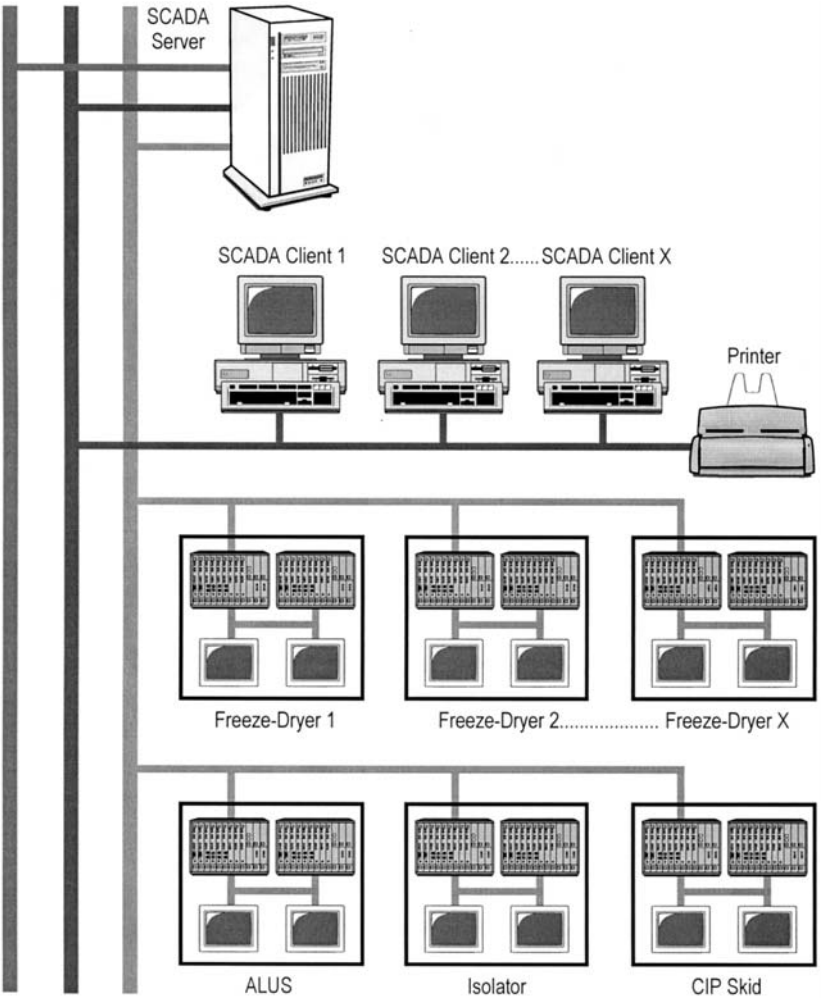

Figure 22 Example of a SCADA (Supervision, Control, and Data Acquisition) solution for several freeze-dryers $(1, 2, \ldots, X)$, one loading and unloading system (ALUS), built into an isolator. Furthermore, a CIP (Clean in Place) system is controlled and monitored, (Steris GmbH, D-50354 Hürth, Germany).

Copyright 2004 by Marcel Dekker, Inc. All Rights Reserved.

The pressure measurements should always be done by capacitance manometers (CAs) and not by thermal conductive gauges. TM depend on the gas mixture (water vapor and permanent gases) and are not reproducible enough for BTM measurements; details are given on pp 327, 328 in [2]. For leak testing no special equipment specifications are required. The leak rate for the chamber, e.g., $<1 \times 10^{-3}$ mbar L/s, and for the condenser, e.g., $<1 \times 10^{-3}$ mbar L/s, should be specified since it might be helpful to measure the chamber and condenser separately. The maximum tolerable leak rate in the two examples is $<1 \times 10^{-2}$ mbar L/s, if the DR data at 0.1%/h should have an error <10%. If a helium leak tester is not available in production, it should be specified for quotation.

The list of data which should be permanently shown to the operator, or shown only if specified events take place, is largely a question of in-house philosophy with a recommendation to have a standard for all operators and not distract them by too much roaming about. In a production plant all available process and machine data should be recorded. Experience teaches that it is easier to analyze the reasons for events if two or more groups of data point in the same direction than if only one group of data is available. The list of data recommended in [2, pp 328–330] is more a bare minimum than a complete list.

G. Cleaning and Sterilization

"The FDA regulations for cleaning validation of production systems can be fulfilled by automated plants and processes in so far as these systems are suitable for Cleaning in Place (CIP)." A CIP system is custom-built for a freeze-dryer, the products to be manufactured, and the cleaning agents and the detergents to be used; a schema of it is shown in Figure 23. The cleaning is dominated by the four T principles [10]:

Temperature:	Thermal effect: a temperature increase of 1°C increases the cleaning efficiency by 5% (over 30°C). With too hot a cleaning medium protein particles will burn onto the surfaces. Precleaning at 40°C is recommended.
Turbulence:	Turbulence as defined by Reynolds number (*Re*) is mostly a function of flow velocity and viscosity. The flow velocity in the pipes should be >2 m/s or *Re* >8000.
Time:	The effect of cleaning time can increase more than pro rata time.
Titration:	The concentration of the chemicals used in detergents, cleaning agents, or acids depends on the degree of equipment contamination.

Copyright 2004 by Marcel Dekker, Inc. All Rights Reserved.

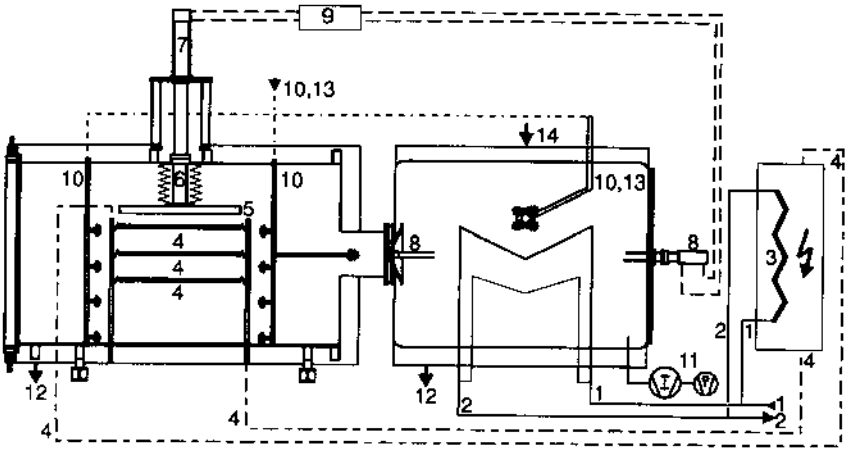

Figure 23 Freeze-drying plant condenser and shelves cooled with LN_2. Clean in Place system in chamber and condenser: 1, LN_2 inlet to condenser and heat exchanger; 2, N_2 outlet from the condenser and heat exchanger; 3, heat exchanger for the brine in the shelves; 4, brine to and from the shelves; 5, pressure plate for closing vials; 6, piston rod with bellows; 7, hydraulic piston for 5 and 6; 8, hydraulically operated valve; 9, hydraulic system; 10 and 13, water and steam inlet; 11, pumping system; 12, water outlet (Steris GmbH, D-50354 Hürth, Germany).

During CIP the following parameters should be documented for validation purposes: water and detergent temperatures, time, pressure, and the conductivity of the drained liquid.

The effect of cleaning can be proved by a 0.1% riboflavin solution; if after cleaning no riboflavin residuals can be detected by UV light, the plant is considered clean.

The sterilization of freeze-dryers is mostly done by ultra-pure steam (water for injection standard: USP XXII or PhEUr equivalent) with a minimum exposure to 121°C for 30 min. The definition of a sterilization process is: a validated process used to render a product or surface free of all forms of viable micro-organisms (EN 556-1: 2001). The principle of Sterilization in Place (SIP) is shown in Figure 24. In section 2.3.4 of [4] more than a dozen design criteria are suggested for a freeze-drying plant to be steam sterilized, a few of which are listed. Filtered "plant steam" contains a large amount of non-condensable gases, while it should contain less than 3.5% and have a dryness value between 0.9 and 1.05. Superheated steam has to be avoided and pressure reduction in the pure steam inlet limited to less than 2:1. All parts to be sterilized should be evacuated to less than 50 mbar; repeated pulsing can help to remove the non-condensable gases.

Copyright 2004 by Marcel Dekker, Inc. All Rights Reserved.

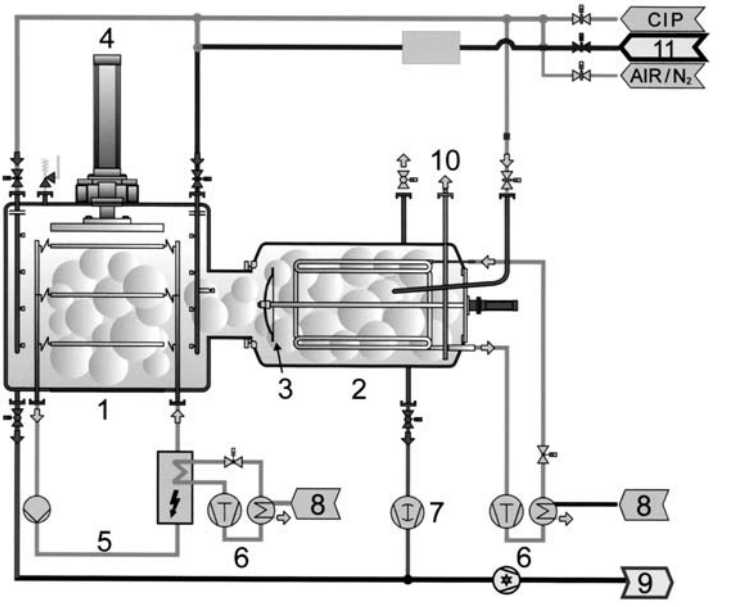

Figure 24 SIP (Sterilize in Place) principle: 1, chamber; 2, condenser; 3, Chamber–condenser valve; 4, hydraulic stoppering system; 5, silicone oil circuit; 6, cooling system; 7, vacuum system; 8, water; 9, drain water; 10, exhaust; 11, steam inlet (from Ref. 4).

The sterilization begins when the sterilization temperature is reached in the "coldest spots," e.g., drain ports and gas inlet filters. The entire process in production plants is normally carried out automatically, controlled, and documented. Depending on the design and size of the plant the time for CIP and SIP can be expected to lie between 8 and 12 h.

To avoid the high pressure during sterilization the VHP process can be used, as on pp 179–182 of [3] and assessed in section 2.3.4 in [4]. The use of VHP requires the following:

- the installation has to be dry, otherwise the H_2O_2 is dissolved in the water;
- the installation has to be pumped down to ≈ 1 mbar, to transport the H_2O_2 vapor quickly to all parts of the plant;
- the material of the plant has to be resistant to H_2O_2, which is proven for stainless steel, aluminum, silicon, viton, and teflon, but not every composition of polyurethane and plexiglass are resistant, e.g., Nylon is not resistant [8];

Copyright 2004 by Marcel Dekker, Inc. All Rights Reserved.

the vaccum pump set has to handle water vapor during the drying of the plant and H_2O_2, when the remaining vapor is pumped off;
long tubes with dead ends should be avoided: a tube of 1 cm diameter and 120 cm length is sterilized up to 80 cm [8].

Nakahira [11] describes his experience with the modification of an existing plant to use the sterilizing process in equipment that cannot be steam sterilized. The advantages were: update of an existing plant, short sterilization time at room temperature, and—compared with ethylenoxide—no risk to the operators and no contamination of the environment.

H. Uniformity and Reliability Consideration

As shown in Section III.E, uniformity within one charge and between charges, the two main reasons for non-uniform products are a non-uniform freezing and a non-uniform temperature distribution among the vials of one charge. Therefore the equipment specification should show how these problems are to be solved. The decision to transport and load the vials from isolators (Figure 2(a) and 2(b)) does not prevent the product from resting for different times on the shelves. As long as T_{sh} during loading is $\sim 5°C$ the different resting times can only influence the freezing by a different product viscosity if the product arrives, for example, at room temperature. Therefore the product should arrive at the loading platform at shelf temperature, which is the situation for the two sample products. Should T_{sh} for another product be, for example, $-50°C$, the product will rest for different times on the shelves and will have a different structure. This cannot be avoided by equipment specifications, but it could be corrected by an additional step during freezing comparable to thermal treatment. The idea is to raise the temperature high enough to soften or partially melt the ice crystals and than start a "second" freezing process common to the whole charge. The whole problem is rather complex and should be discussed under three headings: 1. Confirmation that the non-uniform product structure is due to different resting times at the shelf temperature (this can be done by simulations in the pilot plant). 2. Confirmation that the different structure results in different product qualities outside the accepted tolerances. 3. If headings 1 and 2 are confirmed, electrical resistance measurement (ER) and cryomicroscopy per example can be used to simulate the crystal growth, the influence of the treatment temperature (e.g., $-15°C$), and time on the degree of crystal melting and the final structure after the second freezing. The developed procedure can be checked and confirmed in the pilot plant with simulated loading times. The transfer of the final data to production should be as safe as the transfer of the main or secondary drying data.

Copyright 2004 by Marcel Dekker, Inc. All Rights Reserved.

The process problems resulting from the loading time of precooled shelves is described here in some detail, since it is important to differentiate between non-uniform product quality resulting from the "resting" effect and other effects described in the following. In Section III.E the influence of different kinds of shielding between product and walls/doors on the residual moisture content and on the product temperature was discussed (Figure 12). The consequences of the equipment specifications depend during freezing and MD mainly on the temperature range used: the further away from the average wall/door temperature, the more effective the shielding has to be. In the examples of Figure 12 the freezing step ended at $\sim -50°C$; T_{ice} during MD was $\sim 35°C$. In Figure 12(a) there was no shielding, in 12(b) aluminum frames were placed on the shelves round all vials in each one of the six groups, and in 12(c) the vials on the shelves were enclosed by temperature-controlled shields as shown in Figure 25, position 5. Besides the specification required in Section IV.D, the areas F in Figure 25 have to be dimensioned. A calculation of the different free areas will be too difficult because of the many unknown or uncertain factors. The valve diameter has been estimated and one can compare the necessary F areas with the free areas (B, C, and K in Figure 18). As examples a few assumptions and their consequences are given: F_1 is the free area between two shelves. The amount of water vapor to pass through this area is 50% of the total (in this example). Another critical area is F_2; these two areas should each be large compared with A in Figure 18. By "large" a factor of 3 to 5 is expected; above 5 is helpful in the pressure range below $p_c < 0.04$ mbar. How much is technically possible and economically meaningful is to be decided from case to case. This discussion as part of the specifications is intended to draw the attentions of the engineers to the flow resistances which increase drastically, as shown above, with decreasing pressure. The best uniformity of product quality has to paid for by decreasing flow resistances and additional surfaces to be cleaned and sterilized.

One other reason for a non-uniform product (see Section III.E) can be avoided by respective specifications. A non-uniform heat transfer from the brine in the shelves to the shelf surface can mostly be avoided by calculating and specifying the rate of brine to be circulated, by specifying the inlet and outlet area of the brine in the shelves and the design of the shelf borders. In the two examples freezing should happen at a rate of 1.5°C/min, resp. 0.8°C/min. To simplify the subject only the main part of freezing (90% of total water) from 0°C to −30°C is used in Table 7. The freezing alone in PA would require a brine speed of ~ 0.7 m/s in a channel roughly 20 m long, while in PB a brine speed of ~ 1 m/s in a channel roughly 30 m long would be required. The possible brine speed or the flow resistance depends mainly on the viscosity of the brine between −40°C and −70°C, the design of the

Copyright 2004 by Marcel Dekker, Inc. All Rights Reserved.

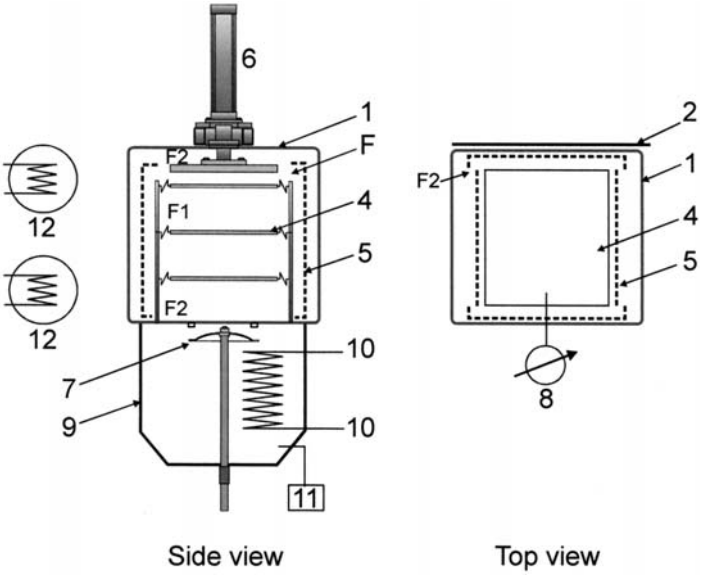

Figure 25 Schema of a freeze-drying plant with temperature-controlled shields between vials and walls: 1, chamber; 2, door with a temperature-controlled shield; 3, temperature-controlled shelves (range optional, max. −80°C to +80°C, cooling rate ($d \sim 15$ mm, 20°C to −50°C) maximum 2°C/min, heating rate (empty, −50°C to 0°C) maximum 3°C/min; 5, overlapping temperature-controlled shields, upper and lowest shelf protect top and bottom; 6, hydraulics for pressing the stoppers into the vials; 7, valve (diameter see Section IV.D); 8, capacitive vacuum gauge; 9, condenser housing; 10, condenser surfaces and temperatures (see Sections IV.B and C); 11, vacuum pump set: roots and two-stage rotary pump: end pressure 1×10^{-3} mbar, alternative: two roots and a dry vaccum pump (Figure 19(c)) from 1000 mbar to 0.02 mbar in loaded plant should be ~12 min; 12, heat exchangers for the brine in shelves and, temperature shields 5, F, space for water vapor flow. Leak rate $< 2 \times 10^{-3}$ mbar L/s.

channels, and their length. In the experience of the author it will be difficult to design a shelf economically in which the product of brine speed (m/s) and channel length (m) exceeds 10. For heat transfer reasons one would try to keep the flow speed as indicated, but the channel length for PA should be reduced; at least for PB it has to be shortened by using multiple brine inlets and outlets on each shelf. The transfer of pilot plant data to a production plant depends very often on the comparability of water vapor flows and heat transfer data of the shelves, but both can be measured before building a production plant: the vapor flow in the pilot plant can be transferred if the

Copyright 2004 by Marcel Dekker, Inc. All Rights Reserved.

Table 7 Limitation of Freezing Time by Shelf Design

Product	PA	PB
Shelf surface (m^2), number of shelves	10, 9	18, 12
Requested freezing time 0–30°C (min)	20	38
Calculated freezing time[a] (min)	33[b]	22
Required brine (L/min)	322	592
Required brine per shelf (L/min)	36	49
If brine channel in the shelf 55 cm × 1.5 cm brine flow (m/s))	0.7[c]	1.0[d]

[a]Calculated by equation (3) ([2], p 279), with $K_{su} = 300\,kJ/m^2\,h\,°C$ and $\Delta T = <35°C$.
[b]A time of 33 min can be achieved by $K_{su} = 495\,kJ/m^2\,h\,°C$, which is very rare, or by lower brine temperature −70°C instead of −50°C, resulting in ~25 min with K_{su}~400.
[c]Channel length in the shelf approx. 20 m.
[d]Channel length in the shelf approx. 30 m.

criteria discussed above are observed. For the shelf it is recommended to build one shelf full scale. It is not easy to use a smaller model and extrapolate the data to a larger shelf. The established data from larger shelves can normally be converted for smaller ones. Such a shelf model is also helpful to check the conditions on the edge of the shelf and at the inlets and outlets of the brine.

V. Troubleshooting

The problems discussed in this section are not due to leaks (see Section IV.F) or the failure of components in the plant. The problems mentioned here are process errors and unsatisfactory product quality.

A. Prolonged Evacuation Time

The condenser temperature (T_{co}) and its related vapor pressure (e.g., −50°C at ~0.04 mbar, −60°C at ~0.01 mbar) will normally define the lowest pressure to be reached in, for example, 20 min. A prolonged evacuation time can be related to water from sterilization or from condenser defrosting which was not completely drained, was frozen during evacuation below ~6 mbar, and "hides" in an area with limited heat input. The lowest pressure to be reached will depend on the ice temperature at an equilibrium between heat input into and possible amount of sublimation from the hide-out. Very often this pressure will be between 1 and 0.1 mbar.

Copyright 2004 by Marcel Dekker, Inc. All Rights Reserved.

Depending on the quantity of ice and the heat transfer it may take from 1/2 h to several hours to remove the ice by sublimation to the condenser. A leak test before the loading of the plant will avoid this effect.

B. Abrupt Pressure Rise After the Heating of Shelves Has Started

T_{co} is correct, but the pressure rises shortly after the heating of the shelves is started. The shelves are more or less covered by ice which condensed during the loading of the vials on cold shelves. The amount of ice depends on the loading time and the relative humidity of the surrounding air. The effect of the sublimation of ice from the heated shelves can lead to a pressure at which the product collapses in minutes (emergency cooling of the shelves is mostly not quick enough to avoid the collapse), or the amount can be so small that the condenser can cope with the additional water vapor at or below the operation pressure (p_c).

In this case T_{co} will rise, but p stays close enough to p_c. To avoid a dangerous pressure rise after loading on cold shelves it is recommended to raise T_{sh} only in small steps from the end freezing temperature ($T_{f,e}$), e.g., $-50°C$, first step $T_{sh} = -45°C$, then $-40°C$, and only after both steps when p_c is no longer exceeded, the final T_{sh}, e.g., $-10°C$, can be applied.

C. Sublimation Front Temperature (T_{ice}) Too High

If the trend of T_{ice} gets too close to the maximum tolerable T_{ice}, a reduction of p_c will stop this trend immediately (Figure 3).

D. Slow Increase of the Chamber Pressure During Main Drying

The increase can be due to two reasons. 1. Permanent gases included or dissolved in the frozen product are freed as the ice sublimates. The amount of gas in frozen product can vary by a factor of almost 100. If the vacuum pumps cannot pump the gases at a pressure substantially lower than the vapor pressure of the ice in the condenser, the condenser will fill up with permanent gas, hinder the transport of vapor to the condenser surface, and form ice with a very low thermal conductivity; this and the permanent gases are the reasons for a pressure increase in the chamber. 2. If the effect happens with a product of low gas content, it is likely that the permanent gases are not sucked off in the lowest area of the condenser (they are heavier than water vapor) and fill the condenser partially or totally with permanent gas, with the effect as above.

Copyright 2004 by Marcel Dekker, Inc. All Rights Reserved.

D. Stoppers "Pop Out" or Slide into Vials

Incompletely frozen concentrates in the product may explosively evaporate during evacuation, and blow some particles to the wall of the vial and some stoppers out of the vials. Stoppers may also slide into the vial neck, practically closing the vial to water vapor. This can happen mostly during freezing when the stoppers shrink too much at low temperatures.

E. Traces of Highly Volatile Components

Highly volatile solvents such as acetone or ethanol have vapor pressures as shown in Figure 26. If they cannot be removed before freezing and drying

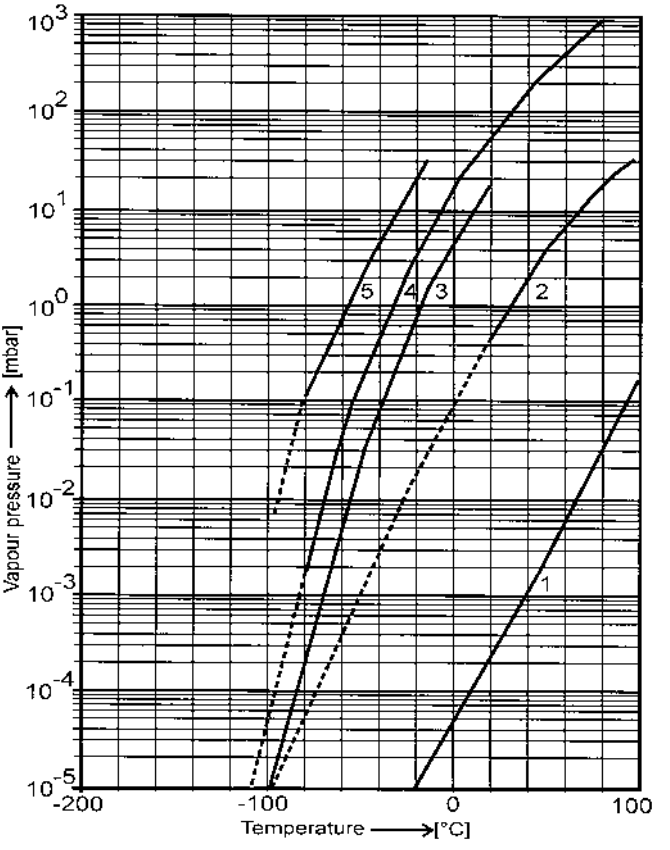

Figure 26 Vapor pressures of solvents as a function of temperature: 1, glycerin; 2, DMSO ($C_3H_8O_3$); 3, water; 4, ethanol; 5, acetone.

Copyright 2004 by Marcel Dekker, Inc. All Rights Reserved.

there are two possibilities: 1. if the amounts are small enough, substantially below 1%, quick freezing can help to distribute the liquid solvent uniformly in the ice and evaporate it together with the sublimation of the ice and pump if off from the condenser by the vacuum system. Acetone and ethanol are both liquids above $-90^{\circ}C$ and have a vapor pressure at $-60^{\circ}C$ of 0.6 mbar and 0.04 mbar respectively. The pumping systems may need condensing and cleaning systems, which are available. 2. If the amounts are too large to be pumped off, no general recommendation can be given, it depends on the type of solvent and its amount. A liquid may drop off the condenser and be stored in a collector at liquid nitrogen temperature or the vapor may directly be condensed at a liquid nitrogen trap. The reproducibility of a freeze-drying process of a product containing highly volatile solvents is at risk. A substantial effort is recommended to remove solvents at least down to traces before freeze-drying.

REFERENCES

1. H Willemer. Development of process data in a pilot plant transferable to production. In: L Rey and JC May, eds. Lyophilization of Pharmaceutical and Biological Products. 2nd ed. New York: Marcel Dekker, 2004 This volume.
2. GW Oetjen. Industrial freeze-drying for pharmaceutical applications. In: L Rey and JC May, eds. Freeze-drying/lyophilization of pharmaceutical and biological products. New York: Marcel Dekker, 1999.
3. GW Oetjen. Freeze-drying. Weinheim: Wiley–VCH Verlag, 1999.
4. GW Oetjen, P Haseley. Freeze-drying. 2nd ed. Weinheim: Wiley–VCH Verlag, in print, 2003.
5. S Corveleyn, S De Smedt, JP Remon. Moisture absorption and desorption of different rubber lyophilization closures. Int J Pharm 159(1): 57–65, 1997.
6. Z Wang, BA Frankel, W Lambert. Determination of moisture in rubber stoppers: effect of Karl Fischer oven temperatures. PDA Pharm Sci Technol 55(3):162–170, 2001.
7. MJ Pikal, S Sham. Interavial distribution of moisture during the secondary drying stage of freeze drying. PDA J Pharm Sci Technol 51(1):17–24, 1997.
8. R Steiner. VHP^{TM} sterilisation of freeze-dryers. ISPE Seminar on Lyophilisation, Antwerp, November 1994, International Society of Pharmaceutical Engineering (ISPE).
9. R Cully. Refrigerants, the environment and the liquid nitrogen option. International Society of Pharmaceutical Engineering (ISPE), Antwerp, 1994
10. F Wolpers. Cleaning in place systems for the pharmaceutical industry. VDMA Seminar, Interphex, Philadelphia, 2001.
11. K Nakahira. Validation of deep vacuum vapor phase hydrogen peroxide sterilizer retrofit to a production lyophilizer. PDA Asian Symposium, Tokyo, 1994.

Copyright 2004 by Marcel Dekker, Inc. All Rights Reserved.

12. P Haseley, GW Oetjen. Equipment data, thermodynamic measurements, and in-process control quality control during freeze-drying. Basel: PDA International Congress, 1998.
13. P Haseley GW Oetjen. The influence of the freezing speed on mannitol solutions during main and secondary drying. 20th International Congress of Refrigeration, Sydney, September 1999.
14. P Haseley, GW Oetjen. Freeze-drying with automated control of residual moisture in model substances and in human albumin products for subsequent viral inactivation. Symposium on the Freeze-drying of Pharmaceuticals and Biologicals, Center for Pharmeceutical Processing Research, Breckenridge, Colorado, August 2001.
15. TP Lin, ChC Hsu. Determination of residual moisture in lyophilized protein pharmaceuticals using a rapid and non-invasive method: near infrared spectroscopy. PDA J Pharm Sci Technol 56:(4): 196–205, 2002.
16. K Diels, R Jaeckel. Vakuum Taschenbuch. 2nd ed. Berlin, Göttingen, Heidelberg: Springer Verlag, 1962, pp 22–24.

Copyright 2004 by Marcel Dekker, Inc. All Rights Reserved.

16

Development of Process Data in a Pilot Plant Transferable to Production

Hanna Willemer
Köln, Germany

I. INTRODUCTION

The development of process data in a pilot plant is based on the data and information supplied by the product development. These data will mainly consist of the product qualities, the behavior during freezing and drying, and the container and stopper used. Furthermore the required residual moisture content and the time schedule for the process are provided.

The main data of the two products are summarized in Table 1. The goal of the development is to supply production with process and plant data as recommended for the manufacture of these products. The data of the examples are intended to illustrate the kind of information given to production.

The laboratory freeze-drying plant did not have automatic BTM and DR measurements. The hydraulic valve between the chamber and condenser was closed and opened manually. The time of closure was measured by a stop watch. The pressure rises were recorded on a high-speed printer, and T_{ice} extrapolated from the pressure plot at the change of slope. The pressure was measured by a capacitive gauge. The relationship between p_c, T_{sh}, and T_{ice} is only viable for the laboratory plant (lab plant); it will be different for the pilot plant and most likely also for the production plant.

Copyright 2004 by Marcel Dekker, Inc. All Rights Reserved.

Table 1

	Product A	Product B
Filling volume (mL/vial)	2.5	150 ml
Layer thickness in the vial (mm)	7	55
Solid content (%)	16	9
Stopper manufacturer and type specified by product development	Igloo type	4 slots
Temperature during loading (°C)	10	5
Heat transfer coefficient (K_{su}) from the heat transfer medium in shelves to the freezing front (kJ/m^2 h °C)	260	115
Freezing:		
Loading: shelf temperature (°C)	−55	5
Subcooling to (°C)	−8/−12	−5/−15
Freezing rate (°C/min) from product development	>1	>0.5
Calculated freezing rate[a] (°C/min)	~1.5	~0.1
Duration of thermal treatment, TT (min)	90	—
T_{sh} during TT (°C)	−35	—
Temperature range of freezing rate (°C)	0/−30	0/−30
End temperature: shelves (°C)	−55	−52
product (°C)	−53	−47
Main drying:		
T_{ice}[b] (°C)	< −38	< − 34
p_c pressure controlled in the lab plant (mbar)	0.08	0.15
T_{sh}[c] shelf temperature in the lab plant (°C).	−5	8
Expected T_{ice} /p_c in the pilot plant (°C/mbar) (see Section II. B)	< −38/0.08	−38/0.1
Heat transfer coefficient from the heat transfer medium to the sublimation front (kJ/m^2 h°C)	90	55
t_{MD} (h) laboratory/estimated[d]	10/4.7	90/61
Change to SD at maxT_{ice}^{e} min^{-2}	2	1
Secondary drying:		
Shelf temperature (°C)	50	45
Total pressure (mbar)/T_{co} (°C)	0.004/−67	0.02/−55
Partial pressure permanent gas (mbar)	< 0.001	< 0.005
t_{SD} (h)	6	25
Termination of SD at DR, dW (%/h, %)	0.04, 1	0.1, <2

(*continued*)

Copyright 2004 by Marcel Dekker, Inc. All Rights Reserved.

Table 1

	Product A	Product B
Subsequent treatment:		
Venting with	N_2	N_2
Venting pressure (mbar)	900	1000
Vial closing with	stoppers	stoppers
Pilot plant requirements:		
Number of loaded shelves	2	1
Number of vials per shelf	100	25
Water content of charge (g)	420	3.410
Solid content of charge (g)	80	340
Desirable chamber volume (L)[f]	100 to 120	100 to 120
Estimated production requirements:		
Vials/charge	10,000	2500
Shelf surface (m^2)	5.5	10
Loading (unloading) time (h)	1.5	2[g]

[a] Calculated by Eq. 3 (p 279 from [2]).
[b] T_{ice} (p 101) from [1] and in Figure 1 in Chapter 15 of this book.
[c] Heat transfer medium cooled, electrically heated.
[d] Estimated by Eq. 4 (p 289 of [2]).
[e] The use of the decrease of T_{ice} at the end of MD is explained in B2 (p 482).
[f] Approx. 1 L volume for 1 g solids.
[g] It is assumed that the hand loading of the large vials in plants of $\sim 10\,m^2$ is operable.

II. PROCESS REQUIREMENT

The general requirement for the pilot plant for product A is to make the necessary amount of product per charge as small as possible since the product is expensive and for the time being difficult to prepare. The task for product B is to define the minimum number of vials which would allow the transfer of data to production. It is decided that two shelves with 100 vials each of product A and one shelf with 25 vials of product B are an economical and technical optimum.

A. Freezing

During loading (1.5 h) the shelves of the production plant at $-55^{\circ}C$ with product A, a structural change between the first and last vials loaded is possible and has to be studied in the pilot plant. The freezing rate of

Copyright 2004 by Marcel Dekker, Inc. All Rights Reserved.

product A can be estimated by equation (1) in [1] as approx. 1.6°C/min in the production plant. If $K_{su} > 160\,kJ/m^2\,h°C$ a freezing rate >1°C/min can be achieved. The freezing rate for product B of 0.5°C/min is not possible with $d = 55\,mm$. With $K_{su} = 115\,kJ/m^2\,h°C$ and $dT = 37°C$ a freezing rate of ~0.1°C/min is estimated. As can be seen from equation (1) an increase to 0.5°C/min is technically not possible, and freezing with liquid N_2 (LN_2) in the large vials and 55 mm product thickness would require a substantial development with the vials and an LN_2 cooling system. Quality management and product development have agreed that the product frozen at 0.1°C/min is acceptable.

The degree of subcooling can influence the actual freezing rate, even if the average rate between 0 and −30°C is the same. The degree of subcooling is difficult to measure (p 285 in [2]) and to influence (pp. 13–14 in [3]). It will be treated as information which is not part of the process control.

The pilot plant studies have to show whether a resting of the first loaded product until the start of drying changes the structure of the first loaded product enough to change the main or secondary drying compared with an immediately dried product. The product quality of both cycles has to be compared. The thermal treatment (TT) of the product reduces the chance of any influence from the different resting time.

To avoid too much ice condensation on the shelves during loading of product A the pilot plant should be kept under a low overpressure of dry air (due point <−40°C).

For the thermal treatment of product A T_{sh} has to be kept at −35°C for 90 min.

B. Main Drying (MD)

1. T_{ice} as a Function of the Operation Pressure p_c and the Shelf Temperature T_{sh}

The temperature at the sublimation front T_{ice}, measured by BTM (pp 99–102 in [2]), has to be <−38°C. In the lab plant this was achieved at $p_c = 0.08$ mbar and $T_{sh} = -5°C$. This relationship applies only for one product, one T_{sh}, in one plant. T_{ice} depends strongly on p_c as shown in Figure 1. T_{ice} as a function of p_c will be measured in the pilot plant.

The calculated main drying time t_{MD} (Table 1) is ~4.7 h. It can be shortened by increasing T_{sh} from −5°C to 0°C or to 5°C to 4.1 h or 3.6 h respectively. In view of a total estimated cycle time of ~17 h from loading to unloading, the saving of 1 h has to be judged in view of the total operation. Besides t_{MD} it is essential to study the uniformity of the process: the main drying and freezing depend mainly on the heat transfer from the heat

Copyright 2004 by Marcel Dekker, Inc. All Rights Reserved.

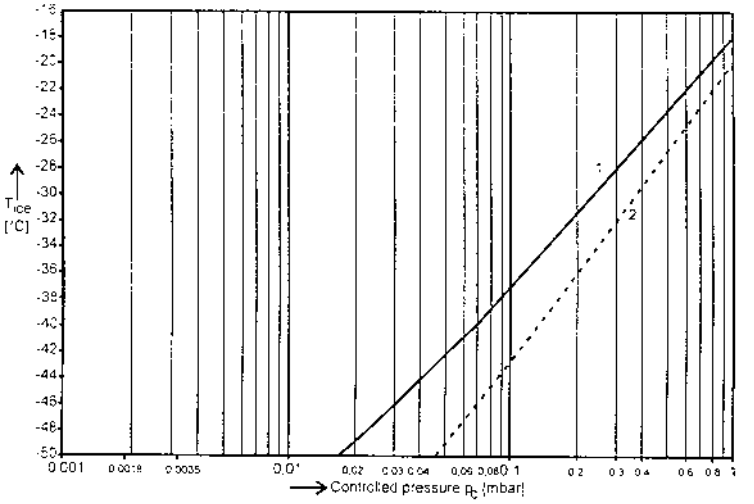

Figure 1 T_{ice} as a function of p_c [1]. The plot shown is only valid for one type of product, in the same vials, in the same plant, and one T_{sh}: 1, T_{ice} as function of p_c; 2, saturation vapor pressure of ice (from Ref. 5).

transfer medium in the shelves to the sublimation—or the freezing zone in the product. With the relatively small shelf surfaces in pilot plants the uniformity of heat transfer in all parts of the shelves may be acceptable, but it will play an important part in production plants. Therefore some details on a uniform heat transfer are discussed in Sections III.E and IV.H [1]. Another influence on the temperature of the product in vials is that of the temperature of the chamber walls and door(s). Some basic facts about the shielding of wall and door influences are given on p 104 and in Figure 23 in [2]. The consequences for the residual moisture (RM) in one charge are shown in Figure 12 in [1]: with no shielding the product in ~50% of the vials on the edge of the shelves shrunk and contained between 7 and 21% RM, while in the center vials RM was between 0.9 and 1.1%. With shielding RM of the product in all vials was between 0.4 and 1%. For product A with the relatively quick temperature changes during TT, the short t_{MD}, and the required low residual moisture dW, a temperature-controlled shielding (case (c) in Figure 12 in [1]) should be tested in the pilot plant. For product B aluminum frames placed on the shelves enclosing groups of vials (solution (b) in Figure 12 of [1]) could be sufficient: no TT, long t_{MD}, and relatively high RM. The different t_{MD} between the lab plant and calculated data show that the calculation by equation (4) is not sufficient for large d: it does not account for the temperature gradient in the ice, which is calculated to be

Copyright 2004 by Marcel Dekker, Inc. All Rights Reserved.

approx. 4°C at $d = 55$ mm and 60 h of t_{MD}. The actual difference may be smaller, since the heat transfer is not only from the bottom to the sublimation front but also from the walls of the vials and by radiation from the upper shelf. For the process requirement it can be assumed that T_{ice} has to be 4°C below the data in Table 1, which results in −38°C or a pressure not of 0.15 mbar but of 0.1 mbar as can be seen from Figure 1. A decrease in T_{sh} would not change the temperature drop in the ice significantly but it would prolong t_{MD}.

2. Change from MD to Secondary Drying (SD)

The change from MD to SD has been done in the lab plant without automation. In the automated pilot plant the time of change can be more precisely defined as shown in Figure 7 of [1]. The maximum average T_{ice} during MD (max.$T_{ice/n}$) is the controlling data by which the change is governed, e.g., max.$T_{ice/n}$ −1°C start $T_{sh,SD}$, max.$T_{ice/n}$ − 3°C stop p_c. The influence of the freezing method, the number of vials per charge, and T_{sh} can be recognized as shown in Figure 2.

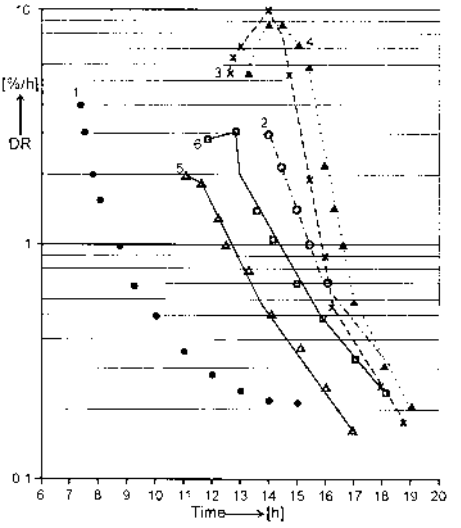

Figure 2 Various influences on the DR data during the change from MD to SD [5]; 1, product is collapsed, DR drops rapidly after too early a change, water is removed by vacuum drying from viscous concentrates; 2, later change due to $T_{sh} = -5$°C (all other $T_{sh} = 0$°C); 3 and 4, product frozen in LN_2, small crystals, long t_{MD}; 5, $T_{ice} = -34.5$°C, 100 vials; 6, $T_{ice} = -32.2$°C, 400 vials in the charge. In 5, $dT = -34.5$°C; in 6, $dT = 32.2$°C; t_{MD} in run 6 ~ 10% longer than in 5. (Figure 2.9 from [5]).

Copyright 2004 by Marcel Dekker, Inc. All Rights Reserved.

3. Secondary Drying (SD)

The pressure and shelf temperature requirements for SD can be taken from the lab plant data (see p 107 in [2]). The automated measurement of the pressure rise permits the calculation of the desorption rate (DR), the desorbed water in % of solids per hour (%/h), by

$$\mathrm{DR} = 2.89 \times 10^2 (V_{\mathrm{ch}}/m_{\mathrm{so}})(\mathrm{d}p/\mathrm{d}t) \quad \text{(desorption of water vapor in \% of solids per h)} \tag{1}$$

where:

V_{ch} = volume of chamber (L)
$\mathrm{d}p$ = pressure increase during $\mathrm{d}t$ (mbar)
$\mathrm{d}t$ = time of pressure increase (s)
m_{so} = mass of solids (g)

From DR data the desorbable water ($\mathrm{d}W$) is calculated as an indicator for the RM content during SD:

$$\mathrm{d}W_t = \int_{t=0}^{t=1} DR\, \mathrm{d}t \tag{2}$$

The secondary drying can be terminated when the desired $\mathrm{d}W$ is reached. The secondary drying for product A requires a total pressure <0.004 mbar or condenser temperatures $<-67^{\circ}$C and permanent gas pressures <0.001 mbar. For product A the pump set has to receive attention in the specifications. The residual moisture calculated from DR can come up with values that are not identical with data from the Karl Fischer (see fig. 1.99.2 in [4]) or the thermogravimetric methods with constant temperature (see fig. 2.94 in [4]).

For uniformity of the RM content see the remarks on shielding in Section B.1. Besides the DR data the plots 2, 3, and 4 in Figure 2 show a change of slope at $\sim$0.6%/h. This change indicates that a certain amount of water was not frozen and is now vacuum dried (different example in fig. 1.73.3 in [5]).

III. PILOT PLANT SPECIFICATION

A. Specifications for the Pilot Plant

Figure 3 is a schematic drawing of the plant and summarizes the specification of the pilot plant, to fulfill the process requirements. The specifications

Copyright 2004 by Marcel Dekker, Inc. All Rights Reserved.

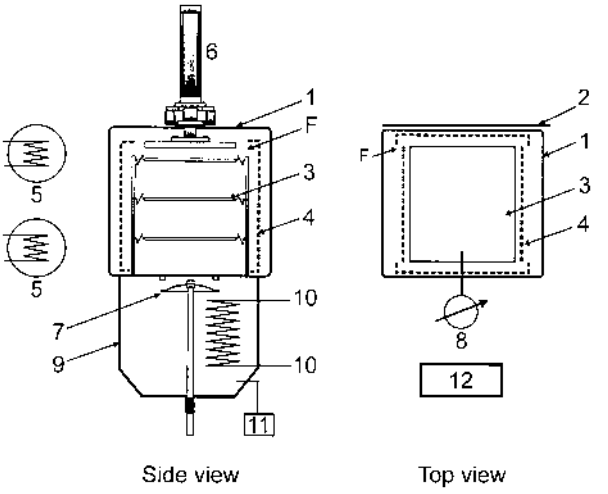

Figure 3 Schematic drawing of the pilot plant and main specifications:

(1) chamber large enough to take up the shelves (3) and the temperature shielding (4), otherwise as small in volume as possible (100 to 120 L) would be acceptable, to keep the ratio volume (L): solid content (g) as close to 1:1 (see III.B [1]). Chamber, door, (2), and condenser (10,11) are operated in a standard laboratory, but it should be possible to place the unit of the three parts in a ''sterile'' operational area, while the rest of the plant remains outside. Therefore the three parts of the plant and a new venting system have to sterilized by a vaporized hydrogen peroxide (VHP®) system; Vacuum pumps and pipeline have to withstand VHP.

(2) Door with temperature controlled shielding.

(3) Temperature-controlled shelves. Two options can be chosen: (1) shelf system adjustable for one pressure plate and two shelves each for 100 vials of product A or for one pressure plate and one shelf for 25 vials with product B, or (2) two independent shelf systems for products A and B. Temperature range -80 to $+80°C$ (if technically impossible, -80 to $+60°C$). Cooling rate between 0 and $-30°C$ at $4°C$/min of the empty shelves, $2°C$/min in a product in vials of 15 mm thickness, heating rate $-50°C$ to $0°C$, $3°C$/min;

(4) Overlapping temperature-controlled shields (not on top; not on bottom if the condenser is below the chamber);

(5) Heat exchangers for cooling and heating of 3 and 4;

(6) Hydraulic for the pressure plate to push the stoppers into the vials;

(7) Valve 100 mm diameter. Required as per Table 1 are: for product A, ~ 90 g/h water vapor at 0.08 mbar, for product B ~ 60 g/h at 0.1 mbar. The vapor flow density as shown in Figure 4 at 0.08 mbar ~ 1.1 to 1.5 g/h cm^2 (depending on the l/d ratio in the plant) and at 0.1 mbar ~ 1.7 to 2.3 g/h cm^2. By these calculations product A requires a valve between 85

Copyright 2004 by Marcel Dekker, Inc. All Rights Reserved.

are limited to those depending on the process. General specifications, e.g., construction, material, electrical, and data system requirements, or standards of the user have to be added.

For some specifications in Figure 3 the following reasons or explanations are given. The sterilization by vaporized hydrogen peroxide (VHP)® is described on pp 324–327 of [3]. The specifications ask for compressor or LN_2 cooling. Without LN_2 it will be difficult to achieve $-80°C$ on the shelves. This temperature is not necessary during MD but can be very helpful during freezing to reach high freezing rates. With $T_{sh} = -50°C$ and the main freezing between -10 and $-20°C$, the difference between average freezing at $-15°C$ and T_{sh} is 35°C; at $T_{sh} = -80°C$ it is 65°C. If approx. 1°C/min freezing rate is possible at $-50°C$, almost 2°C/min becomes possible at $-80°C$. For a pilot plant it is advisable to keep such options open, even if only used to show that 2°C/min does not improve the product quality to an interesting extent. In addition, there may be other considerations for using LN_2: for example, no cooling water and electrical energy for compressors, no mechanical parts in compressors (low maintenance), and no environmental problems with refrigerants. The chamber should be as small as possible to reduce the required amount of solids. The vacuum gauge has a limited reproducibility, for example, of 0.005 mbar, therefore the minimum pressure rise to measure is limited and the smallest DR depends on this minimum dp measurement and the relation of solid content in the chamber to the chamber volume. With today's

---

and 100 mm diameter and B between 60 and 70 mm, therefore 100 mm is specified;

(8) Capacitive vacuum gauge 1–1 × 10^{-4} mbar (0.5–1 × 10^{-4} mbar);

(9) Condenser housing;

(10) Condenser surfaces, 150 g/h water vapor between -50 and $-70°C$, capacity 4 kg ice;

(11) View port condenser surface;

(12) Vacuum pump set, one roots blower, two oil-free pumps in series, end pressure < 1 × 10^{-3} mbar, evacuation time of loaded plant down to 0.08 mbar ~ 12 min. Pressure control during MD either by injection of dry N_2 or by closing and opening the valve between condenser and pump set;

F Areas for water transportation from the vials on the shelves to the condenser. For details see section IV.D of [1];

Leak rates: chamber with cold and heated shelves and condenser with cold surfaces each < 1 × 10^{-3} mbar L/s. To measure DR data of ~0.2 %/h of both products with an influence of the leak rate smaller than 0.002 %/h, the leak rate for the example products, and a chamber of 100 L, a leak rate < 10^{-2} mbar L/s would be sufficient (for details see pp 95–98 in [4]).

Copyright 2004 by Marcel Dekker, Inc. All Rights Reserved.

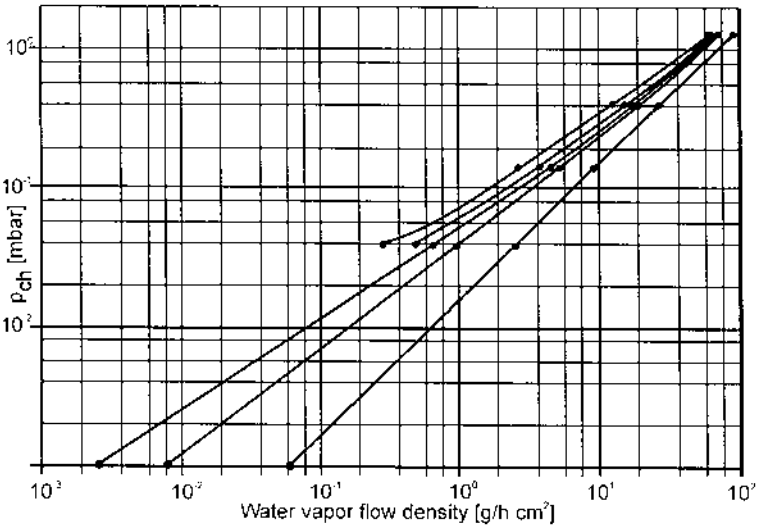

Figure 4 Density of water vapor flow (g/cm^2 h) as function of p_{ch} with jet flow (1) and length (l)/diameter (d) of the connection: 1 (2), 1.6 (3), 2.5 (4), 5 (5) as parameter; (4) and (5) are not plotted below 4×10^{-2} mbar, as these data depend much on the design details of the plant. They should be measured if needed (see Figure 6 in [1]).

capacitive gauges as a rule of thumb, DR data of 0.1%/h can be measured with an error of 10% if the ratio of solids (g) to chamber volume (L) is between 0.5 and 1.0. Larger ratios improve the accuracy, smaller ones decrease it.

Data management and process control should be specified as for the production plant. This is described in Chapter 15, Section IV. F, of this book. Details of the measurement and process control are specified as:

1. During freezing: Record the temperature difference ($dT_{\text{heat transfer medium}}$) in the inlet and outlet of the heat transfer medium in the shelves, frequency optional every 15 s to 3 min in 15 s steps during the main part of freezing. Start the condenser cooling and vacuum pump system. End the freezing when $dT_{\text{heat transfer medium}} < 0.2°C$ for more than 30 min.
2. During main drying: Adjust pressure control by closing and opening the valve between the chamber and condenser or by dry gas injection; T_{ice} by BTM with 60 to 100 measurements per s; calculate maximum average T_{ice} (max. $T_{ice/n}$) and the standard deviation of T_{ice}; the density of water vapor flow as a function of

Copyright 2004 by Marcel Dekker, Inc. All Rights Reserved.

Table 2 Residual Moisture in Product B Measured by the Thermogravimetric Method (RG) (see Figure 12) and Some Data by Karl Fischer (RF)

	RG (%)			
Temperature (°C)	30	60	100	RF (%)
Run 1	—	0.19	0.49	0.7/1.0
	—	0.35	0.61	
	—	0.37	0.56	
	—	0.42	0.56	
	—	0.23	0.41	
		av. 0.31, sd 0.10	av. 0.53, sd 0.08	
Run 2	—	0.32	1.49	1.0–2.0
	—	0.38	1.76	
	—	0.50	1.55	
	—	0.60	1.34	
		av. 0.45, sd 0.12	av. 1.53, sd 0.17	

p_{ch} depends on the land design to be taken from Figure 4 or has to be measured; change from MD to SD if $T_{ice} = \max. T_{ice/n} - 1$ to 3°C (to be chosen).

3. During secondary drying: Measure the pressure rise for DR to be chosen for 30 to 120 s; frequency of measurement to be chosen between 5, 10, 15 min, 0.5 h, and 1 h. Calculate dW from DR with each DR measurement. Terminate SD when the desired dW is reached.

An automated process program is given as an example in Table 2 of [1].

IV. PILOT PLANT QUALIFICATION

A. Qualification Tests

The leak rate of the plant was measured before the first and after the last test: average (av.) 4.2×10^{-4} mbar L/s, standard deviation (sd) 0.24 mbar L/s.

Figure 5 shows T_{sh} and p in the empty pilot plant. The results are summarized as follows:

Quick cooling: 0 to −40°C, 12 min = 3.3°C/min
End temperature of shelves: −80°C

Copyright 2004 by Marcel Dekker, Inc. All Rights Reserved.

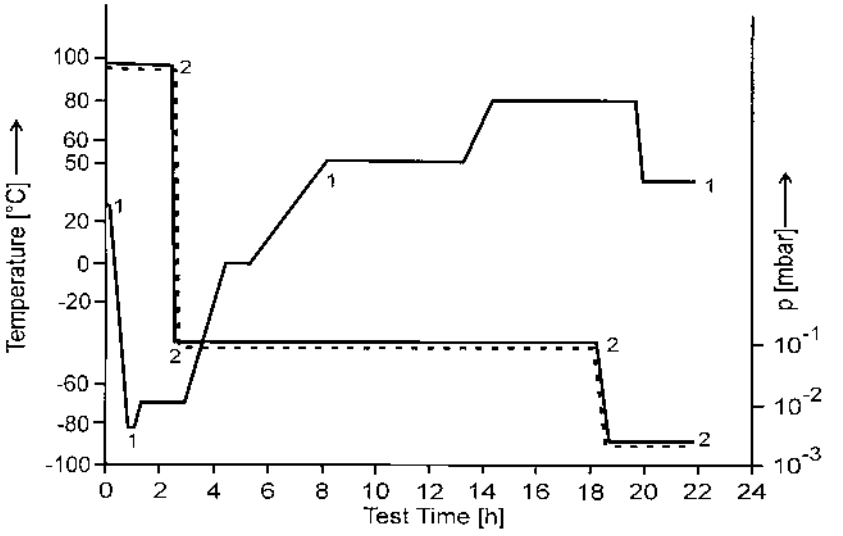

Figure 5 Temperature and pressure during a test run of the empty pilot plant with cold condenser: 1, shelf temperature (°C); 2, pressure as for product A and for B.

Temperature range covered from −80°C, −70°C, 0°C, +50°C, and to +80°C
Controlled heating: −70°C to 0°C, 90 min = 0.8°C/min
Controlled heating: 0 to + 50°C, 168 min = 0.3°C/min
Controlled heating: 50 to 80°C, 60 min = 0.5°C/min
End temperature of shelves: +80°C
Operation pressure control during MD (N_2 injection): 0.08 resp. 0.15 mbar (Table 1)
End pressure with cold condenser: 0.004 mbar
End pressure of pump set: < 0.001 mbar

Figure 6 shows the average data of three test runs with product A. The results can be summarized as follows:

Shelves precooled to −55°C, freezing from 0°C to −40°C in 33 min = 1.2°C/min (calculated 1.5°C/min), minimum freezing rate 1°C/min.
TT 90 min at $T_{sh} = -35$°C (as Table 1).
T_{sh} from −55°C to 0°C (loaded), 1°C min, $T_{sh} = 0$°C (lab. plant −5°C).
The increase to 0°C has not exceeded $T_{ice} = -38$°C, but increased dT in equation (4) to 38°C. In spite of this, t_{MD} is increased.
$p_c = 0.08$ mbar

Copyright 2004 by Marcel Dekker, Inc. All Rights Reserved.

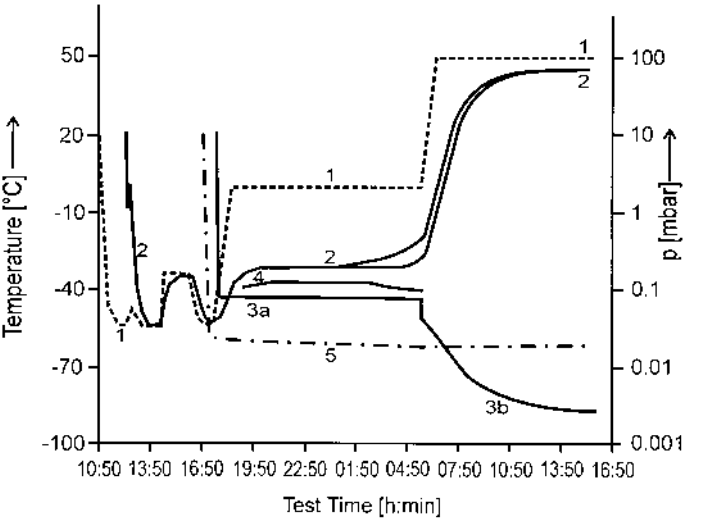

Figure 6 Average T_{sh}, T_{pr}, $p_{c,MD}$, p_{SD}, T_{ice}, T_{co} during three test runs with product A: 1, shelf temperature T_{sh}; 2, product temperature T_{pr} with PT 100 in the product; 3a, p_c during MD; 3b p_{SD} during SD; 4, sublimation front temperature T_{ice}; 5, condenser temperature T_∞.

T_{ice} (av.) $= -38.6°C$, (sd) $0.2°C$ (Table 1 $< -38°C$).
t_{MD} (av.) $= 11.5$ h, (sd) 0.6 h. Lab plant 8 to 10 h, estimated 4, 7 h. The result indicates a much lower heat transfer coefficient K_{tot} (assumed in the calculation at 90 kJ/h m^2 °C) of ~ 40 kJ/h m^2 °C for the vials used. This is in agreement with 1°C/min heating rate with loaded vials, while the empty shelves show a cooling rate of 3.3°C/min. The limiting factor in the heat transfer is not the transfer from the heat transfer medium to the shelf but from the shelf to the vial. This effect is not so severe during freezing since the heat transfer is improved by the atmospheric pressure during freezing.
Change from MD to SD when $T_{ice} = \max.T_{ice/n} - 2°C$ (as Table 1).
$p_{ch,SD}$ drops from 0.08 mbar immediately to 0.05 mbar and finally to 0.004 mbar.

In Figure 7 the plot of T_{ice} of product A as a function of drying time is shown. The three plots for the three runs are identical within drawing accuracy. They allow us to conclude: (1) In the first 6 h the structure of the product is less uniform as to the end of MD; T_{ice} changes abruptly since the sublimation passes through zones of different structures. In the

Copyright 2004 by Marcel Dekker, Inc. All Rights Reserved.

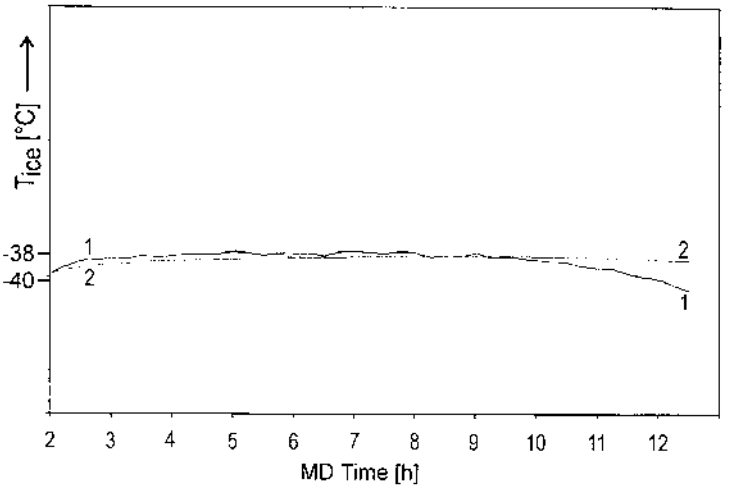

Figure 7 T_{ice} of product A processed with the data of Figure 6 as a function of drying time: 1, T_{ice}; 2, av. T_{ice}.

upper part of the frozen product solids have been concentrated during freezing, pushed up by the ice crystals formed in the lower part. Therefore the lower part of the product has a more uniform structure. (2) The calculated average T_{ice} is very stable with an average deviation of 0.2°C. (3) The change from MD to SD could occur earlier, e.g., at T_{ice} = max. $T_{ice/n} = m^{-2}$ $T_{ice} = 1.0$°C or at 10.5 h of drying.

In Figure 8 the dW data calculated from DR measurements and the residual moisture content is shown for the three runs: RF is the residual moisture content measured by the Karl Fischer method (see e.g. p 111 in [5]). From Figure 8 three conclusions can be drawn: (1) The amount of water detected by dW and Karl Fisher in product A are different. The Karl Fischer method counts water molecules which are not desorbable at 46°C. (2) The RF data are approximately constant at 1.5%. This is in agreement with the concentrated solids in Figure 7; these concentrated solids (highly viscous) will bind water more strongly than freeze-dried particles, so water cannot be removed from the viscous "liquid". This so-called freeze-concentrated part of the product has been reduced by crystallization of some water during TT, but the residual moisture content by RF of product A manufactured by the process as described will remain at ~1.5%, and, measured by dW, 0.06% at ~46°C are the corresponding data (3). The RF data of the three runs are shown in Figure 8: at 22.7 h, 1.2 to 1.5% (av. 1.4%); at 23.2 h, 1.2 to 1.6%

Copyright 2004 by Marcel Dekker, Inc. All Rights Reserved.

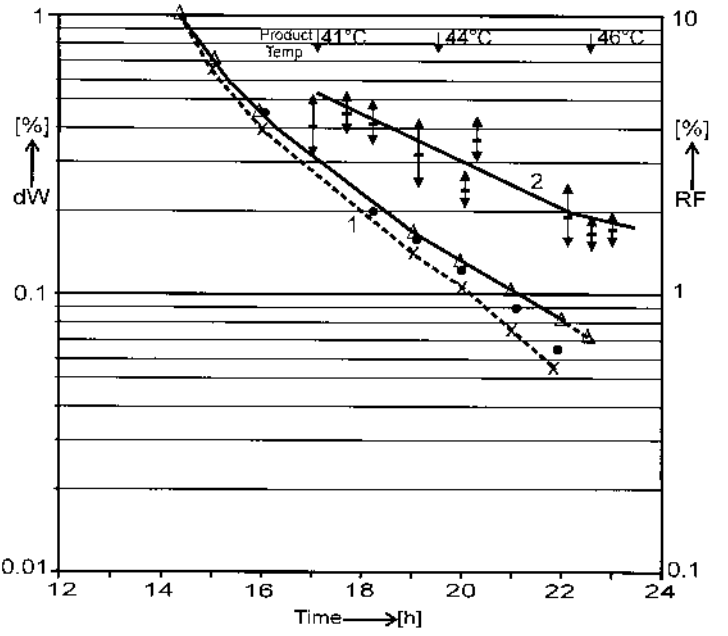

Figure 8 dW and RF (Karl Fischer method) of product A processed with the data of Figure 6 as a function of drying time: 1, dW of the three runs (×,●,Δ); 2, estimated plot of RF, double arrows maximum and minimum RF measured, horizontal line average of three measurements.

(av. 1.4%, sd 0.21%). The average RF within one charge was 1.2%, 1.3%, 1.6% each, with sd from 0.15 to 0.25%. If 1% has to be reached, two possibilities arise: (a) to freeze-dry the product at a lower T_{ice}, e.g., −43°C, to reduce the mobility of the water molecules, which increases the viscosity of the product by several decades; and/or (b) to freeze the product in LN_2 followed by a (different) TT.

Figure 9 shows the average data of two test runs with product B. The results can be summarized as follows:

> Shelves with vials cooled to −55°C, cooling rate = 1.7°C/min, freezing from 0°C to −40°C in 240 min = 0.17°C/min (calculated 0.1°C/min).
> T_{sh} from −55°C to 8°C (loaded), 0.8°C/min.
> p_c = 0.15 mbar.
> In spite of the large *d*. T_{ice} (av.) = −34.7°C, (sd) 0.7°C (Table 1 < −34°C).

Copyright 2004 by Marcel Dekker, Inc. All Rights Reserved.

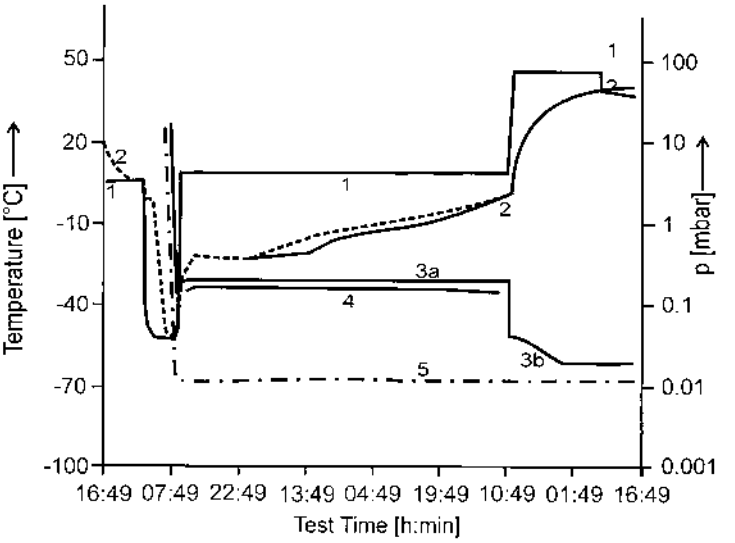

Figure 9 Average T_{sh}, T_{pr}, $p_{c,MD}$, p_{SD}, T_{ice}, T_{co} during two test runs with product B: 1, shelf temperature T_{sh}; 2, product temperature T_{pr} with resistance thermometer PT 100 in the product; 3a, p_c during MD; 3b, p_{SD} during SD; 4, sublimation front temperature T_{ice}; 5, condenser temperature T_{co}.

t_{MD} (av.) = 73.3 h (sd) 1.9 h. Lab plant 90; 61 h calculated. The result indicates a lower heat transfer coefficient K_{tot} (assumed in the calculation at 55 kJ/h m^2 °C) of ~46 kJ/h m^2 °C for the vials used. Change from MD to SD when T_{ice} = max. $T_{ice/n} - 1$°C (as Table 1). $p_{ch,SD}$ drops from 0.15 mbar immediately to 0.05 mbar and finally to 0.02 mbar.

The plot of T_{ice} as a function of drying time shows some instability in the first 10 h. The plots for the two runs deviate by ~1°C. They allow us to conclude: (1) In the first 10 h the temperature gradient in the ice of 55 mm produces a temperature near the bottom which softens or micro-collapses the structure near the bottom, depending on the extent to which ice can sublime between the wall of the vial and a little shrunken product. (2) The calculated average T_{ice} is very stable with an average deviation of 0.2°C within one run. (3) The change from MD to SD could occur earlier, e.g., at T_{ice} = max1.0°C or at 73.3 h of drying. In Figure 10 the dW data calculated from DR measurements are shown for the two runs.

The residual moisture determined by the thermogravimetric analysis (RG) is given in Table 2. The temperature profile 2°C/min from 30 to 100°C is used as the example given in Figure 11.

Copyright 2004 by Marcel Dekker, Inc. All Rights Reserved.

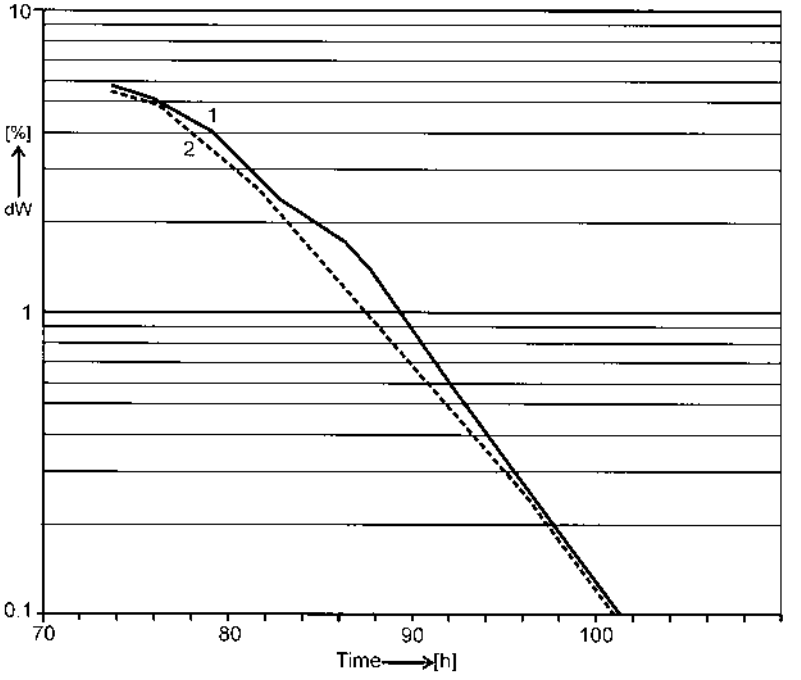

Figure 10 dW for two runs (1 and 2) of product B as a function of time.

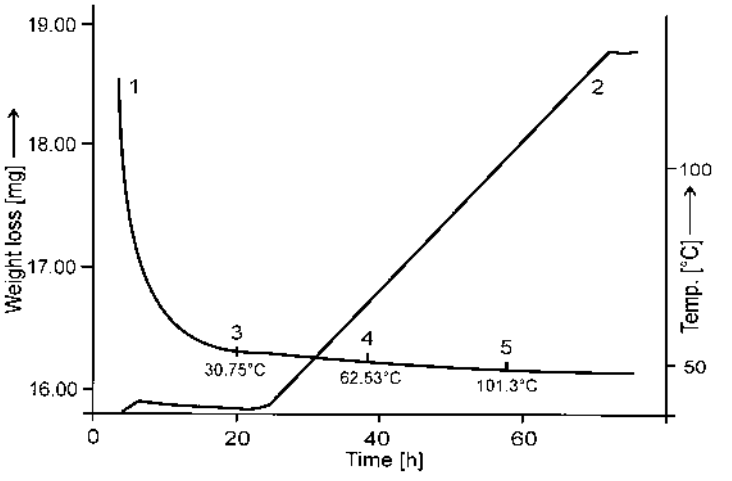

Figure 11 Thermogravimetric analysis of product A, run 1: 1, weight; 2, temperature; 3, no weight loss at 30.75°C; 4, 0.354% weight loss at 62.5°C; 5, 0.613% weight loss at 101.3°C.

Copyright 2004 by Marcel Dekker, Inc. All Rights Reserved.

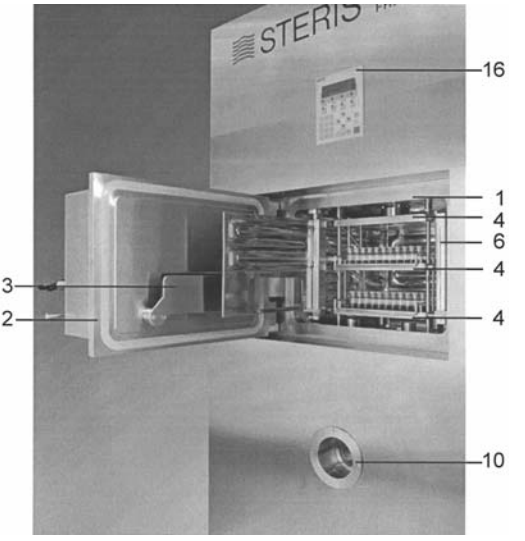

Figure 12 Pilot plant: 1, chamber wall; 2, door and separate temperature-controlled plate open; 3, swiveling cover hides manipulator; 4, temperature-controlled shelves; 6, overlapping temperature-controlled plates; 10, view port in condenser. Steris GmbH, D5034 Hürth, Germany.

Figures 12 and 13 show a pilot plant. In Figure 12 the door and the door shield are open, and the shielding inside the chamber (6) can be seen. In Figure 13 the door is open, but the door shield is closed. The opening in the door shield and its cover (3) are for a manipulator (3) (optional) to close vials during SD.

B. Water Vapor Flow in the Pilot Plant

The water vapor flow of the pilot plant has been calculated in Table 3 by using the data of Figure 4 an opening of the valve with a diameter of 100 mm and the assumption that $l/d = 1.6$. It is obvious that the drying process for product A and B is governed by the heat flow and not by the vapor flow. This opens up the theoretical possibility of reducing the main drying time. Products A and B could both be dried by 0.04 mbar ($T_{ice} = -45°C$) increasing dT from 38 to 45°C, resp. 46 to 53°C. This can reduce t_{MD} from 11 to ~9 h, resp. 73 to 63 h. For product A this could work, but for product B the resulting 54 g/h might be a little too much and only $T_{ice} = -44°C$ might be possible. This idea is only practicable if the valves in the production plant are sufficiently large. The calculation with

Copyright 2004 by Marcel Dekker, Inc. All Rights Reserved.

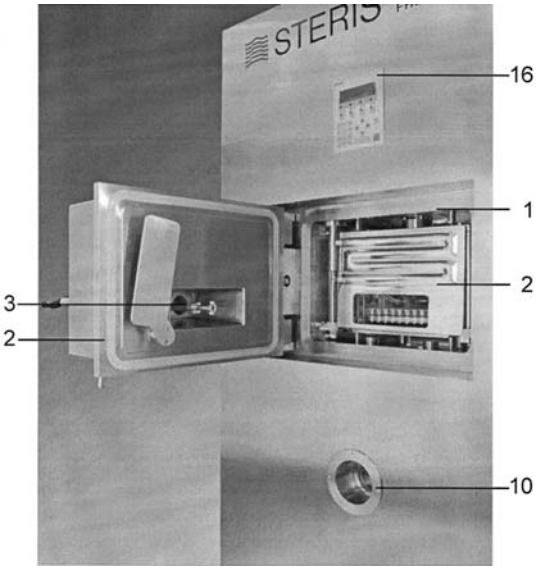

Figure 13 Pilot plant: 1, chamber wall; 2, door open, temperature-controlled plate closed; 3, manipulator, swiveling cover vertical; 10, view port in condenser. Steris GmbH, D5034 Hürth, Germany.

Table 3 Flow Density of Water Vapor at Various Pressures in the Pilot Plant

Pressure (p_c) (mbar)	T_{ice}[a] (°C)	Max. flow density[b] (g/h cm^2)	Max. flow in the pilot plant (g/h)	Flow for product[c]	
				A (g/h)	B (g/h)
0.3	−29	10	785	—	—
0.1	−38	2.6	204	38	—
0.08	−39	1.8	141		46
0.06	−41	1.2	94	—	—
0.04	−45	0.65	51	—	—
0.02	−49	0.25	20	—	—

[a] T_{ice} taken from Figure 1.
[b] Flow density taken from Figure 4.
[c] Necessary flows under the conditions of Table 1.

0.65 g/h cm^2 shows that even for product A the valve has to have a diameter of 1.5 m in the production plant, which is technically not possible. Maximum valve diameters are discussed in Section IV.D of [1]. Nevertheless, the diameter of 100 mm in the pilot plant is useful, and permits the study of processes at low T_{ice} to see which product advantages it might provide.

Copyright 2004 by Marcel Dekker, Inc. All Rights Reserved.

C. Summary and Recommendations for Production

Product A can be freeze-dried in the pilot plant with qualities acceptable to quality management. The transfer of the process data to production is feasible, if the following remarks are taken into account: (1) Product A: The freezing conditions including TT are critical; the water does not crystallize completely; and the temperature uniformity should be assured by temperature-controlled shielding. The main drying time can only be reduced by vials with a better heat transfer behavior; the possible gain compared with the total cycle time has to be judged by production; in the view of the pilot plant department the effort of introducing different vials with all its consequences is not recommended. The plot of T_{ice} during MD should be used to document an acceptable structure of the product during MD. The same applies for the DR data during SD. (2) Product B: The shielding is less critical from the time–temperature point of view, but the unusual thickness of the product presents a uniformity problem. The expected temperature difference during MD from the bottom to the top of the product is less important than expected. The variation of RM between the product in different vials of one charge is larger than expected, since the temperature-controlled shielding is a sure protection against wall and door influences. The configuration of 5×5 vials used on a shielded shelf puts 16 vials in optical contact with the shield, while the others see themselves partially. The easiest way to have all vials below the limit residual moisture content (RM) is to prolong the SD as shown in Figure 12, run 1. The time difference is ~ 97 h compared with 101 h, the RG data (Table 2) at 60°C are 0.45%, sd 0.12 for run 2, and 0.3%, sd 0.10 for run 1. The RF data are 1 to 2% for run 2 and 0.7 to 1.0% for run 1. The loading of the large vials is done by hand. Trays would be used for handling and loading, e.g., for 100 to 150 vials each. The bottom of the tray will be removed when the tray is placed on the shelf, and the vials stand on the shelf, and the remaining frame rests on the shelf. In such a frame a net of metal sheets could be incorporated in such a way as to enclose each vial. They form a very heat conductive and uniform surrounding for each vial. This has not been tried since it is more difficult to clean and sterilize.

ABBREVIATIONS

BTM	Barometric Temperature Measurement,
CA	Capacitive vacuum gauge
d	thickness of layer, diameter
d*p*	*p*ressure rise,
DR	Desorption Rate, desorbed water in % of solids per hour

Copyright 2004 by Marcel Dekker, Inc. All Rights Reserved.

dW	desorbable water
K_{su}	heat transfer coefficient from the heating medium to the sublimation front
LN_2	liquid nitrogen
MD	Main Drying, sublimation drying
p	pressure
p_c	controlled operation pressure during MD
p_{ch}	pressure in the drying chamber
p_{ice}	p_s of ice
p_s	saturation water vapor pressure
RF	residual moisture (Karl Fischer method)
RG	residual moisture content (gravimetric method)
RM	residual moisture
$T_{ice/n}$	sum of all n T_{ice} measurements divided by n

REFERENCES

1. GW Oetjen. Industrial freeze-drying for pharmaceutical applications. This volume.
2. H Willemer. Experimental freeze-drying: procedures and equipment. In: L Rey and JC May, ed. Freeze-drying/Lyophilization of Pharmaceutical and Biological Products. New York: Marcel Dekker, 1999.
3. GW Oetjen. Industrial freeze-drying for pharmaceutical applications. In: L Rey, JC May, ed. Freeze-drying/Lyophilization of Pharmaceutical and Biological Products. New York: Marcel Dekker, 1999.
4. GW Oetjen. Freeze-drying. Weinheim: Wiley–VCH Verlag, 1999.
5. GW Oetjen, P Haseley. Freeze-drying, 2nd ed. Weinheim: Wiley–VCH Verlag, in print.

Copyright 2004 by Marcel Dekker, Inc. All Rights Reserved.

17

Technical Procedures for Operation of Cleaning-in-Place/Sterilization-in-Place Process for Production Freeze-Drying Equipment

Gilles A. Beurel
S.G.D. Serail, Argenteuil, France

The cleaning-in-place/sterilization-in-place (C/SIP) system gives optimal results for the cleaning and sterilization of freeze-dryers. The system consists of four spraying columns situated in strategic areas of the vessels. Cleaning (CIP) and sterilization (SIP) use the same four spraying columns. The CIP operation consists of cleaning the vessels via the rotating spraying columns, which are fitted with a number of spray nozzles, calculated according to the surface to be covered and the position of the shelves. The SIP operation consists of sterilization of vessels via the same rotating spraying columns as for CIP. cGMP imposes different criteria of temperature, pressure, time, and cycle. This system allows a lot of flexibility and all of the vessels are designed according to the rules applied to the appropriate pressure.

The following presentation will acquaint the reader with the C/SIP system.

I. CLEANING IN PLACE

A. Principle

The CIP system (see Figures 1–4) provided in the freeze-dryer utilizes an over pressure spraying system that covers a maximum of the internal surfaces. The system ensures 100% covering of the surfaces to be cleaned.

Copyright 2004 by Marcel Dekker, Inc. All Rights Reserved.

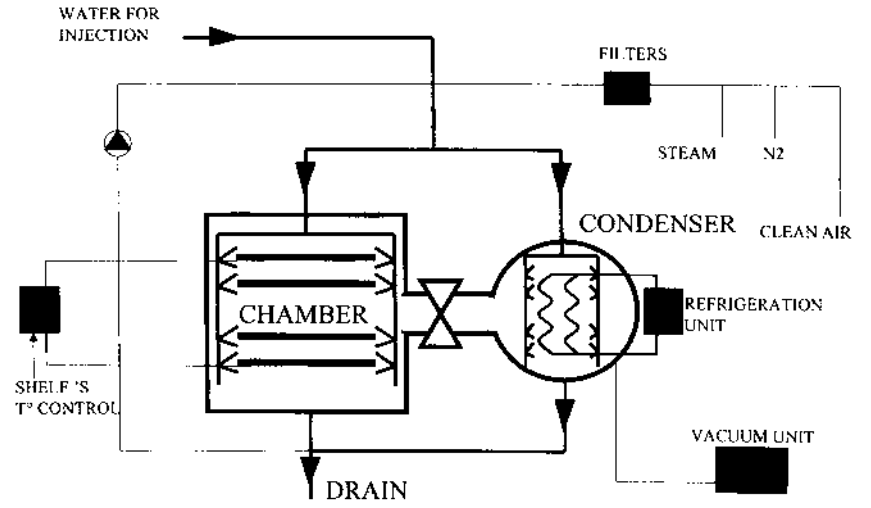

Figure 1 CIP: initial rinsing.

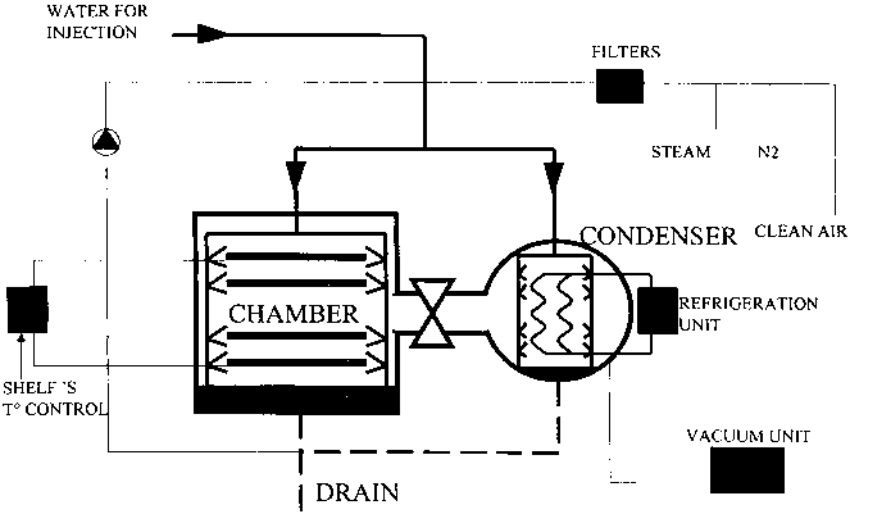

Figure 2 CIP: recirculation filling.

Copyright 2004 by Marcel Dekker, Inc. All Rights Reserved.

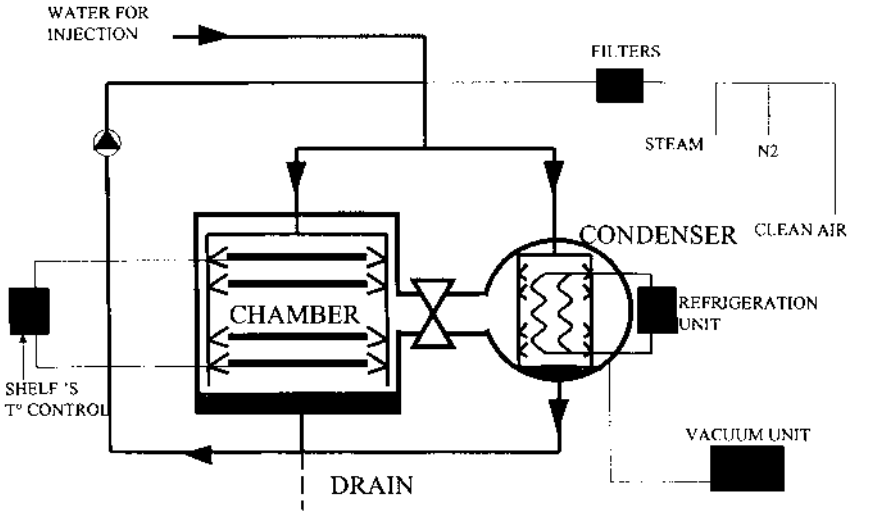

Figure 3 CIP: recirculation deconcentration.

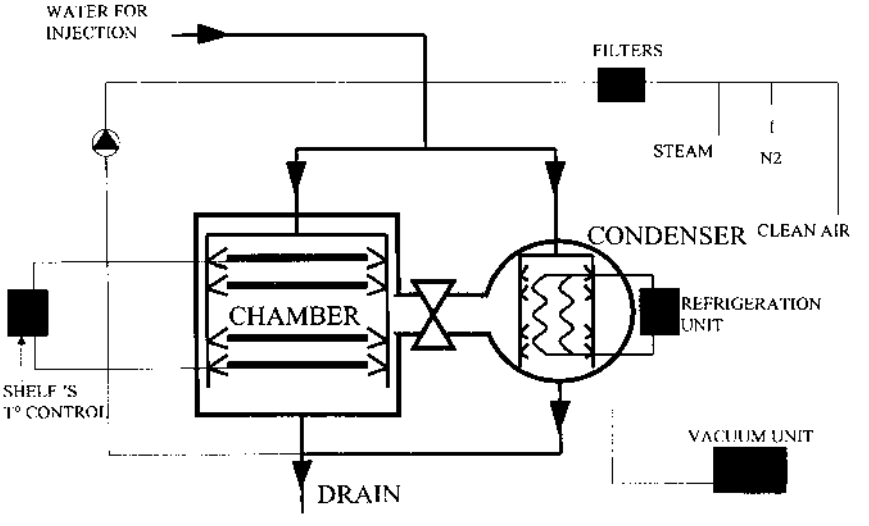

Figure 4 CIP: final rinsing.

Copyright 2004 by Marcel Dekker, Inc. All Rights Reserved.

The conception of overpressure spraying permits the use of various cleaning agents such as water, solvent, etc.

The cleaning cycle consists of three main phases:

Cleaning with reprocessing
Rinsing
Drying (when cleaning is not followed by sterilization).

The proposed system applies only to the freeze-drying chamber but a system could also be adapted to the condenser if required.

B. Description

1. Spraying Column

Four spraying columns are located in strategic areas of the chamber. Each column is fitted with a number of spray nozzles, calculated according to the surface to be covered and the position of the shelves (corking position high and low). Each spraying column is motored in a way that allows a rotational angle of 180° during the operation. One automatic column purging system is provided.

2. Overpressure System

The overpressure system consists of a pump operating with a nominal pressure of 6 bars. The system allows an independent distribution on one of the four spraying columns.

The standard overpressure system is fed with deionized and town water, the recycling capacity being limited by the bottom of the freeze-dryer chamber.

As an option, the system can be supplied as a closed loop for connecting and recycling the cleaning fluid. Such a system would include a collection tank and a filter system.

C. Operation

The operation of the CIP system refers to the above-described elements as well as the vertical shifting of the shelves by the stoppering system. The operation is cycled by a programmable logic controller, the total duration of the cycle being about 1–1/2 h. As mentioned, this operation is divided into three main phases: cleaning, rinsing, and drying.

1. Cleaning

Cleaning consists of spraying through each column. During each cycle, the operating column is fed by the overpressure system while going through

Copyright 2004 by Marcel Dekker, Inc. All Rights Reserved.

the column. At the same time, the shelves are shifted vertically by the stoppering system. Either town water or deionized water, depending on the requirement, can do the cleaning.

A 4 min cycle ensures eight successive sweeps for each column assuring a coverage that statistically is more than enough to obtain excellent cleaning.

2. Final Rinsing

In the same way as cleaning, the rinsing operation is achieved by using water by injection.

3. Drying and Draining

After steaming the chamber, the liquid ring vacuum pump is operated to perform a fast and efficient drying. During this operation, the freeze-dryer is first fed with flowing steam to heat up the chamber and the shelves to the relevant drying temperature. Then the drying operation begins, first using the liquid ring vacuum pump to get rid of the steam and the main part of the condensed water; then by using the ice condenser of the system to remove the remaining moisture. Nevertheless, initially the freeze-dryer will include fluent steam CIP ability.

Fluent steam cycle consists of injecting steam into the freeze-dryer while the drain is open. This creates a high condensation of clean steam in the chamber and the resulting condensates are flowing particulates down to the drain with an associated cleaning effect.

D. CIP Magnetic Coupling

Faced with potential leaks that could causes gaskets of the pneumatic spraying columns rotation system of CIP, Serail has developed a system in which the inlet column of the cleaning agent is fixed. The spraying column makes its rotation through a magnet system.

E. Recirculation Pump

The recirculation pump permits one to make a pass over the different elements to clean again.

F. CIP Skid

The CIP skid includes several catch tanks of cleaner agent as well as the pumps necessary to its distribution. A filtering system can be fitted as well.

Copyright 2004 by Marcel Dekker, Inc. All Rights Reserved.

II. STERILIZATION IN PLACE

A. Principle

The steam sterilization system (see Figures 5–9) used by Serail is designed with "autoclave"-type vessel construction to resist sterilization pressure combined with a control system permitting the validation of the sterilization cycles and eventual determination of the experimental FO sterilization value.

Because pure steam is corrosive, Serail manufactures the chamber, condenser, shelves, coils, and all process piping in 316 L stainless steel. The system is designed to reduce the time of sterilization by fast cooling and inside dry vacuum of the trap and the chamber. The sterilization will take $5H_2O$.

B. Description

1. Chamber and Condenser

The freeze-drying chamber and the condenser are calculated to resist a required sterilization pressure (see technical specifications). For this purpose, the equipment is designed following ASME, CODAP, or equivalent requirements and submitted according to the regulation and control set by the "Lloyd Register" or an equivalent.

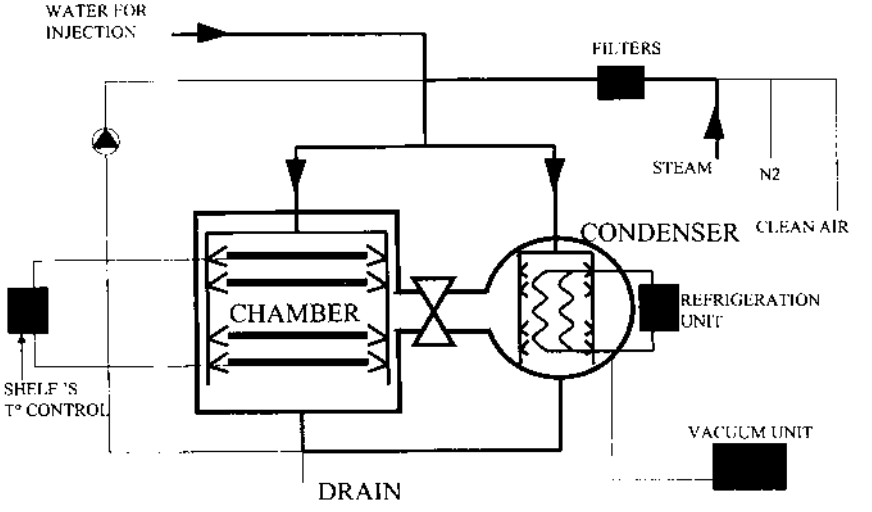

Figure 5 SIP: damping.

Copyright 2004 by Marcel Dekker, Inc. All Rights Reserved.

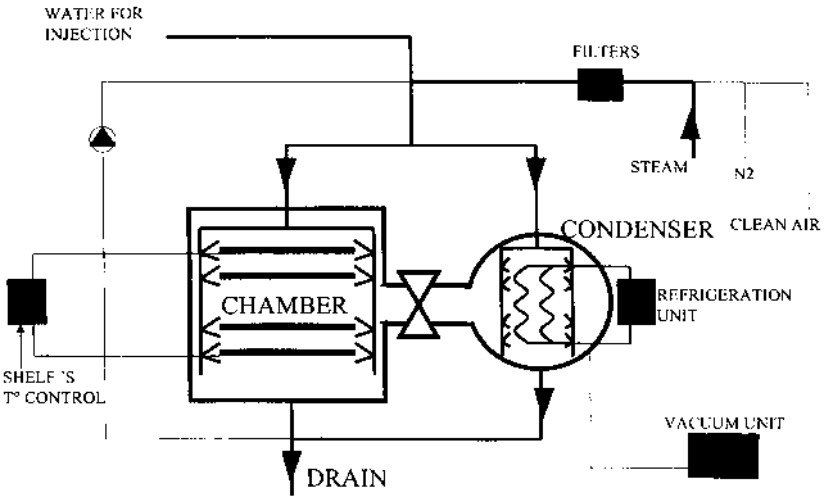

Figure 6 SIP: sterilization.

Both the chamber and the condenser are protected with a safety device (pressure relief valve) as required by these regulations (safety device located on steam manifold). The doors of the sublimation vessel are fitted with a quick latching device. This device works manually or automatically and is interlocked with a closing detection system related to the temperature and the pressure in the vessel (it is impossible to open the doors in case of positive pressure or high temperature). The door gaskets of are the O-ring silicon type (two gaskets including one O-ring gasket and one inflatable gasket).

2. Control

The steam feeding of the chamber is under the full control of the programmable logic controller (PLC) and data acquisition is achieved by the SCADA system during sterilization cycle control. Vacuum gauges are adapted to function in saturated steam and ambient conditions (MKS capacitance manometer 621).

3. Vacuum Pump

One liquid ring vacuum pump is provided to ensure complete evacuation of the steam and quick drying of the chamber and condenser after each sterilization cycle. This pump works under a pressure that is specified in the technical specifications.

Copyright 2004 by Marcel Dekker, Inc. All Rights Reserved.

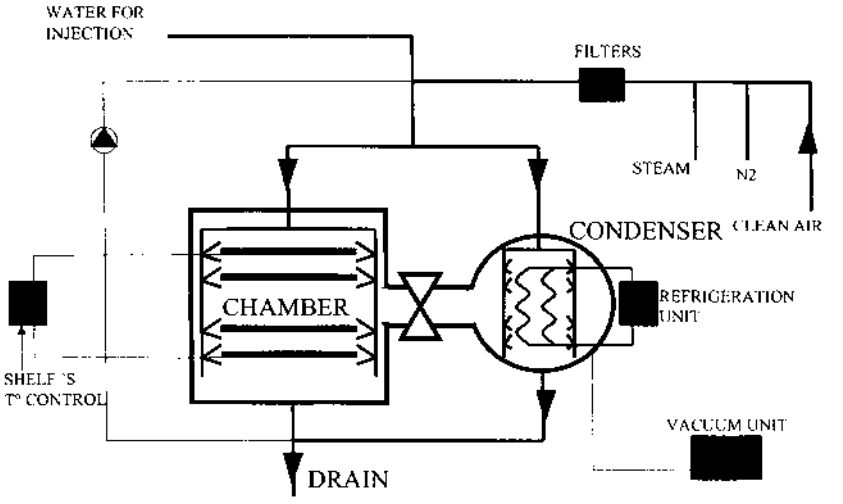

Figure 7 SIP: drying.

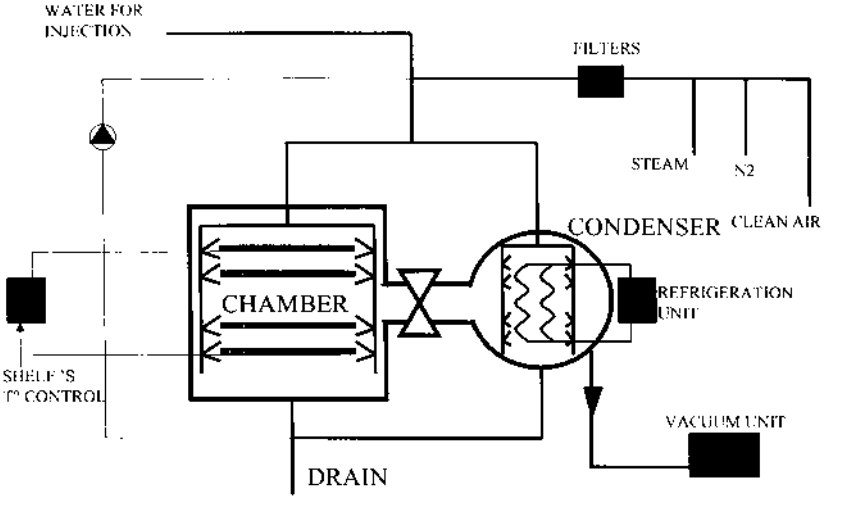

Figure 8 SIP: vacuum test.

C. Operation

The operation is cycled by the PLC. After closing the door, it is possible to initialize the sterilization cycle (checking of the door closing system is ensured by the PLC).

Copyright 2004 by Marcel Dekker, Inc. All Rights Reserved.

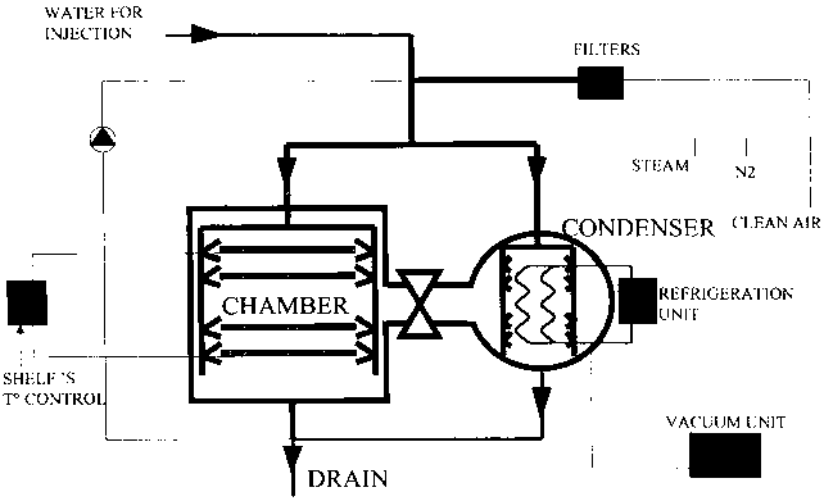

Figure 9 SIP: sterile limit.

A typical sterilization cycle progresses as follows:

1. Primary evacuation
2. First steam injection
3. Secondary evacuation
4. Second steam injection
5. Final evacuation
6. Final steam injection
7. 122°C hold
8. Drying
9. Cooling
10. Vacuum test

With regard to cycle time, the specified flow rate of steam must be available during the different steps of the cycle (see technical data). The operation of cooling and drying permits less time to be taken to keep the freeze-dryer in stand-by position.

This operation has four successive and different phases:

1. Partial vacuum (30 Torr) to dry the liquid ring vacuum pump
2. Cooling of the chamber by circulation of silicon oil in the cooling system
3. Cooling of the trap by circulation of silicon oil in the cooling system

Copyright 2004 by Marcel Dekker, Inc. All Rights Reserved.

4. Cooling of the thermal fluid by circulation in the cooling exchanger

The vacuum test ensures that the sterilization operation does not adversely affect the waterproof status of the freeze dryer.

D. Cooling Exchanger for SIP

The circuit of refrigeration fluid is fitted with a secondary exchanger designed to pull down the temperature from 120°C to around 40°C after each sterilization cycle. This exchanger permits one to increase the disposability time of a freeze-dryer, which Serail puts in place on each sterilizable machine.

E. Cooling System for the Chamber and Condenser

The chamber, walls, and condenser are designed with a cooling system for thermal fluid from the secondary shelf loop connected to the refrigeration media skid.

F. Steaming System

The steam circuit is complete with automatic valves, safety relief valve, and steam traps. The supply of sterile steam is the responsibility of the customer. Steam injection is done through the CIP ports to ensure uniform steam distribution within the chamber.

A safety valve is directly connected on the steam circuit and upstream of the sterile filter in order to prevent any nonsterile microleaks. This 316 L stainless steel safety valve has an automatic pressure release set at 1.7 barg. A 316 L stainless steel rupture disk has a pressure release set at 1.9 barg. The chamber working pressure is 1.5 barg.

III. CONCLUSION

The C/SIP system is an optimal system. This system gives good results in comparison to cGMP. It is automatically operated and carries a limited cost of nonproductivity.

Copyright 2004 by Marcel Dekker, Inc. All Rights Reserved.

18

Global Validation of Freeze-Drying Cycle Parameters by Using Integral HFT Systems

Gilles A. Beurel
S.G.D. Serail, Argenteuil, France

I. INTRODUCTION

Freeze-drying technologies are in permanent evolution, but in the last 10 years, one of the most important targets has become validation of the process cycles in order to ensure the best uniformity and batch reproducibility in product treatment.

This concept of cycle validation is even more important due to the breakthrough of the ALUS (Automatic Loading & Unloading Systems), isolation technologies, and RABS (Restricted Access Biological Systems) which make product temperature control and monitoring very difficult if not almost impossible to handle.

Today, a modern freeze-dryer relies mostly on indirect parameters to ensure repeatability in product treatment. Those indirect parameters have been clearly identified as being shelf temperature profile and pressure profile (vacuum), but, to be consistent, have to be completed with condenser temperature profile which is today an uncontrolled important parameter in sublimation cinematic.

As most of the freeze-dried products nowadays are water based, in the following we will consider the solvent of the product to be water.

Copyright 2004 by Marcel Dekker, Inc. All Rights Reserved.

II. FREEZE-DRYING PROCESS: PHYSICAL FACTS

A. Product Freezing

Process freezing is required for ice crystal formation in the product. Needless to say, the final aspect of the freeze-dried product will mainly depend on the structure of the ice matrix.

Thermal treatment involving double freezing and intermediate rewarming of the product is sometimes required to avoid the solid-like glass form of the ice matrix knowing that the more uniform and the smaller the ice crystals are, the easier is the sublimation and the more consistent the freeze-dried cake is both structurally and cosmetically. This requires a flexible refrigeration system having the capabilities of high instantaneous cooling power and excellent temperature control.

B. Sublimation

Sublimation, which is the first drying step of the lyophilization process, consists in the direct transformation of the free water of the frozen matrix into vapor which is then trapped on the ice condenser of the system.

To achieve this step of the process, the product is heated at a temperature inferior to the lowest eutectic point to avoid any remelting, usually around $-35^{\circ}C$, and the ice condenser is cooled down at a temperature well below the shelf temperature (usually $-55^{\circ}C$) and dependent on the pressure (vacuum) level requested in the chamber.

The difference of temperature between the shelves and the condenser results in a vapor pressure difference above the ice, also called ''driving force,'' which is an essential factor in the sublimation rate. The colder is the ice condenser, the higher is the driving force for the same shelf temperature and pressure (vacuum) set point. This also means that for an identical shelf temperature profile and pressure (vacuum) set point, the sublimation rate can vary in relation to the condenser temperature.

Considering that for a product in a sublimation step at $100\,\mu B$ a temperature variation of the condenser between $-50^{\circ}C$ and $-80^{\circ}C$ results in a vapor pressure difference of approximately 30%, this demonstrates how important condenser temperature control is in terms of validation.

All along the sublimation physical process the pressure (vacuum) level and condenser temperature are linked by the curve of the vapor pressure above the ice, which means that for any value of the vacuum, the condenser has to be at a temperature well inside the sublimation range.

In order to improve the thermal exchanges in the system, all modern freeze-dryers have the capability of introducing gas into the system during

Copyright 2004 by Marcel Dekker, Inc. All Rights Reserved.

sublimation (adjustable leak). This gas, which is incondensable, is permanently evacuated by the vacuum pumps of the system. (See Chapter 1.)

C. Desorption

When all the free water present in the cake in the form of ice crystals has been removed by sublimation, the freeze-drying process has to be terminated by a final desorption step to eliminate the bound water of the product. This desorption step is required to reach a moisture content inferior to around 2%, which is very common for a pharmaceutical freeze-dried product. This step is achieved under high vacuum so that the product can lose a substantial part of its bound water at above zero temperature.

To that end, the shelf temperature, the condenser temperature, and the operation of the pumping system are adjusted so as to enhance the water desorption without affecting the already partially dried product. In most cases, product temperature around $+20^{\circ}C$ to $+30^{\circ}C$ are used whilst the chamber pressure is lowered from 100 μB (used for sublimation) to 10 μB to 30 μB. Under these conditions shelf temperatures are of the order of $+35^{\circ}C$ to $+45^{\circ}C$ and the condenser temperature settles around $-50^{\circ}C$ to $-60^{\circ}C$ or below.

III. FREEZE-DRYING: MECHANICAL HISTORY

A. Shelf Freezing and Heating

Initially, product freezing was achieved by direct expansion of a frigorific fluid in a coil integrated in the shelf on which the product was loaded, but it has been demonstrated that this process was generating discrepancies in the freezing uniformity, mainly because of the physical temperature difference between the shelves, or on the same shelf, due to the expansion of the frigorific fluid.

On the other hand, solid-like glass frozen products require a thermal treatment oriented toward recrystallization. This thermal treatment calls for precise freezing and rewarming cycles which are difficult to achieve when using direct expansion. (See Chapter 1.) In order to address these problems most modern freeze-dryers are fitted with a shelf cooling and heating system using a heat transfer fluid or HTF.

In high-technology freeze-dryers, this temperature uniformity of the shelves during freezing has become even more critical with the expansion of ALUS (Automatic Loading & Unloading System) and RABS (Restricted Access Biological Systems) which are no longer compatible with product temperature recording or monitoring due to the physical impossibility of

Copyright 2004 by Marcel Dekker, Inc. All Rights Reserved.

placing probes in the product. Nowadays, the shelf temperature profile is the first of the indirect, product-related, most important parameters for cycle validation.

B. Vacuum Control

The pumping system of a freeze-dryer is designed to perform the initial evacuation required for sublimation conditions, and then, during the process, to eliminate the incondensable gas resulting from gas introduction through the adjustable leak (mostly gaseous nitrogen today) and the freeze-dryer natural leaks which are usually 20 μB L/S to 30 μB L/S (i.e., around 6 to 9 μB/H for a 30 m^2 freeze-dryer).

The vacuum pump sets are usually vane pumps in combination with blowers or dry pumps. The vacuum control is achieved through a needle valve, and the pressure (vacuum) profile is the second of the indirect, product-related, most important parameters for cycle validation.

C. Condenser Cooling

Condenser cooling and the capability of remaining at low temperature in the range of −50°C to −70°C (in relation to vapor pressure above the ice diagram) are required during the whole freeze-drying process.

Traditionally the condenser cooling and freezing is achieved by direct expansion of frigorific fluids (HFCs allowed by the Montreal protocol), or nowadays liquid nitrogen (LN_2), in the coils or the plates of the ice condenser.

The condensing area of the condenser has to be carefully engineered in relation to the loading area (minimum ratio 1:1) in order to avoid excessive ice thickness which would result in disturbances to and uncontrollability of the temperature gradient through the ice.

It also has to be mentioned that if the freeze-dried product solvent is a mix of water alcohol, for instance, the condenser will have to be fitted with an extra low-temperature condensing unit (i.e., liquid nitrogen or other) located before the vacuum pumps.

The temperature of this ice condenser used to be monitored but not controlled, which meant that the condenser temperature was the result of the thermal equilibrium between the heating system of the shelves and the refrigeration system's maximum available power. However, as already identified for the shelves, the expansion of the frigorific fluids makes condenser temperature control very difficult in terms of uniformity.

In the last 15 years, condenser cooling systems using heat transfer fluid (HTF) have been implemented in industrial freeze-dryers. These systems,

Copyright 2004 by Marcel Dekker, Inc. All Rights Reserved.

which have been initially designed to address the mechanical reliability of the refrigeration systems, have been refined process-wise today under the generic name of integral HFT systems and offer amongst other advantages the capability of controlling the condenser temperature profile.

The condenser temperature profile is the third of the indirect, product-related, most important parameters for cycle validation.

IV. FREEZE-DRYING USING INTEGRAL HTF SYSTEM

Integral HTF systems are an established concept applied to thermal functions of a freeze-dryer. The innovation consists of using the same HTF for heating and cooling both the shelves and the condenser (ice trap) of the freeze-dryer. In an integral HTF system a primary "cold accumulator" loop, and a secondary "hot and cold" loop, achieve the thermal functions of the freeze-dryer, and the cooling/refrigeration agents (HFCs and/or LN_2), which can be used simultaneously, become utilities in the refrigeration system (i.e., mechanical refrigeration system associated to LN_2 backup/booster).

From a validation point of view, it is important to mention that in an integral HTF system the condensing area and temperature remain physically the same product-wise whichever frigorific fluid (HFCs or LN_2) is used on the primary "cold accumulator" loop.

An integral HTF system allows complete specialization of these two loops giving maximum flexibility and dependability to the process. The integral HTF system technology applied to industrial freeze-dryers presents advantages process-wise for both freezing and lyophilization control and validation.

During the freezing process, the "cold accumulator" loop can be used as a thermal flying wheel which results, when operated shelf by shelf, in an almost instantaneous freezing effect on the product. This high freezing rate capability is mostly used in ice crystal size control.

During freeze-drying, mainly sublimation, the integral HTF system gives the capability of controlling the condenser temperature profile thus eliminating all thermal discrepancies resulting in variations of the sublimation rate. This condenser temperature profile should also be linked to the recipe program in order to maintain uniformly the selected adjustable leak flow rate, resulting in a more consistent product freeze-drying process. Using this parameter as part of the recipe allows a very high repeatability from batch to batch in control of the sublimation rate and thus a more accurate global cycle validation.

Finally, condenser temperature control can also be used for control of sublimation rate in the case of high mass transfer at the beginning of

Copyright 2004 by Marcel Dekker, Inc. All Rights Reserved.

the sublimation process, avoiding sublimation peaks which can be harmful to the product. This function is achieved by simultaneous measurements of vapor flux on the condenser in connection with the heat input admitted on shelves.

V. CONCLUSION

Using a freeze-dryer fitted with an integral HTF system drastically extends the field of validation related to the indirect parameters of a freeze-drying cycle by being able to validate on top of the usual shelf temperature profile and pressure (vacuum) profile the third main parameter of the freeze drying cycle, namely, ''the condenser temperature profile.''

Using integral HTF system technology, in steady conditions, the shelf temperature profile is usually validated within the range of $\pm 1^{\circ}C$, and the condenser temperature profile is usually validated within a range of $\pm 2^{\circ}C$ resulting in almost perfect control of the sublimation rate and thus increased uniformity of the product process from batch to batch.

As the extension of ALUS and RABS increases the requirements in terms of cycle validation, an integral HTF system provides today's industrial freeze-dryers with an extended flexibility in operation and total validation capability on all freeze-drying cycle indirect parameters.

Copyright 2004 by Marcel Dekker, Inc. All Rights Reserved.

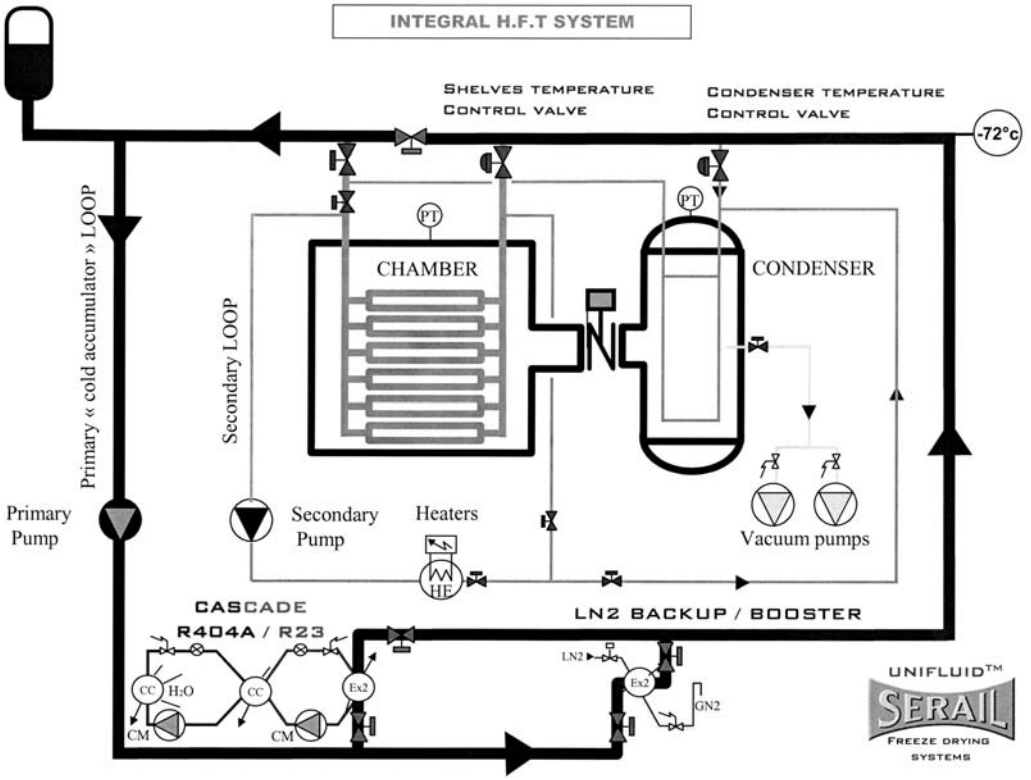

Figure 1 Integral HTF system diagram.

Copyright 2004 by Marcel Dekker, Inc. All Rights Reserved.

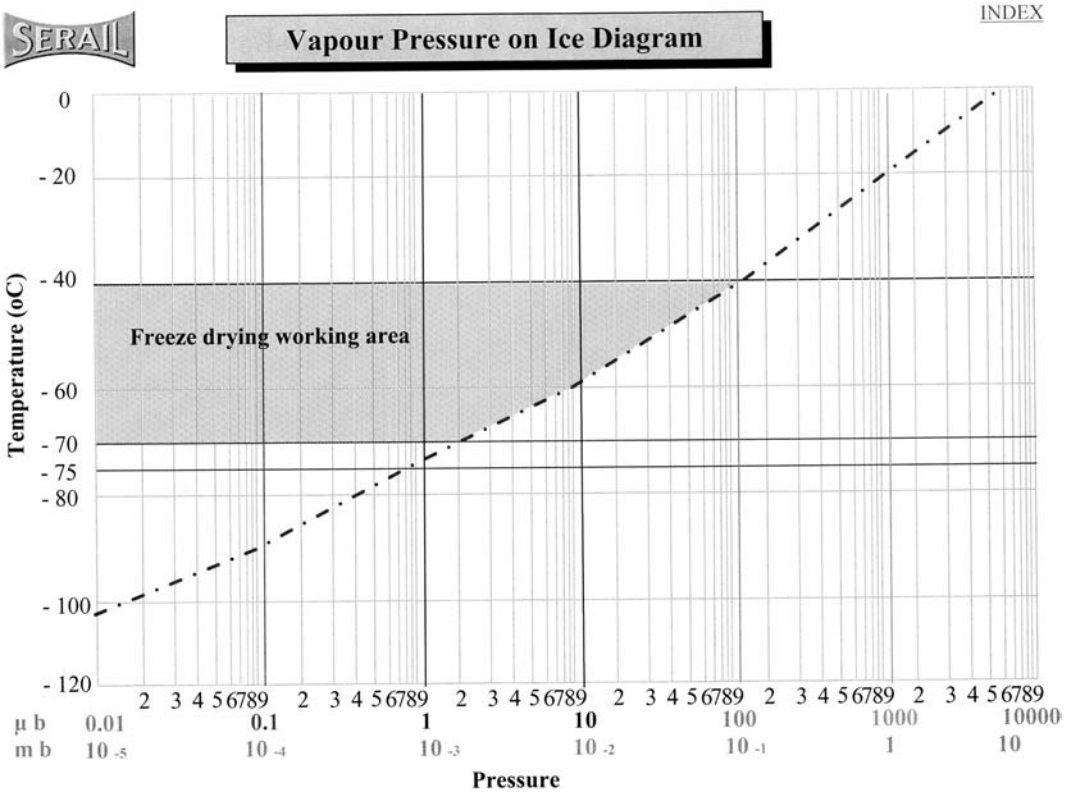

Figure 2 Vapor pressure above the ice diagram.

Copyright 2004 by Marcel Dekker, Inc. All Rights Reserved.

19

Lyophilizer Qualification: Some Practical Advice

Thorsten Fischer
Aventis Behring GmbH,
Marburg, Germany

I. INTRODUCTION

The project described here was initiated by a change control request one year before starting commissioning. The change request identified that an existing lyophilizer required equipping with a new control system, an automatic filter integrity test system, and associated new pipework. Before starting the project the contributing departments of engineering, production, qualification, and quality assurance, analyzed the qualification status of the system. It was found that the implementation of the defined changes would have continued into a major change of the whole system. In this start-up meeting it was determined that a new qualification with the steps IQ (Installation Qualification), OQ (Operational Qualification), and PQ (Performance Qualification) was required. Each protocol was to be pre- and post-approved by all the departments involved.

The qualification exercise included parts of computer and software validation as well as equipment qualification. To ensure a coherent qualification it was determined that portions of the computer and software validation would be subject to an interim approval. This would allow specified computerized systems validation tasks to be completed prior to making equipment operational, and subsequently performance qualification (6,7).

Copyright 2004 by Marcel Dekker, Inc. All Rights Reserved.

II. PROCEDURE

The documents described, namely, System Qualification Procedures (SQPs) and Standard Operating Procedure (SOP) in Figure 1 contain a generic risk assessment for determination of the validation scope and effort on the equipment lyophilizer. They were also used as a generic validation master plan for the project. Management of the project resources, costs, and deadlines was performed with a model created in a standard project planner.

In advance of the qualification a User Requirement Specification (URS) was written by the production and engineering departments. The vendor started detail engineering after approval of the Functional Specification (FS).

The lyophilizer was installed and thoroughly tested during the commissioning and start-up phase.

The qualification activities, as set out in Figure 1, were executed with the support of the vendor and one personnel resource according to Aventis Behring standard qualification procedures for equipment.

Qualification document development is based upon the use of templates that are customized for particular systems and equipment. The SQPs and SOP govern the use of these templates.

A. Installation Qualification

The process for equipment qualification is documented in the Aventis Behring (AB) "System Qualification Procedure" for lyophilizers.

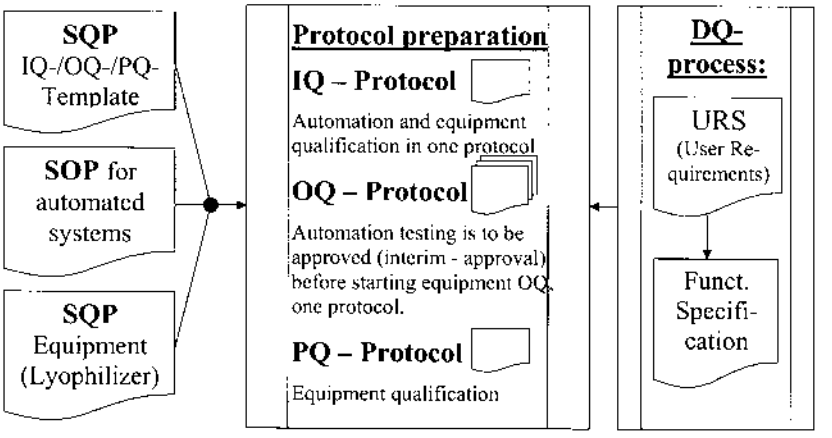

Figure 1 Creation of qualification protocol.

Copyright 2004 by Marcel Dekker, Inc. All Rights Reserved.

Upon completion of the installation and the cycle development phases the IQ phase was initiated. Normally the approach to the IQ phase is similar for each piece of equipment and would differ only in system-specific details.

The IQ verified the following information (testing items 1 to 5 are defined in an SQP for the IQ template):

1. Mechanical equipment installation: verification of the authorized drawings (P&IDs, system schematics, as-built drawings) and component lists including the verification that utilities are installed as required.
2. Mechanical component installation: verification of secondary system components on compliance with specifications.
3. Instruments specifications and calibration: verification of critical and non-critical instruments.
4. Equipment documentation: verification of the technical documentation used during qualification on compliance with basic Good Manufacturing Practice (GMP) rules (6,7).
5. Control system: verification of automation and software parts by performance of additional testing as described below (testing 5.1 to 5.8 is defined in an SOP for qualification of automated systems):

    5.1. Electrical installation: verification of authorized circuit diagrams including the component list.
    5.2. System specifications and drawings: verification of engineering documents as per user requirements, functional specification, software design specification, software integration plan, etc., on compliance with the built system.
    5.3. Hardware installation: verification of secondary automation system components (main components as installed input/output cards, temperature controller, etc.).
    5.4. Wiring termination and pneumatic circuit check: verification that the wiring and pneumatic circuit are installed properly.
    5.5. Input/output (I/O) devices: verification that the I/O devices comply with manufacturers' specification.
    5.6. Configurable switches: verification of the positions of configurable switches (e.g., ***D***ual ***I***n-line ***P***ackage switches).
    5.7. Software installation: verification of each installed software item.
    5.8. Automation system documentation: verification of the technical documentation, used during qualification, on compliance with basic GMP rules (6,7).

Copyright 2004 by Marcel Dekker, Inc. All Rights Reserved.

While executing the electrical installation testing at 5.1 the testing described in 5.2 to 5.6 was also performed with the support of the vendor.

6. System specific testing: verification of aspects defined within the scope of the system qualification procedure for lyophilizers:
   - 6.1. Determination of system equivalence: the equivalence of the present hard- and software with other comparable qualified systems was evaluated within the scope of the IQ. Based on that assessment further additional testing activities were identified with the support of the automation group. The evaluation was documented within the scope of the IQ protocol.
   - 6.2. Chamber door: visual verification of the correct installation of the chamber door and the door sealing.
   - 6.3. Room separation: verification that the lyophilizer was correctly installed into the cleanroom wall and no visual defects were identified in the seals between the lyophilizer front plate and the cleanroom wall.
   - 6.4. Shelves: verification that all shelves were correctly installed and showing no visual damage such as a leakage of heat transfer fluid.

1. Results

In total 16 groups of tests were performed and documented over a 6 week period. The IQ established that the new and existing equipment had been adequately installed and met the relevant acceptance criteria.

Several deviations were identified and promptly resolved. Current documentation requirements meant that the documents for existing parts of the lyophilizer needed substantial supplements and the creation and provision of these were the main issue. Other deviations were of such a minor type that OQ was started without delay and no amendments or addenda to the IQ were required.

The equipment vendor provided execution support. Test execution management and elements of technical support were provided by one AB staff resource. This included solution of deviations, management of document revisions/updates, and data review.

B. Operational Qualification

As a prerequisite for operational qualification of the equipment it was required, as part of the Validation Plan, that major parts of the computer

Copyright 2004 by Marcel Dekker, Inc. All Rights Reserved.

and software validation (CSV) be completed. The CSV testing approach is defined by a separate SOP for Qualification of Automated Systems. To achieve CSV a plan for testing the function of the control system (operator panel, switches, power failure test, etc.) and the visualization program (input, functions, alarm messages, etc.) was prepared and executed with the support of the vendor. This control and visualization functionality was provided through an optional personal computer (PC) connected directly to the control system using a programmable logic controller (PLC).

The following testing was performed for the computer and software validation.

1. Radio frequency interference: verification that the control system has a Certificate of Exportability (CE) that is adequate to show that the system is shielded for interferences.
2. Operator devices (switches, indicator lights installed at the control cabinets): verification that each operator interactive device and indicator light operate as specified.
3. Operator panel: verification of the panel control functions.
4. Security and access: verification that the access is password protected and is active for each specified level.
5. Visualization system: verification of the accuracy and completeness of each screen (equipment schematics, tables, curves, trending, etc.) and the control functions (alarm messages etc.).
6. Alarms: verification of all process-relevant alarms and messages. Testing is performed just below, above, and at the limit.
7. Critical parameters: verification of the programmed critical parameters against specification (e.g., program cycle parameters for time, temperature, pressure, alarm).
8. Power failure: verification of the system condition after a power failure and recovery of the system.
9. Backup: verification that for each software item active on the system there is a backup copy to restore the system.

Further automation testing was defined within the scope of the system-specific qualification procedure and included the following:

10. Network connection: the functioning of the network card was verified. The system boundary ended at the bus connection. Network qualification was performed in a separate protocol and was executed by an automation specialist.
11. Chart recorder: verification of the correct color, description, and range for each channel.

Copyright 2004 by Marcel Dekker, Inc. All Rights Reserved.

12. Recipes: verification that each automated cycle was programmed within its limits in the form of a recipe (lyophilization, sterilization, etc.) and complies with the specification. This test is an additional system-specific test for critical parameters (see 7 above).

1. Interim Result

Tests 1 to 12 were executed in a 2 week period. As noted above, interim approval was required and obtained before the further equipment qualification could continue.

2. Equipment Operational Qualification

Operational equipment testing was performed for the vacuum, temperature, and ventilation system, the stoppering function, and the sterilization process. The qualification of the lyophilizer's Sterilization-in-Place (SIP) system is performed similar to an autoclave and uses biological indicators and accumulated lethality (F_0) determination (2,5).

Additional testing as part of the OQ included:

13. Program cycles: verification of each programmed cycle to ensure that no further cycle development was required; testing was performed by running each programmed cycle (one recipe for lyophilization, SIP cycle, filter integrity test, etc.). The system qualification procedure describes the identification of the most appropriate lyophilization cycle for this test. Testing of the lyophilization cycle for this step is combined with test 18.
14. Vacuum pumps: verification that each pump system is able to reach the lowest pressure, defined in any lyophilization recipe.
15. Vacuum leakage test for chamber and condenser: verification of the system integrity, through a leakage rate test. A leakage rate of less than 10^{-2} mbar L/s was chosen.

    The leakage rate is determined in an empty lyophilizer with running of the condenser cooling. Before starting the test phase it is recommended to evacuate the lyophilizer (chamber and condenser) several hours (e.g., 4 h) to remove the gas (e.g., below 10^{-2} mbar). After stopping the vacuum pumps the test phase begins when pressure is stabilized and has reached 10^{-2} mbar.

    Sometimes virtual leaks might cause a pressure increase directly after stopping the pumps; therefore a stabilization phase is recommended, before starting the test. We have observed that in the range of 10^{-2} to 10^{-1} mbar a representative

Copyright 2004 by Marcel Dekker, Inc. All Rights Reserved.

proportional pressure increase can be monitored with a conductivity detector (vacuum meter based on the Pirani principle (1)). For the test procedure see also Figure 2.

16. Silicon oil pumps: verification of the heat transfer media recycle pump redundancy to ensure that the pumps can replace each other if one of them fails. The test was performed by monitoring the pressure in the pipe before and after failure of a pump.
17. Condenser chilling test: verification of the system cooling rate, normally 2°C/min, by monitoring the temperature at the condensing coils during cooling from 0°C to −60°C (1).
18. Ice capacity: verification that the condenser was able to hold an ice capacity representing a worst-case condenser load. The test is performed with the shortest lyophilization recipe that can be used to load the freeze-dryer with the vial format giving the worst-case load (maximum water to sublime).
19. Automatic stoppering: verification that the lyophilizer can close the vials under vacuum conditions with stoppers. Closure of the vials has been verified with a vacuum tester.
20. Shelf temperature distribution: verification of the temperature homogeneity across all shelves at one time. The shelf temperature mapping is by use of a large number of thermocouples (in our case, five per shelf each, e.g., 70 thermocouples per measurement event), one of the most complex, time-consuming, and error-prone measurements in equipment qualification. It requires an experienced protocol executer for calibration, proper placement

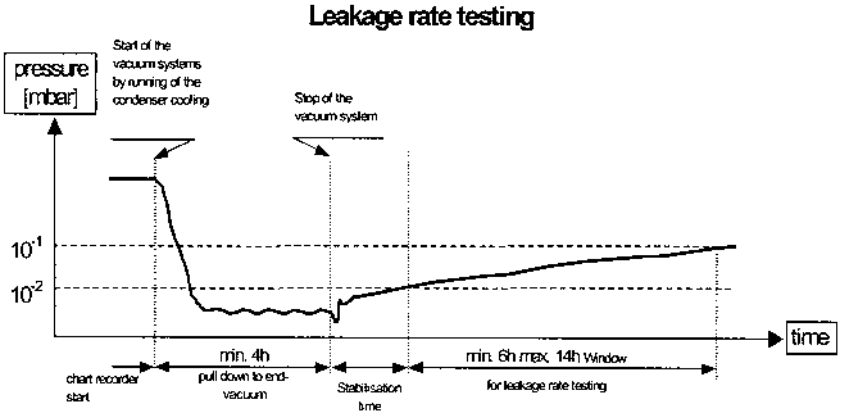

Figure 2 Scheme of vacuum leak rate test procedure.

Copyright 2004 by Marcel Dekker, Inc. All Rights Reserved.

and examination of the thermocouples and their monitored data. Monitoring of the temperatures was recorded with a calibrated data acquisition system, temperature reference bath, Resistance Temperature Detector (RTD), and type K thermocouple. The thermocouples were calibrated before measurement and reverified after the measurement. Use of an automated system is recommended. As the flange is key to a successful qualification it should be made part of the User Requirement that the vendor provide, and show, correct operation of a special vacuum and pressure (for sterilization) resistant flange–thermocouple system. To verify the temperature profile the thermocouple should have good contact with the shelf surface. By the use of lab lifts and a compressible block of isolation material a close surface contact can be provided. See Figure 3.

The temperatures were monitored at the worst-case temperatures of all recipes (e.g., at –45°C, +10°C, +60°C) according a qualification recipe. See Figure 4.

Documentation of the heat transfer from the silicon oil via the shelf to the surface the temperature probes at the silicon oil inlet and outlet pipe were considered an important operational characteristic. This was recorded with the installed calibrated temperature probes.

Results of the measurements are shown in Figure 5: Graph A shows the total run and graphs B, C, and D give a focus at the temperature hold phases.

Figure 6 shows in graph A the results of the measurements across the top shelf and graph B across the bottom shelf at minimum temperature. In graph A one thermocouple shows the effect of an insufficient contact to the shelf. This effect is not visible under vacuum conditions because the compressible isolation material is enlarging its volume under the vacuum and pushing the thermocouple closer to the surface of the shelf.

21. Air ventilation system: verification that the air filter can be automatically tested for integrity. Modern lyophilizers are equipped with an automatic filter–testing unit that verifies the filter integrity by either the water intrusion or the forward flow test method.
22. Sterilization of chamber and condenser: verification of the eight coldest spots within the chamber. These points were then to be used for execution of the performance qualification. Testing was performed using methods similar to those used for an autoclave (2,4,5).

Copyright 2004 by Marcel Dekker, Inc. All Rights Reserved.

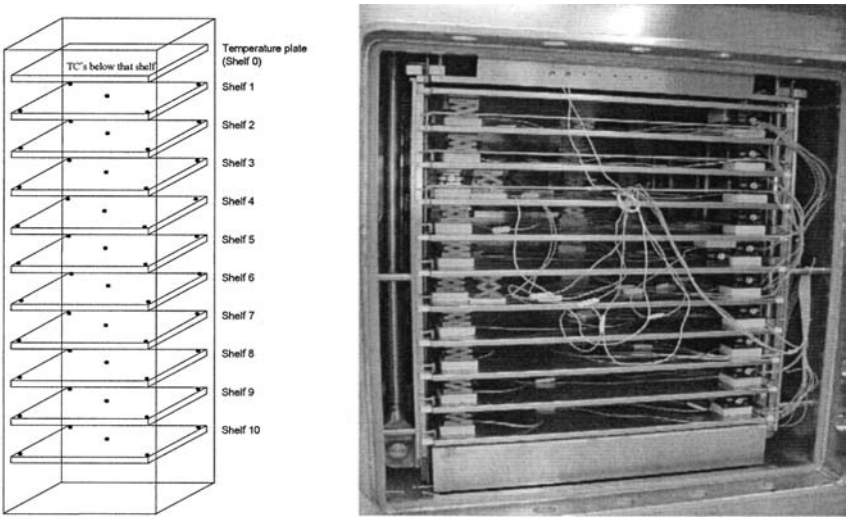

Figure 3 Thermocouple placement for the shelf temperature distribution studies.

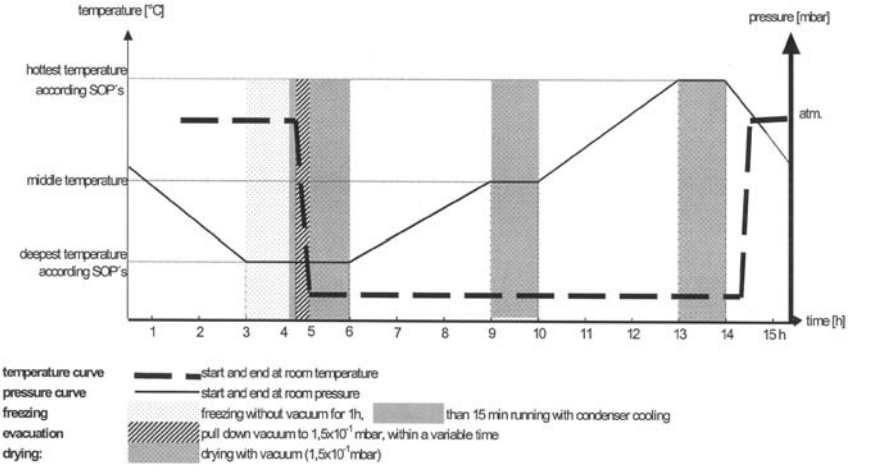
temperature [°C]
pressure [mbar]
hottest temperature according SOP's
middle temperature
deepest temperature according SOP's
atm.
time [h]
1 2 3 4 5 6 7 8 9 10 11 12 13 14 15 h
temperature curve
pressure curve
freezing
evacuation
drying:
start and end at room temperature
start and end at room pressure
freezing without vacuum for 1h,
than 15 min running with condenser cooling
pull down vacuum to 1,5x10-1 mbar, within a variable time
drying with vacuum (1,5x10-1mbar)

Figure 4 Scheme of the qualification recipe.

The thermocouples:

were positioned throughout the chamber and within the anticipated hot and cold regions, at the steam inlet (air filter downstream side), and at the condensate drain;

Copyright 2004 by Marcel Dekker, Inc. All Rights Reserved.

were held in positions with heat- and water-resistant tape;
were positioned at the extremities of the chamber and the condenser, as close as possible to the equipment surface;
had two-point calibration with a midpoint verification prior to the measurement;
were subjected to midpoint verification after the measurement.

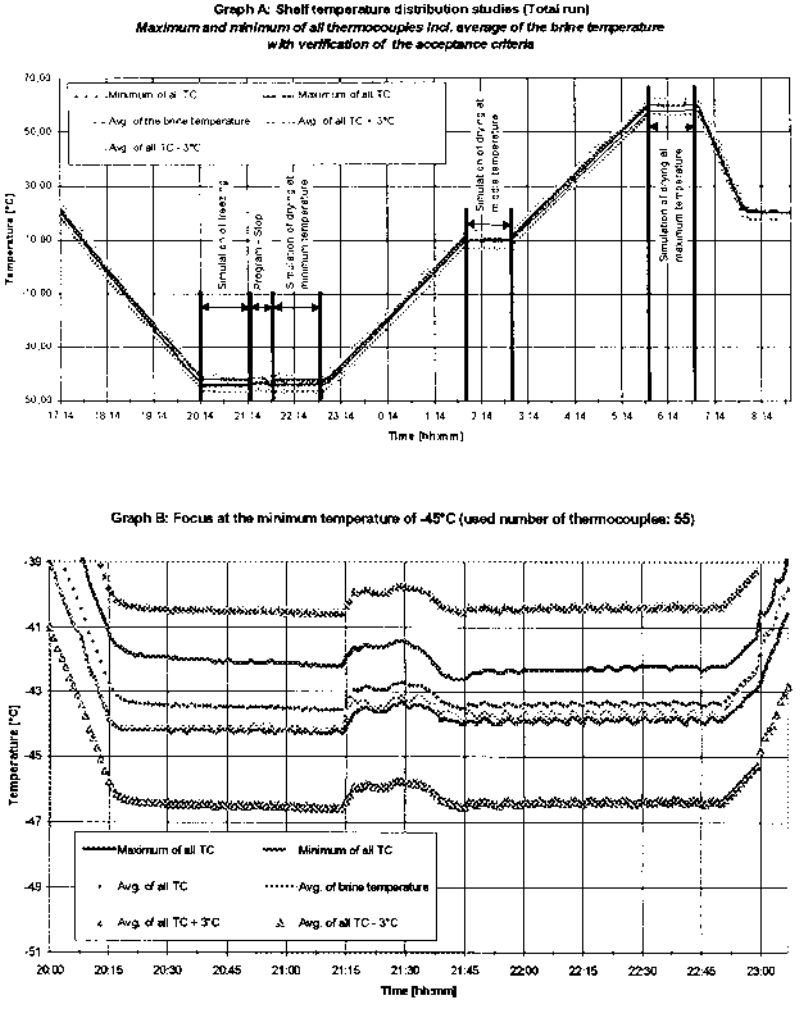
Graph A: Shelf temperature distribution studies (Total run)
Maximum and minimum of all thermocouples incl. average of the brine temperature
with verification of the acceptance criteria
Minimum of all TC
Maximum of all TC
Avg. of the brine temperature
Avg. of all TC + 3°C
Avg. of all TC - 3°C
Temperature [°C]
Time [hh:mm]
Graph B: Focus at the minimum temperature of -45°C (used number of thermocouples: 55)
Maximum of all TC
Minimum of all TC
Avg. of all TC
Avg. of brine temperature
Avg. of all TC + 3°C
Avg. of all TC - 3°C
Temperature [°C]
Time [hh:mm]

Figure 5 Results of the shelf temperature distribution study.

Copyright 2004 by Marcel Dekker, Inc. All Rights Reserved.

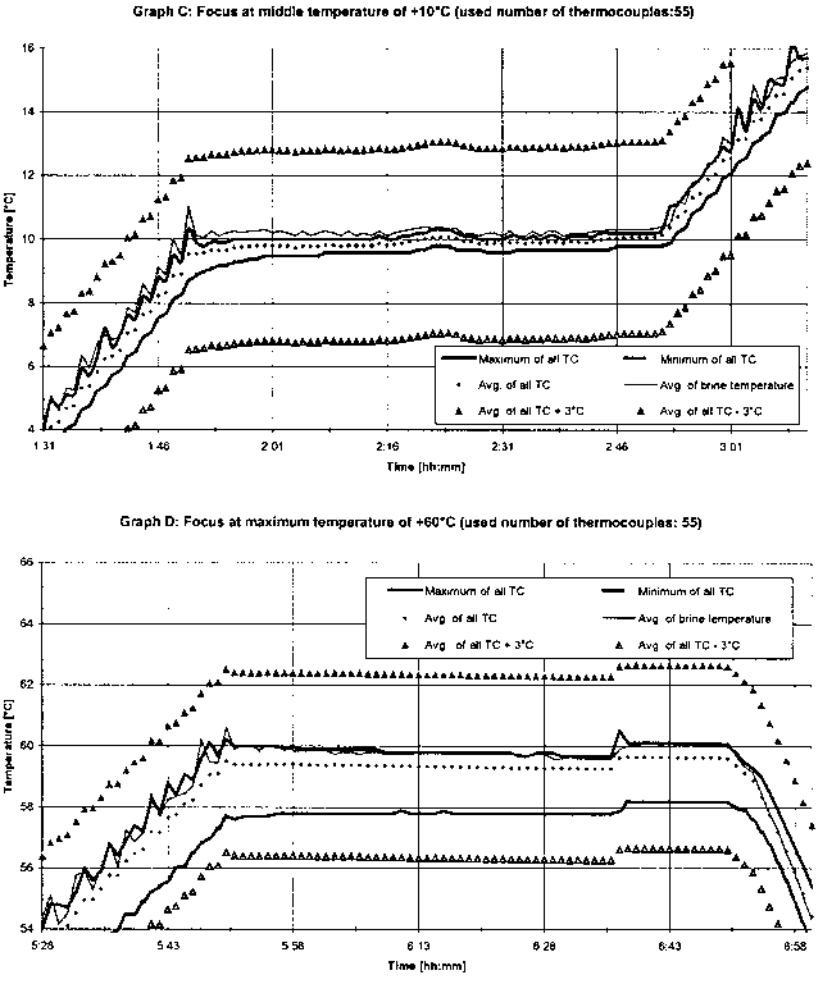
Graph C: Focus at middle temperature of +10°C (used number of thermocouples:55)
Temperature [°C]
Time [hh:mm]
Maximum of all TC
Minimum of all TC
Avg. of all TC
Avg. of brine temperature
Avg. of all TC + 3°C
Avg. of all TC - 3°C
Graph D: Focus at maximum temperature of +60°C (used number of thermocouples: 55)
Temperature [°C]
Time [hh:mm]
Maximum of all TC
Minimum of all TC
Avg. of all TC
Avg. of brine temperature
Avg. of all TC + 3°C
Avg. of all TC - 3°C

Figure 5 Continued

Due to the age of the equipment and the fact that the shelves are pushed from the bottom to the top, the condenser could not be entered for measurements in the condenser. An acceptable compromise in this case may be the evaluation of the installed condenser drain temperature and condenser pressure probes to ensure that they accurately measure saturated steam conditions.

For new lyophilizers it is recommended that the condenser is positioned either below the chamber or can be entered at minimum by a

Copyright 2004 by Marcel Dekker, Inc. All Rights Reserved.

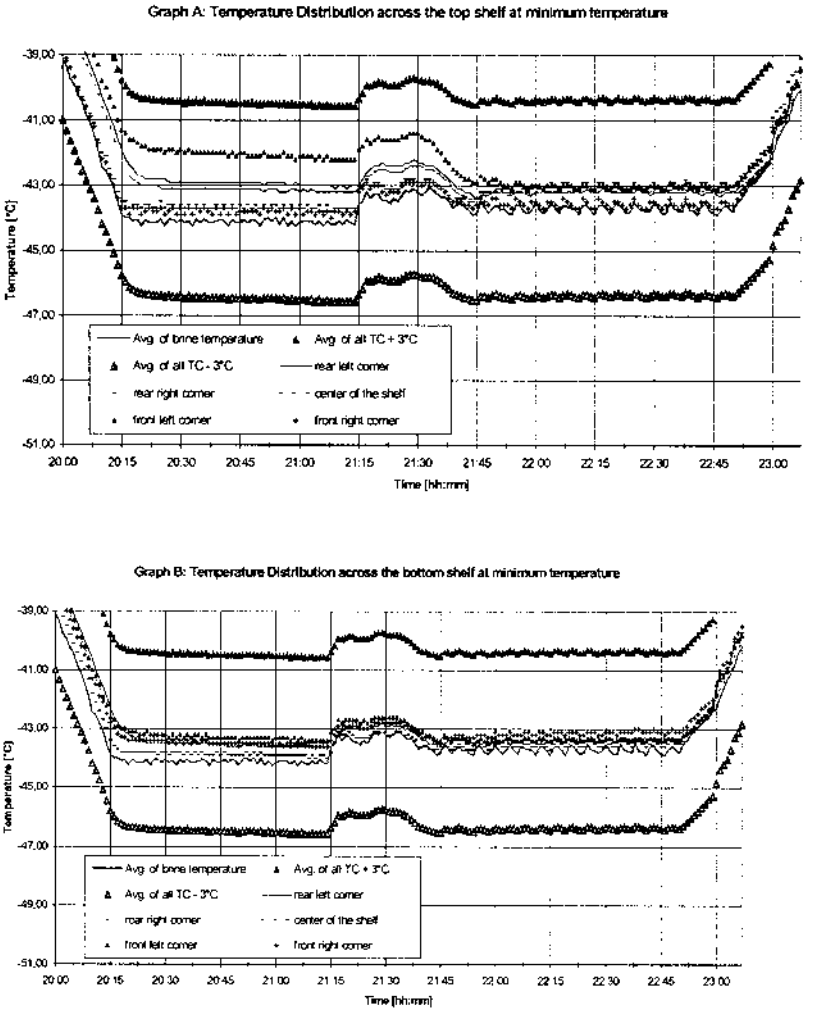

Figure 6 Temperature distribution across the top and the bottom shelves at minimum temperature.

man-hole. For this case, as part of the health and safety assessment for equipment entry, the following points should be considered:

ventilation of the condenser during installation of the thermocouples;
isolation or disconnection of any heating and cooling media;
at minimum, one extra person for safety;
extra lighting.

Copyright 2004 by Marcel Dekker, Inc. All Rights Reserved.

Because of the short time scheduled for the qualification the empty chamber temperature distribution study was combined with the empty chamber temperature penetration study. These studies differ only in the usage of biological indicator (BI), an F_0 (accumulated lethality during the SIP hold period) calculation, and the number of thermocouples. By using the same amount of BIs as thermocouples, the studies could be performed together. A separate performance qualification was established as unnecessary. This approach was documented in the qualification plan.

The testing verified the following items:

Temperatures above or equal to 121°C are recorded during the SIP hold period at all times (see Fig. 7).

Measured temperatures and pressures complied with saturated steam conditions. These were confirmed by an external data acquisition system (external pressure and temperature sensor) (see Fig. 8).

Homogeneous temperature profile: all temperatures measured inside the chamber were within a range of 2°C (see Fig. 7).

Overkill approach provided by the SIP cycle. For the verification the BIs had to fulfill the criteria described below.

Selection of an Adequate BI of Bacillus stearothermophilus for Determination of an Effective Overkill (Biological Evidence). Targets:

1. (a) Verification of a 12 log reduction.
   (b) Use of an adequate BI equivalent to a specific theoretical biological lethality ($F_{\text{bio theo}}$), i.e., $F_{\text{bio theo}} \geq 12$ min.

   Calculation is performed with the certified population (N_0), the population at the end of the SIP cycle (N), and the certified decimal reduction time (D) according to the formula.

$$F = (\log N_0 - \log N)D_T^Z = nD_T^Z$$

To calculate an ideal BI, based on an overkill requiring a 12 log reduction,

$$F = (\log N_0 - \log N)D_T^z$$
$$= (\log 10^{12} - \log 10^{\circ})1.0\,\text{min} = 12 \times 1.0\,\text{min} = 12\,\text{min}$$

Coherence is valid for the lethality F. $F = 12$ describes the criteria to be passed before using the BIs. An example for a purchasable BI is as follows:

$$F_{\text{bio, theo}} = 2.2\ \text{min}\left(\log 10^6 - \log 10^0\right) = 13.2\ \text{min} \geq 12\ \text{min}$$

Copyright 2004 by Marcel Dekker, Inc. All Rights Reserved.

2. A vendor certificate with certified population N and D values is available.
3. Verification of the biological lethality (F_{bio}) by use of the BI with a specific N and D. F_{bio} for determination of the minimum F_0 value is $F_{bio} \geq 15$ min. The basis for F_{bio} is (3)

$$F_{bio} = F^{ATUN}_{121.1^\circ C} = D^{BI}_{121.1^\circ C}\left[\log\left(N_0^{BI}\right) - \left(\log N_F^{ATUN}\right)\right]$$

where:

N_F^{ATUN} = realistic end population after sterilization, if all used BIs show no growth (all test units are negative (ATUN)) (3)

N_0^{BI} = certified starting population of the BI

$$\text{Model}: F_{bio} = 1.0\,\text{min}\left[\log\left(1 \times 10^{12}\right) - \log\left(1 \times 10^{-3}\right)\right] = 15\,\text{min}$$

$$\text{Example}: F_{bio} = 2.2\,\text{min}\left[\log\left(1 \times 10^{6}\right) - \log\left(1 \times 10^{-3}\right)\right] = 19.8\,\text{min}$$

To ensure that conducting the BI and thermographic tests in parallel was acceptable it was essential that each of the three criteria be passed, before using the BI. Thus F_{bio} has to be reached by or exceed the thermographic calculated F_0 value. The calculation follows following formula (5):

$$F_0 = \Delta t \sum \left[10 \exp(T - T_b)/Z\right]$$

where:

T = instantaneous temperature
T_b = base temperature (121.1°C)
Z = value or temperature coefficient (10°C)
Δt = time interval

Testing typically is performed multiple times. In the case of the initial qualification of the sterilization the testing was conducted in triplicate.

3. Results

In total 22 tests were performed for execution of the operational qualification in a total time of 8 weeks. The execution required one full-time and one part-time person. Much of the work was conducted by supervised contractors who had received specific training by AB staff.

Copyright 2004 by Marcel Dekker, Inc. All Rights Reserved.

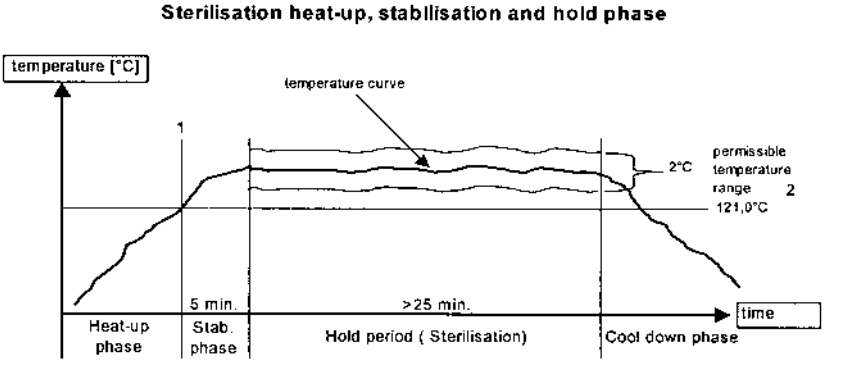

Figure 7 Theoretical sterilization phase.

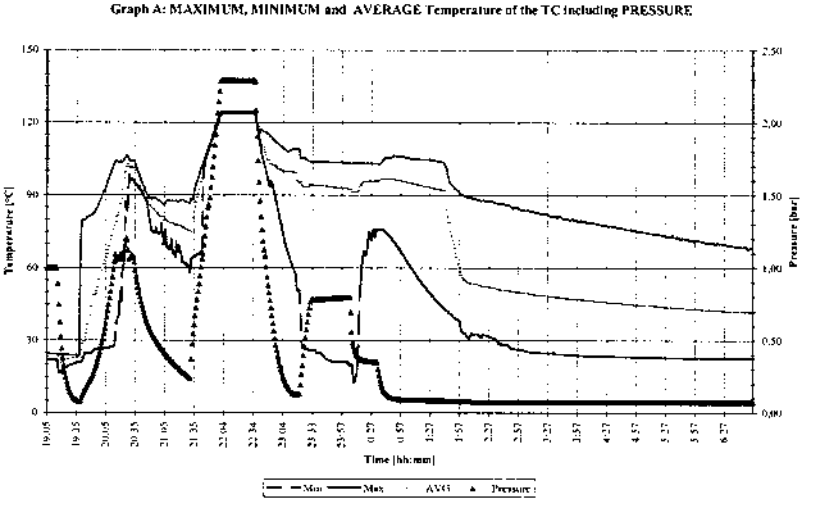

Figure 8 Graphs showing the results of the measurements.

Only minor deviations, relating to control system hardware installation and operational configuration backup, were identified and these were promptly resolved. The support equipment for temperature mapping and BI usage operated well and valuable lessons on probe placement, equipment sealing, and data investigation were learned.

Copyright 2004 by Marcel Dekker, Inc. All Rights Reserved.

C. Final Report

It was recognized at the beginning of the work that the testing would be complicated and to make the results readily understandable to a reviewer a suitable Final Report (FR) structure would be required. To ease the workflow the summaries were generated for each set of test results documented and used as attachments to the FR.

A proper FR also enables a quick review of the system history, and what eventually might be necessary for periodic requalification of the system.

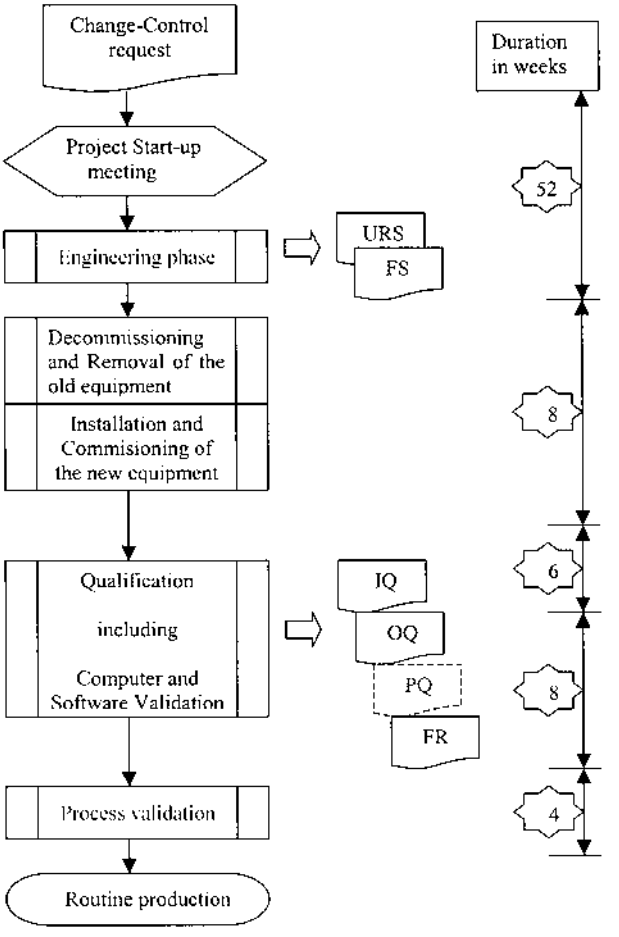

Figure 9 Project flowchart.

Copyright 2004 by Marcel Dekker, Inc. All Rights Reserved.

D. Overall Conclusion

The engineering phase of the project for decommissioning and removal of the old equipment and installation of the new equipment including commissioning and start-up testing on site took 8 weeks. This was followed by the qualification activities in a time of 14 weeks.

After an additional 4 weeks for process validation the upgraded system was completely validated and could be used for routine production. A project flowchart is shown in Figure 9.

The main difficulties encountered in the execution of the project concerned the old documentation of the existing system. One principal recommendation of the project team members, including the vendors, was that review of more focused documentation should be completed during the commissioning and start-up phase to ensure that what is installed is properly documented.

For future work it was established that a clear understanding of roles and responsibilities would smooth progress and ensure that vendor and owner team members better understood other participants' problems and needs.

ACKNOWLEDGMENTS

The author would like to acknowledge the cooperation and support of colleagues at Aventis Behring GmbH, Marburg. In particular Mr. Mathias Klein, Director of Facility Qualification, for his council and direction and Mr. Maurice Shakeshaft of CB Automation Ltd, who assisted in the preparation of the English version of this chapter.

BIBLIOGRAPHY

1. Oetjen, Georg-Wilhelm. Gefriertrocknen. Weinheim: VCH Verlag, 1997.
2. FDA, Guide to Inspections of Lyophilization of Parenterals, 15.02.01.
3. IJ Pflug, KD Evans. PDA Journal of Pharmaceutical Technology 54(2) (March–April), 2000.
4. DIN, Sterilisation Desinfektion Sterilgutversorgung, 1988, Beuth, 2nd ed.
5. PDA, Validation of Steam Sterilization, PDA Technical Report No. 1-Revision, Draft No. 5, January 1999.
6. FDA, 21 CFR Parts 210 and 211, Current Good Manufacturing Practices for Finished Pharmaceuticals.
7. Auterhoff, Gert. EG-Leitfaden einer Guten Herstellungspraxis für Arzneimittel. 5th ed. Aulendorf: ECV Verlag, 1998.

Copyright 2004 by Marcel Dekker, Inc. All Rights Reserved.

20
Lyophilization Process Validation

Christian Bindschaedler
Serono Laboratories S.A., Aubonne, Switzerland

I. INTRODUCTION

The comprehensive validation of freeze-dried products encompasses many topics including the installation and operational qualification of the lyophilizers, the bacterial challenge of the sterile filter, the media simulation studies, the validation of the filling process, and the cleaning validation [1]. This chapter will be restricted to examining the validation of the lyophilization process and several aspects of the manufacturing steps preceding freeze-drying.

The basic purpose of carrying out a validation of the manufacturing process is to establish documented evidence that provides a high degree of assurance that the process consistently produces a product meeting its predetermined specifications and quality attributes. Regardless of which type of validation approach is used, the validation of the lyophilization process includes two complementary aspects:

Examination of the freeze-drying parameters
Examination of product characteristics

While examination of the final product is essential to ensure that the lyophilization process performs consistently and as intended, the monitoring of freeze-drying parameters also ensures that they are maintained within an acceptable range and provides an additional degree of assurance that the process is under control.

Compared to many other pharmaceutical processes, freeze-drying is intrinsically more complex. This is because process parameters and product

Copyright 2004 by Marcel Dekker, Inc. All Rights Reserved.

characteristics are inherently interdependent. The freeze-drying parameters affect the product being freeze-dried, but the converse is also true. A marked impact on the course of freeze-drying may be caused by the chemical composition of the solution and subsequently the thermodynamic and structural properties of the frozen solution, the load of vials or ampoules, the geometrical characteristics of the containers, and the fill volume. The knowledge of the interrelationship between the operating parameters and the product freeze-drying pattern is therefore an important requisite for successful development and validation of new products. For good control of the freeze-drying of formulated products, the following subjects should be mastered:

The thermodynamic and structural properties of the frozen product
The effects of the programmable freeze-drying parameters on dependent process variables
The effects of the dependent process variables on product characteristics
The converse effects of product characteristics on dependent process variables

Before concentrating on process parameters (Section III), we will briefly outline the behavior of the product during the three separate but interdependent stages of freeze-drying: freezing, sublimation (primary drying), and desorption (secondary drying).

II. FREEZE-DRYING FUNDAMENTALS

A. Freezing

1. Thermodynamic Requirements

Freezing of the solution is required to prepare the product for lyophilization. This part of the process is often most critical because the porous structure of the final product will closely reflect that of the initial frozen product. As a consequence, the freezing will affect the progress of primary and secondary drying, as well as the properties of the final product.

The freezing of aqueous solutions occurs in a series of steps. As the solution of drug and excipients is cooled, a temperature is reached where pure ice crystals are nucleated. The crystals progressively grow as the temperature decreases and a continuous network of interstitial phase appears in-between, wherein all the solutes are concentrated. As the cooling goes on, a temperature is reached where no further ice is generated at the

Copyright 2004 by Marcel Dekker, Inc. All Rights Reserved.

expense of the interstitial phase. Depending on the composition of the product, two typical situations may then be encountered:

When the formulated solution contains essentially saline or organic solutes that crystallize easily, the interstitial phase will crystallize out abruptly as an eutectic or a mixture of eutectics. The crystallization results in an immediate hardening of the frozen system, which becomes fully rigid. At this point, the system has reached its maximum temperature for complete solidification (eutectic point, T_e), which is a basic parameter of the freeze-drying process.

When the formulated solution predominantly contains polyols, sugars, or polymers, the interstitial phase does not usually crystallize out upon cooling but increases progressively in viscosity as a glass-like system. In the case where the interstitial phase has effectively the structure of a glass, the frozen system becomes fully rigid once the glass transition temperature (T_g) is reached. In contrast, some amorphous systems may show no such definite transition, but they eventually become very stiff at low temperature, as shown by electrical resistance studies.

Regardless of the freezing behavior of the formulated solution, it is essential to make sure that the temperature of the product is decreased below the temperature where complete solidification is observed. If this condition is not respected, the incompletely frozen interstitial phase will boil or induce pellet partial melting or collapse during lyophilization.

2. Structural Requirements

Although the thermodynamic requirement of freezing below the solidification temperature is compulsory, this condition is not always sufficient to guarantee an easy and satisfactory lyophilization of the product. This is because the structure of the frozen system is affected not only by thermodynamic factors but by kinetic ones.

It is often observed that a very rapid cooling results in small ice crystals, whereas a slow freezing favors the formation of large crystals. The size of ice crystals can have a dramatic effect on the course of lyophilization. A quenching of the formulated solution in liquid nitrogen will generate a glass-like solid with minute embedded ice crystals, which may be very difficult to dry. On the other hand, large ice crystals, resulting in large interconnected pores, will create a structure favorable to sublimation. The large pores offer little resistance to water vapor flow. Thereby the drying is accelerated and the risk of product overheating at the end of primary drying is minimized.

Copyright 2004 by Marcel Dekker, Inc. All Rights Reserved.

However, in some cases the facilitation of primary drying via large ice crystals is counterbalanced by a prolongation of the secondary drying time, owing to the reduced surface area of large pores which limits the rate of water desorption. In some other cases, slow freezing may favor degradation of the active substance due to pH shift and high ionic strength. There is therefore no universal freezing scheme for obtaining an ideal frozen structure. For each formulation, the optimal conditions should be approached by trial-and-error during development and optimization of the freeze-drying cycle. Simple modifications may consist in varying the slope of the freezing ramp, or in replacing the freezing ramp by a step-down freezing including one or several intermediate plateaus. The benefit of these improvements is a more homogeneous temperature distribution inside the containers. This results in a more uniform pore size, and the final product often shows a decreased between-samples variability for residual moisture.

Despite these precautions, a slow freezing process is not always sufficient to ensure a dimensionally stable pellet of good cosmetic appearance. In this respect, formulated solutions that produce interstitial metastable glasses on cooling are sometimes a source of problems. In such systems, devitrification followed by partial erratic recrystallization of the excipient may occur during lyophilization, thereby generating a pellet of poor powdery appearance.

3. Thermal Treatment

The remedy to this situation is to perform a thermal treatment* of the frozen solution. This treatment consists of a controlled rewarming of the solution until devitrification and recrystallization of the excipient occurs, followed by a last freezing step below the solidification temperature. A typical excipient justifiable of such a treatment on thermodynamic grounds is mannitol. In the absence of proteins that maintain the structural integrity of the pellet, mannitol solutions often yield cakes of poor appearance. The induction of mannitol crystallization by rewarming around $-25^{\circ}C$ evades this problem and allows one to obtain elegant pellets that are easy to lyophilize and do not shrink.

In some cases, we have found that amorphous or vitreous solutions that do not crystallize upon rewarming or during lyophilization also benefit from a thermal treatment, but for structural reasons. For such excipients, the rewarming step induces some reorganization of the structure of the

*The concept of thermal treatment was introduced by L. R. Rey in 1960 (Ann NY Acad Sci 85:513–534). See also Chapter 1 of this book.

Copyright 2004 by Marcel Dekker, Inc. All Rights Reserved.

frozen solution involving complex mechanisms, one of which may be the disappearance of small ice crystals via molecular diffusion. The reorganized structure is easier to freeze-dry than the initial one, offers a good safety margin with respect to collapse, and yields pellets of good cosmetic appearance.

B. Primary Drying

1. Thermodynamic Requirements

Once the product is adequately frozen, the next step is the removal of ice, i.e., primary drying. During primary drying, the rate of ice sublimation is dependent on the amount of heat supplied to the product. The temperature of the product equilibrates as a function of two opposite effects: the transfer of heat from the shelf or from the gaseous atmosphere to the product, and the cooling due to ice sublimation. As the ice–vapor interface (moving front) moves toward the bottom of the containers, the rate of ice sublimation tends to diminish because the nascent porous matrix in the upper part of the pellet offers some resistance to vapor flow.

As a result of the lesser ice sublimation, the temperature of the product increases progressively during primary drying. The maximum primary drying product temperature is attained when the sublimation front reaches the bottom of the frozen solution, i.e., when almost all of the ice has disappeared. At this stage, it is essential to make sure that the maximum temperature reached by the product remains consistently lower than the incipient melting temperature of the eutectic T_{im} (for crystalline systems) or the softening or collapse temperature T_c (for vitreous or amorphous systems). If this temperature is exceeded, the crystalline systems will undergo partial liquefaction and the glassy-like ones will yield pellets showing bottom collapse. Inasmuch as they generate a heterogeneous product structure, these defects can in extreme cases jeopardize the efficacy and the stability of the drug product because the altered areas may display different activity and degradation profiles.

In vitreous systems, it is to be noted that the collapse temperature, T_c, can exceed the glass transition temperature T_g by several degrees or more [2]. The retention of pellet structure below T_c arises from the fact that when the frozen solution passes through the glass transition temperature, it returns from a glass to a highly viscous amorphous material. It is only when the viscosity of this material has decreased significantly that the fluidity of the interstitial phase is sufficient to cause collapse.

Copyright 2004 by Marcel Dekker, Inc. All Rights Reserved.

2. Determination of Product Primary Drying Time and Maximum Temperature

Despite the practical importance of determining the point where primary drying terminates, there is no easy or universally recognized method to do this. Part of the difficulty arises from the fact that the boundary between primary and secondary drying is not clear-cut. A reason for this is that the upper part of the cake is subject to a limited water desorption whereas the bottom of the cake is still undergoing sublimation. Another reason is that all of the samples do not necessarily dry at the same rate [3] because freezing–drying is inherently a statistical process in many respects.

Perhaps the best way to determine the end of primary drying, when the lyophilizer design of the main valve allows it to, is to perform pressure rise tests during primary drying [4]. When this testing is not possible, the end of primary drying can be estimated from the freeze-drying graphs according to several approximate methods.

For process review purposes, we determine three endpoints as depicted in Figure 1:

Change in slope of the product temperature traces
Change in slope of the chamber pressure curve (not possible with calibrated leaks)
Change in slope of the condenser temperature trace

The three endpoints generally show an acceptable agreement. The drying times calculated from these three estimates may be somewhat shorter than the real duration of primary drying, but they are reliable enough for comparison purposes.

Although the measurement of product temperature with probes inserted nearly to the bottom of the vials or ampoules is often questioned for many reasons, we use this method routinely to evaluate the duration of primary drying and the maximum primary drying temperature as shown in Figure 1. During prevalidation trials, we have run a series of more or less extreme freeze-drying cycles for sucrose and lactose formulations. The pellets produced were examined for lyophilization-related defects such as melt-back, bottom collapse, or shrinkage. In parallel, differential thermal analysis (DTA) and electrical resistance measurements (see Chapter 1) were carried out to determine the glass transition (T_g) and the softening temperature (T_c) of the frozen solutions. The maximum primary drying product temperature was tabulated for each freeze-drying cycle together with the type, frequency, and severity of cosmetic defects noted in the pellets. In many instances, the maximum product temperature determined from the freeze-drying trace correlated quite well (within $\pm$ 1–2°C) with the

Copyright 2004 by Marcel Dekker, Inc. All Rights Reserved.

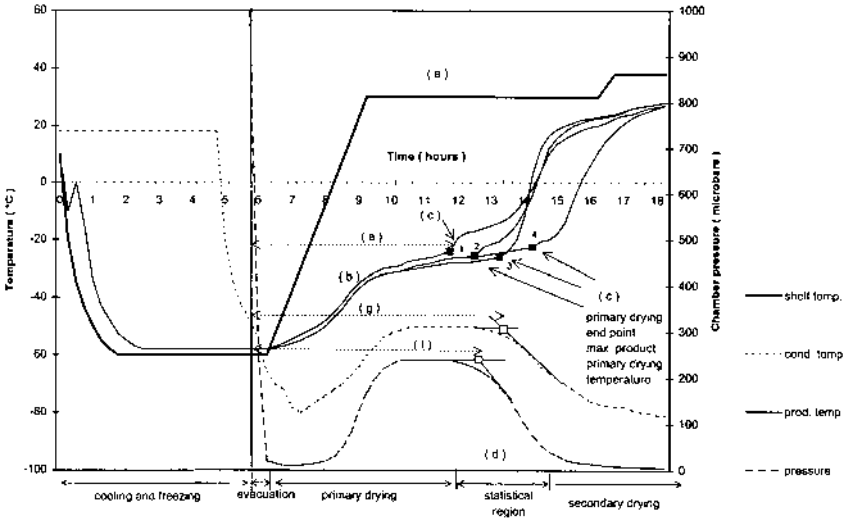

Figure 1 Determination of maximum product primary drying temperature and of product primary drying time. (1) For a given shelf temperature cycle (a), product temperature traces (b) will be achieved. (2) At the end of primary drying, when all the ice has sublimed, an inflection (c) is seen on each of the product temperature traces. (3) The temperature recorded at point c is the maximum product primary drying temperature. During primary drying, the temperature of the product is lower than or equal to the maximum product primary drying temperature. The secondary drying commences after point c. (4) The transition from primary to secondary drying corresponds to a region where transitions are driven by statistical events (d). Therefore, for different product samples, the time to reach the inflection (c) will vary. (5) Based on product temperature traces, the product primary drying time can be defined as the lapse of time from the moment when the vacuum is applied until point c is reached, i.e., time segment e for probe number 1. (6) The product primary drying time can also be determined from the chamber pressure curve (time segment f) or from the condenser temperature trace (time segment g).

temperature range predicted from the cross-examination of pellet appearance, and of DTA and resistivity curves. As the maximum product temperature was exceeding T_g to approach T_c, minor defects (minimal height shrinkage, minimal radial shrinkage, or minimal bottom collapse) were progressively appearing in a few samples. However, after the softening temperature T_c was passed, an increasing proportion of samples displayed significant collapse at the base of the cake. For the above formulations, the softening temperature T_c, which corresponds to the point where a sharp decrease in resistivity is noted on electrical resistance curves (see

Copyright 2004 by Marcel Dekker, Inc. All Rights Reserved.

Chapter 1), was therefore the upper temperature compatible with an acceptable product.

C. Secondary Drying

As the sublimation front moves down to the bottom of the frozen solution, it leaves behind a porous matrix made of solutes and bound water. It is essential that the major part of this water is removed from the matrix to avoid liquefaction and chemical degradation of the active material upon storage. The desorption of the bound water is usually achieved by progressively raising the temperature of the shelves up to the temperature at which drying is completed.

During the transition from primary to secondary drying, care should be taken with glass-like systems to slowly increase the temperature of the shelves, so as to avoid collapse or "retrograde" collapse [2]. Collapse may occur in the frozen part of the cake, if some containers still contain significant amounts of ice while shelf temperature is raised. Retrograde collapse takes place in an upward direction in that part of the cake above the sublimation front that contains no more ice. The dried part of the cake is characterized by a glass transition temperature that increases progressively from the T_g of the frozen solution of the T_g of the final product as the desorption progresses. If the shelf temperature is moved too fast, the glass transition temperature at a given moisture content will be exceeded, thus resulting in collapse in the dried part of the cake.

The time needed to complete desorption is highly dependent on product formulation and drying temperature. Crystalline mannitol usually requires only a short secondary drying, because the amount of bound water is minimal. On the other hand, glass-like systems formulated with sucrose or lactose necessitate a prolonged secondary drying.

III. INDEPENDENT VERSUS DEPENDENT PROCESS PARAMETERS

Besides verifying that the observed values of programmable operating parameters are within the expected range, part of the validation exercise consists of examining the impact of the programmable variables and of their variations on "dependent" process parameters. A control of the dependent parameters and an understanding of how they are related to the programmed variables is essential because the dependent parameters critically affect product properties (Figure 2).

Copyright 2004 by Marcel Dekker, Inc. All Rights Reserved.

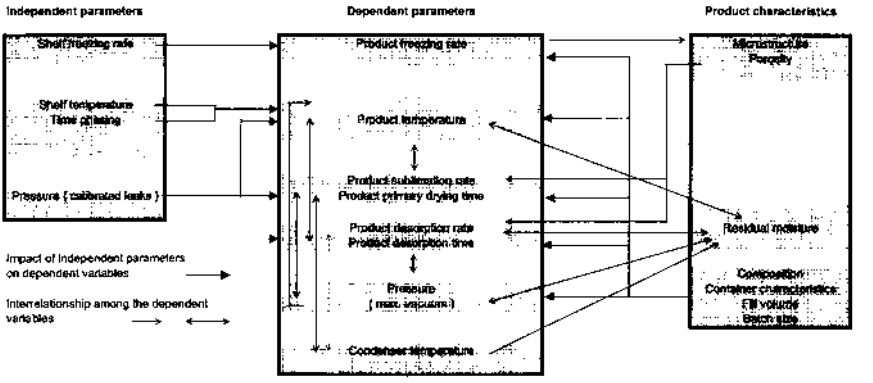

Figure 2 Interrelationship between independent and dependent freeze-drying parameters and product characteristics.

A. Independent Parameters

In freeze-drying runs, there are programmable variables that can be maintained at fixed, predetermined levels, regardless of the actual course of the lyophilization. Under normal conditions, the temperature of the silicon fluid circulated inside the shelves (referred to hereafter as shelf temperature), the time phasing of the temperature plateaus (soaks), and the ramping rate are not affected by the characteristics and load of lyophilized product. The shelf temperature and the observed heating and cooling rates are usually in close agreement with the programmed settings, unless the heating or cooling capacity of the thermoregulating unit is exceeded.

B. Dependent Parameters

In contrast with programmable operating parameters, there are variables that cannot be assigned fixed values during lyophilization because their level is the result of the conjoint effect of several variables on the product being lyophilized.

1. Condenser Temperature

An example of a dependent operating parameter is condenser temperature. During primary drying, condenser temperature equilibrates at different levels, depending on the amount of water being sublimed. For a given formulation and at each time point, the temperature of the condenser is

Copyright 2004 by Marcel Dekker, Inc. All Rights Reserved.

dictated by several variables including the temperature of the shelf, the chamber pressure, the load of product, and the time evolved since the commencement of primary drying.

2. Chamber Pressure

Lyophilization may be performed without pressure control, i.e., under "maximum vacuum." In the absence of pressure control, the pressure generated in the lyophilizing chamber is sustained only by ice sublimation and/or water desorption. Under these conditions, the pressure is to be regarded as a dependent variable, as its actual level is dictated by other parameters such as shelf temperature, time, batch size, and product characteristics.

In contrast with the above situation, chamber pressure becomes an independent programmable variable when a calibrated leak, or successive leaks of different pressure levels, is performed during the lyophilization. A usual way to generate a calibrated leak is to repeatedly inject nitrogen into the chamber so as to maintain the total pressure within a narrow range of values, this independent of the course of ice sublimation or water desorption. Another method for generating a constant pressure inside the chamber is to open and close repeatedly the valve between the condenser and the vacuum pumps, so as to maintain the water vapor pressure within predefined limits.

With regard to process validation, it is essential to note that when the chamber pressure is controlled, the resultant supply of heat to the product and the progress of lyophilization depends on the combined effects of two intensive independent variables: temperature and pressure. This is in contrast with the maximum vacuum process whereby shelf temperature is the only controllable intensive variable.

3. Product Temperature

On most industrial freeze-dryers, the temperature of the product is a "dependent" parameter that cannot be assigned fixed predetermined values. Product temperature results from the conjoint effects of the programmable operating variables, of the formulation being freeze-dried, of the design of product containers, and of the engineering characteristics of the lyophilizer. Although technically feasible, the keeping of a constant product temperature throughout primary drying necessitates a feedback system that regulates the temperature of the shelves as a function of the temperature of the probes inserted in the product or, alternately, as a function of the manometric measurement of product temperature [5]. Such regulating systems are usually restricted to research equipment.

Copyright 2004 by Marcel Dekker, Inc. All Rights Reserved.

4. Product Drying Time

The primary drying time of the product, which can be defined as the time elapsed from the moment when the vacuum is created in the chamber to the disappearance of the last ice crystals in the product, is obviously a dependent parameter as the rate of ice sublimation is controlled by the same factors as product temperature. This is also the case for the secondary drying time of the product, i.e., the time elapsed from the moment when ice sublimation is complete to the end of the cycle. During this period, water is desorbed from the product at a rate dictated both by technical factors and by product characteristics.

5. Shelf Temperature and Pressure Versus Product Temperature During Primary Drying

During primary drying, the temperature of the product is dependent on shelf temperature and on chamber pressure. The higher the temperature of the shelf, the higher the temperature of the product will be. An increase in chamber pressure favors the thermal exchanges at the gas–product interface and the thermal conductivity from the shelf to the tray. More heat is transported to the product and this results in a rise of product temperature.

The functional relationship between product temperature, on the one hand, and shelf temperature and chamber pressure, on the other hand, is affected by many factors including the size and design of the lyophilizer, the characteristics of the product, and the time evolved since the start of primary drying. With a sucrose formulation in vials, we have observed a maximum primary drying product temperature rise of $+5^{\circ}C$ when the shelf temperature was varied from -15 to $+30^{\circ}C$, whereas a pressure variation from 30 to 250 microbars generated an increase of around $+2.5^{\circ}C$. With a lactose formulation in ampoules lyophilized in a larger freeze-dryer equipped with a plate-type condenser, the effect of pressure was found to be predominant: $+6.5^{\circ}C$ for a pressure move from 50 to 300 microbars, versus $+1^{\circ}C$ for a shelf temperature move from 0 to $25^{\circ}C$.

6. Shelf Temperature and Pressure Versus Product Primary Drying Time

An increase in shelf temperature will unambiguously accelerate the primary drying of the product, unless it is excessive and promotes a slowing down of water removal consecutive to collapse or melt-back.

Copyright 2004 by Marcel Dekker, Inc. All Rights Reserved.

The effects of pressure variations, as they occur when pressure is controlled independently via calibrated leaks, are more complicated [6–12]. In many cases, an increase in chamber pressure favors ice sublimation and is reflected in a shorter primary drying time because of the improved thermal exchanges and of the higher product temperature [6,10–12].

However, a slowing down of ice sublimation will be observed if the total pressure in the chamber becomes too close to the pressure above the sublimation interface [9,10,12]. Indeed, for an efficient removal of water vapor from the containers, a sufficient pressure differential must exist between the ice–vapor interface and the chamber. The total pressure above the ice–vapor interface is approximately equal to the saturated vapor pressure of ice at the temperature of the sublimation front, as the headspace contains mostly water vapor [10–12]. Therefore, the pressure gradient that promotes water removal will no longer exist if the pressure level of the calibrated leak exceeds the saturated vapor pressure of ice at the target product temperature.

While a too high pressure in the chamber will prevent water removal, a high sublimation rate will usually be observed when the total pressure in the chamber is approximately one-fourth to one-half of the saturated vapor pressure over ice. At fixed product temperature, a higher vacuum in the chamber would create a larger pressure gradient between the product and the chamber, a condition that favors evaporation. However, in many instances this advantage is not sufficient to offset the poor thermal exchanges associated with high vacuum, especially when the product containers stand on trays. In actuality, the driving force for sublimation increases at relatively low pressures (up to 0.3–0.4 millibars) when chamber pressure is raised because the increase in ice vapor pressure resulting from the elevation of product temperature tends to be greater than the corresponding increase in chamber pressure [10].

7. Maximum Vacuum Versus Pressure-Controlled Lyophilization

Compared to lyophilization under maximum vacuum, the implementation of calibrated leaks during primary drying offers a number of advantages. The primary drying of the product is shortened, and therefore a few hours can be saved on the overall cycle time. In the same equipment, the batch size can be varied within wide limits with minimal effects on cycle time and on product properties. The transposition of the cycle to another freeze-drier and the scale-up operations are facilitated, as the control of the pressure level minimizes the effects of conceptual differences among lyophilizers. Noteworthy differences in drying rate will be attenuated under constant pressure conditions. Technology transfers are also made easier. If the source

Copyright 2004 by Marcel Dekker, Inc. All Rights Reserved.

site cycle is found to be nonoptimal for the receiving site equipment, a small correction of chamber pressure will readily bring the wished result, with no need to adjust shelf temperature.

Although pressure-controlled lyophilization brings significant advantages, a drawback of this technique is to risk promoting collapse in delicate formulations. This is because the assigned pressure modifies the course of sublimation and elevates product temperature in parts of the cycle where little evaporation would occur under maximum vacuum.

IV. SURVEY OF CRITICAL PROCESS PARAMETERS

The selection of the process parameters that need to be quantified and validated requires a knowledge of the many variables that may have an effect on the product. There is no universal validation framework, and the critical parameters should be identified based on the profile of the freeze-drying cycle, as well as on the characteristics, requirements, and release specifications of the product. The present section will be restricted to give examples of process parameters that are frequently assessed in validation reports.

A. Shelf Loading Temperature

The shelf temperature during product loading should be specified and controlled. It should be demonstrated that the product is stable during the storage period in the freeze-dryer prior to freezing. The loading temperature and the eventual holding time following completion of loading should be compatible with obtaining a homogeneous product.

Large differences in temperature between the product loaded first, on the top shelf, and the product loaded last, on the bottom shelf, may lead to different freezing patterns. To verify the uniformity of product temperature, thermocouples may be placed in containers located on different shelves in order to record the cooling and freezing pattern in the various areas. Another possibility for verifying that the structure of ice crystals is homogeneous is to perform a mapping of the residual moisture of the freeze-dried product in the various parts of the lyophilizer. If the loading conditions are not satisfactory, this should be reflected in a significant trend for moisture content from the top to the bottom shelf.

B. Shelf and Product Freezing Rates

The rate at which the product is frozen can have a significant impact on product quality and should be controlled. In scale-up operations,

Copyright 2004 by Marcel Dekker, Inc. All Rights Reserved.

comparable product freezing profiles should be maintained. In critical situations, the range of acceptable rates may be investigated and validated by varying the slope of the freezing ramp while keeping the rest of the cycle constant.

C. Shelf and Product Freezing Temperatures

Considering the inherent temperature variations from sample to sample and from location to location, the product should be frozen at least 5°C below its solidification temperature [13] as determined by DTA and electrical resistance measurements, and a safety margin of not less than 10°C should be observed in terms of shelf temperature.

D. Freezing Time

The freezing duration should be long enough to ensure that the whole volume of solution within a container and the contents of all containers are completely frozen.

E. Shelf Temperature Profile

The shelf temperature during the soaks as well as the duration of the soaks and of the ramps should comply with the settings and should be reproducible to within a set range from batch to batch.

F. Shelf Temperature Ramping Rate

At the beginning of primary drying, the shelf heating rate should not be too high to promote product melting at the base of the cake. At the end of primary drying the ramping rate should not be too high so as to lead to collapse or retrograde collapse.

G. Product Temperature During Primary Drying

Product temperature during primary drying should be consistently maintained below the level where incipient melting or collapse is observed.

H. Pressure During Primary Drying

If the lyophilization is performed under maximum vacuum, the pressure in the chamber reflects the amount of water vapor from the product in transit to the condenser. The maximum pressure during primary drying should be

Copyright 2004 by Marcel Dekker, Inc. All Rights Reserved.

tabulated and should be reproducible to within a set range while keeping the batch size constant. If the chamber pressure is controlled by one or several successive calibrated leaks to maintain specific pressure ranges, then these ranges should be reproducible and comply to within a range with the nominal settings.

I. Pressure During Secondary Drying

For effective desorption, the chamber pressure should be sufficiently low at the terminal stage of secondary drying. A maximum acceptable pressure should be specified.

J. Terminal Drying and Cycle Total Duration

The cycle duration, in particular the terminal drying time, should be substantiated with regard to all product characteristics susceptible to be affected by under- or overdying. A time range should be specified. If the cycle allows a comfortable safety margin with respect to residual moisture, then the cycle can be assigned a fixed duration, with a lower and upper time tolerance. If not, the cycle may be stopped based on a pressure rise test. This test consists of closing temporarily the main valve and recording the pressure rise in the chamber. The lyophilization is discontinued if the recorded pressure rise per minute does not exceed a maximum specified value; otherwise the cycle is continued until the test is passed. The maximum pressure rise value must be compatible with an acceptable level of residual moisture in the product.

For products in vials, cycles of fixed duration are easily implemented, as the vials can be automatically stoppered. However, with ampoules it may be desirable to have cycles of variable duration for schedule-related reasons. An elegant way to avoid variations in freeze-drying duration is to stop the lyophilization after a fixed time and to store the ampoules under dry sterile nitrogen in the lyophilizer until sealing is possible.

The critical segments of the freeze-drying cycle should never be modified in order to satisfy production planning requirements. A possible modification is to prolong the freezing soak. Once the product is fully frozen below its solidification point, no structural changes can be anticipated except perhaps a minimal grain growth. However, if a variable freezing time is allowed, the absence of resultant effects on the product should be substantiated and a range of acceptable freezing times defined.

An alternative is to prolong the last secondary drying step. However, prolonging secondary drying may generate a risk of overdrying and degradation of the active molecule. This point should be carefully assessed.

Copyright 2004 by Marcel Dekker, Inc. All Rights Reserved.

This risk can be at least partially evaded by including in the cycle a terminal soak with a decreased shelf temperature. For example, if secondary drying is effected at 40°C, a subsequent segment at 25°C will act in many instances as a conservation step. The basic reason for this is that at the beginning of secondary drying the moisture decreases quickly to reach asymptotically a minimum value that is highly dependent on the drying temperature. Subsequently, providing that the step at 40°C is long enough, very little additional water will be removed at 25°C no matter how long the drying is. If such cycle variations are allowed, documented evidence should show that they do not affect the product.

K. Partial Batch Size

Partial loading can affect both freezing and drying. When the freezing step is performed rapidly to low temperatures, the rate of product cooling may be dependent on product load. Therefore, if the freezing is critical, the effects of batch size should be substantiated with regard to shelf cooling rate and product freezing pattern.

When the chamber pressure is controlled by calibrated leaks, the load of product in the freeze-dryer usually plays a minimal role, if any, on the product drying rate. However, when lyophilization is achieved under maximum vacuum, the batch size will have some effect on the duration of primary and secondary drying. This is because the chamber pressure is a direct function of the amount of water vapor in transit. As the pressure has an effect on the thermal exchanges during primary drying and on water desorption during secondary drying, partial loading may affect the course of both drying stages. The scenario anticipated for partial loading is a prolongation of product primary drying time (unless there is intimate contact between product and shelves) and a shortening of secondary drying. Therefore, it should be verified that the excess time required to complete primary drying does not result in an increase of the maximum product temperature above the incipient melting or the softening point.

While lyophilizing ampoules on trays under maximum vacuum, we have effectively observed a prolongation of primary drying by 20–30% under partial load conditions. However, in no case was an increase in product temperature noticeable, even when the transition ramp to secondary drying was started before completion of product primary drying.

With regard to product properties, it should be shown that partial batch size does not affect susceptible properties such as residual moisture, reconstitution time, pH, or activity.

Copyright 2004 by Marcel Dekker, Inc. All Rights Reserved.

L. Condenser Temperature

The condenser temperature should be reproducible to within a set range of temperatures for the same batch size.

During primary drying, condenser temperature results from the rate at which water vapor is being condensed. Condensation rate is dependent on the rate at which water is being sublimed from the product. Effective sublimation can only be achieved if a sufficient temperature difference, which corresponds to a driving force, is maintained between the product and the condenser.

For freeze-dryers equipped with a coil condenser cooled down to $-80^{\circ}C$, the increase in temperature consecutive to water condensation is usually not critical even when the sublimation is intensive. In contrast, we have observed in the past a self-accelerated drying effect while using a lyophilizer of the older generation fitted with a plate condenser refrigerated at $-80^{\circ}C$. As the sublimation of ice was becoming intensive, the chamber pressure was rising sharply and the condenser was showing a marked temperature elevation. The pressure rise in turn generated an increase in product temperature, thereby further accelerating the sublimation.

The outcome of this self-accelerating process was a strong increase in condenser temperature (up to $-40^{\circ}C$) and an elevation of product temperature by a few degrees (up to $-30^{\circ}C$). However, the difference of temperature between the product and the condenser temperature was still sufficient to ensure a very rapid drying of the product, much faster than in freeze-dryers equipped with an effective coil condenser cooled at $-80^{\circ}C$. The observation that the primary drying was not impaired is consistent with the exponential decrease of the vapor pressure of ice as temperature is lowered. A sufficient pressure gradient for freeze-drying is established even when the difference of temperature between the product and the condenser is not very large.

Therefore, rather than the hindrance of product drying, the actual risk associated with condenser overloading is the elevation of product temperature, which can result in pellet collapse. For a given target cycle, this eventuality can be ruled out by running a high-pressure/high-temperature cycle that challenges the capacity of the condenser and the product to resist a high sublimation rate. This test may be helpful to define a maximum acceptable condenser temperature below which no pellet collapse is visible.

In contrast with the situation of primary drying, a low-temperature condenser is a great asset during secondary drying for formulations that must be dried to very low residual moisture. As the vapor pressure over ice is 0.5 microbars at $-80^{\circ}C$ versus 11 microbars at $-60^{\circ}C$, the desorption of water can be achieved in a more complete way with a condenser cooled at $-80^{\circ}C$.

Copyright 2004 by Marcel Dekker, Inc. All Rights Reserved.

V. PROSPECTIVE VALIDATION OF CYCLE LIMITS

A. Definition and Aims

Process development, optimization, and prevalidation trials usually yield a cycle believed to be close enough to the optimal freeze-drying conditions. The selected cycle is therefore supposed to represent the target working conditions that will be applied for future production batches. The next step in product development may be to implement a performance qualification of the target process, i.e., to perform a batch-to-batch consistency study using the target cycle. However, prior to carrying out this consistency study, it is useful to demonstrate the robustness of the target cycle with respect to deviations from the target conditions.

The purpose of prospective validation of cycle limits is to implement planned deviations around the target cycle by changing the programmable operating parameters in order to examine the impact of these variations on dependent freeze-drying parameters and on product properties.

The validation of cycle limits recovers two different but complementary approaches: vertical validation and horizontal validation. Vertical validation, the most important approach, consists of varying the shelf temperature around its target values. The chamber pressure may also be varied if the pressure level is independent of shelf temperature, such as in the case of calibrated leaks.

In horizontal validation, it is the time phasing of the segments at constant temperature that is varied. In its simplest form, horizontal validation consists of varying the duration of the terminal secondary drying step and examining the effects of this variation on sensitive properties such as residual moisture, bioactivity, or reconstitution time. If the freeze-dried formulation exhibits a significant risk of collapse, it may be well worth varying also the duration of the primary drying plateau.

In addition to horizontal and vertical validation, a complementary challenge of process robustness may consist in changing the duration of the shelf temperature ramps, i.e., the heating or cooling rate, while keeping the initial and final temperatures unchanged. With delicate formulations, this may be useful for critical parts of the cycle such as the freezing ramp or the transition ramp from primary to secondary drying.

B. Choice of Process Limits

The process limits chosen for the validation of the cycle limits should be wide enough to guarantee that the target cycle is sufficiently robust to withstand the small process fluctuations that occur routinely in industrial freeze-dryers. For example, if the programmed shelf temperature is 30°C

Copyright 2004 by Marcel Dekker, Inc. All Rights Reserved.

and the maximum departure from the programmed values is $\pm 2^{\circ}C$, then the actual shelf temperature may be as low as $28^{\circ}C$ or as high as $32^{\circ}C$. In order to guarantee that the range from $28^{\circ}C$ to $32^{\circ}C$ is effectively covered in terms of actual temperatures, the planned variations around the target shelf temperature should be not less than $\pm 4^{\circ}C$.

On the other hand, the process window defined by the area between the lower and upper limits should correspond to a possible operating range. Therefore, the limits should not be so wide as to produce an unacceptable product. For example, the upper limit may be chosen as the temperature where a few pellets start to display minimal collapse, whereas the lower limit may correspond to a temperature producing a pellet of high residual moisture, but still within specification.

For several validations, we have implemented planned deviations of ± 10–$15^{\circ}C$ around the target temperature during primary drying and of ± 5–$10^{\circ}C$ for secondary drying. The products obtained from these extreme cycles complied with all specifications and the range of the temperature variations was satisfactory for most practical purposes. When the freeze-dried product can accommodate shelf temperature variations of $\pm 10^{\circ}C$ or more, the lyophilization cycle can often be transposed without modifications to another lyophilizer.

It is a common observation that for a same shelf temperature a product may dry at somewhat different rates in two different models of lyophilizers, and that the temperature of the product during primary drying may be marginally higher in one piece of equipment than the other. Consequently, if the optimal shelf temperature is found to be $0^{\circ}C$ during primary drying for a given lyophilizer, the shelf temperature giving an equivalent freeze-drying trace in terms of primary drying product temperature and drying time may be $-5^{\circ}C$ in other equipment. If the robustness of the process has been demonstrated adjustment of the shelf temperature by a few degrees should pose no major problem during a technology transfer.

C. Practical Considerations

The lyophilizer should be loaded to full or at least to half capacity in order for the extreme cycles to be representative of future manufacturing conditions. For this kind of validation, the selected lyophilizer may be somewhat smaller than the ones intended to be used for commercial batches. As the product is not to be released, the load of active product can be completed with placebo if the rate of water evaporation from placebo containers matches that of the active drug. The lyophilizer may be opened at the end of freezing to assess the impact of freezing on product properties, or at various stages of secondary drying to assay residual moisture. The latter

Copyright 2004 by Marcel Dekker, Inc. All Rights Reserved.

operation is helpful to establish the kinetics of drying at various temperatures and to evaluate the time required for secondary drying. A pressure rise test may be effected each time the lyophilizer is opened in order to correlate the pressure rise per unit of time with the residual moisture in the pellets. Based on this correlation, a pressure rise specification for stopping the cycle may be subsequently defined to guarantee a product of acceptable moisture.

The products manufactured from extreme cycles may be placed on real-time and accelerated stability studies to assess their degradation rate compared to the target cycle. If the batches produced under extreme conditions are shown to be stable on storage, this is a good assurance that a small deviation from the target cycle, occasioned say by a compressor failure, will not jeopardize the stability of the batch produced. A strong point of prospective validation for extreme cycles is to facilitate subsequently the management of cycle deviations. In this respect, the batch-to-batch consistency approach is of little value to substantiate abnormal cycles [13]. A validation package including three identical cycle runs will obviously be of no use to assess a significant deviation in a critical part of the cycle, and in the absence of justification for batch release the affected batch should be either placed on stability or rejected.

D. Validation Program

Perhaps the ideal validation program of extreme cycles would consist of varying the independent operating parameters one by one, in order to determine how a punctual change impacts the freeze-drying trace and the final product. Unfortunately, such an extensive testing is usually unrealizable, and therefore a minimum program must be defined.

If the lyophilization is performed under maximum vacuum, the validation may simply consist of running a "high shelf temperature" cycle and a "low shelf temperature" cycle as shown in Figure 3.

If parameters other than shelf temperature are believed to play a critical role, an alternative may be to run, for example, a "low-temperature/low-pressure/short-soaks" cycle followed by a "high-temperature/high-pressure/long-soaks" cycle. The inconvenience is that when many changes are performed simultaneously, the cumulation of these changes may not always result in a "real worst case" because the various independent parameters interact in a complex way.

When the freeze-drying cycle includes a calibrated leak during primary drying, eight vertical deviations can theoretically occur, keeping the segment duration unchanged. The shelf temperature can be normal and the pressure too high or too low or the pressure can be normal and the shelf temperature

Copyright 2004 by Marcel Dekker, Inc. All Rights Reserved.

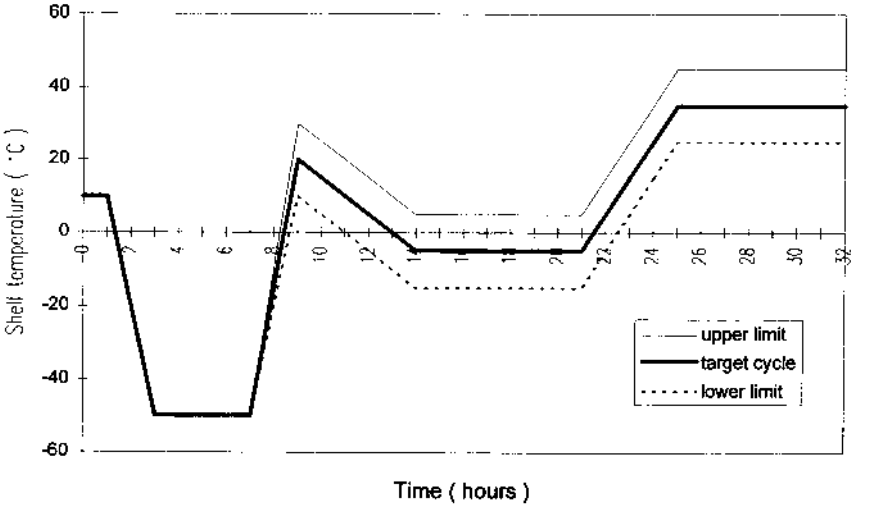

Figure 3 Process window for shelf temperature. The surface area comprised between the lower and upper limits corresponds to temperature range leading to an acceptable product.

Table 1 Combination of Critical Cycles

Shelf temp.	Pressure
High	High
High	Low
Low	High
Low	Low

too high or too low. The four other departures shown in Table 1 represent four extreme conditions that are worth testing.

The high-temperature/low-pressure cycle is often the least critical because it creates conditions favoring ice sublimation.

The low-temperature/low-pressure cycle theoretically results in a low product temperature. However, the drying rate is low and there is a risk that primary drying is not over when the temperature of the shelves is raised. In this case, collapse or retrograde collapse may occur. In addition, final product moisture may be above specification.

Copyright 2004 by Marcel Dekker, Inc. All Rights Reserved.

The combination of high temperature and high pressure promotes a significant elevation of product temperature, especially at the end of primary drying, and this may result in collapse. The condenser temperature may also increase significantly. However, these conditions lead to a high sublimation rate and the cooling effect resulting from ice sublimation limits the rise of product temperature.

In some cases, the low-temperature/high-pressure cycle can be anticipated to be the most damaging to the product because it can create conditions where the rate of ice sublimation is slowed down, thus resulting in product overwarming, collapse, and high residual moisture.

The four deviations shown in Table 1 can be implemented only during primary drying or, alternatively, during the whole cycle. A high temperature during secondary drying will be a test of the resistance of the active substance to thermal degradation. A high pressure during secondary drying does not favor desorption, and this test may be used to define a maximum acceptable pressure level for terminal secondary drying.

VI. PERFORMANCE QUALIFICATION OF THE TARGET CYCLE

A. Definition and Aims

The purpose of carrying out a performance qualification of the target cycle is to demonstrate that the product can be manufactured in a reliable and reproducible manner using the selected freeze-drying process. In order to substantiate process reproducibility, it is commonly accepted that three consecutive successful runs is adequate.

In addition to the qualification of the lyophilization process itself, it is usual to collect liquid samples at various stages of the manufacturing. In this way, the losses in active material or its degradation can be monitored throughout the process.

As the batch-to-batch consistency study is usually the last step preceding the release of the drug product onto the market, it is essential at this time that the batches be manufactured as normal production runs. In particular, production timing should be respected and the validation batches should be full scale or at least representative of the size range of the commercial batches.

The qualification of the target cycle may be carried out in the way of a prospective validation if the batches produced are not for use in humans. In this case, the risk of product contamination is not a critical issue and the taking of in-process samples is facilitated. The obvious

Copyright 2004 by Marcel Dekker, Inc. All Rights Reserved.

drawback of this approach is the sacrifice of active material. More importantly, if a product load is completed with a placebo, the filtration and filling operations will not be representative of a full-size batch, nor will all of the areas within the lyophilizer be occupied by active product. Especially at this stage of product development, the use of a placebo should be carefully considered. Unless the active molecule is present in minute amounts, the placebo formulation will never perfectly match the thermodynamic, structural, and evaporative properties of the active product.

It is therefore often preferable to carry out the batch-to-batch consistency study in a concurrent fashion [1,14], i.e., to manufacture full-scale batches of active product under Good Manufacturing Practices (GMP) conditions, using the standard manufacturing operating procedures. The sterile batches produced are then placed on stability at various temperatures. After a monitoring of product stability and a careful evaluation of the validation data, they may be progressively released onto the market, if the implemented manufacturing process gives full satisfaction.

The performance qualification study normally consists of two parts:

Careful control of in-process parameters and evaluation of the performance of the equipment (***process performance qualification***)

The extensive and rigorous evaluation of product quality (***product performance qualification***)

After each validation run, the batch records and the freeze-drying graphic should be carefully examined. Furthermore, the validation program may include the items developed hereafter.

B. Validation Program

1. Control of the Freeze-Drying Parameters

Shelf Temperature Profile. The shelf temperature during the soaks, the duration of the soaks, and of the ramps should be consistent with the settings and should be reproducible to within a set range from batch to batch.

Dependent Operating Variables. The pressure in the chamber, in particular the maximum pressure during primary drying, the minimum pressure during secondary drying, and the maximum condenser temperature, should be tabulated. If the batch size is kept constant, these parameters should be reproducible for batches produced with the same equipment.

Copyright 2004 by Marcel Dekker, Inc. All Rights Reserved.

Product Temperature Trace. The traces of the different batches should be compared and found in reasonable agreement. Using the method shown in Figure 1, one can tabulate the maximum product temperature at the end of primary drying and the product primary drying time (individual probes and the mean of all).

The pressure curve and the condenser trace may also be used to determine the primary drying time of the product (Figure 1).

2. QC Release Testing of the Final Product

A full quality control testing of the final product should be performed according to the standard analytical operating procedures and release specifications.

3. Visual Inspection of the Final Product

After each run, the full batch of product should be subject to visual inspection, with particular attention paid to lyophilization-related defects [13]. The various defects should be tabulated and the acceptance criteria may state a maximum acceptable level for each defect.

4. Stability Studies

The batches should be placed on real-time and accelerated stability studies.

5. Extensive Analytical Testing of the Product for Uniformity

In contrast with routine QC where a very limited number of samples are tested, a large number of product containers of each batch should be tested for critical analytical properties such as assay, activity or bioactivity, purity, degradation products, residual moisture, and reconstitution time. The purpose of extensive testing is to show that each pellet is typical and representative of the rest of the batch, which is a guarantee of product safety and efficacy as the patients are usually injected with the contents of a single container.

A random sample of product containers may be used for this testing. Alternately, the product may originate from various defined areas within the lyophilizer. The data gathered should be interpreted in terms of descriptive statistics. For each analytical attribute, the mean, the standard deviation, the percentiles, the extreme values, and the normality of the distribution can be determined.

One-tailed or two-tailed confidence limits for the mean content, activity, purity, or residual moisture may also be calculated. For each batch produced, the 99.9999% confidence limits for the mean should be found to

Copyright 2004 by Marcel Dekker, Inc. All Rights Reserved.

be within specifications. For a well-controlled process, 99.9999% one-tailed limits may typically lie in the range of 50–75% of the upper specification limit.

For each analytical property, the proportion of individual pellets lying outside specification may be tabulated. This level should be minimal if the capability of the process and of the lyophilizer is consistent with the specification limits. If the distribution of pellet contents obeys the normal or log-normal law, it is further possible to predict for the whole batch the proportion of samples that can be expected to be outside the specifications. Alternately, process capability indices can be calculated [15].

6. Uniformity of the Product from Various Areas Within the Lyophilizer

This item is discussed in Section VIII.

7. Analytical Testing of In-Process Samples

Liquid samples should be taken at the critical stages of the process, e.g., bulk material, formulated solution before and after filtration, filling solution, filled vials or ampoules at the beginning, middle, and end of filling. When traces of material are to be assayed, care should be taken that the collecting test tubes or containers do not adsorb significant amounts of drug or leach out impurities in the formulated solution.

If they are unstable, the samples of each given step may be analyzed as soon as collected. Alternately, if their stability is sufficient, the different liquid samples may be stored in the refrigerator until the filling is complete and they may be tested at the same time. If the freezing induces no degradation, a third possibility is to freeze the liquid samples and to analyze them at the same time as the samples of finished product.

Whenever feasible, the simultaneous analysis of samples from the different sampling points offers a major advantage, that of enabling a more accurate determination of the losses or variation in purity occurring during manufacture. In actuality, for many analytical methods, the interassay variability tends to be larger than the intraassay variability. As a consequence, when samples from the different production steps are analyzed separately, the results may not be fully comparable, and this may prompt a conclusion of losses or degradation during manufacture while in fact the product is stable.

As an example, the validation program based on liquid sample testing may include the following items:

1. *Sterile filter compatibility testing*. It should be demonstrated that filters of the same surface area as for commercial batches are

Copyright 2004 by Marcel Dekker, Inc. All Rights Reserved.

compatible with the formulation being filtered [16]. The filter should not induce significant degradation of the active product or leach out undesirable substances. The retention of active material inside the filter, in other words the loss on filtration, should be quantified and assessed statistically.

2. *Formulation and filling*. The acceptability of the formulation and filling processes should be evaluated with regard to the level of oxidation or other degradation products. The maximum level of degradation products should be consistently maintained below the specification limit for the final product, but the acceptance criterion may also be a maximum admissible purity decrease over a given step or over the whole production process.

   Special attention should be paid to the compatibility of the plastic tubing that connects the filling tank to the dispensing needles, although this can be the object of a separate validation work. The active material may be adsorbed onto or may diffuse into the tubing, or the tubing may leach out activators or plasticizers into the formulated solution. With sensitive chromatographic methods, these impurities may generate extra peaks that appear in the retention time range where real degradation products are quantified, thus leading to an underestimation of actual product purity.

3. *Assessment of the overall manufacturing process*. When the freeze-dried product is analyzed together with in-process samples, the overall losses in active material throughout the production can be calculated by comparing the mass or the activity of the starting bulk material (or that of the formulated bulk before filtration) with the mass or activity recovery in the freeze-dried product. An estimate of activity variations on freeze-drying is supplied by the comparison of the activity of the filling solution (filling tank or filled containers) with that of the final product.

The losses on manufacture or the variation of purity can be conveniently assessed via two-way analysis of variance (batch versus step) and post hoc comparisons. The acceptance criterion may be that the variation observed, if found significant at $p = 0.05$, should not exceed a predefined maximum admissible level.

To conclude this section, it is worth noting that the process qualification based on liquid samples, although necessary, is not sufficient to qualify all aspects of the stability of the formulated solution. For example, it may happen that the formulated solution has to be stored in the filling tank for a few hours longer than usual. The behavior of the solution during this

Copyright 2004 by Marcel Dekker, Inc. All Rights Reserved.

extra time cannot be safely predicted from the above in-process data. In order to release the batch produced, it is necessary to have a documented study about the stability of the filling solution at different temperatures, over an adequate period of time, e.g., 24 h.

A third aspect of product stability pertains to product uniformity across the shelves (Section VIII.B).

VII. RETROSPECTIVE VALIDATION OF THE FREEZE-DRYING PROCESS

A. Definition and Aims

Retrospective validation is based on the examination of the batch record data of a large number of production batches once the product has entered the market place. As commercial batches are usually produced under admittedly constant operating conditions, the retrospective analysis of freeze-drying data will supply valuable information about the reproducibility of the process, especially if it includes batches produced over a period of several years. However, unless significant deviations have occurred during the production runs, retrospective validation will supply little information about the robustness of the production process. This approach is therefore complementary to the prospective validation of the cycle limits that challenge the robustness of the freeze-drying process. Although retrospective validation proceeds from the same philosophy as concurrent validation, it supplies a more complete picture of the reproducibility and reliability of the process. In contrast with concurrent validation, the retrospective approach supplies documented evidence as to the capability of the process to accommodate factors such as the replacement of lyophilizer components, the maintenance performed in the production unit, or the run-to-run fluctuations that occur in the daily operation of industrial freeze-dryers. Retrospective validation is also a useful tool to substantiate that the change of lots of excipients, vials, or stoppers has no effect on the product.

A retrospective validation of the freeze-drying process will usually consist of two major areas:

Examination of the reproducibility of the freeze-drying parameters, to show that the process and the equipment can be maintained within a state of control

Examination of the reproducibility of product analytical properties, especially those sensitive to lyophilization, to show that acceptable product characteristics can be maintained

The results of the commercial stability program may also be included.

Copyright 2004 by Marcel Dekker, Inc. All Rights Reserved.

B. Validation Program

1. Freeze-Drying Data

The retrospective study of freeze-drying data may include the following parameters for each batch reviewed:

Batch size (percentage of full capacity)
Temperature of shelves during the successive freeze-drying steps
Duration of the soaks and of the temperature ramps
Total cycle time
Maximum pressure in chamber during primary drying, or the pressure level of the calibrated leak
Minimum pressure at the end of secondary drying
Maximum temperature of the condenser
Temperature range of the product at the end of freezing
Maximum primary drying product temperature
Product primary drying time

The data tabulated can be used to calculate the mean values of the various parameters and the standard deviation among the batches. The temperature of the shelves and the duration of the different segments should be reproducible to within defined limits. The extreme values observed and compatible with an acceptable product can be used to define an operating range for each parameter, e.g., for the shelf temperature or the duration of any segment. The highest and lowest pressure values, the highest condenser temperature values, and the highest product temperatures should also be assessed with regard to residual moisture, pellet appearance, and product activity in order to show that they did not affect the product.

The freeze-drying data are also suitable for trend analysis. The reproducibility of the freeze-drying process can be followed over years and the database may be used to trace back the drift of a specific parameter from its initial values.

When the freeze-drying cycle entails one or several segments of a variable duration, statistical testing can be used to compare the analytical properties of the batches with different segment times. For example, if the duration of the freezing step is variable, the batches may be categorized in two groups, "short freezing" and "long freezing". A t test for independent samples can then be performed to verify that the freezing time has no significant effect on properties such as residual moisture, bioactivity, or pH.

If lyophilizers of different types are used to lyophilize a drug product according to the same freeze-drying cycle, useful information about process

Copyright 2004 by Marcel Dekker, Inc. All Rights Reserved.

robustness can sometimes be gained by comparing the values of the dependent parameters. The analytical properties, in particular the activity and the moisture of product batches manufactured in different lyophilizers, also deserve comparison.

When different batch sizes are manufactured within the same lyophilizer, one can assess the effects of loading on the dependent operating variables. Partial and full-size batches should be comparable for pellet cosmetic appearance and for analytical properties such as bioactivity or residual moisture.

The deviations to the normal freeze-drying process that occurred during the period reviewed should be examined for their impact on product properties. The deviation and investigation reports and the stability studies performed on the deviating batches may be referenced.

2. QC Release Data and Visual Inspection

Evaluation of the analytical data should demonstrate that the product consistently achieves its predicted levels of quality, activity, and purity. The visual inspection data should also be assessed, at least for lyophilization-related defects such as collapse or melt-back.

The critical analytical data should be tabulated and analyzed in terms of descriptive statistics (mean, coefficient of variation, extrema), control charts, and trend analysis [17]. If the data of several years are included, yearly means may be calculated, and the significance of the variations from year to year may be investigated by analysis of variance to evaluate the reproducibility of the process.

For each analytical test, the number and frequency of nonconforming batches should be tabulated. An explanation for the failure should be provided, in such a way as to distinguish between process- and nonprocess-related failures.

Based on a large number of batches, the mean content in active material in the final drug product, or its bioactivity, should be found consistent with the claimed content or potency. The extent of the losses throughout manufacturing should be assessed statistically.

Another opportunity of the retrospective validation is to examine the effects on the documented process changes, based on a large number of batches. For example, if the type or the size of the sterile filter has been changed, it may be useful to perform a t test to compare the potency or the drug content of batches produced before and after the change in order to verify that the filters behave similarly for losses on filtration. If during a period the ampoules or vials were provided by an alternative supplier, it may

Copyright 2004 by Marcel Dekker, Inc. All Rights Reserved.

be worth verifying that the glass qualities are equivalent by comparing the pH ranges of the final reconstituted products.

VIII. UNIFORMITY OF THE PRODUCT WITHIN THE LYOPHILIZER

A. Definition and Aims

The study of the properties of the lyophilized product collected from various locations within the lyophilizing chamber, according to a predefined sampling plan, is a useful technique, especially in areas such as troubleshooting, product development, cycle optimization, validation of cycle limits, and batch-to-batch consistency. The main purposes of carrying out a "mapping" of the product within the lyophilizer are the following:

To assess the equivalence of the characteristics of the product arising from the various areas in the chamber
To evaluate the ability of the manufacturing process to yield a homogeneous product
To evaluate the capability of the lyophilizer to yield a homogeneous product

Various product characteristics can be assessed via product mapping. For example, considering protein drug products, typical attributes to be investigated for uniformity may include residual moisture, pellet appearance, immunoassay, protein content, and various impurities or degradation products that may form during filling or freeze-drying. Product nonuniformity may typically be promoted by two factors:

An inadequate filling process and/or holding step in the lyophilizer prior to freeze-drying
A poor freeze-drying cycle or an ineffective lyophilizer

Although it is conceivable during drug development to remove product samples just prior to freezing or at the end of freezing in order to investigate the effects of filling and storage in the lyophilizer, it is often easier to sample the freeze-dried product. Compared to liquid samples, the testing of freeze-dried samples offers several advantages.

The freeze-dried samples are representative of the finished product to be released onto the market.
Providing the product is reconstituted in a small volume of diluent, the resulting solution is more concentrated than the formulated solution before freeze-drying. It is therefore easier to assay minute amounts

Copyright 2004 by Marcel Dekker, Inc. All Rights Reserved.

of drug or impurities and the analytical methods used for QC release can be implemented.

Once the lyophilizer is unloaded, the removing of stoppered vials is compatible with good manufacturing practice and can therefore be implemented in the frame of a concurrent validation.

The disadvantage of collecting samples only after the freeze-drying is that the results may be more difficult to interpret in the case where the product is not of the same characteristics from any position within the lyophilizer, as the differences observed reflect the overall effect of the successive manufacturing steps.

B. Testing of Product Uniformity Across the Shelves

A change of product characteristics across the shelves can have several causes. During filling, the trays supporting the vials or ampoules are usually loaded by small blocks onto the shelves of the freeze-dryer, which are precooled at a defined temperature. Therefore, the product filled first (top shelf) is in contact with the containers and stored for a longer time inside the freeze-dryer than the product filled last (bottom shelf). Conversely, the product filled last remains for a longer time in the filling tank, which may or may not be refrigerated. In addition, the plastic tubing connecting the filling tank to the dispensing needles may interact with the filling solution and this may result in an uneven distribution of the drug substance within the product containers filled first and last.

With sensitive products, it is therefore useful to verify that the expected level of product purity and activity can be consistently maintained throughout the filling and the product loading prior to freeze-drying.

A simple example of mapping is shown in Figure 4A for a performance qualification run for a recombinant drug product filled and released by "mass." Each vial contains only a few micrograms of active protein, and therefore it is important to show that the protein content of the vials is uniform across the shelves of the freeze-dryer. Although no protein material was expected to disappear during lyophilization, the concern here was that protein may be lost during the filling process.

To demonstrate that this was not the case, the shaded trays shown in Figure 4A were sampled and for each tray 3×2 vials were assayed for protein content. The protein content results were analyzed with a two-cell analysis-of-variance model including a factor, the left/right positioning, and a covariate, the shelf number. In order to increase the power of the statistical testing, the shelf number was handled as a covariate and not as a factor, based on the assumption that the filling was progressing at a constant rate.

Copyright 2004 by Marcel Dekker, Inc. All Rights Reserved.

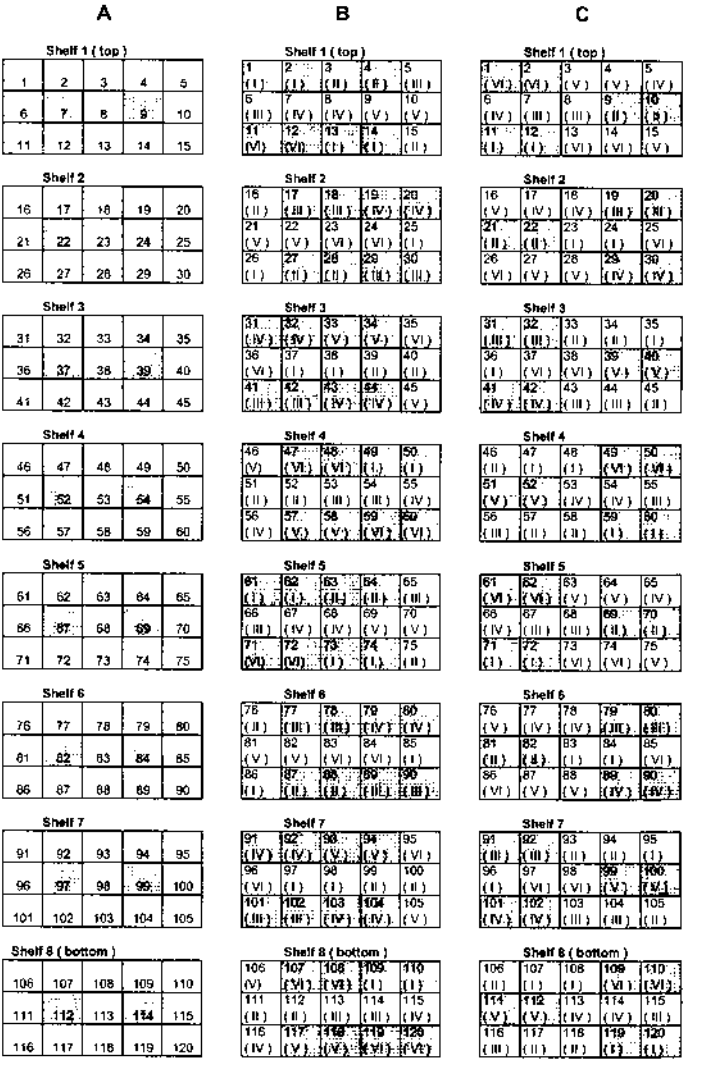

Figure 4 Sampling plans for the determination of product uniformity within the lyophilizer. (A) Uniformity of protein content for a product in vials. (B, C) Uniformity of residual moisture for a product in ampoules. The lyophilizer has eight shelves and each shelf holds 15 trays of product containers. Arabic numerals refer to the tray number and show the order in which the trays are loaded during filling. Roman numerals relate to the sealing sequences. The trays are unloaded by blocks 12, starting from tray 120. As the trays are "sealed" in twos, the first two trays subject to sealing are identified by the number I, the last two trays by the number VI. The trays from which samples are collected for analysis are shaded.

Copyright 2004 by Marcel Dekker, Inc. All Rights Reserved.

In this particular case, the comparison of vials located on the left and on the right side served as a control because no differences of the mean protein content were anticipated. The homogeneity of the protein content across the shelves was demonstrated by the nonsignificance of the slope of the regression line of the protein content versus the shelf number. If the regression mean square had been found to be much larger than the within-mean square (which is a measure of the within-tray variability of protein contents with respect to the content predicted for each tray by the regression line), then there would have been a significant variation trend of protein content across the shelves. The acceptance criterion stated that if the slope was found to be significant at $p = 0.05$, then the variation in protein content from the top to the bottom shelf had to be no more than a given percentage in order for the process to be considered as acceptable.

Sampling layouts similar to the one shown in Figure 4A are appropriate when product heterogeneity reflects a change or a degradation occurring during filling or storage in the lyophilizer prior to freezing. For example, it is reasonable to anticipate a potential increase in oxidation products during filling, reflected as a trend across the shelves, but there is no reason to expect different amounts of oxidized products in product containers coming from two neighboring trays.

C. Testing of the Equivalence of the Product from All Areas Within the Lyophilizer

This situation is more complex when the product property under examination is affected by the freeze-drying process and the equipment. In this case, it should be demonstrated that lyophilization process and the lyophilizer yield a product that consistently achieves its predicted level of quality wherever it comes from in the lyophilizing chamber.

A typical case is that of residual moisture. Pellets from a same batch show inherent differences in moisture content. Residual moisture is dependent on a multitude of factors including the location of the samples in the chamber, their positioning in the middle or at the edge of the trays, and the consistency of the contact between the trays and the shelves.

When looking at process steps, a first potential cause of product heterogeneity is the difference of temperature among the product containers stored in the lyophilizer prior to freezing. The next critical step is freezing because in many freeze-dryers the circulation of silicon fluid inside the shelves is of limited efficiency. Thus, depending on the way the silicon fluid is circulated, all of the shelves will not necessarily cool down at the same rate, especially under full-load conditions. Furthermore, the corner of the shelves corresponding to the fluid inlet will undergo a faster cooling than the corner

Copyright 2004 by Marcel Dekker, Inc. All Rights Reserved.

corresponding to the outlet. The temperature differences will be transmitted to the product, thereby generating variations in the ice crystal structure, with repercussions upon drying. During primary and secondary drying, the rate of water removal from the samples will also be affected by their location with respect to the main valve, and with respect to the inlet and outlet of the silicon fluid.

In extreme cases, the variations in residual moisture may be large enough to have dramatic repercussions on batch stability. For example, the product located in the upper part of the chamber may be found stable whereas the product from the lower part is unstable. It is therefore essential to demonstrate that the batches produced have uniform residual moisture, or at least that the differences observed are too small to jeopardize product stability.

Two of the sampling layouts developed to assess the moisture uniformity of a sucrose-based recombinant drug product in ampoules are shown in Figure 4B and C. When the lyophilization was over, the trays of ampoules were unloaded progressively by blocks of 12, starting from the bottom shelf, and the vacuum was restored in the chamber in the meantime between each unloading operation. This is a standard operating procedure in order to avoid ampoule pickup of excessive amounts of moisture prior to sealing.

Because the validation batches were produced under GMP conditions, it was not possible to recover the opened ampoules during the lyophilizer unloading. The ampoules were therefore collected only after sealing. As the trays of ampoules were "sealed" in twos, the ampoules selected for analysis arose from pairs of trays, and not from individual trays (see Figure 4B and C). The sealing of the ampoules of a pair of trays took about 2.6 min. Thus, the ampoules of the first two trays were exposed to laminated air for a maximum period of 2.6 min and those of the last two trays for 13–15.6 min.

Apart from the compliance with GMPs, the taking of samples after sealing offered a major advantage, that of supplying sealed samples fully representative of routine production. Nevertheless this procedure had a drawback: it did not allow one to distinguish readily between variations in moisture due to sealing and variations resulting from the position of the samples within the lyophilizer.

In order to overcome this problem, the moisture results were analyzed by analysis of variance. The following factors were examined for their effect on the dependent variable "moisture":

Shelf (1 to 8)
Rear–front positioning (rear, front, and, for some layouts, middle)
Left–right positioning (left, right)

Copyright 2004 by Marcel Dekker, Inc. All Rights Reserved.

In addition, the pairs of trays were classified and six groups according to their sealing rank, I to VI (Figure 4B and C), and the sealing rank was handled as a covariate in the analysis-of-variance model. No interaction terms between the main factors or between the covariate and the main factors were defined in the model.

The sampling plan shown in Figure 4B led to a 32-cell orthogonal model and that of Figure 4C to a 24-cell nonorthogonal model. In both models each cell was confounded with a pair of trays. The residual variance, i.e., that between cells, was therefore representative of moisture differences among pairs of trays, whereas the within-cell variance accounted for ampoule-to-ampoule variations within a same pair of trays.

When analyzing the results of each batch, the residual to within-mean square ratio was calculated to determine whether the use of trays had a significant impact on moisture uniformity. In most runs, this F ratio was nonsignificant. This demonstrated that the contact between the trays and the shelves was consistent enough to ensure a homogeneous product when running the target cycle, owing to the relatively slow freezing process and to the time allowed for secondary drying.

For each run, the significance of the factors shelf, rear–front positioning, and left–right positioning, as well as the significance of the regression term associated with the sealing, were assessed with respect to the within + residual mean square. This analysis was complemented by the partitioning of the total variance into components so as to quantify the contribution of each of the following factors to moisture variability:

Shelves
Rear–front positioning
Left–right positioning
Sealing
Tray-to-tray variations
Ampoule-to-ampoule variations (differences among ampoules from a same pair of trays + analytical error)

Based on an overall analysis of seven runs, the contribution of the shelves to moisture variability was found to be only 3.5% (Figure 5). The drying was best under the butterfly valve. It was marginally less efficient for the shelves most remote from the butterfly valve. Virtually no differences were noted when comparing the front, middle, and back rows of trays. The contribution to product variability of left–right positioning was 0.3%. The average moisture content of the samples located on the right side was found to be 272 μg/amp versus 279 μg/amp for the left side. This was consistent with the circulation of silicon fluid inside the shelves from the right to the left side.

Copyright 2004 by Marcel Dekker, Inc. All Rights Reserved.

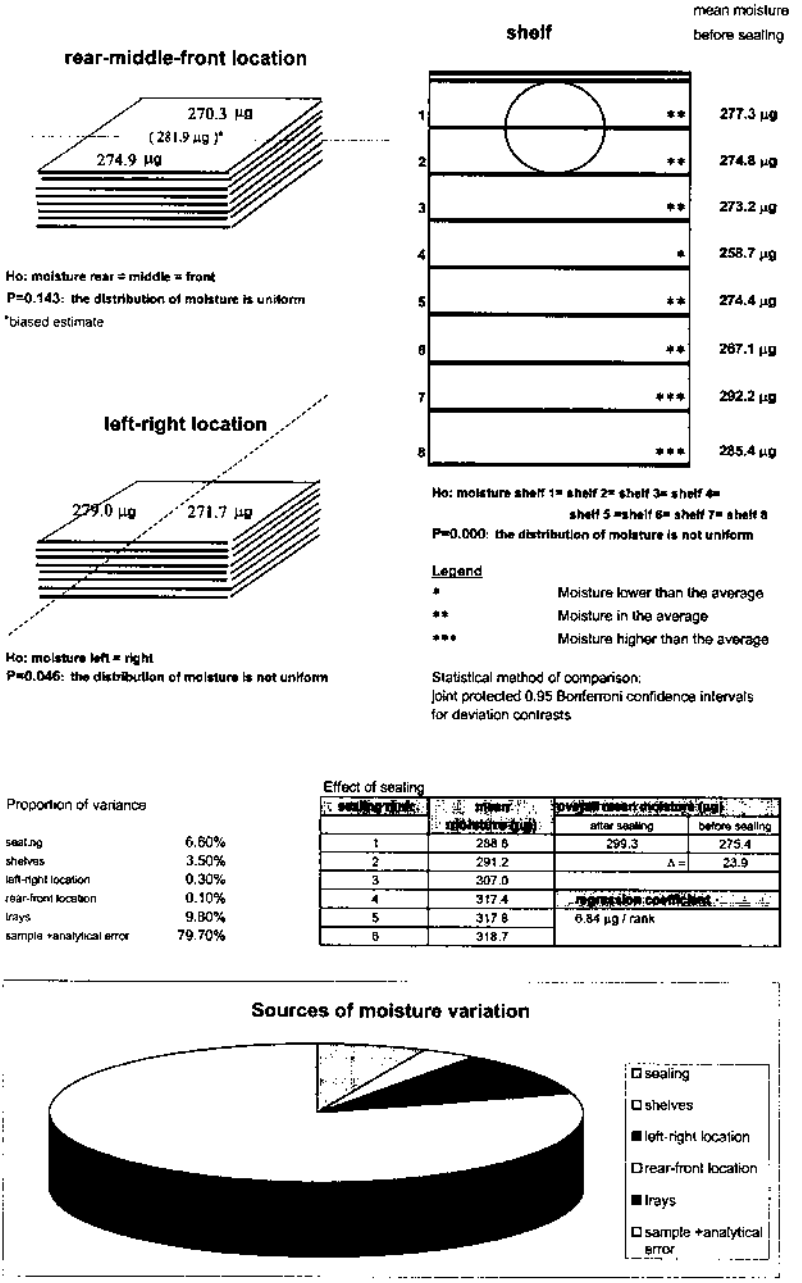

Figure 5 Distribution of product residual moisture within the lyophilizer.

Copyright 2004 by Marcel Dekker, Inc. All Rights Reserved.

The moisture variability resulting from the uptake of moisture during sealing was found to be 6.6% on the average. The increase in moisture upon sealing was calculated (regression coefficient) to be approximately 7 μg per sealing rank. Therefore, the sealing induced a mean moisture increase of 24 μg, and in the worst case the ampoules were calculated to pick up 42 μg water (sealing rank 6).

With regard to the upper specification limit for moisture, this increase was marginal, and it was calculated that there was no risk to breach the specification limit at the relative humidity of the clean room, assuming a cumulation of worst cases.

Finally, for the various runs the moisture variability arising from the trays varied between 0 and 14%, whilst the ampoule-to-ampoule variations represented the major part of the total variance, i.e., 65–95%. Although the differences among ampoules were the major sources of moisture variation, the absolute magnitude of these variations was too small to jeopardize product homogeneity and stability. Indeed, for the batches produced, the coefficient of variation of moisture content (including all sources of variation) did not exceed 15%. As the mean moisture of the final product was approximately half of the maximum allowed content, there was therefore no risk to produce pellets above specification for moisture content.

From these results it was concluded that the lyophilizer was appropriate for the sucrose formulation under validation, as it resulted in minimal moisture variations from the different areas of the chamber. The unloading of the trays by blocks of 12 was also an adequate practice considering the specification range for relative humidity in the clean room.

IX. CONCLUSIONS

The validation of lyophilization cycles is a complicated issue because the process parameters and the characteristics of the product are closely interrelated. The process affects the final product, but the characteristics of the product undergoing lyophilization impact the dependent operating parameters, the freeze-drying pattern, and dictate the basic requirements for a successful process. This interdependence limits the opportunities of using placebo formulations and most of the validation runs must be performed with active product. The high cost and limited availability of some materials, as well as the need to validate the process under conditions that are representative of routine production, justify that part of the validation is performed in a concurrent fashion. The concurrent validation should then be completed by a retrospective review of the data accumulated for

Copyright 2004 by Marcel Dekker, Inc. All Rights Reserved.

commercial batches, so as to track the reproducibility, the reliability, and the trends of the process over a longer period of time.

In the next decade, the increasing demand for high-technology lyophilized products may prompt pharmaceutical companies to optimize and shorten their freeze-drying processes, so as to keep the size of clean room facilities and the manufacturing costs at a reasonable level. In some cases, the redesigned freeze-drying cycles will probably be more extreme or use alternative techniques such as pressure ramping or cyclic pressure lyophilization [18], and it will be of the utmost importance to ensure that the new processes are robust. In this respect, perhaps a promising breakthrough is the emergence of mass spectrometers that can be mounted on the chamber or between the chamber and the condenser. Besides supplying quantitative data about gases in the chamber and vapor components in transit from the product, these spectrometers enable a straightforward evaluation of the effects of a variation of pressure or temperature in terms of water removal from the product. As increasingly sophisticated products and processes emerge, such equipment will prove increasingly useful for cycle optimization, validation, and process compliance.

REFERENCES

1. EH Trappler. Validation of lyophilized products. In: IR Berry and RA Nash, eds. Pharmaceutical Process Validation. 2nd ed. New York: Marcel Dekker, 1993, pp 445–477.
2. AP MacKenzie. Collapse during freeze-drying—qualitative and quantitative aspects. In: SA Goldblith, L Rey and WW Rothmayr, eds. Freeze-Drying and Advanced Food Technology. New York: Academic Press, 1974, pp 277–307.
3. ML Roy, MJ Pikal. Process control in freeze-drying: determination of the end point of sublimation drying by an electronic moisture sensor. J Parenter Sci Technol 43:60–66, 1989.
4. K Murgatroyd. The freeze-drying process. In: P Cameron, ed. Good Pharmaceutical Freeze-Drying Practice. Buffalo Grove, IL: Interpharm Press, 1997, pp 1–58.
5. N Milton, MJ Pikal, ML Roy, SL Nail. Evaluation of manometric temperature measurement as a method of monitoring product temperature during lyophilization. J Pharm Sci Technol 51:7–16, 1997.
6. SL Nail. The effect of chamber pressure on the heat transfer in freeze-drying of parenteral formulations. J Parenter Drug Assoc 34:358–368, 1980.
7. TA Jennings. Effect of pressure on the sublimation rate of ice. J Parenter Sci Technol 40:95–97, 1986.
8. RG Livesey, TWG Rowe. A discussion of the effect of chamber pressure on heat and mass transfer in freeze-drying. J Parenter Sci Technol 41:169–171, 1987.

Copyright 2004 by Marcel Dekker, Inc. All Rights Reserved.

9. TA Jennings. Discussion of primary drying during lyophilization. J Parenter Sci Technol 42:118–121, 1988.
10. MJ Pikal. Freeze-drying of proteins. I. Process design. Pharm Technol Int 37–43, January 1991.
11. MJ Pikal, ML Roy, S Shah, Mass and heat transfer in vial freeze-drying of pharmaceuticals: role of the vial. J Pharm Sci. 73:1224–1237, 1984.
12. MJ Pikal. Use of laboratory data in freeze-drying process design: heat and mass transfer coefficients and the computer simulation of freeze-drying. J Parenter Sci Technol 39:115–139, 1985.
13. FDA Guide to Inspections of Lyophilization of Parenterals. Food and Drug Administration, Rockville, MD, July 1993.
14. E Trappler. Lyophilization. In: MJ Groves and R Murty, eds. Aseptic Pharmaceutical Manufacturing II. Buffalo Grove, IL: Interpharm Press, 1995, pp 291–309.
15. DC Montgomery, Introduction to Statistical Quality Control. New York: John Wiley & Sons, 1996, pp 430–474.
16. V Kumar, R Murty. Validation of aseptic process. In: MJ Groves and R Murty, eds. Aseptic Pharmaceutical Manufacturing II. Buffalo Grove, IL: Interpharm Press, 1995, pp 101–116.
17. DC Montgomery. Introduction to Statistical Quality Control, New York: John Wiley & Sons, 1996, pp 179–312.
18. JD Mellor. Fundamentals of Freeze-Drying. London: Academic Press, 1978.

Copyright 2004 by Marcel Dekker, Inc. All Rights Reserved.

21

A New Development: Irradiation of Freeze-Dried Vaccine and Other Select Biological Products

Louis Rey
Cabinet d'Études, Lausanne, Switzerland

Joan C. May*
Center for Biologics Evaluation and Research,
Food and Drug Administration,
Rockville, Maryland, U.S.A.

I. INTRODUCTION

The U.S. Food and Drug Administration (FDA) regulates a certain number of foods, drugs, and medical devices that have been approved for sterilization by irradiation. For vaccines and other biological products regulated by the Center for Biologics Evaluation and Research of the FDA radiation sterilization has been approved for dispettes (plastic containers) and diluent for vaccines. The approval in both cases is for sterilization using cobalt-60 gamma radiation. Various studies treating the effects of radiation sterilization on biological products have been reported in the literature. Nedugova et al. [1] listed the sterilizing effect of gamma radiation at doses of 20 kGy for liquid preparations and 30 kGy for solid preparations of cholera exotoxin. Terminal sterilization and viral

*This chapter was done in the author's professional capacity but does not necessarily express the opinion of the U.S. Food and Drug Administration.

Copyright 2004 by Marcel Dekker, Inc. All Rights Reserved.

inactivation of blood products have been described by Reid [2]. Bazhanova et al. [3] reported the effects of radiation sterilization on the immunobiological properties of the sorbed protective fraction of *Bordetella pertussis*.

This work reports radiation sterilization dosing levels and their effect on potency for certain vaccines regulated by the FDA. Products were studied varying radiation type, radiation dose, and sample temperature during irradiation. The vaccines have been studied using gamma rays, electron beams, and x-rays with variations in irradiation temperature from room temperature to liquid nitrogen temperature. Radiation dose, typically at the 25 kGy level, was delivered in seconds (electron beam), or hours (X-rays and gamma rays). Molecular sizing potency results and/or IgG and IgM antibody response in mice, ELISA test results, have been determined for Pneumococcal Polysaccharide Type 6B powder, Typhoid Vi Polysaccharide Vaccine, a freeze-dried Haemophilus b Conjugate Vaccine (Tetanus Toxoid Conjugate), the acellular pertussis component of Diphtheria and Tetanus Toxoids and Pertussis Vaccine, Adsorbed (DTaP Vaccine), Polyvalent Pneumococcal Polysaccharide Vaccine, and 7-Valet Pneumococcal Polysaccharide Vaccine.

II. MEASUREMENTS

A. Irradiation

Irradiation of the samples was carried out at a number of facilities:

1. Gamma rays from cobalt-60 were used in the CEA Cadarache, France and also at Studer AG Werk Hard in Daniken, Switzerland.
2. Electron beam using the Rhodotron was performed at Studer AG Werk Hard in Daniken, Switzerland.
3. X-ray irradiation was carried out at RDI IBA (Edgewood, Long Island, New York U.S.A.) and in the laboratory of Louis Rey in Aix-les-Bains, France.
4. Dosimetry [4] was determined using HARWELL (Red and Amber) and Far West technology dosimeters.

B. Molecular Sizing and Potency Assays

Molecular sizing and mouse IgG and IgM antibody response ELISA potency assays were performed at the Center for Biologics Evaluation and Research of the FDA.

Copyright 2004 by Marcel Dekker, Inc. All Rights Reserved.

C. Vaccines Studied

1. Pneumococcal Polysaccharide Type 6B (powder) and Typhoid Vi Polysaccharide Vaccine (liquid)

Table 1 [5] lists the molecular sizing results for samples of a Pneumococcal Polysaccharide Type 6B and Typhoid Vi Polysaccharide Vaccine that had been irradiated (25 kGy) using gamma rays, electron beam, and, in addition, unirradiated control samples. The values for the Kd increased for both irradiated products. This indicated that the molecular size of both products decreased under the chosen irradiation conditions. The Kds for the electron beam irradiated samples of both types of products studied still met their respective product specifications. These results are also examples of gamma irradiation administered in hours and electron beam irradiation administered in seconds at the same 25 kGy dose level having different effects on the samples in that the electron beam caused less of a decrease in molecular size of both samples than the gamma irradiation caused.

2. Freeze-Dried Haemophilus B Conjugate Vaccine (Tetanus Toxoid Conjugate)

The results for the molecular sizing [6–8] for samples of lot A of Haemophilus b Conjugate Vaccine [9] that had been irradiated (25 kGy) using gamma, electron beam, and x-ray sources are listed in Table 2 [5]. Haemophilus B Conjugate Vaccine is an active immunizing agent used to prevent infection by Haemophilus influenza type b (Hib) bacteria which can cause life threatening diseases such as meningitis, epiglottitis, pneumonia, and pericarditis. Irradiation increased the value of the Kd, and, therefore, decreased the molecular size of the polysaccharide. The IgG and IgM ELISA antibody responses [10] for the gamma-irradiated samples, sample

Table 1 Molecular Size Determinations of Irradiated (25 kGy) and Control Pneumococcal Polysaccharides Type 6B and Typhoid Vi Polysaccharide Vaccine

	Molecular sizing (Kd, sepharose CL-4B)	
Radiation type	Pneumococcal Polysaccharide Type 6B (Powder)	Typhoid Vi Polysaccharide Vaccine (Liquid)
Control (no irradiation)	0.02	0.08
Electron beam	0.17	0.23 (in LN_2)
Gamma ray irradiated	0.30	0.76

Copyright 2004 by Marcel Dekker, Inc. All Rights Reserved.

Table 2 Molecular Size Determinations of Irradiated (25 kGy) and Control Samples of Lot A of Haemophilus Influenzae Type b Conjugate Vaccine (Tetanus Toxoid Conjugate)

Irradiation	Molecular sizing for Hib Conjugate Vaccine (freeze-dried) (Kd, Sepharose CL-4B)
Control (no irradiation)	0.24
Electron beam (25 kGy)	0.82
Gamma ray (25 kGy)	0.76
X-ray (25 kGy)	0.83

Table 3 IgG Antibody Response (ELISA OD at 405 nm; 45 min at 25°C) of Gamma Irradiated and Nonirradiation Samples of Lot A of Freeze-dried Haemophilus b Conjugate Vaccine (Tetanus Toxoid Conjugate) and Saline Diluent

	IgG antibody response (ELISA OD unit)			
	Hib Conjugate Vaccine Lot A[a] (freeze-dried)	Hib Conjugate Vaccine Lot A[a] (freeze-dried)	Hib Conjugate Vaccine Lot A[a] control (freeze-dried)	Saline diluent (liquid)
As dilution	25 kGy in LN_2	25 kGy at 0°C	Nonirradiated	Control
1/100	1.08 ± 0.06	0.74 ± 0.25	0.84 ± 0.19	0.28 ± 0.06
1/300	0.80 ± 0.18	0.90 ± 0.16	0.70 ± 0.11	0.32 ± 0.02
1/500	0.37 ± 0.03	0.33 ± 0.06	0.38 ± 0.02	0.32 ± 0.02

[a]Mean and standard deviation of four samples.

control, and saline control are listed in Table 3 [5] and Table 4 [5], respectively. These data indicate that both the IgG and IgM antibody responses were not significantly changed in the irradiated vaccine compared to the vaccine control even though the irradiation has altered the molecular size of the irradiated vaccine.

3. Acellular Pertussis Component of Diphtheria and Tetanus Toxoids and Pertussis Vaccine Adsorbed (Liquid)

Two types of DTaP Vaccine [11,12] have been irradiated with gamma (cobalt-60) radiation at room temperature and X-ray radiation doses at

Copyright 2004 by Marcel Dekker, Inc. All Rights Reserved.

Table 4 IgM Antibody Response (ELISA OD at 405 nm; 45 min at 25°C) of Gamma Irradiated (at Two Temperatures) and Nonirradiation Samples of Lot A of Haemophilus influenza Type b Conjugate Vaccine (Tetanus Toxoid Conjugate) and Saline Diluent

	IgM antibody response (ELISA OD unit)			
	Hib Conjugate Vaccine Lot A[a] (freeze-dried)	Hib Conjugate Vaccine Lot A[a] (freeze-dried)	Hib Conjugate Vaccine Lot A control[a] (freeze-dried)	Saline diluent[a] (liquid)
As dilution	25 kGy in LN_2	25 kGy at 0°C	Nonirradiated	Control
1/100	0.93 ± 0.06	0.75 ± 0.25	0.49 ± 0.19	0.24 ± 0.06
1/300	0.75 ± 0.18	0.87 ± 0.16	0.66 ± 0.11	0.30 ± 0.02
1/500	0.42 ± 0.03	0.52 ± 0.06	0.48 ± 0.02	0.34 ± 0.02

[a]Mean and standard deviation of four samples.

liquid nitrogen temperature. Two DTaP Vaccines have been licensed for use in the U.S.A. Both vaccines have been shown in clinical trials to be safe and effective, but are slightly different formulations. Due to adverse effects associated with whole-cell pertussis vaccine, acellular pertussis vaccines have been developed. Acellular pertussis vaccines contain inactivated pertussis toxin (PT) and may contain one or more other bacterial components, e.g., filamentous hemagglutinin (FHA), a 69-kilodalton outer-membrane protein, pertactin (PRN), and fimbriae types 2 and 3 (FIM). The potency of the acellular pertussis vaccine components of the first type of DTaP Vaccine represented by Lots A and C in this study is evaluated by the antibody response of immunized mice to (PT) and (FHA) measured by enzyme-linked immunosorbent assay (ELISA). The potency of the acellular pertussis vaccine component of the second DTaP Vaccine, represented by Lot B, is evaluated by the antibody response of immunized mice to PT, FHA, PRN, and FIM measured by ELISA.

Samples and control materials were from lots of vaccines licensed in the U.S.A. by the FDA.

For Lots A and C the acellular pertussis components are purified from *B. pertussis* by salt precipitation, ultracentrifugation, and ultrafiltration. After purification, fractions containing PT and FHA are combined to obtain a 1:1 ratio and are treated with formaldehyde to inactivate PT. Each dose of vaccine contains approximately 23.4 μg of protein of inactivated PT (toxoid) and 23.4 μg of protein of FHA, as well as 6.7 limit of flocculation

Copyright 2004 by Marcel Dekker, Inc. All Rights Reserved.

units (Lf) of diphtheria toxoid and 5.0 Lf of tetanus toxoid. The combined components are adsorbed using aluminum potassium sulfate. On July 31, 1996 the FDA licensed this vaccine for use as the initial four doses of the recommended diphtheria, tetanus, and pertussis vaccination series among children aged 6 weeks to 6 years.

For Lot B the acellular pertussis vaccine components are produced from *B. pertussis* cultures grown in Stainer–Scholte medium modified by the addition of casamino acids and dimethyl-betacyclodextrin. Fimbriae types 2 and 3 are extracted from the bacterial cells and the pertussis toxin, FHA, and PRN are prepared from the supernatant. These proteins are purified by sequential filtration, salt precipitation, ultrafiltration, and chromatography. Pertussis toxin is inactivated with glutaraldehyde and FHA is treated with formaldehyde. The individual antigens are adsorbed separately onto aluminum phosphate. Diphtheria and tetanus, toxoids are individually adsorbed onto aluminum phosphate. The adsorbed diphtheria, tetanus, and acellular pertussis components are combined in a sterile isotonic sodium chloride solution containing 2-phenoxyethanol as preservative. Each dose contains 10 μg of PT, 5 μg of FHA, 3 μg of PRN, 5 μg of FIM, as well as 15 Lf of diphtheria toxoid and 5.0 Lf of tetanus toxoid.

Cobalt-60 gamma irradiation was performed at Studer AG Werk Hard in Daniken, Switzerland (Lot A). X-ray irradiations were performed at the laboratory of Professor Louis Rey in Lausanne, Switzerland (Lot A) and IBA, Edgewood, New York, U.S.A. (Lot B and Lot C).

Acellular pertussis antibody response ELISA assays [13] were run in the study of the acellular pertussis vaccine component of the Diphtheria and Tetanus Toxoids and acellular Pertussis Vaccine Adsorbed (DTaP) to assess vaccine potency before and after irradiation of DTaP Vaccine Lots A, B, and C.

Table 5 [14] lists the acellular pertussis vaccine antibody response in mice for samples of Lot A of the DTaP Vaccine characterized by PT and FHA, sample control, and reference vaccine that had been irradiated (25 kGy) using gamma, and X-ray sources. These data indicate that the irradiated vaccine gave equal or better antibody response compared to the vaccine controls for the X-ray irradiated samples held at liquid nitrogen temperature during irradiation.

Similarly, Table 6 [14] lists the antibody response for the x-ray irradiated samples and unirradiated sample controls for both types of DTaP Vaccine. These data also indicate that the X-ray irradiated vaccine with the vaccine at liquid nitrogen temperature gave equal or better acellular pertussis vaccine antibody response results compared to the vaccine controls.

Copyright 2004 by Marcel Dekker, Inc. All Rights Reserved.

Table 5 Acellular Pertussis Vaccine Antibody Response (ELISA OD at 405 nm; 45 min at 25°C) of Gamma Irradiated and Nonirradiated Samples of Lot A of Diphtheria and Tetanus Toxoids and Pertussis (DTaP) Vaccine, Adsorbed Liquid

	Antibody response (ELISA OD unit)			
	DTaP Vaccine Lot A[a] (liquid)	DTaP Vaccine Lot A[a] (liquid)	DTaP Vaccine Lot A control[a](liquid)	Reference vaccine[a] (liquid)
	X-ray, 25 kGy in LN_2	Gamma ray, 25 kGy	Nonirradiated	Nonirradiated
FHA	1315	445	907	691
PT	500	505	206	228

[a]Geometric mean.

Table 6 Acellular Pertussis Vaccine Antibody Response (ELISA) of X-ray Irradiated (at Liquid Nitrogen Temperatures and Two Dose Levels) and Nonirradiated Samples of Lot B and Lot C of Diphtheria and Tetanus Toxoids and Acellular Pertussis Vaccine, Adsorbed

	Acellular Pertussis Vaccine antibody response (ELISA OD unit)			
	DTaP Vaccine Lot B[a] (liquid)	DTaP Vaccine Lot B control[a] (liquid)	DTaP Vaccine Lot C[a] (liquid)	DTaP Vaccine Lot C control[a] (liquid)
	X-ray, 25 kGy in LN_2	Nonirradiated	X-ray, 12 kGy in LN_2	Nonirradiated
FHA	3042	2489	944	1153
PT	595	613	303	295
PRN	180	172	—	—
FIM	798	827	—	—

[a]Geometric mean.

Both types of DTaP Vaccine X-ray irradiated in liquid nitrogen had antibody responses for all of the characterized acellular pertussis vaccine components not significantly different from or greater than the unirradiated controls.

Copyright 2004 by Marcel Dekker, Inc. All Rights Reserved.

Table 7 Mouse IgG and IgM Antibody Response (OD Unit of ELISA) of Four Types of Pneumococcal Polysaccharides Present in X-ray Irradiated Polyvalent Pneumococcal Polysaccharide Vaccine Lot A (Liquid) and of Corresponding Nonirradiation Controls of the Same Polysaccharide Type in Lot A

	Type 9V (liquid)	Type 14 (liquid)	Type 18C (liquid)	Type 19F (liquid)
	IgG antibody response (ELISA OD unit)			
X-ray, 24 kGy, room temp.	0.36 ± 0.02	0.32 ± 0.02	0.33 ± 0.01	0.32 ± 0.01
X-ray, 13 kGy, LN_2	0.37 ± 0.01	0.31 ± 0.01	0.38 ± 0.03	0.34 ± 0.02
Nonirradiated control	0.37 ± 0.01	0.32 ± 0.02	0.49 ± 0.12	0.34 ± 0.02
	IgM antibody response (ELISA OD unit)			
X-ray, 24 kGy, room temp.	0.18 ± 0.01	0.27 ± 0.02	0.23 ± 0.01	0.28 ± 0.02
X-ray, 13 kGy, LN_2	0.18 ± 0.01	0.24 ± 0.02	0.22 ± 0.01	0.31 ± 0.02
Nonirradiated control	0.20 ± 0.02	0.23 ± 0.02	0.25 ± 0.01	0.30 ± 0.03

[a]Geometric mean.

4. Polyvalent Pneumococcal Polysaccharide Vaccine (Liquid)

This vaccine is protective against invasive pneumococcal infections in immunocompetent adults [15]. Table 7 [14] lists the mouse IgG and IgM antibody response of four types of pneumococcal polysaccharide present in X-ray irradiated Polyvalent Pneumococcal Polysaccharide Vaccine Lot A and in a corresponding non-irradiated controls of the same polysaccharide type in Lot A. The type 9V, 14, 18C, and 19F polysaccharide samples were irradiated with X-rays at 24 kGy at room temperature and with X-rays at 13 kGy at liquid nitrogen temperature. In each case for both the IgG and IgM mouse antibody responses there appeared to be no significant difference between the irradiated samples and the controls.

5. 7-Valent Pneumococcal Conjugate Vaccine (Liquid)

This vaccine is indicated for immunization of infants and toddlers against disease caused by *Streptococcus pneumoniae* due to capsular serotypes included in the vaccine (4, 6B, 9V, 14, 18C, 19F, and 23F). *S. pneumoniae* causes invasive infections such as bacteremia, meningitis, pneumonia, and upper respiratory infections including otitis media and sinusitis [16]. Table 8 [14] lists the IgG and IgM mouse antibody responses for types 9V, 14, 18C,

Copyright 2004 by Marcel Dekker, Inc. All Rights Reserved.

Table 8 Mouse IgG and IgM Antibody Response (OD Unit of ELISA) of Four Types of Pneumococcal Conjugates Present in X-ray Irradiated 7-Valent Pneumococcal Conjugate Vaccine Lot A (Liquid) and of Corresponding Nonirradiated Controls of the Same Polysaccharide Type in Lot A

	Type 9V (liquid)	Type 14 (liquid)	Type 18C (liquid)	Type 19F (liquid)
	IgG antibody response (ELISA OD unit)[a]			
X-ray, 8 kGy, LN_2	0.61 ± 0.07	0.73 ± 0.08[c]	0.46 ± 0.02[b]	0.56 ± 0.04[c]
X-ray, 11 kGy, room temp.	0.56 ± 0.01	0.69 ± 0.07[c]	0.58 ± 0.07	0.48 ± 0.04[c]
Nonirradiated Control	0.63 ± 0.01	1.17 ± 0.04	0.51 ± 0.02	0.86 ± 0.08
	IgM antibody response (ELISA OD unit)			
X-ray, 8 kGy, LN_2	0.30 ± 0.02[c]	0.35 ± 0.04[c]	0.53 ± 0.04	0.59 ± 0.03
X-ray, 11 kGy, room temp.	$0.30 + 0.03$[c]	0.22 ± 0.01[c]	0.40 ± 0.06	0.51 ± 0.021
Nonirradiated Control	0.52 ± 0.05	0.72 ± 0.09	0.52 ± 0.04	0.57 ± 0.04

[a] mean $\pm$ standard deviation.
[b] $P < 0.05$.
[c] $P < 0.01$ when antibody response of treated group was compared with nontreated controls.

and 19F of pneumococcal conjugates and corresponding non-irradiated controls. Statistical treatment of the data shows significant lower responses for the irradiated samples compared to the non-irradiated controls for types 14, 18C, and 19F for the IgG antibody response and types 9V and 14 for the IgM antibody response. For the conjugate types that tolerated the irradiation, 9V for the IgG antibody response and 18C and 19F for the IgM antibody response, the values for the X-rays at the 8 kGy dose with the samples at liquid nitrogen temperature during irradiation were consistently closer to the unirradiated controls than the samples irradiated at 11 kGy at room temperature.

II. FUTURE DEVELOPMENTS

Potency tests for the polysaccharide vaccines and the acellular pertussis component of the DTaP Vaccine tolerated the irradiation doses. Molecular sizing experiments indicated some size change for the polysaccharides studied. Further studies are required to determine the specific doses at which sterility is achieved, as well as to determine that the therapeutic effect of the

Copyright 2004 by Marcel Dekker, Inc. All Rights Reserved.

product has not been compromised at the doses necessary to achieve product sterility, and to determine that no deleterious radiolysis products have been formed in the vaccine during the irradiation process.

REFERENCES

1. GI Nedugova, IV Rubtsov, II Samoilenko. Effect of gamma radiation on the immunobiological and immunochemical properties of cholera exotoxin. I. Change in the biological activity of non purified cholera exotoxin as affected by ionizing radiation. Zh Mikrobiol Epidemiol Immunobiol 2:47–51, 1984.
2. BD Reid. The Sterways process: a new approach to inactivating viruses using gamma radiation. Biologicals 26:125–129, 1998.
3. IG Bazhanova, NV Tsevetkova, VF Bulk, GM Mashilova, ES Lazareva. Effect of radiation sterilization on the immunobiological properties of the sorbed protective fraction of Bordetella pertussis. Zh Mikrobiol Immunobiol 3:78–82, 1986.
4. WL McLaughlin, AW Boyd, KH Chadwick, JC McDonald, A Miller. Dosimetry for Radiation Processing. New York: Taylor & Francis, 1989.
5. JC May, L Rey, CJ Lee. Evaluation of some selected vaccines and other biological products irradiated by gamma rays, electron beams, and x-rays. Radiat Phys Chem 63:709–711, 2002.
6. Bureau of Biologics. Molecular sizing of capsular polysaccharide antigens by Sepharose 4B column chromatography. BOB SOP pp 1–5. Food and Drug Administration, 1977.
7. JJ Plumb, SE Yost. Molecular size characterization of Haemophilus influenzae type b polysaccharide-protein conjugates vaccines. Vaccine 14:399–404, 1996.
8. KH Wong et al. Standardization and control of meningococcal vaccines, group A and group C polysaccharides. J Biol Stand 8:197–214, 1977.
9. R Booy et al. Efficacy of Haemophilus influenzae type b conjugate vaccine PRP-T. Lancet 344:362–366, 1994.
10. CS Lu, CJ Lee, P Kind. Immune responses of young mice to pneumococcal type 9V polysaccharide-tetanus toxoid conjugate. Infect Immun 62:2754–2760, 1994.
11. L Gustafsson et al. A controlled trial of a two-component acellular, a five-component acellular, and a whole-cell pertussis vaccine. New Eng J Med 6:349–355, 1996.
12. Centers for Disease Control and Prevention (CDC). Pertussis-United States, 1997–2000. MMWR, 51(4):1–92, 2002.
13. WHO TRS, No. 878, 1998, Annex 2, pp 57–76.
14. JC May, L Rey, CJ Lee, J Arciniega. Evaluation of pneumococcal conjugate and polyvalent vaccines and other biological products irradiated by x-rays and gamma rays. Radiat Phys Chem. In press.

Copyright 2004 by Marcel Dekker, Inc. All Rights Reserved.

15. ED Shapiro, AT Berg, R Austrian, D Schroeder, V Parcells, A Marglis, RK Adair, JD Clemens. The protective efficacy of polyvalent pneumococcal polysaccharide vaccine. New Eng J Med 325:1453–1460, 1991.
16. S Black et al. Efficacy, safety, and immunogenicity of heptavalent pneumococcal conjugate vaccine in children. Pediatr Infect Dis J 19:187–195, 2000.

Copyright 2004 by Marcel Dekker, Inc. All Rights Reserved.

22

Some Leading Edge Prospects in Lyophilization*

Louis Rey
Cabinet d'Études, Lausanne, Switzerland

As is the general case in science, lyophilization has been propelled in the last decades by a push–pull phenomenon between products and technology. New products fulfill new needs, open new markets, but, in turn, request new developments in process and industrialization. Sometimes they are purely genuine, sometimes they are just a consequence of the spin-off of other technologies. This is the reason why I shall switch from basic science to engineering and from technology to consumer acceptance without following a strict rationality.

I. BIOLOGICAL PRODUCTS AND PHARMACEUTICALS

A. Some Basic Issues

For a very long time, freeze-drying has been essentially concerned with the preservation of unstable biochemicals and, more particularly, of injectables. The very first issue was, then, to secure their sterility and safeguard their potency during processing, storage, and reconstitution. At the outset most products were freeze-dried as such, either as a natural substance, such are blood plasma, biosynthetic isolates, or antibiotics, or, else, for vaccines,

*This paper was the basis of a keynote address delivered in Amsterdam at a conference sponsored by the International Society for Lyophilization-Freeze-Drying Inc. LR Rey. Some leading edge prospects in lyophilization. Amer. Pharma. Rev., 6:32–44, 2003.

Copyright 2004 by Marcel Dekker, Inc. All Rights Reserved.

as controlled concentrates of inactivated and/or living cells resulting from selected culture fermentation broths.

Often the product was bulky and resistant (like blood plasma) and could be processed directly. However, as more and more new advances were made, many products became difficult to treat and required the incorporation of a whole set of additives: cryoprotectors, free-radical scavengers, stabilizers, and so on. Today, and with the rocketing development of biotechnology, more and more potent and fragile compounds are produced and, most often, their activity is such that they represent only a few milligrams in the basic formulation. There is, thus, an obvious need to incorporate the active substance into a solid matrix which will prevent it flying away during drying and keep it secluded in a confined stable environment during storage. This means that, on top of the already quoted cryoprotectors, stabilizers, and the like, different bulking agents have to be added like sucrose, mannitol, lactose, etc., the behavior of which might have a major impact on the properties of the active substance. This is particularly true for proteins where a given steric configuration should be preserved during the whole process and withstand the stress of freezing and drying. Carpenter, Pikal, and others have shown that developing a glassy matrix during freezing could substantially reduce the osmotic and mechanical strains on the molecules. This, unfortunately, might also be contrary to the requirements of the drying process itself which is easier to carry from a non-amorphous state. Thus, it might be necessary to mitigate between the conventional freezing and what we called in 1960 a "thermal treatment," most often referred to, today, as an annealing process: double freezing with intermediate rewarming.

Depending upon the products, there might be very narrow margins to that exercise and the endpoint temperatures, velocities of cooling, and rewarming need to be known very accurately by previous laboratory determinations such as differential thermal analysis (DTA) or differential scanning calorimetry (DSC), low temperature electric impedance measurements, velocity of crystallization in the supercooled state, etc.

Moreover, in this context of highly diluted active substances of powerful potency (like for instance Botulinum toxine) there might be a strong interference between the product and the container–closure system. Glass manufacturers like Schott in Germany have pioneered this field showing that a Type I tubing vial might interact with the solution prior to freezing, and this often in an irreversible way. For instance, it might adsorb more than 50% of an active protein (tests have been made with a nicotinic acetylcholine receptor) and equally leach substantial amounts of undesirable glass components (sodium, calcium, boron, aluminum, etc.) into the solution which may also dissolve the inner surface of the container.

Copyright 2004 by Marcel Dekker, Inc. All Rights Reserved.

To obviate these problems, Schott developed the Type I Plus vials in which, thanks to a special high-temperature plasma process (PIVD: Plasma Impulse Chemical Vapor Deposition) a very thin coating (100–200 nm) of pure silica is deposited and strongly bonded to the glass surface (something like a quartz glazing of the inner wall of the vial) which then becomes totally neutral. Much interest is given today to this new process, at a time when regulating agencies, and especially the FDA, are deeply concerned with the effect on the brain and liver of aluminum released from glass in very young infant vaccines. Silica coating affords, then, an excellent protection, still better than some new cyclo olefin polymers (such as Topas 6013) which could also be used to manufacture the entire vial (Schott TopPac^{TM}).

What is true for the container in the "container–closure system" is equally true for the closure alone and, essentially, for the elastomeric stoppers, generally butyl rubber, which cap the vial. Fran DeGrazio from West Pharmaceutical Services has done a lot of research in this field and studied many alternatives to their formulation trying to keep down the extractables (essentially volatile) and leachables and prevent adsorption of oils, waxes, polymers, and others on the freeze-dried plug.

Another critical issue, in the same field, is the determination of the optimum residual moisture, understanding that it could result from the drying process itself obviously, but also from release by the stoppers of water picked up during the sterilization process. Fran DeGrazio, Maninder Hora, and others did show that this phenomenon definitely influences the storage ability of the freeze-dried products which also depends, among other issues, on the quality of the fit between the vial and the stopper which, in turn, depends on how tight the manufacturers can guarantee the dimensional tolerance of their products.

Water is, indeed, a recurrent and unavoidable issue in the whole lyophilization process. Formally regulated by the different responsible agencies, the residual moisture is, indeed, a floating, nebulous concept which is quite difficult to grasp with exactitude. Joan May from the FDA, who has been a leading authority in the field for so many years, knows quite well that neither Karl Fischer titration, thermogravimetry, nor equilibrium water vapor pressure determination could produce the right answer. Moreover, since the first two techniques are destructive, they prevent any follow-up of the "fate" of the water in the product—with time. They titrate the "total water," as a chemical, without discriminating between the part which is free to move and exchange between the stopper and the cake and the one, bound to the cake, which is often essential to maintain, within the freeze-dried active substance, the tridimensional structure, which is at the root of its potency. The equilibrium water vapor pressure that we have introduced (see Ch. 1, p. 24) solves the follow-up issue since it is a non-intrusive,

Copyright 2004 by Marcel Dekker, Inc. All Rights Reserved.

non-destructive technique, but it gives an "indirect" reading of the water content. Finally, we know that, in the dry product itself and without any interference from the container–closure system, there are movements of water with time and, that, during storage, the ratio between "free" and the different types of "bound" water changes and might impact the final potency.

These are only limited glimpses of the basic issues that any professional has to challenge when performing freeze-drying of biological products and pharmaceuticals.

B. A Few New Original Technologies

Since it would be impossible to deal with all these fundamental problems, let us have a general look at several interesting breakthroughs which could be applied to the lyophilization of biological products and pharmaceuticals.

1. Inert Carriers

The first idea is, when dealing with a highly diluted active substance, to try and get rid of the bulking agent. One possibility is to enclose the liquid to be dried into a porous matrix where it will be kept, in the course of drying, and thus prevented from flying away with the water vapor stream. Porous polymers, sintered metals, ceramics, porous glass (such as Vycor), inorganic textiles, multilamellar pads, etc., could, at first glance, carry a solution provided they simultaneously demonstrate a certain number of properties:

- They can adsorb the liquid solution as easily as a hydrophilic material and withstand freezing and drying without mechanical rupture.
- They do not interact with any element of the formulation.
- They are clean and deprived of residues, particles, or contaminants.
- They hold enough liquid per unit volume, which means that they present, at least, 30 to 50% porosity.
- They can be shaped as well-defined geometrical units (e.g., disks, rods, spheres) to be incorporated into the vial.
- Their pore structure is thin enough to hold the solution but wide enough to let the water vapor escape from the frozen liquid, which means an open-pore structure, a "sponge" with interconnecting interstitial channels.
- They release the active enclosed, adsorbed product when they are flooded with the reconstitution fluid.

In our own experience, fulfilling these requirements is not an easy task and, actually, very few products are capable of providing this complete set of properties. Whilst most of the structural issues can be solved, the most

Copyright 2004 by Marcel Dekker, Inc. All Rights Reserved.

difficult, by far, remains the latter one: the ''carrier'' should release the totality or at least a major known amount of the active substance at the time of reconstitution. To that end, developments have been made to ''exhaust'' the carrier by percolating the dissolution fluid through it under pressure, as would be done with a conventional on-line filter. Special syringes have been manufactured where the original solution to be dried is pumped through the carrier, then allowed to dry there, and finally extracted by the reconstitution fluid using the same type of mechanism.

Today, the inert carrier issue is still under development and it is more than likely that the enormous amount of research which is currently devoted to new materials, whether glass and glass derivatives, polymers, fibers, etc., will generate some challenging contributions in this area.

Before closing this particular topic, I believe that it is useful to recall that for some dermatological and surgical uses, and also in the vast field of cosmetics, freeze-dried carriers have been in use for several years. Generally, they consist of natural products like collagen, agar–agar, vegetal extracts which are doped with very small amounts of active substances, freeze-dried, and used as dressings on burns, scars, bleeding areas, or as beauty masks for the face and/or eyelids. Depending upon their formulation, they can either be stripped off after release of the active compound or else remain in situ where they dissolve away in a rather short time in the case of dressings or are easily washed out of the beauty masks.

Whilst carrier technology appears as rather specific to the pharmaceutical and cosmetic industries, the next developments that I would like to present are, actually, the results of technology transfer from the food industry, namely, soft ice, continuous freeze-drying, and radiation treatment.

2. Soft-Ice

Everybody is familiar with the concept of sherbets and soft ice-creams. They are basically frozen plastic pastes which present a high viscosity at relatively moderate negative temperatures. They are not free-flowing but can be stirred, mixed under moderate mechanical strength, and can incorporate solid particles like chocolate crumbs, fruit, nuts, and so on without losing their structure. Their rheological properties are rather complex and highly dependent on temperature. They are most generally commercialized as such but might also be the first step of a more elaborate process. For instance, in the freeze-drying of coffee, we start with the production of a viscous concentrated coffee extract which is turned into a plastic icy foam by injection of carbon dioxide under pressure in a rotative, scraped surface heat exchanger. There, the liquid is converted into

Copyright 2004 by Marcel Dekker, Inc. All Rights Reserved.

a sherbet-like foamy paste which is spread over a metallic belt conveyor and frozen hard in a cold room. Then, it is broken, ground and/or sliced, sifted, and finally fed into the freeze-drying plant.

In the preparation of many pharmaceuticals we know that some components in the formulation are not compatible. For instance, if we mix acetyl salicylic acid with sodium bicarbonate in solution, there is an immediate reaction and a vigorous release of carbon dioxide. Nevertheless, it might be of interest to freeze-dry them together in order to have instant sparkling aspirin, but this is not possible and the only way around this is to compact the products together in the dry state. The resulting tablet is not very stable and it takes a relatively long time to get back into solution.

Conversely, if such reactive substances are mixed together at low temperature after incorporation in a soft ice, they will not react and the resulting paste can be molded in appropriate shapes and hardened by further cooling. The material can then be freeze-dried without difficulty. In that state, lyophilized aspirin, for instance, is perfectly stable and, when water is added back, it reconstitutes as a sparkling fluid in a few seconds because of its high porosity.

The "soft ice" technology is thus a very precious tool for preparing complex products, most often for oral route. Pure chemicals, drugs, vitamins, and mineral salts can be successfully freeze-dried in that way in rather elaborate formulations since it is possible to mix together "sherbets-lines" issued from different solutions and even add to the whole other solid ingredients as finely dispersed powders. The key to success in that process is a good control of the temperature of the icy paste which is generally prepared in a cylindrical double-wall heat exchanger with a continuous scraped surface maintained at temperatures between $-4^{\circ}C$ and $-20^{\circ}C$ depending on the nature of the treated products. When the soft ice mixture is duly completed it can be molded by conventional equipment in plastic blisters and frozen hard in a blast tunnel. Then this material can enter the freeze-dryer. It is altogether a rather simple on-line galenic process.

3. Continuous Freeze-Drying

Any chemical engineer dreams of a continuous process because it is easy to control and gives manufactured products a standard equal quality. Freeze-drying has not escaped this trend and, as early as the 1960s, semi-continuous and continuous equipment has been designed and built for the food industry. Leybold was among the very first to do it and G. W. Oetjen developed the CQC process into an industrial reality for milk products. The operation was, indeed, sequenced into several phases. The frozen products,

Copyright 2004 by Marcel Dekker, Inc. All Rights Reserved.

most often in granular form, were loaded on trays placed on a special carrier, and hung on a monorail which traveled all along the freeze-drying tunnel between heating plates in successive steps through vacuum locks closed by sliding gates. From the entrance lock to the outlet the total cycle time was on the order of several hours.

An alternative to this system was introduced by Atlas, which pioneered the so-called ''Conrad'' System in which the loading of the frozen goods was done tray by tray through a small side lock. Coffee, milk, but also vegetables, fish fillets, and meat have been successfully treated in this way, essentially by radiant heat.

Quite obviously this technology worked, but it was still a semi-continuous process and the food industry was eager to develop a fully automated continuous operation for one of its leading products on the international market: instant coffee. I had the opportunity to participate in this development very closely and I can tell you that it was very difficult because most steps of the instant coffee processing had to be revised. As a mere example, extraction needed to be completely revisited because the extract being dried at low temperature did not ''benefit,'' if we can say so, from the ''positive effects'' of the high temperature found in conventional spay-dryers which stripped off what were called the negative aromas. Freezing of the concentrated extract proved equally touchy since density, color, and brittleness of the frozen foams had to be made just right. Grinding happened to be one of the most delicate issues because a regular granule size had to be reached without releasing a large amount of fines which would have to be sifted away and recycled. Finally, sublimation and desorption in the tunnel were additional critical steps as during primary drying any interstitial melting could alter the color of the final product and also in the course of desorption overdrying could result in a substantial loss of volatile aromas. Finally, from a purely engineering standpoint, drying several tonnes of frozen coffee extracts per day on a continuous basis required a completely new design of the equipment.

Thus, it is not surprising that it was only in the mid 1960s that a fully continuous line was introduced. In one of the most advanced designs granulated frozen extract is fed continuously into the dryer through a rotating lock and deposited on a 20 to 30 m long vibrating tray on which it travels as a fluidized bed. It moves, indeed, on its own water vapor cushion all along the heated surface, which provides the energy for sublimation. During that long transport, the granules are guided by vertical ribs into parallel channels and great care is taken to prevent attrition from mechanical chocks between the granules themselves and with the surface and walls of the tray. Though limited, attrition nevertheless does occur and generates a lot of ''dust'' which has to be stopped by a long semi-cylindrical

Copyright 2004 by Marcel Dekker, Inc. All Rights Reserved.

screen deployed all over the vibrating tray. In that way, the fines are not carried away with the vapor stream toward the condenser and the pumps.

Under these circumstances, it can be easily appreciated that a continuous freeze-drying plant is a highly sophisticated piece of equipment which most often is designed and put together by the food industry itself, which keeps the whole development strictly confidential and assembles different components purchased from multiple unconnected manufacturers.

The efficiency of a vibrating tray freeze-dryer is enormous and the drying times drop by more than an order of magnitude. We are speaking in terms of minutes instead of hours and throughputs of tens of tonnes per day are no longer unrealistic. Moreover, the process is ''intellectually clean'' and the end product constant in quality.

This is the reason why, for a very long time, I have been dreaming about introducing that technology to the processing of biologicals and pharmaceuticals. Indeed, despite the elaborate design proposed by equipment manufacturers and the care that the drug companies take in their freeze-drying operations we are still facing the recurrent problem of potential heterogeneity between vials and ampoules within the same single batch. The spatial distribution of 10,000 to 100,000 vials in a multishelf freeze-drying cabinet remains a problem. Some sit close to the door, some right in the middle, others near the condenser, some in the upper shelves, others lower down, and, to be serious, they do not dry in the same way. I know that drug manufacturers claim that all the products they release are within very strict standards and I know, also, that the regulatory agencies keep a close eye on this issue and are more and more stringent on the validation tests. Nevertheless, the homogeneity of a single batch is still a matter of deep concern. Can we solve that problem? I believe so.

A very simple idea is to switch to a semi-continuous or continuous process as is done in the food industry. Let us forget about the holy paradigm that a vial which has been initially loaded with a given volume of solution has to remain so until it is capped with its freeze-dried cake inside and placed in a commercial box. Let us try to consider instead a process in which the initial solution is distributed as individual droplets frozen into spherical granules of given geometry, continuously fed into a vacuum chamber, and spread on a heated conveyor. On that tray, most probably a vibrating tray, they glide self-suspended on their water vapor cushion as a thin, regular, fluidized cloud at a well-controlled operating pressure fit for sublimation, say a hundred microbar. At the end of the tray they reach a transfer lock which discharges them onto another conveyor placed in a second chamber fit for desorption and secondary drying at pressures of some tens of microbars. Finally, they enter an ultimate lock and are discharged into a receiving bin under dry neutral atmosphere. The efficiency

Copyright 2004 by Marcel Dekker, Inc. All Rights Reserved.

of such a process is tremendous, and if we have granules of size 1 to 3 mm the whole freeze-drying operation might take less than 30 min!

Now, at the end of the process, we have a population of granules, all dried under the same conditions, all equal in quality and size, that can be numbered and fed into dry sterile vials as so many distribution machines can do. The result is a batch of identical vials containing, say, 100 ± 1 freeze-dried granules instead of a more or less regular cake, painfully manufactured over several days. Moreover, product "elegance" is maximized and, in that dispersed form, reconstitution takes a matter of seconds.

This is not wishful thinking since we already have the basic knowledge, the practical know-how, and multiyear experience of this type of operation. It is just a change of mindset, a new approach which deviates from historical practice. Unfortunately, we know that this is sometimes more difficult to pass.

Some people will claim that instant coffee manufacturers do not care about sterility, that individual freezing of small droplets is a difficult undertaking, that, maybe mechanically, the granules will not prove resistant to the process. I know quite well that nothing yet has been completely solved, but equally I know that we do have industrial solutions to those specific issues and I have not the slightest doubt that they can be successfully challenged if, at the same time, some developments are made on the formulation side.

4. Irradiation Technology

Almost a hundred years have elapsed since Becquerel, Roentgen, Pierre and Marie Curie, and other pioneers discovered the fascinating world of radiant energy, but it was in the 1930s and the following decade that the main advances were made, inter alia, with the introduction of van de Graaff accelerators, cyclotrons, and the like. As usual these developments did benefit from the war and in the 1940s and 1950s an enormous amount of basic and applied research was done in this field and within almost every compartment of Science: radioisotopes for medicine, fundamental approaches on the structure of atoms and in particle physics, the design and operation of nuclear reactors, and last but not least strategic atomic weaponry.

At first sight, all these developments had little to do with the very basic, down-to-earth needs of the food industry. However, this business was still struggling to meet a geographically large, year-round consumer market with seasonal localized natural resources, and the profession needed ways and means to collect and preserve these unstable products of agricultural or marine origin. Heat treatment, sterilization, or pasteurization, cold storage,

Copyright 2004 by Marcel Dekker, Inc. All Rights Reserved.

and distribution were, of course, the practice at the time but sometimes they did not give all the expected results. This is the reason why, in the early 1960s, some pioneers like Henri Vidal, from the refrigeration industry, thought that it could be of interest to try and use radiant energy. Numerous tests were done, then, with the gamma rays of cobalt-60 and it was shown, among many other things, that it was possible to prevent germination in stored potatoes, and to radio-pasteurize and radio-sterilize natural and processed perishable products. Some years later, the same type of development was achieved with electron beams. Of course, this process was not universal and often it altered substantially the organoleptic properties of the treated goods. There was, also, in medical circles, some deep concern about the remnant free radicals generated in the irradiated products: they were supposed to lead to cancer. For more than 40 years, this question has been debated, most often, unfortunately, in emotional terms, as the media raised concerns and fears in the public at large on nuclear issues, confusing altogether irradiated and radioactive. Today the situation is still unsettled and only a limited number of food items are authorized for processing by radiation: spices, shrimps, ground meat, fish fillets, poultry legs. However, views are evolving as another threat comes into the limelight: risks due to chemicals. In the wake of this it is interesting to see that even the most ardent environmentalists have began to prefer irradiated products to those that have been exposed to ethylene oxide or methyl-bromide!

In the meantime, nonetheless, irradiation technologies became highly sophisticated. Today large cobalt sources, powerful accelerators (such as the Rhodotron), and high-energy x-ray beams process thousands of tonnes different products every year sterilizing frozen shrimps, cross-linking plastic films, energy cables, or water tubing, sterilizing surgical garments and medical equipment, syringes, prosthesis, dressings for extended wounds—and even, at the end of 2001, sterilizing Congressional and Governmental mail due to fear of criminal anthrax contamination!

Here we are today, and again, once more, it is of interest to see how irradiation could couple with lyophilization.

The first obvious issue is to resort to radiant energy to sterilize the container–closure system for injectables. Indeed, glass vials and elastomeric closures can definitely be made sterile by irradiation with gamma rays, electron beams and x-rays, thus preventing the undesirable water uptake resulting from steam treatment. However, if high doses are applied (10 to 25 kGy) some modifications do occur. Glass vials turn brown: butyl rubber becomes sticky and fails the multiple needle penetration test. However, solutions to these problems do exist and, for glass for instance, Schott has developed a cerium doted glass which remains perfectly clean at 25 kGy.

Copyright 2004 by Marcel Dekker, Inc. All Rights Reserved.

It has even been shown (very recently) that, contrary to some previous claims, radiation treatment does not induce extra brittleness in the vials whichever radiation sources are used: gamma, x-rays, or e-beams (Thürk). On the stopper side some preliminary work done by Fran deGrazio showed also that there were some specific formulations well adapted to irradiation. More research is on its way and it looks promising.

The second input that radiation technology could give to lyophilization concerns the products themselves. Let us go back, if you agree, to what I said a little while ago. In a large freeze-drying cabinet holding 10,000 to 100,000 vials we are not completely sure that all vials are strictly identical at the end of the run, and what is valid for their physicochemical properties, residual moisture, and potency is equally valid for their sterility. Can we really rely on a handful of tests on isolated vials to claim that the whole batch is 100% sterile? We know, quite well, that the key answer to this question lies before us and that the only way to secure final sterility is to make sure that the whole process has been duly carried out from the beginning under strictly sterile conditions. This compulsory requirement, unfortunately, is difficult to fulfill and, as evidenced, it adds tremendously to the overall cost; on that latter point we know quite well the feelings of the National Health Programs. Moreover, there are some new active substances which do not come out sterile from their manufacturing process and which are both heat-labile and difficult to filtrate because of their large molecular weight. How can we solve this issue when most sterilizing chemicals are now forbidden or, at least, earmarked as merthiolate!

This is precisely where we can resort to irradiation.

Let us consider a clean plant where solutions to be freeze-dried are prepared with care, under hygienic conditions. Let us secure the filling of the vials, the loading of the freeze-dryer, the freeze-drying itself, the neutral gas vacuum rupture, the driving in of the stoppers, and the unloading of the batch under clean hygienic conditions. Up to now, we have not mentioned sterile processing once and we know that, at that point, the freeze-dried product and its container are not sterile. Let us go ahead anyway, place the aluminum flip-off overseals, and finally package the whole lot into their retail and distribution units. All these operations can be done on-line, even freeze-drying, if we adopt the continuous process that I described earlier. Then irradiation comes in. The finished products can enter a gamma plant or be run under the horn of an e-beam or the window of an x-ray tube and be sterilized in depth, right to the very core of the active substance, and what is valid for one of them is valid for all of them since the radiation treatment is a well-defined physical process which relies exclusively on purely parametric settings. Using this technology we are able

Copyright 2004 by Marcel Dekker, Inc. All Rights Reserved.

to secure a 100% guarantee of sterility and at the same time substantially decrease the manufacturing cost.

Well, it sounds nice—too much maybe. It is too soon for sure because, to the extent of our present knowledge, this process does not have a universal value. Indeed, to be sure that we can resort to irradiation technologies for the terminal sterilization of the finished freeze-dried pharmaceutical products we have to fulfill three important requirements:

1. We should be assured that, at the dose which is delivered, total sterility has been achieved. This depends, in turn, on the initial level of contamination of the product: 25 kGy is the regulatory figure but 5 or even 2 kGy might prove to be enough if the whole process has been done in a clean, hygienic way provided that the initial bioburden is low.
2. At the delivered dose we have to be sure that the therapeutic value of the product has not been impaired, that it has retained its physiological activity, and that its final potency, after irradiation, is in line with regulatory requirements.
3. Even if 1 and 2 are met and we have a sterile and active product, we should be assured that no special foreign element which might have a deleterious effect on health could appear by radiolysis within the other ingredients of the formulation.

Should these three requirements be fulfilled, then we can resort to irradiation. As you will easily understand, there is no direct protocol that can give an overall answer and this development has to be done on a case-by-case basis, each special manufacturing scheme being duly validated. It is, no doubt, a lengthy process which will require a substantial amount of basic and applied research. But we do not start from scratch: a lot has already been done and it lies on the optimistic side. However, to carry on this work, and since it is a new approach for pharmaceuticals, we still need to solve the following issues:

What does the delivered radiation dose really mean? Is 25 kGy an absolute prerequisite or is it just the upper value?

Are 5 and 10 kGy of the same significance if they are delivered by gamma rays, x-rays, or e-beams?

Is the effect of a single dose independent of the dose rate? In other words, do we get the same result if we give 10 kGy in 5 h with gamma rays, in 30 min with x-rays, or in 5 s with e-beams?

Does the irradiation temperature play a significant role and is it not better, for certain delicate products, to carry out the irradiation under negative temperatures?

Copyright 2004 by Marcel Dekker, Inc. All Rights Reserved.

These are some of the different points that need to be clarified but we do already have some answers.

We have shown, for instance, together with Aguettant, that, in solution, heparin, morphine, and apomorphine were almost totally destroyed by irradiation but that, if they were irradiated in the frozen state, at a low enough temperature, 100% of the activity/potency could be preserved. Nevertheless, at these low temperatures, in the frozen state, they became totally sterile under irradiation even after a massive initial contamination with *Bacillus pumillus*.

In very recent experiments done in close collaboration with the Center for Biologics Research and Evaluation of the U.S. FDA (see Ch. 21), Joan May and I have been able to demonstrate that we could safeguard the potency and chemical integrity of different polysaccharides of major significance in injectable vaccines which had received up to 25 kGy from gamma rays (in Celestin, Marcoule and Cigal, Cadarache), e-beams (at Studer's Werk), and x-rays (at RDI IBA).

The road now looks much more open. It is a rough but worthwhile exercise, since it can result in a much easier processing of sterile injectables with increased security and a substantial decrease in cost. Moreover, it appears to be a smart process easily coupled with continuous freeze-drying.

II. CHEMICALS AND NON-AQUEOUS SOLVENTS

Water ice is not the unique substance which can go directly from the solid state into vapor and we know that, within different temperature ranges, many organic and some mineral solvents can do it. Thus, actually, there is no reason to limit lyophilization to the single field of aqueous products and, in that sense, there is also no reason to restrict freezing and drying to the pharmaceutical, biological, and medical fields as well as to cosmetics and food.

This was our reasoning in the mid 1960s when my colleagues and I we developed freeze-drying from non-aqueous media. At that time, a substantial amount of basic research was done, special equipment built, some processes developed, patents applied for, and sometimes granted!

My purpose today is not to indulge in some nostalgic considerations of the past, neither to dwell too long on a topic which lies somewhat outside the main theme of this book, but the ideas are still in the pipeline and they might trigger some interesting new ventures even in the most conventional areas of freeze-drying.

Since it is a rather diversified field, I shall try to scan it quickly and point out what appears to me as the promising issues.

Copyright 2004 by Marcel Dekker, Inc. All Rights Reserved.

A. The Use of Non-Aqueous Co-Solvent Systems

This is the first area that, indeed, is still in the field of "classical freeze-drying." An excellent review of these developments is given in this book by Dirk Teagarden and David Baker and I shall not attempt to supersede what they have already described.

The very basic idea is, then, to freeze-dry aqueous solutions which contain substantial amounts of organic solvents because their presence brings a marked improvement in the results, for instance: increasing the rate of sublimation and chemical stability both of the pre-dried bulk solution and of the dried product; improving wettability, solubility, and reconstitution of the dry product; enhancing sterility assurance, etc. Of course, there are also many potential drawbacks: toxicity concerns, operational hazards, presence of undesirable contaminants, and, as can be readily understood, increased cost and adverse regulatory issues. However, in some cases the balance proved to be positive and, in the Caverject® Sterile Powder Project, Pharmacia was able to prepare stabilized Prostaglandin E_1 by freeze-drying a 20% (v/v) tert-butanol/water co-solvent system.

In my views it is a very encouraging step and I am absolutely convinced that many more attempts should be made in that way using other solvents. This, in fact, is already the case for Annamycin (Tert-Butanol, Dimethyl-sulfoxide, water), Cephalothin sodium (50% w/w Isopropyl alcohol/water), Dioleoylphosphatidylcholine (Cyclohexane), and many others.

We can even use a pure non-aqueous solvent alone. In 1964 we reported on some successful experiments done with phospholipids freeze-dried out of carbon tetrachloride solutions using glycol disterate as the bulking agent.

No doubt there are a great number of products which could be studied along these lines, still bearing in mind, however, that, under present regulations, most of these processes can fail on pure toxicity and tolerance issues.

These issues, however, are less stringent for products which do not penetrate the body by oral or parenteral routes and there are still very large openings for solvent freeze-drying in dermatology or in the cosmetic field, though, of course, great care still has to be taken with their systemic penetration through the skin, if any.

B. Complex Freeze-Drying

In that specific area, freeze-drying can offer even more if we consider the processing of different solvents mixed together. We discussed the behavior of these systems in 1966, introducing then the concept of "complex

Copyright 2004 by Marcel Dekker, Inc. All Rights Reserved.

freeze-drying'' which is closely linked to the physical characteristics of the different solvents.

Depending on their miscibility, freezing point, and saturated vapor pressure in the solid state, we found two different freeze-drying strategies, as follows.

1. Joint Complex Freeze-Drying

This refers to solutions made of two or more solvents, either easily miscible or emulsified together, containing two or more active solutions and their accompanying ingredients (including the ad hoc bulking agents).

After freezing, they can be dried by sublimation under vacuum according to two different modes:

Simultaneous lyophilization: Both/or more solvents sublime at the same velocity and thus the freeze-drying boundary moves inside the frozen mass at a constant speed. This is typical, for instance, of a mixture of dioxane and water.

Stepwise or ''scaled'' lyophilization: One of the solvents is more volatile than the other because of its higher vapor pressure in the frozen state and it disappears first, followed at different speeds by the others. The frozen mass, then, is ''carved'' from the inside along the crystallized pathway of the first solvent and in this open network, the ''islands'' of the second solvent are progressively extracted. This is the case for a mixed solution of cyclohexane and water. When 100 p. 100 of the cyclohexane has already been sublimated away when more than 85% of the water ice is still there.

2. Successive Freeze-Drying

In that process the system under investigation is freeze-dried several times in succession resulting in a final dry product that has an intermingled structure of interlocked membranes. To that end we should make sure that each ''new'' solvent does not dissolve the material coming from the preceding ones. In 1966 we gave, for instance, the following example:

1. A 1 p. 100 solution of polystyrene in carbon tetrachloride is freeze-dried.
2. The resulting plug is impregnated by a 2 p. 100 solution of dextran in water and freeze-dried.

The final cake when imbedded into an acrylic resin and sliced for microscopic examination showed a very nice structure with a regular lattice

Copyright 2004 by Marcel Dekker, Inc. All Rights Reserved.

of polystyrene membranes in which a sublattice of dextran membranes is enclosed.

We also observed this whole process in real time using a specially built freeze-drying microscope allowing direct observation of the freezing process and of the movement of the drying boundaries in a thin film.

Needless to say, this sequenced freeze-drying operation could be repeated, say with a 2 p. 100 maltose solution in diethylamine, resulting in a triple intermingled network of three compounds: polystyrene, dextran, and maltose and so on.

These complex porous bodies have interesting properties and could, for instance, be used as "intelligent" filters on gases or fluids, each component of the freeze-dried mass having its own selectivity and retaining those substances with which it can interact. When the filtration is over, it is possible, then, to extract the three "collections" one by one using the original solvents. That process was, at the time, felt to be of interest for the selective retention of aromas and was patented by the Nestlé Company with which I was then associated.

C. Mineral Solvents

Organic solvents are not the only ones to be used in freeze-drying and, during the same period, we devoted a large amount of effort to evaluating the opportunities offered by some selected fluids of mineral origin. The results were promising and we believe that, today, they can prime new developments in what remains an open and challenging field.

In this brief review I shall refer only to two particular compounds: ammonia and carbon dioxide.

1. Ammonia

Liquid ammonia (NH_3) is a most interesting solvent where reactions NH_2–H do occur, similar in a way to the OH–H reactions which are found in water. Alkaline metals can react with ammonia giving soluble amidures which most often do not resist the transfer to room temperature. Many organic substances too, like amino acids, phospho lipids, certain polymers, are soluble in liquid ammonia at atmospheric pressure at temperatures between $-40^{\circ}C$ and $-70^{\circ}C$. Their solutions can then be distributed in vials, frozen with liquid nitrogen, set into a freeze-dryer, and placed under a vacuum. Under those conditions solid ammonia will easily sublime at temperatures as low as $-130^{\circ}C$ and pressures around 20 μbar leaving a dry porous cake containing the original substance (incorporated if required in

Copyright 2004 by Marcel Dekker, Inc. All Rights Reserved.

an appropriate bulking agent) which, now being stable, can be brought back to room temperature.

On that basis we attempted to see whether we could stabilize transient free radicals generated by irradiation at liquid nitrogen temperature. To that end we prepared a 10% solution of l-lysine in liquid ammonia at $-70^{\circ}C$ and froze it with liquid nitrogen down to $-196^{\circ}C$. At that temperature we irradiated the system with a dose of 10 kGy of gamma rays from a cobalt-60 source (in CEA, Saclay).

The same experiment was done in parallel with a 10 p. 100 solution of l-lysine in water. In both cases, the activated frozen material gave, at $-196^{\circ}C$, a strong paramagnetic signal after irradiation. However, if the temperature rose over $-100^{\circ}C$, this signal almost completely disappeared; at the same time, evidence of the recombination of free radicals in the solid state could be witnessed by thermoluminescence, essentially below $-100^{\circ}C$.

Thus, instead of rewarming the irradiated solutions, we placed them in two different freeze-drying cabinets and sublimed the solvents under reduced pressure:

at $-30^{\circ}C$ and 100 μbar for the frozen water solution;
at $-120^{\circ}C$ and 25 μbar for the frozen ammonia solution.

When the products were dried they were brought back to room temperature, placed under nitrogen gas, and tested with ESR equipment. We could detect, then, a very faint signal for the product issuing from the water solution (relative intensity: 2000), whilst the lysine dried from the ammonia solution gave a very strong response, 300 times bigger (relative intensity: 6,000,000).

This result was confirmed with other substances and showed in evidence that unstable free radicals by irradiation generated at liquid nitrogen temperature could be preserved and stabilized at room temperature by freeze-drying of their solution in ammonia at very low temperatures. This, of course, would be strictly impossible in a water solution.

We are convinced that physicochemists have not yet exhausted the possibilities offered by this technology.

2. Carbon Dioxide

Amongst the many solvents that can be used to extract and dissolve natural and artificial chemicals, carbon dioxide in its liquid form is one of the most interesting not only because of its physical properties, but also because of its lack of toxicity. Sparkling mineral waters and soft drinks are good examples. The only serious drawback in handling liquid CO_2 is that it is

Copyright 2004 by Marcel Dekker, Inc. All Rights Reserved.

compulsory to operate under pressure and, to that end, we designed with Air Liquide, and also within the Nestlé company, different laboratory and pilot equipment with which we carried many experiments over several years. Let me just quote two of them which involved freeze-drying.

In the first one we made use of a pressure reactor in stainless steel, containing a certain amount of dry black tea, through which liquid CO_2 could percolate at $-35°C$ and 13 bar. Under those circumstances and with continuous stirring, and a loop recirculation, the solvent extracts a large amount of the main aromatic compounds of tea, essentially the most fragile and volatile ones.

The aromatic CO_2 is then separated away and expanded through a nozzle giving a fluffy carbonic snow at $-78.8°C$. This aromatic snow is then mixed on-line with an instant tea powder coming from a conventional spray-dryer and, as it sublimes away, it releases directly into the dry product the delicate aromas extracted from the unprocessed tea. What, indeed, was achieved is direct freeze-drying of frozen carbonic acid at atmospheric pressure and low temperature.

In the other set of experiments, more connected with the pharmaceutical or chemical industries, we directly dissolved an active substance—or a more complex formulation including a bulking agent—in liquid CO_2 under agitation. This operation was carried out in a special stainless steel tray sitting on a shelf inside a pressure vessel. As in the preceding case, the operation was done at $-35°C$ and 13 bar with a given volume of liquid CO_2. When it was felt that the dissolution was done, liquid nitrogen was fed into the underlying shelf and the solution slowly frozen. During that time and before reaching $-78.8°C$, the decreasing CO_2 pressure was compensated by a controlled injection of nitrogen gas to keep the vessel pressure around 10 bar. Finally, near $-80°C$, the whole material was frozen hard and further subcooled to $-100°C/-110°C$. The nitrogen pressure was released and the vessel brought back to 1 bar.

In the stainless steel vessel there is, now, a solid disk of deep frozen carbonic acid ice which is ready to sublimate if we provide the appropriate energy (thanks, for instance, to an electric heater placed on the supporting shelf). Then solid CO_2 evaporates and the drying boundary recedes progressively inside the frozen slab leaving behind a dry, solid, porous cake. What is remarkable is that, right to the very last core of sublimating ice, this operation is done at temperatures below or at least equal to $-78.8°C$ and at atmospheric pressure at a relatively good rate. Indeed, depending upon the nature and concentration of the starting solution, we observed that the freeze-drying boundary sinks inside at a speed of 3 to 15 mm/h.

These are only two examples of what can be achieved with CO_2 and it is our firm conviction that many new products and/or ingredients used by

Copyright 2004 by Marcel Dekker, Inc. All Rights Reserved.

the pharmaceutical and especially the cosmetic industry could be processed successfully with this technology.

D. Freeze-Drying and the Major Chemical Industry

In switching from water to co-solvents, then to organic solvents, and further to mineral solvents we have progressively shifted from classical pharmaceutical practices to more advanced "exotic" technologies which open the door to major chemical industries.

Indeed, if we can make indiscriminate use of solvents—except for the usual regulations applied to chemical plants—we can visualize many potential areas in which freeze-drying has already brought and could bring new exciting developments. Let us quote just a few of them:

Preparation of porous, expanded, fats, polymers, and fibers.

Preparation of catalysts by freeze-drying their metallic salts which, when expanded as dry porous cakes, can be turned into oxides by heating, then reduced by hydrogen as dispersed metals.

Preparation of filters in slabs or in powders suitable to be placed on air channels in fluidized beds or else as selective adsorbants on process lines. In recent years we made interesting approaches at COGEMA in this field using freeze-dried silica and alumina for the retention of radionuclides, acid droplets, and contaminants in the ventilation ducts of nuclear plants. Besides their great efficiency and low pressure drop the most interesting feature of these freeze-dried filters is that they can withstand extreme pH conditions and high temperatures.

As a sideline, preparation of "absolute" filters with the same freeze-dried silica beads to control air ventilation in highly sensitive laboratories for bacteriology, virology, genetic engineering, P4 labs, etc.

Preparation of pigments and dyes for cosmetics, paints, and coatings. Exploratory work has proved very promising. Freeze-dried pigments (most often from their organic solutions) are of higher quality, bright, glittering, with fresh colors.

Decontamination of low- to medium-activity liquid wastes from nuclear centers. Very advanced work has been done in the past by CEA on this issue and the results were excellent since decontamination factors of 10^6 or even better could be achieved (Rey, Cerré, and Mestre), much better than by single effect or even multiple effect evaporation.

This listing, of course, is in no way limiting and there are many other areas in the chemical industry where lyophilization could be used. Is this

Copyright 2004 by Marcel Dekker, Inc. All Rights Reserved.

century-old technology suitable to meet this challenge? Shall we not stumble across pure engineering problems and costs as we enter an industrial area where the daily batches might be several orders of magnitude higher than in the food industry? My own feeling is definitely positive. Yes, lyophilization can afford to enter these new areas. The continuous process developed for pharmaceuticals and foods can be easily scaled up to handle hundreds of tonnes per day if needed and the component industries are already able to deliver the corresponding equipment. Large vacuum plants are no threat to the different manufacturers who already build them for steel degassing and casting. As far as the energy requirements are concerned—and since they play a critical role in freeze-drying where phase changes are made four times (freeze–sublimate–condense the vapors–defrost the condenser!)—we can find a solution if the freeze-drying plant is positioned in the close vicinity of one of these huge storage areas devoted to LNG (Liquefied Natural Gas). Indeed, there, we have very low temperatures available at almost no cost since the liquid methane has to be converted into a simple gas anyway to be fed into the network. Today, this major refrigeration capacity is poorly used. Moreover, the liquefied gas can be boiled under pressure and thus provide mechanical energy to drive turbines, alternators, and pumps. Finally, the outgoing gas can still be burnt to deliver the necessary heat for sublimation. Whilst I am convinced that neither a food industry nor a pharmaceutical plant manufacturing ethical products will ever settle on the premises or even in the close vicinity of a refinery or a petrochemical complex, it is pretty clear that a pure chemical industry would do it right away.

At the end of this incomplete review I feel that lyophilization will not remain an exclusive technique for a select few. It will move as cryogenics did, and today when Air Liquide or BOC deliver liquid oxygen by the hundreds of tonnes we are pretty far away from the isolated dewar of liquid air prepared a century ago by Georges Claude. I have not the slightest doubt that lyophilization can follow this route.

Copyright 2004 by Marcel Dekker, Inc. All Rights Reserved.

"...[a] **clear** and **comprehensive** book, readily accessible to the diversified group of potential users of freeze drying in the pharmaceutical industry."—*Bioseparation*

"...contributors range from theoreticians to experts with considerable practical experience...**very useful**."—*European Journal of Pharmaceutics and Biopharmaceutics*

"...a **good acquisition** for anyone contemplating the development of a lyophilized product."—*Pharmaceutical Development and Technology*

about the second edition . . .

Thoroughly acquainting the reader with freeze-drying fundamentals—including water properties critical to the process and mechanisms and means of protein stabilization—***Freeze-Drying/Lyophilization of Pharmaceutical and Biological Products, Second Edition*** carves practical guidelines from the **very latest** theoretical research, technologies, and industrial procedures—ensuring the best execution of steps from closure preparation and regulatory control of products to equipment sterilization and process validation.

Unveils innovations currently advancing the field, including LYOGUARD® packaging for bulk freeze-drying and the irradiation of pharmaceutical and biological products.

The 13 chapters new to this ***Second Edition*** provide state-of-the-art information on freeze-drying using nonaqueous cosolvent systems...formulation characterization, and molecular mobility determination via NMR relaxation...modern closure and container options for lyophilization...selection of advanced glassware for freeze-drying...specific considerations in the freeze-drying of biological standards...developing process data to facilitate the move from pilot plant to production...the use of integral HFT systems in the global validation of cycle parameters...contemporary opinions and guidelines for lyophilizer qualification...the technological horizon for freeze-drying...and many more topics.

about the editors . . .

LOUIS REY is a Scientific Advisor based in Lausanne, Switzerland. He has been a Regent's Lecturer and Visiting Professor at the University of California, Los Angeles, and the University of Alaska, Fairbanks. The author, coauthor, or editor of 16 books and 130 papers and notes in eight languages, he has also presented over 250 lectures worldwide. Dr. Rey has worked as a research scientist at the Centre National de la Recherche Scientifique, Paris, France, and as Head of Corporate Research and Development for Nestlé, Vevey, Switzerland. He is a Fellow of the New York Academy of Sciences and the Academy of Savoy, and has managed the International Courses on Lyophilization. Dr. Rey received the M.A. (1952) and Ph.D. (1958) degrees from the Sorbonne, Paris, France.

JOAN C. MAY is the Director of the Laboratory of Analytical Chemistry for the Center for Biologics Evaluation and Research (CBER) of the U.S. Food and Drug Administration, Rockville, Maryland. The author or coauthor of many articles and the coeditor of several books on freeze-drying processes, she is a member of the American Chemical Society and the North American Thermal Analysis Society. Dr. May received the B.S. degree (1965) from Nazareth College, Rochester, New York, the M.S. degree (1968) from the University of Wisconsin–Madison, and the Ph.D. degree (1971) in analytical chemistry from the University of Notre Dame, Notre Dame, Indiana.

Printed in the United States of America

MARCEL DEKKER, INC.
NEW YORK • BASEL

ISBN 0-8247-4868-9